Phytoremediation of metal-contaminated chromium asbestos mines of Jharkhand: Ecological recycling through vermicomposting

A thesis submitted to

Jadavpur University

In partial fulfilment of the requirements for the degree of

Doctor of Philosophy (Science)

By

Sonali Banerjee (M.Sc.)

Index No: – 84/22/Life Sc./27

Department of Life science & Bio-technology

Jadavpur University

And

Agricultural and Ecological Research Unit

Indian Statistical Institute, Giridih

June 2025

INDIAN STATISTICAL INSTITUTE

Pradip Bhattacharyya, PhD
Associate Professor
Biological Science Division
Agricultural & Ecological Research Unit

Rose Villa, New Barganda
Giridih, Jharkhand - 815 301, India
06532-226688 (O), (91) 09859986548 (mobile)
pradip.bhattacharyya@gmail.com

Dated:

Certificate from the supervisor

This is to certify that the thesis entitled **"Phytoremediation of metal-contaminated chromium asbestos mines of Jharkhand: Ecological recycling through vermicomposting"** submitted by **Smt. Sonali Banerjee** who got her name registered on **03.03.2022** for the award of **Ph.D. (Science)** Degree of **Jadavpur University, Department of Life Science and Biotechnology**, is absolutely based upon her work under the supervision of **Dr. Pradip Bhattacharyya** and that neither this thesis nor any part of it has been submitted for either any degree/ diploma or any other academic award anywhere before.

Pradip Bhattacharyya

Pradip Bhattacharyya, Ph.D
Associate Professor
Agricultural and Ecological Research Unit
Indian Statistical Institute
New Barganda, Giridih - 815301
Jharkhand, India

Dedications……!!!!!

To **Lord Jagannath**, whose divine grace, strength, and guidance have been my constant source of inspiration.

To **my Supervisor**, **Dr. Pradip Bhattacharyya**, whose support, mentorship, and encouragement have been invaluable throughout this journey.

To **my Baba**, who wished to see "**Dr.**" before my name. I may not have become the doctor you imagined, but I fulfilled that dream in my own way.

To **my Maa**, who once dreamed dreams she could not pursue, but chose to live them through me. She always told my father, "***My girl will do what I could not.***" Your faith gave me wings. This journey is yours as much as mine.

To **Sayak**, who believed in me, saw my potential, and lifted me when I lost faith in myself.

DECLARATION OF ORIGINALITY

I, Sonali Banerjee, Index No.: 84/22/Life Sc./27, hereby declare that this Ph.D. thesis entitled **"Phytoremediation of metal-contaminated chromium asbestos mines of Jharkhand: Ecological recycling through vermicomposting"** represents my original work carried out as a doctoral scholar at Agricultural and Ecological Research Unit, **Indian Statistical Institute**, **Giridih, Jharkhand.** The work contained in the thesis is original and has been done by myself under the supervision of my supervisor, **Dr. Pradip Bhattacharyya**. To the best of my knowledge, it does not contain any material previously published by others or written by any other person. The work has not been submitted to Jadavpur University or any other Institute for any other degree or diploma. Any input from sources other than myself or others with whom I have collaborated on this study has been acknowledged. I have given due credit to them by citing them in the text of the thesis and giving their details in the references. When I have used writing from another source, I have always put it in quotation marks and give credit where credit is due by citing the source and providing all necessary information in the references.

Date: 17.06.2025

Sonali Banerjee

(Sonali Banerjee)

Acknowledgement

I express my deepest gratitude to my supervisor, **Dr. Pradip Bhattacharyya**, Associate Professor, Agricultural and Ecological Research Unit, Indian Statistical Institute, Giridih. Sir, you are truly different. When I first came to Giridih, my first time away from home, you guided me not only in research but in life. You showed me the way when everything felt unfamiliar. Your constant support, encouragement, and belief in me helped me push through the moments when I doubted myself. You always motivated me, gave me firm deadlines, and reminded me of what I was capable of. Even when I struggled to meet those expectations, I never felt alone because your belief in me never wavered. Today, I realize that without your guidance and steady hand, I could not have shaped myself or my research journey the way it is now. For that, I am sincerely grateful. I truly believe I could not have had a better mentor.

I would like to sincerely thank **Dr. Abhisek Mukherjee**, Associate Professor, Agricultural and Ecological Research Unit, Indian Statistical Institute, Giridih, for his invaluable guidance and support throughout my research journey. From the early days of my PhD, Sir, you joined us in the field, worked as if it were your own project, and offered insightful feedback and constant encouragement to improve my work. Beyond academics, your kindness touched every part of this journey — from treating us to delicious meals, playing badminton, to being there whenever I needed help, in any form. I am truly grateful for everything. I would like to express my heartfelt thanks to **Dr. Hari Charan Behera,** Associate Professor, Sociological Research Unit, Indian Statistical Institute, Giridih, for his constant support and for playing badminton with us — a refreshing break during my PhD journey.

A special thank you to **Dr. Sudipta Tripathi,** Assistant Professor, School of Environment and Disaster Management, Ramakrishna Mission Vivekananda Educational and Research Institute— without your motivation and unwavering support, I wouldn't have taken the first steps toward pursuing a PhD. You helped me in every possible way, and I'm truly grateful. I would like to express my sincere gratitude to **Prof. Dibyendu Sarkar**, Department of Civil, Environmental, and Ocean Engineering, Stevens Institute of Technology, USA, and **Prof. Rupali Datta**, Department of Biological Sciences, Michigan Technological University, USA, for their invaluable guidance, thoughtful insights, and continued support throughout my research journey. Their encouragement and timely input have been instrumental in shaping my work. I am sincerely thankful to **Dr. Jajati Mandal**, University of Salford, UK, for his valuable collaboration and insightful contributions throughout my research journey. Your support and input have been truly helpful and appreciated. I am also thankful to **Prof. Biren Panja,** Professor, Department of Plant Pathology, BCKV, for your support and guidance in working with mycorrhizal cultures, especially when I was new to the subject. I am very grateful for your support. I extend my thanks to **Dr. Satya Sundar Bhattacharya,** Associate Professor, Department of Environmental Science, Tezpur University**,** for helping with sample analysis in the early stages and for providing a welcoming environment at Tezpur University through your suggestions and the warm presence of your scholars. I am grateful to the **Indian Statistical Institute** for the opportunity to join as a Junior Research Fellow, for providing a supportive research environment, instrumental facilities, as well as the fellowship and other necessary assistance throughout my work. I would also like to sincerely thank the

Department of Life Science & Biotechnology, **Jadavpur University**, and all its faculty members for allowing me to register as a Ph.D. candidate and for their continued support.

I would like to express my deepest love and gratitude to Late Mr. **Hari Sankar Shaw**, fondly known to us as **"Hari da",** Assistant Farm Manager at ISI-Giridih. His fatherly care, constant support, and the homely environment he created meant to me during my Ph.D. journey. Whenever I faced a problem, I could always turn to Hari da, and he would resolve it within moments — his presence was truly a blessing.

I'm also very grateful to **Ramesh ji and Santosh ji** for their kind help and generosity. My heartfelt thanks go to **Sonu Da, Chhotelal Bhaiya, Aslam Da, Suman Da, Dewson Da, Sandip Da, Rashid Da, Khisku Da,** and **Kaleswar ji** for their unwavering support, from sampling to daily lab maintenance; their dedication made everything run smoothly. Honestly, it's hard to imagine my lab life without them. Also, I would like to extend my heartfelt thanks to all the security personnel for always ensuring a safe and secure environment on campus.

Beyond the farm staff, I extend my sincere thanks to **Samsul da, Ajit da, Naquib ji, Asif ji, Pradeep ji, Vikas ji, Tudu ji,** and other members at ISI-Giridih, whose help with official matters ensured a hassle-free working environment. My warmest appreciation also goes to **Rakesh da, Azhar da, Sulekha di, and Zoya di** for the comforting and delicious meals served at our canteen. A special thank you to **Suresh ji** for tirelessly helping with travel and field sampling. I would like to thank **Manash da, Surajit da,** and other staff members at ISI-Kolkata for their guidance, travel support, and help with official work. Lastly, I want to express my gratitude to all the staff members of **Jadavpur University**, especially **Azizur da** from the Ph.D. Cell (Science), for his incredible support. He was always ready to assist with any official matter and helped make my entire research journey smoother.

I would like to thank all of my lab mates at ISI-Giridih. My senior, **Saibal da,** I would like to express my heartfelt gratitude for his immense support throughout my research journey. In the early days, your strict nature and frequent scoldings for my mistakes made me nervous, but they were always followed by guidance and genuine care. You not only taught me every experiment with dedication but also guided me throughout my research journey. Over time, you evolved from a strict senior into a beloved elder brother—someone I could rely on both professionally and personally. Your unwavering support in and beyond the lab has shaped who I am today. I'll always be thankful and will cherish our bond.

I want to sincerely thank all my seniors, **Priyanka di, Sampad da, Shuvrodeb da, Kasturi di, Annanya di, Sandip da, Pranamita di, Tapadhara di, and Adrija di** for their constant support and guidance. Whether it was inside the lab or beyond, you were always there with advice, encouragement, and a friendly helping hand. Your presence created a positive and motivating work environment, and I'm truly grateful for all the moments of support and learning I've received from each of you.

Suvasri, a dear friend from my M.Sc. days, and we began our Ph.D. journey together—just like two new kids at ISI Giridih. Over time, we not only worked and lived together but also built a home and a beautiful friendship. You've become one of my closest companions and my go-to problem solver, always ready with a quick fix or practical advice. Through all the

highs and lows of my Ph.D. journey, you stood by me. We've fought, laughed, cried, gone on trips, and shared it all. I've truly cherished every moment we shared. Thank you for letting me be a part of your journey. **Shreya,** you've been an amazing friend, a constant source of motivation and positivity. Your caring nature and helpful advice always came just when I needed them most. You're also a fantastic trip planner with a great sense of aesthetics — the Australia trip wouldn't have been the same without you. The bond we shared, me, Suvasri, and you, became truly special and something I'll always treasure.

Rupsha, we've shared so many moments—starting from field sampling, lab work, to our visit to Tezpur University. Even our early work trips turned into cherished memories filled with laughter. You've also been a wonderful dancer, always bringing energy wherever you go. Grateful for all the memories you've added to my journey.

Sonam, from being my junior, you became someone very close to me. Your unwavering support, constant help in my research, and your genuinely kind heart touched me deeply. You stood by me when I needed someone the most, and without you, this journey would have felt incomplete. I'm truly, deeply grateful to you, from the bottom of my heart.

I would like to thank **Sumit** and **Gourav**, for their constant support and ever-helpful nature. Their assistance was invaluable to my research, especially during the sampling time, which wouldn't have been possible without you guys**. Sumit**, you have the heart of a child, always eager to help. Even though we had to do quite a bit of convincing to get you to do things, and also, teasing you was one of our favourite pastimes! And **Gourav**, your kindness truly stands out. Your advice is always thoughtful and genuinely helpful. You always listened patiently whenever I shared something, and you took it gracefully. That thoughtfulness and openness mean a lot to me. Beyond work, we shared a wonderful bond filled with laughter and memories, from picnics to trips, that I will always cherish.

I would like to extend my heartfelt thanks to **Riddhi** and **Sristi** for their unwavering love and support throughout my journey. **Riddhi**, you stood by me during one of the most difficult phases of my life, encouraging me, lifting me up when I felt lost, and giving me the strength to carry on. In the lab, and of course, your playful teasing and affection brought warmth and lightness to even the heaviest days. I'll always cherish that. **Sristi**, though you joined as one of my juniors, you soon became a wonderful friend and neighbour. Especially during the final, most intense stretch of my PhD, you were always there, your readiness to help, your kindness. This kind of support is something I will carry in my heart always.

I'm truly thankful to my dear juniors, **Annewsa**, **Jyoti**, and **Sreeya**, for always being there with their immense support. To Debatri, Sayantika, Ambika, and Sohail, though we've known each other for a shorter time, I've genuinely cherished your presence. Wishing each of you all the very best for your future journeys.

I would like to express my special thanks to **Madhurima** for her constant support, her warm and loving nature, and for being such a wonderful friend. The bond we share has been truly special and has brought me comfort and strength during my journey. Also, thank **Sreemoye** for her constant cooperation and the memories in Giridih and Rishop trip.
Beyond the lab, my heartfelt gratitude goes to my landlord, **Uncleji**, who embraced me like his own child. He always expressed pride in my pursuit of a PhD and would often say, "**You**

make me proud." His warmth, encouragement, and fatherly support meant a lot to me throughout this journey. Most importantly, my deepest gratitude goes to "**Giridih**"—a place that became so much more than just where I pursued my research. It nurtured me, shaped my resilience, and helped me grow not just as a researcher but as a person. Giridih taught me to adapt, to endure, and to find joy in simplicity. It became my strength, and above all, my "**OWN HOME**".

I'm deeply grateful to my friends—**Suchana, Baisakhi, Arijit, Tanay, Arko, and Rohit**—for their unwavering support, uplifting words, and the countless moments of laughter that helped me recharge and stay balanced. A heartfelt thanks also goes to **Shrestha, Priyanka, Hrishikesh, Suman, Suzana, Prithwish, and Aindrila** for creating beautiful memories and offering much-needed escapes from the intense pace of PhD life. Your presence made my journey lighter and so much more joyful.

Last but not least, I would like to express my deepest gratitude to my family, my big strength, **my Maa (Mrs. Namita Banerjee)** and **Baba (Mr. Indrajit Banerjee)**, for their unwavering support, sacrifices, endless patience, and constant encouragement throughout this journey. A special thank you and all my love to **my little sister, Soumi Banerjee**. From being my wardrobe manager to stepping in as my advisor when I needed it most, you've always supported me and made sure I had everything I needed. I'm truly grateful for your constant help and presence in my life.

I would also like to express my deepest gratitude to **my Mama (Dr. Subhas Chandra Mukhopadhyay)**, and **Maima (Dr. Krishanthi Jayasundera Mukhopadhyay)** for your constant encouragement to pursue my PhD. Also, thanks to my brother, **Hiroshi,** and sister, **Sakura**, for their incredible support during my conference trip to Australia meant a lot to me. I am truly overwhelmed by the love, care, and all the thoughtful arrangements you made for me. Your unwavering support has left a lasting impact on my journey.

Sayak, I'm truly and deeply grateful to you. Words like 'thank you' feel far too small to express what your presence has meant to me. You've been my constant, my strength, my unwavering support through every challenge, setback, and moment of doubt during this journey. Your belief in me, even when I struggled to believe in myself. I also want to sincerely thank **Kakima and Kaku**—from the bottom of my heart—for their unconditional love, kindness, and the warmth with which they embraced me as one of their own. Your family has been a true blessing in my life.

Finally, from the bottom of my heart, I thank each of you who shared this journey with me. My experiences here have shown me, beyond a doubt, that "**HARD WORK**" truly pays off.

Place: Kolkata

Sonali Banerjee

Date: 17.06.2025 Sonali Banerjee

ABSTRACT

Index No. 84/22/Life Sc./27

Title: Phytoremediation of metal-contaminated chromium asbestos mines of Jharkhand: Ecological recycling through vermicomposting

Submitted by: Sonali Banerjee

Chromite-asbestos mining generates substantial amounts of toxic waste (CAMW), leading to the contamination of adjacent agricultural lands with potentially toxic elements (PTEs). This study investigates PTE concentrations, identifies their sources, assesses associated health-dietary risks through probabilistic models and examines the combined impact of soil alkalinity and bioavailable PTEs on microbial diversity in the chromite-asbestos mining region of India. The soil, tailings, and rice grains samples were collected and studied across the region. The results revealed that the PTEs concentration was significantly above the permissible limit in site 1 (mine waste dumping area) and site 2 (mine waste contaminated soil) as compared with site 3 (uncontaminated soil). The Positive matrix factorization, Self-organizing map, and spatial distribution map analysis identified the source of PTEs pollution in this region. The Free ion activity model (FIAM) was applied to detect the solubility of PTEs in polluted soil and their probable transfer from soil to rice grain. The hazard quotient values were significantly higher than the safe (FIAM-HQ < 0.5) for Cr (1.50E+00), and Ni (1.32E+00). Severity adjustment margin of exposure (SAMOE) results indicates that raw rice grains contaminated with PTEs pose a high health risk to humans [Cr: 0.001; Ni: 0.002]. Boiled rice showed a moderate risk (Cr: 0.011; Ni: 0.013), while rice (without husk) reflected a high (class 5) dietary risk. Compared to adults (5.08E-05), children (1.88E-03) were more vulnerable to total carcinogenic risk via the ingestion pathway. The study observed a decline in microbial attributes, with *Proteobacteria* constituting 57.18% of the bacterial community, highlighting their predominance in the contaminated soil. Therefore, efficient management is necessary for the mitigation of PTEs.

In recent decades, bio-based approaches (mycophytoremediation and vermi-technology) present a promising strategy for environmental restoration worldwide. Furthermore, the present investigation assessed the impact of AMF (*Glomus hoi*, *Funneliformis coronatum*, *Claroideoglomus claroideum*, and *Claroideoglomus etunicatum*) on the growth and PTEs accumulation abilities of vetiver (*Chrysopogon zizanioides*) in a soil contaminated with CAMW. *Glomus hoi* showed high efficiency in improving soil quality, mitigating PTEs stress, accumulating PTEs in the roots (Ni: 27.44%, Cr: 21.74%), and promoting healthy plant growth. This study also explores the post-remediation management of PTE-enriched vetiver plants (PTE-EV) obtained after myco-phytoremediation, where significant accumulation of PTEs occurred in plant tissues. To prevent re-contamination from exposed shoot parts, PTE-EV was vermi-remediated with cow dung, effectively neutralizing acidity, boosting NPK levels, and stabilizing organic carbon mineralization. Another critical aspect is the widespread generation of CAMW, rich in PTEs, poses a major environmental threat and currently lacks sustainable recycling solutions. This study also introduces vermi-remediation technology to sustainably and efficiently transform CAMW into a valuable organic fertilizer, offering a practical solution for waste management and soil restoration. The findings revealed bioavailable PTEs levels were significantly reduced up to 80% in vermibeds. Therefore, this study highlights the potential of vermicomposted PTE-EV and vermicomposted CAMW as effective organic amendments for diverse agricultural systems, including crops like tomato, chilli, sesame, and rice. Results showed that combining vermicomposted PTE-EV/CAMW with chemical fertilizers led to negligible PTE levels in edible crops, supporting their use as sustainable alternatives to traditional manure for long-term soil health and waste management. Overall, we believe this study represents a foundational step toward advancing eco-friendly bioremediation of toxic CAMW, supporting sustainable management, and promoting long-term ecosystem health.

Sonali Banerjee
Signature of Student

Pradip Bhattacharyya
Signature of Supervisor

Pradip Bhattacharyya, Ph.D
Associate Professor
Agricultural and Ecological Research Unit
Indian Statistical Institute
New Barganda, Giridih - 815301
Jharkhand, India

Thesis Title: Phytoremediation of metal-contaminated chromium asbestos mines of Jharkhand: Ecological recycling through vermicomposting

SYNOPSIS

The land of mines and minerals, Jharkhand, is one of India's leading states in mining activities. Over the past few decades, the rapid growth of the mining sector and the abundant disposal of mine waste have led to the contamination of nearby agricultural soils with potentially toxic elements (PTEs) such as Cr, Ni, Cd, Cu, and Pb. This has raised serious environmental and human health concerns. The research is focused on the chromium-asbestos mine situated in the Roro hills, Chaibasa district, Jharkhand. Due to its toxic nature, lack of nutrients, poor water retention, and non-biodegradable properties, chromium mine waste poses a serious threat to the ecosystem. Crops commonly grown on or near these mine sites (mainly rice) tend to absorb and accumulate high levels of PTEs in their roots, shoots, and grains. This, in turn, poses a significant risk to the food chain. Therefore, mitigation of soil contaminated with hazardous waste requires innovative strategies. However, most current methods are often unsustainable, expensive, and can produce secondary waste or negatively impact soil properties. In contrast, using the appropriate combination of plants and beneficial microorganisms offers an eco-friendly solution. This approach can help reduce soil toxicity, support the re-vegetation of polluted sites, improve long-term soil health, and prevent erosion by stabilizing the soil surface. While microbe-assisted phytoremediation offers several benefits, one concern is the potential for recontamination. If plants absorb PTEs and later shed their shoots back into the field, these harmful elements can re-enter the soil. To address this issue, an innovative and cost-effective solution lies in vermitechnology. This approach involves using earthworms to convert PTEs-contaminated plant material into nutrient-rich organic compost. Farmers can then apply this compost to their fields to enhance soil fertility and crop productivity. Altogether, this integrated method presents a holistic strategy for waste management, PTEs detoxification, and soil health improvement, contributing significantly to global research efforts.

Evaluation of Soil Properties, PTEs Concentration, and Distribution Pattern

The chromium-asbestos mine area contains a variety of potentially toxic elements (PTEs), and based on their concentration gradients, the site is categorized into three distinct zones: Site 1: the tailing dumping area, Site 2: tailing-affected agricultural field, and Site 3: uncontaminated agricultural field. The pH levels across most sampling sites ranged from slightly acidic (6.038 ± 0.22) to slightly alkaline (7.65 ± 0.28), which can lead to the formation of carbonic acid. Acidic soils tend to increase the mobility of PTEs, while alkaline soils can reduce their mobility by forming stable complexes. Both electrical conductivity (EC) and organic carbon (OC) content showed statistically significant differences ($p < 0.05$) among the three sites. EC readings suggest that the uncontaminated site (Site 3) has better electrical conductivity, making it more suitable for crop production compared to Sites 1 and 2. Additionally, OC levels were lower at the tailings site and the contaminated agricultural site than at the uncontaminated site.The levels of available nitrogen (N) and phosphorus (P)

were significantly lower in Site 1 and Site 2 compared to Site 3. A similar result was obtained for exchangeable cations [potassium (K), sodium (Na), calcium (Ca), and magnesium (Mg)]. The cation exchange capacity (CEC) across sites ranged from 13.33 to 23.40 cmol kg^{-1}. Soil texture also varied notably between the zones. The agricultural land in site 2, which is contaminated by chromium-asbestos mine waste, was predominantly sandy, with an average sand content of 91.6%. In contrast, Site 3, the uncontaminated area, had a higher percentage of silt and clay, averaging 16.9%. Various soil microbial (microbial biomass carbon, microbial respiration) and enzymatic activities (dehydrogenase, urease, phosphatase, glucosidase, and fluorescein diacetate) varied significantly across the three sites. Site 1 showed minimal microbial and enzymatic activity, followed by Site 2, while Site 3 exhibited the highest levels. This trend is attributed to the toxic nature of chromium-asbestos mine waste, which has a severely detrimental impact on soil biology, particularly in Sites 1 and 2. To support these findings, soil metagenomic analysis was conducted using samples from Site 2 (contaminated) and Site 3 (uncontaminated). The results revealed that *Proteobacteria* made up 57.18% of the microbial community in the contaminated soil, highlighting their significant presence. This high abundance is likely due to *Proteobacteria's* ability to adapt to environments with elevated levels of PTEs. Additionally, there was a significant difference ($p < 0.05$) in the abundance of *Acidobacteria* between the contaminated soil (7.12%) and the uncontaminated soil (2.01%). This variation may be linked to the slightly more acidic conditions observed in Site 2. To assess the levels of potentially toxic elements (PTEs), soil samples were collected from all three sites, digested, and analyzed using an atomic absorption spectrophotometer. The results showed that both total and DTPA-extractable concentrations of PTEs were significantly higher in Site 1 [(Total_Cr: 2018.24 ± 88.35 mg kg^{-1}, DTPA_Cr: 10.05 ± 0.42 mg kg^{-1}); (Total_Ni: 1484.88 ± 47.67 mg kg^{-1}, DTPA_Ni: 7.82 ± 0.61 mg kg^{-1})] and site 2 [(Total_Cr: 1350.60 ± 76.90 mg kg^{-1}, DTPA_Cr: 7.41 ± 0.87 mg kg^{-1}); (Total_Ni: 1059.95 ± 33.8 mg kg^{-1}, DTPA_Ni: 5.91 ± 0.36 mg kg^{-1})] as compared with site 3 [(Total_Cr: 96.22 ± 4.5 mg kg^{-1}, DTPA_Cr: 3.36 ± 0.89 mg kg^{-1}); (Total_Ni: 263.45 ± 10.7 mg kg^{-1}, DTPA_Ni: 3.91 ± 0.75 mg kg^{-1})]. The above observations revealed that agricultural soils in both Site 1 and Site 2 are heavily contaminated with PTEs. However, since Site 1 is a tailing dump with no agricultural activity, Sites 2 and 3 were selected for assessing PTEs concentrations in crops, as this directly impacts the food chain. Rice, being a staple food across South Asian countries, was chosen for the study. The analysis showed significantly higher concentrations of PTEs in the roots, shoots, and grains of rice grown in Site 2 compared to Site 3, with levels exceeding the permissible limits set by the WHO. Alarmingly, not just the raw rice grains, but also the cooked rice retained these toxic elements, posing a direct threat to human health through ingestion. Long-term consumption of such contaminated food can lead to serious health risks. To further validate these findings, two statistical models were applied: the Free Ion Activity Model (FIAM) and the SAMOE (Severity Adjusted Margin of Exposure) risk thermometer. FIAM results indicated that the movement and uptake of PTEs in rice parts are influenced by soil pH and organic carbon content. The SAMOE model categorized the risk level of rice grains as high (Class 5), while cooked rice was rated as moderate risk (Class 4). Overall, prolonged exposure to mining waste and consumption of contaminated food not only threatens human health but also disrupt the broader ecosystem. To analyze the distribution patterns of PTEs, various models

such as geospatial distribution (GIS), positive matrix factorization model (PMF), and self-organising map (SOM) were employed. The GIS results indicated that PTEs concentrations were significantly higher in areas close to the mining site. The PMF model was particularly useful in identifying the specific sources of pollution, revealing that both mining operations and natural geological source were the main contributors to contamination in the region. Meanwhile, the SOM model effectively illustrated the distribution patterns of PTEs across the study area.

Tolerance assay of Vetiver grass via hydroponic system

A hydroponic system (soil-less medium) allows plants to easily absorb nutrients directly from water. This experiment was conducted to assess vetiver's ability to tolerate high concentrations of PTEs, mainly Cr. This study also observed the biochemical and physiological responses, and determined Cr distribution and translocation pattern in the plant parts. Initially, vetiver plants were acclimated in hydroponic containers filled with nutrient solution for 30 days. After acclimation, the plants were transferred to fresh media containing varying concentrations of Cr (0, 5, 10, 15, 20, 50, and 100 mg kg^{-1}) and maintained for another 21 days. Results showed that Cr accumulated more in the roots than in the shoots at all time points. Vetiver demonstrated the ability to tolerate high level of Cr concentrations. Moreover, stress-related enzyme and biochemical properties activities were increased in roots compared to shoots. These findings suggest that vetiver is an effective accumulator of chromium and can be considered a promising candidate for phytoremediation.

Boosting phytoremediation efficiency through appropriate mycorrhizal culture

Vetiver is a well-recognized plant for use in bioremediation purposes. To enhance its efficacy, vetiver plants inoculated with arbuscular mycorrhizal fungi (AMF) were introduced into the contaminated soil samples. For experimental purposes, the samples were collected from a waste-contaminated area near the chromium-asbestos mining site. Vetiver plants were cultivated at the Experimental Agricultural Farm of the Indian Statistical Institute (ISI) in Jharkhand, India. AMF cultures including *Glomus hoi* (M1), *Funneliformis coronatum* (M2), *Claroideoglomus claroideum* (M3), and *Claroideoglomus etunicatum* (M4) were sourced from The Energy and Resources Institute (TERI), New Delhi. A pot experiment was carried out in the greenhouse at ISI's Experimental Farm using a completely randomized design (CRD) with five treatment groups, each replicated three times. The experiment was conducted for 60 days, after which the concentrations of PTEs were measured in the vetiver roots, shoots, and soil. Following the experiment, a significant reduction in bioavailable trace elements (TEs) in the soil was observed during both the WS-TEs phase (around 77%–89%) and the EX-phase (around 74%–87%) when vetiver was inoculated with M1 (*Glomus hoi*). In contrast, control plants showed much lower reductions (WS-TEs: 16%–42%; EX-TEs: 8%–28%) as shown in Fig. S2. Among the other AMF treatments (M2, M3, and M4), the least reduction in TEs was recorded with M4 (*Claroideoglomus etunicatum*). The findings revealed that vetiver plants treated with all four AMF species accumulated significantly greater amounts of trace elements (Cr, Ni, Cd, Pb, and Cu) in their roots. Specifically, plants inoculated with *Glomus hoi* showed increased root concentrations of Pb (33.21%), Cu (32.44%), Cd (27.79%), Ni (27.44%), and Cr (21.74%) compared to the control group.

Among these elements, Cr and Ni were most abundant in the shoots of AMF-inoculated plants, followed by Cd, Pb, and Cu. The highest percentage of root colonization was observed in the M1 treatment, while no colonization was detected in the control plants. Inoculation with AMF not only enhanced phytoremediation efficiency but also contributed to improved soil fertility.

Conversion of PTE-enriched vetiver plant through vermicomposting technology and assessing the efficiency of the vermi-remediating products

Although mycorrhiza-assisted phytoremediation has many advantages, a key concern is the risk of recontamination. After absorbing PTEs by plants and later shedding their shoots onto the soil, these harmful substances can again contaminate the environment. A promising, low-cost solution to this problem is vermi-technology, which uses earthworms to break down PTE-contaminated plant material and transform it into nutrient-rich organic compost. For this experiment, vetiver plants enriched with PTEs from the earlier mycorrhiza-assisted phytoremediation study were used. The shoot portions were dried, ground, and then introduced into a setup with the earthworm species *Eisenia fetida*. However, within 10 to 14 days, a 100% mortality rate was observed among the earthworms. This was likely due to the high concentration of PTEs in the plant material, which had a direct negative impact on earthworm survival. Following this, the fine plant material was mixed with cow dung in two different ratios (T1: 1:1 and T2: 2:1), while cow dung (T3) alone served as the control. The mixtures were left to homogenize for 14 days before introducing the earthworms, at a rate of 10 *Eisenia fetida* per kilogram of material. The experiment was carried out over a period of 90 days. At the end of the trial, measurements were taken for earthworm population, PTE content in the earthworm gut, and the bioavailable fraction of PTEs in the substrate. Result revealed that the earthworm population was rapidly increased in the T3 and T1 treatments as compared with T2. Using the freeze-kill method, PTE content in the earthworm gut was assessed. The highest concentration of PTEs was detected in earthworms from Treatment T2, followed by T1, while only trace amounts were found in T3. This pattern is likely due to the fact that T2 contained twice the amount of PTE-contaminated plant material, whereas the cow dung-only treatment (T3) had the lowest PTE levels. During the initial phase, the concentration of bioavailable PTEs was higher in treatments T1 and T2. However, after 90 days, once the vermicompost had matured, these levels dropped significantly. To assess the effectiveness of the two vermicompost products, both pot and field experiments were conducted using different crops. For the experiments, we used tomato plants in pots and rice in the field trials. Two types of vermicomposted products (1:1 ratio and 2:1 ratio) were introduced as treatments. We also included a control group without any organic or inorganic fertilizer, and another treatment with just NPK fertilizer. One more treatment involved the direct application of plant material enriched with potentially toxic elements (PTEs). The tomato experiment was conducted for 60–70 days, while the rice experiment was carried out for 110–120 days, with three replications for each. Result indicated that the treatments involving vermicomposted products showed negligible levels of bioavailable PTEs in the shoots and grains of both tomato and rice. Most of the PTEs were found in the plant roots section. Additionally, the treatment with direct application of PTE-enriched plant material estimated the presence of PTEs in the rice grain and tomato. Overall, the combination of a 1:1

mix of vermicomposted product with half the recommended dose of fertilizer resulted in better growth and yield in both the pot and field experiments. Therefore, the integration of different bioremediation technologies provides a holistic and sustainable strategy for mitigating soil PTEs contamination. Also, this approach contributes to the generation of nutrient-rich organic compost. Such a system holds significant promise for improving soil health and agricultural productivity in mining-impacted regions, while also offering a scalable model for sustainable remediation practices at a global level.

Conclusion

The study illuminates that a comprehensive, eco-friendly approach integrating phytoremediation, microbial inoculation, and vermicomposting can effectively address the complex issue of soil contamination by potentially toxic elements in mining-impacted regions. The use of vetiver grass amended with mycorrhizal fungi such as *Glomus hoi*, significantly enhanced the uptake and immobilization of PTEs in contaminated soils, particularly Cr and Ni. However, the challenge of safe disposal of PTE-enriched biomass was effectively overcome through vermi-technology, where mixing contaminated plant material with cow dung in a 1:1 ratio proved most beneficial. This treatment not only reduced the bioavailability of PTEs but also resulted in the production of valuable organic amendments, which improved plant growth and yield of the crops. Moreover, the results highlight soil properties, microbial and enzymatic activities, and PTEs distribution patterns vary significantly across contamination gradients, reinforcing the need for site-specific interventions. The combination of these green technologies offers a sustainable and scalable solution, improving soil health, supporting safer agriculture, and minimizing environmental and health risks. This integrated strategy holds great promise not only for rehabilitating contaminated lands in mining areas but also as a replicable model for sustainable remediation worldwide.

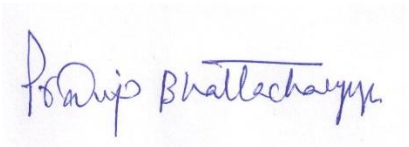

Pradip Bhattacharyya

Sonali Banerjee

Table of contents

List of Tables

List of Figures

Introduction

Chapter 1: Introduction

1. Investigation Scenario

The land of mines and minerals, 'India' is the producer of chromium ore in the world. Jharkhand is one of the leading states of chromium ore production according to the Indian Bureau of Mines IBM (2013) and it holds the sole chromium mine that is situated at the Roro hills, Chaibasa, India. In the past few decades, the rapid development of mining sectors mining activities, and abrupt dumping of mine wastes in surroundings causes the contamination of PTEs (Cr, Ni, Cd, Cu, and Pb) in nearby agricultural field soil and thereby raising critical health concerns for the environment as well as human (Mileusnic et al., 2014; Nawab et al., 2015). During monsoons, due to heavy rainfall and wind blow, these toxic mine wastes are easily carried out from the abundant and active mine site to the nearby area and polluted the water streams, agricultural soil, and crops (Kumar and Maiti, 2015). The release of PTEs into the environment occurs through natural processes such as weathering or erosion from rocks, as well as anthropogenic processes such as mining, industrialization, dumping sludge, and fuel production, all of which have detrimental impacts on natural ecosystems (Nawab et al., 2018; Nawab et al., 2019). As a result of its toxicity, easy accumulation, devoid of nutrients, low water holding capacity, and non-biodegradable nature of chromium mine waste, is a threat to the ecosystem. These poisonous PTEs from chromium asbestos mines cause several diseases including lung cancer, skin cancer, kidney damage, skin irritation, brain damage, etc. (Kapoor et al., 2022). In the long run, PTEs poisoning has had a serious ecological impact such as affecting soil function, soil quality, and degrading organic pollutants.

1.1 PTEs pollution enumeration and health risk assessment surrounding chromium-asbestos mine sites

Various indices (pollution index PI, contamination index CI, ecological risk assessment ERI, and geo-accumulation index Igeo) have been determined to estimate soil pollution by PTEs in agricultural soil (Proshad et al., 2020). It is common to use total soil PTEs content as an index of metal hazard, however, this does not take into account soil properties as they affect metal solubility and bioavailability. As a consequence, such indices are not always relevant for both protecting human health from PTEs hazards and judging whether agricultural land is suitable for growing crops. The human body exposure pathways (ingestion, inhalation, and dermal)

have been assessed to investigate the health hazard caused by PTEs as they have high biotoxicity and persistence in nature (Oluwasola et al., 2021). Therefore, PTEs need to be understood for the safety purpose of human health, for children especially who tend to eat and drink frequently and are more likely to ingest PTEs accidentally (Jin et al., 2019). In light of the fact that existing health risk assessment depends on the conventional models with few deterministic factors but due to variation in specific individuals and uncertainty of concentration, it is difficult to consider the point estimation method for determining the most dangerous element for living beings (Brtnicky et al., 2019). This method either over or underestimate the level of risk (Yang et al., 2019). In probability risk analysis, MCS is one of the most effective approaches since it identifies risk management priorities based on the guidelines and determines whether the risk exceeds the threshold value (Tong et al., 2019). The sources of potential soil pollution, particularly those that can be attributed to human activities, need to be identified and quantified in order to effectively control PTE-related health risks (Hou and Li, 2017). In combination, SOM and cluster analysis provide a logical way of comparing quantitative characteristics among diverse groups of PTEs (Nakagawa et al., 2020). In accordance with USEPA (2014), the PMF model can estimate the positive contribution of each point and help allocate each element's contribution (Tian et al., 2018). The accuracy of the PMF model is limited as it relies on researcher’s explanation for the background data of the study site (Li et al., 2020). So, in this study area, to enhance the accuracy of source identification, the collaboration of PMF with Pearson’s correlation analysis originated. In addition to SOM's ability to recognize and classify elements, and the application of PMF may further substantiate its results with regards to apportioning the contribution of diverse sources. Thus, on the basis of both concentration- and source-oriented health risks caused by soil PTEs, the probabilistic risk estimation methods were employed to accurately identify the riskiest PTEs. The application of spatial distribution maps (GIS) to investigate the patterns of soil bioavailable PTEs in agricultural soils affected by mining activities. Therefore, this combine multi model approach would estimates the joint ecological and human health risks, determines the priority pollution sources, and controls and manages these sources to protect ecosystems and living beings in the chromium-asbestos mines region,

Toxic PTEs are easily leached out from the chromium mine tailings and contaminate the adjacent agricultural land and water bodies during monsoons amid intense rainfall and runoff water (Kumar and Maiti, 2015). To assess the toxicity of PTEs in mine waste-polluted soils, the Toxicity Characterized Leaching Procedure (TCLP) method by USEPA is regarded as a

worldwide benchmark test for PTEs leachability as well as determining the movement of contaminants in liquid, solid, and multiphase wastes (Yu et al., 2014). The chemical nature of contaminants determines their mobility and toxicity in soils (Mandal et al., 2019). For the assessment of bioavailability in PTEs polluted soil, it is necessary to be aware of the PTEs content, species, and leachability under different environmental conditions at the mine waste dumpsite (Chezom et al., 2013). The TCLP Hazard Quotient [TCLP-HQ] is an additional effective strategy for determining the compatibility of soil for the production of food items in relation to the risk to human health posed by the consumption of PTEs in the diet (Golui et al., 2020). In this context, proper evaluation of PTEs leachability and accumulation pattern in soil is crucial. So, in the modern era of research with soft computational data-driven statistical models, many machine learning (ML) algorithms have been applied to foresee soil PTEs leachability trends despite little data and complicated soil systems in mining locations (Sengupta et al., 2021). Additionally, it emphasized cross-validating various ML algorithms and employed the best-fit one to foretell each PTE's leachability patterns. Meanwhile, the geostatistical method can also be implemented to evaluate the leachable-accessibility pattern of various PTEs in soil systems through spatial distribution data (Mondal et al., 2017).

The total PTEs concentration could overstate the health risk, and only a small amount (less than 100%) of PTEs can disintegrate from the soil into digestive fluids (stomach and intestinal) after being consumed. In light of this, bio-accessible PTEs have become more prevalent to conduct more precise risk assessments (Wang et al., 2023). As part of in-vivo animal bioassays, swine, mice, and rats have been used to evaluate PTEs bioavailability in soil. However, animal models are complex, time-consuming, and expensive, making them unpracticable (Denys et al., 2012; Li et al., 2019). To overcome this limitation, a modified in vitro test has been developed to determine the bio-accessibility of PTEs in mine waste-polluted soils using a variety of tests, including the stomach phase (S-phase) and intestinal phase (I-phase) tests (Sarkar and Dutta 2003). The probability distribution pattern analysis utilizes various reliable techniques to determine the bio-accessible significance of PTEs and evaluate the potential risks posed by the various forms of PTEs (Ghosh et al., 2023a).

1.2 Evaluation of PTEs level in agricultural crop and dietary risk determination

Major crops mainly rice, wheat, maize, vegetables etc. grown on mine sites significantly accumulate a high concentration of PTEs (Cr, Ni, Cu, Pb) in their body parts (root, shoot, and grain) that leads to a potential threat to the food chain (Nawab et al., 2016; Zhao and Wang,

2020). Ingestion of these PTEs contaminated crops grown on agricultural fields near mining sites causes significant human health risk including carcinogenic and non-carcinogenic risks (Khan et al., 2018; Zakir et al., 2021). The safety of food is of great concern for health and well-being. Despite dietary diversity, staple foods provide the majority of our nutritional intake. The staple food of more than half of the world's population, rice (*Oryza sativa* L.), forms an integral part of the diet of Southeast and East Asians (Chan, 2014). The potential of rice to accumulate PTEs is around three times that of other crops, leading to it being more susceptible to PTEs pollution near mines area. The accumulation of PTEs in rice (WH) also influences protein and amylose content. The disposal of mine waste in agricultural fields close to the chromium mine, areas in which locally farmed cooked rice (boiled rice) is grown, poses a significant threat to the villagers (Kumar and Maiti, 2015). Rice produced on chromium waste-contaminated land accumulates PTEs, which can lead to a variety of illnesses including mesothelioma, skin cancer, and brain impairment (Kapoor et al., 2022).

In order to estimate safe limit of each PTEs in chromium-asbestos mine waste-contaminated soil, multiple approaches have been considered. It is critically important to predicting how well toxic elements are solubilized in soil and how they are transferred from soil to plants to determine the risk of PTEs contamination of soil. Firstly, to assess the threat of PTEs contaminated soils in terms of Hazard Quotient (HQ), several authors have successfully used simple approaches like FIAM to predict the uptake of PTEs by plants (Golui et al., 2017; Kumari et al., 2021). Soil pore water is the foremost important factor to predict risk. Hence, the PTE concentration in pore water affects the bioavailability of PTEs in crops and ecotoxicity to microbes (Golui et al., 2021). Using FIAM, villagers of Roro mines, Jharkhand were exposed to health risks linked with the consumption of contaminated rice grain when the FIAM-Hazard quotient (HQ) exceeded 1. Similarly, FIAM predictability in rice, wheat, and maize in Bihar and West Bengal was reported earlier (Maity et al., 2020). Further, this model will facilitate soil contamination risk assessment in routine. Considering that soil-crop-food transmission of PTEs to humans is a persistent process, health risk analysis can be a useful tool for evaluating the efficacy of interventions. Secondly, to determine the human health risk from PTEs through dietary intake, the severity-adjusted margin of exposure (SAMOE) viz “Risk Thermometer”, SAMOE-Target cancer risk (SAMOE-TCR), and Fuzzy-TOPSIS rank can be determined (Chowdhury et al., 2020). These parameters evaluate the potential ecological risk that PTEs pose to the health of animal as well as human when they have consumed rice parts (husk, without husk rice, boiled rice and starch). For forecasting the

dietary risk of PTEs contamination to living beings, artificial neural networks (ANN) model that resemble the human brain is implemented (Cho et al., 2011). Moreover, to obtain a broader perspective on the actual health risk scenario of chromium mine area, the decision-making trial and evaluation laboratory (DEMATEL) approach has been taken into account. DEMATEL uses survey questionnaires to first prioritize the relevance of the criteria and then create causal links between the criteria (Shieh et al., 2010).

1.3 Soil microbial-enzymatic aspect in mine site: An insight through bacteriome analysis

Soil is the natural habitat for a diverse range of living organisms, encompassing plants, animals, and microorganisms (Kuang et al., 2016). Microorganisms, being the most predominant group present on Earth, serve a vital role in maintaining the biological activity and biodiversity within the soil. Since soil microorganisms are highly sensitive to changes in their environment, they are frequently used as accurate stress indicators of the environment (Schloter et al., 2003). Nevertheless, both anthropogenic and natural stressors have the potential to induce disturbances in microbial biodiversity. The alteration of microbial communities is strongly linked to variations in physicochemical factors, such as pH, temperature, and cationic stress (Xiong et al., 2012). Additionally, imbalances in nutrient levels (Zhang et al., 2017), improper agricultural practices (such as pesticide and chemical fertilizer usage), industrial effluents, mining activities, and the presence of toxic potential hazardous elements (PTEs) have been recognized as key factors that influence changes in microbial communities (Sarma et al., 2022; Banerjee et al., 2023). Numerous investigations undertaken on the mining site revealed that mining activities generate a variety of toxic PTEs (Cr, Cd, Ni, Pb, and Cu) forms (water-soluble, exchangeable, and oxide-bound) which influence the structure and function of the microbial community, resulting in a decrease in their overall abundance and activity (Tripathy et al., 2014). For instance, elements (bioavailable forms) such as Cr, Ni, and Cd can initiate oxidative stress and denaturation of microorganisms (Booth et al., 2015). On the other hand, Cu and Pb result in the degradation of cytoplasmic molecules, DNA structure, cell membrane, lipids, and other proteins (Olaniran et al., 2013). However, there is evidence that microbes can display resistance and persist existence in environments contaminated with PTEs. Hence, it is imperative to have a comprehensive understanding of the microbial diversity and functionality inside chromium-asbestos mine waste (CAMW)-contaminated agricultural soil, as this knowledge is crucial for comprehending the ecological processes occurring within chromium-asbestos mine soil ecosystems (Bruins et al., 2000).

Microbial biomass carbon (MBC), microbial respiration, fluorescein diacetate activity (FDA), and various enzymatic activities such as dehydrogenase (DHG), urease (U), glucosidase (BG), and alkaline phosphatase (AP) have been widely used as potent indicators of soil health in numerous studies, helping assess the extent of disturbance experienced by microbial populations (Ghosh et al., 2024). The eco-enzymatic stoichiometry approach has been extensively employed to elucidate the constraints on microbial metabolism, particularly concerning C, N, or P limitations (Cui et al., 2018). In order to discern the attributes of soil microbial metabolism, Moorhead et al. (2013) put forth a method involving the computation of the "length" and "angle" of the vector within the enzymatic C:N versus C:P acquisition activity ratio. This approach enables the quantification of the relative allocation of resources towards C versus nutrient acquisition (vector length), as well as P versus N acquisition (vector angle). Consequently, this approach shows promise in elucidating the metabolic response of microorganisms under stress conditions. It is a widely acknowledged fact that a significant proportion of microorganisms cannot be successfully culturable using synthetic media (Handelsman, 2004). In order to assess the collective behavior of microorganisms, culture-independent approaches (16s rDNA metagenomics analysis) are employed to ascertain the diversity, evolution, abundance, and activity of soil microbial populations (Riesenfeld et al., 2004). Microbial community analysis has emerged as an effective strategy for enhancing our understanding of soil microbiology and global micro-ecology. Consequently, this facilitates our ability to progress towards enhanced environmental governance, preservation, and long-term viability.

1.4 Synergistic impact of soil PTEs and alkalinity on soil health

Apart from the toxicity of PTEs in chromium mine sites, alkalinity in soil systems also has a major effect on microbial populations. Recent research has indicated that inadequate irrigation practices and the recycling of industrial waste materials can lead to an increase in soil alkalinity, specifically in potassium and magnesium levels (Rengasamy, 2002). Potassium, being a monovalent cation, can exert a comparable influence on sodium (Rengasamy, 2006; Arienzo et al., 2009). Therefore, instead of sodium adsorption ratio (SAR), and exchangeable sodium percentage (ESP), the 'monovalent cation ratio' (MCAR) indices have been developed by Smiles and Smith (2004) to estimate proper alkalinity in soil. According to Rengasamy (2002), the increased hydration energy of magnesium ions relative to other monovalent and divalent cations causes clay dispersion and swelling. Another crucial metric, the cation ratio of soil structural stability (CROSS) index, has been used to ascertain

the actual alkalinity levels in the soil to reconcile all the disparities (Rengasamy, 2002). Several studies have explored the influence of various alkalinity indices on soil structure, yet limited literature addresses their impact, including CROSS, MCAR, ECR, and MH, on soil microbial diversity

1.5 Various remediation strategies: An insight through bio-based approach(s)

Moreover, soil microorganisms play a vital role in restoring soil health and quality, breaking down organic matter, and facilitating nutrient exchange between soil and plants (Fierer, 2017). However, they are highly sensitive to environmental shifts, which can significantly alter ecosystem functions (Coban et al., 2022). Soil enzymes are also vulnerable to PTEs, being key in nutrient cycles (Lopez et al., 2019). Enzyme activities, especially those of glucosidase, phosphatase, and dehydrogenase, decline steadily as concentrations of PTEs (Cd, Cr, Pb, and Ni) increase, making them reliable indicators of soil and environmental health (Jha et al., 2023). In recent times, the mining sector has emerged as a significant contributor to the global economy, while simultaneously producing substantial quantities of hazardous toxic waste. Remediation of soil polluted with hazardous waste necessitates novel strategies; unfortunately, the majority of existing approaches are neither sustainable nor cost-effective and can substantially generates secondary waste as well as alter the soil properties (Mukherjee et al., 2022). Therefore, managing toxic waste upon the completion of mining activities has become a crucial aspect of ecological restoration (Midhat et al., 2019). For this purpose, to detoxify toxic elements-rich chromium waste, various physical, chemical, and microbiological techniques are available. However, these methods are often costly and can have negative environmental impacts. Therefore, the suitable environmental agents (combination of appropriate plants microorganisms and earthworms) could remediate soil toxicity, enhance re-vegetation of polluted areas, promote long-term soil stability, and mitigate erosion by facilitating surface stabilization. Therefore, this innovative, holistic, green-sustainable approach not only mitigates PTEs toxicity but also facilitates gradual restoration of damaged ecosystems (Siyar et al., 2020).

1.6 Mycorrhiza-assisted phytoremediation approach

An emerging in-situ eco-friendly restoration technology, “Mycor-phytoremediation”, employs natural agents [native or exotic plant species and symbiotic arbuscular mycorrhizal fungi (AMF)] for remediation of PTEs from toxic mine waste amended soils. Its affordability, compatibility with ecological principles, and sustainability nature serve as a one of the most

promising, widely recognised bio-remedial technology (Singh et al., 2019). Out of the different strategies used in phytoremediation, "phytostabilization (immobilization of PTEs within the soil, limiting mobility and bioavailability)" and "phytoextraction" (the mobilization, uptake, and sequestration of PTEs within plant tissues, facilitating their removal from contaminated sites)" have proven to be the most popular and successful techniques (Gravand et al., 2021). Another promising technology mediated by AMF which forms symbiotic association with plant roots and enhance plant nutrition, improve overall health, boosts the phytoremediation efficiency and plants' capacity to withstand and adapt to stress caused by PTEs (Verma et al., 2021). Certain plants have shown remarkable capability in extracting, and sequestering substantial level of PTEs and are often recognized as promising choices for phytoremediation (Roy and Pandey, 2020). The perennial, fast growing C4 grass, *Chrysopogon zizanioides* L., (Vetiver: Poaceae family) is native to South and Southeast Asia and it has ability to tolerates abiotic stress (including drought, salinity, PTEs stress, and water logging) with its massive deep roots, making it ideal for soil erosion control and challenging environments (Oshunsanya et al., 2019; Singh et al., 2021). It exhibits exceptional tolerance to high concentrations of toxic elements like Cd, As, Cr, Cu, Pb, Hg, Ni, Se, and Zn while also adapting to diverse soil conditions, including a wide pH range and low fertility (Banerjee et al., 2019). More than 80% of terrestrial plants are symbiotically associated with AMF, a crucial component of soil microbiota. Vetiver also possesses a symbiotic association with AMF (extensive hyphal networks), which promotes nutrient absorption (especially phosphorus), and plays a crucial role in soil restoration (Nanjundappa et al., 2019). Moreover, AMF generates hydrophobic glycoprotein, particularly glomalin-related soil proteins (GRSP) in soil, which plays a crucial role in improving nutrient availability, enhancing PTEs sequestration, and soil aggregation (Agnihotri et al., 2022). The AMF also mitigates PTEs toxicity which is achieved by PTEs immobilization within hyphae and storing PTEs within fungal vacuoles (Mohammadi et al., 2011). This association between plants and AMF promotes growth, development, biomass production even under PTEs stress condition (Giovannini et al., 2020).

AMF assisted phytoremediation using vetiver grass is a promising approach for developing sustainable productivity, improving soil health, and protecting plants from PTEs stress (Dhalaria et al., 2020). After the uptake of PTEs by the plant-microbe system, the accumulated metals are sequestered within the plant biomass. Hence, the safe and efficient recycling of this biomass is crucial for completing the remediation process and prevent

secondary environmental contamination. Additionally, CAMW by-products raise ecological concerns due to their toxicity, presence of harmful PTEs, tendency to accumulate, lack of nutrients, poor water retention, and resistance to biodegradation (Kumar and Maiti, 2015). The high concentration of PTEs in agricultural soil poses an alarming situation to sustainable farming practices.

1.7 Vermi-remediation approach

In this background, "Vermi-composting technology (VCT)", can be considered as a nutrient rich, environment-friendly, sustainable and cost-effective approach to detoxify the plant biomass (Wang et al., 2018). It is often utilized as a soil conditioner or organic amendment to enhance soil quality and crop productivity, owing to its substantial content of humified organic matter and its remarkable capabilities in water retention, soil aeration, drainage, porosity, and promoting bacterial development, rendering it an exceptional soil conditioner (Tejada et al., 2010). Chakraborty et al. (2024) also showed that the application of vermicompost drastically decreased the availability of PTEs in plants. Additionally, following the myco-phytoremediation process, the PTEs become concentrated in the plant biomass. Therefore, safely and efficiently recycling this biomass is essential to require another remediation process to avoid secondary environmental contamination. VCT has proven effective in treating various industrial wastes and other biobased waste, including steel waste (Jha et al., 2023), and tannery waste (Vig et al., 2011). It also stabilizes organic materials via the interaction of microbes and earthworms, and has been suggested as a valuable resource for soil restoration and the enhancement of soil organic carbon content and quality. *Epigeic* earthworms can reduce the bioavailability of PTEs through detoxification processes involving metallothioneins and similar proteins (Hussain et al., 2021). The effectiveness of earthworms in degrading industrial waste is largely influenced by their feed composition. The mixing ratio and composition of feed stocks in vermibeds play a crucial role in determining earthworm degradation efficiency and the quality of the final product (Ramnarain et al., 2019). In microbial cell membrane, the key components are phospholipid fatty acid (PLFA) and microorganisms adjust the configuration of these fatty acids to adapt to environmental fluctuations (Quideau et al., 2016). Furthermore, studies have shown that PLFA-based analysis of microbial community structure offers superior accuracy compared to DNA fingerprinting or PCR approaches (Ramsey et al., 2006).

1.8 Crop experiment

Therefore, combination of all bio-based approaches establishes a sustainable framework for utilising CAMW-vermicompost and PTE-enriched vetiver vermicompost (PTE-EVVc) in agriculture area. The application and efficacy of this transformed waste as an organic amendment has several potential advantages regarding crop yield, soil nutrient status, microbial response, and biochemical characteristics of the crop. The vermicompost serves as nutrient-rich organic soil amendment, enhancing soil fertility and boosting crop yields. Different crops, like sesame (oil seed crop), chilli (horticultural crop), tomato (vegetable), and rice (cereal) etc. have been widely utilized as a test crop for evaluating the efficiency of the vermicomposted product through pot and field trials.

Sesame (*Sesamum indicum* L.) is one of the most ancient oil-seed crops and holds a significant role in both the Indian and global agricultural sectors. Sesame is a member of the Pedaliaceae family and contains 40-50% oil. A notable characteristic of sesame is its resilience and capacity to endure adverse climatic and environmental circumstances. Sesame pods are abundant in fatty acids such as oleic, palmitic, vitamins (A, E, and B), and stearic acids (Kurdiya et al., 2020). Another important horticultural crop i.e chilli (*Capsicum annum* L.) belongs to the family of Solanaceae and is one of the most extensively grown spices, greatly valued for its pungency, taste, and medicinal properties. Being a native of America, it has become a central component in global culinary traditions (Wahocho et al., 2016). Worldwide, China and India are the leading producers of chillies, accounting for over half of the total production, and play a key role in the nation's economy (Tripodi et al., 2019). Chillies are prevalent in various culinary, agricultural markets and offer enormous health benefits. A wide range of bioactive chemicals are present in chilli, including capsaicin, beta-carotene, ascorbic acid, flavonoids, and phenolic compounds, which have the ability to combat various infections and diseases (Das et al., 2016). Capsaicin ($C_{18}H_{27}NO_3$; N-vanillyl-8-methyl-6-nonenamide) is a phenylalkylamide alkaloid that imparts “pungency” and “hotness” to chillies. It is synthesised by the condensation of 8-methyl-6-nonenoyl-CoA and vanillylamine (Keyhaninejad et al., 2014). Capsaicin is significant in mitigating gastric ulcers through the selective stimulation of afferent nerves in the gastric mucosa, which inhibits acid secretion, enhances mucus production, and primarily accelerates gastric mucosal blood flow, thereby facilitating ulcer prevention and healing (Kang et al., 1996). Hence, chilli has achieved global recognition due to its pharmacological properties, therapeutic potential, and its economic and cultural significance (Prasad et al., 2005). Tomatoes (*Solanum lycopersicum*

L.) are well acquainted globally as a popular horticultural crop for the presence of various antioxidant crops such as phenolics, flavonoids, lycopene, and ascorbic acid content (Meena et al., 2017). Tomatoes are considered an essential component of a balanced diet due to its multiple health benefits, including anti-cancer properties, cardiovascular disease-preventing capacity (Ghosh et al., 2025). Rice (*Oryza sativa* L.) is a staple food crop that supports a large portion of the global population (Tahir et al., 2020). Unlike many other cereals, rice cultivation involves a distinctive ecological transition (from flooded fields to wetland conditions) before eventually integrating into a terrestrial ecosystem (Sarkar et al., 2023). This unique adaptation adds an ecological intrigue to rice farming beyond its economic value (Dash et al., 2011). Therefore, this study offers an integrated approach to pollution evaluation and mitigation by transforming waste into nutrient-rich organic compost, simultaneously supporting sustainable agriculture and effective waste management for ecosystem.

Review of Literature

Chapter 2: Review of Literature

2. Background

Human-driven activities such as agriculture, mining, industrial processes, and the extensive use of fertilizers and pesticides have led to an escalating demand for land resources since the twentieth century (Cheng, 2016). Potentially toxic element (PTEs) pollution, desertification of land, ecological imbalance of land, soil erosion, land degradation, environmental damage, and decreased soil fertility are all major environmental factors that have severe effects on soil, water, and air (Nosrati and Collins, 2019; Vaverková et al., 2019). PTEs pollution is an unadorned environmental phenomenon worldwide. Metal mining and mineral ore processing have a dual effect on the economy and environment. From one perspective, it provides economic benefits to the country, and simultaneously it causes environmental pollution. Abundant and active mines are the prime source of toxic PTEs. During rainy season, due to heavy rainfall and strong winds run-off water washes down the toxic waste material to agricultural fields, and surrounding water bodies simultaneously causing air, water, and soil pollution. PTE pollution has an irreversible, long-term residual effect, and toxicity that poses an immense threat to the living beings as well as the environment (Dhaliwal et al., 2020). Once these toxic PTEs are released into the surrounding ecosystem, it could migrate to a distant area, accumulate in various biotic, abiotic components of the system, and adversely affect the food chain, human health, and environment (Peralta-Videa et al, 2009). Lead (Pb), chromium (Cr), mercury (Hg), cadmium (Cd), and arsenic (As) have lethal effects in humans, plants, and animals but depending on the concentration; a few metals such as zinc (Zn), copper (Cu), manganese (Mn) and iron (Fe) have another role as an essential micronutrient needed for metabolic activity (Schneegurt et al., 2001; Mohan et al., 2007). PTEs contamination significantly alters soil characteristics and the surrounding micro-environment. Microorganisms, serving as dynamic bio-indicators, respond to these changes through variations in microbial biomass, respiration rates, and enzyme activity under PTE stress conditions (Hinojosa et al., 2005). Long term or short-term exposure to various toxic PTEs causes significant changes in physiological and ecological parameters including a reduction in basal respiration, microbial biomass, and an increase in metabolic entropy (qCO2) (Crowley, 2008; Zhao et al., 2020). The degree of PTE pollution has been evaluated by

several indices like pollution load index (PLI) and geo-accumulation index (Igeo) (Duncan et al., 2018; Hamad et al., 2019).

Factors such as, plant life cycle, plant biomass, bioaccessibility, and bioavailability of PTEs in soil can influence the metal removal process (Ali et al., 2013). Various physical and chemical methods are available for decontamination of toxic PTEs which are usually cost-intensive. Given the limitations of conventional cleanup techniques, bio-logical approaches could be looked into as a potential alternative mitigation option. In some places, bioremediation, phytoremediation of soils contaminated with organic or inorganic pollutants, such as pesticides and hydrocarbons, has become widely accepted. The popularity of bioremediation and phytoremediation for the reclamation of PTE-polluted soils is growing despite the fact that it has substantial disadvantages due to its economic viability. The term phytoremediation is defined as a green, eco-friendly, low-cost, holistic approach to cleaning up toxic contaminants from the environment by a plant-based system (Ali et al., 2013). Numerous phytoremediation projects have been carried out over the past few decades, and as a result, novel phytoremediation techniques, creative concepts, and research have emerged. Several phytoremediation works have been done in the last few decades and new phytoremediation strategies, innovative ideas, and research have evolved as a result. More than 500 plant species have been identified as potent PTEs hyperaccumulators (Ye et al., 2020). A long-time span is required for plants to remediate the high metal contaminated area. Remediation through plant or phytoremediation is one of the most promising eco-friendly management strategies for reducing toxic contaminates (Burges et al., 2018).

In past few decades researchers have worked with various types of plants, their potentiality, and their remediation mechanisms strategies for a better understanding of the phytoremediation process. Plants like *Cymbopogon citrates* (China et al., 2014), *Helianthus petiolaris* (Saran et al., 2020), *Helianthus annuus* (Lothe et al., 2016), *Bryophyllum laetivirens* (Li et al., 2020), *Cordyline fruticosa* (Herlina et al., 2020), etc. are widely used to remediate PTEs (Pb, Cd, Cr, Cu, As) and their removal mechanisms have been extensively studied by several researchers in last few years. Vetiver grass (*Chrysopogon zizanioides*) has been widely used for rehabilitation of mine tailings in several countries like China and Australia. Vetiver is a perennial grass with a huge root system (3-4 m), 1-2 m tall, and non-invasive in nature (Andra et al., 2009). Also, Vetiver grass has a strong symbiotic association in the rhizosphere region with a wide range of soil microbes especially with arbuscular mycorrhizal fungi (AMF) which stipulates phytohormones and essential nutrients for plant

development (Bahraminia et al., 2016). The most advantageous properties of mycorrhizal root colonization are an increase in the root surface area to enhance the phytoremediation/phytostabilization potential.

Numerous studies have been conducted in the past focusing on mining activities and PTEs contamination, exploring their effects on soil, plants, water resources, ecosystems, and living organisms. Previous studies also examine bioremediation approaches, utilizing plants and microorganisms to mitigate the adverse impacts of PTEs effectively. This review aims to provide a comprehensive overview of PTEs pollution in agricultural soil caused by various mining activities and its associated environmental impacts. Through meta-analysis, the study assesses PTEs contamination and examines the global distribution of key pollutants, including Cr, Ni, Cd, Pb, and Cu in mining-affected regions worldwide. This article also sheds light on the role of different plant species and microbes (especially AMF), in mitigating the PTEs stress condition while supporting plant growth and nutrient uptake. Additionally, through meta-analysis, the study evaluates the efficiency of AMF as a remediation strategy for mine-impacted soils contaminated with PTEs such as Cd, Cu, Ni, and Pb.

2.1 Mines and associated potentially toxic elements (PTEs)

According to the ancient Kautilya's Arthshastra, "Mines are Nation's treasury". Mineral resources from mines are abundant in nature. Exploitation of these minerals enhances world's economy and development but at the same time, surface mining, especially open cast mining causes severe environmental problem (i.e loss of surface vegetation, destruction of soil structure etc.). Mines are the source of various metals and minerals like iron and ferro-alloys (Fe, Cr, Co, Mn, Mo, Ni etc.), non-ferrous metals (Al, Sb, As, Bi, Cd, Cu, Pb, Hg, Li, Zn etc.), precious metals (Au, Pd, Pt, Ag), industrial minerals (perlite, sulfur, vermiculite, feldspar, graphite, gypsum, kaolin, etc.) and mineral fuels (uranium, petroleum, cooking coal, natural gas etc.). China is the largest producer of total minerals followed by United States, Russia, Australia, and India etc. (Reichl and Schatz, 2020).

2.2 Chromium-Asbestos mines and its status regarding pollution

Ferrochromium is only natural and economical resources of chromium produced in Chromium mines by carbothermic smelting (Beukes et al., 2010). It is a crystalline alloy generally composed of chromium and iron compounds. Globally, South Africa grasp most Chromium ores followed by Kazakhstan, India, Albania, and Turkey (ICDA, 2022). The active and abandoned mine wastes are the reservoirs of PTEs which have lethal effects on

water, soil, and living beings (Fernández-Caliani et al., 2009). These mine wastes are generally composed of different types of toxic PTEs mainly chromium (Cr) and Nickel (Ni) along with other metals such as Cu, Cd, Pb, Ni and Mn are present in lesser quantity (Bueno et al., 2009). Chromium (Cr) is generally utilized by different industrial activities such as processing and finishing of leather, production of refractory steel by stainless steel industry, electroplating cleaning agent, muds drilling, production of chromic acid and other chemicals, and use to preserve food for a short time (Shanker et al., 2005). Chromium exhibits different levels of toxicity depending on its chemical form, pH, reacts with other elements and solubility index (Thatoi et al., 2014). Cr (VI) exhibits high toxicity and bioavailability due to it has better solubility than Cr (III) (Abyaneh and Fazaelipoor, 2016). For humans and mammals, lack of Cr (III) in diet can causes metabolic deterioration, cardiac problem, diabetes but excess presence in the body has harmful health effects (WHO, 1996). Hexavalent chromium tends to act as a strong oxidizing agent; therefore Cr (VI) is 10-100 times more toxic than Cr (III) (Zayed et al., 1998). The toxicity level of hexavalent chromium for plant in solution is as low as 0.5mg kg^{-1} and 5 mg kg^{-1} for soil (Turner and Rust, 1971). Highly carcinogenic chromium and asbestos exposure may lead to cancer, mesothelioma, pneumoconiosis, skin irritations, and other respiratory problems such as irritation larynx and pharynx, edema, coughing, asthma etc. (Bloise et al., 2008; Pugnaloni et al., 2013). Cr is mostly accumulated in the root than shoot due to its less mobility in root vacuoles but in case of Ni, accumulation is higher in shoot than root due to greater mobility of Ni through xylem tissue (Pulford et al., 2001; Shanker et al., 2005). The Cr and Ni concentration in Roro Chromium mine waste soil is 3120 mg kg^{-1} and 1620 mg kg^{-1} respectively which exceeds the safety level (Cr :75-100 mg kg^{-1}; Ni: 100 mg kg^{-1}) of metals present in soil (IS, 1993) (Fig. 1). Similar studies in Almadén mine site in Spain and southern Togo mine sites, Cr and Ni concentration has 86–35 Cr mg kg^{-1} and 21.2–126 Ni mg kg^{-1}) and (182–1029 Cr mg kg^{-1} and 15–432 Ni mg kg^{-1}) respectively due to deposition of mine tailings in agricultural soil (Gnandi and Tobschall, 2002; Bueno, et al. 2009). In Daduk mine area of Korea, due to dispersion of metals from tailings and watercourses, various types of PTEs are reported in nearby paddy fields (Lee et al., 2001). Another study in Co Dinh mine of Vietnam, high level of potentially toxic elements is also detected in rice field (5750 Cr mg kg^{-1}, 375 Co mg kg^{-1} and 5590 Ni mg kg^{-1}) (Kien et al., 2010). Based on dynamic translocation factor (TF dyn>1), Cr and Ni accumulation is higher in plant parts of *Oryza sativa* growing in the contaminated agricultural fields which might have potential risk of transfer of toxic PTEs to livestock or human (Kien et al., 2010; Kumar and Maiti, 2014).

Fig. 1: Chromium-asbestos mine, Jharkhand, India

2.3 Bio-based remediation strategies

Worldwide, the immense development in industrial sectors especially mining, metal, energy supply, agriculture, chemical production, and transport causes significant pollution of the ecosystem. Globally, PTEs contamination is one of the serious nuisances to the environment as well as for living beings (Sun et al., 2012; Cachada et al., 2018). As we know remediation of PTEss is very much complicated than any other organic pollutants. Various traditional, mechanical and chemical techniques such as electrochemical treatments, thermal methods, incineration, excavation, vitrification, chemical oxidation, and solvent extraction are widely utilized to remove or destroy these toxic PTEs in soil. However, these methods are often costly, time-intensive, and labor-demanding. Moreover, they can lead to soil degradation, and generate secondary waste materials, posing additional environmental management challenges (Khan et al., 2018). Bio-remediation techniques have gained a lot of attention due to its cost-effectiveness, viability, no generation of secondary waste and eco-friendly (Akande et al., 2018; ALAM et al., 2018). It includes plants, various microbes (bacteria, fungi, mycorrhiza etc) which are utilized to decontaminate the hazardous compounds from soil. For soil purification, the applications of plant alone or association with microorganisms that helps to stabilize, mineralize, transfer, remove the PTEs (Wang et al., 2018)

2.3.1 Phytoremediation

The term ‘Phytoremediation’ is derived from Greek (‘phyton’) and Latin (‘remedium’) which means ‘plant’ and ‘to correct’ respectively (Cunningham et al., 1996). By the definition, phytoremediation is a bioremediation process in which plants (alone or in association with microbes) are used as purifying agents to remove, stabilize or destroy the PTEs from air, water, and soil in an eco-friendly manner (Wani et al., 2012). Table 1 showed different types of mechanisms of phytoremediation.

Table 1: Different types of mechanisms of phytoremediation

Type	Process	Agents	Contaminates	References
Phytoextraction/ Phytoabsorption/ Phytoaccumulation/ phytosequestration	• Removal, absorption, translocation of metals and organics from soil and water • Chelating agent enhance metal accumulation ability of plant (metal-cheated complex) in plant roots, shoots and leaf's part • In case of organics various detoxifying enzymes help in sequestration process	• Chelating agents (EDTA, DTPA, EDDS etc) • Detoxifying enzymes (cytochrome P450 enzymes (CYP), glutathione S-transferases (GSTs)	• Metals (As, Cu, Zn, Pb, Cd etc.) • Organic pollutants (phthalic esters, polycyclic aromatic hydrocarbons (PAHs), hydrophobic pollutants)	Sun et al., 2012; Hamdi et al., 2012; Attinti et al., 2017
Phytodegradation/ phytotransformation	• Plant uptake the complex toxic compounds and plant enzymes help to degrade or transform it into less harmful substances • Break down into low molecular weight compound via plant metabolic process	• Plant secretes enzymes (dehalogenases, oxygenases, and reductases)	• Pharmaceuticals, Pesticides, Petroleum hydrocarbons, Insecticides, Surfactants etc. • TNT, DNT, tetracycline, IBP	Topal et al., 2015; Zazouli et al., 2014
Phytostabilization	• Plant immobilizes the toxic compounds in soil and water • Rhizosphere induced absorption, precipitation or accumulation of metals within plant root zone • Prevent mobility of metal in above ground part of plant and lowers bioavailability of metal in food chain	• Amide, Sulfonate, Hydroxyl, Carboxyl, Sulfhydryl, Phosphate, Microbes (Mycorrhizal fungus)	• Mining waste containing toxic metals (Cr, Fe, As, Zn, Pb, Cd, Mn, Cu, and Ni)	Andra et al., 2009; Guo et al., 2016; Farahat et al., 2018
Phytovolatilization	• Plant uptake organic or inorganic contaminants and transform into volatile compounds • These volatile substances release to the atmosphere by transpiration or radial diffusion of leaves, stem and roots.	• Volatized by plant leaves in a form of dimethylselenide	• Toxic metals like Hg, As, Se • Trichloroethylene (TCE), Tetrachloroethylene, Perchloroethylene (PCE)	Limmer and Burken, 2016; Peter et al., 2017

Phytostimulation/ Rhizodegradation	• Degradation of pollutants by the help of rhizospheric microbes • Root release enzyme and exudates that degrades the pollutants • Microbes transform the toxic hazardous compounds into nontoxic form.	• Microbes (bacteria, fungus)	• PAHs (polyaromatic hydrocarbons) Perchlorates • Phenanthrene (Ph) Pyrene (Py)	Jia et al., 2016; Gkorezis et al., 2016
Phytofiltration Rhizofiltration/	• Removal of heavy metal by plant through absorption, concentration and precipitation within root tissue	• Plant rhizosphere • Rhizospheric microorganisms	• Heavy metals or radionuclides (Ra, U, and Cs)	Lee and Yang, 2010; Kumar et al., 2017

The pictorial representation is in Fig. 2. Generally, plants can extract essential nutrients (Fe, Zn, Ni, Mn, and Cu) as well as non-essential metals (Cr, Cd, As, Pb and Hg) which are not required in their physiological process and can store an enormous amount of the PTEs (hyper-accumulator) in their parts from contaminated soil and water (Tangahu et al., 2011).

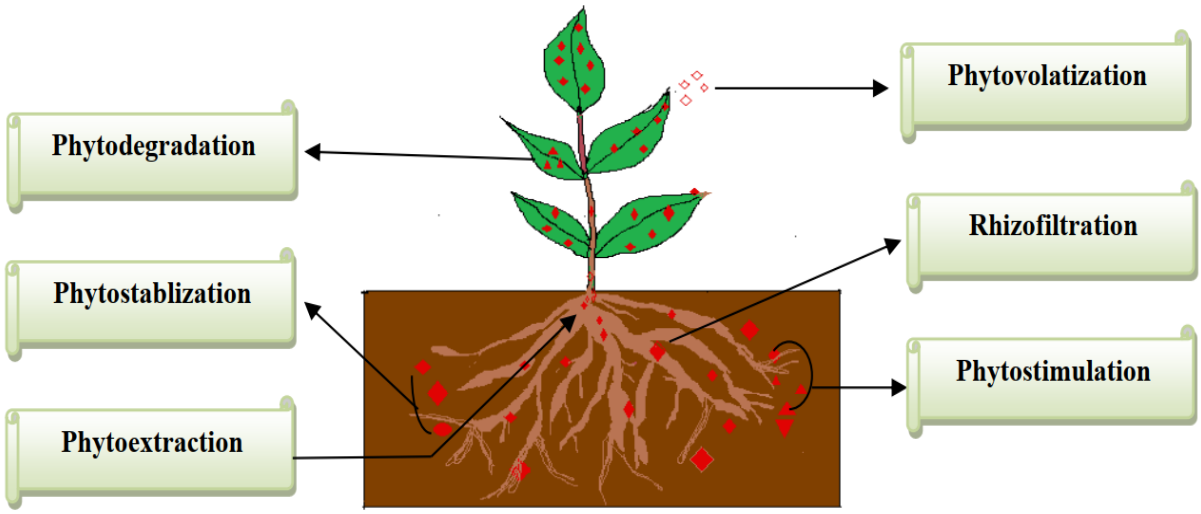

Fig. 2: Pictorial representation of different types of phytoremediation mechanisms

There are several studies have been done regarding different mechanisms of phytoremediation strategies, as shown in Table 2. There are many advantages of phytoremediation listed as follows – 1) inexpensive technology (60%-80% lesser than traditional process); 2) minimize soil deterioration; 3) solar-driven remediation process; 4) no generation of secondary hazardous compounds; 5) suitable and broad-spectrum treatment; 6) sustainable and environment-friendly technique, however, one limitation is there, that plant requires time for their growth and development (Morikawa and Erkin, 2003). Several plant species have demonstrated the ability to absorb, bioaccumulate, immobilize, and degrade PTEs from contaminated sites.

Table 2: Summary of research works on different mechanisms of phytoremediation strategies

Process	Plant	PTEs	Experiment	Research outcome	Research site	References
Phytostablization	*Cymbopogon citrates*	Cu, Ni, Pb	Outside pot experiment 3 treatments with lemon grass T_1: Tailing (100%) T_2: Tailings (97.5%) +Chicken manure (2.5%) T_3: Tailings (97.5%) + Chicken manure (1.25%) + Soil (1.25%) Exposure time: 6months	➢ Limited growth of plant on tailings. ➢ Additives like chicken manure and soil increases the growth of the plant ➢ Only chicken manure increases metal accumulation (Cu,Ni, Pb) in shoot than root ➢ Mixture of chicken manure and soil decreased metal accumulation expect Pb in root and shoot.	Mosaboni, Jharkhand India	China et al., 2014
	Lavandula dentate L.	Cr	Green house pot experiment (box: 80cmx 60cm x 40cm) (light/dark: 16h/8h; temperature: 18°C -30°C; water hoalding capacity: 60%-70%) Treatment: T_1: Cr contaminated soil + 2.5% biochar + 2.5% oyster shell waste T_2: Cr contaminated soil +2.5% oyster shell waste+ 2.5% citrus peel T_3: Cr contaminated soil without amendments T_4: Uncontaminated soil Exposure time: 41 days and 104 days	➢ High concentration (>8000mg/kg Cr) affects theplant growth and plant biomass ➢ T_1 and T_2 showed that the water-soluble fraction of Cr concentration is reduced by plant in T1 and T2 ➢ In un-amendment soil, high Cr concentration in shoots than roots ➢ Biochar, oyster shell and citrus peel enhances the phytostablization ability of the plant.	Qingdao, China	Ye et al., 2020
	Helianthus petiolaris	Pb and Cd	Growth chamber (25°Cday/ 19°C night; Photoperiod 16/8 Treatment for short term: Cd: 0, 1, 3, 5, 10, 20 mg/kg $CdCl_2$ Pb: 0, 50, 100, 250, 500, 1000 mgkg $Pb(NO_3)_2$ Exposure time: 32 days Pot experiment (Pots: one and a half liter) Treatments for long term: Cd: 0, 10, 50, 100 mg/kg Pb: 0, 100, 500, 1000 mg/kg Exposure time: 3months	➢ *H. petiolaris* grows upto 50mg/kg for Cd and 1000mg/kg Pb ➢ Accumulates more than 3 times the soil Cd content in the aerial parts ➢ Up to 1000mg/kg concentration of Pb, no symptoms of phytotoxicity were observed.	Poland	Saran et al., 2020
	Pennisetum purpureum cv. Mott	As, Mn	Pot experiment (5kg per pot) Treatments: T_1: Mine tailings without amendments T_2: Mine tailings with 1 %, 3% and 5% cow manure	➢ Biochar and cow manure enhances the stability and immobility of As and Mn in tailings. ➢ It also decreases accumulation and	Thailand	Kowitwiwat and Sampanpanish, 2020

Process	Plant	PTEs	Experiment	Research outcome	Research site	References
			T_3: Mine tailings with 1%, 3% and 5% biochar Exposure time: 30, 60, 90, 120 days	uptake capacity of P. purpureum at 5% biochar treatment and enhance the growth and improve the tailing properties ➢ The reduction percentage of uptake and accumulation in shoot and root was78.6% and 63.9% for As and 72.5% and 69.3% for Mn, respectively.		
	Vetiveria zizanioides L.	Pb	Hydroponic experiment Experimental tanks: 40 × 10 × 10 cm Concentration: 0, 400, 1200 mg/ L Condition: 16-h, 24 ± 2°C/8-h, 20 ± 1°C light/dark Relative humidity: 60% Experiment duration: 7 days	➢ Vetiver accumulated up to 13,200 and 19,800 mg/kg of dry weight of root in presence of 400 mg/L and 1200mg/L of Pb ➢ No toxicity symptoms appears in vetiver in presence of Pb (Upto 2300 mg/kg of dry weight)	USA	Andra et al., 2009
Phytoextraction/ Phytoabsorption/ Phytoaccumulation/ phytosequestration	*Helianthus annuus*	Cr	Pot experiment in green house (Plastic pots; Temperatures: 18-28 ℃; Humidity: 75%; Photoperiod: 16/8 h light/dark) Treatments: Different concentration of Cr (0, 75, 150 ppm) and Fe^0 nano powder (0, 1 and 2%) Exposure time: 8 weeks	➢ Sunflower has the ability to accumulate more Cr in shoot portion than in root portion. ➢ BAF value of Cr was higher in treatment (150ppm) indicates plant ability to uptake metal ions. ➢ By increasing concentration of Cr, TF value was decreased ➢ Fe^0 (1% and 2%) nano particle application increases the activities of anti-oxidant enzymes and improves the activity of sunflower in Cr stress conditions.	Iran	Mohammadi et al., 2020
	Conocarpus lancifolius	Pb, Zn, Cd	Green house experiment under natural environment (Average temperature :28 ± 1.5°C and relative humidity: 55 ± 5) Plastic pots with 8kg soil Treatments: T_1: 20 plants irrigated with 300ml tap water T_2: 20 plants irrigated with waste water Irrigation time – 4tines in a week Experiment duration: 6 weeks	➢ In waste water, C. *lancifolius* increases 30% in growth parameters and biomass production compared to control. ➢ 34% increased net CO_2 assimilation rate. ➢ High accumulation of Zn, Pb and Cd in roots followed by leaves and shoots ➢ High translocation of Zn and Cd from root to shoot	Faisalabad, Pakisthan	Rasheed et al., 2020

Process	Plant	PTEs	Experiment	Research outcome	Research site	References
	Cordyline fruticose	Pb	Pot experiment (pots having 30.35cm in diameter) Treatments: Soil mix with vermicompost (2:1) Pb Concentration: T_0: 27.47mg/kg T_1: 250mg/kg T_2: 375 mg/kg Exposure time : 30, 60, 90 days	➢ Pb concentration higher in roots than in shoots and stems ➢ Pb has low solubility and translocation power ➢ TF<1 in T_2 and T_0 except T_1 after 30days ➢ BAF< 1 in T_1 and T_2 except T_0 after 30days ➢ Lead tolerant plant	Java, Indonesia	Herlina et al., 2020
Phytodegradation/ phytotransformation	*Arabidopsis thaliana*	2,4-DNT	Hydroponic experiment under controlled condition 2,4-DNT concentration 0,8,15,30 mg/L added to 15days old seedlings Experiment duration: 10 days	➢ Only 5% of the initial concentration remained in the medium ➢ Aminonitrotoluenes detected in plant tissue extract from the plants exposed to 2,4-DNT	USA	Yoon et al., 2008
	Azolla Filiculoides	Bisphenol A (BPA)	Hydroponic experiment under natural condition (Natural light and ambient temperature 30°C) Plastic containers (capacity of 200 ml) Concentration: 5, 10, 25, 50 ppm BPA Experiment duration: 20 days	➢ Removal efficiency of azolla more than 95% in presence of 5ppm BPA ➢ Reduction in growth rate at higher concentration (50 ppm)	Iran	Zazouli et al., 2014
Phyto-volatilization	*Pteris Vittata*	As	Pot experiment (Greenhouse) Concentration: 6540 ± 380 mg/kg soil Temperature: 25 (night) to 45◦C (day) in summer 10 (night) to 25 ◦C (day) in winter Experiment duration: 18 months	➢ 37% arsenite and 63% arsenate (both form of As) present in sample ➢ 90% of total As removed from As-contaminated soil by plant	Japan	Sakakibara et al., 2010
	Salicornia bigelovii	Se	Pot experiment (9 cm or 25 cm in diameter) Green house experiment Concentration: 2.5 mg/kg and 10mg/kg Condition: 14 h/10 h day/night cycle Amendment: 10 g/pot pickleweed shoot tissues Experiment duration: 4 months	➢ Average Se volatilization Treatment: 1.78 ± 0.99 µg/day per pot Control: 0.82 ± 0.12 µg/day per pot ➢ Volatilization of Se has significantly increased by the presence of pickleweed shoot	USA	Shrestha et al., 2006
	Avicennia marina	Phenanthrene and pyrene	Pot experiment, green house Top: 20 cm in diameter, Bottom: 14 cm in diameter, height: 20 cm	➢ Removal efficiency of Ph and Py in rhizosphere zones was 83.8–86.2% and 68.5–69.1% respectively	China	Jia et al., 2016

Process	Plant	PTEs	Experiment	Research outcome	Research site	References
Phytostimulation/ Rhizodegradation			Concentration: 5, 10, and 50 mg/kg soil Condition: 12 h/12 h day/night cycle, Relative humidity: 85%, Temperature: 22 - 26 ◦C Experiment duration: 120 days	➢ Plant roots significantly improved dissipation of phenanthrene and pyrene.		
	Sebastiania Commersonia na	TPH	Pot experiment (22 cm × 24 cm) Greenhouse experiment Concentration:25, 50, 75 g/kg soil Temperature: 25-30◦C and Relative humidity: 85 to 90%Experiment duration: 424 days	➢ No appearance of TPH toxicity symptoms on plant tissues ➢ After 60 days plant growth, higher than 60% reduction of TPH showed ➢ More than 94% reduction of petroleum hydrocarbon after 424 days	Brazil	Ramos et al., 2009
Phytofiltration Rhizofiltration/	*Brassica juncea*	U	Hydroponic experiment Concentration: 25–5000 µM Flask: 250 mL Temperature: 25 ◦C Experiment duration: 10–12 day	➢ Plant accumulated 20-23% U from solution ➢ In higher concentration (1000–5000 µM U), hairy root growth of the plant was retarded	India	Eapen et al., 2003
	Helianthus annuus	U	Hydroponic experiment (Green house) Experiments jars—12 cm × 12 cm × 8 cm, Concentration: 30–646 µg/L; Temperature: 25 ◦C Relative humidity: 80% Experiment duration: 72 hours	➢ Within 24 hrs, 80% U contamination was removed from ground water ➢ At pH 3-5, maximum removal of U occurred. ➢ Accumulation higher in plant roots	Korea	Lee and Yang, 2010

Techniques like phytoextraction and phytostabilization are commonly used for remediating PTEs-polluted sites. Some examples include *Cymbopogon citrates*, *Helianthus petiolaris*, *Chrysopogon zizanioides L, Pennisetum purpureum* cv. Mott, *Conocarpus lancifolius*, and *Cordyline fruticose* etc (Andra et al., 2009; China et al., 2014; Herlina et al., 2020; Rasheed et al., 2020; Kowitwiwat and Sampanpanish, 2020; Saran et al., 2020). These species are key in cleaning contaminated soils either by extracting PTEs into their tissues or stabilizing them in the soil. Vegetation helps limit pollutant transport, reduce wind dispersion, and prevent water erosion (Perronnet et al., 2000). Unlike conventional methods that disturb soil physical properties, phyto-strategies maintain and enhance soil quality. Successful phytoremediation implementation requires considerations of biomass production, PTEs concentration in plant material, and the time needed for soil remediation (Robinson et al., 1998). Phytodegradation involves the uptake of toxic compounds by plants, where plant enzymes break down these substances into less harmful forms (Sun et al., 2012; Hamdi et al., 2012). Plant species like *Arabidopsis thaliana* and *Azolla filiculoides* are used for phytodegradation of pollutants such as 2,4-DNT and Bisphenol A in the USA and Iran (Yoon et al., 2008; Zazouli et al., 2014). Phytovolatilization occurs when plants transform the contaminant into volatile compounds and emit into the atmosphere through transpiration or radial diffusion from their leaves, stems, and roots (Limmer and Burken, 2016; Peter et al., 2017). Rhizodegradation is the breakdown of contaminants facilitated by rhizospheric microorganisms, where root-released enzymes and exudates help decompose pollutants into non-toxic forms (Jia et al., 2016; Gkorezis et al., 2016). Plants like Pteris vittata (Sakakibara et al., 2010) and Salicornia bigelovii (Shrestha et al., 2006) are involved in phytovolatilization of arsenic and selenium in Japan and the USA, respectively. The efficacy of phytoremediation depends on selecting appropriate plant species and various environmental factors. Overall, phytoremediation is a complex process involving multiple plant mechanisms. Understanding these processes can enhance plant adaptation to metal stress and improve efficiency, providing sustainable solutions for PTEs contamination and ecosystem restoration.

2.3.2 Arbuscular-mycorrhizal remediation

Naturally plants interact constantly with large number of microorganisms in their rhizospheric region. Beneficial microorganisms especially arbuscular mycorrhizal fungi (AMF) have a symbiotic association with plant roots where AMF increases plant nutrient uptake ability, improves biomass accumulation, amplifies photosynthesis capacity, and provide protection against PTEs toxicity, successively, plant provides exudates of amino

acids, carbon, photosynthetic product to the AMF for growth and developments (Mitra et al., 2020).

Around 80% terrestrial plants and 90% agricultural plants have mycorrhizal association in their roots where fungal hyphae enter in the cortical cells of plant roots forming vesicles, hyphae and arbuscles (Smith and Read, 2010). Fig. 3 denotes the schematic diagram of PTEs detoxification mechanism through AMF. AMF helps in immobilization of PTEss by binding them at cortical region, prevent translocation to the upper ground part (shoot, stem, leaves) and prevent damage of leaves.

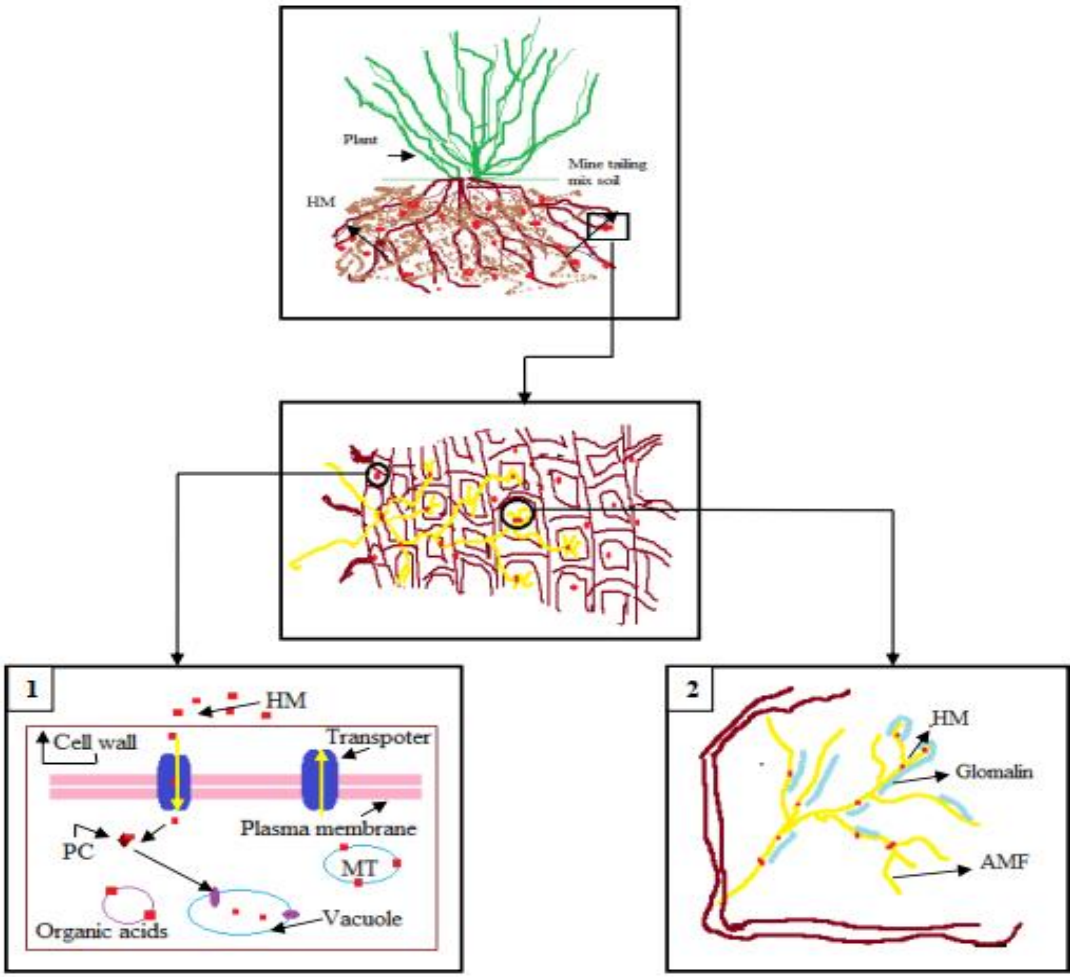

Fig. 3: Schematic representation provides an idea of PTE (HM) detoxification mechanisms in plant through arbuscular mycorrhizal fungi (AMF). 1) PTEs in mine tailing mix soil binds on phytochelatins (PC), metallothionein (MT), organic acids and transported across the cell wall and plasma membrane through ion selective transporter for HM sequestration on the vacuole 2) Transport HMs on AMF hyphae, export it on plant cells via arbuscules and immobilize metals, reclaim soil water holding capacity due to glomalin production.

Plants are categorized based on TF value into hyper accumulator (TF>1) and non- hyper accumulator (TF<1). The translocation factor (TF) is higher in non-mycorrhizal associated plant than in mycorrhizal associated plant (Arshad et al., 2008). Endomycorrhizal fungi AMF, belongs to phylum *Glomeromycota* which considered as an eco-friendly sustainable strategy to enhance plant growth, increase shoot biomass, improving soil health and water uptake capacity, provide protection to the plant against biotic, abiotic stress and detoxify PTEs induced stress (Mishra et al., 2019). *Glomeromycota* are obligated symbiotic organisms, so they require around 20% of carbon from host plant cell for their survival and simultaneously they provide water and nutrients (P, N) through their arbuscles, intracellular and extracellular hyphae to the host plant (Parniske, 2008). AMF combat the PTEs stress by immobilization, precipitation, chelation and sequestration in rhizosphere, vacuoles and activates the plant anti-oxidant defense system (Mitra et al., 2020). Another way of defense mechanisms of AMF is to secrets a hydrophobic unique glycoprotein called 'Glomalin' which is composed of (39-59%) carbon, (0.03-0.1%) phosphorus, (3-5%) nitrogen, (4-6%) hydrogen, (33-49%) oxygen and trace amount of iron (Schindler et al., 2007; Zhang et al., 2017). This protein is basically N-linked glycoprotein produced from the spores and hyphae of AMF which helps in soil aggregation, cellular function, toxic PTEs stress, carbon storage etc. (Emran et al., 2012; Wu et al., 2015). Easily extractable glomalin-related soil protein (EE-GRSP) and total glomalin-related soil protein (T-GRSP) both are simply quantified from soil with the help of citrate buffer (Wright and Upadhyaya, 1996).

For plant growth and nutrition, AMF increase the surface area with the help of extracellular and intracellular hyphae for better absorption of nutrient, water and the ions which are generally present in immobilize form in soil. AMF also improves the plant ability to acquire nutrient from nutrient depleted zone of rhizosphere (Smith and Read, 2010; Smith and Smith, 2011). As stated by Nakmee et al., (2016), native species of AMF *Glomus aggregatum*, *Acaulospora scrobiculata*, *F. mosseae* provide a positive effect on plant nutrient uptake (total N, P, K), enhance plant biomass, leaf number and plant height of sorghum. It was observed that those wheat plants inoculated with AMF culture (*F. mosseae* and *R. intraradices*) contain 1.13-2.76 times higher concentration of Zn than non-inoculated wheat plants (Coccina et al., 2019). Various abiotic stresses like salinity, PTEs, drought, flooding, extreme temperature etc. AMF community withstand independently against these unfavorable stress condition for its host plant and provide sufficient water in drought stress, supply nutrients (phosphorus) and balance osmotic pressure in flooding stress condition (Zhu et al., 2017; Caradonia et al., 2019). Under drought condition, tomato plant containing AMF (*R. intraradices*) colonization

on their roots, provides sufficient water-nutrient to the tomato plant for better growth during water stress situation. Inoculation with *G. etunicatum* enhances total chlorophyll content, root- shoot height- weight, increased N, P, K, Ca, Zn, Cu concentration, flavonoids content, soluble sugar, proline, glycine betaine, polyamine, POD, CAT activity in *Pistaciavera* L under stress condition (Abbaspour et al., 2012). Studies raveled that *G. etunicatum, F. mosseae,* and *R. irregularis* increased the growth, grain yield of *Triticum aestivum* L. and regulates nutrient uptake capacity and decreases Na^+ and Cl^- concentration at the time of salinity stress (Daei et al., 2009). According to Hashem et al., (2016) oxidative stress generates high concentration malonaldehyde and hydrogen peroxide on *Solanum lycopersicum* L. AMF strain (*Glomus mosseae, Glomus intraradices,* and *Glomus etunicatum*) helps to decrease the concentration of these elements and boost up plant defense system against Cd stress. AMF also provide protection against biotic stress. Various pathogens such as root-rot fungi, pathogenic bacteria, nematodes, and other harmful microorganisms can cause various plant diseases. However, the presence of AMF significantly reduces pathogen-induced damage and infection by enhancing nutrient availability, stimulating root growth, and improving root morphology. Additionally, AMF secrete beneficial enzymes in the rhizosphere, strengthening plant defenses and enabling plants to better withstand biotic stress (Vos et al., 2012; Spagnoletti et al., 2020). Fusarium wilt causes damage on *Cicer arietinum* L plant but treatment with AMF strain (*Glomus hoi*) provide protection against wilt disease and increase the nitrogen and phosphate content in treated plants as compared with non-treated plants (Singh et al., 2010). Similarly, *Glomus sp*. synthesis antimicrobial compounds which helps to arrest the mycelia growth of *Fusarium oxysporum,* on *L. esculentum* plants and increase chlorophyll, N, P, K content of the plants. Also in *Capsicum annum*, *Glomus sp*. reduces the activity of pathogen *Pythium aphanidermatum* and provide better yield of the plant (Kumari and Prabina, 2019; Kumari and Srimeena, 2019).

Previous literature denotes that AMF increased shoot accumulation of Cr, Pb, and As in *Jatropha multifida* grown in Malaysian landfill soils (Hassan et al., 2025), *Zea mays* and *Cicer arietinum* indicated reduced PTE uptake and improved physiological traits when inoculated with various AMF species (Cheema and Garg, 2024; Singh et al., 2019). Similarly, maize (HemmatiTabar et al., 2023), Chickpea (Cheema and Garg, 2024), safflower (Salari et al., 2024), Sweet sorghum (Cheng et al., 2021) and *Lallemantia iberica* (Ansari et al., 2021) demonstrated enhanced tolerance to Ni As, and Pb, respectively, under AMF influence as depicted in Table 3.

Table 3: Summary of previous research works on plant-associated arbuscular mycorrhizal fungi in PTEs remediation

Country	Experimental details	Result obtained	Reference
Malaysia	In this experiment, the treatment group included *Jatropha multifida* grown in landfill-contaminated soil with AMF inoculation, while the control group consisted of *J. multifida* grown in the same contaminated soil without AMF. The study was carried out for 120 days. The AMF consortium used for inoculation was composed of isolates primarily including *Fusarium chlamydosporum, F. equiseti, Aspergillus niger, A. fumigatus, Trametes versicolor, Paecilomyces lilacinus, Perenniporia subtephropora, Penicillium cataractum, Antrodia serealis, Daldinia starbaeckii, Phanerochaete concrescens, Polyporales* sp., and *Cerrena aurantiopora*.	This study showed that in presence of AMF enhanced TEs uptake, and phytoremediation potential of *Jatropha multifida* L. AMF inoculation significantly promoted the growth of *J. multifida* and improved its resilience in contaminated landfill soil. In AMF-inoculated plants, notable accumulation of TEs was observed in shoots [Cr (320.77 ± 73.58 mg/kg), Pb (320.10 ± 51.68 mg/kg), and As (10.23 ± 3.07 mg/kg)] and in roots [Cr (124.61 ± 19.26 mg/kg) and Pb (67.52 ± 15.18 mg/kg)] compared to uninoculated controls. Overall, AMF inoculation significantly improved the health and phytoremediation capacity of *J. multifida* in metal/metalloid-polluted environments.	Hassan et al., (2025)
India	A pot experiment was conducted using chickpea (*Cicer arietinum* L.) to evaluate the effects of three AMF species [*Funneliformis mosseae, Claroideoglomus claroideum,* and *Rhizoglomus intraradices*] Seeds were sown in earthen pots filled with soil. The experiment followed with fiveAs	The study demonstrated that the three AMF species effectively reduced As uptake by promoting nutrient absorption, regulating proline and glutathione (GSH) metabolism, and strengthening antioxidant defences. Among the combinations, the HC 3 genotype inoculated with *R. intraradices* showed the highest efficiency,	Cheema and Garg, (2024)

	treatments (0, AsV40, AsV60, AsIII5, and AsIII10), four AMF treatments, and two chickpea genotypes (HC3 and C235). Plants were harvested 90 days after sowing.	offering strong functional synergy with the symbiosomes.	
Iran	A pot experiment was conducted to evaluate the impact of two AMF species, *Rhizophagus irregularis* and *Funneliformis mosseae*, on the tolerance and accumulation of As in safflower (*Carthamus tinctorius* L), in soils amended with different arsenate concentrations (0, 25, 50, and 100 mg/kg). The experiment was conducted for 45 days.	The findings showed that both AMF species formed successful symbiotic associations with safflower. However, *Rhizophagus irregularis* demonstrated higher root colonization and mycorrhizal activity, particularly at 100 mg/kg arsenic concentration. Both fungi significantly improved safflower's tolerance to arsenic by promoting its retention in the roots, enhancing phosphorus uptake, and boosting antioxidant enzyme activity, highlighting their effectiveness in supporting phytostabilization in safflower.	Salari et al., (2024)
Nigeria	A field experiment was carried out using spent engine oil, which contains TEs, applied to soil at three different concentrations: 0 ml (0 L/ha), 400 ml (1000 L/ha), and 800 ml (2000 L/ha). The experiment also incorporated various soil amendments, including cow dung, poultry manure, *Glomus hoi* (a mycorrhizal fungus), and *Gliricidia sepium* leaves and control.	The study showed that each amendment, when combined with contaminated soil, had a positive effect in reducing the impact of spent engine oil. Amendments like cow dung, poultry manure, *Glomus hoi*, and *Gliricidia sepium* leaves helped enhance the condition and quality of soils affected by the oil contamination. These organic amendments can	Adebiyi and Salami, (2023)

	Maize (*Zea mays*) seeds were sown in the plot and the experiment was conducted for 1 year.	significantly reduce the TEs uptake of soils contaminated with spent-engine oil	
China	The experiment was carried out in a greenhouse, where soil was uniformly mixed with AMF inoculum (*Funneliformis mosseae* BGCXJ03A). As was applied at concentrations of 0, 25, and 50 mg/kg, while iron was added at 0 and 50 mg/kg. *Zea mays* L. ND108 served as the test crop, and the study was conducted for 56-day.	Under low to moderate arsenic stress, the combined application of arbuscular mycorrhizal fungi and iron compounds worked synergistically to enhance phosphorus uptake and suppress As absorption. This increased the phosphorus-to-As uptake ratio, ultimately supporting better maize growth.	Zhou et al., (2023)
Iran	A pot experiment was conducted with maize plant *(Zea mays* L.) using a completely randomized design to assess the interaction between AMF inoculation and varying Ni concentrations. The treatments included four levels of Ni: 0 mg/kg, 50 mg/kg, 100 mg/kg, and 250 mg/kg, along with the inoculation with *Claroideoglomus etunicatum* (AMF) and control (devoid of AMF). The plants were grown in a greenhouse for 90 days.	Result showed that Inoculation with AMF significantly influenced nickel distribution in plants. At the Ni 250 level, inoculated roots had 29% more Ni than non-inoculated plant, while Ni levels in the shoots were 30% and 33% lower at Ni100 and Ni250, respectively. Additionally, soil glomalin increased with Ni up to 100 mg/kg, and inoculated plants showed higher phosphorus content in both shoots and roots compared to uninoculated plants.	HemmatiTabar et al., (2023)
Spain	In this investigation, TE-contaminated soil was added to each pot, and then inoculated with three AMF species: *Rhizoglomu scustos* (Custos); *Rhizoglomus*	In heavily contaminated soil, plants inoculated with the indigenous *Aznalcóllar* fungus showed higher TEs accumulation, particularly in the shoots. In contrast,	Silva-Castro et al., (2022)

	sp. (Aznalcollar); *Rhizophagus irregularis* (Intraradices) and control. Wheat (*Triticum aestivum* L.) was planted in each pot, and the experiment was conducted over a period of 45 days.	*Custos* and *Intraradices* demonstrated greater bioaccumulation in less-contaminated soil. All AMF treatments enhanced soil enzyme activity and plant antioxidant responses. Overall, *Aznalcóllar* supported phytoremediation, while *Custos* and *Intraradices* contributed more to wheat bio-protection in TE-contaminated conditions.	
Iran	The experiment included treatments with four levels of Pb contamination (0, 300, 600, and 900 mg Pb/kg soil), three mycorrhizal conditions (non-inoculated, inoculated with *Funneliformis mosseae*, and *Rhizophagus intraradices*), and three levels of putrescine (Put) application (no Put, 0.5 mM, and 1 mM foliar spray). *Lallemantia iberica* was used as the test plant in Pb-contaminated soil. The experiment was conducted for 52 days after sowing.	Result showed that AMF inoculation enhanced plant growth, stress defense, and tolerance while reducing translocation factor, Pb accumulation, under Pb stress. The combination of 0.5 mM putrescine with *Funneliformis mosseae* led to notable improvements, including a 13% increase in shoot biomass, 14.4% greater shoot tolerance, and reduced shoot Pb concentration by 28.1%. In contrast, combining 1 mM putrescine with *Rhizophagus intraradices* had adverse effects on all measured parameters. Overall, the *Funneliformis mosseae* and 0.5 mM putrescine combination proved most effective in lowering Pb accumulation in *L.iberica*, supporting its potential for phytostabilization.	Ansari et al., (2021)

China	The individual and combined effects of arbuscular mycorrhizal (AM) fungi and nano zero-valent iron (nZVI), a three-factor experimental design was employed. The factors included for pot experiment: (1) two AM fungal treatments (either inoculated or non-inoculated with *Acaulospora mellea* ZZ), (2) two types of nZVI (S-nZVI and B-nZVI), and (3) six levels of nZVI concentrations (0, 50, 100, 200, 500, and 1000 mg/kg). Sweet sorghum was used as the test plant for the experiment and experimental duration was 60 days.	AMF inoculation alone proved effective in immobilizing heavy metals in the soil and reducing their uptake by plants. Despite the potential fungitoxic effects of nZVI, AMF were still able to successfully colonize plant roots. Overall, the combination of AM inoculation with low nZVI concentrations (100 mg/kg) showed a synergistic effect, further enhancing TEs immobilization in the soil.	Cheng et al., (2021)
China	The experiment was designed as a two-factorial setup, involving two Pb levels (0 and 800 mg/kg) and two AMF treatments (with and without inoculation). *Medicago truncatula* was used as the test plant, and the AMF inoculum consisted of *Rhizophagus irregularis* (BGC BJ09). The experiment was conducted for 12 weeks	The results indicate that AM inoculation can enhance plant growth and promote lead (Pb) immobilization within the cell wall by boosting polysaccharide levels in pectin and hemicellulose, as well as by stimulating cell wall peroxidase activity.	Zhang et al., (2021)
Philippines	Inorganic mercury chloride ($HgCl_2$) was applied to soil at concentrations of 0, 2, 4, and 6 ppm per 2 kg of soil, which was placed in plastic pots. Each treatment	The study emphasizes the impact of AMF inoculation on both the uptake of inorganic mercury and the growth of *Chrysopogon zizanoides* (vetiver). The findings showed	Bretaña et al., (2019)

	was inoculated with two commercially available AMF inoculants, *Mykovam*™ and *Glomus* sp.. Pots without AMF served as the control. Vetiver was used as the test plant, and the experiment was carried out for 4 weeks.	that AMF inoculation significantly improved the plant's growth. Moreover, it enhanced mercury absorption by the plant, even at higher mercury concentrations.	
India	A pot experiment was carried out using tannery sludge rich in toxic elements (TEs), which was inoculated with mycorrhizal cultures (*R. fasciculatus, R. intraradices, F. mosseae and G. aggregatum*) and control (devoid of AMF). Maize (*Zea mays*) seeds were sown in the pot, and the experiment was maintained for 3 months.	AMF injection enhanced root development, facilitating improved phytoextraction and phytostabilization processes, as well as soil enzyme activities. Among four AMF species, *F. mosseae* was the most effective for multi-TEs-polluted areas, as it enhanced TEs accumulation in maize roots while limiting translocation to the shoots.	Singh et al., (2019)
Brazil	Soil mixed with coal mine waste was placed in pots and amended with various AMF species, including *Acaulospora colombiana*, Acaulospora morrowiae, *Acaulospora scrobiculata, Dentiscutata heterogama, Gigaspora margarita, Rhizophagus clarus* and control. Vetiver was used as the test plant, and the experiment was conducted for 165 days.	The study highlights the positive impact of specific AMF species (*G. margarita*, *R. clarus*, and *A. morrowiae*) on vetiver growth in coal mine waste substrates. Plants inoculated with *A. colombiana*, *A. morrowiae*, and *A. scrobiculata*, showed the highest root accumulation of Cu and Zn. Notably, *G. margarita* promoted the higher biomass production and led to elevated TEs accumulation in the plant.	Meyer et al., (2017)

USA	Vetiver plants, and AMF were transplanted into plastic columns filled with As-spiked soil and grown for 4 weeks. As was introduced into the soil using sodium hydrogenarsenate heptahydrate ($Na_2AsO_4 \cdot 7H_2O$) at concentrations of 0, 12.5, 25, and 50 mg/kg of dry soil. The AMF inoculum (*Glomus* spp.) consisted of an equal mixture of spores from three *Glomus* species: *G. intraradices, G. mosseae*, and *G. aggregatum.*	The study indicated that AMF inoculation promoted plant growth, primarily by enhancing root development. Although As uptake by vetiver was not significantly influenced by the *Glomus* spp. inoculum, most of the absorbed As remained in the roots, indicating limited translocation to the shoots when grown in As-spiked soil.	Caporale et al., (2014)
India	Earthen pots were filled with soil contaminated by chromite-asbestos mine waste and amended with different AMF cultures. These included *Glomus hoi*, *Funneliformis coronatum*, *Claroideoglomus claroideum*, and *Claroideoglomus etunicatum*, along with a control group without AMF. Vetiver was used as the test plant, and the experiment was carried out for two months.	The result depicted that among four AMF species tested, *Glomus hoi* and *Funneliformis coronatum* proved to be the most effective for soils contaminated with multiple TEs. They significantly boosted glomalin production, which in turn enhanced the accumulation of TEs in vetiver roots while restricting their movement to the shoots. The higher TEs accumulation in the roots (Ni: 27.44%, Cr: 21.74%) was observed in presence of *Glomus hoi*. Also, model-based analysis (PLS-SEM and sobol model) also validates the presence of AMF enhances phytoremediation efficiency of vetiver plant.	Present Study

Vetiver grass has been studied in the PTEs remediation of overburden sites (including mercury-laden soils, coal mine overburden, arsenic-enriched soils, and iron ore dumps etc.); industrial activities (such as tannery sludge, fly ash etc.) (Caporale et al., 2014; Mayer et al., 2017; Singh et al., 2019; Banerjee et al., 2019; Bretaña et al., 2019).

2.3.2.1 Evaluation of AMF as a tool to remediate metals through meta-analysis

Research works published between 2005 and 2022 were searched in Web of Science database and selected based on their reporting quality. The keywords were 'Arbuscular mycorrhizal fungi', 'Mine', 'Soil', 'World', 'Cadmium', 'Nickel', 'Lead', "Copper" and "Chromium". After the assessment of >250 peer-reviewed articles, the articles were excluded based on the following reasons: a) Lacking in analytical techniques (not mentioning the QA/QC), b) remediation through other microbes c) Graphical representation of data. To conclude, a total of 24 studies comprising of 9, 12, 7 and 5 studies for Cd, Pb, Cu and Ni respectively were included in for meta-analysis, which assessed the efficacy of AMF in remediating metal-contaminated mine soils (Table 4).

Table 4: Summary of research works on arbuscular mycorrhizal fungi in toxic metal remediation

Country	Metal	Type of experiment	Name of AMF	Inherent total metal concentration in soil (mg kg^{-1})	Experimental dose (mg kg^{-1})	Plant metal content (mg kg^{-1})	Test Crop	Effect of AMF inoculation	Reference
South Africa	Ni	Pot experiment	Native AMF sp. (*Gigaspora* sp. and *Glomus tenue*)	650		7020	*Berkheya coddii* Roessle	↓	Orlowska et al. 2011
South Africa	Ni	Pot experiment	Native AMF	650		724	*Berkheya coddii* Roessle	↑	Orłowska et al. 2013
France	Ni	Pot experiment	*Glomus etunicatum* SFONL		60	881	*Cloezia artensis*	↓	Amir et al. 2013
Taiwan	Ni	Pot experiment	AMF	459.5		90.1	*Ipomoea aquatica* Forsk.	↓	Lam and Lia 2018
South Africa	Ni	Pot experiment	AMF	634.25		66.10	*Colosphospermum mopane*,	↓	Manyiwa and Ultra, 2022
China	Pb	Pot experiment	AMF		600	259.81	*Kummerowia striata*	↑	Chen et al. 2005
China	Pb	Pot experiment	*Glomus mosseae* and *Glomus intraradices*	4418		1.11	*Leucaena leucocephala*	–	Ma et al.2006
Spain	Pb	Pot experiment	*Glomus deserticola*	595.96		284.1	*Eucalyptus globulus*	↑	Arriagada et al. 2007

USA	Pb	Pot experiment	*Glomus mosseae*		1200	2179	*Chrysopogon zizanioides* (L.)	↑	Punamiya et al. 2010
China	Pb	Field experiment	*Glomus intraradices* and *Glomus mosseae*	209		12.6	*Chrysopogon zizanioides* (L.)	–	Wu et al. 2010
USA	Pb	Pot experiment	*Glomus deserticola*	4620		3.89	*Prosopis juliflora*	–	Solís-Domínguez et al. 2011
China	Pb	Pot experiment	AMF	3683	1500	2655	*Viola baoshanensis*	↑	Zhong et al. 2012
Iran	Pb	Pot experiment	*Glomus versiforme*		800	119.80	*Chrysopogon zizanioides*	–	Bahraminia et al. 2016
Brazil	Pb	Pot experiment	*Acaulospora scrobiculata*	125		103	*Chrysopogon zizanioides* (L.)	↑	Meyer et al. 2017
China	Pb	Pot experiment	*Gaeumannomyces cylindrosporus*		1000	252.25	*Zea mays* L	↑	Yihui et al. 2017
China	Pb	Pot experiment	*Diversispora spurcum*	1426.7		732.9	*Cynodon dactylon* (L.) Pers.	↑	Zhan et al. 2019
Mexico	Pb	Pot experiment	*Rhizophagus irregularis*	640		237.97	*Parkinsonia aculeata* L	↑	González-Villaloboset et al.2021
Spain	Cd	Pot experiment	*Glomus deserticola*	21.48		7.4	*Eucalyptus globulus*	↑	Arriagada et al. 2007

Brazil	Cd	Pot experiment	*Glomus intraradices*		0.02	885	*Helianthus annuus* L.	↑	de Andrade et al. 2008
China	Cd	Field experiment	Glomus intraradices and *Glomus mosseae*	2.25		939	*Chrysopogon zizanioides* (L.)	↓	Wu et al. 2010
China	Cd	Pot experiment	AMF	113	200	6952	*Viola baoshanensis*	↑	Zhong et al. 2012
China	Cd	Pot experiment	*Glomus caledonium* 90036	1.54		1.44	*Sedum alfredii* Hance	↓	Hu et al. 2013
Canada	Cd	Pot experiment	*Rhizophagus irregularis*	0.75	40	256.44	*Helianthus annuus* L.	↑	Hassan et al. 2013
China	Cd	Pot experiment	*Glomus constrictum*		112	8.27	*Zea mays* L.	↓	Liu et al. 2014
China	Cd	Pot experiment	*Diversispora spurcum*	16.9		14.5	*Cynodon dactylon* (L.) Pers.	↑	Zhan et al. 2019
China	Cd	Field experiment	AMF	19.02		4.8	*Zea mays* L.	↓	He et al. 2020
Brazil	Cu	Pot experiment	*Glomus etunicatum*			125.71	Leucaena leucocephala	↑	Lins et al. 2006
China	Cu	Pot experiment	*Glomus mosseae*	232		1267.34	*Lolium perenne*	↑	Chen et al. 2005
South Africa	Cu	Pot experiment	Native AMF sp. (*Gigaspora* sp. and	55		108(29)	*Berkheya coddii* Roessle	↑	Orlowska et al. 2011

			Glomus tenue)						
USA	Cu	Pot experiment	Native AMF	653		21.5	*Prosopis juliflora*	↑	Solís-Domínguez et al. 2011
South Africa	Cu	Pot experiment	Native AMF	55		26	*Berkheya coddii* Roessle	↑	Orłowska et al. 2013
Brazil	Cu	Pot experiment	*Glomus margarita*	17.7		102	*Chrysopogon zizanioides* (L.)	↓	Meyer et al. 2017
South Africa	Cu	Pot experiment	AMF	768.13		250.11	*Colosphospermum mopane*,	↓	Manyiwa and Ultra, 2022

↑ PTE uptake increased in shoot/root of AMF infected plant as compared with control

↓ PTE uptake decreased in shoot/root of AMF infected plant as compared with control

– Non significant

Studies reporting remediation of Cr with AMF was not found during the systemic review. The PRISMA flowchart is displayed in Fig. 4.

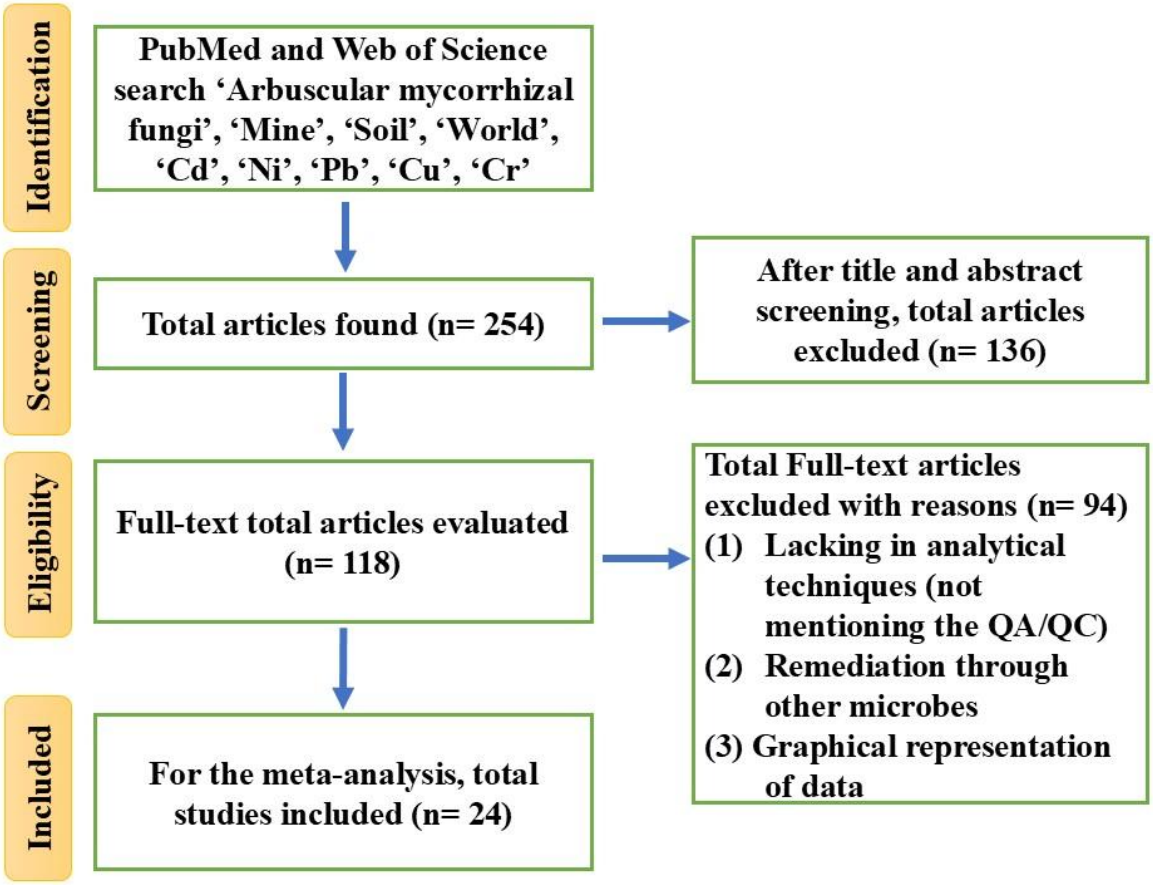

Fig. 4: The PRISMA flowchart showed the selection of articles eligible for meta-analysis

From RE models at (Fig. 5(a, b, c, d)), the overall mean value for Pb, Cd, Ni, and Cu were 1.34 (CIs: 1.19-1.49), 1.08 (CIs: 0.86-1.31), 0.79 (CIs: 0.53-1.05), and 1.46 (CIs: 1.02-1.90) respectively. The data showed statistical significance at $p < 0.05$. The inconsistency index (I^2) of Pb, Cd, Ni, and Cu was 92.94%, 96.39%, 99.30%, and 98.89% respectively, indicating substantial heterogeneity.

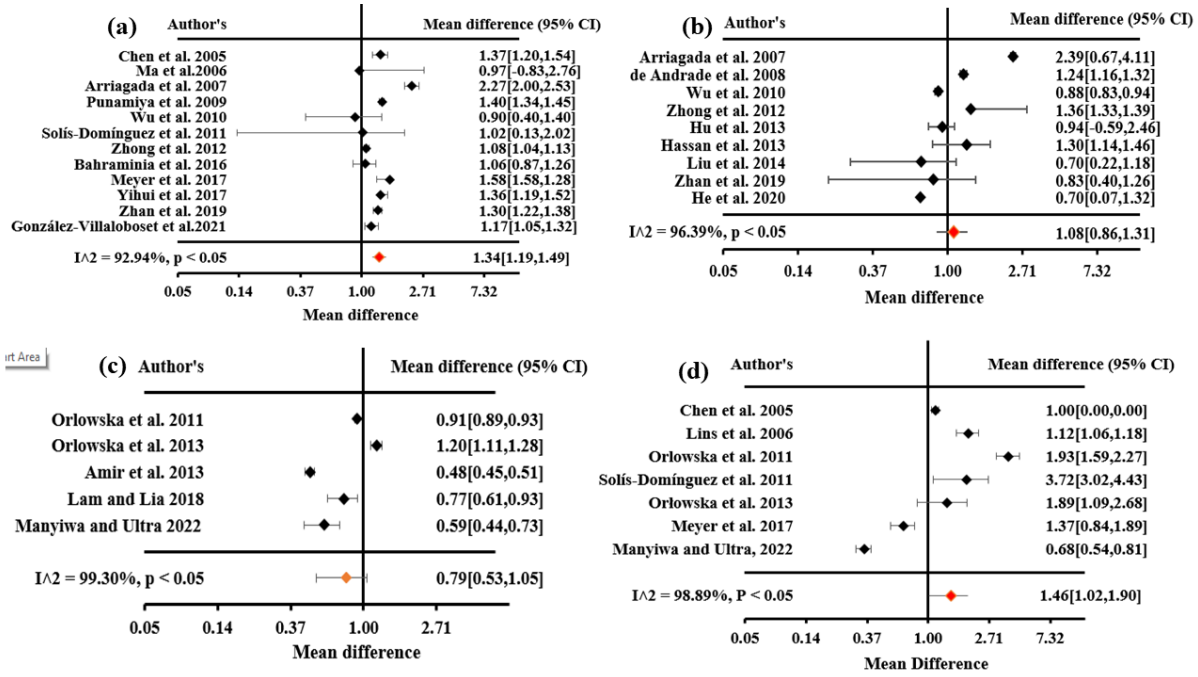

Fig. 5: Forest plot indicates the mean difference of individual observation regarding the PTEs accumulation level in plants in the presence of mycorrhizal infection in different countries. [(a) – Pb; (b)- Cd; (c)- Ni and (d) - Cu]

The positive effect size for all the metals indicated that the AMF has the ability to reduce the metal accumulation capacity in plants. The studies from USA (Punamiya et al., 2010), China (Zhan et al., 2019), Mexico (González-Villalobos et al., 2021), etc. indicate that the Pb accumulation in plants has increased by AMF (*Diversispora spurcum, Glomus mosseae, Rhizophagus irregularis*) except (Wu et al., 2010; Solís-Domínguez et al., 2011; Bahraminia et al., 2016), the CIs value overlapped the line of zero showing non-significance (Fig. 5a). The case studies from Spain (Arriagada et al., 2007), Brazil (de Andrade et al., 2008), China (Zhong et al., 2012), and Canada (Hassan et al., 2013) showed that the accumulation of Cd in plant systems has increased in presence of AMF infection of *Glomus deserticola, Glomus intraradices* and *R. irregularis*. Other studies from China (Wu et al., 2010; Hu et al., 2013; Liu et al., 2014; He et al., 2020), the Cd accumulation in plant was decreased (*Glomus constrictum, Glomus caledonium,* and *Glomus intraradices*) (Fig. 5b). For Ni and Cu, the accumulation in decreases in the presence of AMF (*Glomus tenue, Glomus margarita*) (Orłowska et al., 2011; Lam and Lai, 2018; Manyiwa and Ultra Jr, 2022) and simultaneously increase the accumulation by the help of *Glomus mosseae, Glomus etunicatum* (Chen et al. 2005; Lins et al., 2006) (Fig. 5c and 5d). Plant roots are symbiotically associated with AMF, which increases plant nutrient uptake ability, increases biomass accumulation, increases

photosynthesis capacity, and modulates metal toxicity. Through the formation of extracellular and intracellular hyphae, AMF increases soil surface area for better absorption of soil nutrients (N, and P), PTEs (Cr, Ni, Cd, Pb, and Cu), improve root growth, root morphology, secrets various proteins like glomalin (Amir et al., 2013; Lam and Lai, 2018; Zhan et al., 2019; Manyiwa and Ultra Jr, 2022). In this paradigm, the presence or absence of AMF in plant systems could impact the accumulation capacity of PTEs, thus increasing or decreasing ecosystem risk.

2.3.3 Vermi-remediation technology: an innovative approach

The use of biological agents for managing different types of waste offers an effective strategy to reduce toxicity and mitigate environmental risks associated with improper disposal. Among these, vermi-remediation technology is a sophisticated technique that enhances the breakdown of persistent organic materials. Relying on the mutual interaction between earthworms and microorganisms, it proves to be more efficient than conventional composting approaches (Piearce et al., 1990; Bhattacharya and Kim, 2016). This process produces stable, nutrient-rich material that is both aesthetically pleasing and biologically advantageous as earthworms and microorganisms gradually break down solid waste. However, in the vermicomposting process, humification fixes a large amount of organic C. For the formation of metal-humus complexes, these stable, refractory humic components are essential. A rather congruent organic product with a substantial amount of organic matter and organic carbon is the result of the vermicomposting process. Furthermore, it lowers PTEs pollution and has easily accessible micronutrients, NPK, and a range of enzyme activities (Sharma et al., 2005). The nature and quantity of source material or underlying materials used in vermibeds affect the final quality of vermicompost. The metabolic process and the degree to which waste can be converted into an organic amendment are significantly impacted by factors such as substrate and its quality (Ramnarain et al., 2019). Vermicomposting, which mineralizes a variety of solid organic wastes, yields compost of higher quality than other composting technologies (Suthar et al., 2012).

2.3.3.1 Earthworm activity and mechanism in PTEs removal

Earthworms (Class *Clitellata)* have a significant impact on the biology, chemical balance, and physical structure of soil (Domínguez et al., 2018). They prefer moderate temperatures (20–25 °C) and moisture (60–75%). They have a life cycle of approximately 220 days and lays 300–400 eggs.

Earthworms are divided into the following groups according to their habitat:

- *Epigeic*: Surface-dwellers, feed on organic waste.
- *Endogeic*: Digs in soil rich in organic matter
- *Anecic*: Dwells in deep, dug vertical burrows.

Particularly, *epigeic* worms are favoured for the bioconversion of solid waste. They can also be divided into two groups based on how they feed: geophages (soil feeders, such as endo- and anecics) and detritivores (surface waste feeders, such as epigeics). Species such as *Eisenia fetida, Eisenia andrei*, and *Dendrobaena veneta* are the most often utilized species in vermicomposting; they are chosen for their quick reproductive cycles and capacity to tolerate a wide range of moisture and temperature conditions. *Eisenia andrei* is consistently red, but *Eisenia fetida,* also referred to as the "tiger worm," has light stripes. As potent decomposers, earthworms assimilate or expel the vast majority of the material that they ingest into extremely nutrient-dense castings. Their strong gizzards grind up substrate, which promotes microbial breakdown and nutrient transformation. Their gizzards expand the surface area available for microbial action by mechanically grinding convoluted substrates into tiny fragments (Bhattacharya and Kim, 2016). At the same time, their gut diversity transforms insoluble nutrients into soluble forms that are accessible to the body (Goswami et al., 2014). The detoxification of waste harbouring PTEs is an important upside of vermicomposting. Earthworms' gastrointestinal tissue possesses cysteine-rich proteins known as metallothionein's, which facilitate them to bioaccumulate metals. It's interesting to mention that *Eisenia fetida* that is exposed to PTEs exhibits a stimulation of metallothionein isoforms, which promotes PTEs sequestration while preserving redox balance and metal-ion homeostasis.

The efficiency of waste stabilization and mineralization is greatly influenced by the kind of earthworms used. Surface feeders, or *epigeic* species, are especially good in vermi-stabilizing solid waste (Bhattacharya and Kim, 2016). An *epigeic* worm called *Eisenia fetida* efficiently breaks down industrial waste, including coal ash from thermal plants, paper mills, and tea factories. For example, vermicomposting fly ash enhanced with cattle manure reduces soluble PTEs including Cd, Cr, and Pb while increasing readily mineralizable N, accessible P, and K. Research indicates that when vermicomposting fly ash combined with calf dung, *E. fetida* and *E. eugeniae* can significantly lower concentrations of Zn and Pb, Cd by around 51%, Cu by more than 50%, and Cr by up to 59%. Additionally, consecutive extraction investigations

show that earthworms reduce mobility and toxicity (e.g., in sewage sludge) by converting metals into more stable, recalcitrant organic- or mineral-bound fractions.

In brief, vermicomposting has several adventurous aspects.

1. Robust process: During vermicompost, earthworms mechanically grind substrates and harbour microbial communities that solubilize nutrients, resulting in a robust process.

2. PTEs detoxification: PTEs are stabilized into less accessible components and accumulation, aided by gut metallothioneins.

3. Performance of the species: *Epigeic* worms, specifically *E. fetida* and *E. andrei*, are exceptional in swiftly breaking down waste, reproducing, and withstanding the effects of PTEs.

2.4 Evaluating the effectiveness of vermicomposted product on agricultural productivity and soil vitality through crop experiment

Vermicompost has been shown to improve soil health and agricultural productivity in a number of recent studies. Vermicomposting industrial wastes, such as steel waste slag, oil sludge, red mud, and tannery waste, and incorporating them into agricultural soils either by alone or in conjunction with organic and inorganic amendments has been the subject of recent research (Sarkar et al., 2023, Chakraborty et al., 2022, Jha et al., 2024, Charan et al., 2024). Vermicomposted steel waste slag has been demonstrated to enhance a number of soil physicochemical characteristics and increase plant vigor when added to soil. These results, which came from well-monitored vermicomposting trials, offered compelling justification for assessing the agronomic potential of these composts for improving soil fertility and stimulating crop development (Jha et al., 2023). Green gram, or *Vigna radiata* L., was used as a test crop in a pot experiment to confirm the efficacy of vermicomposted red mud. Vermicompost application significantly improved plant growth parameters, suggesting that it has potential as a soil amendment (Charan et al., 2024). When applied at realistic agronomic rates during short-term cropping of rice, experimental vermicompost made from oil sludge showed no adverse effects on crop output metrics or important soil quality indicators like pH, organic carbon content, or cation exchange capacity. This shows that such vermicompost can be used in the field without affecting the productivity or health of the soil. (Sarkar et al., 2023). *Eisenia fetida* was used in parallel vermicomposting of tannery waste in order to assess the plant's effectiveness in cleaning up hazardous substrates. The study also sought to

comprehend how the process affected the enzyme profiles, microbial activity, and the organization of the microbial community during metal detoxification. The findings showed that a 1:1 co-vermicomposting ratio between tannery waste and cow dung considerably decreased the microbial population's exposure to metal-induced stress. Important enzymes, including urease, phosphatase, and dehydrogenase, were among the many microbial species and enzymatic activities that were significantly increased by this therapy (Chakraborty et al., 2022). In a nutshell, vermicomposting with industrial waste has demonstrated significant promise in enhancing soil qualities and promoting crop growth, especially when paired with organic substrates like cow dung. In furtherance of helping with PTEs detoxification, earthworms and microbial communities act in concert to improve nutrient availability, which promotes sustainable waste management and increased agricultural yield. Several industrial wastes, including paper mill and textile sludge, have been effectively transformed into vermicompost, showing positive impacts on soil fertility (Ravindran et al., 2008; Das et al., 2016). However, no studies have yet explored the vermicomposting of chromium-asbestos mine waste (CAMW) and PTE-enriched vetiver (PTE-EV), nor their potential application in agriculture.

2.5 Research gaps identification, defining the problem, and possible solutions

India, often referred to as the “land of mines and minerals,” and particularly the state of Jharkhand, is home to a variety of mines such as those for coal, mica, copper, iron, uranium, and chromium-asbestos. Large-scale mining operations generate toxic mine waste, which frequently leach PTEs into nearby soils and contaminate ecosystems on a global scale (Kumar and Maity, 2014). Chromium-asbestos mine waste (CAMW), an extremely lethal byproduct, has given rise to significant environmental hazards globally. Uncontrolled mining activities and inappropriate disposal of mine waste containing PTEs have resulted in the pollution of nearby agricultural fields, ultimately lowering crop yield and quality. The presence of hazardous PTEs such as Cr, Ni, Pb, and Cu in soil contaminated by CAMW poses a major challenge due to their non-biodegradable nature and persistence in the environment. These PTEs can be absorbed by crops through soil-plant interactions, potentially entering the food chain and posing serious health risks to humans (Seleiman et al., 2020). Additionally, the high concentration of PTEs in CAMW-affected agricultural soils significantly threatens the sustainability of farming practices. These hazardous PTEs influence the structure and function of microbial communities (Tripathy et al., 2014). Therefore, a comprehensive and systematic investigation into the levels, spatial distribution,

potential health and dietary risks, effects on soil microbial activity, and feasible remediation approaches for PTEs is essential at the chromium-asbestos mine site in Jharkhand, India. In light of this, the present study seeks to address these critical gaps and provide insight into this underexplored area.

To the best of our knowledge, there is a lack of substantial research focusing on health risk assessment related to PTEs in the chromium-asbestos mine region of India. Existing studies have not comprehensively examined the bioavailability of PTEs in contaminated soils, their accumulation in staple crops like rice, and the subsequent implications for the food chain. Furthermore, limited information exists on the bio-accessibility and leachability of PTEs across different rice components (husk, without husk, cooked rice, and starch). The dynamic behaviour of soil PTEs leachability and its future health risk implications, particularly in relation to rice consumption, remains largely unexplored, though such insight is vital for soil and crop quality management. Additionally, the synergistic impact of bioavailable PTEs and soil alkalinity on microbial dynamics in soils impacted by chromium-asbestos mine waste has not been systematically studied. This study aims to fill these critical gaps by integrating assessments of PTE bioavailability, food chain transfer, source identification, leaching potential, and combined ecological impacts to support targeted risk mitigation and sustainable land use in the region.

Remediation of soils polluted with hazardous waste, such as those impacted by chromium-asbestos mine residues, requires innovative, eco-friendly, and economically viable strategies. However, most existing remediation techniques are neither sustainable nor cost-effective and can substantially generate secondary pollution and negative alterations to soil physicochemical properties (Mukherjee et al., 2024). Although phytoremediation using resilient plant species has gained attention, its full potential remains underexplored, particularly in combination with microbial consortia. Vetiver grass (*Chrysopogon zizanioides*) has been widely recognized for its effectiveness in the remediation of PTEs-contaminated environments, including coal mine overburden, iron ore dumps, tannery sludge, and fly ash (Mayer et al., 2017; Singh et al., 2019; Banerjee et al., 2019). However, its capacity for Cr remediation under hydroponic conditions remains inadequately studied. More critically, there is a lack of comprehensive research on vetiver's mycophytoremediation potential, particularly its synergistic interactions with arbuscular mycorrhizal fungi (AMF), in soils contaminated with chromium-asbestos mine waste. Moreover, comparative effectiveness of different AMF species (*Glomus hoi, Claroideoglomus etunicatum,*

Claroideoglomus claroideum, and Funneliformis coronatum) in enhancing vetiver's remediation potential has not been systematically assessed. This study addresses these critical gaps by simulating field conditions and evaluating the role of AMF-assisted vetiver in remediating and restoring chromium-asbestos mine-affected soils, thus offering a novel bio-based solution for managing such complex environmental challenges.

Post-mycophytoremediation, PTEs are sequestered within plant tissues mainly shoot section, necessitating safe and sustainable recycling strategies to prevent secondary environmental contamination. Similarly, improper disposal of CAMW, rich in PTEs, severely threatens soil health and crop productivity. Although vermicomposting has emerged as a sustainable biotechnological tool for converting organic and inorganic wastes into nutrient-rich amendments, two critical gaps remain unaddressed. First, the transformation of PTE-enriched vetiver (PTE-EV) into stabilized organic manure via vermicomposting remains underexplored, particularly with respect to its effects on soil biochemical parameters and crop performance. Second, while earthworms are known to facilitate the detoxification of industrial waste, the conversion of CAMW into safe and effective vermicompost and its isolated application in agriculture have received limited scientific attention. Moreover, no comprehensive studies have assessed the individual agronomic implications of these two vermicompost types, PTE-EV-derived manure and CAMW-derived compost, on soil nutrient status, microbial activity, PTEs bioavailability, crop yield, and plant biochemical traits. This dual-gap highlights the urgent need for systematic research to validate the efficacy, safety, and environmental sustainability of these recycled products in agricultural systems.

Henceforth, the subsequent objectives were taken into consideration for this current research.

2.6 Objectives of research

1. To assess the physico-chemical characteristics, microbial dynamics, and levels of potentially toxic elements (PTEs) in soil and crops cultivated on fields contaminated with chromium-asbestos mine waste (CAMW), India.
2. To determine Cr-tolerance of vetiver grass (*Chrysopogon zizanioides*) via hydroponic system through the analysis of physiological and biochemical parameters.
3. To evaluate the efficacy of phytoremediation potential of vetiver grown on soil contaminated with toxic mine wastes (CAMW) in presence of four different mycorrhizal cultures.

4. To transform these PTE-enriched vetiver (PTE-EV) and chromium-asbestos mine waste (CAMW) into beneficial organic products through a foremost effective technology (vermi-remediation) using earthworm species.
5. To assess the efficiency of reclaimed vermi-remediating products through pot and field trials with different agriculture crops.

Methodology and Instrumentation

Chapter 3: Methodology and Instrumentation

3. Orientation of the investigation

This thesis sheds light on a comprehensive insight into the contamination levels of PTEs, their spatial distribution, source allocation, accumulation in agricultural crops (particularly rice), the associated health and dietary risks, their effects on microbial dynamics, and the development of sustainable bioremediation strategies. The final focus lies on the agricultural utilization of composts derived from vermi-remediation of PTE-enriched vetiver and chromium-asbestos mine waste (CAMW). To systematically achieve the research objectives, the entire study has been organized into five sequential phases. The graphical abstract represents entire research plan (Fig. 6).

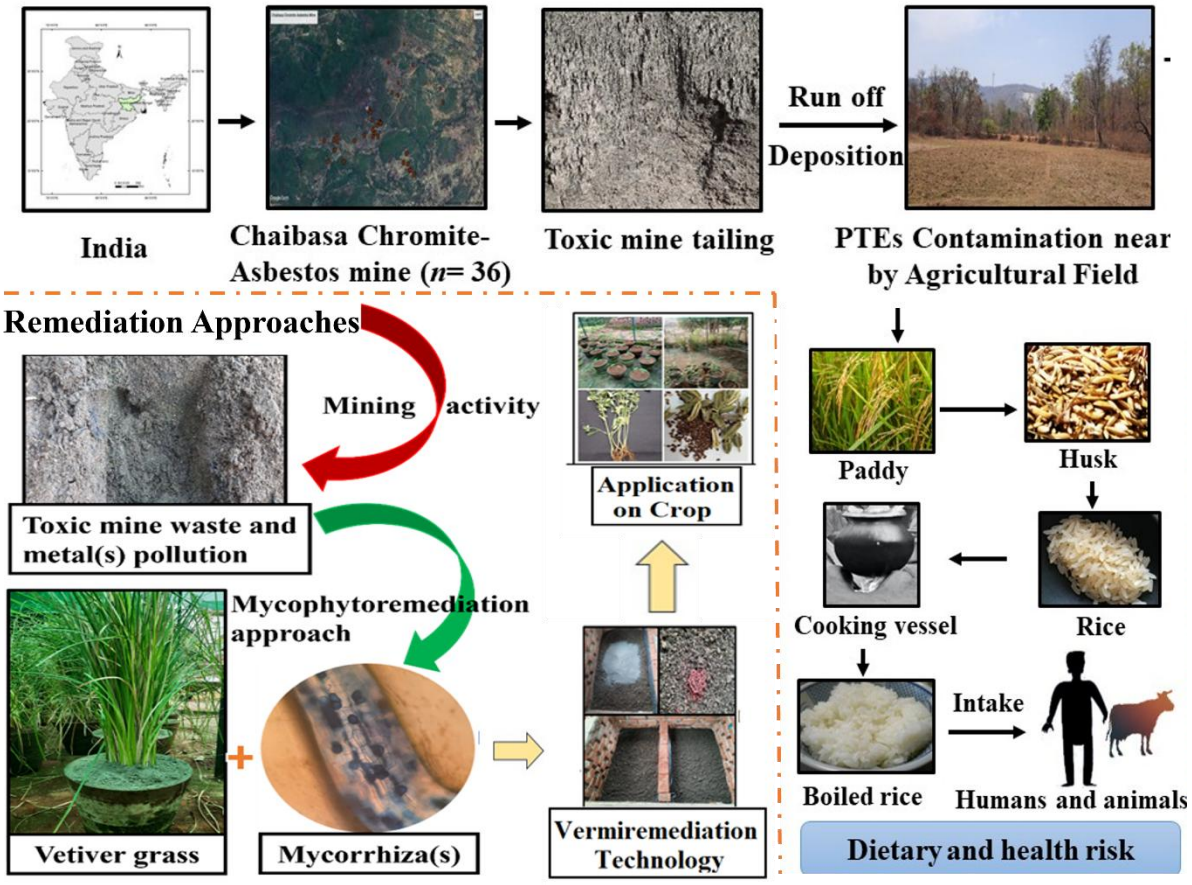

Fig. 6: Graphical representation depicts the overview of the complete research work

Phase I: Environmental assessment and impact analysis

This phase addressed the first set of objectives, focusing on the quantification and distribution of PTEs in the chromium-asbestos mining region of Jharkhand, India. Source apportionment, distribution pattern, probabilistic human health risk assessments, dietary intake risks from rice consumption, and the effects of PTEs on different rice plant components were examined. Additionally, the synergistic impact of PTEs and soil alkalinity on microbial diversity and soil health was explored using advanced statistical and multi-model approaches.

Phase II: Vetiver phyto-tolerance and accumulation study

In this phase, the second objective was pursued by investigating the tolerance, uptake capacity, and physiological responses of vetiver (*Chrysopogon zizanioides*) under different Cr concentrations in a hydroponic system. Biochemical indicators and plant growth metrics were measured to evaluate vetiver's potential for phytoremediation in Cr-contaminated environments.

Phase III: Mycophytoremediation of CAMW-contaminated soil

This phase focused on the third objective, which explored the use of arbuscular mycorrhizal fungi (AMF)-assisted phytoremediation for detoxifying CAMW-contaminated soil. The remediation efficacy of vetiver in symbiosis with different AMF strains (*Glomus hoi*, *Funneliformis coronatum*, *Claroideoglomus claroideum*, and *Claroideoglomus etunicatum*) was assessed in terms of PTEs uptake, soil improvement, and microbial interactions.

Phase IV: Vermi-remediation of contaminated PTE-enriched plant and CAMW (mine waste)

The fourth phase dealt with the conversion of hazardous PTE-laden vetiver shoot (PTE-EV) and CAMW into nutrient-rich, low-toxicity compost using the *epigeic* earthworm *Eisenia fetida*. This phase evaluated the potential of vermicomposting as a sustainable and eco-friendly technique to sanitize and valorize contaminated waste.

Phase V: Agricultural application of vermicompost

In the final phase, vermicompost derived from PTE-EV (mixed with cow dung) and CAMW (mixed with cow dung) were tested in four crop systems: sesame, tomato, chili (pot trials), and rice (field trial). The agronomic performance and soil quality parameters were compared with conventional fertilizer treatments to evaluate the effectiveness of the composts. PTEs

concentrations in harvested crops were also measured to ensure their safety for consumption and confirm the viability of this approach for sustainable agriculture.

3.1 Selection of study area and geomorphological characteristics

The study area was strategically selected based on the severity of pollution caused by chromium-asbestos mining activities. Located in Roro hills, Jharkhand, India, hosts one of the most environmentally degraded chromium-asbestos mining regions in the country. The area is situated approximately 22 km from Chaibasa town, falling under the Chaibasa Forest Division, and lies within the latitude N22◦29.30′ and longitude E85◦38.84′ (Banerjee et al., 2023). This region has experienced extensive environmental degradation due to long-term unregulated mining operations, making it an ideal site for assessing pollution levels and exploring remediation strategies.

The Roro chromium-asbestos mine, operated as an opencast mining site for many years before closing in 1983, leaving behind around 0.7 million tons of hazardous mine waste (CAMW) in this area. This waste is fine, loose, and homogeneous, lacking essential nutrients. The poor nutritional content and high levels of PTEs (Ni, Cd, Cr, Cu, and Pb) result in limited coverage of vegetation. Mostly tropical climatic condition with high temperature has been observed during the summer and cold in the winter. The yearly rainfall during the monsoon is roughly 1422 mm, and over 80% of it falls during this time throughout the area. Natural calamities, including wind, rainfall, and water erosion, have transported substantial quantities of hazardous mining waste into agricultural fields, resulting in a huge concentration of PTEs in these areas. These toxic wastes have a severe environmental impact, leading to soil and water contamination, biodiversity loss, and soil degradation. The local population comes into contact with this waste during daily activities, leading to skin rashes, lung cancer, and other major health complications (Banerjee et al., 2025). Mining activities were eventually abandoned without adequate post-closure remediation or containment of waste, resulting in heaps of overburden and tailings rich in PTEs, primarily Cr, and Ni. These tailings and waste dumps, spread over several hectares, are loosely consolidated and highly prone to wind and water erosion, posing serious health and environmental risks. The area’s dry deciduous forest ecosystem has been severely disrupted, and local communities face risks from airborne asbestos fibers, PTEs leaching into agricultural lands, and contaminated soil (Banerjee et al., 2025). Despite being a major environmental hotspot, the site has seen limited scientific interventions toward reclamation or sustainable reuse of the degraded land and waste

materials. Given these characteristics, Roro Hills (chromium-asbestos mine) serve as a critical model location for the study and application of innovative bioremediation, mycophytoremediation, and vermicomposting strategies for PTEs detoxification and ecological restoration.

3.2 Sampling points distribution, collection of samples, and preservation process

A simple random sampling method (W-pattern) was applied to obtain samples (0-15cm) from three separate locations [site 1: mine waste dumping area (6 samples), site 2: mine waste contaminated soil (15 samples), and zone 3: uncontaminated soil (15 samples)] in January 2020, as depicted in Fig. 7.

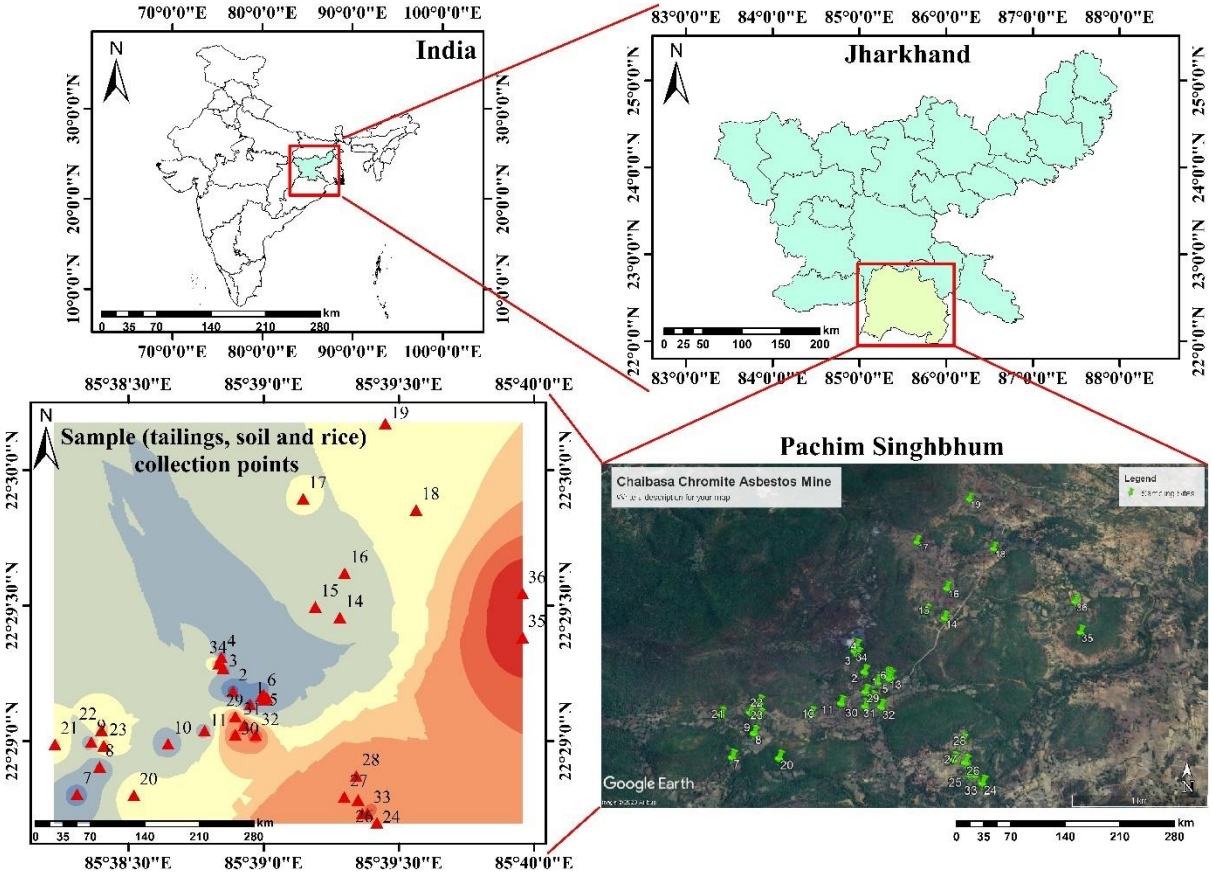

Fig. 7: The map illustrates the study region of chromium-asbestos mines

The samples were brought to the laboratory in sealed and properly labelled zip-lock bags. The soil samples were dried in the air, processed (with a mesh size of 2 mm and 0.2 mm), and

then stored in plastic containers within the laboratory. These plastic containers containing soil samples were stored at 4℃ for microbiological analysis. The microbiological studies were conducted using samples in their natural field moist state, whereas air-dried soil samples were used for physicochemical, and PTEs analysis. The total rice plant was uprooted from the agricultural soil. For the collection of rice samples, site 2 (15 samples) and 3 (15 samples) were considered, as site 1 was a mine tailings dumpsite where no agricultural activity occurs. The rice plant samples underwent an initial washing process using tap water, followed by a further washing using double distilled water. Then the Rice roots, shoots, and grains were carefully separated, appropriately labeled, and placed in a hot air oven at a temperature of 55°C for 24 hours prior to assessment. The soil sampling procedure was followed using a standardized method derived from Page et al. (1982).

3.3 Quality control, quality assurance, and calibration procedure

Analytical graded reagents were used for experimental purposes. Glassware was properly washed with a 10% HNO_3 solution initially for 24hrs, then rinsed with double distilled water (three times) before use in the experiment. This study follows a regressive quality control model, which is explained by the fact that all instruments used in the study were calibrated regularly. A blank was run after every ten samples analyzed to ensure that the instruments were accurate. All the analyses for samples were conducted in triplicate with blank samples simultaneously for quality control. We analyzed the mean values of each PTEs (Cr, Ni, Cd, Cu, and Pb) in triplicate, with a relative standard deviation (RSD) of <10%. Each PTEs concentration were assessed using an atomic absorption spectrophotometer (AAS-816, Systronics, India). Standard stock solutions of respective metal ions (1000 mg/L, Sigma-Aldrich grade) in 1% (v/v) HNO_3 were used for calibration standards ranging from 0.1 to 10 mg/L except for Cd (range 0.1 to 1 mg/L). The standard curve was developed based on the range of each PTEs and then analysis was carried out. To enhance clarity, the standard curves of each PTEs have been included (Fig. 8) for reference.

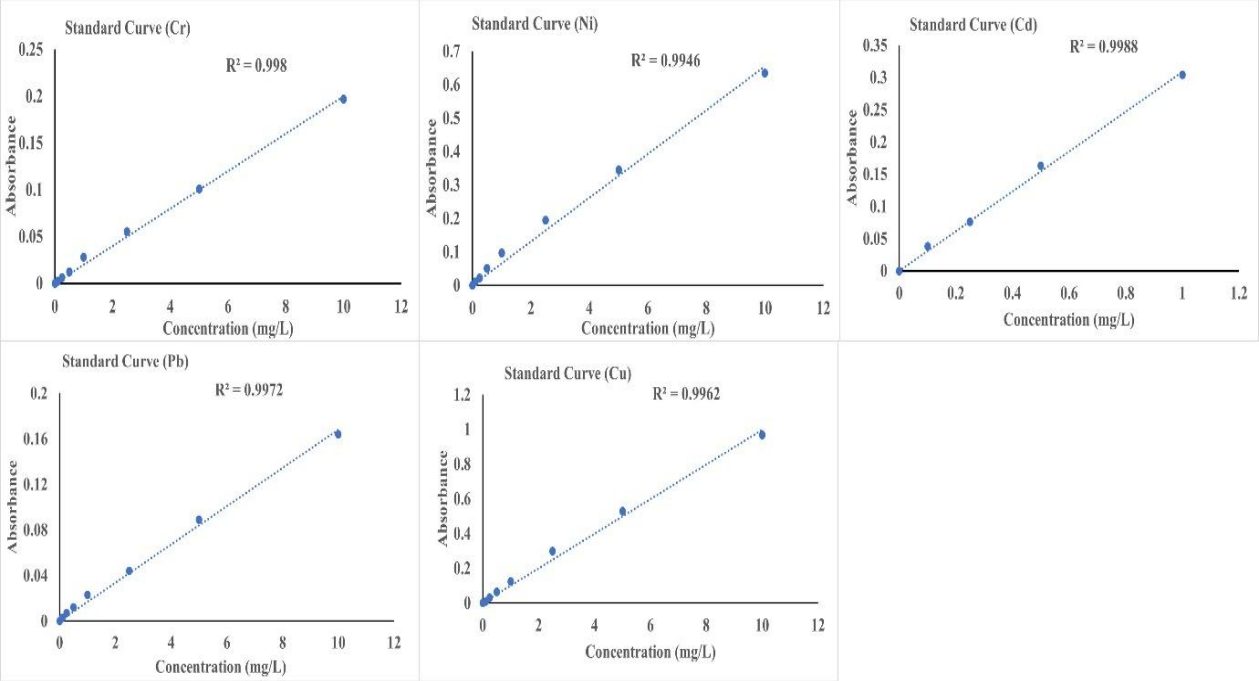

Fig. 8: Standard curve preparation of each PTEs (Cr, Ni, Cd, Pb, and Cu)

The PTEs analysis consisted of three procedures: an initial calibration verification (ICV) using a 1 mg/L standard (tested for > 95% recovery), a continuous calibration verification (CCV) after every 10 samples, and the addition of reagent blanks after the ICV and every CCV. Certified reference material SRM 2710 in 1% (v/v) HNO_3 was used to determine the accuracy and reproducibility of the tested samples. Reliable data accuracy was obtained from the recovery percentage of PTEs in the tested samples. Eventually, the certified material was digested in an ultrapure mixture of acids, and the acquired results were differentiated with SRM2710 values to establish the precision of the procedure for PTEs (Table 5).

Table 5: Recovery percentage of certified material (SRM2710)

PTEs	SRM 2710 (mg kg^{-1})	AAS measured (mg kg^{-1})	Recovery (%)
Pb	5104	5072	99.37
Ni	10	9.89	98.90
Cd	19	18.79	98.89
Cr	17	16.85	99.12
Cu	2700	2712	99.56

As it is a standard reference solution with a certified PTEs content that was diluted three times and compared with the concentration measured. Findings indicate a <10% deviation from the standard solution. Regarding detection limits, the AAS method employed in this study had sufficiently low limits of detection (LOD) and limits of quantification (LOQ) to accurately measure even trace levels of TEs. The LOD and LOQ values have been included (Table 6). Therefore, the method used was highly sensitive and precise, enabling reliable detection of TEs at low concentrations, which is crucial for assessing their environmental significance in this study.

Table 6: The detection limit of an atomic absorption spectrophotometer (AAS-816)

Potentially Toxic Elements (PTEs)	LoD (mg/kg)	LoQ (mg/kg)
Cr	0.015	0.65
Cd	0.05	0.25
Cu	0.08	0.2
Ni	0.07	0.25
Pb	0.02	0.03

3.4 General soil properties

3.4.1 Physico-chemical parameters

Agricultural soil parameters such as pH, EC, total organic carbon (TOC) available nitrogen (N), and phosphorous (P), exchangeable potassium (K), sodium (Na), calcium (Ca), magnesium (Mg), and cation exchange capacity (CEC) were examined (Page et al., 1982). The pH (soil: water ratio 1:2.5) was determined using a digital pH meter. The EC was measured using a digital conductivity meter, with a soil-to-water ratio of 1:5. The organic carbon content was quantified using (1N) potassium dichromate and concentrated sulphuric acid. Subsequently, excess dichromate was titrated utilizing (0.5N) ferrous ammonium sulphate. The available N in the soil was determined using an alkaline potassium permanganate (0.32%) solution followed by steam distillation using a Kjeldahl apparatus. The soil P availability was determined by employing Olsen's reagent (0.5M $NaHCO_3$), ammonium molybdate, and stannous chloride. The resulting molybdophosphoric blue complex was then analyzed employing a spectrophotometer. The K, Na, Ca, and Mg content in the soils was extracted utilizing a (1M) ammonium acetate solution (pH:7) and then measured using a flame photometer (Na and K) and atomic absorption spectrophotometer (Ca

and Mg). The CEC in the soil samples was measured using an (1N) ammonium acetate solution followed by steam distillation employing a Kjeldahl instrument (Page et al., 1982). The particle size analyser was used to estimate the soil's particle-size distribution, and Brady (1990) used the triangular textural diagram to identify the soil's textural class based on the % concentrations of sand, silt, and clay.

3.4.2 Alkalinity indices evaluation

Various soil alkalinity predicted indices including sodium adsorption ratio (SAR), exchangeable sodium percentage (ESP), exchangeable cation ratio (ECR), cation ratio of soil structural stability (CROSS), and monovalent cation ratio (MCAR), and magnesium hazard (MH) were calculated based on Na, K, Ca, Mg cations to assess soil structural stability, clay dispersion, and their impact on both soil structure and microbial community (Rengasamy and Marchuk, 2011).

3.4.3 Insight into different forms of potentially toxic elements (PTEs)

3.4.3.1 PTEs in soil samples

The samples were digested with mixture of acids including hydrofluoric acid (HF)- perchloric acid ($HClO^{4-}$)- sulfuric acid (H_2SO_4)- nitric acid (HNO_3) in a platinum crucible until the solution turns colorless. After that digested solution was filtered and measured the total PTEs in the solution using atomic absorption spectroscopy (AAS 816, Systronics, India) (Page et al., 1982).

The DTPA extractable bioavailable forms of PTEs in samples were used as an extractant using 0.005(M) DTPA (diethylene triamine penta acetic acid), and after filtration, the concentration was determined through AAS (Lindsey and Norvel, 1978).

The toxicity characterized leaching procedure (TCLP) method by USEPA is regarded as a worldwide benchmark test for PTEs leachability as well as determining the movement of contaminants in liquid, solid, and multiphase wastes (Yu et al., 2014). The probable toxicity of PTEs (Cr, Ni, Cd, Pb, and Cu) from the chromium-asbestos mine area was evaluated using the USEPA-TCLP test. Samples (pH > 5) were gently mixed with extraction fluid 2 (solution containing glacial acetic acid with pH 2.88) (Sun et al., 2006). The leachable form of PTEs was collected by the filtration method using Whatman No. 42 filter paper, and the concentration of PTEs in filtrate solution was measured employing AAS.

The bio-accessible forms of PTEs in samples were estimated according to a modified approach by Sarkar and Dutta (2003). The stomach phase (S-phase) and intestinal phase (I-phase) were the two stages of the bio-accessible form of PTEs. The gastric phase solution (0.15 M NaCl mixed with 1% porcine pepsin and pH adjusted at 1.8± 0.05 using HCL) and intestinal phase solution (addition of 525 mg of bile salt extract and 52.5 mg of pancreatin and followed by adjusting the pH to 7.0± 0.05 using $NaHCO_3$ solution). The procedure mimics the human body system in vitro. After incubation at 37°C, filtrates were collected from both phases and measured the concentration of PTEs was measured through AAS.

Sequential extraction of different forms including water-soluble (Ws), exchangeable (Ex), carbonate-bound (Car), Fe-Mn oxide-bound (Ox), organic-bound (Or), and mineral-bound (Min) of PTEs (Cr, Ni, Cu, Cd, and Pb) in samples were chemically fractionated and progressively extracted using a standard process by Tessier et al., (1979). The bioavailable fraction (BA) is often represented by a combination of water-soluble and exchangeable fractions. The water-soluble fraction was extracted from the soil sample with distilled water, while the exchangeable phase was extracted using 0.5M Mg $(NO_3)_2$. After that, carbonate-bound (Car), Fe-Mn oxide-bound (Ox), organic-bound (Or), and mineral-bound (Min) was extracted using 1(M) sodium acetate, 0.08(M) hydroxyl-amine hydrochloride mix with acetic acid, 0.02(M) nitric acid mix with peroxide and ammonium acetate, and concentrated nitric acid.

3.4.3.2 PTEs in rice samples

The PTEs content in rice plant parts (dried roots, shoots and raw rice grain) were digested with a mixture of di-acid [4:1 HNO_3:$HClO_4$(v/v)] in a conical flask placed on an electric mantel at 190℃ until the color changed. The PTEs concentration in the digested solution was measured by AAS following the method as described (Li et al., 2018).

In most Asian countries, including India, cooking rice in extra water (1:10) was a traditional practice, and after cooking, excess water was drained out in the form of starch. Prior to cooking, the husk was removed from the rice grain samples and thoroughly cleaned with distilled water. For cooking, distilled water was added to a container containing rice (husk removed), which was then placed on a hot plate. Both the surplus water (starch) and the boiled rice were collected when the rice was fully cooked. To obtain the total PTEs concentration, rice grain sections husk (H), without husk rice (WH), boiled rice (BR), and

starch (ST) were digested with a di-acid mixture (HNO_3:$HClO_4$) (Chowdhury et al., 2020). The PTEs concentration was measured using AAS

A similar procedure was used for the bio-accessible forms (S and I) of PTEs in various rice sections (H, WH, BR, ST), as outlined by Sarkar and Dutta (2003). Porcine pepsin, bile salt extract and pancreatin were used in the respective phases and obtained the filtrate solution after completion of the procedure. The PTEs was determined using AAS.

3.4.3.3 Determination of plants' PTEs accumulation pattern and PTEs mobility indexes

To evaluate the mobility and accumulation patterns of PTEs in several sections of vetiver (shoot and root), two crucial indices, particularly the plant bioaccumulation factor (PBAF) and plant translocation factor (PTF), were adopted. The PBAF evaluates the capacity of a plant to uptake PTEs from the soil to the plant shoot, while the PBCF denotes the capability of plant to uptake PTEs from the soil to the root. Additionally, PTF indicates the plant's ability to translocate PTEs from the root to the shoot (Singh et al., 2019).

$$\text{Plant Bioaccumulation Factor (PBAF)} = \frac{Shoot\ _{PTEs}}{Soil\ p_{TEs}} \quad (1)$$

$$\text{Plant Bioconcentration Factor (PBCF)} = \frac{Root\ p_{TEs}}{Soil\ _{PTEs}} \quad (2)$$

$$\text{Plant Translocation Factor (PTF)} = \frac{Shoot\ p_{TEs}}{Root\ _{PTEs}} \quad (3)$$

3.4.4 Insight into microbial properties and community diversity

3.4.4.1 Microbial-enzymatic attributes

The microbial activity includes microbial biomass—carbon (MBC), nitrogen (MBN), phosphorus (MBP)—and respiration (substrate-induced respiration: SIR, and basal soil respiration: BSR) were analyzed based on respective protocols (Alef, 1995; Brookes et al., 1985; Joergensen et al., 2011). Additionally, enzyme activity for β-glucosidase (BG), urease (U), alkaline phosphatase (AP), and acid phosphatase (APP), dehydrogenase (DHG) following methods by Tabatabai, (1994), as well as fluorescein diacetate (FDA) hydrolysis (Schnrer and Rosswall, 1982) was evaluated using standard protocol.

3.4.4.2 Microbial nutrient limitation via vector analysis

The determination of the stoichiometry of enzyme activities in this study region was conducted using the vector analysis technique, as described by Moorhead et al., (2013). The

measurements of length and angle, referred to as "Vector L" and "Vector A" respectively, were approximated in order to assess the extent of microbial nutrition constraint using the provided equations.

$$\text{Vector L (unitless)} = \sqrt{X^2 + Y^2} \quad (4)$$

$$\text{Vector A (degree)} = \text{Degrees (Atan2 (X, Y))} \quad (5)$$

Here:

$$X = \frac{\text{Enzyme C (BG)}}{\text{Enzyme C (BG)} + \text{Enzyme P (AP)}}, Y = \frac{\text{Enzyme C (BG)}}{\text{Enzyme C (BG)} + \text{Enzyme N(U)}}$$

3.4.4.3 Soil total DNA and Illumina MiSeq 16S rDNA amplicon sequencing

The total soil DNA per site was extracted using the Xploregen soil kit, following a standardized technique. The V3-V4 region of the 16S rDNA was amplified by polymerase chain reaction (PCR) utilizing the primers V34F (5' AGAGTTTGATGMTGGCTCAG3') and V34R (5' TTACCGCGGCMGCSGGCAC3'). The amplicons generated through polymerase chain reaction (PCR) were subjected to purification using Ampure beads in order to eliminate any residual primers. Subsequently, an additional 8 cycles of PCR were conducted. The DNA extracted from the moist samples was evaluated for both its quality and quantity using NanoDrop. DNA samples with an absorbance ratio A260/A280 more than 1.9 were selected for further analysis. Following the purification of the libraries, a quantitative analysis was conducted with the Qubit dsDNA High Sensitivity test kit. Afterward, the sequencing process was conducted utilising an Illumina MiSeq 2x300PE V3-V4 sequencing kit. The raw sequencing reads produced by the Illumina Miseq platform underwent a series of quality control steps. These included filtering out high-quality reads based on their score value, removing reads that contained primer/adaptor sequences, and trimming the read length. Additionally, various aspects of the reads were assessed, such as base quality score distribution, sequence quality score distribution, PCR amplification issues, average base content per read, and overrepresented sequences. The goal of these steps was to retain only the reads of high quality. The National Centre for Biotechnology Information (NCBI) database was utilised for the analysis of the 16s V3-V4 region. Additional examination of the sequenced samples encompassed the identification of chimaera, the clustering of operational taxonomic units (OTUs), the selection of representative sequences, and the assignment of taxonomic classifications. The bacterial community analysis focused on assessing alpha diversity within each site and beta diversity between sites. Alpha diversity encompasses various aspects of community diversity, including the Shannon, Simpson and Fischer

diversity. It also takes into account evenness, as measured by the Shannon equitability index, and richness, as estimated by the abundance-based coverage estimator (Chao1). The Whittaker beta diversity index was a dissimilarity measure that was calculated using abundance or relative abundance data (Narendrula-kotha and Nkongolo 2017).

3.5 Insight into biochemical characteristics and antioxidant enzyme activity

The biochemical properties, including chlorophyll a, chlorophyll b, total chlorophyll, total carotenoid, total soluble sugar, proline, protein, were measured using a modified methodology by Singh et al. (2019). The antioxidant activity, which includes catalase, guaiacol peroxidase, and superoxide dismutase, was assessed using a standardized technique described by Banerjee et al., (2019). Lycopene, capsaicin, titratable acidity, ascorbic acid, and pungency were carried out using a modified standard protocol (Das et al., 2016; Tripodi et al., 2019). The protein and amylose content in rice (without husk) were estimated by the modified standard protocol of Lowry et al. (1951) and Liu et al. (2023), respectively.

3.6 Insight into growth properties of plants: an agronomic perspective

The plants were carefully uprooted, removing soil from the roots by gentle tapping, and properly washed under tap water. Excess water in the roots was eliminated by blotting papers followed by drying the samples in a hot air oven (55°C for 48 hours). The dry weight (g) of root and shoot was recorded subsequently. Similarly, the fresh weight (g) was estimated using an electronic balance prior to drying (Mayer et al., 2017). The height or length (cm) was estimated using a scale. The agronomic traits estimated for chilli plants were plant height, fresh weight of chilli, No of chilli/plant, length of chilli, and yield (g/plant). These measurements were recorded based on the standard protocol described by Wahocho et al., (2016). In case of sesame and tomato, shoot length, root length, and yield were considered for the evaluation, while in case of rice, plant height, 1000 grain weight (g), straw yield (t/ha), and grain yield (t/ha) were taken (Jha et al., 2024; Chakraborty et al., 2024)

3.7 Insight into arbuscular mycorrhizal fungi (AMF)

3.7.1 Evaluation of root colonization percentage

Following the procedure by Phillips and Hayman (1970), AMF root colonization rate was determined. In this process, roots from each treatment were thoroughly washed, sectioned into 1 cm root length, and placed in 10% KOH (water bath at 80ºC) for 1 hour. After rinsing with distilled water, the roots were immersed in 0.1N HCl for 30 minutes, washed again, and

stained with 0.05% Trypan blue to observe hyphae, arbuscules, and vesicles. De-stained root segments were analyzed for AMF colonization under a light microscope

3.7.2 Glomalin-related soil protein (GRSP) determination

The GRSP fractions (easily extractable: EE and difficultly extractable: DE) of each treatment were measured using the modified approach described by Anandakumar et al., (2024). Approximately, 1g of rhizosphere soil was processed for GRSP extraction. For EE-GRSP, the sample was mixed with 20 mM citrate solution (pH 7.0), autoclaved at 121ºC for 30 minutes, and centrifuged at 10,000 rpm for 10 minutes. This process was performed twice, and the supernatant was collected for EE-GRSP analysis. Then the remaining soil residue was used to extract DE-GRSP with 50 mM citrate solution (pH 8.0), autoclaved at 121ºC for 60 minutes, and centrifuged. EE-GRSP and DE-GRSP concentrations were measured using the Lowry assay (Lowry et al., 1951) with bovine serum albumin as the standard, and T-GRSP was calculated as their sum (EE and DE), expressed in mg g^{-1} of soil.

3.8 Vermi-remediation technology: an insight into earthworm dynamics, nutrient benefit ratio, and phospholipid fatty acid profiling (PLFA)

3.8.1 Earthworm population enumeration

Earthworm populations were systematically monitored during the vermicomposting process. To achieve this, feedstock materials were spread on trays (aluminum), and the finer feedstock particles were filtered through a iron mesh (3–4 mm). The vermibeds were divided into ten equal plots. Earthworms were then meticulously collected from the designated areas by hand for counting. The counts were noted and averages were computed for consistency. After recording the counts, the earthworms, along with the feedstocks, were returned to their designated containers. At the conclusion of the study period (90 days), earthworms were separated from the vermi units, and the vermi-processed materials were collected for analysis.

3.8.2 Analysis of PTEs content in earthworm gut

At the end of the 90-day incubation period, 5 adult earthworms from each replicate were selected for gut TEs accumulation analysis. The earthworms were rinsed with de-ionized water and then placed on moist filter paper at room temperature (27±2°C) overnight for gut clearance (removal of faecal matter). Afterward, the worms were euthanized by freezing, and the samples underwent di-acid digestion using an HNO_3–$HClO_4$ mixture (4:1 ratio) (Charan et al., 2024). The concentrations of PTEs accumulated in the gut were measured using AAS.

Subsequently, the effectiveness of earthworms in accumulating TEs from each feedstock was then assessed by calculating the earthworm bioaccumulation factor (BAF) (Mondal et al., 2020).

$$\text{Bioaccumulation factor (BAF)} = \frac{\text{PTEs in earthworm gut}}{\text{bioavailable PTEs in substrate}} \quad (6)$$

3.8.3 Assessment of stress enzymes in earthworms

The activities of specific enzymes including super oxide dismutase (SOD), catalase (CAT), and peroxidase (POX) in earthworms are considered rapid and predictive indicators of their response to environmental stress (PTEs stress). These enzymes play a crucial role in safeguarding organisms against PTEs stress (Chao et al., 2016). For this experiment, earthworms were randomly selected from each treatment at intervals (0, 30, 60, and 90 days). Before analysis, their guts were cleansed for 24 hours. A pre-cooled 0.1 mol/L PBS solution (pH 7.4) [1:9 ratio (m/v)] was added, and the earthworms were ground thoroughly. The mixture was centrifuged at 4°C and 3000 rpm for 15 minutes. The resulting supernatants were used immediately to measure SOD, CAT, and POX contents and then aliquoted and stored at −80°C for further analysis (Chao et al., 2016; Wang et al., 2020).

3.8.4 Nutrient benefit ratio and PTEs removal ratio of vermicomposted products

To evaluate the nutrient status of vermicomposted product and cow dung, a nutritional benefit ratio (NBR) was applied following a standardized formula (Sahariah et al., 2015). It was calculated based on different physicochemical properties, which are indicators of physico-chemical properties.

$$\text{Nutritional benefit ratio (NBR)} = \frac{\text{Mean 90 D concentration} - \text{Mean 0 D concentration}}{\text{Mean 0 D concentration}} \quad (7)$$

A modified formula was utilized to evaluate the removal efficiency ratio of bioavailable PTEs during vermicomposting.

$$\text{PTEs removal ratio} = \frac{\text{0 D mean PTEs concentration} - \text{90 D mean PTEs concentration}}{\text{0 D mean PTEs concentration}} \quad (8)$$

3.8.5 PLFA analysis: An aspect for identifying fatty acid diversity and microbial communities, and model-based estimation

The PLFA assay was conducted on vermicompost samples after 90 days of incubation according to the standard protocol to evaluate the microbial diversity (Hussain et al., 2018). In a nutshell, freshly collected samples (2g) were dried overnight in a centrifugal evaporator

(temperature 30°C) (Eppendorf-AG-5301) and then extracted using the Bligh–Dyer extractant [K_2HPO_4: methanol: chloroform (4:10:5)]. Lipids were isolated using solid phase extraction, and the resultant samples were combined with hexane for gas chromatographic and PLFA analysis. Microbial communities were identified using Sherlock software (Luo et al., 2016). The diversity of fatty acid profiles was subsequently calculated using various indices [Shannon diversity (SDI), Shannon evenness (SEI), and Evar (EVI)] as outlined in formulas (9), (10), and (11). to assess the impact of fatty acid richness on feedstock combinations (Chakraborty et al., 2022).

$$\text{Diversity index (Shannon): SDI} = \sum_{i=1}^{n}(\text{qi lnqi}) \quad (9)$$

Here, qi: Sum total of each fatty acids relative abundance

n: Fatty acids number

$$\text{Evenness index (Shannon): SEI} = \text{SDI}/\ln R \quad (10)$$

where R: Tested fatty acids number

If SEI is closer to 1, it denotes a more even distribution, while closer to 0 indicates a less even distribution.

$$\text{Evar index: EVI} = 1-2/\pi \arctan\{\sum \ln(yR) - \sum \ln(y1)/R)2/R\} \quad (11)$$

y: Sum total of fatty acids relative abundance

This research also employs the Sobol sensitivity model to identify the most influential parameters for evaluating PLFA-based microbial diversity under the stress of PTEs (Kumar et al., 2020). The model-based approach SOBOL sensitivity analysis was also employed to identify and validate the most relevant PLFA factors that govern soil microbial community structure under the stress conditions of PTEs. SSM was conducted using Python software(version 3.10).

3.9 Application of different indices and models for validation of the findings

3.9.1 Distribution pattern, and source allocation of different forms of PTEs at chromium-asbestos mine region

3.9.1.1 Spatial pattern of PTEs determination using ArcGIS

The distribution pattern of different forms of PTEs, including total, bioavailable, and leachable, was evaluated using geospatial analysis. Kriging interpolation was used for the spatial distribution of total PTEs and the factor score acquired from PMF analysis (ArcGIS version 10.4). The spatial dispersion of the soil PTE levels through leaching (TCLP) was carried out using the inverse distance weighted (IDW) interpolation approach. In the area of GIScience, the IDW interpolation method was frequently used to estimate the spatial data of unknown sites from nearby known sites (Ghosh et al., 2023b). Also, the geographical distribution of bioavailable PTEs, alkalinity indexes, and microbial community was plotted using IDW (ArcGIS version 10.4).

3.9.1.2 PTEs Pattern identification through Self-organizing map (SOM)

Artificial neural web (SOM) was developed to analyze the complex dataset and identify the pattern of PTEs and alkalinity indices in soil samples (Nakagawa et al., 2020). The similar color density denotes positive correlation whereas different color designates a negative correlation in the component plane. As part of the self-learning process, neurons are projected into two-dimensional units in order to improve the visualization. A heuristic equation was followed for choosing the number of neurons (Bhuiyan et al. 2021).

$$m = 5\ x\ \sqrt{n} \qquad (12)$$

Here, ‘m’ denotes SOM nodes quantity and ‘n’ represents the input data quantity. The dataset was trained applying R-programming language (V.4.2.2).

3.9.1.3 Source allocation of PTEs using Positive matrix factorization model (PMF)

PMF was comprehensive model and applied for source allotment (Yan et al. 2019). Concentration of evaluating parameters (different form of PTEs concentration and alkalinity constituents like Na, K, Ca, Mg) and uncertainty values derived from equations were the two important files used as input to the PMF model (Jiang et al., 2019). The analysis was carried

out using EPA-PMF version 5.0. by optimizing various factors, Q value denoting the best fit data by model (Huang et al., 2021)

$$X_{ij} = \sum_{k=1}^{P} g_{ik} f_{kj} + e_{ij} \quad (13)$$

$$Q = \sum_{i=1}^{n} \sum_{j=1}^{m} \left(\frac{x_{ij} - \sum_{k=1}^{p} g_{ik} f_{kj}}{u_{ij}} \right)^2 \quad (14)$$

$$\text{For } c \leq \text{MDL}, \; u_{ij} = \frac{5}{6} \text{ MDL} \quad (15)$$

$$\text{Else}, \; u_{ij} = \sqrt{(Error fraction \; x \; c)^2 + \left(\frac{MDL}{2}\right)^2} \quad (16)$$

Here, i, j, and k = Samples number, elements and different sources respectively; X_{ij} = The concentration of element j in sample i (mg kg^{-1}); g_{ik} = The contribution source k in sample i (mg kg^{-1}); f_{kj} = The amount of element j in source k; eij = The residual part; uij = The uncertainty of element j in sample i; MDL = The species-specific method detection limit; Error fraction = the percentage of measurement of uncertainty (Goswami and Kamadhad, 2023).

3.9.2 Different indices indicate soil PTEs contamination level

Roro and Tilasud villages are located at the foothill of the Roro mines. At that time, a considerable number of local villagers were involved in mining activity as mine workers. After the extraction of valuable minerals from the mines, toxic wastes were dumped abundantly on the top of Roro hills. Due to rainfall and wind blow, the toxic waste was spread over the adjacent agricultural field and contaminated the ecosystem. As a result, local villagers came into contact with harmful toxic mines waste. Due to this, the possible risk on ecosystem from mines waste was analysed.

3.9.2.1 Pollution index (PI)

Multi-element effects play a critical role in the study of PTEs contamination. The PI was evaluated to quantify the potential pollution of multi-PTEs of tailings and soils. The formula of PI was showed below (Equeenuddin et al., 2013).

$$Pollution \; Index \; (PI) = \frac{\frac{Cr}{100} + \frac{Ni}{100} + \frac{Pb}{100} + \frac{Cd}{100} + \frac{Cu}{100}}{5} \quad (17)$$

This PI formula depicts the ratio of PTEs concentration in samples to the assumed permissible levels. The permissible limits of individual metals were Cr = 100 mg kg^{-1}; Ni = 100 mg kg^{-1}; Pb = 100 mg kg^{-1}; Cd = 100 mg kg^{-1}; Cu = 100 mg kg^{-1}, according to Kabata-Pendias and Pendias (2001), Ferreira et al. (2022).

3.9.2.2 Contamination index (CI)

The contamination index was used to determine the total contamination level in a specific area. It was calculated against the background value of respective PTEs. The background values of individual PTEs were Cr = 36.7 mg kg^{-1}, Ni = 36.7 mg kg^{-1}, Pb = 48.78 mg kg^{-1}, Cd = 50.8 mg kg^{-1}, Cu = 116 mg kg^{-1} (Liao et al., 2022). The following equation was used to evaluate the contamination index (Rang et al. 1987; Weissmannová and Pavlovský, 2017).

$$Contamination\ index\ (CI) = \sum \frac{C_n}{B_n} \qquad (18)$$

Where, C_n is the concentration of each PTEs in the sample and B_n is the background value of each PTEs (Likuku et al., 2013).

3.9.2.3 Geo-accumulation index (I_{geo})

According to Mondal et al., (2017), the geo-accumulation index was applied to evaluate the probable accumulation pattern of various toxic elements (PTEs) in the environment. The formula was here below.

$$Geo - accumulation\ (Igeo) = \log_2 \frac{C_n}{1.5\ B_n} \qquad (19)$$

Here, the constant value of 1.5 is taken to evaluate the environmental variation of the toxic elements in the sample with anthropogenic activities. The reference value of B_n was collected from the annual report of Soil and Land Use Survey of India (SLUSI, 2013-2014).

3.9.2.4 Ecological risk index (ERI)

Yang et al., (2009) state that by aggregating the change in PTEs with respect to background reference values and toxicological factors, ERI was used to determine changes in toxic elements. The equation was shown below.

$$Ecological\ risk\ index\ (ERI) = \sum \frac{T_i\ x\ C_n}{B_n} \qquad (20)$$

In this equation, T_i was the toxic response factor for each given metal. The value of T_i for Cr, Ni, Cd, Pb, and Cu were 2, 2, 30, 5, and 5 respectively (Ferreira et al., 2022).

3.9.3 Health risk assessment using total PTEs concentration

The upper surface of the soil is more susceptible to metal pollution than underground soil. Various human activities like mining, overburden of materials, use of chemicals and fertilizers, dumping of toxic material, etc. mainly influence the contamination of the topsoil (wang et al., 2020). Therefore, PTEs on the upper surface of soil plays an important role in human health. Thus, human health risk (HHR) assessment is required.

3.9.3.1 Ingestion, inhalation, and dermal analysis pathways for non-carcinogenic risk assessment

Three important pathways through which the human body is exposed to upper surface of soil. Human body intake these polluted particulates from soil through nose, oral, mouth and skin. three pathways i.e ingestion, inhalation, and dermal were considered for non-carcinogenic risk assessment and the equation was derived from US Environment Protection Agency (USEPA., 1989; De Miguel et al., 2007; Huang et al., 2022). Non-carcinogenic risk of child and adult was determined following three formulas for each different exposure pathways.

$$ADD_{ingestion} = \frac{C \times IngR \times EF \times ED}{BW \times AT} \times 10^{-6} \quad (21)$$

$$ADD_{inhalation} = \frac{C \times InhR \times EF \times ED}{PEF \times BW \times AT} \quad (22)$$

$$ADD_{dermal} = \frac{C \times SA \times SAF \times ABS_{dermal} \times EF \times ED}{BW \times AT} \times 10^{-6} \quad (23)$$

Here, $ADD_{\text{ingestion or inhalation or dermal}}$ were the daily intake of PTEs from soil (mg kg $^{-1}$ day^{-1}). The exposure parameters for risk assessment were followed according to Chabukdhara and Nema, 2013).

3.9.3.2 Hazard quotient and hazard index

Hazard quotient (HQ) and hazard index (HI) were basically helps to determine the non-cancer risk. They were evaluated after the calculation ingestion, inhalation and dermal pathways following standard equation (US EPA, 1989 and Chabukdhara and Nema 2013).

$$HQ = \frac{Intake_{(ingestion\ or\ inhalation\ or\ dermal)}}{Reference\ dose\ (R_f\ D)} \quad (24)$$

$$HI = \sum HQ_{ex}P = HQ_{ingestion} + HQ_{inhalation} + HQ_{dermal} \quad (25)$$

The R_fD means the reference dose i.e., the harmless exposure limits for human in their lifespan. While, $_{ex}P_s$ denotes the three different pathways.

3.9.3.3 Cancer risk assessment via three pathways on human

The probability of growing cancer after an exposure to a carcinogen was assessment of cancer risk whereas total carcinogenic risk (TCR) was determined of an individual to develop cancer over a life span. TCR basically the summation of potential cancer risk of all PTEs. For estimation $ADD_{\text{ingestion or inhalation or dermal}}$ was multiplied by the CPFs factor (cancer potency factors) and it was different for each PTEs (Weissmannová and Pavlovský.,2017). Carcinogenic risk (CR) and total carcinogenic risk (TCR) were estimated following equations.

$$Carcinogenic\ risk\ (CR) = ADD \times SF \times ADAF \qquad (26)$$

$$TCR = \sum CR \qquad (27)$$

3.9.3.4 Probabilistic models for risk assessment using Monte Carlo simulation model

The sensitivity and uncertainty analysis were accomplished by MCS method using Crystal Ball software (version11.1.1, Oracle, Inc., USA).

3.9.4 Health risk prediction through different indices and models using leachable and bio-accessible PTEs

The human health risk was evaluated through three probable body exposure pathways (noses, mouths, and skin). For leachable PTEs, the health risk indices were determined via TCLP-$ADIL_{ingestion}$, TCLP-$ADIL_{inhalation}$, and TCLP-$ADIL_{dermal}$ routes. After calculating these three routes using basic formulas, the hazard quotient (TCLP-HQ) and hazard index (TCLP-HI) were used to determine non-cancer risk. The cancer risk from PTEs was calculated by estimating carcinogenic risk (TCLP-CR) and total carcinogenic risk (TCLP-TCR). For bioaccessible PTEs, the health risk indexes ($ADI_{ingestion}$), hazard quotient (bio-accessible-HQ), carcinogenic risk (bio-accessible-CR), total carcinogenic risk (bio-accessible-TCR) were estimated (USEPA 1989; Huang et al., 2022). The input parameters and equations are depicted in Table 7 for health risk assessment according to the reports [USEPA (1989); Chabukdhara and Nema (2013); mospi.gov.in (NSSO 2010); Jharkhand CSO forum 2020-2021 (Jo and Biswakarma 2021) and Ghosh et al., (2023a)]. In order to forecast the variability associated with health risk in the population (child and adult), a mathematical tool

"MCS" was employed in this study using Crystal Ball software (version 11.1.1.1, Oracle, Inc., USA) (Ghosh et al., 2023a).

Table 7: The input values and equation of health risk assessment [mospi.gov.in (NSSO 2010); Jharkhand CSO forum 2020-2021 (Jo and Biswakarma 2021); Ghosh et al., (2023a) and USEPA (1989)]

Input Parameters	Unit	Value		Equations of health risk assessment
		Adult	Child	
Average daily intake (*ADI*-Soil)	mg/day	100	200	$ADI_{ingestion} = \frac{C \times IngR \times EF \times ED}{BW \times AT} \times 10^{-6}$
Average daily intake (*ADI*-Rice)	gm/day	278		$ADI_{inhalation} = \frac{C \times InhR \times EF \times ED}{PEF \times BW \times AT}$
Inhalation	m^3/day	20	7.6	$ADI_{dermal} = \frac{C \times SA \times SAF \times ABS_{dermal} \times EF \times ED}{BW \times AT} \times 10^{-6}$
Dermal (Skin surface area: *SA*)	m^2	0.57	0.28	
Dermal (Skin adherence factor: *SAF*)	mg/cm^2	0.07	0.2	$HQ = \frac{Intake_{(ingestion\ or\ inhalation\ or\ dermal)}}{Reference\ dose}$
Dermal absorption fraction (*ABS*)	Unitless	0.001		$HI = \sum HQ_{ex}P = HQ_{ingestion} + HQ_{inhalation} + HQ_{dermal}$
Exposure duration (*ED*)	Years	24	6	$CR = ADI_{(ingestion\ or\ inhalation\ or\ dermal)} \times SF \times ADAF$
Exposure frequency (*EF*)	days/year	365	365	$TCR = \sum CR$
Average body weight (*BW*)	Kg	60	15	
Average exposure time (*AT*)	Days	ED * 365		
Partial emission fraction (*PEF*)	m^3/kg	$1.36 * 10^9$		
Unit conversion factor (*CF*)	Dimensionless	$1 * 10^{-6}$		

3.9.5 Prediction models of PTEs uptake in rice grain and its impact assessment

3.9.5.1 Free ion activity model (FIAM)

An integrated solubility model FIAM (free ion activity model) was implemented for the prediction of PTEs uptake in rice grains grown on chromium-asbestos mine tailings contaminated agricultural soil. A basic Freundlich equation (pH-dependent was used to predict the free ion activity of PTEs in the soil pore water (Golui et al. 2014; Golui et al., 2021). Transfer factor (TF) was evaluated as the quotient of PTEs content in the plant to metal(loid) activity in the soil. The following equation was used to calculate TF.

$$TF = \log \frac{[M_{plant}]}{(M^{n+})} \quad (28)$$

Where, $[M_{plant}]$ is PTEs content in plant and (M^{n+}) is the free metal ion activity in soil solution.

The equation of Freundlich was applied to predict the free ion of activity of PTEs in as follows (Mandal et al., 2019):

$$p\,(M^{n+}) = \{\, p\,[M_c] + k_1 + k_2\,[pH]\,\}/n_F \quad (29)$$

Here, (M^{n+}) is the free ion activity of PTEs in mine tailings contaminated soil; M_c is the labile pool of PTEs in soil presumed to be exclusively adsorbed on the humas (mol kg^{-1} carbon); k_1 and k_2 are empirical, PTEs-specific constants; and n_F is the power term from the Freundlich equation (Golui et al. 2020). In this context, 0.005(M) DTPA extractable-PTEs were used as estimates of the labile pool. For the prediction of PTEs uptake by plants, the equation (iii) was derived by combining the equation (i) and (ii) as follows:

$$p[M_{plant}] = C + \beta_1 p\,[M_c] + \beta_2 [pH] \quad (30)$$

Where, $C = k_1/n_F$ - log TF, $\beta_1 = 1/n_F$, $\beta_2 = k_2/n_F$ and C, β_1, and β_2 are empirical metal(loid) and plant-specific coefficients. By non-linear error minimization, equation (iii) was parameterized using "SOLVER" facilities in Microsoft Excel 2019.

3.9.5.2 Risk assessment

Human health risk for PTEs intake through the consumption of rice grains grown on mine tailing's contaminated soil was calculated based on FIAM-HQ using the United States Environmental Protection Agency (USEPA) protocol (IRIS, 2020).

$$FIAM - HQ = \frac{ADD}{R_fD} \quad (31)$$

Here, *ADD* is the average daily dose (mg kg body $weight^{-1}$ day^{-1}) and R_fD is the reference dose of different PTEs (Cr: 0.3, Ni: 0.02, Cd: 0.001, Pb: 0.0035, and Cu: 0.5) (IRIS, 2020; WHO, 1996). If HQ > 1, the *ADD* of each PTEs exceeds the R_fD values, suggesting that there is a potential risk associated with PTEs intake through rice grain consumption. The recommended daily consumption of rice grain was considered to be 0.2 kg/day and for an adult, the average body weight was assumed to be 68 kg for the calculation of FIAM-HQ (Kumar et al., 2021). Thus, the FIAM-HQ of an adult was estimated as follows:

$$FIAM - HQ = \frac{M_{plant} \times W}{R_f D \times 68} \quad (32)$$

Here, M_{plant} is PTEs content (mg kg^{-1}) in rice grain grown on tailings contaminated soil; W is the daily intake of rice grain. This toxic limit value of extractable PTEs in soil was taken based on a particular pH and organic carbon content under the FIAM model framework.

3.9.5.3 Risk thermometer prediction and Severity adjustment margin of exposure (SAMOE) of PTEs: Assessment of risks associated with dietary exposure to PTEs

According to the Swedish National Food Agency, the risk thermometer is an effective method for risk characterization (Sengupta et al., 2021). Based on health based tolerable daily intake (TDI), risk thermometers assess the estimated exposure to a PTEs in food. The equation is used to calculate the human dietary to PTEs through rice intake as follow (Chowdhury et al., 2020):

$$SAMOE = \frac{TDI}{(AF_{BMR} \times AF \times SF \times E)} \quad (33)$$

Where, TDI value for each PTEs is different i.e TDI for Cr: 1.0 mg/kg, Ni: 1.63 mg/kg, Cd: 0.3 mg/kg, Pb: 5.0 mg/kg and Cu: 30 mg/kg (Kohzadi et al., 2019); AF_{BMR} : non-linear relation in dose range (1/10); BMR- Benchmark response; AF (Assessment factors) = a factor of 10 (conservative assessment); SF (Severity factor) = 100 (For cancer, the most severe category); E = Different exposure factor (here, the concentration of PTEs.

3.9.5.4 Estimation of target cancer risk through SAMOE approach (SAMOE-TCR)

Among the factors that contribute to dietary risk assessment, TCR is of particular importance since it categorizes a human's lifetime exposure to carcinogens. The calculation of SAMOE-TCR is based on following formula (Bhattacharyya et al., 2021).

$$SAMOE - TCR = \frac{E_{fr} \times Ed \times F_{ir} \times C \times CPS_o}{BW_a \times AT_c} * 10^{-3} \quad (34)$$

Here, E_{fr} : exposure frequency to PTEs (365 days); Ed: exposure duration (70yeras); F_{ir}: food ingestion rate in grams per day; C = PTEs concentration; CPS_o : oral cancer slope for Cr: 0.5 (mg kg^{-1} day^{-1}), Ni: 1.7 (mg kg^{-1} day^{-1}), Cd: 0.38 (mg kg^{-1} day^{-1}), Pb: 0.0085(mg kg^{-1} day^{-1}), and Cu: 0 (mg kg^{-1} day^{-1}) respectively (Onuoha et al., 2016); BW_a : Body weight (68 kg); AT_c: averaged carcinogenic exposure time (365days x 70 years), 10^{-3} : unit conversion factor.

3.9.5.5 Risk assessment of rice sample: An insight through Fuzzy-TOPSIS, Health-dietary indices

Rice is the major staple grain in the vicinity of the research. The health indices, including $ADIR_{ingestion}$, hazard quotient (HQR), and carcinogenic risk (CRR) were calculated based on rice parts (WH, BR) (Shao et al., 2023; and Neisi et al., 2024). The dietary health risk assessment was evaluated via ranking approaches. The SAMOE-risk thermometer was a risk characterization method that estimates the risk level of PTEs content in the husk, without husk rice, boiled rice, and starch. Each of the PTEs and their SAMOE (SAMOE-PTEs) values has been used to assess dietary consumption exposure class following standard equations (Joardar et al., 2023). Also, SAMOE-TCR was crucial to dietary risk assessment since it categorizes a human being's lifetime carcinogen exposure.

Another approach, the Fuzzy-TOPSIS technique, was employed to determine the actual risk in rice sections based on synergetic performance score rank. Information entropy determines which alternative was closest to the Si+ and farthest from the Si- in the TOPSIS approach (Saif-Ud-Din et al., 2022).

3.9.6 PTEs contribution assessment on rice components using machine-learning approaches

In order to identify the most appropriate model to forecast the contribution of the different leachable PTEs from the chromium-asbestos mine tailings waste to rice parts (H, WH, BR, and ST), seven ML approaches have been implemented, including linear regression (LR), multivariate adaptive regression spline (MARS), support vector machine regression (SVM), random forest (RF), K nearest neighbour (KNN), extreme gradient boosting (XGB), and regression tree (RTtree). In this investigation, the correlation coefficient (r) value and root mean square error (RMSE) were used to assess model accuracy and the best-fit model based on actual and predicted values using R-software (4.3) (Taylor 1990, Mahammad et al., 2023).

An artificial neural network (ANN), was an effective technique for identifying pattern classifications of datasets and predicting health risk by PTEs (Cho et al., 2011; Ostad-Ali-Askari et al., 2017). In this research, ANN was applied to predict the risk-related effects on soil bio-accessible phases (S or I) of particular PTEs and which parts of rice (husk, without husk rice, boiled rice, and starch) were most affected by these PTEs.

A survey questionnaire was designed to gather the necessary information from the residents of Roro village in the chromium mine area. The survey results were then taken into account for health risk assessment using one structural modelling tool, the "decision-making trial and

evaluation laboratory (Fuzzy-DEMATEL)" method. It also used causal diagrams (digraphs) to show systems interconnectedness. The matrix and equations were followed by Shieh et al. (2010).

3.9.7 Evaluating the mycophytoremedial potency utilizing novel machine learning approaches

3.9.7.1 Partial least squares structural equation modeling (PLS-SEM)

PLS-SEM regarded as an appropriate statistical tool for examining causal relationships between various components in ecological studies (Pandey et al., 2021). It is crucial to identify the way through which different AMF amendments can affect the mycophytoremediation efficacy (MPRE) of vetiver grass. In this model, soil health quality (MBC, BSR, SIR), soil bioavailable PTEs (Cr, Cd, Ni, Cu and Pb), AMF attributes (colonization percentage, EEG, DEG), stress enzymes (PRO, SOD, CAT, GPOD), and plant growth (root length, plant biomass) were treated as exogenous latent variables, while mycophytoremediation efficiency was denoted as the endogenous latent variable. The validity of the PLS-SEM model has been evaluated based on R^2 values. The PLS-SEM model was analyzed using SmartPLS software (version 4.1.0.9).

3.9.7.2 Sobol sensitivity assay

Sobol's sensitivity analysis conducted in Python software (version 3.10), is a variance-based model designed to quantify the impact of different parameters on the total variance of the model's output, irrespective of specific conditions, as elucidated by Nossent et al., (2011). This work utilized innovative Sobol analysis to evaluate the absorption patterns of TEs in the presence of potent AMF cultures, highlighting their direct impact on the mycophytoremedial potential of the vetiver plant.

3.10 Statistical analysis

Statistical analysis was applied to assess the data variations across different parameters. Data normality and homogeneity of variances were evaluated using the Shapiro-Wilk test, and Bartlett’s test, respectively. After confirming the data followed a normal distribution and variance homogeneity, a parametric test (one-way, two-way ANOVA) and t-test were conducted to compare the means across treatments. Mean separation was then carried out using the least significant difference (LSD) test at a 5% significance level ($p < 0.05$). All

statistical analyses were conducted using R software (version 4.3.0) and SPSS (version 25). The bar plots, violine plots, box-and-whisker plots, line plots, dot plots, were generated in Origin software (version 2024b) and Sigma Plot (14.5). The Pearson correlation and Principal components analysis (PCA) to explore the relationship between microbial diversity and PTEs dynamics were conducted using R-Studio (version 4.3.1).

Results and Discussions

Chapter 4: Results and Discussions

Objective: 1

4.1 Assessing the physico-chemical characteristics, microbial dynamics, and levels of PTEs in soil and crops cultivated on fields contaminated with CAMW

As outlined in Section 3.2, three sites were selected for evaluating PTE contamination. Although Site 1 is a waste dumpsite with no ongoing agricultural activity, it was included for assessing general soil properties and conducting preliminary risk assessments. However, since the core focus of this study is on agricultural land, particularly crop systems that serve as a direct route for PTEs to enter the food chain, sites 2 and 3 were chosen for detailed investigation. These two sites were also utilized to assess the impact of toxic PTEs on soil microbial activity.

4.1.1 Characterization of soil physico-chemical properties

Physico-chemical properties of PTEs contaminated agricultural soil, and tailings from Roro mines in Jharkhand are described in Table 8. Most sampling sites had pH values that ranged from slightly acidic (6.04 ± 0.22) to slightly alkaline (7.65 ± 0.28), leading to carbonic acid formation. These carbonic acids and toxic mine waste deposition play a significant role in regulating soil reactions. As acidic soil increases the mobility of PTEs and alkaline soil forms a complex to decrease the mobility (Acosta et al., 2011).

Table 8: Physicochemical parameters, PTEs level and alkalinity indices of chromium-asbestos mine soil (Mean ± Standard deviation)

Properties	Site 1 (mean ± SD)	Site 2 (mean ± SD)	Site 3 (mean ± SD)
pH	6.04 ± 0.22	6.81 ± 0.34	7.65 ± 0.28
EC (ds m^{-1})	0.28 ± 0.1	0.52 ± 0.19	1.10 ± 0.27
TOC (%)	0.19 ± 0.04	0.72 ± 0.17	1.09 ± 0.18
CO_3 (%)	-	1.88 ± 0.11	2.33 ± 0.19
HCO_3 (%)	-	0.31 ± 0.024	0.40 ± 0.031
Avl. N (mg/kg)	4.19 ± 0.16	30.26 ± 2.70	58.11 ± 3.27
Avl. P (mg/kg)	6.32 ± 0.31	22.46 ± 3.18	27.95 ± 3.58

Avl. K (mg/kg)	7.27 ± 0.51	50.84 ± 6.17	40.31 ± 5.27
Avl. Na (mg/kg)	13.48 ± 0.63	31.32 ± 4.29	22.95 ± 1.97
Avl. Ca (mg/kg)	90.46 ± 7.09	395.13 ± 37.56	716.32 ± 86.74
Avl. Mg (mg/kg)	106.73 ± 6.82	684.29 ± 57.46	939.17 ± 95.68
CEC (meq/100gm)	4.02 ± 0.21	13.33 ± 1.39	23.4 ± 1.83
Sand (%)	-	91.6 ± 7.47	83.1 ± 9.13
Slit (%)	-	7.2 ± 0.59	14.3 ± 0.97
Clay (%)	-	1.2 ± 0.03	2.6 ± 0.04
Textural class	-	Sandy	Loamy Sand
Total_Cr (mg/kg)	2018.24 ± 88.35	1350.60 ± 76.90	96.22 ± 4.5
Total_Ni (mg/kg)	1484.88 ± 47.67	1059.95 ± 33.8	263.45 ± 10.7
Total_Cd (mg/kg)	8.08 ± 0.43	5.51 ± 0.25	2.00 ± 0.07
Total_Pb (mg/kg)	159.58 ± 7.84	107.92 ± 4.85	63.91 ± 2.09
Total_Cu (mg/kg)	162 ± 8.52	88.22 ± 3.42	47.82 ± 1.01
DTPA_Cr (mg/kg)	10.05 ± 0.42	7.41 ± 0.87	3.36 ± 0.89
DTPA_Ni (mg/kg)	7.82 ± 0.61	5.91 ± 0.36	3.91 ± 0.75
DTPA_Cd (mg/kg)	0.08 ± 0.005	0.06 ± 0.004	0.04 ± 0.002
DTPA_Pb (mg/kg)	3.92 ± 0.23	1.61 ± 0.12	0.86 ± 0.06
DTPA_Cu (mg/kg)	12.96 ± 1.02	7.35 ± 1.75	4.32 ± 0.79
SAR	-	0.069 ± 0.0004	0.042 ± 0.0003
ECR (%)	-	2.641 ± 0.31	1.364 ± 0.16
ESP	-	1.721 ± 0.19	0.863 ± 0.07
MCAR	-	0.135 ± 0.01	0.085 ± 0.009
CROSS	-	0.127 ± 0.02	0.078 ± 0.003
MH	-	74.095 ± 6.59	68.601 ± 5.97

EC and OC varied statistically (p<0.05) among the 3 sites. EC is a key factor for crop production in agricultural soil. The results indicate that the uncontaminated site (site 3) has relatively better electrical conductivity for crop production as compared with site 2 and site 1. Organic carbon mainly improves soil structure, water retention, water drainage capacity, soil aeration, nutrients leaching, etc (Zeng et al., 2011). Generally, PTEs became less accessible to plants when they were bound to organic carbon (Dey et al., 2021). In this present scenario, OC content is less in the tailings site and contaminated site than uncontaminated site. The reason behind this is that toxic mine wastes may have lowered the organic carbon content of mine-tailings site samples, and contaminated site samples compared to uncontaminated site samples.

Since toxic mine wastes in the chromium-asbestos mining area are not nutrient-rich but contain various PTEs. The available nitrogen, and phosphorus (P) content was significantly (p_avl.N = 0.0002; p_avl.P = 0.0001) lower in in site 1 and site 2 as compared with site 2. The decreased levels of nitrogen and organic carbon in site 1 and site 2 due to presence of toxic waste, can be attributed to nitrogen volatilization and reduced organic matter content, leading to strain on the microbial community and subsequently affecting nitrogen mineralization (Kizildag et al., 2013). The mean value of exchangeable K, Na, Ca, Mg were in site 1 (7.27 mg/kg, 13.48 mg/kg, 90.46 mg/kg, and 106.73 mg/kg); site 2 (50.84 mg/kg, 31.32 mg/kg, 395.13 mg/kg, and 684.29 mg/kg) and site 3 (40.31 mg/kg, 22.95 mg/kg, 716.32 mg/kg and 939.17 mg/kg) respectively. Cation exchange capacity (CEC) was in between 4.06 cmol/kg and 23.40 cmol/kg among the 3 sites. The elevated pH, and EC observed in site 3, in contrast to site 2 and site 1, can be attributed to the greater presence of Ca, and Mg ions in these areas. Compared to site 3, site 2 had lower average carbonate and water-soluble bicarbonate contents, whereas site 1 has a negligeable content as site 1 is tailings dumping site (Table 8). The agricultural fields within the vicinity of chromium-asbestos mine area experience a scarcity of rainfall, resulting in the evaporation of water and the emergence of drought-like conditions (Banerjee et al., 2023). In this scenario, the combination of carbonate and bicarbonate ions with Ca or Mg ions may result in the precipitation of calcium carbonate or magnesium carbonate under conditions of drying. This precipitation process subsequently leads to an elevation in pH inside site 3. The agricultural fields in site 2, which were contaminated by waste from a chromium-asbestos mine, were primarily constituted of sand with an average value of 91.6%. In contrast, the uncontaminated field in site 3 had a maximum silt and clay percentage of 16.9%. The particle size distribution exhibited significant variations across different sites, indicating that mining operations had resulted in disturbances within the region.

4.1.2 Evaluation of Total and Bioavailable (DTPA-extractable) PTEs

The mean total and DTPA extractable PTEs concentration among the three sites are depicted in Table 8. Results showed that all the PTEs concentration mainly Cr followed by Ni, Cd, Pb, and Cu in site 1, site 2 sample was significantly higher as compared to site 3[{Cr_{Total} (LSD: 133.76; $p = 0.004$), Ni_{Total} (LSD: 88.83; $p = 0.006$), Cd_{Total} (LSD: 0.57; $p = 0.007$), Pb_{Total} (LSD: 6.77; $p = 0.009$), Cu_{Total} (LSD: 7.90; $p = 0.005$)} and { Cr_{DTPA} (LSD: 0.46; $p = 0.001$), Ni_{DTPA} (LSD: 0.39; $p = 0.003$), Cd_{DTPA} (LSD: 0.004; $p = 0.001$), Pb_{DTPA} (LSD: 0.14; $p = 0.002$), Cu_{DTPA} (LSD: 0.71; $p = 0.002$)}]. As a result of toxic chromium-asbestos mine wastes deposition in the agricultural field, and the low pH and low OC content of the soil, there is a risk of

chromium, and nickel poisoning in the Roro mining area. The current situation has created a concern for animal, plant, and human health.

4.1.3 Leachable PTEs concentration around the chromium-asbestos mines area

A TCLP was a crucial tool for investigating the bio-accessibility of PTEs at the chromium mine site. In our study, Fig. 9 illustrates the results of the bio-accessible form of each PTE via TCLP. The observation revealed that the leachable-Cu concentration (LSD-Cu_{TCLP}: 0.30, *p:* 0.0008) was significantly below the permissible limit of USEPA in three sites of this mine region (USEPA 1990). Cr, Ni, and Cd concentrations were significantly higher in site 1 and site 2 (LSD-Cr_{TCLP}: 2.34, *p:* 0.0007; LSD-Ni_{TCLP}: 1.22, *p:* 0.0009; LSD-Cd_{TCLP}: 0.23, *p*: 0.0002) than in site 3, due to the deposition of mine tailings waste in the tailings site and contaminated site. But Pb-leachable element concentration was higher in site 1 (LSD-Pb_{TCLP}: 0.42, *p:* 0.0001). As a result of long-term mining and the abandonment of chromium-asbestos mine tailings without any treatment, PTEs have been leached out of the tailings and accumulated over time into the nearby agricultural soil. TCLP results also indicate that Cr and Ni accumulation was found to be maximum around the mines and also exceeds the standards of TCLP-PTEs (USEPA 1990; CPCBI 2012).

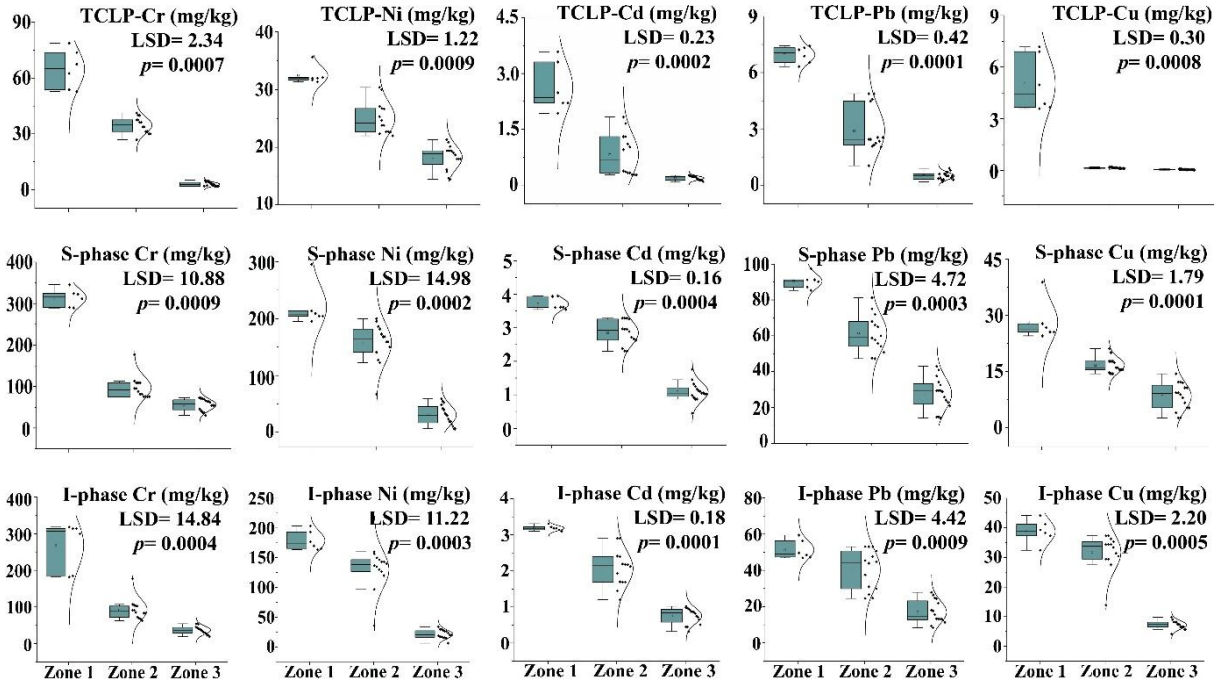

Fig. 9: Violin plot demonstrating the leachable and bio-accessible concentration of PTEs among the three zones. Here, Zone 1= Site 1, Zone 2 = Site 2, and Zone 3: Site 3

4.1.4 Bio-accessibility investigation of PTEs though stomach-intestinal phases

As the TCLP approach does not distinguish between stomach and intestinal phases (Yu et al., 2014), a study of actual bio-accessibility was necessary to understand the impact of PTEs on human health. Bio-accessibility was basically a physiological solubility of PTEs in the human stomach-intestinal tract (S-I). The agricultural soil was considered a key factor for the bio-accessibility test. In this research work, bio-accessible fractions (S and I phases) of PTEs extracted from three sites were shown in Fig. 9. Results showed that, in both the fractions, all the PTEs concentrations were significantly higher in site 1 and site 2 as compared with site 3. In the S-phase, the PTEs bio-accessibility percentage of this studied area was in the order of (site 1: SPCr-52.77%, IPCr: 47.22%; SPNi: 55.42%, IPNi: 44.57%; SPCd- 53.89%, IPCd: 46.10%; SPPb: 63.69%, IPPb: 36.30%, and SPCu: 42.53, IPCu: 57.46%; site 2: SPCr: 51.16%, IPCr: 48.83%; SPNi: 54.71%, IPNi: 45.28%; SPCd: 57.98%, IPCd: 42.01%; SPPb: 60.29%, IPPb: 39.70% and SPCu: 34.50, IPCu: 65.49%; and site 3: SPCr: 60.26%, IPCr: 39.73; SPNi: 59.08%, IPNi: 40.91%; SPCd: 58.96%, IPCd: 41.03; SPPb: 61.97%, IPPb: 38.02%; and SPCu: 53.97%, IPCu: 46.02%). Based on this percentage, Cr, Ni, Cd, and Pb exhibited high S-phase bio-accessibility in sites 1 and 2 except Cu, which showed high bio-accessibility in the I-Phase. The bio-accessibility of PTEs concentrations was increased in the S-phase as a result of the disposal of toxic tailings in the chromium-asbestos mines region. In S-phase, the pH was acidic in nature, which facilitates PTEs' easy dissolution and ability to pass the intestinal wall (Bosso et al., 2008; Saminathan et al., 2010). Simultaneously, bio-accessible PTEs in the S and I phases showed a strong positive correlation with the leachable (TCLP) concentration of PTEs [SPCr: 0.80***, IPCr: 0.87***; SPNi: 0.92***, IPNi: 0.88***; SPCd: 0.98***, IPCd: 0.97***; SPPb: 0.78***, IPPb: 0.90***; and SPCu: 0.83***, IPCu: 0.87***] as depicted in Fig. 10. Our results and Yu et al. (2014) observation were in accordance.

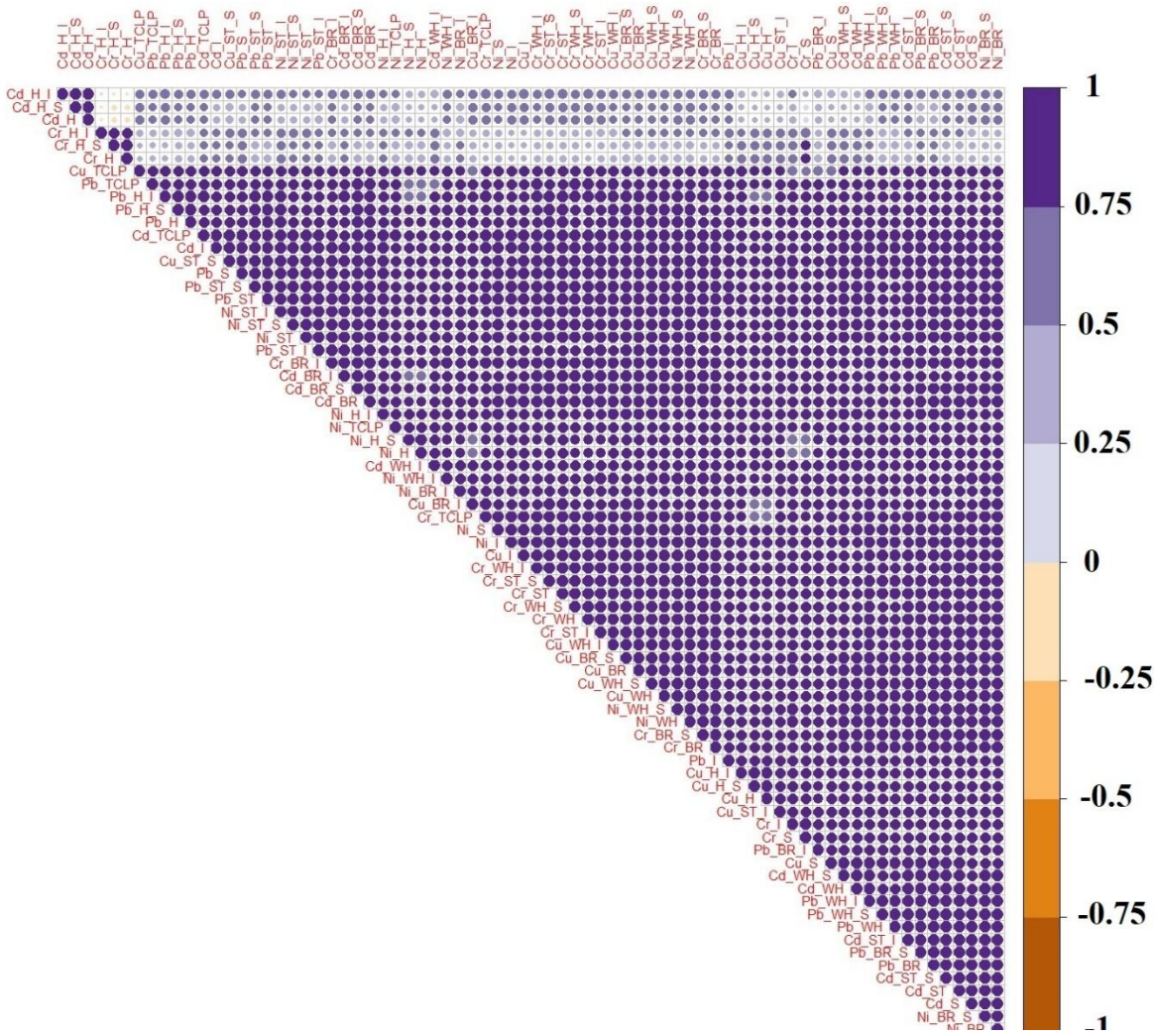

Fig. 10: The correlations plot depicts the relationships between TCLP, bioaccessible forms, and rice components. (Each point on the figure reflects correlation coefficients and their corresponding significance values, which are indicated by different colours)

4.1.5 Distribution pattern of total PTEs using different model across the mining site

4.1.5.1 Geostatistical approach of total PTEs pattern distribution

A geostatistical analysis of Chromium-asbestos mine sites revealed the presence of total PTEs (Cr, Ni, Cd, Pb, and Cu). The characteristics parameters of the best-fit semi-variogram models and ordinary kriging method for PTEs content of these study area are shown (Fig. 11 and Table 9).

Table 9: Semi-variogram characteristics parameters used in geostatistical modelling of total PTEs content. RMSE – root mean square error; AIC – Akaike Information Criterion; MSE – mean square error; RMSSE – root mean square standard error; G – Goodness-of-prediction; ASE – average standard error

Total PTEs	Nugget	Partial sill	Nugget/Sill*100	Spatial dependency	Model	RMSE	AIC	MSE	RMSSE	G	ASE
Cr	597.95	597954.8	0.0990	Moderate	Gaussian	544.1	517.32	0.082	1.476	68.18	573.83
Ni	0.529	324305.62	0.0001	Strong	Spherical	400.41	517.99	0.022	0.99	69.85	421.85
Cd	0.239	0.545	43.85	Strong	Gaussian	2.03	153.47	0.007	1.00	99.99	2.03
Pb	1.03	0.148	695.94	Moderate	Spherical	21.85	311.21	0.121	1.45	98.63	14.76
Cu	0.532	0.283	187.98	Strong	Spherical	24.35	320.54	0.013	0.81	97.84	30.63

Combined partial sill, nugget, and standard deviation represent the maximum variance and reflect regional variation between data pairs. Cd, Ni, Cu nugget effect is low in the chromium-asbestos mine site, indicating sufficient sampling density to explain the data spatial structures. To express the semi variograms in this assessment, the spherical model was used for Ni, Pb and Cu contents, while the gaussian model was used for Cr and Ni. For all elements the nugget to sill ratio was used to illustrate mild to strong spatial variations and also determining factor for geographical area, soil, weather and human entities. Near-zero MSE values and 1% RMSSE values for this study's prediction model supported its validity (Mondal et al., 2017).

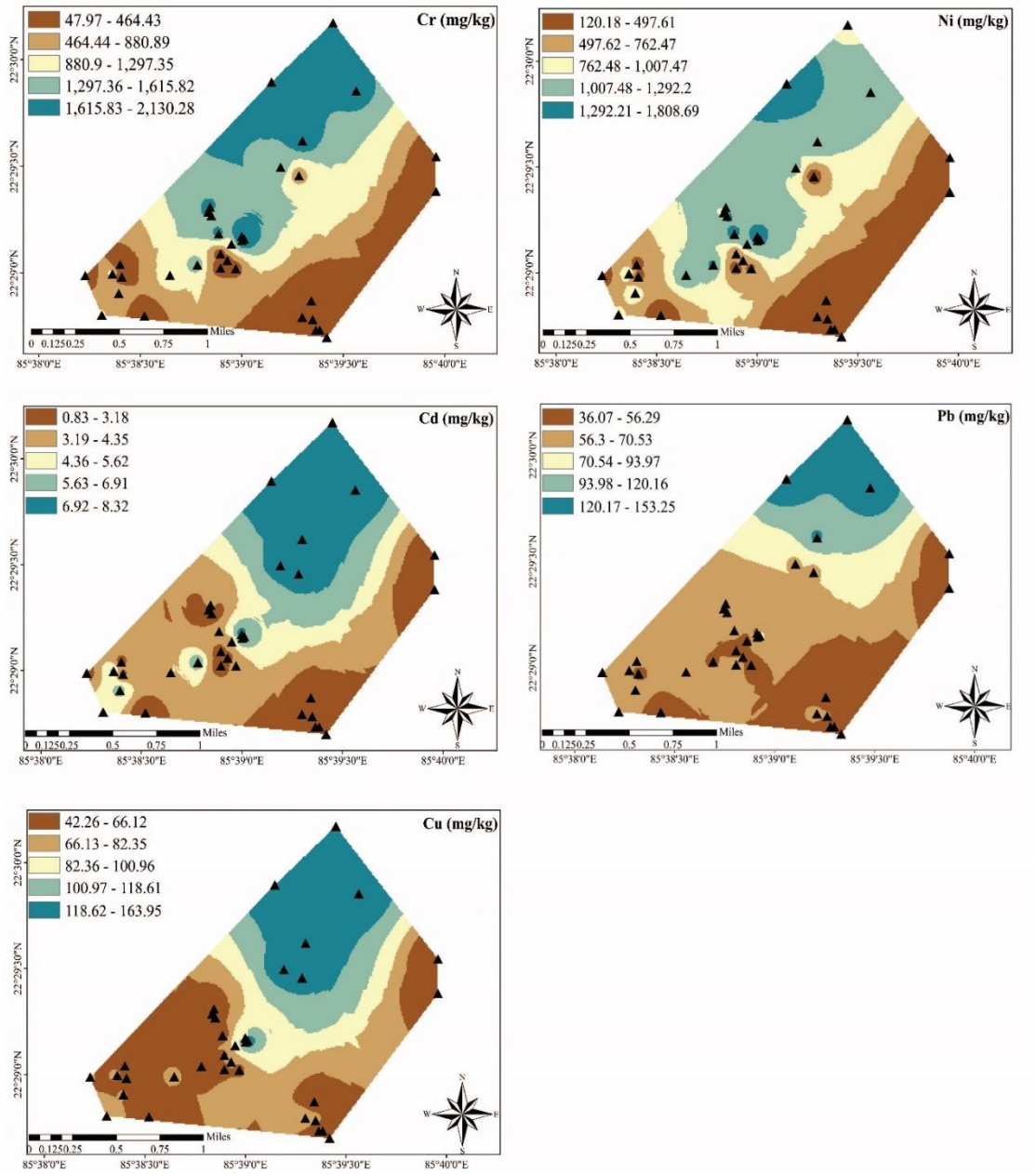

Fig. 11: Maps showing the spatial distribution of total PTEs (Cr, Ni, Cd, Pb, Cu) in Chromium-asbestos mine waste contaminated soils.

4.1.5.2 Spatial distribution pattern of leachable-PTEs at chromium-asbestos mines area

For the purpose of identifying patterns and making predictions about various leachable PTEs levels in the mining region, inverse distance weighting (IDW) was employed (Ghosh et al., 2023b). For the purpose of predicting leachable-PTEs pattern in this mining area, IDW was used to visualize varying amounts of Cr, Ni, Cd, Pb, and Cu, as shown in Fig. 12. According to this GIS map, higher concentrations of Cr, Ni, Cd, Pb, and Cu were observed (western section) close to the chromium-asbestos tailing dumpsite, but PTEs concentrations were

decreased in the uncontaminated area (northern section). In Fig. 12, the dark blue colour demonstrates the higher contamination, while the other colour depicts relatively less contamination in this chromium-asbestos mining area. The main source of this observation was the deposition of toxic mine waste and mining activities at the chromium-asbestos mine in the western site, which resulted in increased concentrations of PTEs, particularly Cr and Ni. This contamination affected agricultural soil, crops, and water, causing significant impact to the ecosystem. In contrast, the northern section, located farther from the mining dumpsite, exhibited lower PTE concentrations, leading to reduced contamination and less harmful effects on the environment. The results were consistent with the findings of Ghosh et al. (2023b), which highlighted that mines and mining activities are the primary sources of PTEs pollution and have a detrimental effect on agricultural soil and crops.

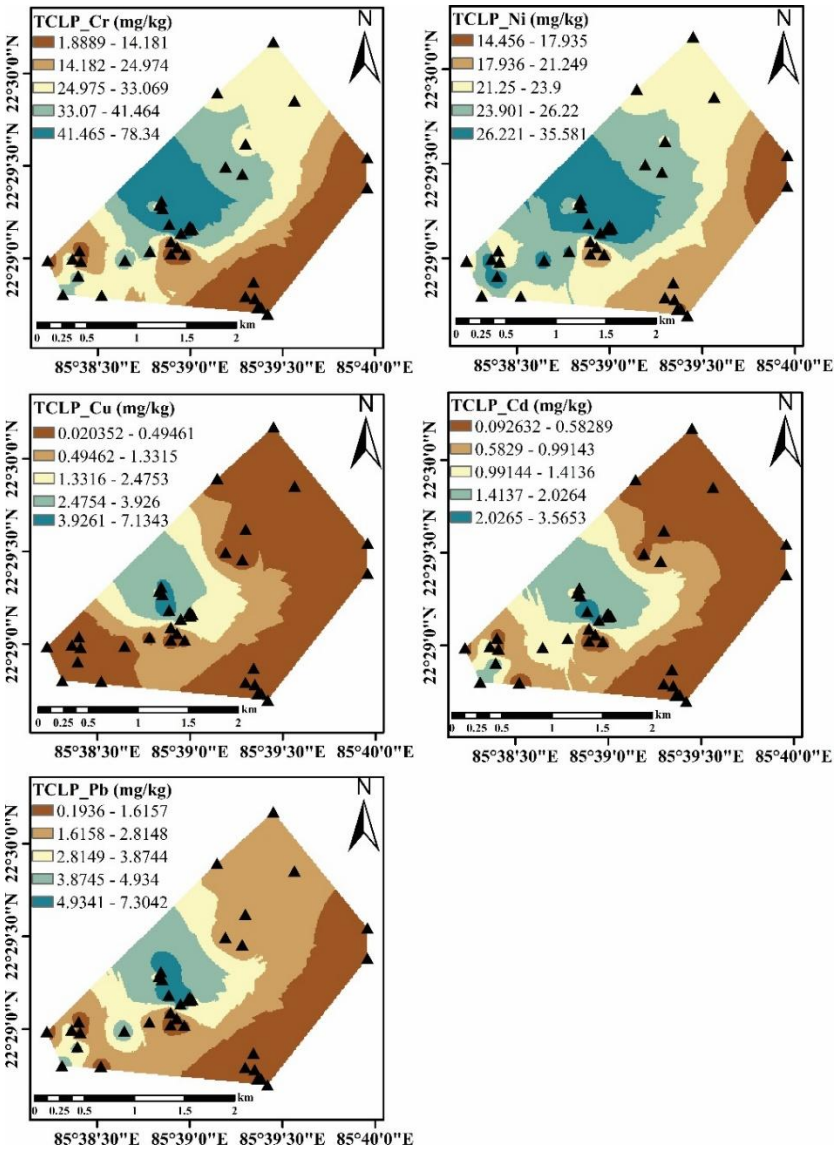

Fig. 12: An illustration of the spatial distribution pattern of different leachable-PTEs in Chromium-asbestos mines

4.1.5.3 PTEs distribution using self-organizing map

SOM (self-organizing map) can be used to reveal significant information in interpretations that are hard to find with traditional approaches and the output were represented (Fig. 13a-c). By using SOM, this study explores a quantitative method of estimating PTEs distributions in soil as well as classifying and treating different sources of pollution. To demonstrate the importance of variables delivered by each SOM unit for each hexagon, color ranked plots were constructed in order to show the closer analogy between samples' characteristics based on their smaller hexagonal spaces. Each neuron's weight vectors and its neighbours form a unified distance matrix (U-matrix). Similarly, colored components in a component plane indicate positive correlation between variables, while different colors indicate negative correlation. Fig. 13a showed higher concentrations for all PTEs in the upper left neurons. The right upper quadrant neurons had more prominence for sites 1, neuron in left lower to upper for site 2, while the right lower quadrant neurons had more prominence for sites 3 (Fig. 13b). In addition, a U-matrix clustered by location of sample sites was prepared using the SOM algorithm (Fig. 13c).

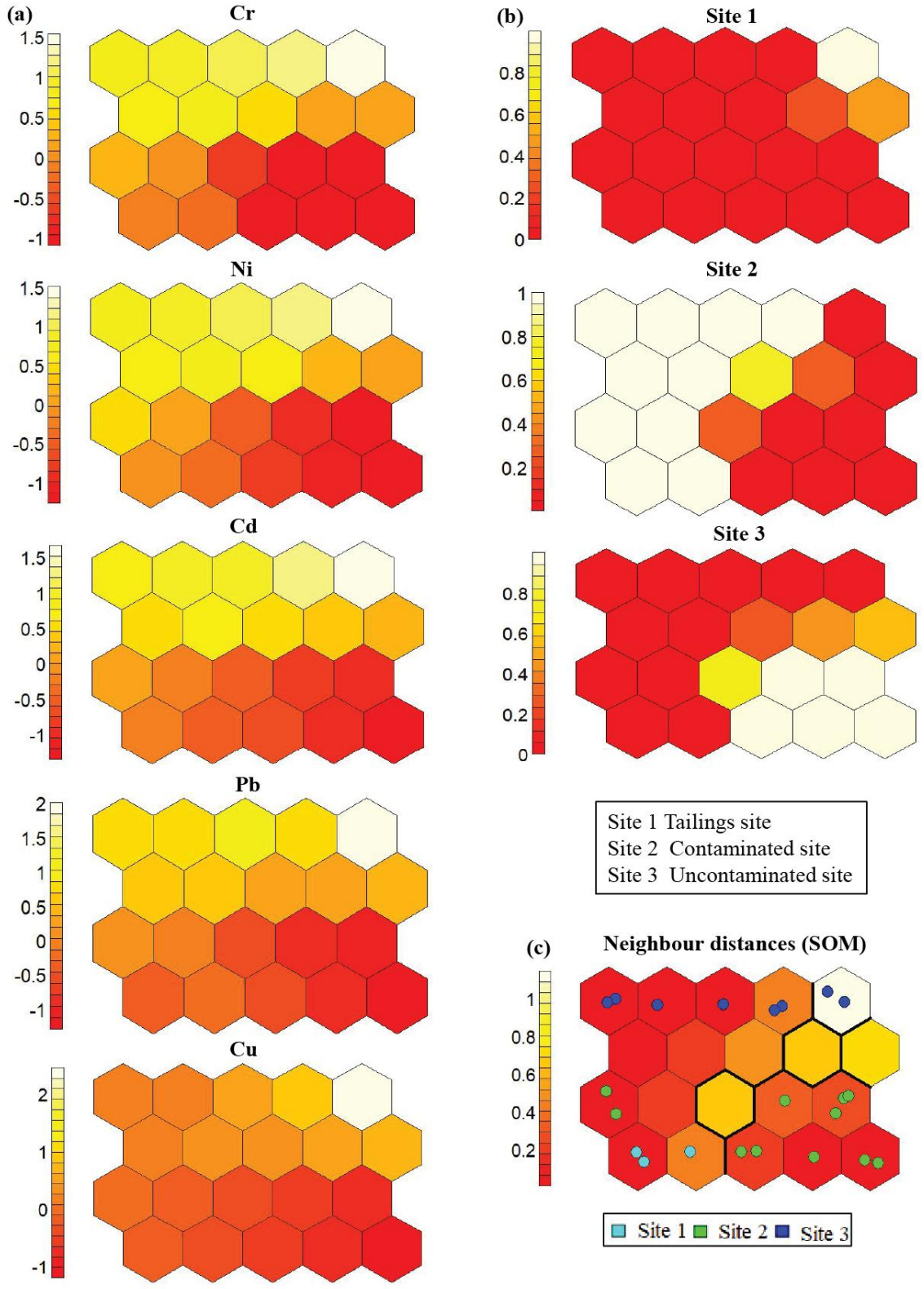

Fig. 13: (a) Distribution of each PTEs in Chromium-asbestos mine waste contaminated soils through self-organizing map (SOM); (b) Site wise PTEs concentration distribution maps; (c) Clustering of U-matrix denotes the three sampling sites.

4.1.5.4 Source-oriented distribution of PTEs utilizing positive matrix factorization model

As a perspicuous method, the PMF was employed to inspect and identify the sources of the five PTEs in this region. The PMF model evaluates the 'Q' value by repeating the model for several factors (1-6 factors). In our experiment, the model ran for 100 times to find the least stable Q value, and then extracted the optimum number of factors (four factors) based on the lowest and stable Q values (Chai et al., 2021). The S/N ratio (signal to noise) of the 5 selected PTEs were greater than 2 which indicate the strong data accuracy and confirms the model's rationality. The regression between observed concentrations and predicted concentrations are shown in supplementary fig. 5. Model coefficient value (R^2) greater than 0.9 indicated strong correlation between those PTEs, so it was appropriate to use the model for demonstration purposes and results were reliable. Fig. 14 (a-c) shows how each PTEs contributes to the PMF model as well as the associated precise factors profiles and correlation matrix.

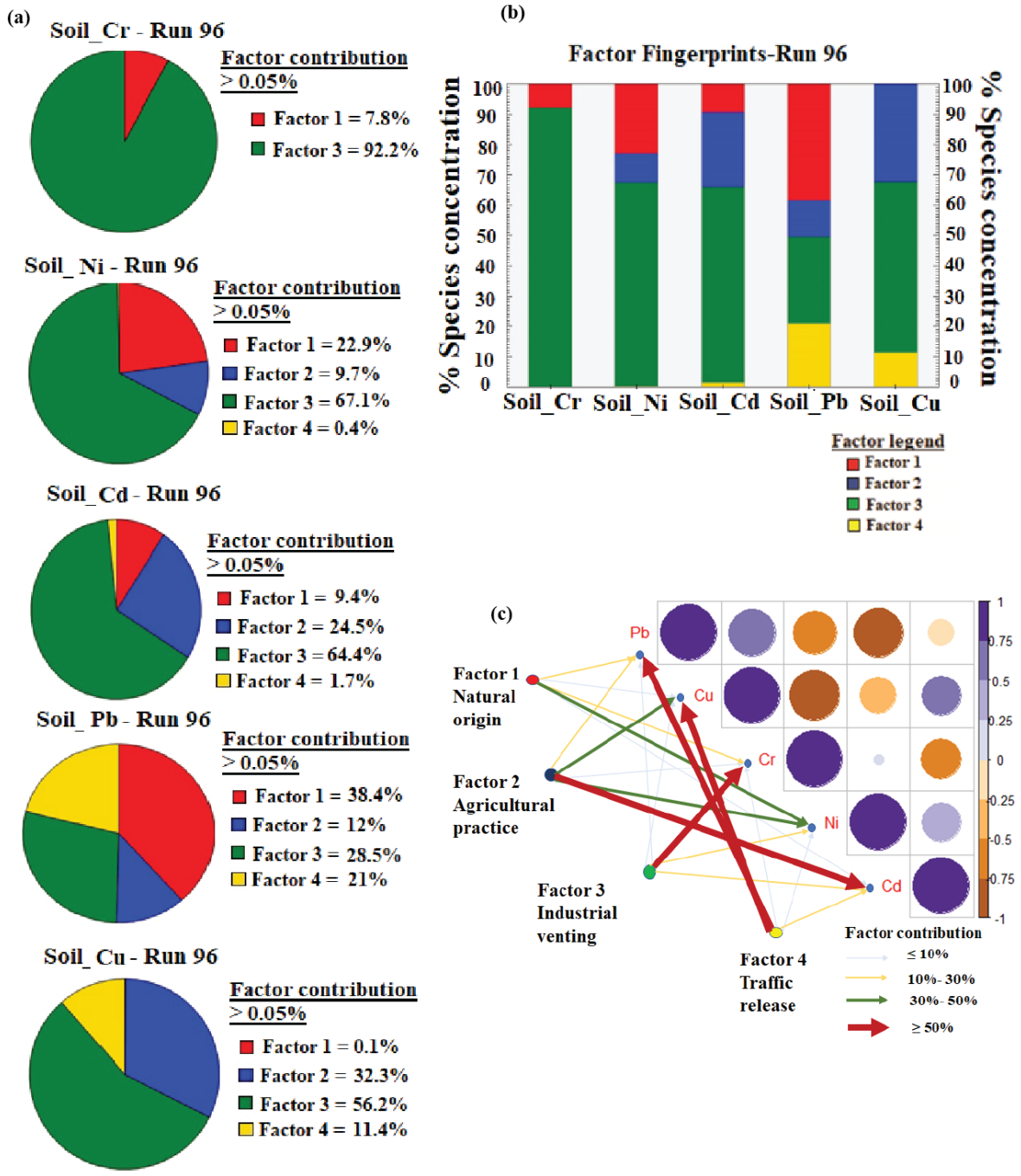

Fig. 14: Source allocation of PTEs in Chromium-asbestos mine waste contaminated soils of the study location (a) the contribution percentage of each factor by PMF; (b) PMF model factor profiles of PTEs in Chromium-asbestos mine waste soils; (c) PMF model integrated with Pearson correlation analysis to detect the correlation between PTEs

Fig. 15 illustrates the analysis of the four PMF factors.

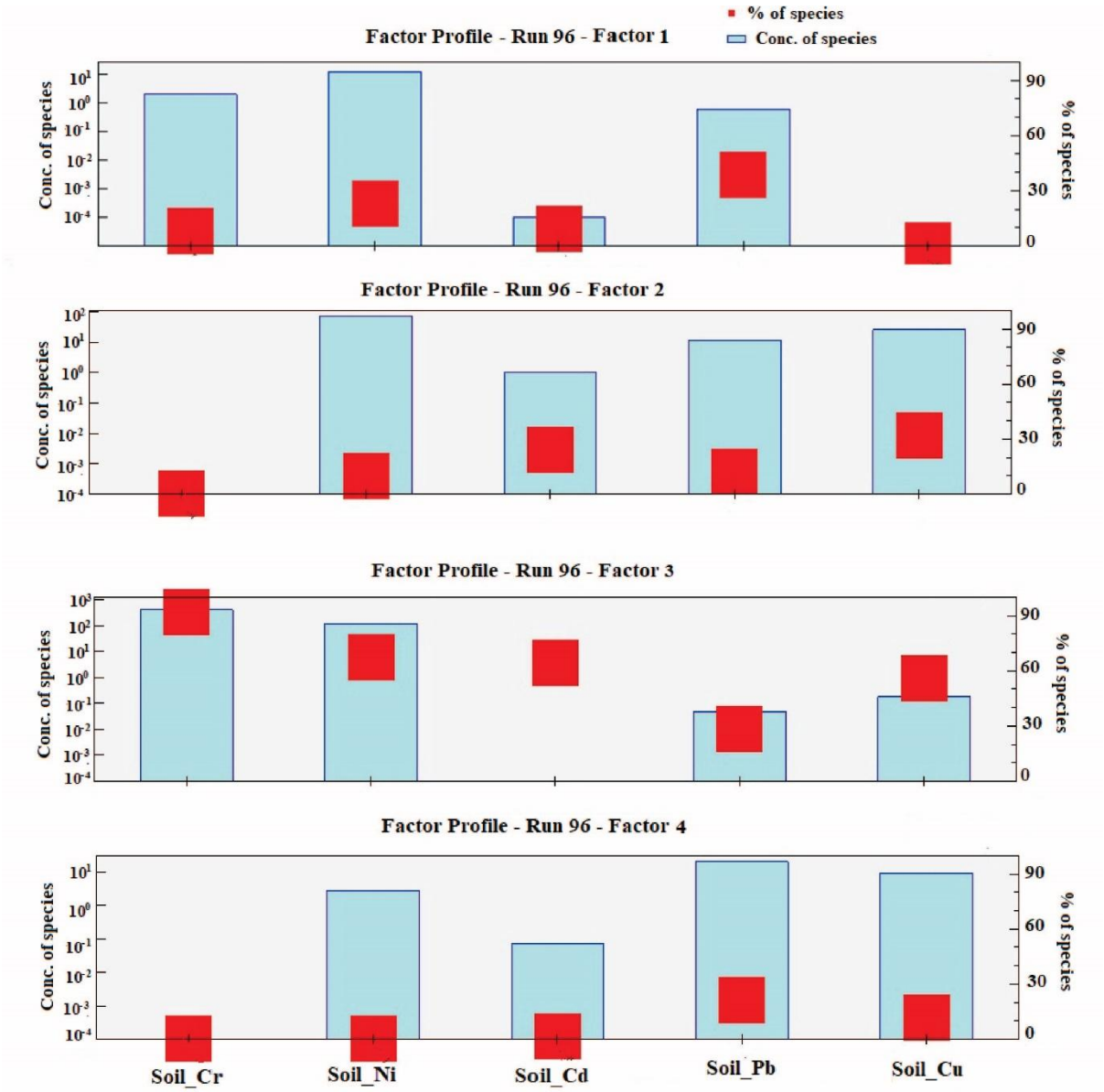

Fig. 15: Percentage contribution of PTEs to the four factors

The spatial distributions of PTE concentrations by GIS methods based on factor score were shown in Fig. (16a-d) as evidence of source apportionment. In this study, the PMF results denote that Factor 1 contributed to mainly Pb (38%; factor 2 loaded on Cu (32%) and Cd (24%); Factor 3 weighted on Cr (92%), and Ni (67%), and last factor 4 was dominated by Pb (21%) (Fig. 14b). A total variance of 15.72% was attributed to Factor 1, which was predominated by Pb, Ni, Cd, and Cr. The *Igeo* of Pb, and Cd also showed moderate to low contamination whereas Cr, Ni exhibits maximum contamination in site1 and site 2 as compared with site3. These PTEs are the primary industrial elements found in industrial waste mainly mining waste residue,

waste water, metal smelting, alloy processing, cement production, and apparel industry (Liu et al. 2020; Huang et al., 2022). In Fig 16a, spatial distribution indicate that the northern part was heavily loaded where mine waste dumping sites delivered contamination to the nearby water bodies and agricultural land (Fig 16a).

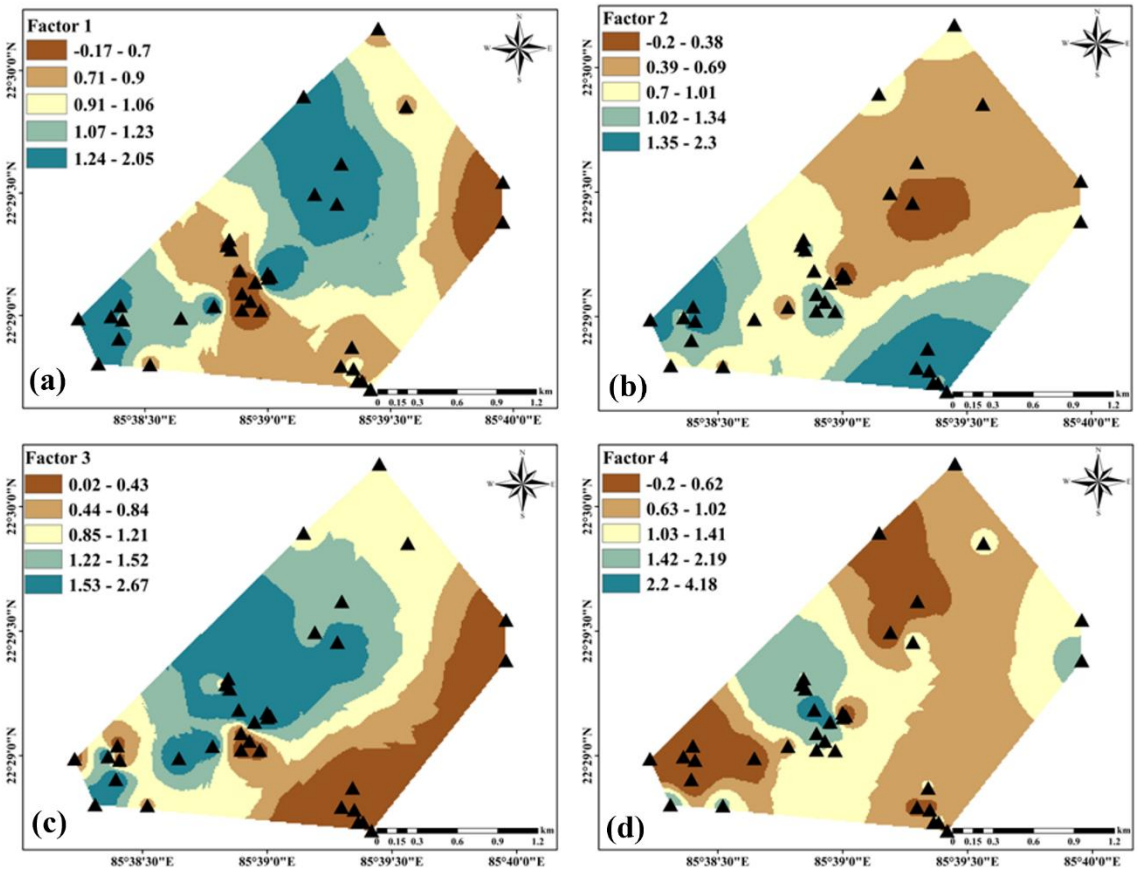

Fig. 16: An illustration of the spatial distribution of factors (a-d) derived from the PMF model

Reports regarding PTEs contamination from mine waste, industrial waste, textile industry, pharmacy etc. reported earlier (Ayub et al., 2020: Jiang et al., 2021). Accordingly, factor 1 was classified as industrial activities. Factor 2, which was dominantly composed of Cu, Cd, and Pb was ascribed to a total variance of 15.70%. In GIS map, factor 2 was located on the southern portion where agricultural lands were contaminated with deposited toxic waste (Fig. 16b). Due to the application of various fertilizers, herbicide, insecticides and pesticides, high concentrations of Cu, Pb and Cd are present in the agricultural soil (Cai et al. 2019; Huang et al. 2022). Additional studies have shown that Cu and its compounds are linked to fungicides, pesticides, and animal manure (Luo et al., 2009). Inorganic lead (Pb) was used in the preparation of insecticides and herbicides (Belon et al., 2012). As mentioned above, factor 2

could be associated with agricultural practices. In terms of total contribution, factor 3 made up 61.68%. It is mainly allied to the soil core material of the lithogenic source. It was primarily weighted on Cr, and Ni and a positive correlation was found between Cr and Ni. In this work, north-western portion of the area was loaded with factors 3 (Fig. 16c). Furthermore, our spatial distribution analysis in the study area reveals that Cr and Ni in the agricultural area is primarily released from chromium asbestos mines. Similarly, the *Igeo* index also revealed that Cr and Ni contamination was higher on site1 and site 2 than site 3. Previous researchers have found that these PTEs in the soil comes from soil parent material (Jiang et al., 2021; Huang et al., 2022). Therefore, factor 3 might be related to natural sources. The last factor, factor 4 contributes (6.9% of total variance) mainly to Pb followed by Cd and Cu. In terms of spatial distribution, Pb and Cu were very similar, and Cd exhibited some similarity, as well (Fig. 16d). Village areas and roads were the sites of the hotspots of these PTEs. Transportation, combustion of vehicle fuel, lead acid batteries and catalytic agents are the major sources of lead production. Similar nature of research reached similar conclusion (Du et al., 2019; Jiang et al., 2021; Hung et al., 2022). Cd and Cu are mainly obtained from smelting activities in industries, vehicle transporting, tires, lubricants and road traffic (Jiang et al., 2020; Hung et al. 2022). As analyzed above, Factor 4 might be determined as traffic emissions. This result indicates that the PMF model was capable of analyzing the quantitative sources of PTEs in soil, and that the result was more accurate. In site 1 and site 2, natural and industrial contamination have always been considered the most important sources of PTEs pollution and might pose a significant impact on human health risks. Since Cr and Ni were loaded most with these two factors, they were identified as priority contaminants for further risk reduction.

4.1.6 Soil pollution level determination through different indices

Total PTEs concentrations were substantially higher in the soils of chromium-asbestos mines area which are eventually subjected to mine toxic waste disposal. Thus, it can immensely pollute the ecosystem and human health. So, in this research, this issue has addressed through the assessment of different indices and human health hazards.

The pollution index (PI) is a useful tool to quantify the potential degree of contamination by PTEs in tailings and soils. Calculation of PI involved averaging the concentration ratios of all PTEs in a sample against their assumed permissible levels. The results of the pollution index (PI) are demonstrated (Fig. 17). In site 1 (6.50) and site 2 (4.42), the average PI value is significantly ($p < 0.05$) higher pollution (above the permissible limit PI >1) than in site 3 (0.85).

There is a danger of soil contamination in roro mines areas from Cr followed by Ni which has a pollution index (PI) higher than those of Cd, Pb, and Cu, as shown in this study.

The contamination index was used to quantify the total contamination level in a particular area. In this context, CI is estimated in the Chromium-asbestos mines area and represented in Fig. 17. In Roro mines, the average CI value for site 1, site 2, and site 3 is 17.20, 11.76, and 2.19 respectively. Here results indicate that the PTEs contamination is higher in the tailings site (site1), and contamination site (site 2) as compared with the uncontaminated site (site 3). The CI for all analyzed PTEs decreased in the sequence of Cr>Ni>Pb>Cu>Cd. A significant ($p < 0.05$) increase in the CI value above than permissible limit in site 1 and site 2 due to the presence of toxic mine waste in the soils. The CI values generally ranged from low to extremely high at Roro mines and Cr had a considerable influence on soil quality.

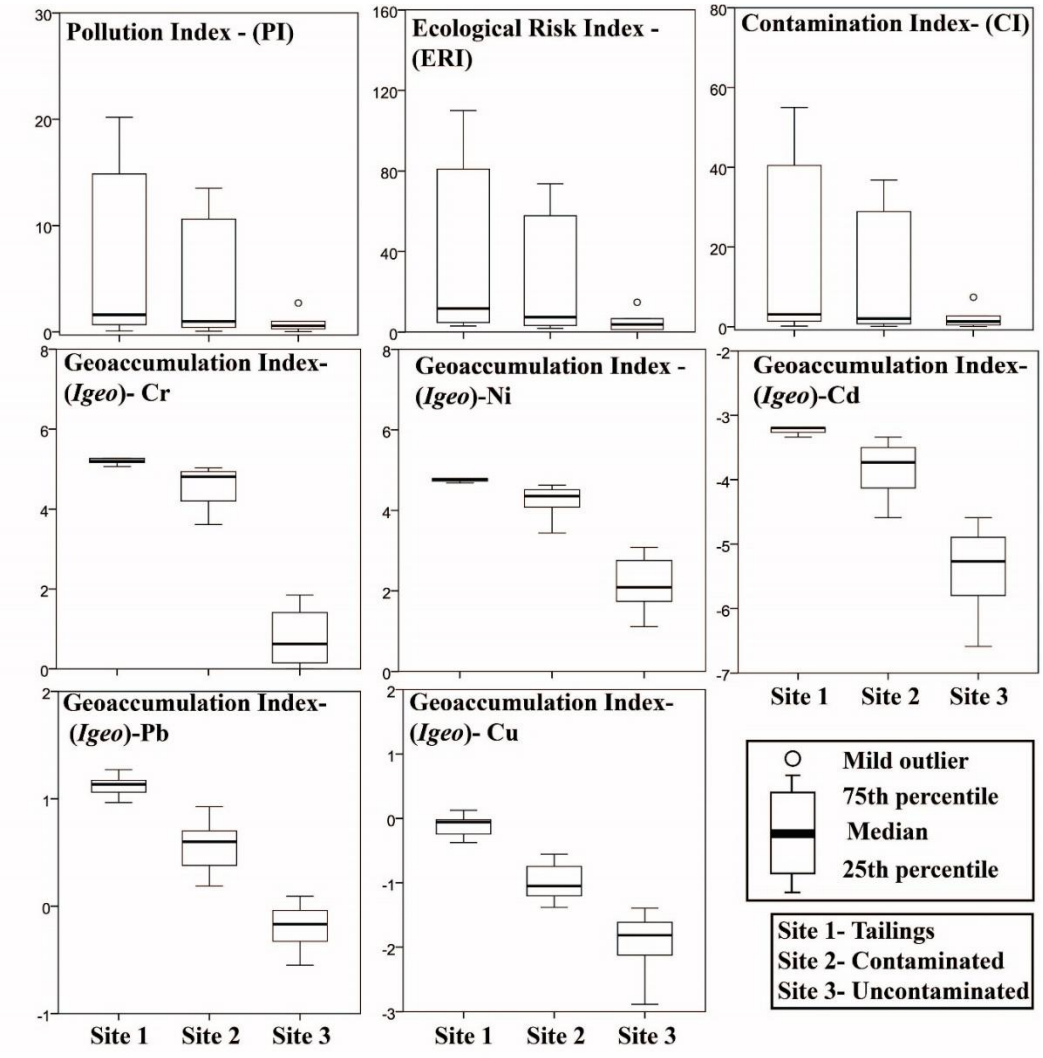

Fig. 17: Box-whisker plot indicating the different index comparisons among the three sites in regards to pollution index (PI), Ecological risk index (ERI), Contamination index (CI) and geoaccumulation index (*Igeo*) of Chromium-asbestos mine waste contaminated soils

Fig. 17 denotes the ecological risk index (ERI) for all PTEs in the soil and the order of PTEs-ERI is Cr>Ni>Pb>Cu>Cd according to their ERI. In the present study, all the estimated PTEs appear to pose low to moderate risk to the ecosystem as ERI values were less than 300. ERI value of Pb, Cd, and Cu contributes least to the overall environmental risk. Despite Cr and Ni apparently posing a huge threat for the ecosystem and living beings within the Roro mine area, measured ERI values are trending towards the moderate category. Hence the living beings in this area are prone to probable ecological concerns from Cr and Ni contamination in soil.

Basically, the geo-accumulation index (I_{geo}) was an effective index for the evaluation of the probable accumulation pattern of PTEs in the ecosystem. In this study area, (I_{geo}) values (Fig. 17) showed low to extreme contamination ($0 \geq I_{geo} \leq 5$) throughout the Roro mines area due to the presence of PTEs (Cr, Ni, Pb, Cd, and Cu) respectively. Hence the mean geo-accumulation index (I_{geo}), for Cr and Ni showed extremely contaminated, Pb showed moderately to extremely contaminated and Cu and Cd showed low contaminated soils. The trend of contamination in the CI coincides with all other indices (PI, ERI, *Igeo*), illustrating the high level of pollution and health risk for all living entities. These indices have shown similar results in earlier studies (Mondal et al., 2017; Kahangwa, 2022; Omeka et al., 2022; Wang et al., 2022)

4.1.7 Humans non-carcinogenic and carcinogenic health risks assessment through total PTEs

PTEs can cause detrimental effects on human health depending on their average daily intake. Any PTEs can be harmful even at very low concentrations, exposure time, and dosage (Roy and Bhattacharya, 2022). In light of this, it becomes vital that individual PTEs are evaluated based on their hazards posed by a variety of exposure routes (ingestion, inhalation, dermal exposure). Tables (10, 11, 12) show non-carcinogenic risks, carcinogenic risk from PTEs, HQ (hazard quotient), and aggregate HI (hazard index) through three exposure pathways in children and adults. In our study, a mean significant non-carcinogenic risk was observed from PTEs for adults and children in three sites of chromium asbestos mine area [$ADD_{ingestion}$: 7.39E-04, $ADD_{inhalation}$: 1.08E-07 and ADD_{dermal}: 6.21E-11 for adult; $ADD_{ingestion}$: 5.91E-03, $ADD_{inhalation}$: 1.65E-07 and ADD_{dermal}: 3.48E-10 for children]. Over three exposure pathways for both adults and children, site1 showed significantly higher non-carcinogenic risk than sites 2 and 3 (Table 10).

Table 10: Non-carcinogenic risk (three exposure pathway) values on adults and children

Total PTEs	Adult			Child		
Site 1	$ADD_{Ingestion}$	$ADD_{inhalation}$	ADD_{dermal}	$ADD_{Ingestion}$	$ADD_{Inhalation}$	ADD_{dermal}
Cr	3.22E-2	4.74E-7	1.28E-9	2.58E-2	7.21E-7	7.23E-9
Ni	2.37E-3	3.49E-7	9.47E-10	1.89E-2	5.30E-7	5.32E-9
Cu	2.58E-4	3.80E-8	1.03E-10	2.07E-3	5.79E-8	5.80E-10
Cd	1.29E-5	1.90E-9	5.15E-12	1.03E-4	2.89E-9	2.89E-11
Pb	2.55E-4	3.75E-8	1.02E-10	2.04E-3	5.70E-8	5.71E-10
Site 2						
Cr	2.15E-3	3.17E-7	8.61E-10	1.72E-2	4.82E-7	4.84E-9
Ni	1.69E-3	2.49E-7	6.76E-10	1.32E-2	3.79E-7	3.79E-9
Cu	1.41E-4	2.07E-8	5.63E-11	1.12E-3	3.15E-8	3.16E-10
Cd	8.82E-6	1.30E-9	3.52E-12	7.05E-5	1.97E-9	1.97E-11
Pb	1.72E-4	2.54E-8	6.88E-11	1.37E-3	3.86E-8	3.86E-10
Site 3						
Cr	1.59E-4	2.34E-8	6.35E-11	1.27E-3	3.56E-8	3.57E-10
Ni	4.34E-4	6.39E-8	1.73E-10	3.47E-3	9.71E-8	9.73E-10
Cu	7.77E-5	1.14E-8	3.10E-11	6.21E-4	1.74E-8	1.74E-10
Cd	3.28E-6	4.82E-10	1.31E-12	2.62E-5	7.33E-10	7.35E-12
Pb	1.03E-4	1.52E-8	4.13E-11	8.28E-4	2.31E-8	2.32E-10

The HQs of all the PTEs for both adults and children were <1 among all sites of the Roro mines area. A significant difference was found between site 1 and sites 2 and 3 in terms of their hazard quotients (HQs) for different exposure pathways (Table 12). The average health risk index (HI) values for adults and children in this area were below the USEPA's limit (HI>1) (USEPA's, 2014) denoting no possible non-carcinogenic risk. Therefore, both children and adults were most likely to be exposed through ingestion. Among the three sites of Roro mines, the sequence of hazard pathways was: ingestion > dermal > inhalation. Also, it was observed that HI values were higher among children than in adults for all elements and all exposure pathways. Thus, the results shed light on the fact that children are more susceptible to environmental PTEs. Similar results were seen in some reports that children are more sufferers and ingestion was the most common pathway for health hazards (Huang et al., 2021; Alyousef et al., 2022).

Table 11: Carcinogenic risk (three exposure pathway) values on adults and children

Total PTEs	Adult			Child		
Site 1	$CR_{Ingestion}$	$CR_{inhalation}$	CR_{dermal}	$CR_{Ingestion}$	$CR_{Inhalation}$	CR_{dermal}
Cr	1.55E-3	2.37E-7	6.43E-10	5.80E-2	1.62E-6	1.62E-8
Ni	2.15E-3	3.17E-7	8.61E-10	7.77E-2	2.17E-6	2.17E-8
Cd	4.90E-6	7.21E-10	1.95E-12	1.76E-4	4.93E-9	4.94E-11
Pb	1.07E-5	1.57E-9	4.27E-12	3.85E-4	1.07E-8	1.07E-10
Site 2						
Cr	9.87E-4	1.58E-7	4.30E-10	3.88E-2	1.08E-6	1.08E-8
Ni	1.54E-3	2.26E-7	6.15E-10	5.54E-2	1.55E-6	1.55E-8
Cd	3.34E-6	4.92E-10	1.33E-12	1.20E-4	3.36E-9	3.37E-11
Pb	7.24E-6	1.06E-9	2.89E-12	2.60E-4	7.28E-9	7.30E-11
Site 3						
Cr	6.97E-5	1.17E-8	3.17E-11	c	8.00E-8	8.02E-10
Ni	3.95E-4	5.81E-8	1.57E-10	1.42E-2	3.97E-7	3.98E-9
Cd	1.24E-6	1.83E-10	4.97E-13	4.48E-5	1.25E9	1.25E-11
Pb	4.34E-6	6.39E-10	1.73E-12	1.56E-4	4.37E-9	4.38E-11

PTEs like Cr, Ni, Cd, and Pb are immensely carcinogenic substances. Table 11 denotes the (CR) carcinogenic risk and (TCR) total carcinogenic risk for children and adults were determined from the three different pathways among the three sites of chromium-asbestos mines. The maximum tolerable limit for total cancer risk (TCR) varies between 10^{-6} to 10^{-4} (Li et al. 2020). In our experiment, significant risks were observed (above the permissible limit) from Cr [adult: 1.56E-03; children: 5.81E-02] and Ni [adult: 2.16E-03; children: 7.77E-02] for both adults and children (Table 11). Also, children showed higher carcinogenic risk (CR) than adults from these PTEs via pathways (ingestion>inhalation>dermal). CR values from three sites showed a carcinogenic risk level order of site1>site2>site3. The carcinogenic risk from total PTEs concentration has been reported earlier although (Xiao et al., 2020; Roy and Bhattacharya, 2022). Similar results were observed for children's carcinogenic effect from Cr in Iran (Najmeddin et al., 2018). For Pb and Cd, the range of TCR fell within no carcinogenic risk effects (10^{-6} to 10^{-4}) (Fig. 18).

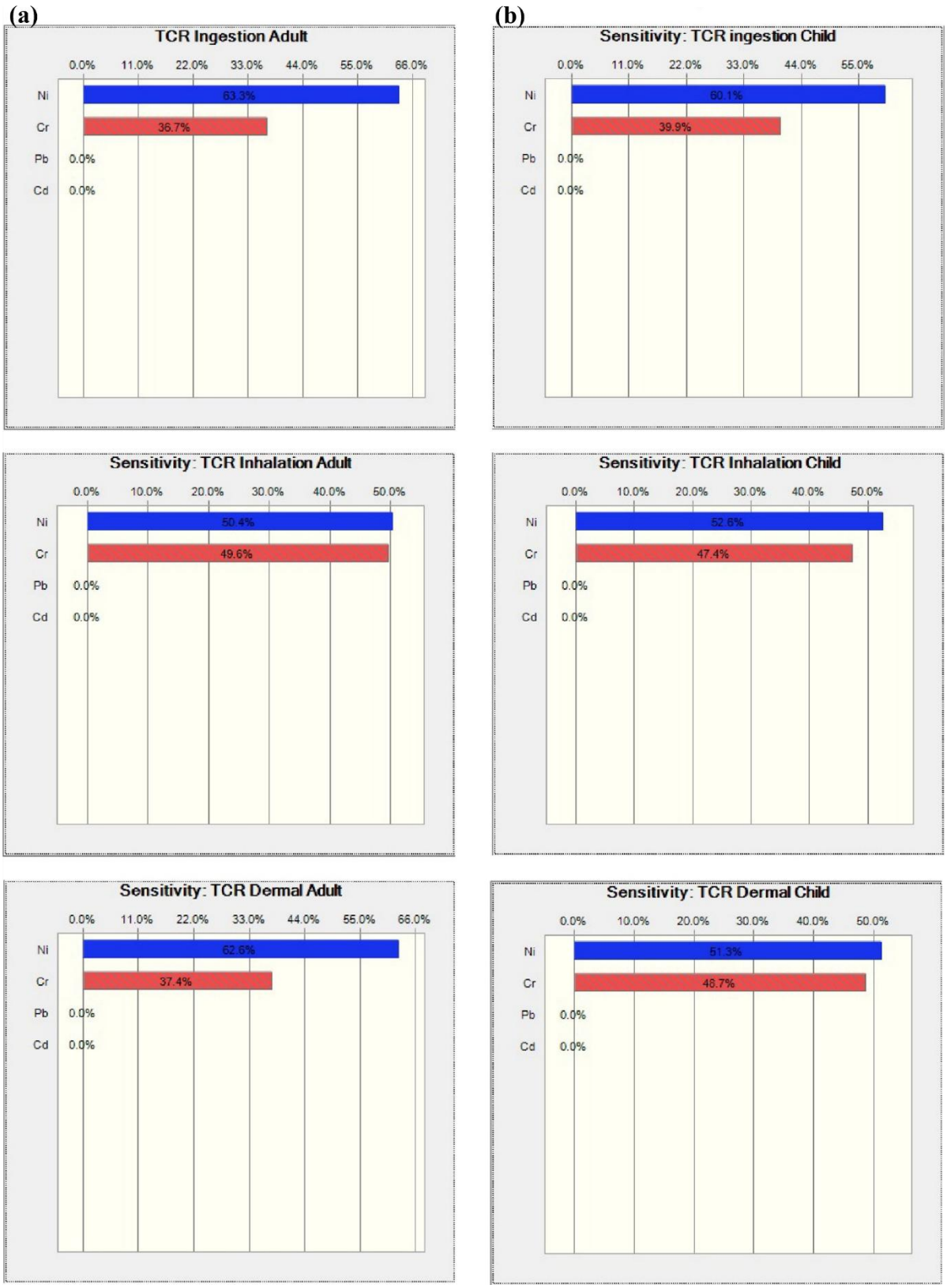

Fig. 18: Sensitivity analysis of total carcinogenic risk (TCR) in (a) adults and (b) children

Thus, the risk was mainly from Cr followed by Ni in the chromium-asbestos mining area. Due to mining activity and dumping the toxic mine waste on the soil, the Cr and Ni concentration in the soil increased tremendously. Reports suggested similar work of increasing concentrations of Cr and Ni in mine-impacted soil (Alyousef et al., 2022). Thus, necessary measures should be taken to mitigate cancer risk.

4.1.8 Predictable health risk assessment through concentration-oriented evaluation of PTEs

In addition, the Monte-Carlo simulation (MCS) method was used to assess health risk evaluation to avoid mistakes caused by deterministic parameters being overestimated or underestimated. In chromium-asbestos mine areas, the non-carcinogenic and carcinogenic effects (on children and adults) of PTEs have been evaluated through three different pathways (ingestion, ingestion, and dermal) using MCS, and the data were represented (Tables 10, 11). The non-carcinogenic risk was inconsequential for both adults and children. The mean value of PTE's single non-carcinogenic risk index was below 1. Apart from this, the mean HQ values trend of adults and children was Cr>Ni>Pb>Cd (Table 12).

Table 12: Calculation of hazards quotients (HQ) and hazards indexes (HI) for adults and children

Total PTEs	**Adult**				**Child**			
Site 1	$HQ_{Ingestion}$	$HQ_{inhalation}$	HQ_{dermal}	**HI**	$HQ_{Ingestion}$	$HQ_{Inhalation}$	HQ_{dermal}	**HI**
Cr	2.15E-3	3.16E-7	1.07E-4	2.17E-3	1.72E-2	4.80E-7	6.02E-4	1.73E-2
Ni	1.58E-3	2.33E-7	7.89E-5	1.59E-3	1.26E-2	3.53E7	4.42E-4	1.27E-2
Cu	6.47E-3	9.51E-7	4.30E-8	6.47E-3	5.17E-2	1.44E-6	2.41E-7	5.17E-2
Cd	1.94E-3	1.89E-6	2.57E-6	1.29E-2	1.03E-1	2.88E-6	1.44E-5	1.03E-1
Pb	6.37E-2	9.37E-6	9.69E-7	6.37E-2	5.10E-1	1.42E-5	5.44E-6	5.10E-1
Site 2								
Cr	1.43E-3	2.11E-7	2.00E-4	1.45E-3	1.15E-2	3.21E-7	1.12E-3	1.15E-2
Ni	1.12E-3	1.66E-7	1.57E-4	1.14E-3	9.03E-3	2.52E-7	8.85E-4	9.09E-3
Cu	3.52E-3	5.18E-7	6.56E-8	3.52E-3	2.82E-2	7.87E-7	3.68E-7	2.82E-2
Cd	8.81E-4	1.29E-6	4.92E-6	8.81E-3	7.05E-2	1.97E-6	2.76E-5	7.05E-2
Pb	4.31E-2	6.34E-6	1.83E-6	4.31E-2	3.44E-1	9.63E-6	1.03E-5	3.44E-1
Site 3								
Cr	1.06E-4	1.56E-8	1.69E-5	1.07E-4	8.49E-4	2.37E-8	9.51E-5	8.55E-4
Ni	2.89E-4	4.25E-8	4.62E-5	2.92E-4	2.31E-2	6.47E-8	2.59E-4	2.33E-3
Cu	1.94E-3	2.85E-7	4.13E-8	1.94E-3	1.55E-2	4.34E-7	2.32E-7	1.55E-2
Cd	3.28E-3	4.82E-7	2.09E-6	3.28E-3	2.62E-2	7.33E-7	1.17E-5	2.62E-2
Pb	2.58E-2	3.80E-6	1.25E-6	2.58E-2	2.07E-1	5.78E-6	7.06E-6	2.07E-1

To recapitulate, the average values of HI for adults and children were 1.18E-02 and 9.41E-02 respectively. HQ and HI values were below than guideline limit (USEPA 2021). The probability model shown in Fig. 19 indicates that the TCR cannot be negligible across all PTEs studied, while individual PTEs carcinogenic risk (CR) values were different.

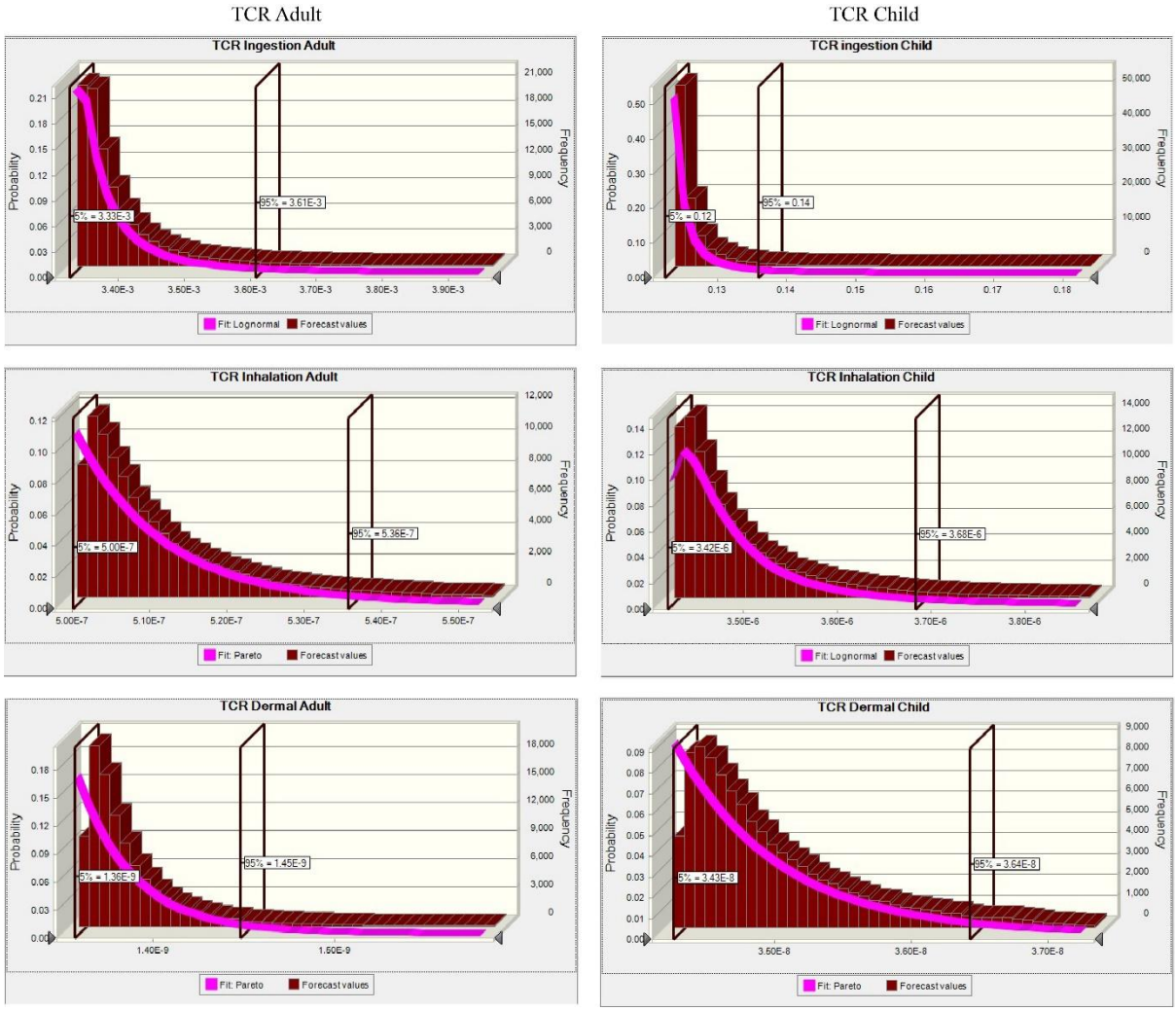

Fig. 19: Probability distribution plot of TCR for adult and child by ingestion, inhalation and dermal through Monte Carlo simulation model

The TCR values for Cr and Ni exceeded the permissible threshold of 10^{-6} indicating a high potential risk of cancer-causing. The TCR revealed that the probable risk of each PTEs was as follows: Cr>Ni>Pb>Cd. The health risk via soil ingestion was the most crucial pathway for carcinogenic risk for both adults and children and children are the maximum sufferer of hazards. Cr was established as the dominant PTEs of carcinogenic risk (CR) by differentiating the actual mean of carcinogenic risk value for both adults and children. In adults and children, Cr and Ni concentrations contribute to cancer risk (Wang et al., 2022). In the three sites, the contribution of PTEs concentration was the highest, and also recognized as a prime factor followed by the soil intake rate, RfD, and SF. The positive impact on HI and CR is due to the negative contribution of body weight. Furthermore, the population of the Roro mine should avoid consuming contaminated food, water, reduce agricultural and household activity near

mining sites. The risk assessment in the chromium-asbestos mine area of India should pay closer attention to PTEs exposure to Cr for especially children.

4.1.9 Health risk assessment using Leachable PTEs

PTEs in the soil's top layer significantly impact human health, as the upper surface of soil close to mining areas was more sensitive to PTEs pollution than beneath the soil (Wang et al., 2020). Tables (13-15) illustrate children's and adults' non-cancerous risk (NCR), cancer-causing risks (CR), hazard quotient (TCLP-HQ), and hazard index (TCLP-HI) through three exposure pathways. In this study, site 1 showed a considerably greater NCR ($ADIL_{ingestion}$: 1.07E-04, $ADIL_{inhalation}$: 1.58E-08, and $ADIL_{dermal}$: 4.29E-11 for adults; $ADIL_{ingestion}$: 8.60E-04, $ADIl_{inhalation}$: 2.40E-08 and $ADIL_{dermal}$: 2.41E-10 for child) as compared with sites 2 and 3 along three exposure paths (Table 13). The average ADIL value for these leachable-PTEs via ingestion of soil varied in order as Cr > Ni > Pb > Cu > Cd for both adults and children in site 1 and site 2.

Table 13: Non-carcinogenic risk of leachable-PTEs values on adults and children

PTEs	**Adult**			**Child**		
Site 1	$ADIL_{ingestion}$	$ADIL_{inhalation}$	$ADIL_{dermal}$	$ADIL_{ingestion}$	$ADIL_{inhalation}$	$ADIL_{dermal}$
Cr	1.07E-04	1.58E-08	4.29E-11	8.60E-04	2.40E-08	2.41E-10
Ni	5.20E-05	7.65E-09	2.07E-11	4.16E-04	1.16E-08	1.16E-10
Cu	8.47E-06	1.25E-09	3.38E-12	6.77E-05	1.89E-09	1.90E-11
Cd	4.41E-06	6.48E-10	1.76E-12	3.53E-05	9.85E-10	9.88E-12
Pb	1.12E-05	1.65E-09	4.48E-12	8.99E-05	2.51E-09	2.52E-11
Site 2						
Cr	5.54E-05	8.15E-09	2.21E-11	4.43E-04	1.24E-08	1.24E-10
Ni	4.01E-05	5.89E-09	1.60E-11	3.21E-04	8.96E-09	8.97E-11
Cu	2.35E-07	3.45E-11	9.37E-14	1.88E-06	5.25E-11	5.26E-13
Cd	1.49E-06	2.19E-10	5.93E-13	1.19E-05	3.32E-10	3.33E-12
Pb	4.64E-06	6.82E-10	1.85E-12	3.71E-05	1.04E-09	1.04E-11
Site 3						
Cr	4.77E-06	7.02E-10	1.90E-12	3.82E-05	1.07E-09	1.07E-11
Ni	2.92E-05	4.30E-09	1.17E-11	2.34E-04	6.53E-09	6.55E-11
Cu	8.41E-08	1.24E-11	3.35E-14	6.73E-07	1.88E-11	1.88E-13
Cd	2.99E-07	4.40E-11	1.19E-13	2.40E-06	6.69E-11	6.71E-13
Pb	7.80E-07	1.15E-10	3.11E-13	6.24E-06	1.74E-10	1.75E-12

As site 1 and 2 soils were highly contaminated with chromium mine tailing waste, Cr and Ni were found to be major contributors to the ADIL of leachable-PTEs. Similar trends were observed in other various studies (Ghosh et al., 2023a). The probable NCR of each leachable-PTEs exposure was determined based on the HQ value. Among all three sites of the chromium mining area, the HQ values of all the leachable-PTEs for both adults and children were less than 1 (Table 14).

Table 14: Hazards quotients (HQ) and hazards indexes (HI) of leachable -PTEs for adults and children

PTEs	Adult				Child			
Site 1	$HQ_{ingestion}$	$HQ_{inhalation}$	HQ_{dermal}	**HI**	$HQ_{ingestion}$	$HQ_{inhalation}$	HQ_{dermal}	**HI**
Cr	7.17E-05	1.05E-08	7.15E-07	7.24E-05	5.73E-04	1.60E-08	4.01E-06	5.77E-04
Ni	3.47E-05	5.10E-09	3.46E-07	3.50E-05	2.77E-04	7.75E-09	1.94E-06	2.79E-04
Cu	2.12E-04	3.11E-08	2.82E-10	2.12E-04	1.69E-03	4.73E-08	1.58E-09	1.69E-03
Cd	4.41E-03	6.48E-07	1.76E-07	4.41E-03	3.53E-02	9.85E-07	9.88E-07	3.53E-02
Pb	2.81E-03	4.13E-07	8.54E-09	2.81E-03	2.25E-02	6.28E-07	4.80E-08	2.25E-02
Site 2								
Cr	3.70E-05	5.43E-09	3.69E-07	3.73E-05	2.96E-04	8.26E-09	2.07E-06	2.98E-04
Ni	2.67E-05	3.93E-09	2.66E-07	2.70E-05	2.14E-04	5.97E-09	1.50E-06	2.15E-04
Cu	5.87E-06	8.64E-10	7.81E-12	5.87E-06	4.70E-05	1.31E-09	4.38E-11	4.70E-05
Cd	1.49E-03	2.19E-07	5.93E-08	1.49E-03	1.19E-02	3.32E-07	3.33E-07	1.19E-02
Pb	1.16E-03	1.71E-07	3.52E-09	1.16E-03	9.28E-03	2.59E-07	1.98E-08	9.28E-03
Site 3								
Cr	3.18E-06	4.68E-10	3.17E-08	3.21E-06	2.55E-05	7.11E-10	1.78E-07	2.56E-05
Ni	1.95E-05	2.87E-09	1.94E-07	1.97E-05	1.56E-04	4.36E-09	1.09E-06	1.57E-04
Cu	2.10E-06	3.09E-10	2.80E-12	2.10E-06	1.68E-05	4.70E-10	1.57E-11	1.68E-05
Cd	2.99E-04	4.40E-08	1.19E-08	2.99E-04	2.40E-03	6.69E-08	6.71E-08	2.40E-03
Pb	1.95E-04	2.87E-08	5.93E-10	1.95E-04	1.56E-03	4.36E-08	3.33E-09	1.56E-03

Research conducted by Adedeji et al. (2020), based on the HQ values, the Cd and Pb in soil were determined to be 2.50E-05 and 2.42E-03, respectively. Contrastingly, Kan et al. (2021) found that the HQ values for Pb (1.85) exceeded the range of 1. The order of hazard paths for adults and children was as follows among the three sites of chromium mines: ingestion, dermal, and inhalation, respectively. Adults and children's average health risk index (HI) values in this region were below the USEPA's limit (HI > 1) (USEPA 2004), indicating no probable NCR threats (Table 14). While other studies showed that HI values for all leachable-PTEs were less than 1, that means the concentration of PTEs might pose a minute health impact on both adults and children (Alyousef et al., 2022). The risk of acquiring any type of cancer at any point in one's life as a result of having been exposed to a carcinogenic factor. When humans are exposed to soil TCLP-PTEs, including Cr, Ni, Cd, Cu, and Pb can cause cancer. CR of each PTE via three different pathways was demonstrated in Table 15.

Table 15: Carcinogenic risk information of leachable PTEs on adults and children

PTEs	Adult			Child		
Site 1	$CR_{ingestion}$	$CR_{inhalation}$	CR_{dermal}	$CR_{ingestion}$	$CR_{inhalation}$	CR_{dermal}
Cr	4.77E-05	7.90E-09	2.14E-11	1.93E-03	5.41E-08	5.42E-10
Ni	4.73E-05	6.96E-09	1.89E-11	1.70E-03	4.76E-08	4.77E-10
Cd	1.68E-06	2.46E-10	6.68E-13	6.03E-05	1.69E-09	1.69E-11
Pb	4.72E-07	6.94E-11	1.88E-13	1.70E-05	4.75E-10	4.76E-12
Site 2						
Cr	2.55E-05	4.08E-09	1.11E-11	9.98E-04	2.79E-08	2.79E-10
Ni	3.65E-05	5.36E-09	1.45E-11	1.31E-03	3.67E-08	3.68E-10
Cd	5.65E-07	8.31E-11	2.25E-13	2.03E-05	5.68E-10	5.70E-12
Pb	1.95E-07	2.86E-11	7.77E-14	7.01E-06	1.96E-10	1.96E-12
Site 3						
Cr	2.29E-06	3.51E-10	9.52E-13	8.59E-05	2.40E-09	2.41E-11
Ni	2.66E-05	3.91E-09	1.06E-11	9.58E-04	2.68E-08	2.68E-10
Cd	1.14E-07	1.67E-11	4.54E-14	4.10E-06	1.14E-10	1.15E-12
Pb	3.28E-08	4.82E-12	1.31E-14	1.18E-06	3.29E-11	3.30E-13

The results showed that children in sites 1 and 2 were more likely to get cancer through ingestion than children in site 3. The carcinogenic risk was found in this area in the following order: site 1 > site 2 > site 3, based on the CR value of each TCLP-PTE. Ni and Cr showed a higher cancer risk for children (1.70E-03; 1.93E-03) as compared with adults (4.73E-05; 4.77E-05) in this study.

4.1.10 Risk prediction of Leachable PTEs by MCS model

Additionally, the Monte Carlo Simulation (MCS) approach was employed to evaluate health risks (TCR) in order to prevent errors imposed by predictable parameters that were either overstated or underestimated. The 10^{-6} to 10^{-4} range represents the maximum tolerated level for total cancer risk (TCR) (Li et al., 2020). According to the probability distribution plot of MCS, children (1.88E-03) were more susceptible to TCR via ingestion than adults (5.08E-05) (Fig. 20).

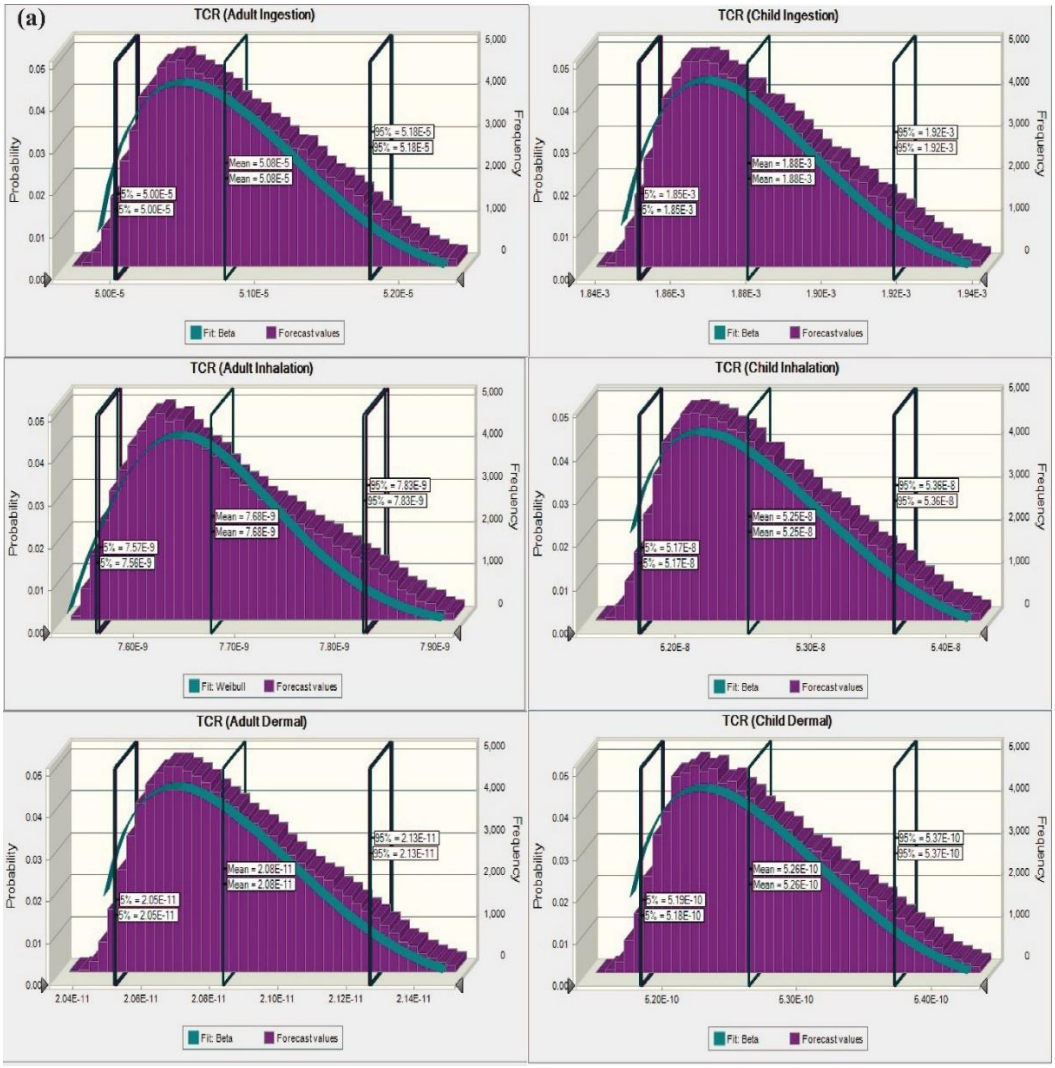

Fig. 20: Monte Carlo simulation distribution plot of leachable PTEs TCR for adults and children through body exposure pathways

Furthermore, as stated by Zeng et al. (2015), children are in a stage of development where they have reduced detoxification, toxin removal capabilities, and metabolism. Chen et al. (2023) similarly found that the carcinogenic risks linked to different routes of exposure were greater for children compared to adults. In addition, the sensitivity analysis revealed that Cr and Ni contributed to cancerous risk the most for three pathways as well as for both child and adult populations (Fig. 21).

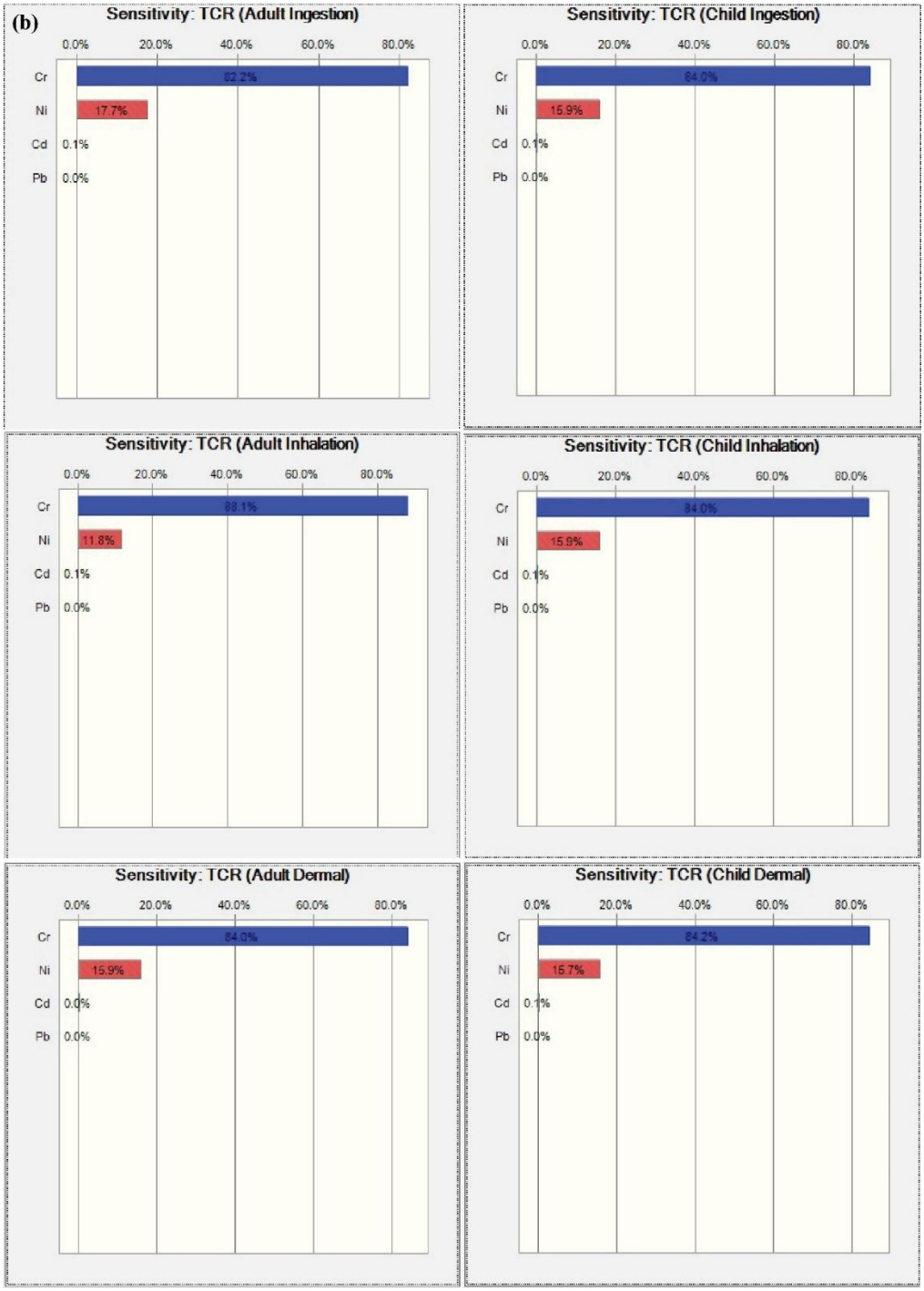

Fig. 21: Total carcinogenic risk (TCR) from leachable PTEs in adults and children showed by sensitivity plot

In contrast, Ahmad et al. (2021) and Wang et al. (2023) reported that the CR for Ni and Pb were below the permissible range in Pakistan and China, respectively. Similarly, in China and Iran, the CR of Ni has been measured to be 2.15E-03 and 1.13E-02, which exceeds the tolerable threshold of 10^{-4}. Therefore, local people in this area have the potential to cause cancer (Taghavi et al., 2024; Liu et al., 2024). For other elements like Cd, Cu, and Pb, the mean value of leachable-PTEs falls within the range of no NCR effects. Similar research regarding rising Cr and Ni concentrations in mine-impacted soil has been reported (Roy and Bhattacharya 2022). Through this research, we discovered that the persistent dumping of tailings waste close to agricultural land can accelerate the accumulation of leachable-PTEs in the soil, which could represent a threat to human health in a few decades.

4.1.11 Risk assessment from bioaccessible PTEs (HQ, HI, NCR, CR, TCR) of adult and child

Ingestion of PTEs' bio-accessible portion, which can easily be absorbed in the stomach and intestinal tract, affects human health. Hence, ingestion alone was taken into account for risk evaluation (Moreira et al., 2018). According to previously published studies (Qing et al., 2015; Wei et al., 2015), ingestion was the main exposure pathway for human health. In this work, Table 16 depicts the $ADI_{ingestion}$ and HQ for adults and children owing to PTEs exposure in mine waste-contaminated agricultural soils.

Table 16: Non- carcinogenic risk and hazard quotient values of bio-accessible PTEs (Stomach and Intestinal)

PTEs	Adult		Child		Adult		Child	
Site 1	$ADIS_{ingestion}$	$ADII_{ingestion}$	$ADIS_{ingestion}$	$ADII_{ingestion}$	$HQS_{ingestion}$	$HQI_{ingestion}$	$HQS_{ingestion}$	$HQI_{ingestion}$
Cr	5.10E-04	4.56E-04	4.08E-03	3.65E-03	3.40E-04	3.04E-04	2.72E-03	2.43E-03
Ni	3.60E-04	2.90E-04	2.88E-03	2.32E-03	2.40E-04	1.93E-04	1.92E-03	1.55E-03
Cu	4.62E-05	6.25E-05	3.70E-04	5.00E-04	1.16E-03	1.56E-03	9.25E-03	1.25E-02
Cd	5.99E-06	5.12E-06	4.79E-05	4.10E-05	5.99E-03	5.12E-03	4.79E-02	4.10E-02
Pb	1.46E-04	8.34E-05	1.17E-03	6.67E-04	3.66E-02	2.08E-02	2.92E-01	1.67E-01
Site 2								
Cr	1.56E-04	1.49E-04	1.25E-03	1.19E-03	1.04E-04	9.90E-05	8.30E-04	7.92E-04
Ni	2.51E-04	2.08E-04	2.01E-03	1.66E-03	1.67E-04	1.39E-04	1.34E-03	1.11E-03
Cu	2.68E-05	5.08E-05	2.14E-04	4.06E-04	6.69E-04	1.27E-03	5.35E-03	1.02E-02
Cd	4.56E-06	3.30E-06	3.65E-05	2.64E-05	4.56E-03	3.30E-03	3.65E-02	2.64E-02
Pb	9.81E-05	6.46E-05	7.85E-04	5.17E-04	2.45E-02	1.61E-02	1.96E-01	1.29E-01
Site 3								
Cr	8.98E-05	5.92E-05	7.18E-04	4.73E-04	5.98E-05	3.95E-05	4.79E-04	3.16E-04
Ni	4.90E-05	3.39E-05	3.92E-04	2.72E-04	3.27E-05	2.26E-05	2.61E-04	1.81E-04
Cu	1.35E-05	1.15E-05	1.08E-04	9.19E-05	3.37E-04	2.87E-04	2.69E-03	2.30E-03
Cd	1.74E-06	1.21E-06	1.39E-05	9.68E-06	1.74E-03	1.21E-03	1.39E-02	9.68E-03
Pb	4.42E-05	2.71E-05	3.53E-04	2.17E-04	1.10E-02	6.78E-03	8.83E-02	5.42E-02

In both S-phase and I-phase, the average $ADI_{ingestion}$ results for children and adults were as follows: Cr > Ni > Pb > Cu > Cd. Since the allowable limit for risk was 1, the HQ analysis of both the S-phase and the I-phase showed that there was no noncarcinogenic risk (NCR) for either adults or children (Table 17).

Table 17: Carcinogenic risk values of bio-accessible PTEs via ingestion

PTEs	Adult		Child	
Site 1	$CRS_{ingestion}$	$CRI_{ingestion}$	$CRS_{ingestion}$	$CRI_{ingestion}$
Cr	2.28E-04	2.06E-04	9.18E-03	8.21E-03
Ni	3.28E-04	2.64E-04	1.18E-02	9.49E-03
Cd	2.28E-06	1.95E-06	8.19E-05	7.01E-05
Pb	6.14E-06	3.50E-06	2.21E-04	1.26E-04
Site 2				
Cr	7.19E-05	6.73E-05	2.80E-03	2.67E-03
Ni	2.28E-04	1.89E-04	8.22E-03	6.81E-03
Cd	1.73E-06	1.25E-06	6.23E-05	4.52E-05
Pb	4.12E-06	2.71E-06	1.48E-04	9.77E-05
Site 3				
Cr	4.12E-05	2.69E-05	1.62E-03	1.07E-03
Ni	4.46E-05	3.09E-05	1.61E-03	1.11E-03
Cd	6.60E-07	4.60E-07	2.38E-05	1.65E-05
Pb	1.86E-06	1.14E-06	6.68E-05	4.10E-05

The study conducted by Ugbede et al. (2024) found that the HQ of Cd in adults and children in Nigeria was greater than 1, indicating non-carcinogenic health hazards in this area. According to Wang and Cheng's (2023) research, children in Lhasa farming soil were exposed to non-carcinogenic levels of PTEs, with ingestion being the primary mode of exposure. To forecast the uncertainty related to cancer risk in the population (both children and adults), the MCS analysis was applied. The MCS-distribution plot analysis revealed that child (7.08E-03) and adult (1.89E-04) via I-phase were more receptive to TCR than S-phase [child (8.57E-03) and adult (2.31E-04)] (Fig. 23).

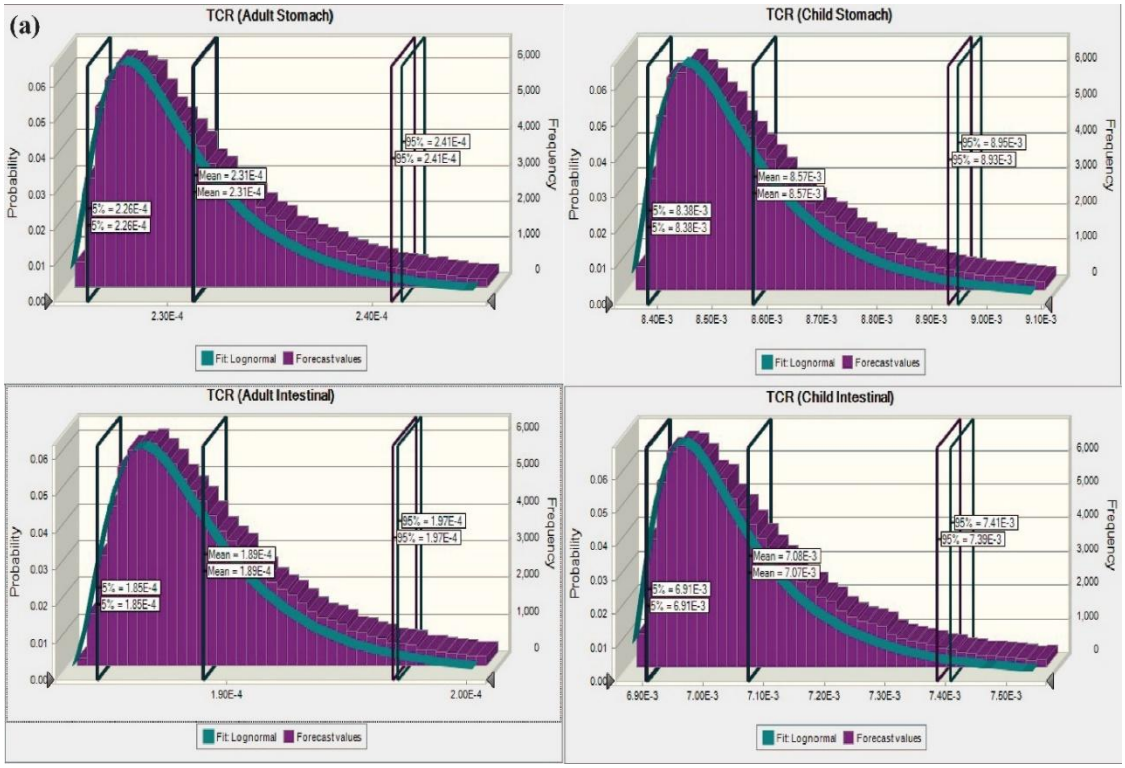

Fig. 23: Probability distribution function for bio-accessible (Stomach and Intestinal) PTEs

Reports (Yang et al., 2022) obtained that the CR for Cr and Ni exceeded the permissible range of 10^{-4}, with values of 4.39E-02 and 4.88E-03, respectively. Similarly, in this study, the maximum contribution of each PTE towards cancer risk in both phases (S and I phases) resides in Ni and Cr, according to MCS-sensitivity analysis (Fig. 24).

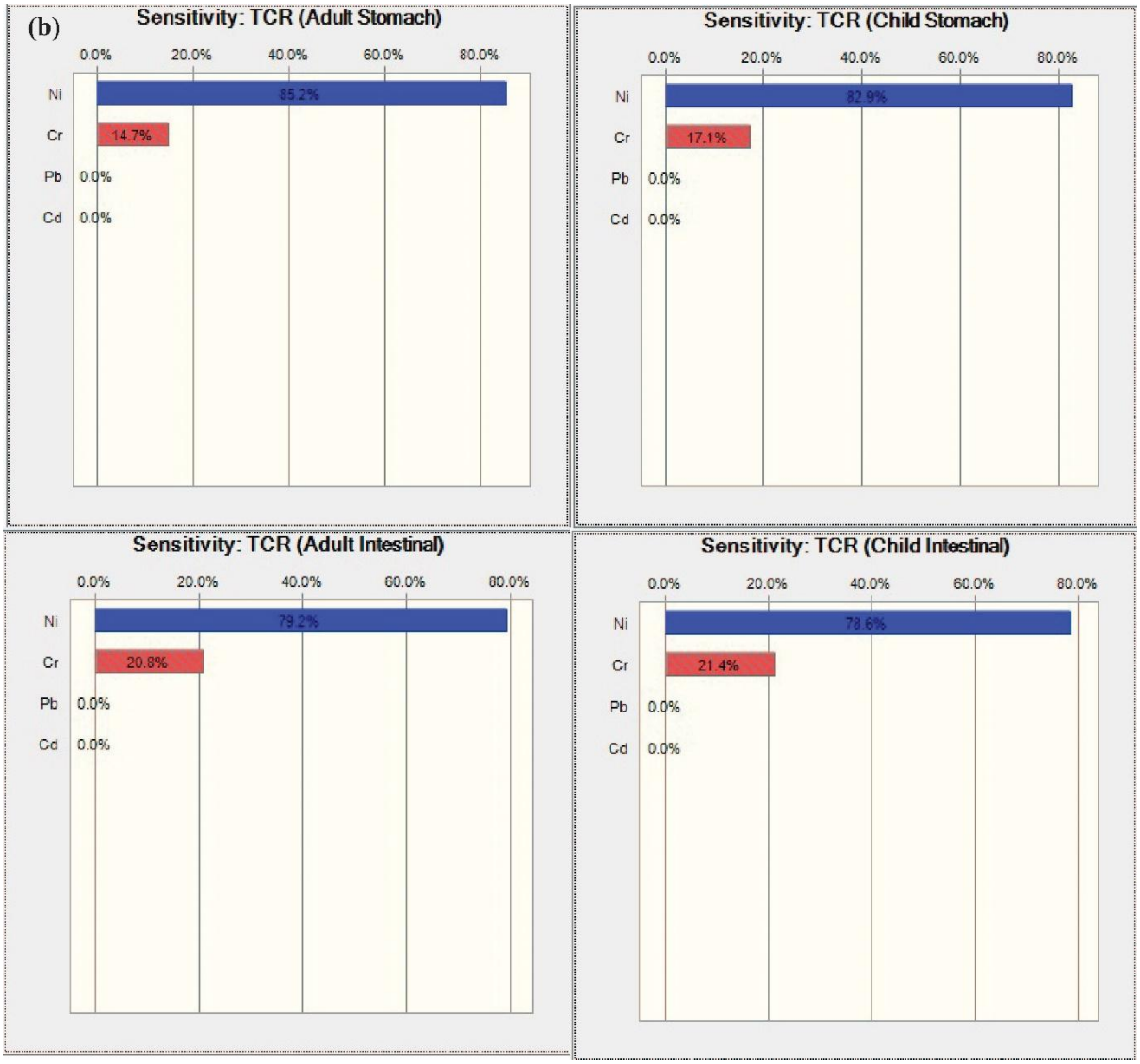

Fig. 24: Contribution of bio-accessible PTEs to adult and child (Stomach and Intestinal)

People who reside in the nearby chromium mine area were at greater risk, and their children are particularly vulnerable since they have intake the food and have a tendency to play on the agricultural field. Therefore, the risk assessment in the chromium-asbestos mines of India has to pay more consideration to PTEs exposure to Cr and Ni, especially for children. Based on the findings, the bio-accessible forms of PTEs were available for plant uptake and simultaneously posed a potential risk for ecosystems via food chains.

Since site 1 has been identified as a toxic mine tailing dumping area with high concentrations of PTEs that pose serious threats to all forms of life. This fact was established from aforementioned analysis. Also, there was no agricultural land for cultivation of crops, therefore, it was excluded from further investigation. As our key focus is the impact of PTEs on agricultural land, soil microbial community and the direct exposure of local residents to these elements in areas surrounding the mine. Consequently, only Site 2 (CAMW-contaminated agricultural site) and Site 3 (uncontaminated agricultural site) were chosen for further investigation, which includes rice sample collection, sequential extraction of PTEs, alkalinity indices and assessment of microbial activity.

4.1.12 Sequential extraction assay of PTEs and their bioavailable-spatial pattern through GIS

The distribution of PTE forms in the soil is shown in Fig. 25. The precise determination of potential toxicity was mostly based on the bioavailable fraction of PTEs, particularly the water-soluble (Ws) and exchangeable (Ex) forms. All the forms of PTEs were found to be elevated in site 2 compared to site 3. The occurrence of PTEs (Cr, Ni, Cd, Pb, and Cu) in soil demonstrates diverse patterns of distribution, ranging from easily extractable forms to more enduring and resilient forms, owing to a range of interactions with soil constituents (Bhattacharyya et al., 2008). The presence of toxic chromium-asbestos mine waste on agricultural land (site 2) resulted in the highest concentrations of bioavailable forms of Cr (Ws: 31.08 mg/kg, $p = 0.0001$; Ex: 80.76 mg/kg, $p = 0.0003$) and Ni (Ws: 13.90 mg/kg, $p = 0.0007$; Ex: 27.53 mg/kg, $p = 0.0003$) compared to others PTEs (Cd, Cu and Pb). The other predominant fractions, particularly Fe (III) and Mn (IV) oxides, exhibited the highest levels of PTEs binding, suggesting that the Ws and Ex fractions may experience a future increase due to the reductive dissolution of Fe (III)/Mn (IV). This phenomenon is anticipated as submerged paddy soils typically exist in a highly anoxic environment. The Ox-bound phases of all the PTEs exhibited a statistically significant increase inside the contaminated site. The other phases, mainly Car, Or, and Min bound PTEs, showed statistical insignificance. In contrast, the spatial distribution map reveals that the north-western region had a notable concentration of all bioavailable PTEs (Fig. 26), since mining activities affected nearby areas through the discharge of chromium-asbestos mine waste. Therefore, the findings of this study demonstrate that the bioavailable and oxide forms of PTEs (mainly Cr and Ni) were identified as the key soil stressors (Ghosh et al., 2023b).

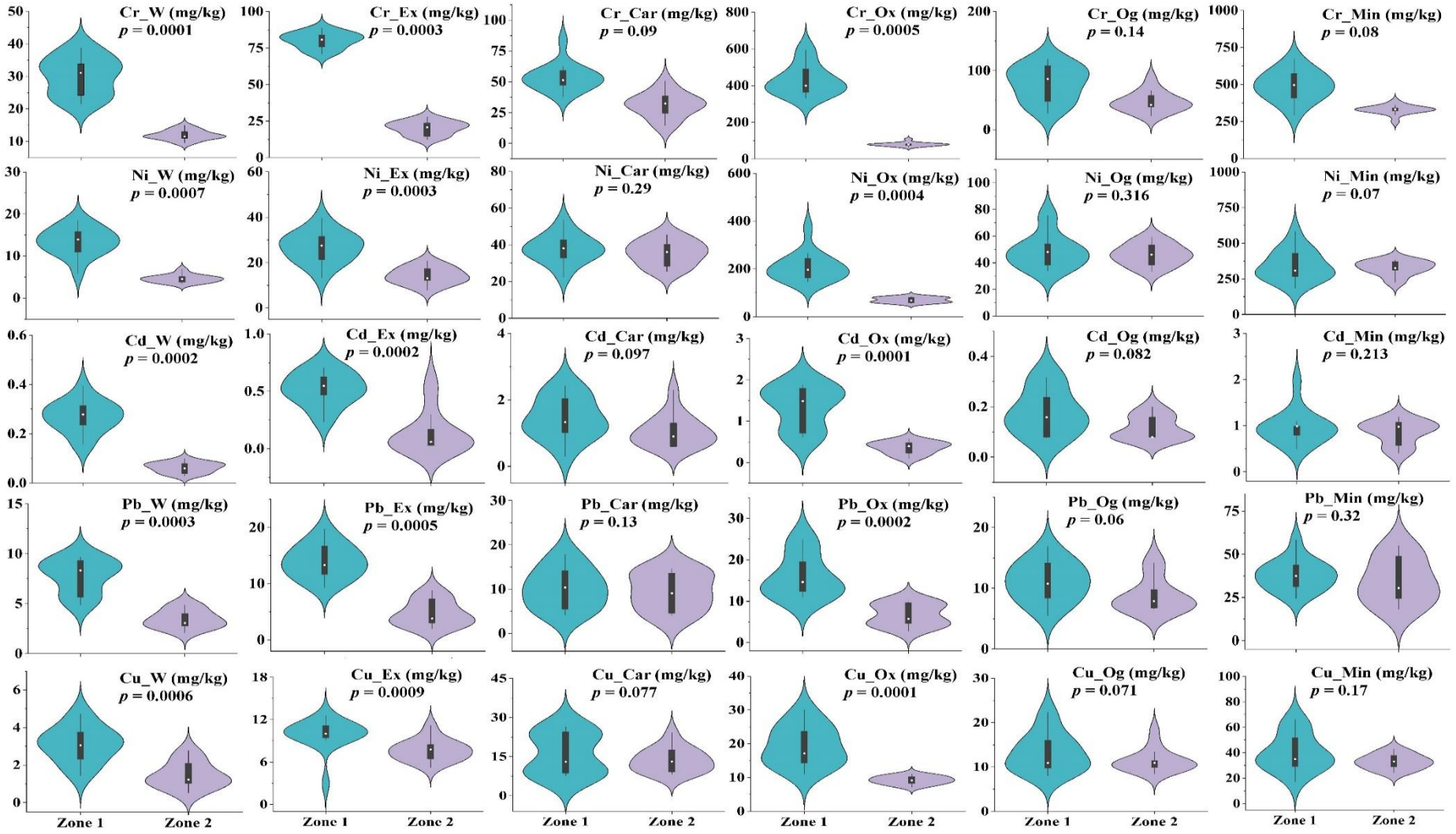

Fig. 25: Sequential extraction of PHEs from chromium-asbestos waste amended soil

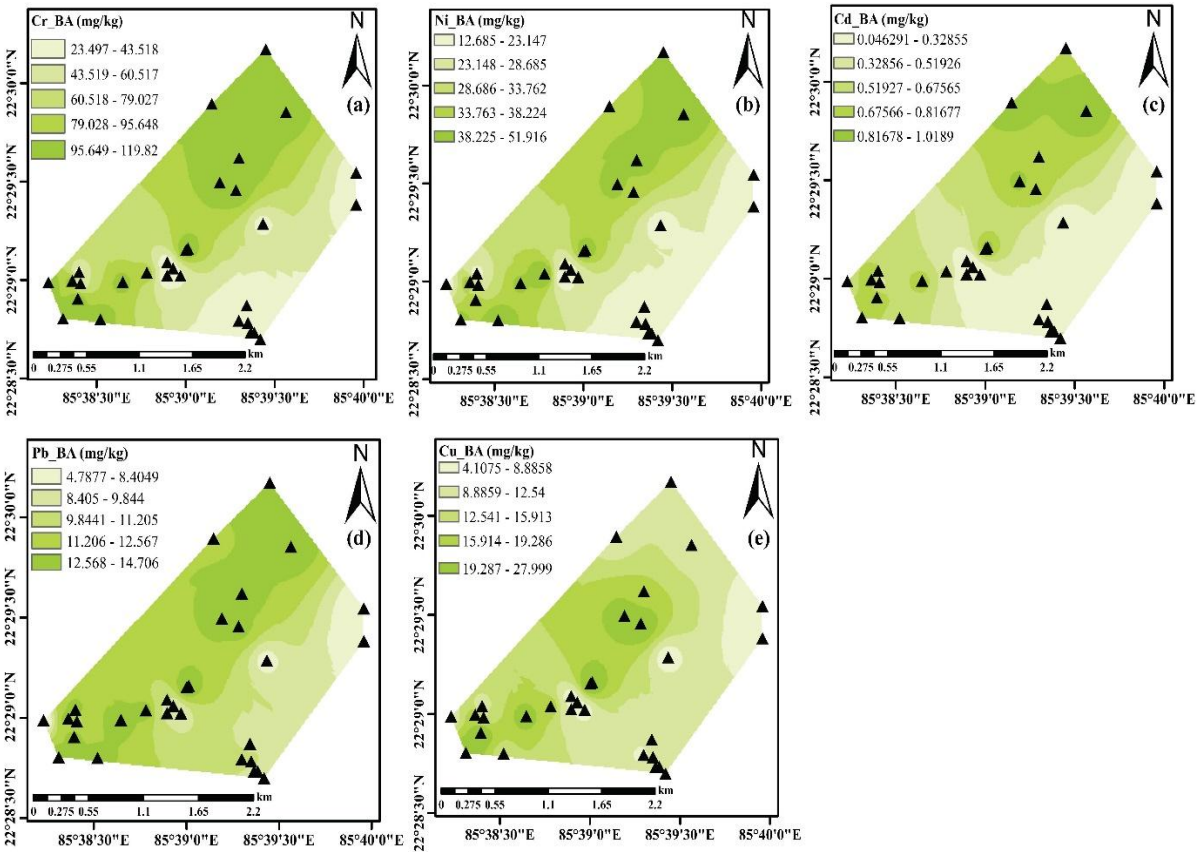

Fig. 26: Geospatial distribution of bioavailable PTEs (Cr, NI, Cd, Pb, and Cu) in the chromium-asbestos mine site

4.1.13 Total PTEs content in different parts of rice plants

As we considered site 1 as a toxic mine tailing dumping site, there was no agricultural land for cultivation of crops (basically rice), so we were only considering site 2 (contaminated site) and site 3 (uncontaminated site) for the collection of rice samples. The total concentration of PTEs in different plant parts of rice including root, shoot, and raw grains was estimated from site 2 and site 3 and depicted in Fig. 27. The results of site 2 showed that PTEs concentration in the roots and shoots was significantly above the permissible limit (WHO 1996) than in site 3 [{Cr_{root} (p = 0.005), Ni_{root} (p = 0.003), Cd_{root} (p = 0.0001), Pb_{root} (p = 0.0003), Cu_{root} (p = 0.0002)} and {Cr_{shoot} (p = 0.00001), Ni_{shoot} (p = 0.0002), Cd_{shoot} (p = 0.0001), Pb_{shoot} (p = 0.0005), Cu_{shoot} (p = 0.0005)}]. In this context, PTEs concentration in raw rice grain is also significantly higher in site 2 than in site 3 [Cr_{grain} (p = 0.0003), Ni_{grain} (p = 0.0001), Cd_{grain} (p = 0.0003), Pb_{grain} (p = 0.0005), Cu_{grain} (p = 0.0001)]. Nawab et al., (2016) and Khan et al., (2018) their findings result supported our observation. A positive correlation was observed between bioavailable-DTPA extractable PTEs concentration and rice grains [Cr_{DTPA} (r = 0.95***),

Ni_{DTPA} (r = 0.91***), Cd_{DTPA} (r = 0.92***), Pb_{DTPA} (r = 0.95***) and Cu_{DTPA} (r = 0.93***)]. Positive correlation results showed that in site 2 PTEs accumulation in rice grain is higher than site 3. Thus, the findings were in line with reports of Zhou et al., (2014) which was stated that a strong correlation between bioavailable forms of toxic PTEs and rice grain uptake of PTEs. Rice grain in site 2 contain high levels of PTEs, mainly Cr and Ni, which may pose a threat to human health and the food chain.

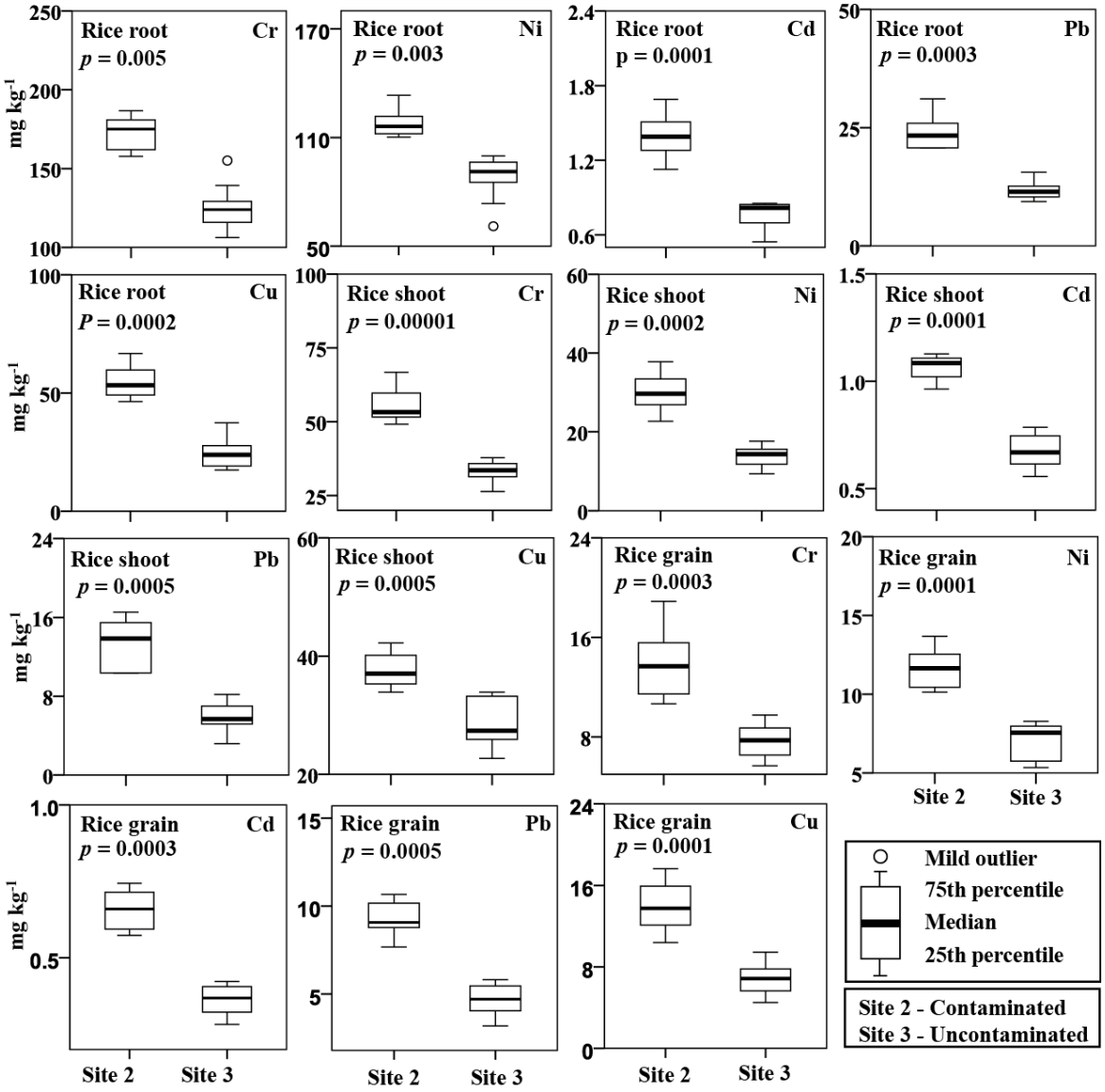

Fig. 27: Box-whisker plot demonstrating the comparison between the two sites in terms of PTEs content in rice root, shoot, and grain

4.1.14 FIAM (Free ion activity model) of PTEs and risk assessment through FIAM-HQ

Prediction of PTEs (Cr, Ni, Cd, Pb, and Cu) uptake by rice grains in the Roro mines area was done by solubility-free ion activity model (FIAM). Crop-specific model parameters (C, β1, and β2), and the prediction coefficient of FIAM are demonstrated (Table 18 and Fig. 28).

Table 18: FIAM parameters for predicting uptake of PTEs by rice as a function of pH, Walkley Black organic-C and DTPA extractable PTEs, FIAM-HQ for intake of PTEs through consumption of rice grains grown on mine waste contaminated soils, and dietary risk (SAMOE-TCR and SAMOE) of PTEs from mine-contaminated rice grains. The upper threshold level for PTEs: (a)Singh et al. 2018;(b) Kohzadi et al. 2019

Potential toxic elements (PTEs)	Constant	β1	β2	R^2	FIAM-HQ	SAMOE-TCR	PTEs level in Grain (mg/kg)	SAMOE	Upper threshold level for PTEs(mg/kg)
Cr	-2.834	0.222	0.112	0.997	1.50E+00	3.08E-02	10.477	0.001	1[a]
Ni	-2.582	0.203	0.078	0.989	1.32E+00	9.25E-02	9.253	0.002	1.63[b]
Cd	-1.802	0.199	0.160	0.987	1.43E-03	1.12E-03	0.500	0.007	0.3[a]
Pb	-2.952	0.211	0.195	0.979	5.55E+00	3.40E-04	6.800	0.008	5[a]
Cu	0.493	-0.363	0.712	0.693	5.82E-02		10.180	0.035	30[a]

Results revealed that variability of PTEs in rice grain could be interpreted by solubility-free ion activity model (FIAM) based on soil pH, soil organic carbon (OC) and DTPA extractable PTEs. Previously it was reported by Meena et al., (2016) that soil pH and soil OC are the crucial factors that govern the solubility of PTEs in polluted areas. This model (FIAM) throws light on the fact that without measuring the solubility of metalloids, it describes the relocation of PTEs from soil solution to plant. Further, pH and OC mainly controlled the solubility of metalloids (Golui et al., 2017; Mandal et al., 2019; Raj et al., 2022). In this study, β1 and β2 values in the FIAM model are positive for all the PTEs except β1-Cu. As evidenced by model parameters β1 and β2 (positive value), the transfer of PTEs from soil to rice grain is negatively affected by pH and OC. Therefore, PTEs content in rice grain will decrease as either increase in pH or OC. In Roro mine, PTEs solubility is significantly higher in site 2 as compared with site 3 due to pH and OC content decreasing in site 2 and increasing in site 3. So PTEs are available for uptake in rice grain. Numerous studies showed similar results between the mobility of metalloids and pH and OC (Golui et al., 2017; Mandal et al., 2019).

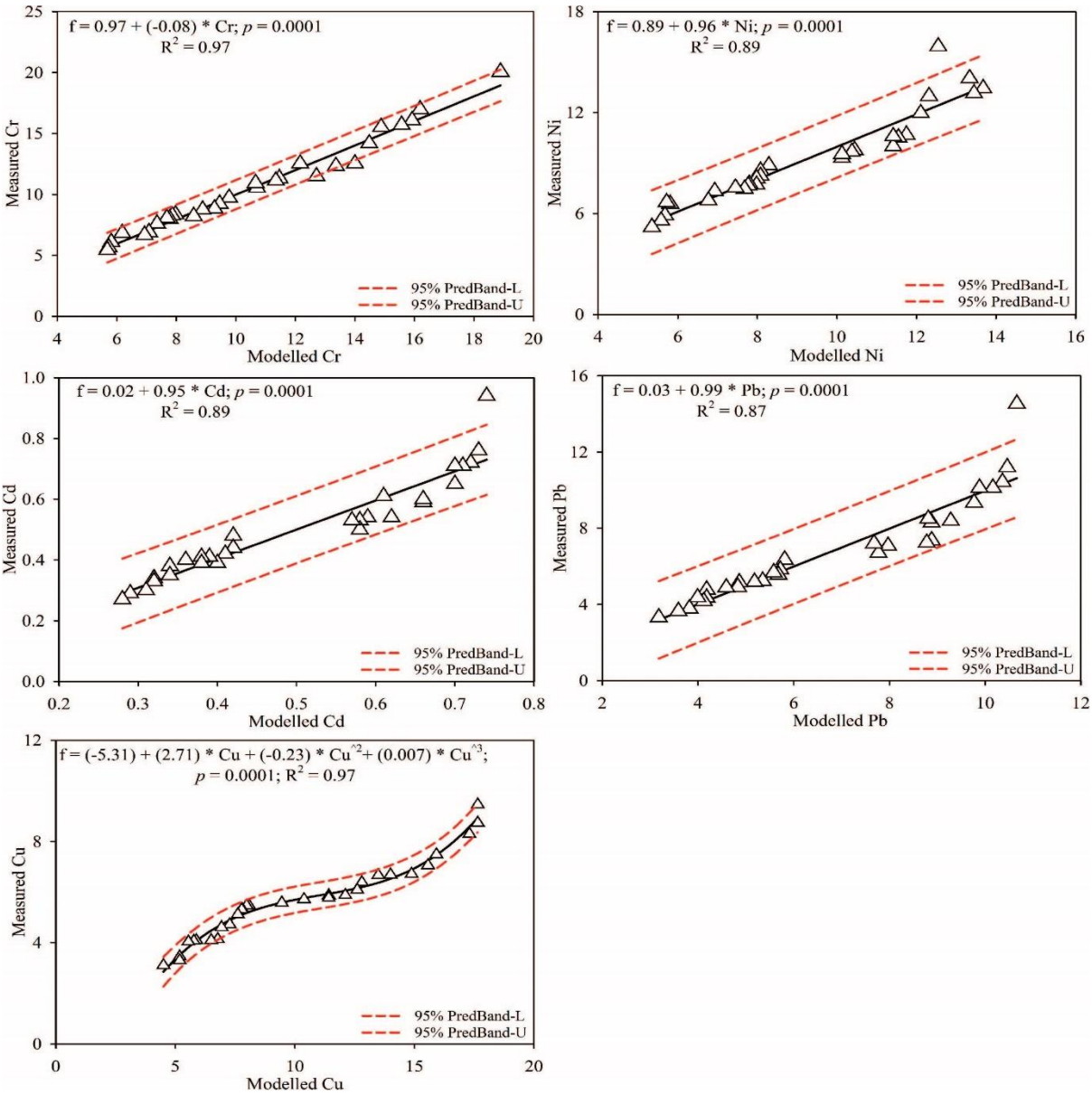

Fig. 28: FIAM analysis showed the comparison between measured and predicted PTEs (Cr, Ni, Cd, Pb and Cu) content in rice grain in Chromium-asbestos mine waste contaminated soil

This study determined the human health risk associated with PTEs uptake in rice grain by using the FIAM model's hazard quotient (HQ). Among the staple foods of India, rice contributes a significant portion of the diet. In light of this, the safe limit of FIAM-HQ for staple food (rice) has been set at 0.5 (Raj et al., 2022). Rice grains are considered to pose a health menace to humans when FIAM-HQ > 0.5. In Table 18, the average value of FIAM-HQ for Cr, Ni, and, Pb are 1.50, 1.32, and Pb (5.55). These results indicated that the hazard quotient values are higher than the safe (FIAM-HQ < 0.5) for Cr, Ni, and, Pb except Cd (1.43E-03) and Cu (5.82E-02). So, human consumption of rice grown on these agricultural soils of Roro mines may not

be recommended. Similar work has been done by Golui et al., (2021) that, wheat grown on PTEs contaminated soil is not recommended for human consumption predicted by FIAM-HQ.

4.1.15 Risk thermometer and dietary exposure assessment through SAMOE

The daily exposure of humans to PTEs is assessed in order to understand possible health risks. Through the application of a 'Risk thermometer', human health risk has been estimated from food. Fig 29 shows the 'Risk thermometer' for PTEs in raw rice grain, along with the SAMOE value, risk class, and concern level. The Risk thermometer scale is used to measure the PTEs toxicity mainly Cr and Ni in raw rice grains and the results indicate that the raw rice grain accounts for high health risk (Class 5) [Cr_{SAMOE}: 0.001; Ni_{SAMOE}: 0.002; Cd_{SAMOE}: 0.007; Pb_{SAMOE}: 0.008] for humans. But Cu content in rice grain shows moderate to high risk (Cu_{SAMOE}: 0.035). Apparently, the consumption of rice imposes health risks for human beings in this chromium-asbestos mines area due to the deposition of mine waste, high Cr and Ni concentrations in the rice grain as well as in the soil are observed (Kumar and Maiti, 2015). The experiment indicates that rice consumption may not be safe for humans and prolonged intake of this rice grain may lead to Cr, Ni, Pb and Cd poisoning in near future.

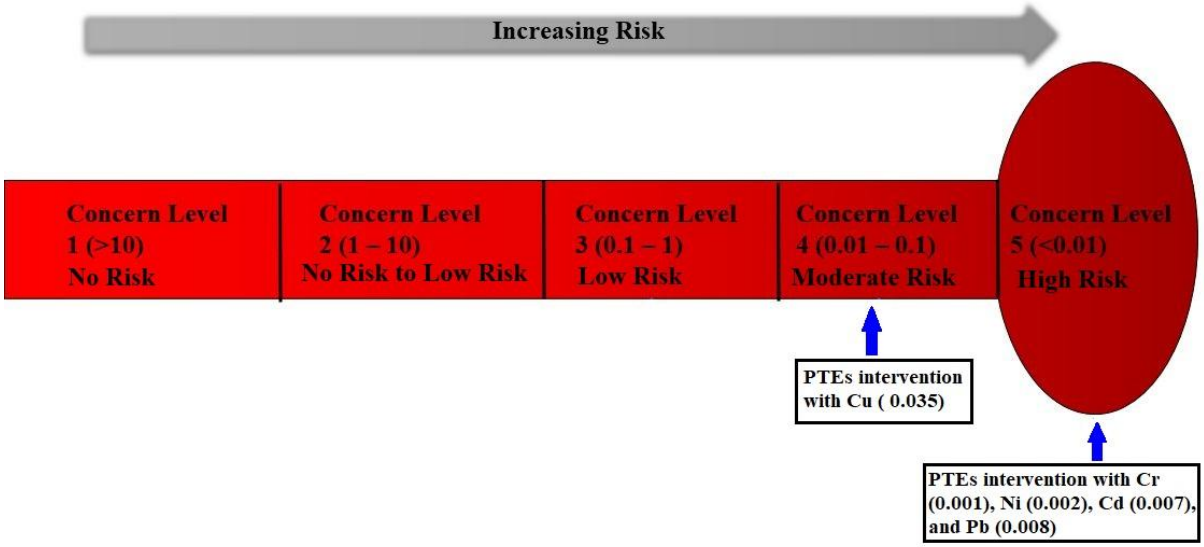

Fig. 29: Risk thermometer scale shows the risk of PTEs (Cr, Ni, Cd. Pb and Cu) through consumption of rice grown on Chromium-asbestos mine waste contaminated soil

Assessment of SAMOE-target cancer risk (SAMOE-TCR) through consumption of contaminated rice grain was reported in Table 18. The SAMOE-TCR of rice grain value was significantly higher for Cr (3.08E-02), Ni (9.25E-02) and Cd (1.12E-03) than the tolerable limit of 10^{-4} except Pb (3.40E-04) (Li et al., 2020). In our study, we observed that the risk of cancer associated with rice grains from the Roro mine is high. Researchers have reported an increased

risk of cancer occurrence through dietary exposure to PTEs (Cr, Ni, Cd, Pb, and Cu) (Kormokar et al., 2022).

4.1.16 PTEs content (total and bioaccessible forms) in different plant parts of rice

In the chromium-asbestos mine region, site 1 was a toxic mine tailing disposal site, so no rice crops were cultivated there; hence only sites 2 and 3 were considered for the collection of rice grain samples. In this scenario, total PTEs concentrations in different portions of rice (H, WH, BR, ST) can vary depending on various parameters like variety, origin, and cooking process used (Mandal et al., 2019). Before cooking, the husk was removed from the raw rice grain. In site 2, all the total PTEs concentrations especially, Cr and Ni in rice grain decreased, by 30%-45%, 37%-53% respectively, and for other element concentrations (Cd: 55%-78%, Pb: 50%-66% and Cu: 58%-82%) decreased after the removal of the husk as shown in Fig. 30.

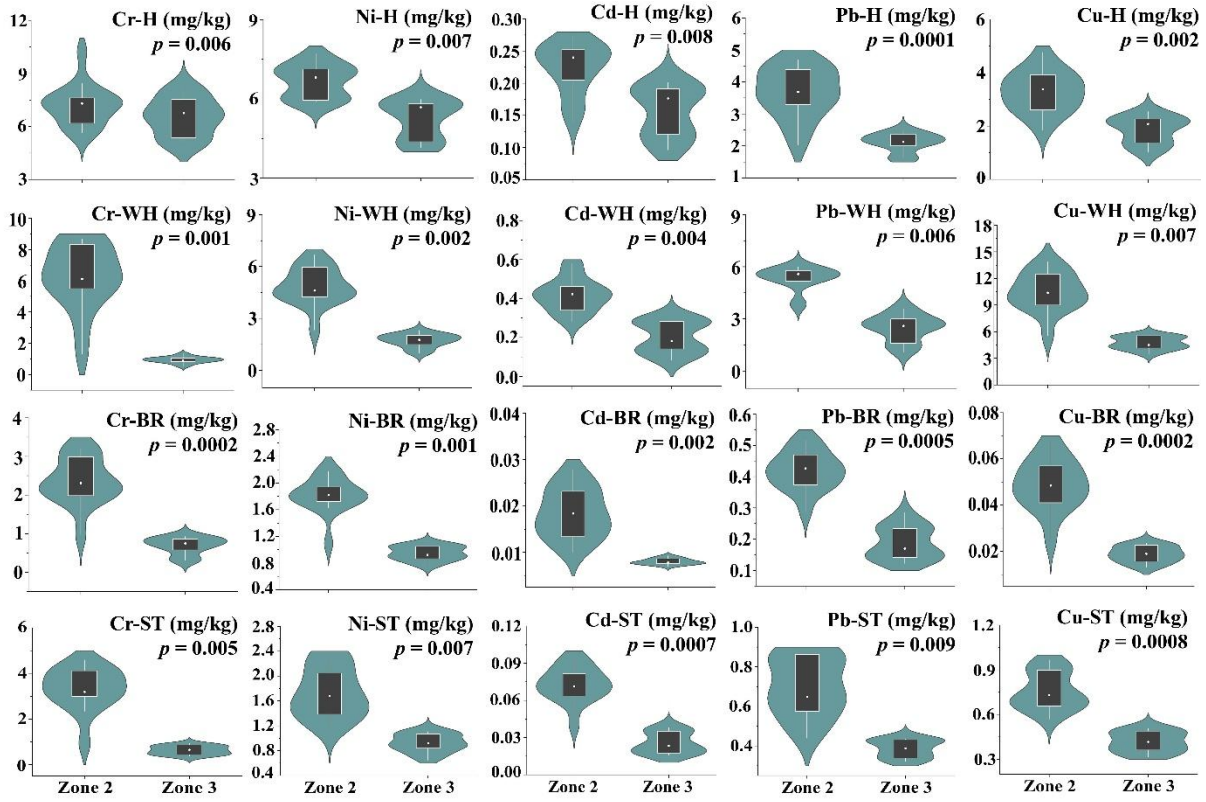

Fig. 30: Violin plots compared PTEs in rice sections (husk-H, without husk-WH, boiled rice-BR, and starch-ST) between the two sites. Here, Zone 1= Site 1, Zone 2 = Site 2, and Zone 3: Site 3

Similarly, following the removal of the husk, the concentrations of all the bioaccessible PTEs, particularly Cr and Ni in rice grain, dropped by approx. 46%, 63%, respectively in the S-phase and 47%, 42% in the I phase (Fig. 31, 32). In accordance with the traditional approach, at the time of cooking, rice was dissolved in excess water and after that, surplus water was drained off in the form of starch. To assess the real risk posed by consuming BR, we also measured the PTEs concentration in dry BR and ST as depicted in Fig. 30.

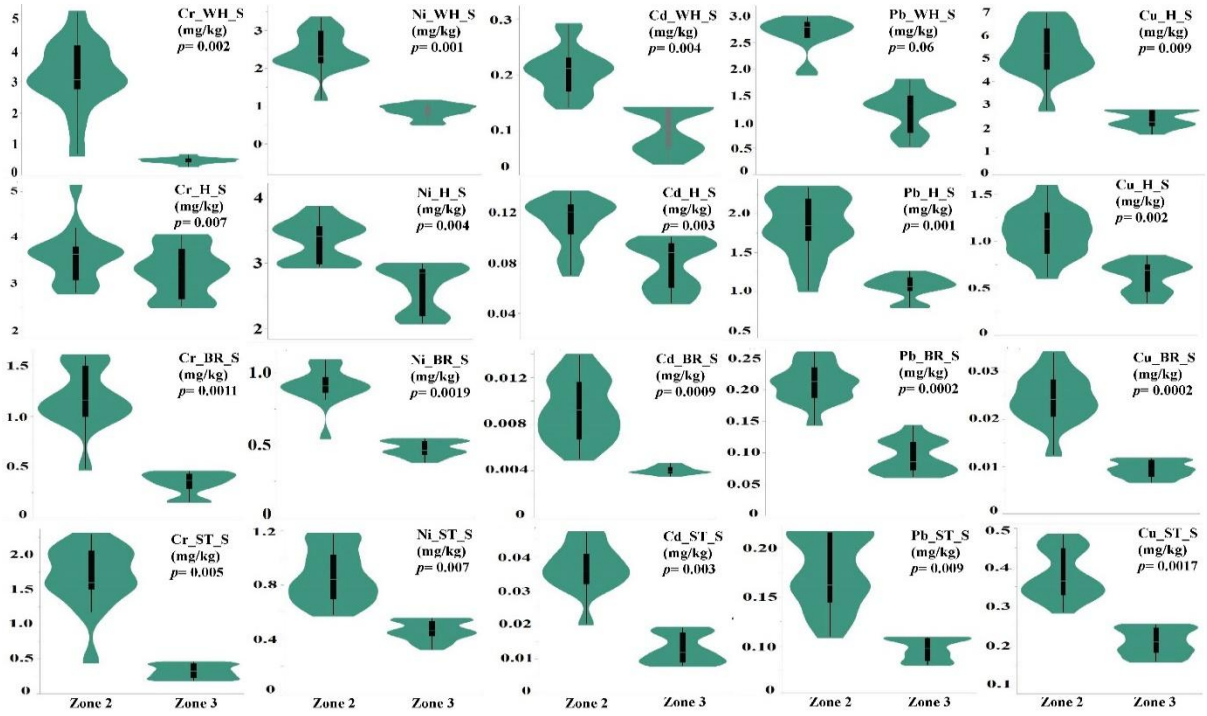

Fig. 31: The violin graphs illustrate the concentration of bioaccessible PTEs (S-phase) in several parts of rice (husk-H, without husk-WH, boiled rice-BR, and starch-ST) at two different zones. Zone 2 = Site 2, and Zone 3: Site 3

Post-cooking, total PTEs concentration in dry BR decreased by 27%-51% for Cr, 50%-75% for Ni, and 85%-90% for other elements (Cd, Pb, and Cu) in site 2. Concurrently, the percentage of bioaccessible PTEs in dry BR reduced by 62%–80% for Cr and Ni for both phases. As a result, mainly Cr and Ni concentrations in rice (WH) and BR were above the permissible limit of raw rice in the contaminated site (site 2). A similar type of study has been done in the case of As, where the arsenic concentration in raw and cooked rice was significantly higher in contaminated site samples than in uncontaminated site samples (Mridha et al., 2022). In starch, PTEs concentration was determined and depicted in Fig 30. This study also found that the supernatant liquid (ST) contained a higher amount of Cr and Ni in site 2 as compared with site

3. t-test statistical analysis suggested that for rice PTEs content, a significant difference was observed in contaminated and uncontaminated sites.

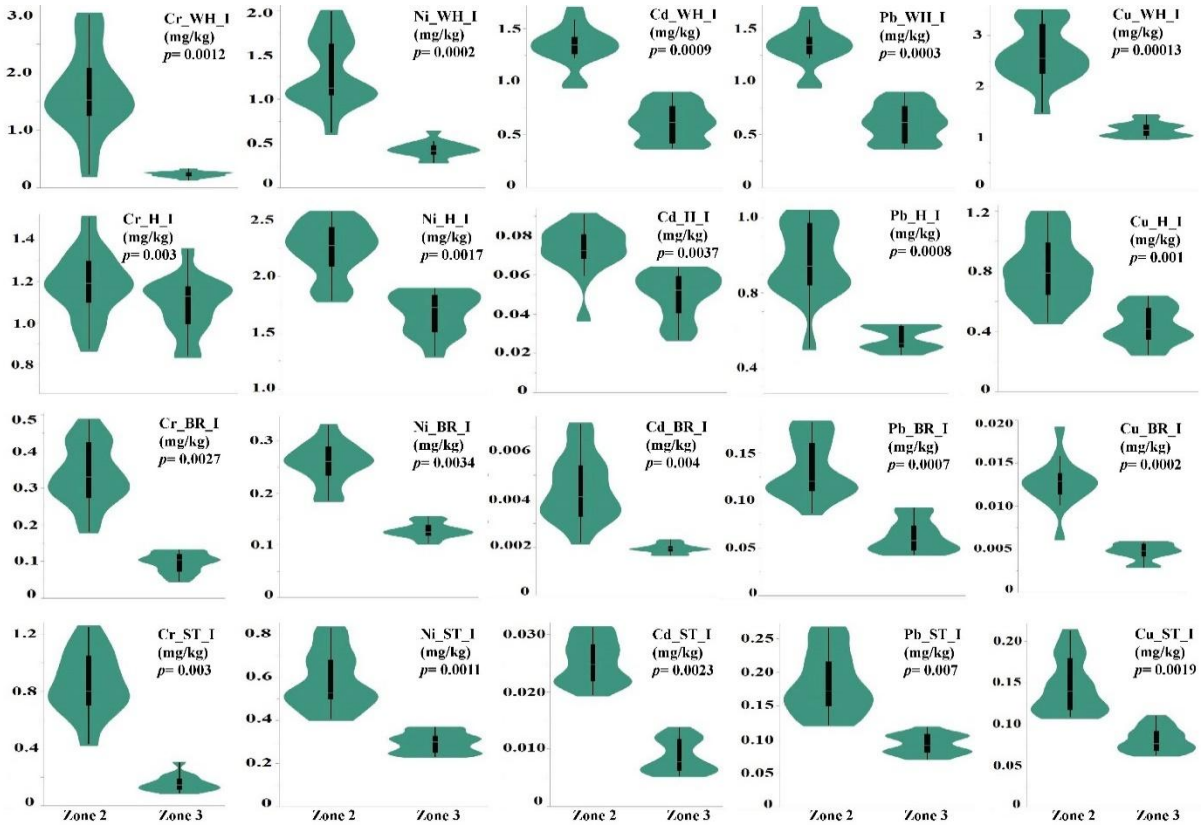

Fig. 32: The violin plots depict the levels of bioaccessible PTEs (I- phase) in various components of rice (husk-H, without husk-WH, boiling rice-BR, and starch-ST) at two distinct zones (Zone 2 = Site 2; Zone 3 = Site 3)

A highly significant positive correlation (>0.80***) was observed between bio-accessible fractions of PTEs (S and I phases) concentration and different rice grain portions (Fig. S4). TCLP leachable-PTEs concentration and different rice grain parts also showed a significant positive correlation with each other (Fig. 10). A strong correlation was reported earlier between bioavailable forms of toxic PTEs and rice grain uptake of PTEs (Zhou et al., 2014; Ghosh et al., 2024). Rice grain and cooked rice contain high levels of PTEs, mainly Cr and Ni, which may pose a risk to human health and the food chain. Similar results were found in the phyto-available potions of metals in wheat and spinach (Golui et al., 2020).

4.1.17 Health risk evaluation through ingestion of rice (WH and BR)

In India, food intake is predominantly centered around rice, considered the main carbohydrate source (Kumar et al., 2024). Prior research has demonstrated that rice exhibits a propensity for

PTEs at greater concentrations in comparison to other crops (Khanam et al., 2020). In this study, Table 19 depicts the health risk assessment (carcinogenic and non-carcinogenic) through rice consumption for adults.

Table 19: Non-carcinogenic risk, Hazards quotients (HQ), and Carcinogenic risk values of rice-PTEs (without husk-WH, and boiled rice-BR) values on adults of the studied area

WH-PTEs	Adult			BR-PTEs	Adult		
Site 2	$ADIR_{ingestion}$	$HQR_{ingestion}$	$CRR_{ingestion}$	**Site 2**	$ADIR_{ingestion}$	$HQR_{ingestion}$	$CRR_{ingestion}$
Cr	2.78E-04	1.85E-04	1.28E-04	**Cr**	1.04E-04	6.96E-05	4.89E-05
Ni	2.15E-04	1.44E-04	1.48E-04	**Ni**	8.07E-05	5.38E-05	6.14E-05
Cu	4.66E-04	1.16E-02		**Cu**	2.17E-06	5.43E-05	
Cd	1.85E-05	1.85E-02	5.85E-06	**Cd**	8.19E-07	8.19E-04	2.28E-07
Pb	2.37E-04	5.94E-02	8.56E-06	**Pb**	1.86E-05	4.65E-03	6.50E-07
Site 3				**Site 3**			
Cr	4.16E-05	2.77E-05	1.96E-05	**Cr**	3.07E-05	2.05E-05	1.45E-05
Ni	7.68E-05	5.12E-05	6.42E-05	**Ni**	4.22E-05	2.81E-05	3.66E-05
Cu	2.10E-04	5.25E-03		**Cu**	8.33E-07	2.08E-05	
Cd	8.98E-06	8.98E-03	2.92E-06	**Cd**	3.55E-07	3.55E-04	1.30E-07
Pb	1.10E-04	2.75E-02	4.06E-06	**Pb**	8.32E-08	2.08E-03	3.06E-07

The findings indicated that the *ADIR* values for Cr and Ni in site 2 for WH-rice were 2.78E-05 and 2.15E-05, respectively, whereas the values for BR-rice were 1.04E-05 and 8.07E-06, respectively. The assessment of the non-carcinogenic risk linked to PTEs in rice parts for adults revealed that the hazard quotients (HQ) were below 1 for both WH and BR rice. Thus, consuming rice in the studied area (site 2 and site 3) was not related to a non-carcinogenic risk of toxic PTEs. The elevated levels of soil PTEs may facilitate the transfer of these elements into the food chain via the intake of rice (both WH and BR), leading to detrimental effects for both animals and humans (Chowdhury et al., 2022). Similarly, Bhatti et al., (2020), Yang et al., (2022), and Neisi et al., (2024) obtained comparable findings for rice, wheat, and maize, accordingly. Pb and Cd were determined to be related to the highest HQ values for BR rice and WH rice. According to Setia et al. (2021) the concentration of Cd and Cr in rice grown in India surpassed an HQ value of 1. The findings indicate that consuming rice cultivated in the region might lead to non-carcinogenic health hazards. The HQs for Cd, Ni, and Pb in wheat from China are 2.81E-02, 3.88E-02, and 2.51E-02, respectively. These PTEs pose a non-carcinogenic risk for adults (Chen et al., 2020). In this study, the assessment of the cancer-causing risk posed by PTEs in rice (both WH and BR in site 2) revealed that the CRs for both groups were found to be above $1*10^{-6}$ in case of Ni and Cr. The agricultural land of this studied

area was contaminated by toxic PTEs as a result of mining activities, and the ingestion of rice in this region might potentially cause carcinogenic risks to both humans and animals. Similarly, Pirsaheb et al. (2021) conducted a study revealing that the region of Iran is unsuitable for rice cultivation due to the presence of elevated concentrations of PTEs, which represent a threat to food safety. Cd, and Ni are identified as the PTEs that have the greatest risk of causing cancer in this region. Likewise, Caicedo-Rivas et al. (2022) and Yang et al. (2022) reported similar findings to rice and maize in the Colombian Pacific and China. Hence, the long-term ingestion of rice in this chromium-asbestos mine area holds the potential to induce cancer in people in the foreseeable future.

4.1.18 Dietary risk assessment through rank-based approach

The Swedish National Food Agency has exhibited a new procedure for risk characterization termed “Risk Thermometer” (Sand et al., 2015). The average PTEs concentration values of H, WH, BR, and ST were taken into account in determining risk factors. The calculations related to the 'Severity Adjusted Margin of Exposure' (SAMOE) value of each PTE, as well as their risk of class and concern levels, have been shown in Table 20.

Table 20: Dietary health risk assessment of rice components using SAMOE and SAMOE-TCR

	Husk		Rice (Without husk)		Boiled rice		Starch	
PTEs	**SAMOE**	**SAMOE-TCR**	**SAMOE**	**SAMOE-TCR**	**SAMOE**	**SAMOE-TCR**	**SAMOE**	**SAMOE-TCR**
Cr	0.001	2.02E-02	0.007	1.06E-02	0.011	4.47E-03	0.010	5.83E-03
Ni	0.003	5.96E-02	0.007	4.55E-02	0.013	1.38E-02	0.014	1.33E-02
Cd	0.017	4.25E-04	0.013	6.92E-04	0.277	2.95E-05	0.086	1.10E-04
Pb	0.019	1.44E-04	0.016	1.96E-04	0.204	1.51E-05	0.103	2.71E-05
Cu	0.136		0.047		11.522		0.573	

Depending on their PTEs concentration, the various rice components exhibited distinct levels of risk that ranged from class 3 to class 5, except Cu (class 1) in boiled rice. The findings show that rice (WH) and husk (H) ($H_{CrSAMOE}$: 0.001, $H_{NiSAMOE}$: 0.003; $WH_{CrSAMOE}$: 0.007; $WH_{NiSAMOE}$: 0.007) account for significant health risk (Class 5). In case of boiled rice and starch, the moderate risk (class 4) was observed for Cr and Ni. When compared to rice (WH), the SAMOE value of each PTE for the boiling rice showed a precise declining trend. Rice parts all demonstrated a moderate to low risk for Pb, Cu, and Cd, as shown in Fig. 33. According to Banerjee et al. (2023), substantial quantities of Cr and Ni have been found in both the rice and the soil, suggesting that consuming rice poses health hazards to populations that reside near

chromium-asbestos mines. Similarly, the SAMOE-TCR value of different rice portions was significantly higher for [H: Cr (2.02E-02), Ni (5.96E-02); WH: Cr (1.06E-02), Ni (4.55E-02); BR: Cr (4.47E-03), Ni (1.38E-02); and ST: Cr (5.83E-03), Ni (1.33E-02)] than the tolerable limit of 10^{-4}, with the exception of Cd and Pb. From this experiment, ingesting rice may not be safe (causing cancer risk) for humans, and long-term intake of this cooked rice, starch may result in poisoning with Cr, Ni, Pb, and Cd in the future.

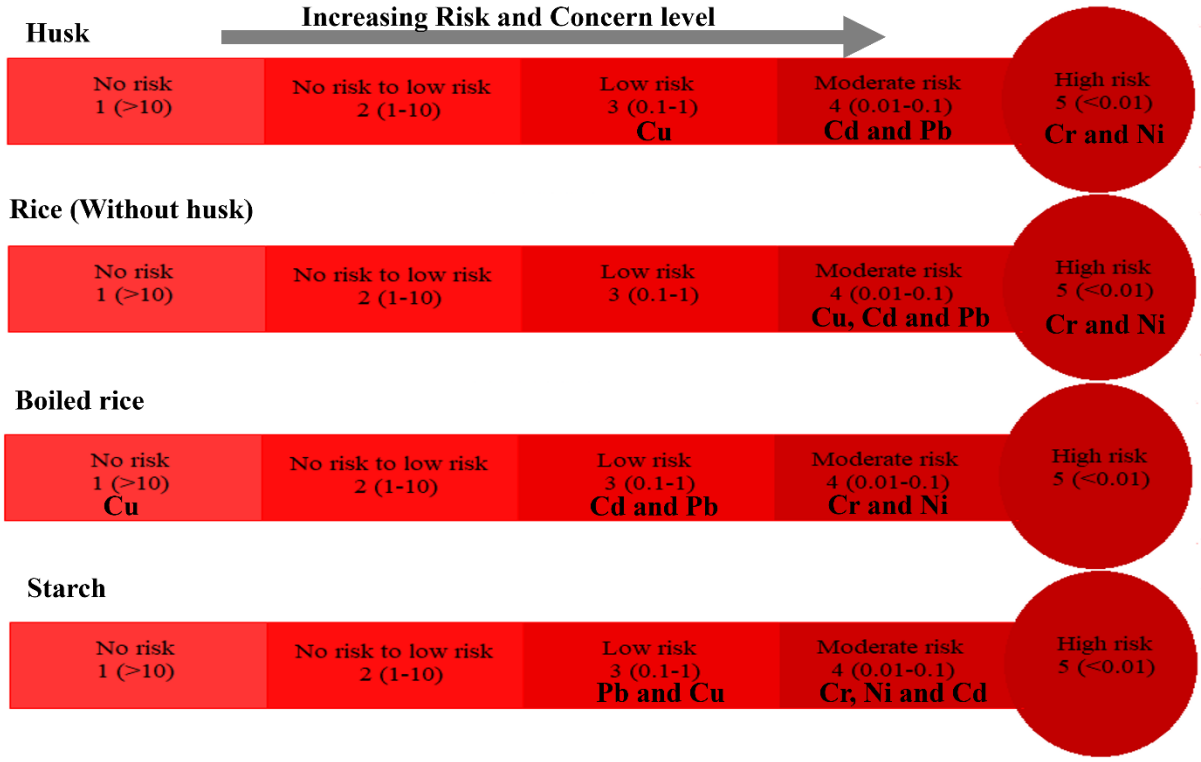

Fig. 33: Risk thermometer scale illustrates the risk of PTEs (Cr, Ni, Cd, Pb, and Cu) in rice (husk, without husk, boiling rice, starch) produced on Chromium-asbestos mine waste polluted soil

Simultaneously, the Fuzzy-TOPSIS multi-criteria decision-making (MCDM) approach was utilized in order to discover the best possible alternatives (PTEs), considering the PTEs concentrations found in rice portions (husk, without husk, boiled rice and starch). For the purpose of this experiment, the alternatives "A = Cr, Ni, Cd, Pb, Cu" were evaluated based on the criteria "Husk, without husk rice, boiled rice, starch." The ideal best and ideal worst values were shown in Table 21, and the criteria weights of the estimated concentration of PTEs from rice portions were calculated through the entropy technique as follows: [site 2: 0.163, 0.149, 0.424, 0.262; and site 3: Wj = 0.202, 0.214, 0.415, 0.167], respectively. From Table 21, the

order of PTEs accumulation in rice parts was observed in site 2 (Cr > Ni > Cu > Pb > Cd) and in site 3 (Ni > Cr > Cu > Pb > Cd).

Table 21: Overall performance score values and rank (Fuzzy-TOPSIS) of different PTEs contribution to rice

	Site 2				Site 3			
PTEs	**Si+**	**Si-**	**Pi**	**Rank**	**Si+**	**Si-**	**Pi**	**Rank**
Cr	0.113	0.401	0.780	1	0.227	0.254	0.528	2
Ni	0.174	0.282	0.619	2	0.162	0.356	0.687	1
Cd	0.410	0.104	0.203	5	0.389	0.146	0.273	5
Pb	0.334	0.102	0.234	4	0.292	0.155	0.346	4
Cu	0.372	0.130	0.259	3	0.334	0.208	0.384	3

Based on the ranking of the performance scores (Pi), Cr (0.78) and Ni (0.61) were found to be the primary contributors to the health risk in the rice portions found in site 2. Our results were in line with Saif-Ud-Din et al. (2022), who assessed risk based on the accumulation of PTEs in various food sources.

4.1.19 PTEs Influence on protein and amylose content of rice sample (without husk)

In site 2, the agricultural land was severely contaminated with toxic PTEs due to the deposition of chromium mine tailings. Hence, the rice grain (WH) from the contaminated site accumulates a considerable level of toxic PTEs. Generally, protein supplies nutrients (amino acids), while amylose regulates whether cooked rice will be sticky or firm (Nakamura et al., 2016). The rice sample mainly grown in site 2 ($protein_{mean}$: 1.76; $amylose_{mean}$: 12.13) region showed significantly ($p_{protein}$: 0.006, $p_{amylose}$: 0.002) lower content of protein and amylose as compared with site 3 ($protein_{mean}$: 5.31; $amylose_{mean}$: 26.72). The protein and amylose content of rice (without husk) in site 2 was decreased by 66.91% and 54.61% compared to site 3. A significant negative correlation (>0.89) was observed between PTEs concentration in rice (without husk), and the protein, amylose content. Therefore, a rise in the concentration of PTEs in rice parts would cause a reduction in protein and amylose content, which would have an adverse effect on the nutritional quality and taste of cooked rice.

4.1.20 Model based prediction of health risk from PTEs (soil-rice system)

4.1.20.1 Health risk evaluation from leachable PTEs via different ML approaches

Likewise, machine learning (ML) was an excellent strategy that has evolved as a useful tool for predicting soil leachable-PTEs pollution employing basic correlations within data sets (Sengupta et al., 2021). To predict the dynamics of leachable-PTEs and their accumulation in

the soil-rice system, out of seven ML approaches, the best-fit model for each leachable-PTE has been determined on the basis of its reliability tests and Taylor diagram Fig. 34.

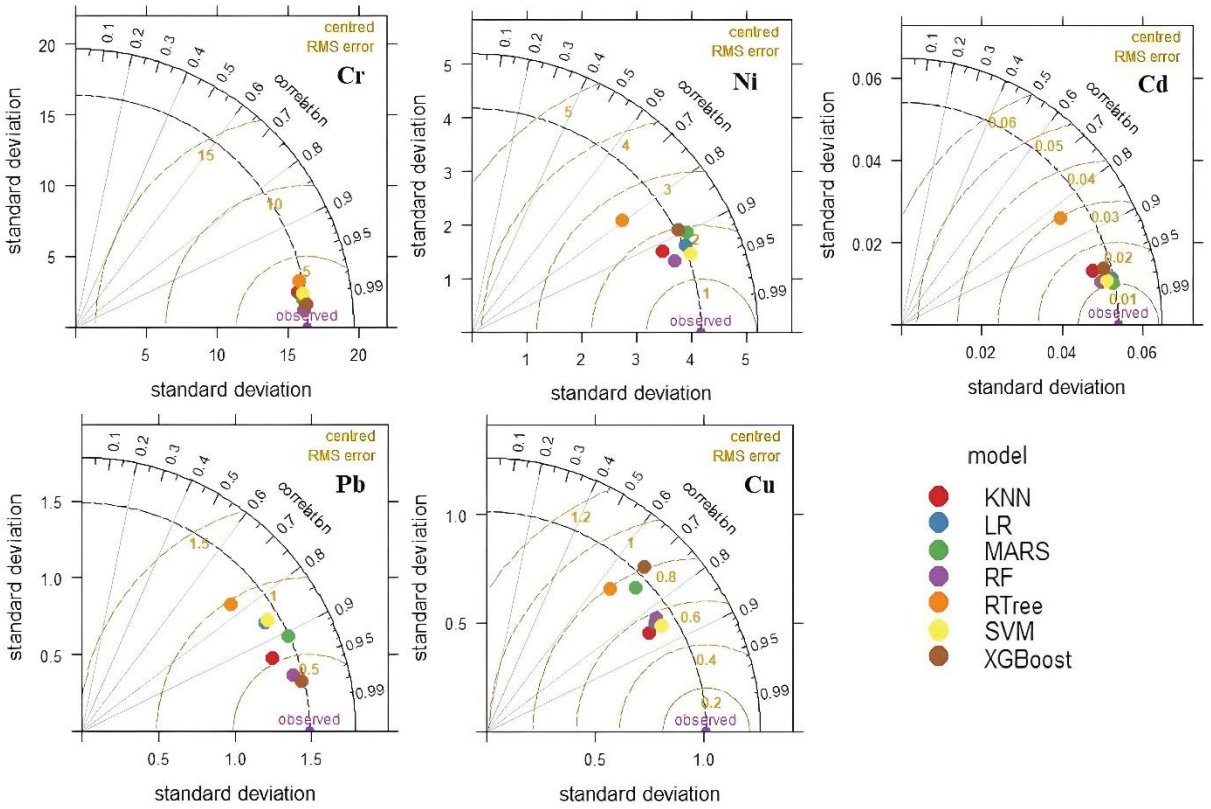

Fig. 34: Taylor diagram comparing model accuracy based on RMSE, and r of different leachable-PTEs. linear regression (LR), multivariate adaptive regression spline (MARS), support vector machine regression (SVM), random forest (RF), K nearest neighbour (KNN), extreme gradient boosting (XGB), and regression tree (RTtree)

The outcome demonstrates that most PTEs have forecasts that they were comparable to training and testing data. The valuable prediction of the PTEs leachability related to the toxicity and accumulation of PTEs in the soil-rice system was found in the current investigation through the use of multiple regression models. Thus, during the training phase, RMSE was calculated from observed and forecasted values and used to evaluate the models' performance. The measurement of the centered RMS error was displayed as the distance from the observed (real observation). The model with a lower RMSE was more accurate. Using the Taylor diagram for each PTE, various ML algorithms have also been evaluated for validity and accuracy. A Taylor diagram was a visual representation of the parameters SD, r, and RMSE. In close proximity to the observed line, this identifies the best-fit model (Fig. 34). The findings demonstrated that the RF was the most accurate model ($RMSE_{TCLP\text{-}Cr}$: 1.21 and $RMSE_{TCLP\text{-}Ni}$: 1.40 respectively) for contribution assessment of TCLP-Cr, TCLP-Ni on different parts of rice-PTEs content (H,

WH, BR, and ST). This was followed by the LR, GBM, MARS, SVM, KNN, and Rtree with their respective RMSE values in-case of TCLP-Cr. In-case of TCLP-Cu, KNN was the best-fit model for determining PTEs toxicity in rice parts (Table 22).

Table 22: RMSE and r values of different machine learning models

	Cr		Ni		Cd		Pb		Cu	
	RMSE	**r**	**RMSE**	**r**	**RMSE**	**r**	**RMSE**	**R**	**RMSE**	**R**
LR	2.320	0.996	2.656	0.922	0.00013	0.989	0.564	0.861	0.297	0.840
MARS	4.039	0.992	3.534	0.902	0.00010	0.989	0.390	0.908	0.525	0.720
SVM	5.648	0.989	2.134	0.938	0.00012	0.989	0.576	0.860	0.275	0.854
XGB	2.644	0.995	3.758	0.891	0.00020	0.989	0.107	0.975	0.635	0.692
RF	1.486	0.997	1.968	0.940	0.00012	0.983	0.140	0.967	0.318	0.830
KNN	6.838	0.987	2.700	0.917	0.00021	0.961	0.282	0.933	0.270	0.854
Rtree	10.446	0.980	6.280	0.793	0.00086	0.856	0.921	0.760	0.628	0.652

GBM accurately predicted PTEs (TCLP-Pb) toxicity on rice sections. For TCLP-Cd, MARS was the most suitable model, followed by SVM > RF > LR > GBM > KNN > Rtree. Among all the PTEs, the Rtree regressor exhibited the least desirable performance. In the chromium mining area, ML algorithms indicate that accumulation of PTEs in rice might be influenced by leachable-PTEs and long-term consumption of this rice would have a detrimental effect on the health of well-beings. The implications of these predictions for soil and crop management are significant, as the mobility and bioavailability of PTEs play a crucial role in the quality and safety of rice. The insights from these predictions inform agricultural practices, such as choosing rice cultivars that accumulate lower levels of PTEs, adjusting fertilization practices, and employing land management strategies like crop rotation. From a food safety standpoint, machine learning insights help address the potential health risks linked to high levels of PTE accumulation in rice.

4.1.20.2 Bio-accessible PTEs contribution on rice portion based on ANN model

In this study, ANN was also utilized to assess the suitable health risk caused by the bio-accessible-PTEs phases in this chromium mining region and provide a clearer picture of the imminent risk from different PTEs in various rice parts. By contrasting the actual and predicted levels of bio accessible-PTEs concentration in different parts of rice, the accuracy of the ANN model was evaluated. Fig. 35 depicts the percentage contribution of each PTEs in various rice parts. The order of contribution pattern was CrH > CrBR > NiBR > CrWH > CdST > CdWH > CrST > CuST > CuWH > CuBR > PbWH > PbBR > NiST > NiH > PbST > CuH > CdH > NiWH > CdBR > PbH. From this model, we observed that in-case of husk and boiled rice, Cr

was the foremost important factor towards the contribution of health risk. Long-term consumption of husk by animals and boiled rice by humans might cause health risks according to the ANN model prediction, as Cr was a highly carcinogenic substance. Also in Fig. 6, it was revealed that Cr from the I phase and Ni from the S-phase were the maximum contributors of PTEs concentration in different portions of rice. This finding was consistent with a prior study by Cho et al. (2011), which found that ANN performed better in predicting PTEs contamination. According to our findings, all of the aforementioned models (SAMOE, Fuzzy-TOPSIS, and ANN) suggest that consuming rice produced from chromium mine area poses an unacceptable risk to both human and animal health.

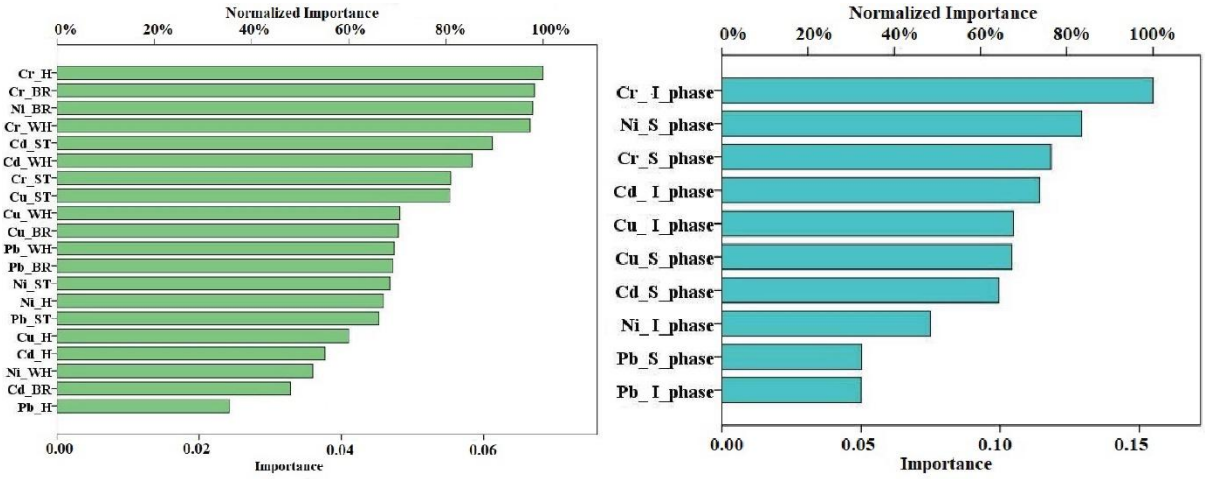

Fig. 35: ANN model showed the contribution of bio-accessible PTEs on rice parts

4.1.21 Survey- based risk evaluation based the on Fuzzy-DEMATEL approach

The finding of the survey work was considered for analysis of the potential health risks posed by villagers of the chromium-asbestos mine area. From the questionaries, seven criteria's direct and indirect effects were shown in Table 23. The average of the elements in matrix T was used to determine the threshold value, which was 1.8953. According to the Table 23, the seven criteria's relevance can be ranked in order of priority as E>C>D>F>G>A>B based on ($r_i + c_i$) values, with ingestion of starch-rice (E) ranking as the most important criterion with a value of 28.70 and child population (B) ranking as the least important criterion with a value of 24.10. In accordance with (r_i-c_i) values, (A) adult population, (C) body weight of the population, (D) consumption rate of cooked rice, and (F) exposure time on the mining site were net causes, whereas (B) child population, (E) ingestion of starch-rice, and (G) disease symptoms/sickness occur on the population were net recipients. In particular, Table 23. demonstrates that criterion

B (child populations) was not impacted by the others but affected by C (body weight of the population), E (ingestion of starch-rice), and F (exposure time on the mining site). Any pair of criteria B, C, D, E, F was mutually impacted by each other as shown in the digraph (Fig. 36).

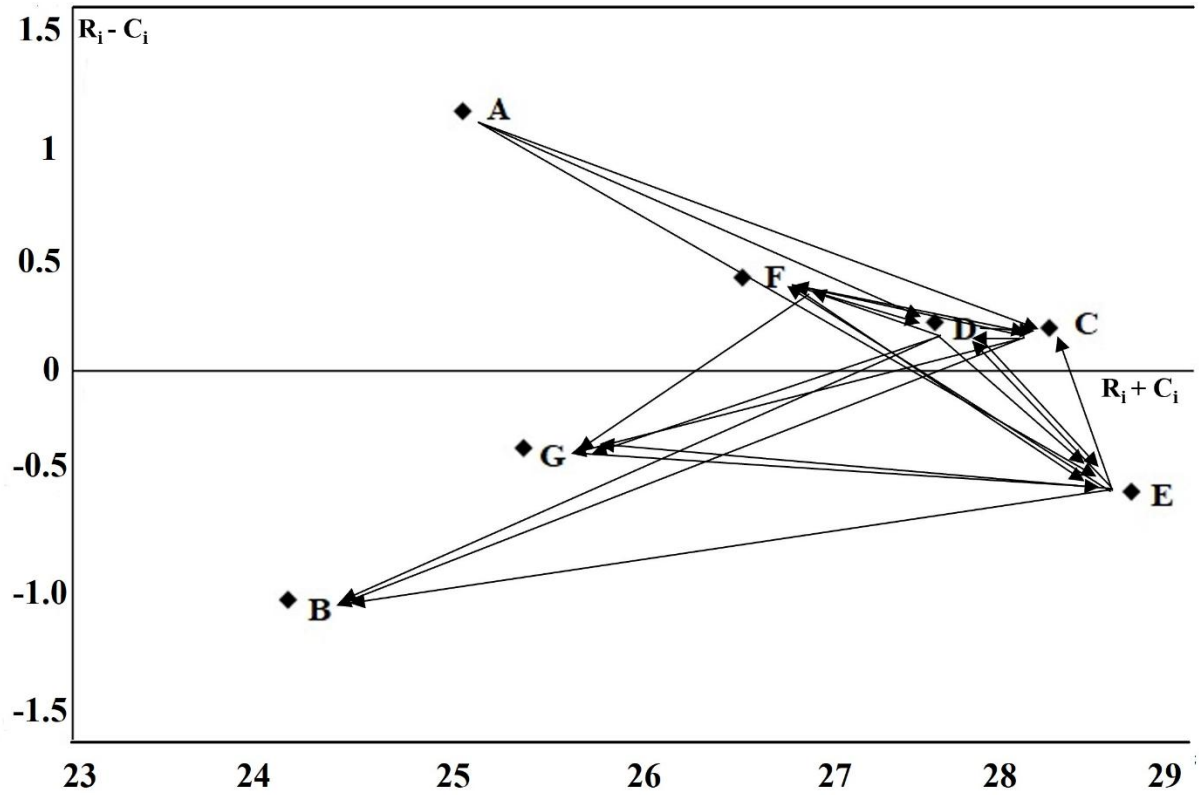

Fig. 36: The digraph illustrates the causal relationships between these seven criteria (DEMATEL approach).

In a nutshell, the authorities in charge of environmental protection ought to focus more of their attention on the four causes (A, C, D, and F) rather than the receiver (B, E, and G). The consumption of starch-rice and cooked rice, over an extended period of time, sourced from mining sites, was associated with substantial health risks for both adults and children.

Table 23: Depicts the direct and indirect effects of seven criteria (DEMATEL approach)

	Criteria	r_i	c_i	$r_i + c_i$	$r_i - c_i$
A	Adult population	13.08	11.98	25.06	1.10
B	Child population	11.56	12.55	24.11	-0.99
C	Body weight of the population	14.22	14.04	28.26	0.17
D	Consumption rate of cooked rice	13.92	13.72	27.64	0.20
E	Ingestion of starch-rice	14.09	14.62	28.71	-0.53
F	Exposure duration on the mining site	13.49	13.10	26.58	0.39
G	Disease symptoms/sickness occurs on population	12.52	12.87	25.39	-0.34

4.1.22 Source allocation of alkalinity employing PMF-factor geospatial distribution model

The PMF model, a systematic approach to investigate and ascertain the origins of alkalinity in this area. With the purpose of validating the findings of source apportionment, the contributions of factors in the PMF model were examined by calculating Pearson correlation coefficients (Fig. 37). The residual matrix was constructed using the minimum objective function (Q), resulting in the identification of four factors in the PMF model (Hsu et al., 2017).

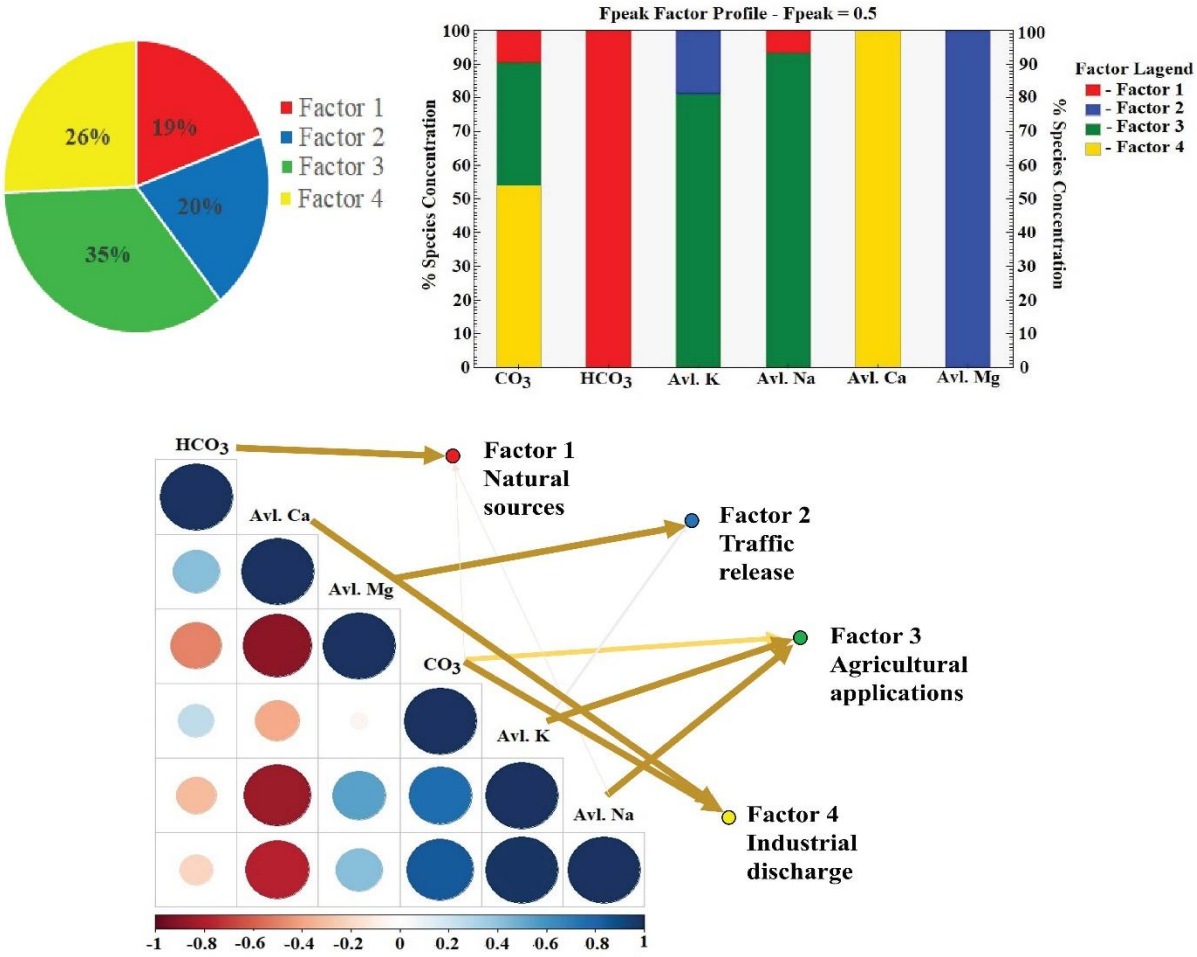

Fig. 37: Distribution of soil alkalinity constituents originating from chromium-asbestos mining waste in the contaminated soils at the study site. (a) The PMF analysis determines the percentage contribution of each factor. (b) The PMF model generates factor profiles for alkalinity constituents in Chromium-asbestos mining waste soils. (c) The PMF model combined with Pearson correlation analysis to identify correlations between soil alkalinity components

Fig. 38. illustrates the correspondence between the predicted and observed values with the signal-to-noise ratio. The PMF model was run 20 times to determine the least Q value. The findings of this study indicate that Factor 1 primarily contributed to the presence of HCO_3 (100%), CO_3 (9.5%), and Na (6.7%). Factor 2 had a strong association with K (18.7%) and Mg

(100%). Factor 3 was characterized by high loadings of Na (93.3%), K (81.3%), and CO_3 (36.6%). Lastly, Factor 4 was predominantly influenced by Ca (100%) and CO_3 (53.9%) (Fig. 39 a b).

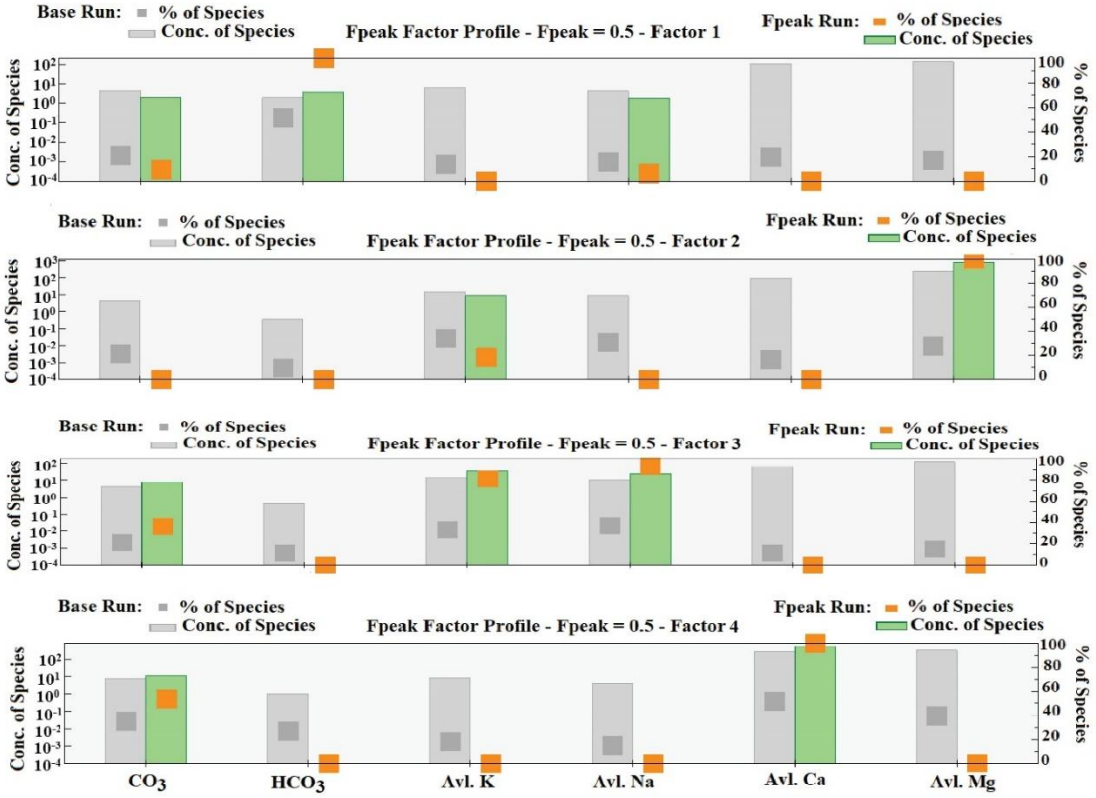

Fig. 38: Percentage contribution of soil alkalinity constituents in chromium-asbestos mine waste contaminated soils of the study location through positive matrix factorization model (PMF)

Factor 1 exhibited a dominant influence on the observed variation, accounting for a cumulative total of 19%. This factor was primarily characterized by the presence of HCO_3, CO_3, and Na. Factor 1 (mainly the northern portion) mostly pertains to the soil core material derived from lithogenic sources (basically rocks: dolomite, limestone, igneous rocks, and mines) as observed through the factor-GIS model (Fig. 39a). The weathering of rocks and mining waste can be the sources of HCO_3, CO_3, and Na. Factor 2 (traffic), which mostly consisted of K and Mg, accounted for a cumulative variance of 20%. Village areas and highways near mining sites were the geographic centre (mainly the southern portion) in terms of spatial distribution (Fig. 39b). Mainly, transportation, the combustion of vehicle fuel, batteries, tires, fuel additives, and engine wear were identified as the primary sources of K and Mg. Our research findings were consistent with previous research (Jiang et al., 2021; Huang et al., 2022). Nevertheless, the impact of lithogenic and transportation sources was rather least significant, particularly in

comparison to anthropogenic activities. Effective management of mining operations can play a crucial role in safeguarding the environment, in conjunction with appropriate agricultural practices. In relation to the overall contribution, factor 3 (mining industrial activities), accounted for 35% (north portion), while factor 4 (agricultural activities), accounted for 26% (southwestern portion) as depicted in (Fig. 39c, d). The mining sector engages in the extraction of significant quantities of mine waste, which serves as a valuable source of Na, K, and CO_3. Disposal of this mine waste in close proximity to agricultural fields leads to an elevation in alkalinity (Ghosh et al., 2023a). While, the agricultural activities predominate in the area surrounding the chromium-asbestos mine, with rainfed rice being the main crop. The increase in Ca and CO_3 content can be attributed to the use of different fertilizers, lime applications, and pesticide usage (Ozyhar et al., 2022). The findings of the PMF model reveal a significant influence of factor 3 on soil alkalinity. The mining industrial activities have been historically prevalent, with the dumping waste site serving as the primary repository for soil alkalinity.

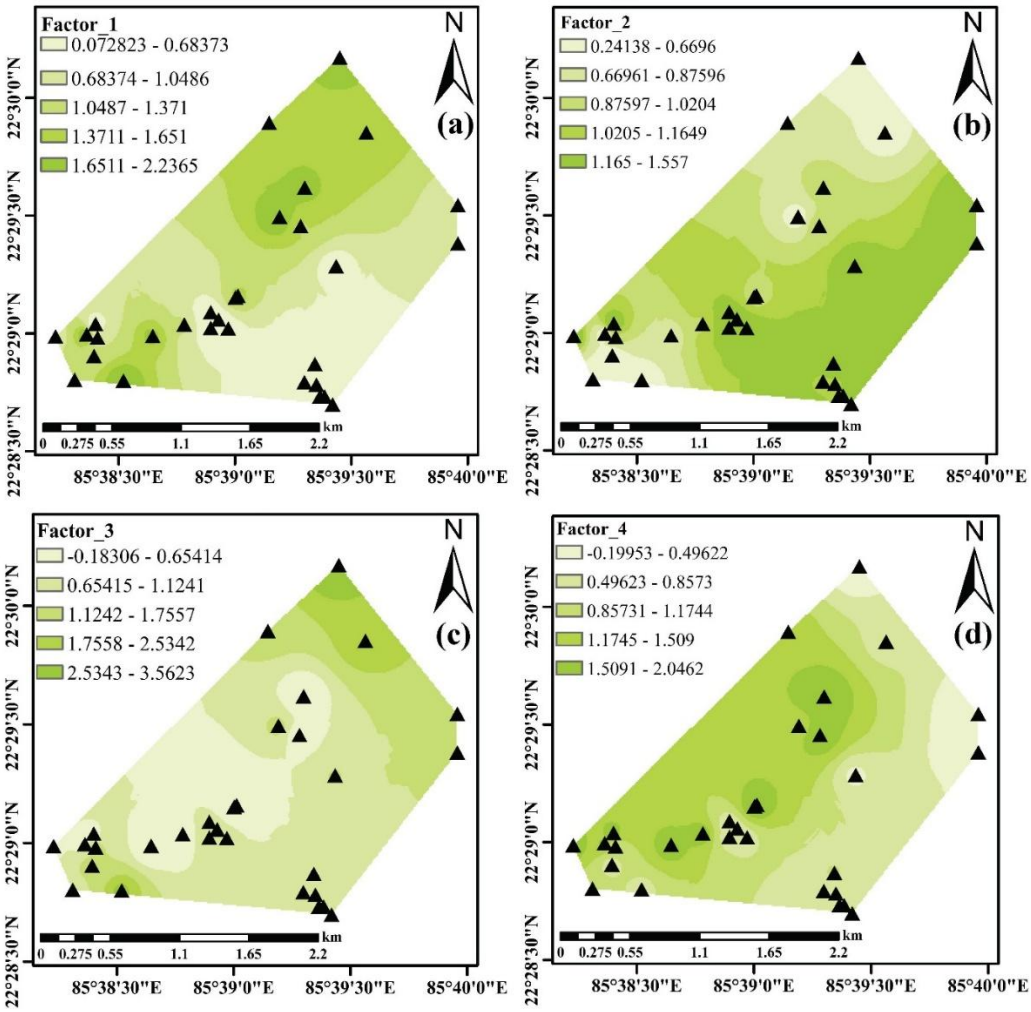

Fig. 39: A depiction of the spatial arrangement of factors (a–d) obtained from the PMF model

4.1.23 Pattern distribution of soil alkalinity indices and bioavailable PTEs

The SOM network analysis was used to investigate and contrast the patterns of various bioavailable PTEs and different alkalinity indices of chromium-asbestos mine sites. Fig. 40 illustrates the component plane results accompanied by the representation of each individual variable. Color-ranked plots were employed to visually depict the strong correlation among sample characteristics, as indicated by their placement within smaller hexagonal spaces. Notably, as the distance between each hexagon expands, the distinctions between the sample characteristics become increasingly evident (Nakagawa et al., 2020). The weight vectors of each neuron and its neighboring neurons collectively constitute a U-matrix (unified distance matrix). Components that share the same color in a component plane suggest a positive correlation between variables, whereas distinct colors imply a negative correlation (Ghosh et al., 2023a).

Fig. 40 (a-k) denotes all of the bioavailable PTEs and alkalinity indices have a similar pattern of mapping. In each of these cases except Cu (upper left), shows a greater correlation value from the left lower to upper left region (Fig. 4e). Similarly in the upper left neurons, all of the alkalinity parameters had greater values except MH (lower left). For site 1 neurons are more prominent in the upper left and lower left to right quadrant, whereas site 2 neurons are more prominent in the upper center to upper left quadrant (Fig. 4l, m). Subsequently, the self-organizing map (SOM) algorithm was employed to generate a clustered U-matrix, as depicted in Fig. 4n. The distribution of neurons was primarily concentrated in sites 1, and 2, housing 7, and 13 neurons accordingly. Intriguingly, the correlation between bioavailable PTEs and alkalinity parameters was highly comparable, providing clear evidence of their availability and mobility in soil.

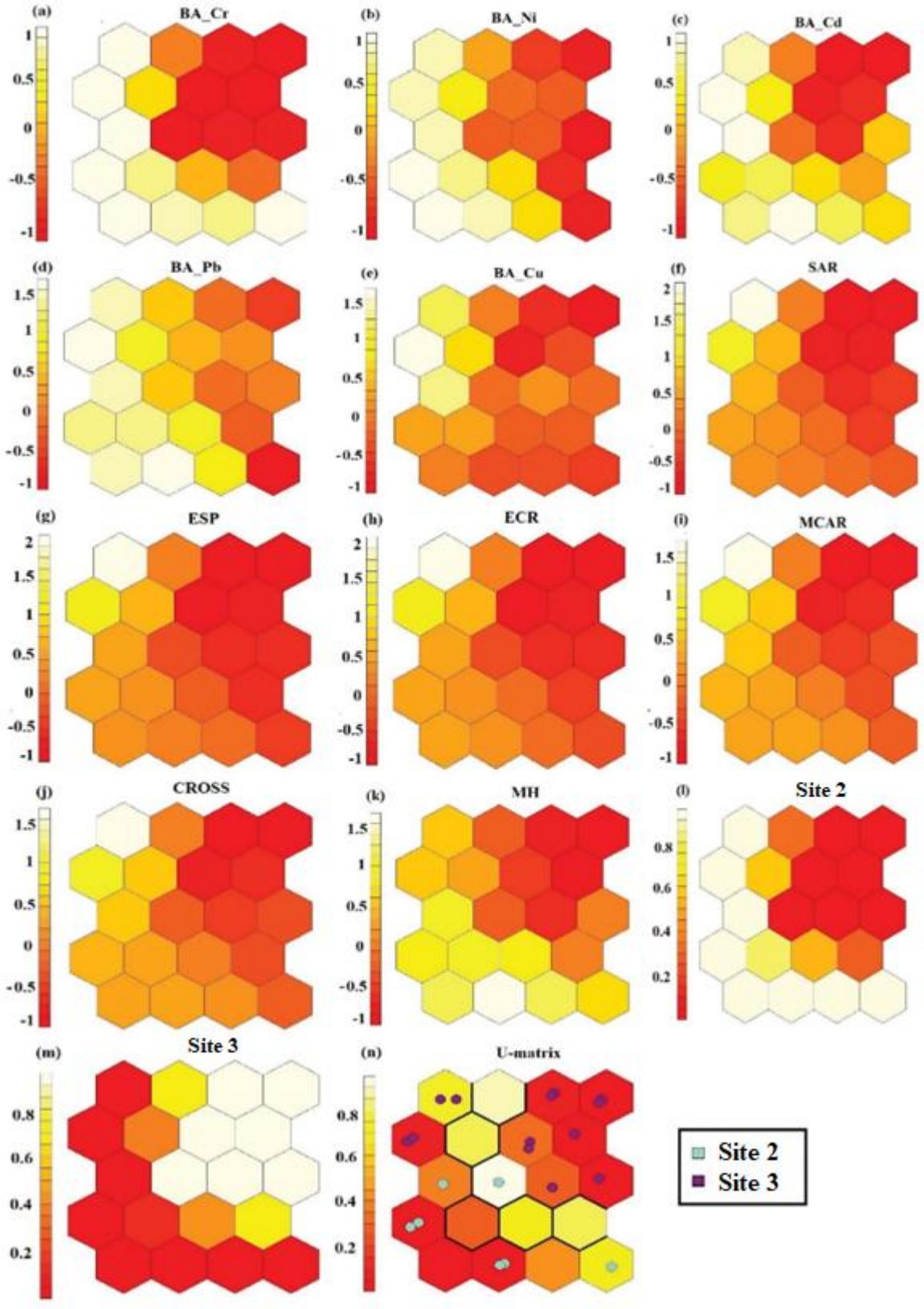

Fig. 40: Allocation of each PTEs and alkalinity indices in Chromium-asbestos mine waste contaminated soils via self-organizing map (SOM); (b) Site-wise PTEs concentration distribution maps; (c) Clustering of U-matrix denotes the two sampling locations

4.1.24 Different indices of alkalinity and its pattern identification by GIS

Table 8 demonstrates several indices of alkalinity (SAR, ESP, ECR, CROSS, MCAR, and MH). In our study area, the SAR, and ESP values exhibited a relatively low magnitude within both sites, which can be attributed to the low levels of exchangeable Na content. However, the aforementioned indexes did not take into account the influence of exchangeable K in soil, despite the fact that K has been found to have a comparable impact on clay dispersion as Na. Conversely, an elevated concentration of Mg can lead to structural degradation and an increased dispersion of clay particles. The present study revealed that the concentration of exchangeable K was relatively higher than that of exchangeable Na. This finding implies that the presence of K, in conjunction with Ca and Mg, has a notable impact on the occurrence of alkalinity in this region. The main significant indices, including ECR, MCAR, and CROSS, which encompass the comprehensive impact of Na, K, Ca, and Mg on soil, indicate that the values of ECR, MCAR, and CROSS were higher in site 2 than in site 3. Since K, Ca and Mg levels were quite high, the CROSS index was more accurate in predicting soil behavior than ECR, and MCAR. According to the findings of (Rengasamy et al., 1986), the increased dispersion of clay in soil with high levels of magnesium can be attributed to the radius and hydration energy of magnesium ions in comparison to calcium ions. The MH index exhibited a significant increase in site 2, reaching a value of 74.09%. The majority of soil samples obtained from site 2 were classified as being in a hazardous category. The alkalinity indicators exhibited greater values in site 2 in comparison to site 3. The above findings were further corroborated by the GIS mapping. The findings reveal that the spatial pattern of these indices (SAR and ESP), wherein the map exhibited a considerably lower contribution of these indices due to might less availability of Na, as depicted in the Fig. 41. In-case of MCAR, ECR, and CROSS, it was observed that the south-western site exhibited a significant elevation of alkalinity. Conversely, for MH, the northern region had a substantial elevation of alkalinity (mainly for Mg), since these locations were mostly used for the disposal of toxic mining waste. The aforementioned indices collectively indicate that the huge abundance of alkalinity levels in soil contaminated with chromium waste (site 2) was elevated, which might have posed hazardous stress effects on the soil microbial diversity. This observation was consistent with previous reports (Tripathi et al., 2007; Boyrahmadi and Raiesi 2018; Gao et al., 2019).

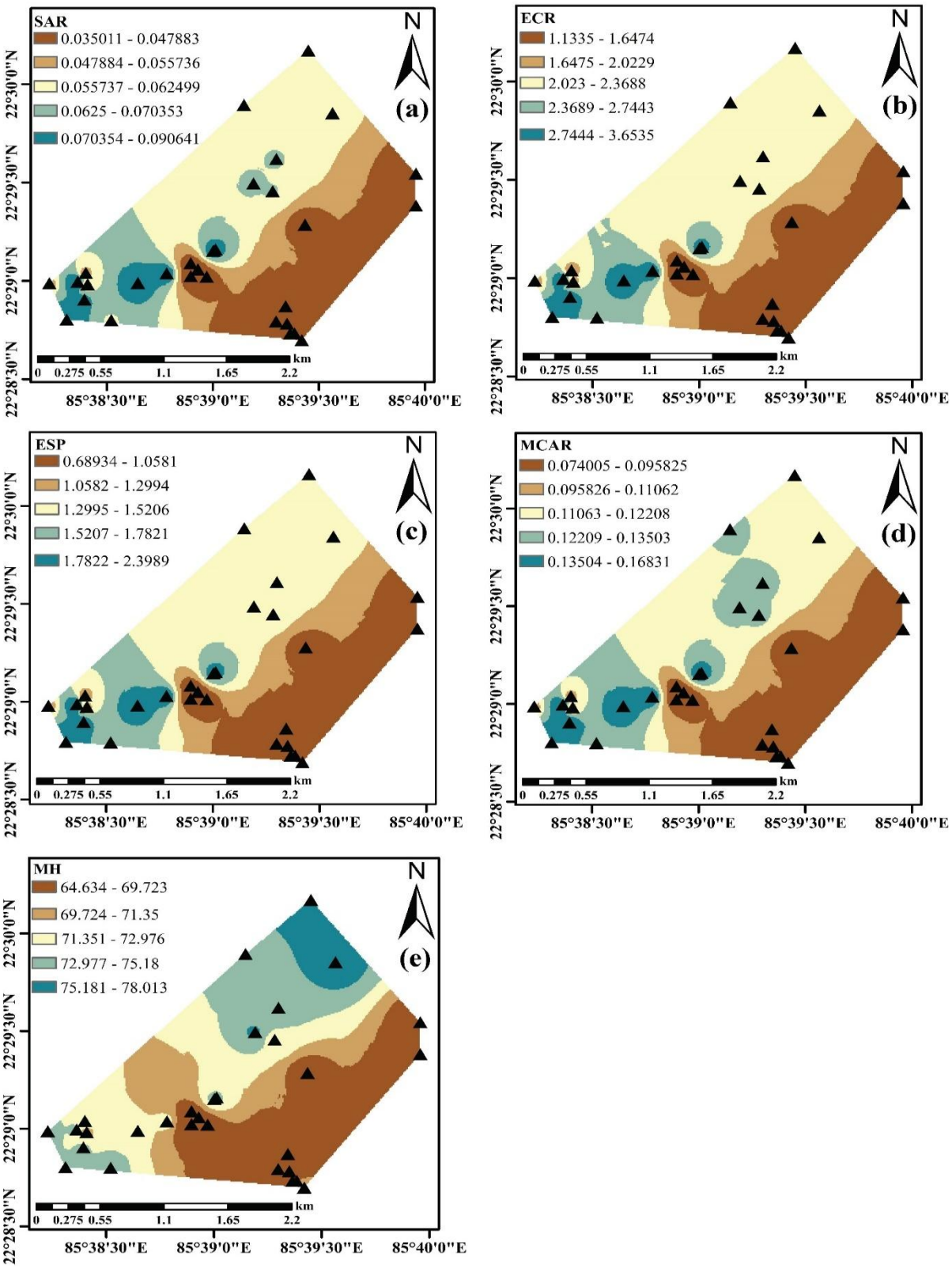

Fig. 41: The geostatistical map denotes the distribution pattern of alkalinity indices surround the chromium-asbestos mining area

4.1.25 Microbial and enzymatic activities of soil and their geospatial footprints

The microbial and enzymatic activities were represented in Fig. 42. The level of MBC in soil contaminated by a chromium-asbestos mine waste (site 2: range 173.12-417.66 mg/kg) exhibited a substantial decrease (p = 0.0008) when compared to uncontaminated soil (site 3: range 420.78-603.96 mg/kg). The coexistence of two stressors, (PTEs, and alkalinity) in site 2 results in a decrease in the synthesis of total soil microbial biomass. The presence of microbial biomass carbon within organic matter was crucial, as any impediment to MBC can have significant implications for nutrient cycling and the availability of minerals for plant growth (Tang et al., 2019; Ghosh et al., 2023b). However, MBC can also function as an indicator of soil quality, providing an early and effective warning of soil deterioration caused by the presence of both PTEs and alkalinity (Bhattacharyya et al., 2008). Concurrently, the assessment of microbial respiration basically, the levels of BSR and SIR level in site 2 (BSRmean: 2.07 mg CO_2/g soil/h at 22°C; SIRmean 7.17 mg CO_2/g soil/h at 22°C) exhibited a significant (pBSR = 0.006; pSIR = 0.001) decline as compared to site 3. Microbial respiration, which serves as a key indicator of environmental stress, can be employed to identify microbial communities that are metabolically either active or dormant (Dilly, 2005). Moreover, under stressful situations, microbial respiration acts as a reliable predictor of soil microbial response to disturbance (Tripathy et al., 2014). The activity of the FDA (fluorescein diacetate) was seen to be significantly (p = 0.009) decreased in soil that was contaminated (site 2: mean 11.75 mg fluorescein/g soil/h), suggesting that the microbial cells might be unable to generate fluorescein in the presence of stress-inducing conditions caused by elevated levels of toxic mine waste inside the soil. The enzymes like dehydrogenase (DHG), β-glucosidase (BG), urease (U), and alkaline phosphatase (AP) activities were significantly varied between the two sites of the chromium-asbestos mine site, represented in Fig. 42.

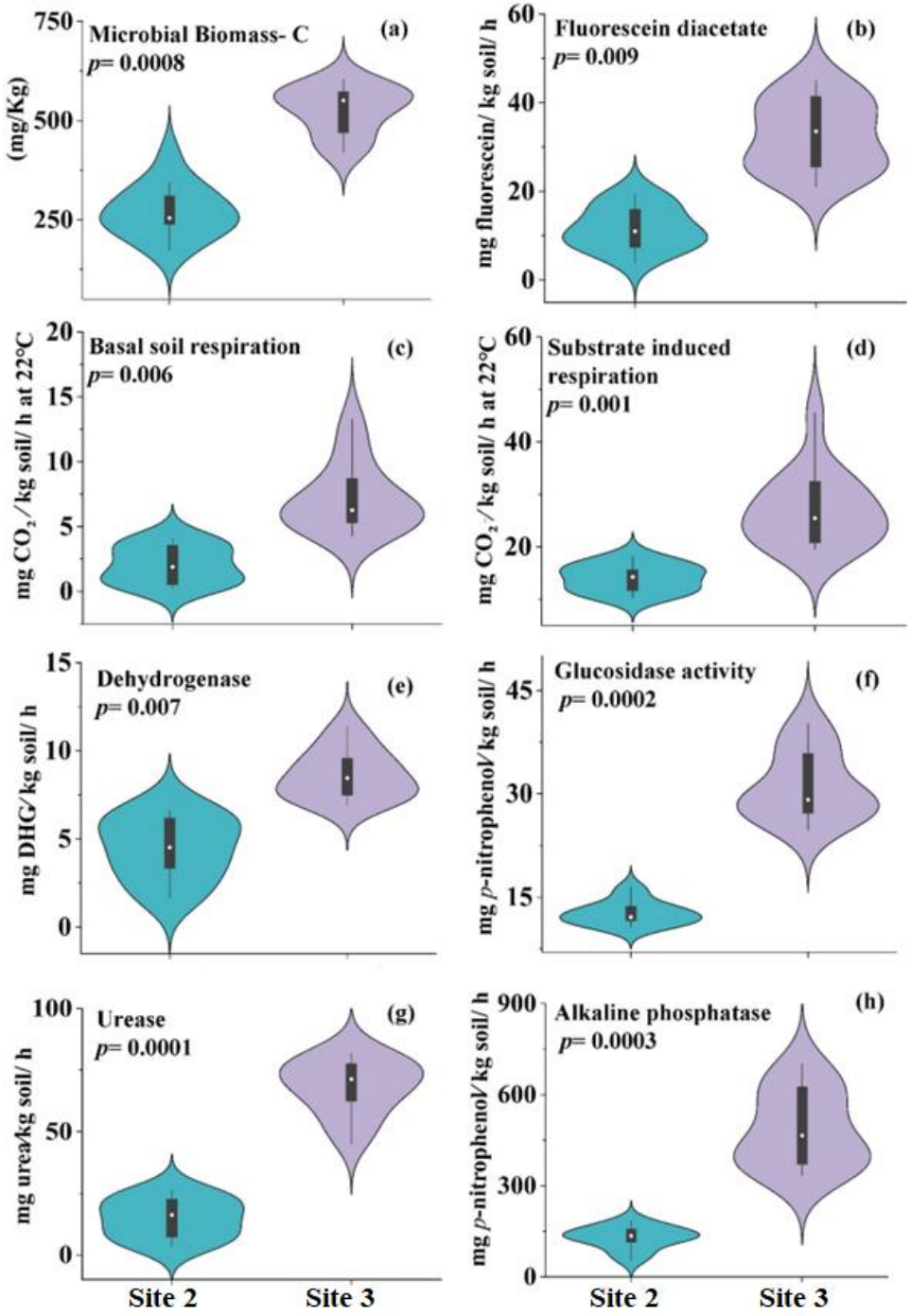

Fig. 42: Violin plots illustrating distinctions in soil microbial and enzymatic activities between two separate zones (Contaminated: Site 2 and Uncontaminated: Site 3)

The enzyme activities in site 2 were reduced as compared with site 3. This result indicated that the presence of sulfhydryl groups in the enzyme catalytic site plays a crucial role by interacting with PTEs and forming PTEs-sulfide complexes. Therefore, it might have the ability to render enzyme activity or cause enzyme denaturation (Tripathy et al., 2014). Similarly, a GIS map demonstrated that the microbial and enzymatic activity was reduced in the northwest to

southwest, with these regions primarily being identified as dumping site of toxic mine waste (Fig. 43).

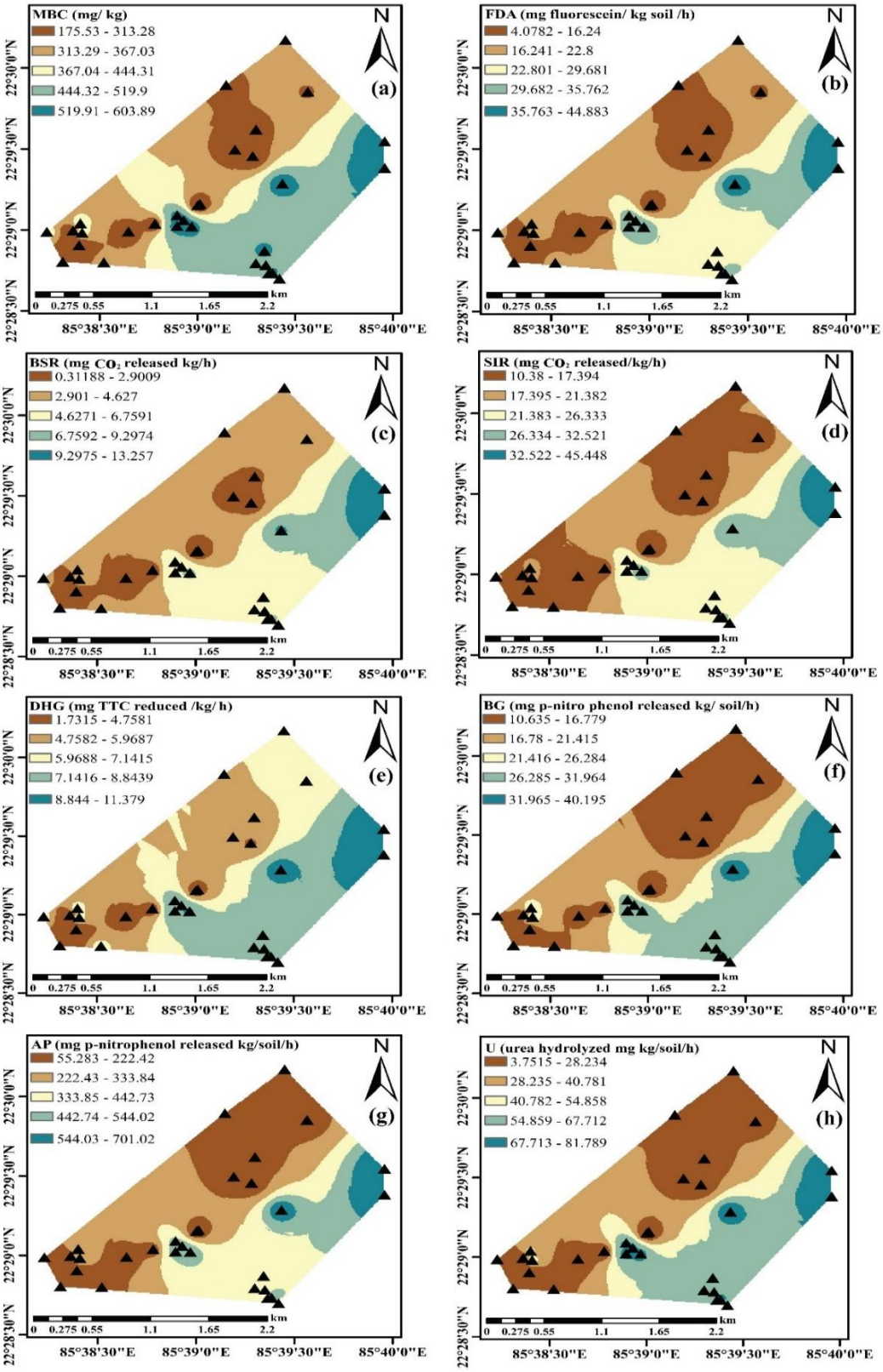

Fig. 43: The spatial distribution of microbial and enzymatic parameters around the chromium-asbestos mining region

PTEs were extremely abundant in these contaminated regions (site 2) due to the deposition of toxic mining waste, which might interact with microbial activity and disrupt it compared to site 3 (uncontaminated site). Hence, microbes are believed to be the gatekeeper of enzymatic regulation, so they have the ability to respond to any changes in the environment and provide minute information on enzyme catalytic mechanisms associated with biological systems (Bhattacharyya et al., 2008).

4.1.26 Microbial metabolism limitation assay via vector analysis

The vector length and angle were determined by integrating the activities of enzymes involved in carbon (C), nitrogen (N), and phosphorus (P) cycle (Table 24).

Table 24: Enzymatic stoichiometry relative proportion and their variation in vector angle, length under stressed condition

Metric	Site 1 (Mean ± SD)	Site 2 (Mean ± SD)
BG/BG+AP	0.09 ± 0.006	0.06 ± 0.003
BG/BG+U	0.5 ± 0.02	0.31 ± 0.01
ln (AP)	4.82 ± 0.52	6.15 ± 0.72
ln (U)	2.52 ± 0.19	4.21 ± 0.38
ln (BG)	2.53 ± 0.13	3.42 ± 0.26
Length	0.51 ± 0.04	0.32 ± 0.02
Angle	79.23 ± 6.43	78.89 ± 6.91

Individual enzyme activity in soil samples from site 2 was lower than that from site 3 (Fig. 1). The length of the vector was greater in site 2 (0.51) in comparison to site 3 (0.32) suggesting that there was a significant limitation on C availability, resulting in a higher proportion of carbon acquisition compared to nutrient acquisition. Soil samples with lower vector lengths indicate lower C limitation (Sinsabaugh et al., 2008). Similarly, sites 2 (79.23◦) and 3 (78.89◦) had vector angles above 45◦, indicating a stronger P limitation and the lowest values for BG/(BG + AP) for both sites. Environmental variables include PTEs content and soil alkalinity, while the species variables consist of microbial enzymes, vector length, and vector angle. Similar research (Lagomarsino et al., 2011) revealed that under stressful conditions, there was a significant decrease in microbial population.

4.1.27 Microbial community analysis

4.1.27.1 Bacterial community composition

Bacterial taxonomic classification was conducted on the PTEs-contaminated (site 2) and uncontaminated sites (site 3) of the chromium-asbestos mine, utilizing operational taxonomic units (OTUs) and reads. The raw reads generated in this project have been deposited in the NCBI Short Read Archive (SRA) database (Accession number: PRJNA1083037). The distribution of bacterial phylum in site 2 (24,752 reads) and site 3 (52,352 reads) was evaluated, revealing that both types of soil were predominantly populated by *Proteobacteria*. Additionally, *Actinobacteria*, *Acidobacteria*, *Bacteroides*, *Firmicutes*, *Chloroflexi*, and other phyla were present, although their relative abundance differed between the two sites. The abundance of *Proteobacteria* in the contaminated soils (site 2) was significant, comprising 57.18% of the total population. Furthermore, among the *Proteobacteria* phyla, the contaminated soil exhibited a larger proportion of γ-*Proteobacteria* (38.61%) and α-*Proteobacteria* (8.93%) classes compared to the uncontaminated sites (site 3) (Fig. 44). The abundance of the β and δ Proteobacterial phyla was also found to be higher in both alkaline environments and regions polluted with PTEs (site 2). These findings were corroborated by several studies (Valenzuela-Encinas et al., 2009; Keshri et al., 2013). Therefore, the *Proteobacteria* phylum is well known for its capacity to demonstrate the complexity of habitats and effectively degrade a wide range of complex organic compounds, allowing it to adapt to diverse stressful conditions (Pereira et al., 2014). Numerous reports were available of *Proteobacteria* phyla that are prevalent in various mining areas (Desai et al., 2009; Halter et al., 2011; Narendrula-kotha and Nkongolo, 2017) and that have been found in both PTE-contaminated and alkaline environments (Mwirichia et al., 2011; Nielsen et al., 2014; Yan et al., 2016). The prevalence of *Proteobacteria* showed an increase with higher levels of Pb, Cr, Cd, and Ni pollution, in contrast to *Actinobacteria*, *Acidobacteria,and Firmicutes* in site 2 (Fig. 44).

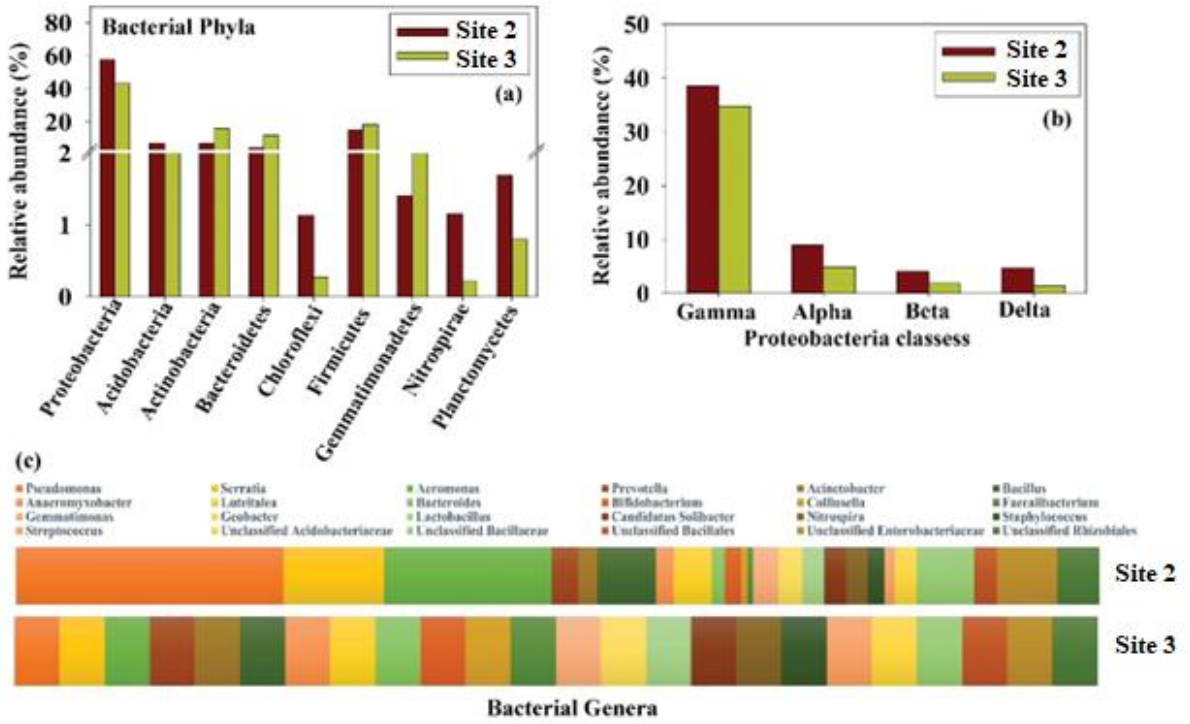

Fig. 44: Graphs illustrating the relative abundance of bacterial community. (a) Distribution percentage of bacterial phyla (b) Distribution percentage of bacterial class (c) Distribution percentage of bacterial genera through metagenomics analysis

The increase in abundance might be attributed to the capacity of *Proteobacteria* to acclimate to high concentrations of PTEs environment. Previous research has also shown evidence that PTEs reduce microbial diversity by promoting the growth of *Proteobacteria* and suppressing the abundance of *Acidobacteria* and *Actinobacteria* in polluted areas (Gołębiewski et al., 2014). Also, other reports suggested that *Proteobacteria* was more prevalent than *Firmicutes* in the alkaline environments (Qinghai, China), and (Elmenteita, Kenya) (Dong et al., 2006; Mwirichia et al., 2011). Site 2 shows contamination resulting from prolonged exposure to lethal levels of Cr and Ni, as well as other bioavailable forms of other PTEs that are poisonous. Additionally, this site displayed a high concentration of Ca and Mg. A decline in both overall diversity and phylogenetic diversity was detected might be due to the presence of high level of PTEs and alkalinity, indicating that numerous bacterial species were unable to persist (Keshri et al., 2013; Narendrula-kotha and Nkongolo, 2017). A notable transition in the bacterial population at the phylum level from contaminated sites to the control site implies that these particular bacterial phyla may possess a high degree of tolerance towards PTEs and alkalinity environment (Mwirichia et al., 2011; Nielsen et al., 2014). Research has further indicated that

the majority of *Proteobacteria* were classified as nitrogen-fixing and photosynthetic bacteria. These bacteria were crucial for the carbon and nitrogen cycles, as well as for preserving the overall stability of the ecosystem (Nordlund et al., 2004; Li et al., 2021). It was also well known that the majority of the pure-culture isolates that are capable of converting or resistant to Cr or other PTEs (Ni, Pb, Cd, and Cu) belong to the bacterial phyla *Proteobacteria*, *Actinobacteria*, and *Firmicutes* (Ozyhar et al., 2022). Previous research has indicated that chronic exposure to PTEs contamination and soil alkalinity was likely to have detrimental impacts on the structure and, eventually, the functioning of the community, leading to a loss of species (Chodak et al., 2013). The abundance of *Acidobacteria*, *Firmicutes*, *Actinobacteria*, and other bacterial phyla exhibited variations throughout the soil systems. There was a notable (p <0.05) disparity in the prevalence of *Acidobacteria* between the contaminated (7.12%) and uncontaminated (2.01%) soil systems (Fig. 44). This discrepancy can be attributed to the slightly higher acidity seen in the site 2. Paul et al. (2016) also established the adaptation of *Acidobacteria* in PTEs-polluted environments. The decline in *Acidobacteria* population in uncontaminated soils can perhaps be attributed to the elevated pH levels, rather than the presence of PTEs. It was widely recognized that pH exerts significant control over the quantity and variety of *Acidobacteria*. The bacterial diversity analysis also revealed a significant decrease ($p<0.01$) in the actinobacterial population within site 2 (6.71%) in comparison to site 3 (16.08%). *Actinobacteria*, which was highly prevalent in soil ecosystems, exhibits a reduction in abundance within PTEs and alkalinity-stressed habitats. The findings of our study are consistent with the literature that *Actinobacteria*, experience a decrease in population within PTEs-contaminated site (Gołębiewski et al., 2014; Chodak et al., 2015). The phylum *Actinobacteria* exhibited a notable rise in an uncontaminated environment, likely attributed to the existence of low levels of bioavailable PTEs. This phylum serves a vital role in managing different stressors owing to its strong metabolic activities and rapid colonization capabilities (Valverde et al., 2012; Narendrula-kotha and Nkongolo, 2017). On the other hand, the population of *Firmicutes* showed a significant difference between the two soil conditions, with 14.87% in the contaminated site and 18.45% in the uncontaminated site. Phylum *Firmicutes* exhibit resistance to drought and possess the ability to thrive in harsh conditions (Chodak et al., 2015). Therefore, the presence of *Firmicutes* in our research area may be attributed to the arid climate of the region under study and the ability of *Firmicutes* to withstand dry conditions, alkaline stress and PTEs toxicity, as shown in previous research (Navarro-Noya et al., 2010; Lopez-Lopez et al. 2010; Gołębiewski et al., 2014). Specifically, *Bacteroides* accounted for 4.31% of the population in the contaminated site and 11.83% in the uncontaminated site, while *Chloroflexi*

accounted for 1.13% in the contaminated site. The phylum *Bacteroidetes* has been noted to be extremely diverse and has been observed in stressful environments (such as PTEs and alkaline stress) and agricultural lands (Gołębiewski et al., 2014; Ma et al., 2015). According to Kirchman (2002) and Keshri et al. (2013), they are often typically lithotrophic or aerobic chemoorganotrophic and have a variety of metabolic capacities that allow them to break down a wide range of organic molecules under extreme condition like alkaline stress and PTEs stress. Most organisms in the *Chloroflexi* phylum were uncultured, despite their capability to inhabit many harsh habitats, including PTEs-contaminated and alkalinity-affected soils (Pereira et al., 2014; Tebo et al., 2015; Choure et al., 2021). The phyla *Firmicutes, Bacteroides* and *Chloroflexi* have been observed to possess PTEs tolerance (Cu, Cd, Pb) abilities, making them more prevalent in contaminated populations (Zhang et al., 2017; Pai et al., 2018). The other phyla *Planctomycetes*, *Armatimonadetes*, *Cyanobacteria*, *Gemmatimonadetes*, *Verrucomicrobia*, *Ignavibacteriae*, *Fusobacteria*, and *Nitrospirae* were found to be infrequent, accounting for less than 2% of all recognized phyla worldwide. The *Planctomycetes* exhibited a decreased relative abundance of taxa in the Ca-high environment (García-Galdeano et al., 2021). Also, the presence of *Gemmatimonadetes* in polluted areas has been shown in the literature (Navarro-Noya et al., 2010; Pereira et al., 2014). Since submerged rice farming is performed in these areas, the accumulation of mine tailings in agricultural fields might have led to increased microaerophilic conditions, which may have contributed to the presence of *Verrucomicrobia* phyla. Several studies have documented a prevalence of *Verrucomicrobia* in soil samples (Fierer et al., 2013).

At the taxonomic level of genus, the two sites exhibited significant variation in populations of various bacterial genera including *Pseudomonas*, *Aeromonas*, *Serratia*, *Bacillus*, Unclassified *Enterobacteriaceae*, *Prevotella*, *Bifidobacterium*, *Staphylococcus*, *Gemmatiomonas, Geobacter,* Unclassified *Clostridiales*, *Nitrospira*, *Candidatus Solibacter*, *Candidatus Koribacter*, *Luteitalea* and Unclassified *Acidobacteriaceae.* The abundance of the *Pseudomonas* genus was significantly higher in site 2 compared to site 3. The existence of an abundance of *Pseudomonas* genus from the *Proteobacteria* phylum in these soils suggests that it has a high resistance to pollution from Cr, Cd, Pb, and Ni. This resistance has been well-documented in studies conducted by Kaur et al. (2015). *Pseudomonas* has genes that encode enzymes responsible for PTEs resistance (Li et al., 2015). *Gemmatiomonas* has been observed in several habitats exhibiting a slightly alkaline pH (Pereira et al., 2014), which might explain the prevalence of *Gemmatiomonas* in these soils. The genus *Geobacter* had a high prevalence

in these research sites, suggesting that it is resistant to high concentrations of Cd, Pb, and Cr. Therefore, a significant presence of *Geobacter* has been documented in soils contaminated with PTEs (Gołębiewski et al., 2014). The abundance of *Luteitalea* (2.07%), Unclassified *Acidobacteriaceae* (1.18%), *Candidatus Solibacter* (1.20%), and *Candidatus Koribacter* (1.95%) was found to be much greater in the PTEs contaminated soils, indicating a notable presence of these *acidobacterial* species in the predominantly acidic soil, While certain genera, such *Clostridium*, *Lactobacillus*, and *Acinetobacter*, were exclusively identified in soil that had been polluted (mining activity) with PTEs (mostly with high levels of Cr pollution), indicating that they were naturally resistant to this substance. The abundance of *Serratia* (5.5%), well-known for its capacity to produce strong plant growth-promoting rhizobacteria (PGPRs) that can enhance tolerance to PTEs stress, was seen to be markedly increased in the soils site 2 compared to site 3. The presence of *Nitrospira*, an aerobic chemolithoautotrophic nitrite-oxidizing bacteria that plays a vital part in nitrification, may suggest nitrification in alkaline soil (Feng et al., 2018). The involvement of *Bacillus* and *Lactobacillus* in chromate detoxification has been investigated by Xu et al. (2015) and Mishra et al. (2012). Another study conducted by Kang et al. (2014), the researchers assessed the capacity of *Pseudomonas aeruginosa* to reduce chromium (Cr). The ion transport mechanism involves the use of a transporter protein (ChrA), derived from the bacterium *Pseudomonas aeruginosa*. This protein has been observed to facilitate the efflux of cytoplasmic chromate (Alvarez et al., 1999).

4.1.27.2 Bacterial species richness and diversity indices

The α-diversity (species richness and/ or evenness) within a microbial population displayed variation across the two sites represented in Fig. 45. The estimation of bacterial community richness was performed by rarefying the OTUs table. The rarefaction curves were utilized to assess the species richness and evenness of the samples by a comparison of OTUs and the number of sequences per sample (Fig. 45b). The α-diversity index (Shannon, Simpson, Fischer, and Chao1) exhibited a decrease in site 2 compared to site 3 (Fig. 45c). The Whittaker's beta diversity coefficient was calculated to be 0.15828, suggesting a low level of dissimilarity in species composition across the two sites. The beta diversity index is a numerical measure that varies from 0 to 1. A value of 0 signifies a minimal or negligible dissimilarity in the species composition across various sites, while a value of 1 represents the highest possible dissimilarity in composition. From metagenomics analysis, out of the total (447 OTUs), 406 OTUs were detected in site 2 (contaminated site) and 384 OTUs were found in site 3 (uncontaminated site).

According to the Venn diagram, only 14.1% (63 OTUs) in site 2 and 9.17% (41 OTUs) in site 3 were unique to each location, supporting the beta diversity (Fig. 45a).

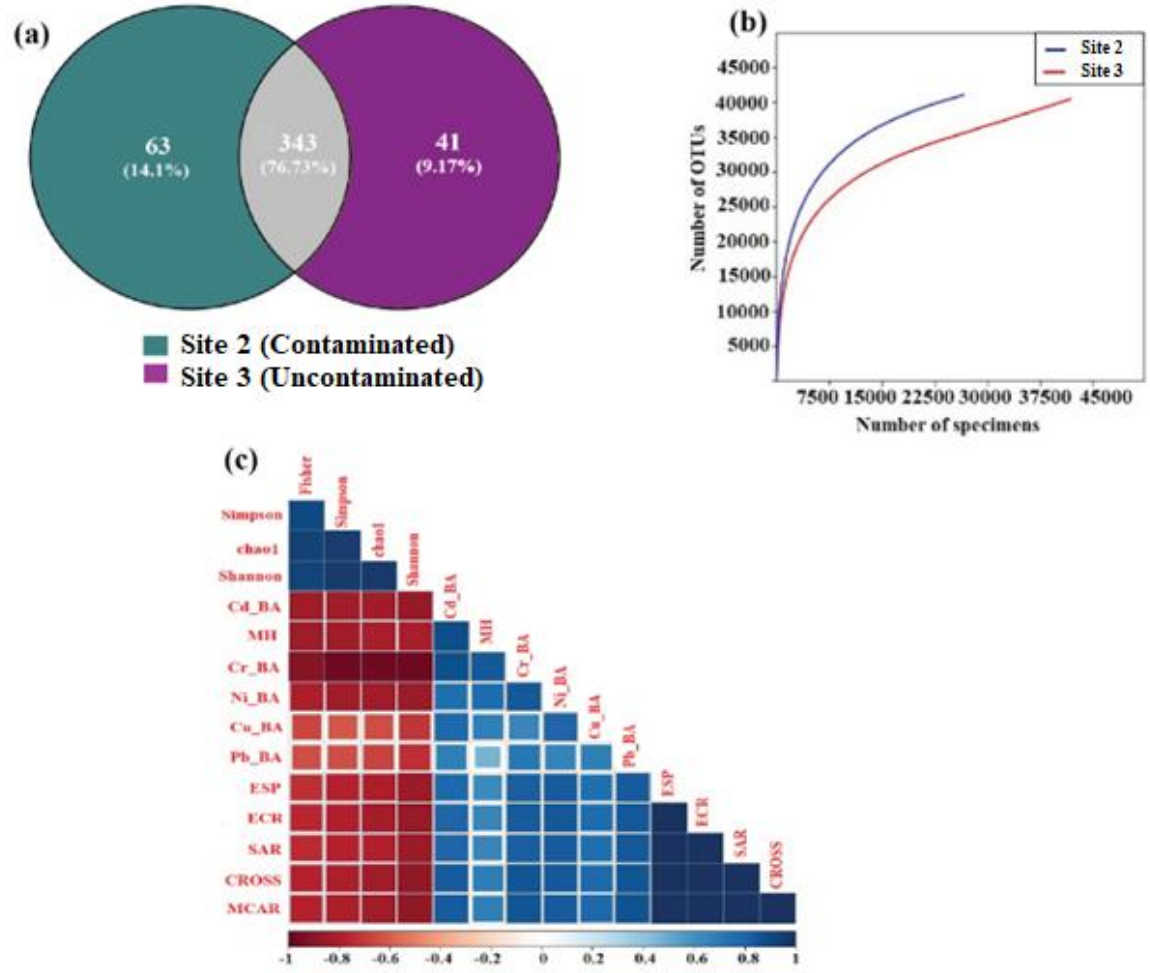

Fig. 45: Venn diagram illustrating the dispersion of Operational Taxonomic Units (OTUs) b) The rarefaction curve investigates the alpha diversity. c) The synergistic impact of PTEs pollution, and alkalinity indices, on the evenness metrics of soil microbial community

There was a notable ($p < 0.05$) negative relationship among bioavailable PTEs, alkalinity indices and all alpha diversity indicators. These findings suggest that the synergistic effect of various PTEs (Cr, Ni, Cd, Cu, and Pb) and alkaline indices (mainly CROSS, ECR, MCAR and MH) in soil have a detrimental impact on the microbial population within the community. These results support the hypothesis of a synergistic stress effect of alkalinity and PTEs on the microflora (Fig. 45c).

4.1.28 Evaluation of microbial community responses towards soil stressors using model

Assessing the combined effects of PTEs and alkalinity on the soil microbial population and their enzyme activity was one of the prime goals of this research. A correlational analysis was conducted by Pearsons to investigate the relationship between soil stressors and soil microbial parameters. Fig. 46 indicates a significant (1% level) negative relationship was observed between the alkalinity measurements (SAR, ESP, ECR, CROSS, and MCAR) and all the microbiological parameters. Hence, the microbial population in this region was impacted by the rise in alkalinity indices. Moreover, the bioavailable fractions of PTEs (Ws, Ex, and Ox) also exhibited a significant (1% level) inverse relationship with the microbial populations. So, the agricultural soil at the chromium-asbestos mine site had a decline in microbial population as a result of the elevated concentration of different PTEs (Fig. 46).

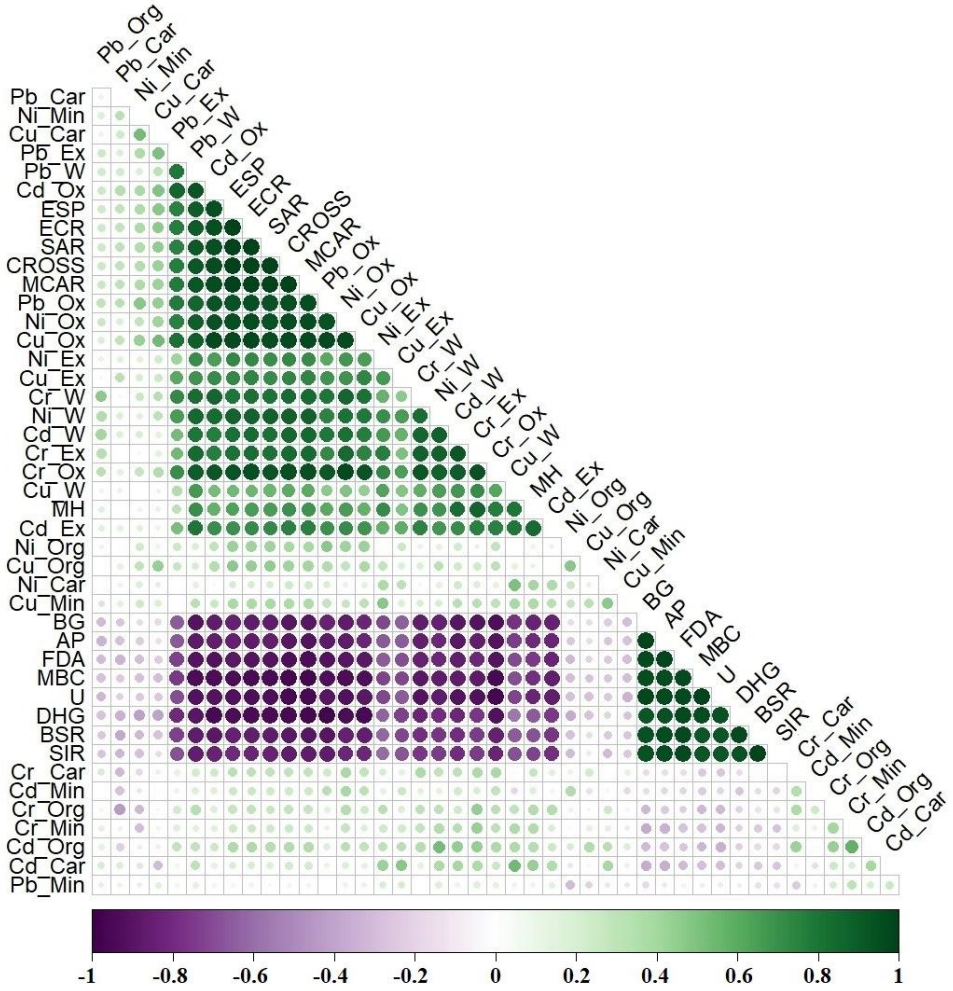

Fig. 46: The Pearson correlation assesses the relationships between different fractions of PTEs, alkalinity indices, and various enzymatic-microbial parameters at a chromium-asbestos mining waste site. [The correlation coefficient and significance level are represented by each coloured point]

In contrast, the GIS map revealed that the concentration of bioavailable PTEs and alkalinity indices was higher in the northwest to the southwest region, as compared with microbial activities due to the presence of toxic mine waste in the agricultural soil (Fig. 26, 41). Hence, the correlation assay and GIS distribution uncovered a notable impact of the combination of alkalinity and bioavailable PTEs on the microbial population, demonstrating a synergistic effect. The GIS mapping provided additional support for the aforementioned conclusions (Fig. 21, 41, 43).

A subsequent investigation, namely the Principal Component investigation (PCA), was performed to examine the relationship between alkalinity parameters, various concentrations of PTEs, and all microbiological characteristics. The application of principal component analysis (PCA) demonstrated that the initial two dimensions, referred to as Dim-1 and Dim-2, accounted for a total of 91.9% of the overall variation (Fig. 47).

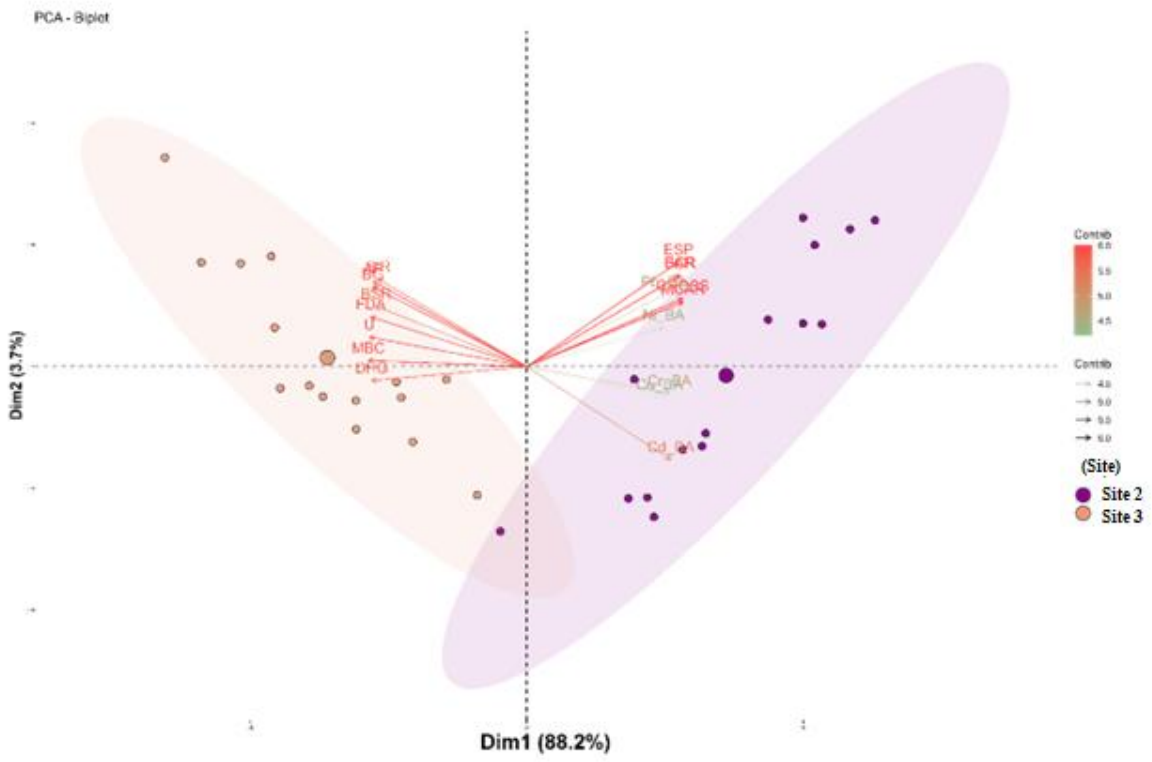

Fig. 47: Principal component analysis demonstrates an association between alkalinity, PTEs fractions, and microbiological metrics

The eigenvalues of Dim-1 and Dim-2 accounted for 88.2% and 3.7% of the total explained variance, respectively. In Dim-1, a positive correlation was discovered between the alkalinity parameters (MCAR, ECR, ESP, CROSS, SAR) and the bioavailable percentages of PTEs. All the microbiological parameters were observed to exhibit negative values in relation to both

Dim-1 and Dim-2. The abundance of bioavailable fractions of PTEs and abundance of alkalinity exhibits a decline as the distance from chromium-asbestos mines increases, although a contrasting pattern was seen in relation to soil microbial and enzymatic activities. Therefore, utilizing PCA was an effective approach to maximize the coverage of variance within the data (Ghosh et al., 2024).

This study also aimed to provide seven novel techniques in the field of machine learning for the prediction of alterations in soil microflora caused by prevalent stressors (alkalinity indices and PTEs stress) in the region (Fig. 48).

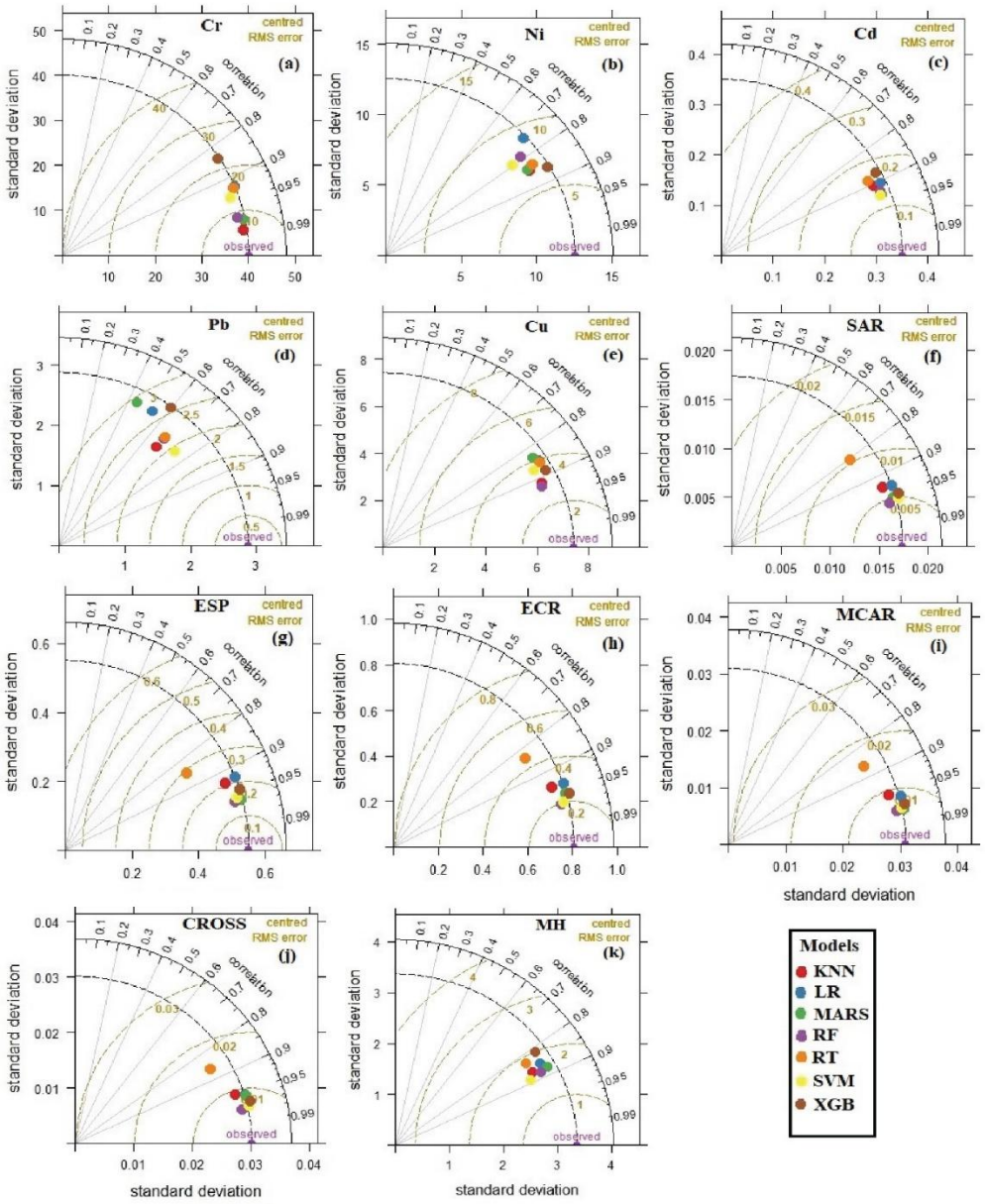

Fig. 48. RMSE, r, and SD-based Taylor diagram illustrating the accuracy of the various machine learning models

The accuracy of a model was determined by a lower RMSE and a higher correlation coefficient (r). Based on the findings, it can be concluded that the RF model demonstrates superior performance in predicting the synergistic influence of stressors (PTEs and alkalinity) on the microbial community. The RMSE and r value of the RF model are represented in Table 25.

Table 25: Root Mean Square Error (RMSE) and correlation coefficient (r) values for different machine learning techniques

		Machine learning models						
Parameters		**LR**	**RT**	**RF**	**XGB**	**MARS**	**SVM**	**KNN**
	r	0.957	0.865	0.978	0.969	0.959	0.974	0.952
CROSS	**RMSE**	0.009	0.015	0.006	0.008	0.009	0.007	0.009
	r	0.938	0.833	0.970	0.958	0.955	0.969	0.938
ECR	**RMSE**	0.281	0.443	0.194	0.232	0.239	0.199	0.275
	r	0.962	0.865	0.980	0.974	0.979	0.977	0.956
MCAR	**RMSE**	0.008	0.015	0.006	0.007	0.006	0.006	0.009
	r	0.857	0.833	0.881	0.815	0.876	0.889	0.871
MH	**RMSE**	1.721	1.844	1.568	1.984	1.620	1.534	1.633
	r	0.923	0.852	0.964	0.947	0.962	0.959	0.926
ESP	**RMSE**	0.213	0.290	0.144	0.177	0.149	0.155	0.204
	r	0.934	0.804	0.965	0.952	0.956	0.959	0.931
SAR	**RMSE**	0.006	0.010	0.005	0.005	0.005	0.005	0.006
	r	0.922	0.925	0.975	0.842	0.980	0.943	0.990
BA_Cr	**RMSE**	15.495	15.350	8.722	22.096	7.952	13.154	5.622
	r	0.906	0.885	0.924	0.875	0.931	0.932	0.904
BA_Cd	**RMSE**	0.148	0.162	0.132	0.170	0.126	0.125	0.148
	r	0.851	0.859	0.921	0.887	0.837	0.873	0.914
BA_Cu	**RMSE**	3.910	3.812	2.853	3.437	4.067	3.576	3.001
	r	0.739	0.834	0.787	0.863	0.841	0.796	0.844
BA_Ni	**RMSE**	8.854	6.962	7.750	6.524	6.737	7.538	6.684
	r	0.538	0.667	0.666	0.595	0.443	0.746	0.668
BA_Pb	**RMSE**	2.626	2.171	2.161	2.534	2.883	1.911	2.131

Subsequently, the algorithms employed are SVM, GBM, MARS, and KNN. RT was identified as the least effective performer within the models. The predictive capability of Random Forest (RF) was purported to be superior due to its reliance on numerical evidence, which provides a robust and adaptable framework (Moorhead et al., 2013). The utilization of this machine learning methodology has the capability to offer a precise and resilient resolution in comprehending the immediate soil health, hence rendering it highly advantageous for practical implementations in the real world.

All the aforementioned findings offer valuable insights into the extent of PTEs contamination and its potential impact on the food chain in agricultural regions near mining sites. However, this study has a few limitations, including the selection of different rice varieties and different vegetable crops and seasonal variations, which could affect the uptake of PTEs in rice parts

and also influence food chain risk. Additionally, the local people residing in this area are reluctant to grow crops and vegetables across different seasons due to water scarcity (as cultivation solely depends on rainfall), lack of funding, and inadequate agricultural facilities. This study emphasizes the future potential of adopting various remediation techniques, particularly bioremediation (including phytoremediation/microbial remediation), as efficient, cost-effective, and sustainable approaches for managing toxic mine waste. Additionally, the results provide policymakers and authorities with critical information on PTE pollution, enabling them to develop effective waste management policies and contribute to environmental protection.

Objective: 2

4.2 Determining Cr-tolerance of vetiver grass (*Chrysopogon zizanioides*) via hydroponic system

This study assessed the effectiveness of the vetiver (*Chrysopogon zizanioides*, ecotype: Sunshine) plant (efficacy of phytoremediation technology) in remediating Cr in a hydroponic system. This method offers a comprehensive insight of the vetiver system's capacity for chromium removal. Vetiver plants were acclimatized for 30 days in a hydroponic system and subsequently transplanted to plastic tanks (12 L capacity) holding 10 L of nutrient medium, which was continually aerated using air circulation tubing. The hydroponics experiment was carried out at the greenhouse of the Experimental Agricultural Farm, Indian Statistical Institute (ISI), Jharkhand, India. Vetiver grass tillers with comparable biomass and height (22–28 g fresh weight per tank) were utilized for the hydroponic experiment (Fig. 49).

Fig. 49: Hydroponic system set up with vetiver and different doses of Cr

The fundamental nutritional media employed for vetiver acclimatization was a modified Hoagland's solution, as delineated by Sahi et al. (2002). Following the 30-day acclimatization phase, a fresh nutritional medium was prepared using potassium dichromate ($K_2Cr_2O_7$) as the Cr source, added at concentrations of 0, 5, 10, 15, 20, 50, 75, and 100 mg Cr L^{-1}. Deionized water was utilized in the preparation of the nutritional medium and Cr solutions. The experiment was carried out over a duration of 21 days, with intervals of 7 days. The treatment combinations were set up in a complete randomized design (CRD) consisting of 8 treatments, each replicated 3 times. The greenhouse maintained an average temperature of 27.0 °C ± 1, a humidity level of 60% ± 5, and a light/dark cycle of 14 hours of light and 10 hours of darkness. A thorough investigation was performed, including the accumulation of Cr in different plant sections (root, shoot), biochemical parameters (total chlorophyll, protein), stress osmolyte (proline), and growth characteristics (root length, shoot length, plant biomass fresh weight).

4.2.1 Temporal changes of Cr content in water during the hydroponic experiment

The Cr concentration in water (hydroponic tank) was periodically monitored to assess its uptake pattern and concentration over time. The results, illustrated in the corresponding Fig. 50(a), showed that different Cr concentrations were initially (0 day) maintained and measured at 7-day intervals. After 7 days, a significant reduction (LSD_Day: 0.024; *p*: 0.002) in Cr levels was observed at lower concentrations (5, 10, 15, and 20 mg L^{-1}), indicating that vetiver effectively absorbed Cr through both roots and shoots. In contrast, Cr levels at higher concentrations decreased more gradually. By day 14, Cr in the lower concentration treatments was nearly undetectable, suggesting efficient uptake by vetiver. However, at higher concentrations, Cr levels approached a saturation point, and by day 21, there was almost no detectable change in Cr concentration compared to day 14. The most substantial reduction in Cr (at 75 mg L^{-1}) occurred by day 14. During this period, vetiver showed no visible physiological symptoms. However, at 75 and 100 mg L^{-1}, signs of stress such as leaf yellowing, decolorization appeared by day 21, and in the 100 mg L^{-1} treatment, symptoms were already evident by day 14. The result was consistent with Andra et al., (2009), who demonstrated lead uptake in a hydroponic system utilising vetiver.

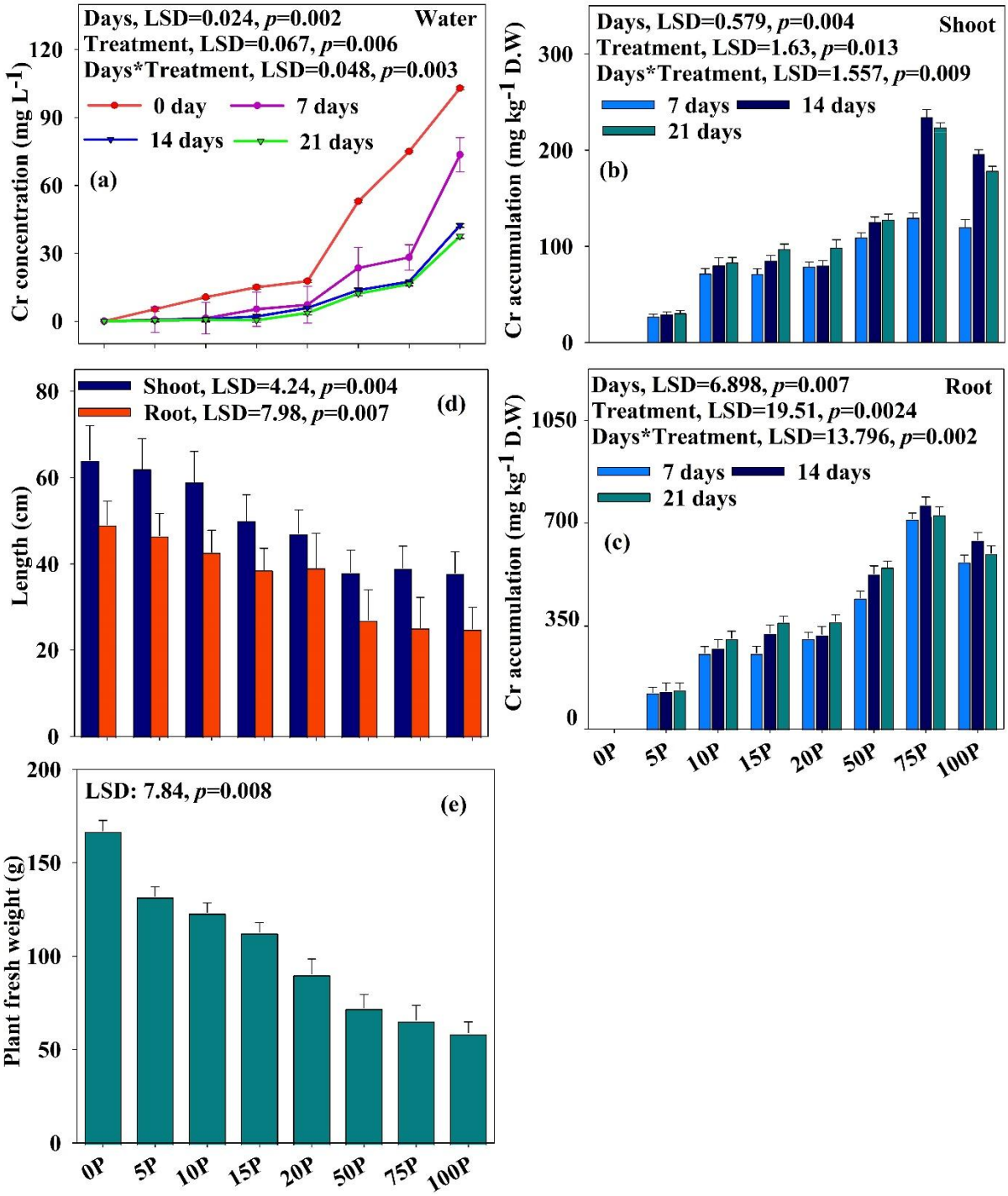

Fig. 50: Different attributes evaluation during the hydroponic experiment. (a) Changes of Cr concentration in water, Cr accumulation in shoots (b) and roots (c) of vetiver, and length (d) and fresh weight (e) of vetiver plant

4.2.2 Periodic changes of Cr accumulation pattern in the root and shoot of vetiver plant during the experiment

The variation in Cr accumulation in the roots and shoots of vetiver plants is illustrated in the Fig. 50 (b,c). Overall, Cr concentration was consistently higher in the roots compared to the shoots. At day 7, plants exposed to lower Cr concentrations (5, 10, 15, and 20 mg L^{-1}) showed a significant increase in Cr uptake in both roots (LSD_Day: 6.898; *p*: 0.007) and shoots (LSD_Day: 0.579; *p*: 0.004). In treatments with higher concentrations (75 and 100 mg L^{-1}), Cr uptake was also substantial when compared to the control. In the control set, plants had no detectable Cr in either roots or shoots due to the absence of Cr exposure. Plants in the control group exhibited no physiological symptoms. By day 14, Cr uptake reached its peak across both plant parts and all concentration levels. Interestingly, plants exposed to a moderate dose (50 mg L^{-1}) exhibited uptake patterns similar to those observed at lower concentrations. However, by day 21, Cr uptake in the lower concentration treatments remained relatively unchanged, while in the higher concentrations, uptake was very low due to saturation, and the plants began to exhibit physiological stress symptoms, such as chlorosis. The highest accumulation and tolerance to Cr were observed at 75 mg L^{-1} by day 14. Notably, Cr translocation from root to shoot was limited, indicating that vetiver primarily retains Cr in its root system. This characteristic supports its role in phyto-stabilization. Similar observations were reported by Andra et al. (2009), and Baker et al. (1994) suggested that the immobilization of metals in roots serves as a plant's exclusion strategy to mitigate metal toxicity.

4.2.3 Growth properties and biochemical attributes evaluation after harvest under different Cr dose

The assessment of various growth parameters and biochemical traits of vetiver after harvest is shown in Fig. 50 (d, e), 51. Key growth indicators such as root length, shoot length, and overall biomass were noticeably affected by different concentrations of Cr (Fig. 50 d, e). Both the length and biomass of the vetiver plants increased significantly ($p < 0.05$) compared to their initial values before acclimatization, indicating that the plants continued to grow throughout the experimental period. In the control group, where no Cr was added, the plants appeared healthy and showed robust growth. However, as the Cr concentration increased from 5 mg L^{-1} to 100 mg L^{-1}, there was a clear decline in both root and shoot lengths, as well as a reduction in biomass at harvest. This decline can be attributed to the toxic effects of Cr, which interfere

with the plant's physiological functions and ultimately hampers its growth. A comparable result was achieved by Andra et al. (2009) with Pb.

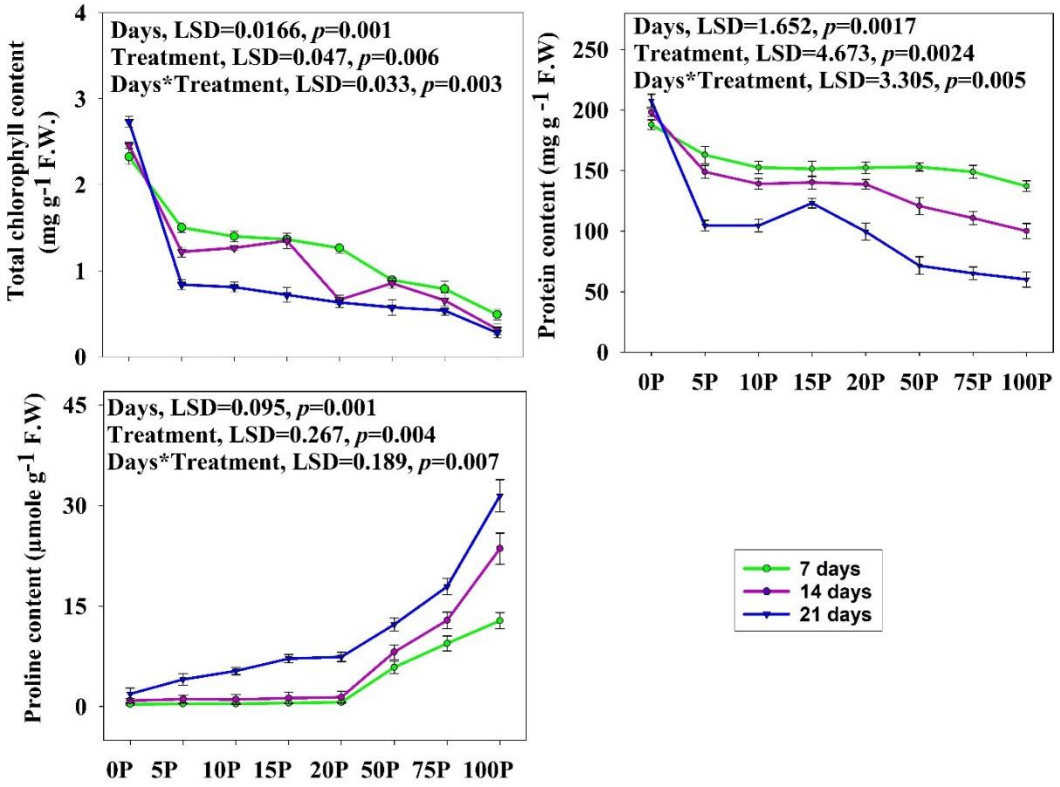

Fig. 51: Periodic changes of biochemical parameters (total chlorophyll, protein, and proline) estimation in vetiver shoot

In addition, key biochemical attributes were primarily analyzed in the shoots of vetiver plants to assess their response to stress. The main parameters measured included total chlorophyll, total protein, and the important osmolyte proline. These were evaluated periodically and are presented in the corresponding Fig. 51. Total Chlorophyll (LSD_Day: 0.0166; *p*: 0.001) and protein (LSD_Day: 1.652; *p*: 0.0017) levels showed a significant decline at higher Cr concentrations from day 7 to day 21, with the most pronounced decrease observed in the 100 mg L^{-1} treatment compared to the control. This reduction in chlorophyll content is likely due to metal accumulation in plant tissues, which may have disrupted the photosynthetic electron transport chain, leading to decreased chlorophyll synthesis (Patra et al., 2018). Furthermore, metal toxicity in treatments may result in reduced protein content, corroborating the findings of Farhangi-Abriz et al., (2017). Conversely, proline content (LSD_Day: 0.095; *p*: 0.001) increased with rising Cr concentrations, regardless of the duration of exposure. This suggests an adaptive response, as proline functions as an effective osmoregulator that helps protect plants from oxidative stress under adverse conditions (Yang et al., 2025).

Objective: 3

4.3 Enhancing Mycophytoremediation Potential of *Chrysopogon zizanioides* in Chromium-Asbestos Mine Waste Soil Using Arbuscular Mycorrhizal Fungi

This study evaluated the effectiveness of the vetiver-AMF system (mycophytoremediation technology) in remediating chromium-asbestos mine waste-contaminated field soil over a two-month period. A comprehensive analysis was conducted, which included the accumulation of trace elements (PTEs) in various plant parts in the presence of AMF infection, antioxidant enzyme activity, changes in soil properties, plant physiological and biochemical assessments, and the percentage of AMF colonization. This approach provides a detailed understanding of the vetiver system's potential for mycophytoremediation. The pot experiment was conducted at the greenhouse of Experimental Agricultural Farm, Indian Statistical Institute (ISI), Jharkhand, India. The treatment combinations were set up in a completely randomized design (CRD) with five treatments, each treatment being repeated three times. The treatment details are depicted in Table 26.

Table 26: The treatment details of mycophytoremediation experiment

Treatments	Depiction
C1 (Control)	Soil contaminated with CAMW + Vetiver plant
M1	Soil contaminated with CAMW + Vetiver plant + *Glomus hoi*
M2	Soil contaminated with CAMW + Vetiver plant + *Funneliformis coronatum*
M3	Soil contaminated with CAMW + Vetiver plant + *Claroideoglomus claroideum*
M4	Soil contaminated with CAMW + Vetiver plant + *Claroideoglomus etunicatum*

Earthen pots (measuring 23 cm in diameter and 20 cm in depth) were filled with 10.0 kg of chromium waste-contaminated soil. Vetiver plants (*Chrysopogon zizanioides*, ecotype: Sunshine) were pruned uniformly, ensuring root lengths of 10-12 cm and shoot lengths of 20-25 cm. An amount of 100 g of mycorrhizal inoculums per kg of substrate, (including fungal spores, and mycelium), was administered at a depth of 4-5.0 cm below the surface of sterilized roots (treated with 0.1% mercuric chloride for 4-5 minutes) of the Vetiver plant. The control treatment, which did not involve mycorrhizal activity, was given an equivalent quantity of soil. The greenhouse was kept at an average temperature of 27.0 °C ± 1, with a humidity level of 60% ± 5, and a light/dark cycle of 14 hours of light followed by 10 hours of darkness. The soil

moisture was maintained at around 60% of its field capacity. The plants were then harvested after a period of two months.

4.3.1 Physico-chemical properties of soil among the treatments (initial and post-harvest)

Table 27 summarizes the initial (0 day) physicochemical properties of soil contaminated with chromium-asbestos mine-waste. Initially, the soil exhibited a slightly acidic pH and contained low levels of total organic carbon (TOC) and nutrients.

Table 27: Initial physico-chemical and microbial-enzymatic properties of soil contaminated with chromium-asbestos mine-waste

Parameters	Mean ± SD
pH	6.37 ± 0.41
TOC (%)	0.37 ± 0.012
AN (mg kg^{-1})	23.97 ± 1.09
AP (mg kg^{-1})	18.74 ± 1.01
AK (mg kg^{-1})	104.64 ± 6.17
MBC (mg kg^{-1})	213.12 ± 13.16
BSR (mg CO_2 released $kg^{-1}h^{-1}$)	4.14 ± 0.27
SIR (mg CO_2 released $kg^{-1}h^{-1}$)	10.38 ± 0.76
FDA (mg fluorescein kg^{-1} soil h^{-1})	14.17 ± 1.13
DHG (mg TPF released kg^{-1} soil h^{-1})	3.78 ± 0.21
BG (mg *p*-nitrophenol released kg^{-1} soil h^{-1})	9.76 ± 0.68
U (mg urea hydrolysed kg^{-1} soil h^{-1})	13.75 ± 0.92
APP (mg *p*-nitrophenol released kg^{-1} soil h^{-1})	38.98 ± 2.04

Soil essential nutrients such as available nitrogen (AN), available phosphorus (AP), and available potassium (AK) were measured at 23.97 ± 1.23 mg kg^{-1}, 19.74 ± 0.87 mg kg^{-1}, and 104.64 ± 3.87 mg kg^{-1}, respectively, at the initial phase (0 day) of the experiment. After 60 days of the mycophytoremediation pot experiment, treatments enriched with different AMF species exhibited a significant increase in soil properties compared to the control vetiver plants (devoid of AMF) (Table 28).

Table 28: Physico-chemical properties of different treatment soil at time of harvest

Treatment	pH	OC (%)	AN (mg kg^{-1})	AP (mg kg^{-1})	AK (mg kg^{-1})
C1	6.62 ± 0.36	0.43 ± 0.035	27.29 ± 2.09	21.14 ± 1.51	147.81 ± 6.31
M1	6.93 ± 0.39	0.649 ± 0.041	43.16 ± 3.32	31.97 ± 2.28	229.25 ± 12.10
M2	6.73 ± 0.27	0.561 ± 0.024	37.69 ± 2.89	27.84 ± 1.98	183.97 ± 9.33
M3	6.67 ± 0.21	0.494 ± 0.021	33.17 ± 2.55	23.87 ± 1.70	172.76 ± 8.39
M4	6.61 ± 0.22	0.57 ± 0.032	34.89 ± 2.68	22.19 ± 1.58	163.34 ± 8.12

C1: Control plant (without AMF); **M1:** *Glomus hoi;* **M2:** *Funneliformis coronatum*; **M3:** *Claroideoglomus claroideum*; **M4:** *Claroideoglomus etunicatum*

The soil pH increased in the presence of M1 infection, reaching a neutral range compared to other AMF species. The shift in soil pH towards neutrality was likely due to the AMF promoting plant growth, stimulating microbial activity, and triggering the production of oxidative enzymes (Chelangat et al., 2021). Soil nutrients, including TOC, AN, AP, and AK, were significantly higher in the presence of *Glomus hoi* (M1), followed by *Funneliformis coronatum* (M2), *Claroideoglomus claroideum* (M3), and *Claroideoglomus etunicatum* (M4) depicted in Table 28. AMF increases the carbon content in soil by producing residues deposited in the soil, releasing enzymes (hydrolytic enzymes) that help break down plant and microbial matter, and boosting plant growth (Treseder and Holden, 2013). It also improves plant nutrient absorption, which leads to more photosynthesis and the production of carbon-rich compounds like carbohydrates. This, in turn, increases microbial activity, available carbon, and other nutrients in the soil (Agnihotri et al., 2022). AMF is essential for enhancing the availability of P in the soil which breaks down soil substrates and releases accessible phosphate through their metabolic process (Fall et al., 2022). AMF plays a role in mobilizing inorganic nitrogen, such as ammonium ions (NH_4^+), from the soil (Casieri et al., 2013). Like AP, AMF also improves the absorption of AK in nutrient-deficient soils (Dominguez-Nuñez et al., 2016). The AMF mycelium is capable of absorbing nitrogen in multiple forms, including ammonium (NH_4^+), nitrates (NO_3^-), and amino acids (Jansa et al., 2019). It has also been shown that mycorrhizal associations may play a crucial role in the breakdown and mineralization of plant organic matter, helping to mobilize nutrients, especially nitrogen, to support the host plant.

4.3.2 Sequential extraction of different forms of PTEs in soil contaminated with chromium-asbestos mine waste across treatments

Table 29 shows the distribution of TE forms in chromium mine waste-contaminated soil initially. The assessment of potential toxicity and accumulation patterns primarily relied on the bioavailable fractions of TEs, especially the water-soluble phase (WS), and exchangeable phase (EX) forms. The presence of toxic mine waste in the soil resulted in significantly higher levels of PTEs such as Cd, Ni, and Cr compared to other PTEs like Cu and Pb at the initial time.

Table 29: Initial PTEs concentration at different phases (mg kg^{-1}) of soil containing Chromium-asbestos mine waste

Soil_Cr_Phases	Concentration (Mean ± SD)	Soil_Ni_Phases	Concentration (Mean ± SD)	Soil_Cd_Phases	Concentration (Mean ± SD)	Soil_Pb_Phases	Concentration (Mean ± SD)	Soil_Cu_Phases	Concentration (Mean ± SD)
Cr-WS	28.8 ± 1.67	**Ni-WS**	17.90 ± 1.23	**Cd-WS**	0.349 ± 0.014	**Pb-WS**	8.89 ± 0.35	**Cu-WS**	4.74 ± 0.203
Cr-EX	51.04± 4.51	**Ni-EX**	31.76 ± 1.68	**Cd-EX**	0.579 ± 0.021	**Pb-EX**	19.76 ± 1.11	**Cu-EX**	11.42 ± 0.96
Cr-CAR	39.32 ± 2.76	**Ni-CAR**	36.71 ± 2.14	**Cd-CAR**	1.110 ± 0.045	**Pb-CAR**	12.13 ± 0.83	**Cu-CAR**	26.67 ± 1.53
Cr-OX	229.61 ± 17.13	**Ni-OX**	196.41 ± 12.33	**Cd-OX**	1.738 ± 0.063	**Pb-OX**	21.67 ± 1.13	**Cu-OX**	27.14 ± 1.82
Cr-ORG	27.32 ± 1.43	**Ni-ORG**	33.95 ± 2.03	**Cd-ORG**	0.238 ± 0.011	**Pb-ORG**	11.63 ± 0.89	**Cu-ORG**	16.21 ± 1.07
Cr-MIN	662.80 ± 46.23	**Ni-MIN**	489.74 ± 27.86	**Cd-MIN**	1.990 ± 0.009	**Pb-MIN**	68.25 ± 4.17	**Cu-MIN**	66.14 ± 4.79

Generally, PTEs shows varying distribution patterns in the soil, from easily extractable forms to more persistent and stable ones, due to various interactions with soil components (Bhattacharyya et al., 2008). At the beginning, the concentrations of WS-PTEs (Cr: 28.8 mg kg^{-1}, Ni: 17.90 mg kg^{-1}, and Pb: 8.89 mg kg^{-1}) EX-PTEs (Cr: 51.04 mg kg^{-1}, Ni: 31.76 mg kg^{-1}, and Pb: 19.77 mg kg^{-1}), OX-PTEs (Cr: 229.62 mg kg^{-1}, Ni: 196.41 mg kg^{-1}, and Pb: 21.68 mg kg^{-1}), and other TE phases are significantly higher in the waste amended soil (Table 29). The presence of hazardous toxic mine waste and the presence of PTEs deteriorate soil structure, adversely impacting the overall ecosystem. This also hinders natural plant growth and disrupts soil microbial activity (Banerjee et al., 2024). To address this issue, a pot experiment was conducted using a combination of vetiver plants and four different AMF cultures. Following the pot experiment, the concentration of bioavailable PTEs in the soil significantly decreased in the WS-PTEs phase (approximately 77%-89%) and the EX-phase (approximately 74%-87%) in the presence of M1 infection, compared to the control plants (approximately WS-PTEs: 16%-42%; EX-PTEs: 8%-28%) (Fig. 52). Among the other AMF infections, such as M2, M3, and M4, the lowest decrease in PTEs was observed with M4 (*Claroideoglomus etunicatum*). Microorganisms like bacteria, fungi, and arbuscular mycorrhizal fungi (AMF) are key agents in mitigating PTEs toxicity in soil (Singh et al., 2019). The other dominant fractions, particularly Fe (III) and Mn (IV) oxides, exhibited the highest levels of PTEs binding in the control treatment. However, in the presence of M1 infection, the OX-PTEs levels showed a slight decrease, followed by reductions observed with as M2, M3, and M4 compared to the control (C1) as illustrated in Fig. 52.

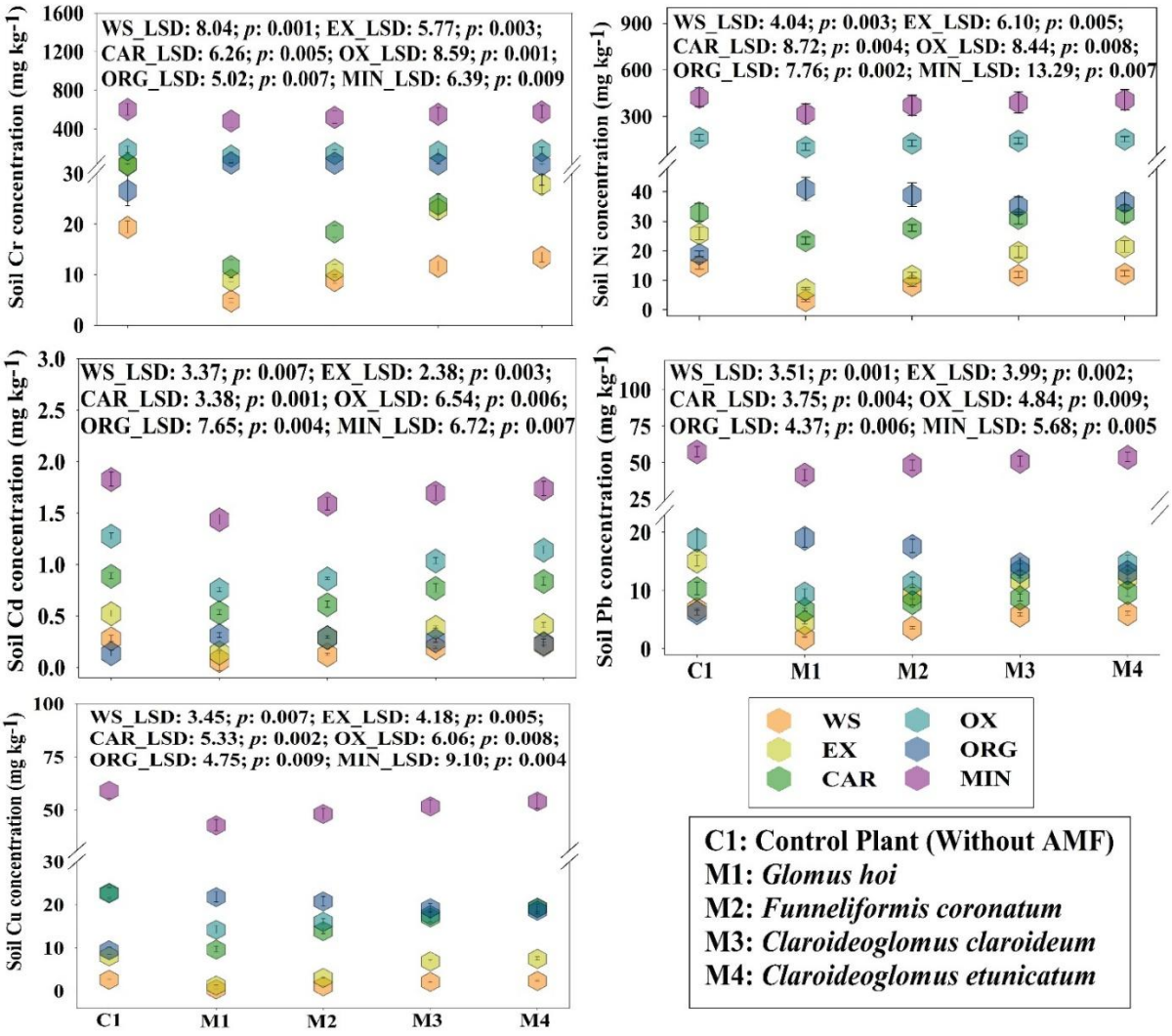

Fig. 52: Sequential extraction of different PTEs forms in soil contaminated with chromium-asbestos mine-waste at post-harvest. Here, **C1:** Control plant (without AMF); **M1:** *Glomus hoi;* **M2:** *Funneliformis coronatum*; **M3:** *Claroideoglomus claroideum*; **M4:** *Claroideoglomus etunicatum*

This suggests that the reductive dissolution of Fe (III) and Mn (IV) may occur in the presence of AMF infection. In the Org-bound phases, PTEs accumulation in the soil showed a slight increase in the presence of AMF infection, likely due to the secretion of glomalin protein, which facilitates the sequestration of toxic PTEs in the soil. The order of PTEs content increase under AMF infection was: *Glomus hoi* > *Funneliformis coronatum* > *Claroideoglomus claroideum* > *Claroideoglomus etunicatum*. Other phases like CAR, and Min bound phases of PTEs were slightly decreased as compared with the C1 plant. This pot experiment demonstrated that the presence of AMF infection in vetiver roots enhances the plant's ability to accumulate PTEs, leading to increased uptake compared to plants without infection. AMF species such as *Glomus*

hoi and *Funneliformis coronatum* enhance the remediation potential of the vetiver plant more effectively than other species.

4.3.3 PTEs accumulation pattern in the shoots and roots of vetiver infected by various AMF

The accumulation of PTEs in both the shoots and roots varied depending on the AMF inoculant, leading to varying phytoextraction/phytostabilization patterns observed at harvest (Fig. 53). The results showed that plants treated with all four AMF species accumulated significantly higher levels of PTEs (Cr, Ni, Cd, Pb, and Cu) in their root tissues. The PTEs levels varied depending on the AMF inoculation, affecting both shoots and roots. Some fungi increased PTEs concentrations, while others reduced them in the plants. The concentrations of Pb, Cu, Cd, Ni, and Cr in the roots of *Glomus hoi*-treated plants were higher by 33.21%, 32.44%, 27.79%, 27.44%, and 21.74%, respectively, compared to the C1 (Fig. 53). Ma et al. (2019) found that inoculating *Helianthus annuus* with the AMF *Claroideoglomus claroideum* (BEG210) boosted Ni accumulation in plants grown in Ni-contaminated saline soils, compared to the non-inoculated control (C1). Similarly, plants inoculated with M4 had the highest concentrations of PTEs, particularly Cr and Ni, in the roots followed by M3, and M2. Several studies have reported that AMF employs mechanisms that facilitate PTEs accumulation in root tissue while limiting their transfer to the shoots, thereby enhancing the phytostabilization process (Singh et al., 2019) Additionally, In the control plants, the Cr, Pb, and Ni concentrations in roots were 389.39 mg kg^{-1}, 61.96 mg kg^{-1}, and 209.21 mg kg^{-1}. Furthermore, AMF functions as a biofilter, preventing the transfer of PTEs from the roots to the shoots, in contrast to the control plants. Plants inoculated with M1, M2 and M3, along with the control group (C1), showed the highest concentrations of Cr, Ni, and Pb in the roots. Interestingly, AMF accumulate PTEs in their extrametrical hyphae and extra-hyphal slime, effectively sequestering them near the roots and limiting their absorption by the plant's shoots (Danesh et al., 2013).

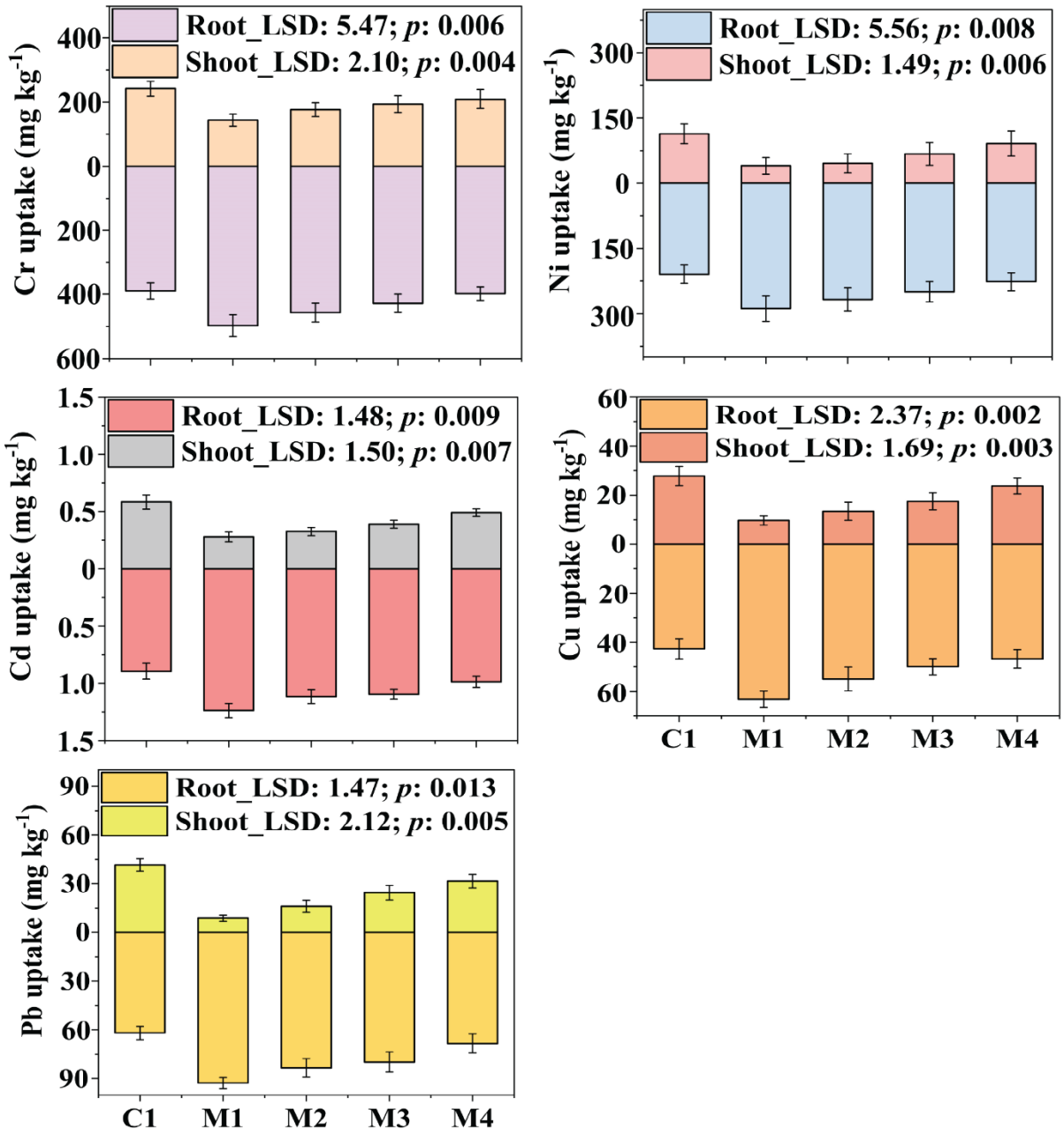

Fig. 53: Accumulation of PTEs in root and shoot of vetiver plant in presence of four different AMF treatments and control (devoid of AMF) at post-harvest. Here, **C1:** Control plant (without AMF); **M1:** *Glomus hoi;* **M2:** *Funneliformis coronatum*; **M3:** *Claroideoglomus claroideum*; **M4:** *Claroideoglomus etunicatum*

Among the analyzed elements, Cr and Ni were found in the highest concentrations in the shoots, followed by Cd, Pb, and Cu in the AMF-infected plants as depicted in Fig. 53. These concentrations are considered harmful or toxic to the majority of plant species (Kabata-Pendias 2011). Plant growth in the control pots (C1) was hindered due to PTEs toxicity, whereas growth improved in the AMF-treated pots. This occurred in control plots because of PTEs ionic

properties, their ability to bind to various cellular ligands, and their interaction with native essential metals. Elements like Cu and Pb exhibited lower concentrations in the plant shoots, likely due to their strong affinity for the roots, which prevents their translocation to the shoots (Mayer, 2017). Cd is known to compete with cellular zinc, ultimately interfering with enzyme activities. Similarly, other PTEs have been reported to disrupt oxidative phosphorylation and affect membrane permeability (Singh et al., 2019). The highest accumulation of PTEs in vetiver shoots was observed in the case of *C. etunicatum* (M4) compared to the other species. Among the fungi tested, inoculation of vetiver with *Glomus hoi* significantly decreased the levels of PTEs, particularly Cr, and Ni, in the shoots, followed by *Funneliformis coronatum* (M2), compared to the control (C1) treatment. The beneficial role of AMF has been documented by numerous researchers in limiting the translocation of PTEs from colonized roots to shoots in highly PTEs-polluted soils.

4.3.4 Microbiological and enzymatic parameters among different treatments

Fig. 54 denotes the periodical variation of microbial properties among the treatments during experiment. AMF species significantly influenced plant root site and soil microbial activity as indicated by MBC (T_LSD: 3.37, *p*: 0.002). A consistent periodic increase in MBC was observed across all AMF inoculums, with the M1 treatment (527.66 mg kg^{-1}) showing the highest microbial activity, while the Plant treatment (devoid of AMF) C1 exhibited the lowest MBC (338.32 mg kg^{-1}). This outcome highlights the role of mycorrhizal roots in creating a sink demand for carbon and nitrogen. AMF mineralizes waste, leading to an increase in soil microbial populations, which subsequently elevates the MBC content in the plant root site. This rise in MBC enhances enzyme activity, improving the availability of plant nutrients. The Basal soil respiration (BSR) was highest (T_LSD: 0.36, *p*: 0.004) in the M1 treatment and lowest in the M4 treatment, depicted in Fig. 54. Similarly, substrate-induced respiration peaked in the *Glomus hoi* (M1) treatment as compared with C1 treatment. Microbial respiration serves as a reliable predictor of the soil microbial response to disturbances under stress conditions (Tripathy et al., 2014).

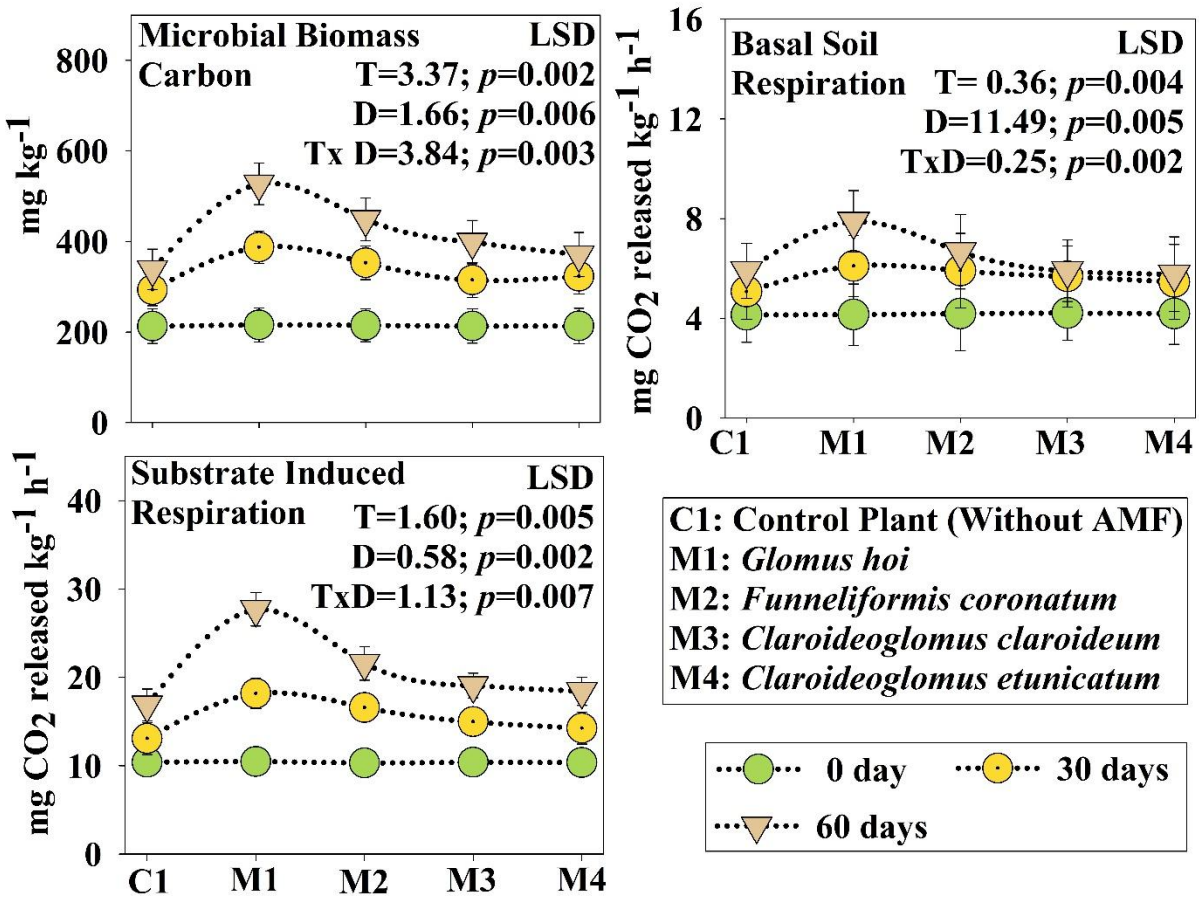

Fig. 54: Temporal dynamics of microbial properties of chromium-mine waste contaminated soil with and without four different AMF treatment. Here, **C1:** Control plant (without AMF); **M1:** *Glomus hoi;* **M2:** *Funneliformis coronatum*; **M3:** *Claroideoglomus claroideum*; **M4:** *Claroideoglomus etunicatum*

The enzyme activities fluorescein diacetate (FDA), dehydrogenase (DHG), acid phosphatase (APP), Urease (U) as well as β-glucosidase (BG), serve as indicators of microbial establishment and growth in the soil (Singh et al., 2019). The temporal variation of enzymatic parameters were represented in Fig. 55. The AMF treatments influenced enzyme activity, resulting in statistically significant differences from the C1 ($p < 0.05$). FDA hydrolytic activity was low in control treatments but significantly (T_LSD: 3.94, *p*: 0.006) higher in the M1 treatment (47.35 mg fluorescein kg soil^{-1} h^{-1}) followed by M2 (38.06 mg fluorescein kg soil^{-1} h^{-1}), and M3 (31.24 mg fluorescein kg soil^{-1} h^{-1}). This result suggests that microbial cells in the control treatment produce less fluorescein due to stress from toxic mine waste, while AMF-treated pots show higher fluorescein activity, highlighting AMF's role in reducing stress, boosting microbial activity, and improving nutrient availability. The results DHG activity significantly increased periodically (D_LSD: 1.04, *p*: 0.007) in the AMF-treated pots compared to the C1. DHG is an oxidoreductase enzyme found only in viable cells. DHG enzyme activity, the most sensitive

among those tested, increased significantly (T_LSD: 3.29, *p*: 0.009) with M1 inoculation, demonstrating the best AMF performance, while the *C. etunicatum* (M4) showed the lowest performance. The maximum U, and BG activity was observed at the time of harvest in case of M1 (46.26 mg urea kg soil^{-1} h^{-1} and 43.84 mg PNP kg soil^{-1} h^{-1}) treatment followed by M2 (39.03 mg urea kg soil^{-1} h^{-1} and 34.7 mg PNP kg soil^{-1} h^{-1}), M3 (28.06 mg urea kg soil^{-1} h^{-1} and 26.62 mg PNP kg soil^{-1} h^{-1}), and M4 (26.67 mg urea kg soil^{-1} h^{-1} and 22.11 mg PNP kg soil^{-1} h^{-1}) (Fig. 55).

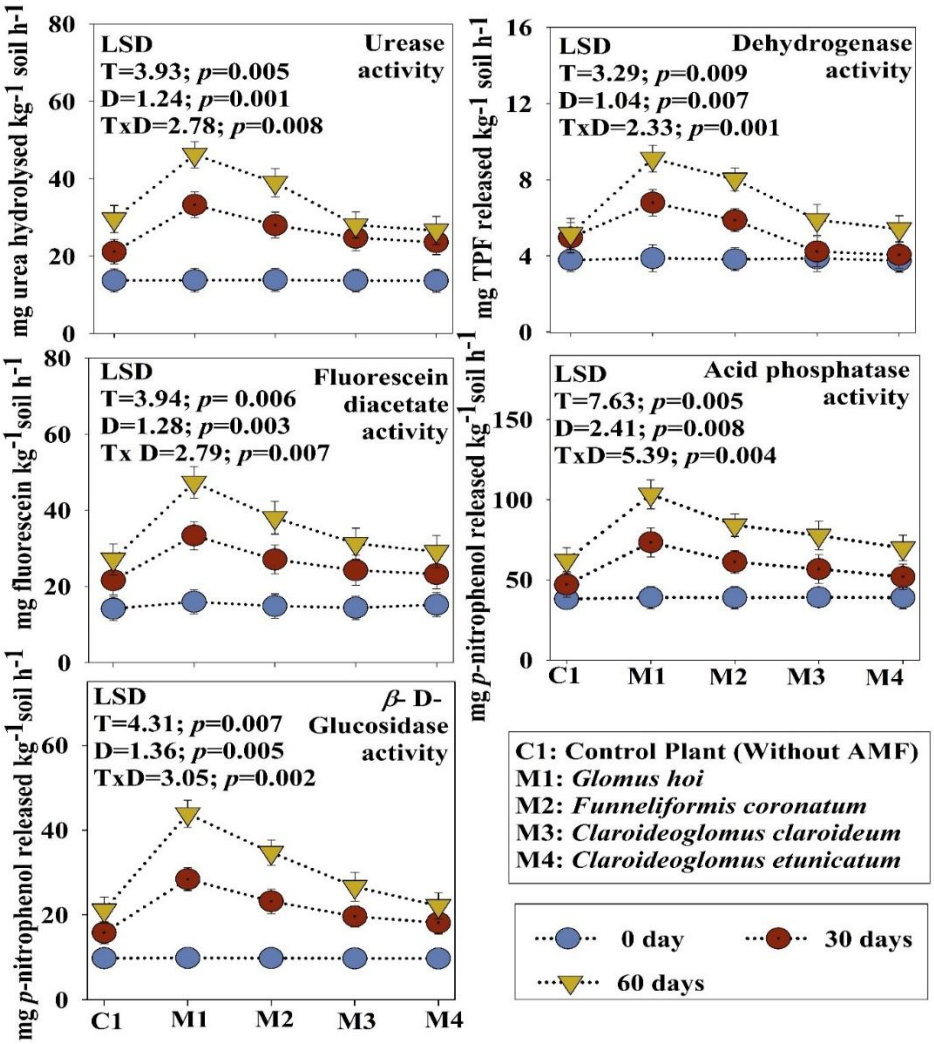

Fig. 55: Periodic variation of enzymatic attributes of chromium-mine waste contaminated soil with and without four different AMF treatment. Here, **C1:** Control plant (without AMF); **M1:** *Glomus hoi;* **M2:** *Funneliformis coronatum*; **M3:** *Claroideoglomus claroideum*; **M4:** *Claroideoglomus etunicatum*

The BG enzyme catalyzes the hydrolysis of cellobiose into glucose, providing energy for microbes, while urease enzyme activity facilitates the hydrolysis of urea into ammonia, increasing pH and releasing NH_3 as the first step in nitrification. The result is consistent with

similar findings by Medina et al. (2006) following soil inoculation with *Glomus mosseae*. The overall trend for APP activity across treatments was M1 > M2 > M3> M4 > C1. Acid phosphatase (APP) activity results indicated that M1 and M2 mycorrhizal isolates were the most effective in promoting hydrolytic processes. AMF treatments improved APP enzyme activity as well as soil and plant phosphorus levels. This improvement is attributed to AMF's ability to convert inorganic phosphate into soluble forms through exchange reactions, chelation, acidification, and the production of organic acids, H^+, and metabolites. Additionally, phosphate-solubilizing bacteria, known for mineralizing organic phosphorus and producing phosphatase, play a crucial complementary role in this process. Additionally, the significant increase in AMF root colonization percentage in the *Glomus hoi* and *Funneliformis coronatum* treatments led to enhanced enzyme activities in the vetiver rhizospheric soil (Fig. 56b). The mycophytoremediation of chromium-asbestos mine waste-contaminated soil was evident through the enhancement of soil biological properties and enzyme activities, which were reflected in the rhizosphere of AMF-treated plants.

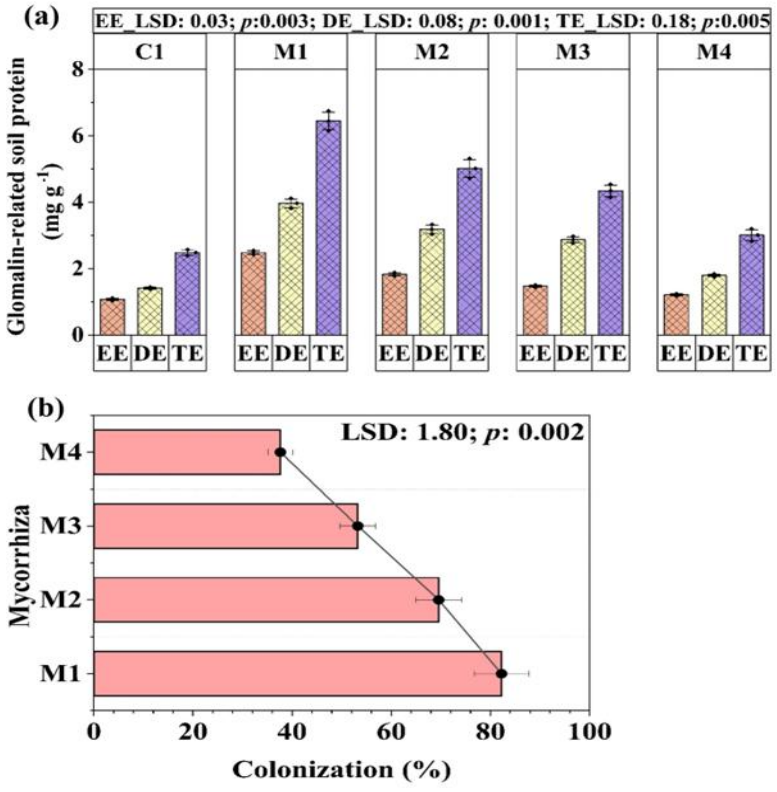

Fig. 56: The AMF attributes including **(a)** Fractions of glomalin-related soil proteins properties of chromium-mine waste contaminated soil with and without four different AMF treatment (post-harvest); **(b)** The colonization percentage of among the AMF treatments at post-harvest. Here, **C1:** Control plant (without AMF); **M1:** *Glomus hoi;* **M2:** *Funneliformis coronatum*; **M3:** *Claroideoglomus claroideum*; **M4:** *Claroideoglomus etunicatum*

4.3.5 Translocation and bio-concentration factor of PTEs across treatments with or without AMF

In AMF treatments, the translocation factor (TF) for Cd, Pb, Cr, Ni, and Cu was significantly below 1 compared to the control, depicted in Table 30. According to TF values, plants are classified as hyperaccumulators (TF > 1) or non-hyperaccumulators (TF < 1) (Singh et al., 2010). However, AMF restricted PTEs movement from roots to shoots, resulting in lower TF values for Ni, Cr, Cd, and Pb. M1 was the most effective AMF species in reducing the translocation of Ni, Cr, Cd, and Pb from roots to shoots, while control plants exhibited higher TF values. TF values below 1 indicate limited Cr and Ni transport from roots to shoots. A similar trend was observed by Gheju et al., (2009) regarding TF.

Table 30: Bioconcentration factor and Translocation factor of PTEs in vetiver plants across treatments

Bioconcentration factor (BCF)					
AMF culture	**BCF_Cr**	**BCF_Ni**	**BCF_Cd**	**BCF_Pb**	**BCF_Cu**
C1	0.441	0.308	0.180	0.539	0.341
M1	0.739	0.580	0.378	1.111	0.697
M2	0.618	0.457	0.293	0.848	0.530
M3	0.536	0.396	0.250	0.756	0.434
M4	0.472	0.341	0.214	0.621	0.385
Translocation factor (TF)					
AMF culture	**TF_Cr**	**TF_Ni**	**TF_Cd**	**TF_Pb**	**TF_Cu**
C1	0.621	0.544	0.654	0.671	0.652
M1	0.289	0.138	0.226	0.095	0.155
M2	0.387	0.170	0.293	0.193	0.246
M3	0.454	0.269	0.358	0.306	0.352
M4	0.526	0.403	0.498	0.460	0.508

C1: Control plant (without AMF); **M1:** *Glomus hoi;* **M2:** *Funneliformis coronatum*; **M3:** *Claroideoglomus claroideum*; **M4:** *Claroideoglomus etunicatum*

The bio-concentration factor (BCF) of plants was increased with AMF inoculation, whereas control plants showed the lowest BCF values (Table 30). Among the AMF species, M1 exhibited the highest BCF values, with 0.73 for Cr, 0.58 for Ni, 0.37 for Cd, and 1.11 for Pb, compared to the control C1 (no AMF). The BCF for PTEs followed the order: Pb > Cr > Cu > Ni > Cd. AMF effectively restricted the translocation of trace elements (PTEs) to the shoots, likely due to their binding to chitin in fungal cell walls and the sequestration of toxic metals in

vesicles (Gohre and Paszkowski, 2006). Additionally, this study found that the micronutrient Cu accumulated at higher levels in the roots of AMF-inoculated plants compared to controls. Liu et al. (2000) highlighted the role of AMF in enhancing the uptake of PTEs and nutrients through extra-radical hyphae, which provide an expanded surface area for the absorption of immobile nutrients.

4.3.6 Glomalin-related soil protein fraction across various treatments

AMF colonization and inoculation significantly influenced GRSP and its fractions in the vetiver rhizosphere soil (Fig. 56a, 57). AMF inoculation led to a 1.31–1.48-fold increase in EE-GRSP compared to non-inoculated treatments. GRSP plays an essential role in enhancing soil structure and biochemical properties critical for soil fertility (Wang et al., 2023).

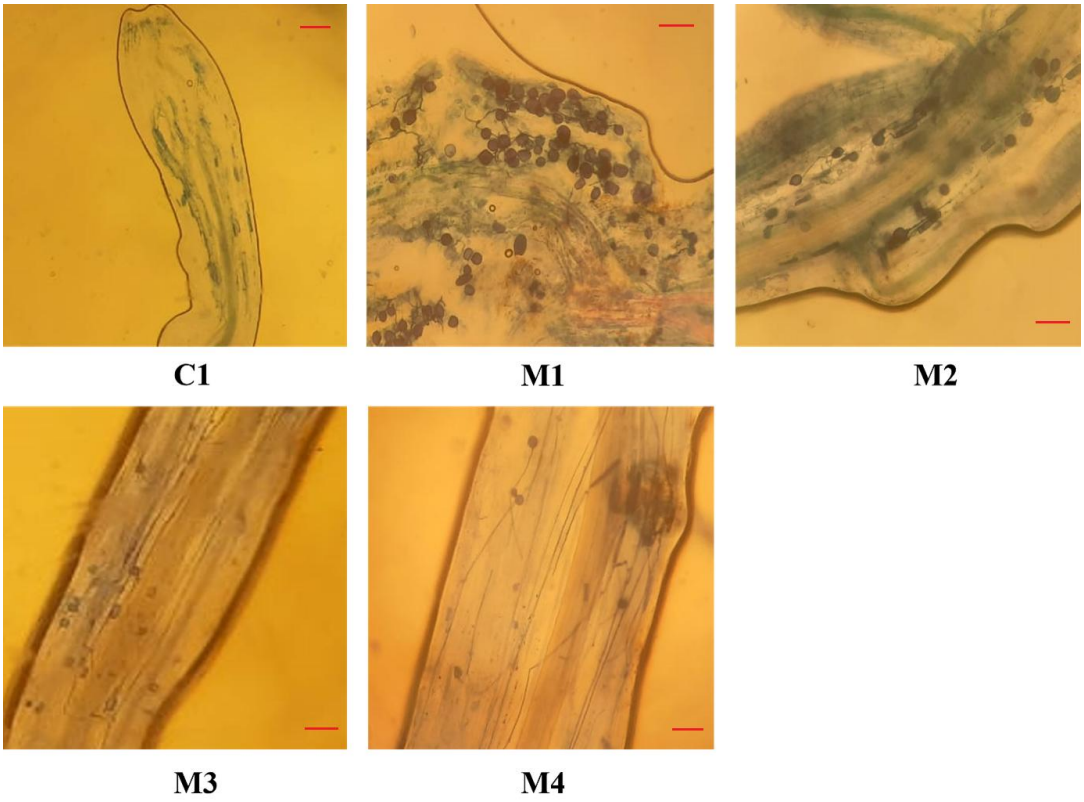

Fig. 57: The root staining shows the different structure of Arbuscular mycorrhizal fungi (AMF) including hyphae, arbusclues, vesicles among different treatments With and without AMF amendment and evaluated root colonization percentage. Here, **C1:** Control plant (without AMF); **M1:** *Glomus hoi;* **M2:** *Funneliformis coronatum*; **M3:** *Claroideoglomus claroideum*; **M4:** *Claroideoglomus etunicatum*

It increases soil carbon and nitrogen storage, stabilizes soil aggregates, and protects organic matter from microbial degradation. In this study, DE-GRSP levels were markedly higher in the rhizosphere soil of plants infected with M1, showing a 2.81-fold increase, followed by M2,

M3, and M4. T-GRSP levels in the vetiver rhizosphere soil were 2.59 times higher in the M1 treatment compared to the uninoculated control (Fig. 56a). Bedini et al. (2009) observed a significant rise in EE-GRSP and TGRSP levels in *Medicago sativa* inoculated with *Funneliformis mosseae* and *Glomus intraradices*. However, the effect of GRSP on soil quality depends on various factors, including host plant species, AMF diversity, environmental conditions, and the application of chemicals or synthetic fertilizers (Anandakumar et al., 2024).

4.3.7 Phosphorus uptake potential of vetiver plant with or without AMF treatments

Across all treatments, the phosphorus levels in plant shoots and roots were significantly higher in AMF-infected treatment as compared to the non-infected plant (control: C1), illustrated in Fig. 58. At harvest, inoculation with M1 led to a 1.91-fold increase in phosphorus content in the roots and a 2.39-fold increase in the shoots. High root colonization by *Glomus hoi* showed a positive correlation (shoot_r: 0.84, root_r: 0.45) with increased P uptake. This was followed by *Funneliformis coronatum* and *Claroideoglomus claroideum,* which enhanced phosphorus levels by 1.83 folds and 1.57 folds in shoots as well as 1.69 folds and 1.41 in roots, respectively. The phosphorus uptake with *Claroideoglomus etunicatum* (M4) was the lowest and closely resembled that of the control treatment. AMF-colonized roots effectively absorbed significant amounts of phosphorus and transported it to other plant parts, even under PTEs-contaminated soils. Supporting these findings, research has shown that AMF enhances the root surface area, including fine roots and root hairs, to optimize the uptake of nutrients and various ions (Mackay et al., 2017).

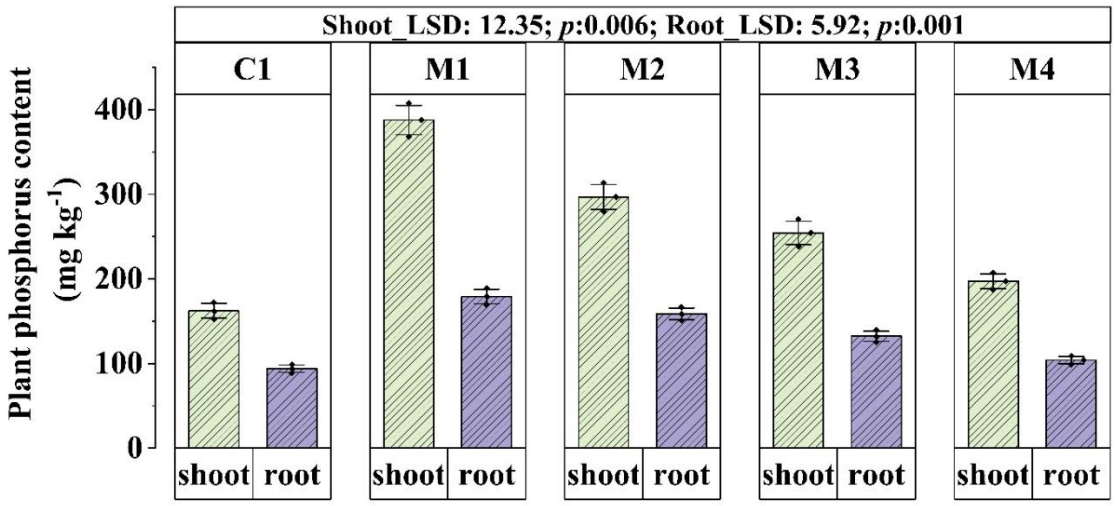

Fig. 58: Total phosphorus content in root and shoot of vetiver with and without four different AMF treatment. Here, **C1:** Control plant (without AMF); **M1:** *Glomus hoi;* **M2:** *Funneliformis coronatum*; **M3:** *Claroideoglomus claroideum*; **M4:** *Claroideoglomus etunicatum*

4.3.8 Biochemical attributes and antioxidant defence activity among the treatments

The chlorophyll content (total chlorophyll, chlorophyll a, and chlorophyll b) and carotenoid levels varied significantly across the treatments (Fig. 59). Plants treated with *Glomus hoi* exhibited the highest levels of chlorophyll a, chlorophyll b, and total chlorophyll, showing increases of 1.32-fold, 1.48-fold, and 1.36-fold, respectively, compared to the control. Similarly, the highest carotenoid content was observed in plants treated with M1, followed by those treated with M2, M3, and M4. In contrast, C1 (without AMF treatment) showed reduced chlorophyll content, likely due to the uptake of PTEs in plant tissues, which may have disrupted the photosynthetic electron transport chain and subsequently reduced chlorophyll pigment levels (Patra et al., 2018). In contrast, Andrade et al. (2008) reported that mycorrhizal inoculation enhanced nutrient uptake in plants and increased chlorophyll content. The total soluble sugar content was significantly higher in AMF amended treatment as compared with control (shoot_LSD: 0.112, *p*: 0.001; root_LSD: 0.415, *p*: 0.017). It plays an important role in plant osmotic balance. Similarly, proline content was found to be lower in control plants (both shoot and root) compared to those inoculated with AMF (Fig. 59). The highest proline accumulation was observed in plants treated with M1 (root: 2.07folds, and shoot: 1.98 folds), which provided greater resistance to PTEs stress, depicted in Fig. 59.

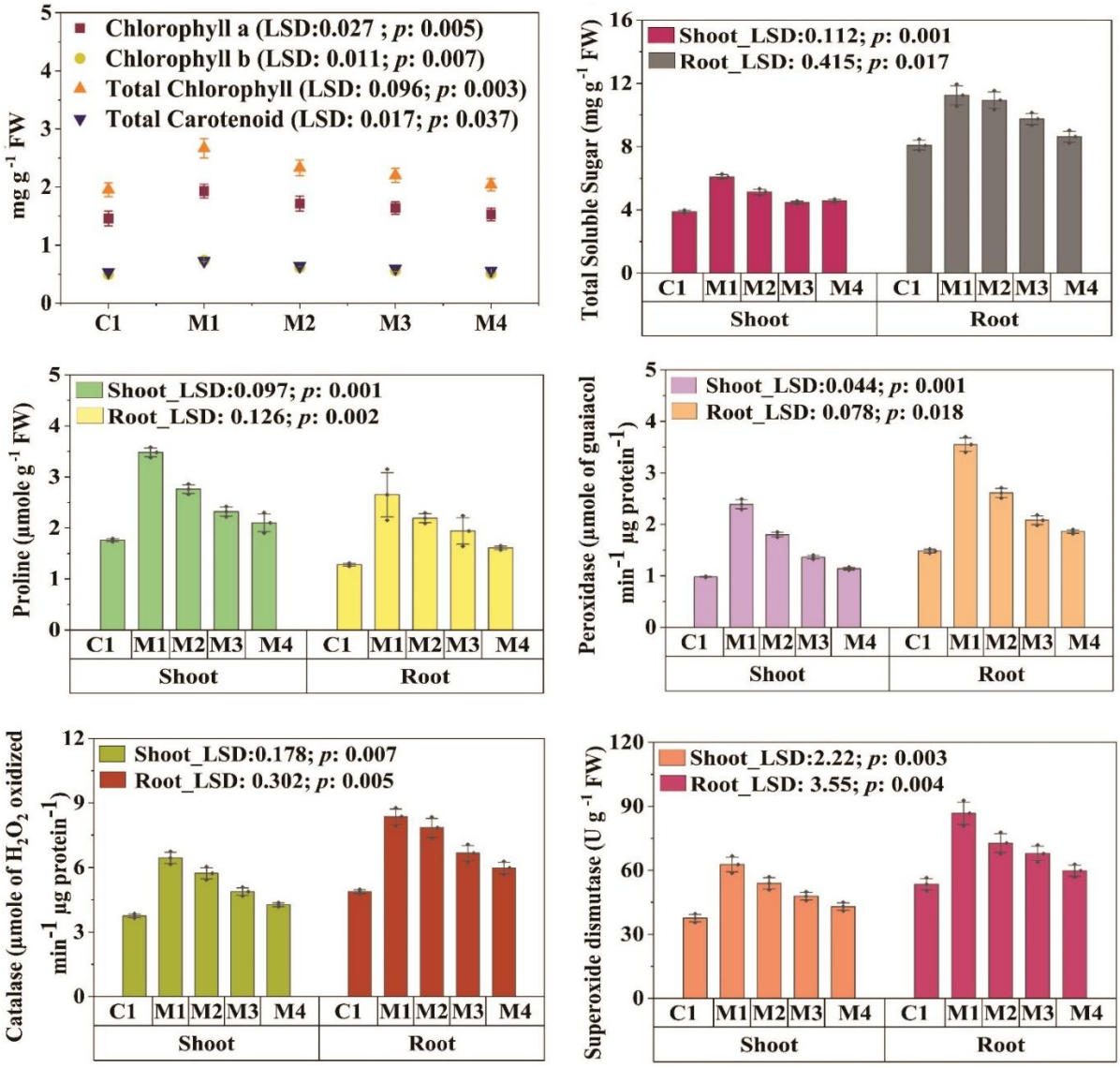

Fig. 59: The biochemical parameters and antioxidant enzymes properties of vetiver plant (root and shoot) across the treatments (post-harvest). Here, **M1:** *Glomus hoi;* **M2:** *Funneliformis coronatum*; **M3:** *Claroideoglomus claroideum*; **M4:** *Claroideoglomus etunicatum*

Proline is a highly effective osmoregulator, known to protect plants from oxidative damage under stress conditions. The results align with He et al. (2020), who reported that under PTEs stress, corn plants inoculated with AMF exhibited significantly higher levels of soluble sugar and proline than non-inoculated plants. The accumulation of osmoregulatory substances is a typical stress response, and plant symbiotic fungi contribute to maintaining subcellular structural stability by promoting this accumulation, thereby alleviating stress on the host plant. Fig. 59 illustrates the antioxidant enzyme activity in response to PTE stress. The activities of SOD, CAT, and GPOD in the shoots and roots of AMF-infected vetiver plants were

significantly higher than those in control plants when grown in mine waste-contaminated soil. Among the AMF-infected plants, M1 exhibited the highest SOD activity (shoot: 1.66 folds, root: 1.62 folds) followed by M2 (shoot: 1.43 folds, root: 1.36 folds), M3 (shoot: 1.27 folds, root: 1.26 folds), and M4 (shoot: 1.14 folds, root: 1.11 folds) (Fig. 4). Similarly, CAT activity was significantly elevated (shoot_LSD: 0.178; *p*: 0.007; root_LSD: 0.302; *p*: 0.005) in *Glomus hoi* compared to control plants. Additionally, a similar pattern was observed, with GPOD activity in both the roots and shoots of vetiver plants increasing in the presence of AMF compared to the control group. In response to increased oxidative stress induced by PTEs, plants activate these antioxidant enzymes to neutralize reactive oxygen species (ROS) and minimize damage (Banerjee et al., 2019). In our study, AMF infection led to increased antioxidant activity, which helped reduce TE-induced ROS in the vetiver plants growing in chromium-asbestos mine tailing-contaminated soil. A similar pattern was observed by Wang et al. (2016), who reported that AMF inoculation mitigated phytotoxicity by decreasing ROS production and boosting antioxidant activity.

4.3.9 Plant growth properties in presence of different AMF species

The shoot and root lengths as well as weight (fresh and dry) of vetiver grown on chromium-asbestos mine waste-contaminated soil, with and without AMF inoculation, were presented in Fig. 60. Among the AMF treatments, M1, and M2 resulted in a significant increase in shoot and root lengths at the time of harvest followed by M3 and M4. The mean shoot length of vetiver grown with AMF (*Glomus hoi* and *Funneliformis coronatum*) was 124.5± 13.21 cm and 110.3 ± 8.76 cm, while the root length was 73.4 ± 5.12 cm and 62.7 ± 3.69 cm, respectively. The increased shoot and root length of vetiver can be directly attributed to higher root colonization by M1 and M2, which improved nutrient and phosphorus uptake. A similar trend of AMF was observed in both fresh weight and dry weight. The shoot and root lengths, as well as biomass production (dry weight), were significantly lower in vetiver plants grown in the C1 treatment. AMF-treated plants appeared healthy, showing no signs of stress such as discoloration, wilting, or necrosis. In contrast, plants in the control group (without AMF) exhibited stunted growth. To assess the impact of AMF on the root system, the plants were taken out from the pots at the end of the experiment. The roots exhibited a dense, mesh-like growth that held the mine-soil together, a characteristic considered ideal for an effective "phyto-stabilizer". The dense root system developed through AMF infection can aid in preventing the toxic effect (secretion of GRSP) of PTEs from the contaminated mine waste soil (Gohre and Paszkowski 2006). In line with our findings, other studies have also confirmed the

significant increase in shoot and root length, as well as biomass (fresh and dry weight), of *L. usitatissimum* and *Sesamum indicum* with the application of *G. intraradices* and *G. fasciculatum* (Amna et al., 2015).

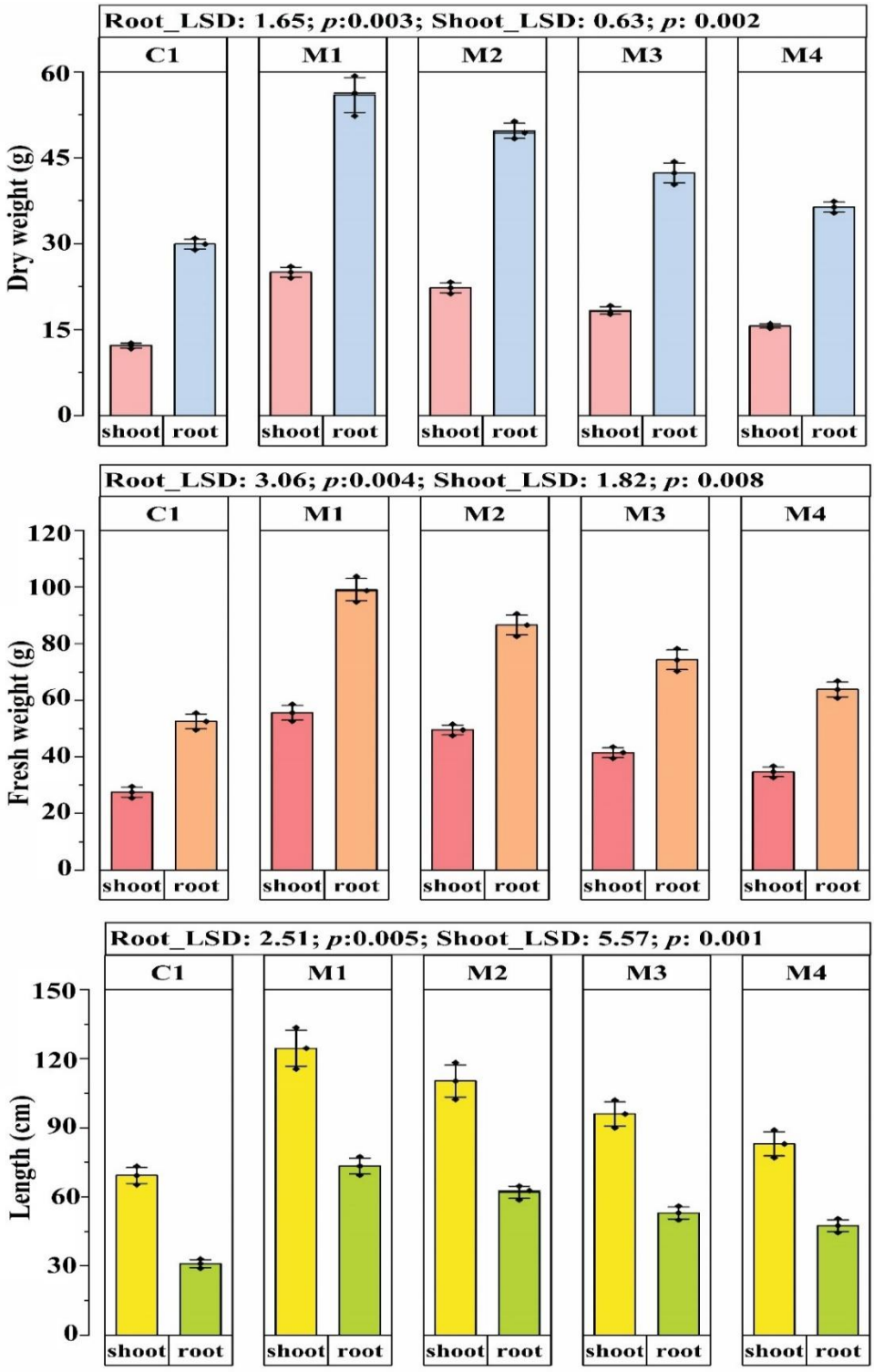

Fig. 60: The growth properties of vetiver plant (root and shoot) across the treatments (post-harvest). Here, **M1:** *Glomus hoi;* **M2:** *Funneliformis coronatum*; **M3:** *Claroideoglomus claroideum*; **M4:** *Claroideoglomus etunicatum*

4.3.10 Statistical model analysis to evaluate the efficiency of mycophytoremediation approach

The heatmap (Fig. 61) correspond to the Pearsons' correlation and Principal component analysis (PCA) (Fig. S6) among different parameters (AMF attributes [colonization percentage (CP), glomalin protein fractions (EEG, DEG)], bioavailable soil PTEs (Cr_BA, Cd_BA, Ni_BA, Cu_BA, and Pb_BA), soil microbial-enzymatic properties [microbial biomass carbon (MBC), substrate induced respiration (SIR), basal soil respiration (BSR), acid phosphatase (APP), dehydrogenase (DHG), urease (U), β-glucosidase (BG) and fluoresceine diacetate (FDA)], soil quality (pH, TOC, AP, AN, and AK), PTEs root accumulation (RA_Cr, RA_Cd, RA_Ni, RA_Cu, and RA_Pb), stress enzyme (PRO, SOD, CAT, and POD) and plant growth properties (RL, and DW) at the time of post-harvest. The AMF attributes (CP, EEG, DEG) showed negative correlation with bioavailable soil PTEs (rCr_BA: -0.61, -0.77, -0.07; rCd_BA: -0.60, -0.75, -0.08; rCu_BA: -0.69, -0.84, -0.21; rNi_BA: -0.84, -0.88, -0.24; and rPb_BA: -0.50, -0.66, -0.05) while, other parameters had a positive correlation with each other (Fig. 61). A significant positive correlation was observed between PTEs in roots (RA_Cr, RA_Cd, RA_Ni, RA_Cu, and RA_Pb) and the AMF attributes (rCP: 0.70, 0.45, 0.69, 0.62, 0.71; rEEG: 0.70, 0.34, 0.76, 0.44, 0.53; rDEG: 0.62, 0.45, 0.71, 0.48, 0.32). Following harvest, the vetiver plant absorbs toxic PTEs from the soil, facilitated by the presence of AMF, which helps the plant store these PTEs in its root system. Overall, from this analysis depicts that the presence of AMF in the treatments reduces PTEs in contaminated soil, promotes the secretion of stress enzymes to mitigate stress, and improves soil quality and plant growth, thereby enhancing the remediation potential of the vetiver plant.

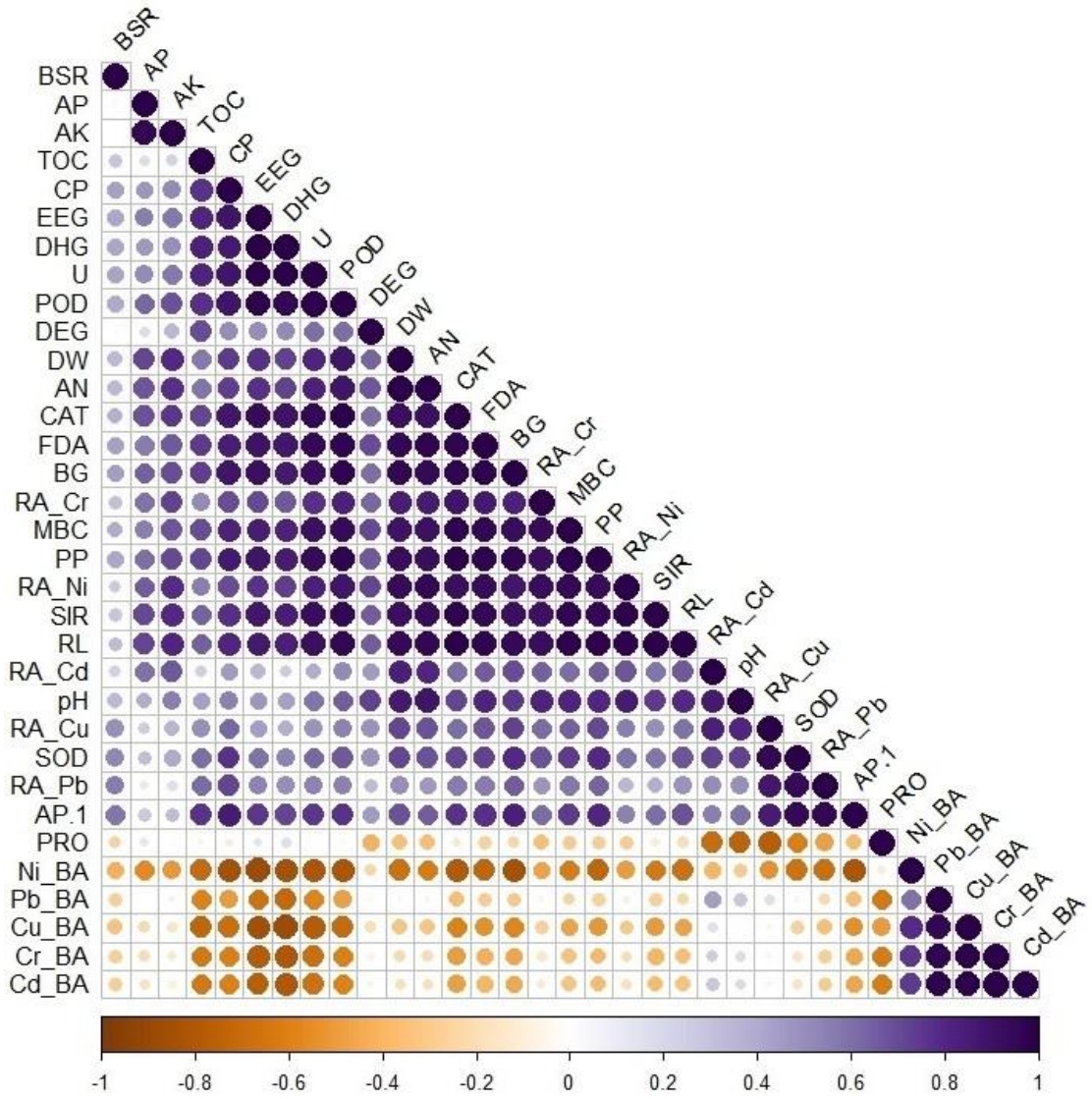

Fig. 61: The Pearson correlation plot showing the relationship among different parameters including soil quality, microbial-enzymatic attributes, soil bioavailable PTEs, stress enzymes, plant growth properties, AMF attributes and root PTEs accumulation at post-harvest. Here, two different colour denotes positive (violet) and negative (brown) correlation among treatments during experiment

A subsequent investigation, PCA was performed to examine the relationship between different parameters and results indicate a closer association between AMF attributes soil microbial-enzymatic properties, soil quality, PTEs root accumulation, stress enzyme, and plant growth properties (Fig. 62). The application of PCA revealed that the first two dimensions, Dim-1 and Dim-2, together explained 82.3% of the total variation. The eigenvalues for Dim-1 and Dim-2 contributed 63.8% and 18.5%, respectively, to the total explained variance (Fig. 62). The positive association was observed between AMF attributes with other parameters including

root PTEs accumulation, growth parameters, and overall soil health quality whereas a negative association was found between AMF attributes and soil bioavailable PTEs. The result indicates that the inclusion of AMF in the treatments helps decrease PTEs in contaminated soil, stimulates the release of stress enzymes to alleviate stress, and boosts both soil quality and plant growth, ultimately enhancing the vetiver plant's remediation potential.

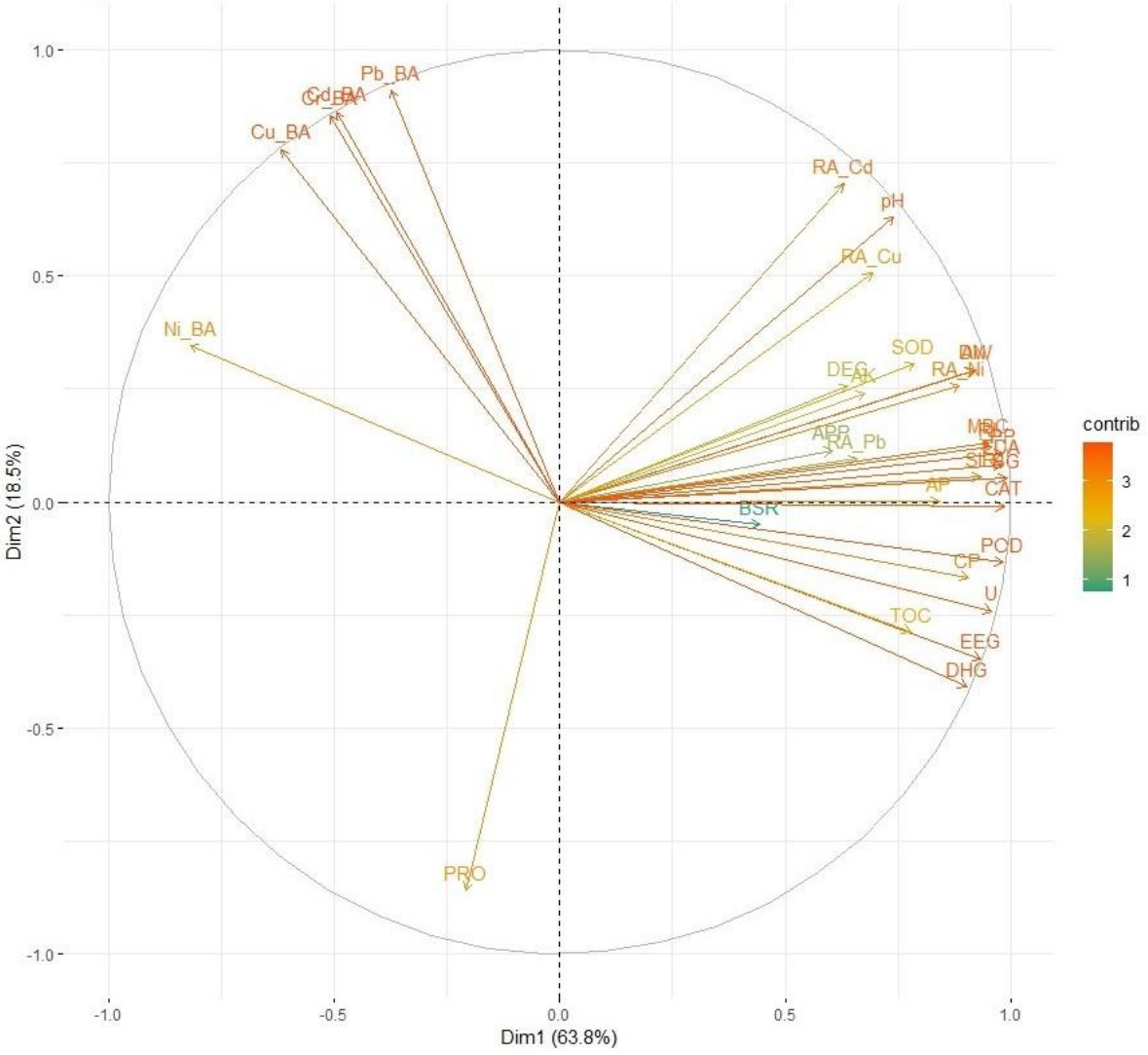

Fig. 62: Principal components analysis (PCA) plot showing the relationship among various attributes including soil quality, microbial-enzymatic attributes, soil bioavailable PTEs, stress enzymes, plant growth properties, AMF attributes and root PTEs accumulation at post-harvest

The path analyzing the mycophytoremediation efficacy of vetiver plant (MPRE) was demonstrated through the PLS-SEM model presented in Fig. 63, considering four different AMF amendments. The variance inflation factor (VIF) and path coefficient for different AMF treatments were depicted in Tables 31, 32.

Table 31: Variance inflation factors (VIF) for each indicator construct of different AMF treatments

Construct	M1_VIF	M2_VIF	M3_VIF	M4_VIF
AMF Attributes				
Colonization	2.546	1.512	2.307	2.617
EEG	2.976	2.559	2.663	2.706
DEG	2.129	2.200	2.106	1.087
Soil PTEs				
Cr	1.979	2.192	3.008	1.419
Ni	1.526	1.373	2.121	1.738
Cd	3.008	2.005	3.905	2.089
Pb	1.237	1.933	1.744	1.407
Cu	4.179	2.934	2.123	2.178
Soil Quality				
MBC	1.828	2.387	1.702	1.037
BSR	1.561	1.116	1.075	1.078
SIR	1.259	2.230	1.771	1.045
Stress Enzymes				
PRO	1.479	1.628	1.131	1.123
SOD	1.317	2.193	1.252	3.054
CAT	1.805	3.274	1.348	1.564
GPOD	1.266	2.693	1.076	2.187
Plant Growth				
Root length	8.133	1.635	1.094	1.117
Root biomass	8.133	1.635	1.094	1.117
Mycophytoremediation efficiency (MPRE)				
Root_Cr	3.988	3.041	3.724	1.822
Root_Ni	3.694	1.636	2.452	2.331
Root_Cd	1.254	4.037	3.232	2.264
Root_Pb	1.912	9.329	2.468	1.827
Root_Cu	1.614	4.695	1.817	1.328

M1: *Glomus hoi;* **M2:** *Funneliformis coronatum*; **M3:** *Claroideoglomus claroideum*; **M4:** *Claroideoglomus etunicatum*

Table 32: Path coefficient of the paths from exogenous latent variables to endogenous latent variables and also between exogenous latent variables of mycophytoremediation experiment

Path	M1_Path coefficient	M2_Path coefficient	M3_Path coefficient	M4_Path coefficient
AMF Attributes -> MPRE	0.412	0.705	0.246	0.425
AMF Attributes -> Plant Growth	1.167	0.837	0.33	-0.061
AMF Attributes -> Soil Quality	0.953	0.643	0.641	0.647
AMF Attributes -> Soil PTEs	0.899	0.723	0.755	0.778
Plant Growth -> MPRE	-0.034	-0.678	0.43	0.503
Soil Quality -> Plant Growth	-0.238	0.052	0.562	0.771
Soil PTEs -> MPRE	0.126	-0.033	0.224	-0.391
Soil PTEs -> Stress enzymes	0.886	0.891	0.646	0.773
Stress enzymes -> MPRE	0.478	0.937	0.259	0.527

The analysis showed that the presence of AMF had the maximum impact on MPRE, primarily influenced by the plant's defence mechanisms (stress enzyme secretion), with a positive relationship indicated by M1_ß = 0.478, M2_ß = 0.937, M3_ß = 0.259, and M4_ß = 0.527. The direct and indirect paths explaining the main target variable (MPRE) were significant based on the R^2 value (M1_MPRE: 0.888, M2_MPRE: 0.909, M3_MPRE: 0.871, and M4_MPRE: 0.604). The attributes of AMF had a strong positive impact on soil quality (0.953), plant growth (1.167), and soil PTEs (0.899), with the maximum effect observed in M1. The presence of AMF culture (M1) in the vetiver plant roots aids in the accumulation of toxic PTEs from the soil while also enhancing soil quality, which in turn promotes proper growth of vetiver plant. Similar trend was observed in case of other AMF mediated treatment (M2, M3, and M4). In the presence of M1 and M3, soil PTEs have a positive relationship on MPRE, whereas a negative relationship between soil PTEs and MPRE was observed in the presence of M2 and M4. Furthermore, a positive influence was observed between soil PTEs and stress enzymes in all treatments. Under PTEs stress conditions, the plant secretes various stress enzymes to counteract the stress without compromising its phytoremediation efficiency. The presence of AMF culture also enhances the phytoremediation process by expanding the root surface area through their hyphal structure, which aids in the absorption of PTEs, thereby boosting overall efficiency. Overall, the current study showed that the vetiver plant performed more effectively under the AMF-amended treatments, particularly in the presence of M1 AMF (*Glomus hoi*). This finding is supported by the results of the PLS-SEM model (Fig. 63), which displayed a higher path coefficient value through the direct path and the appropriate association AMF culture would improve the efficacy of mycophytoremediation potential.

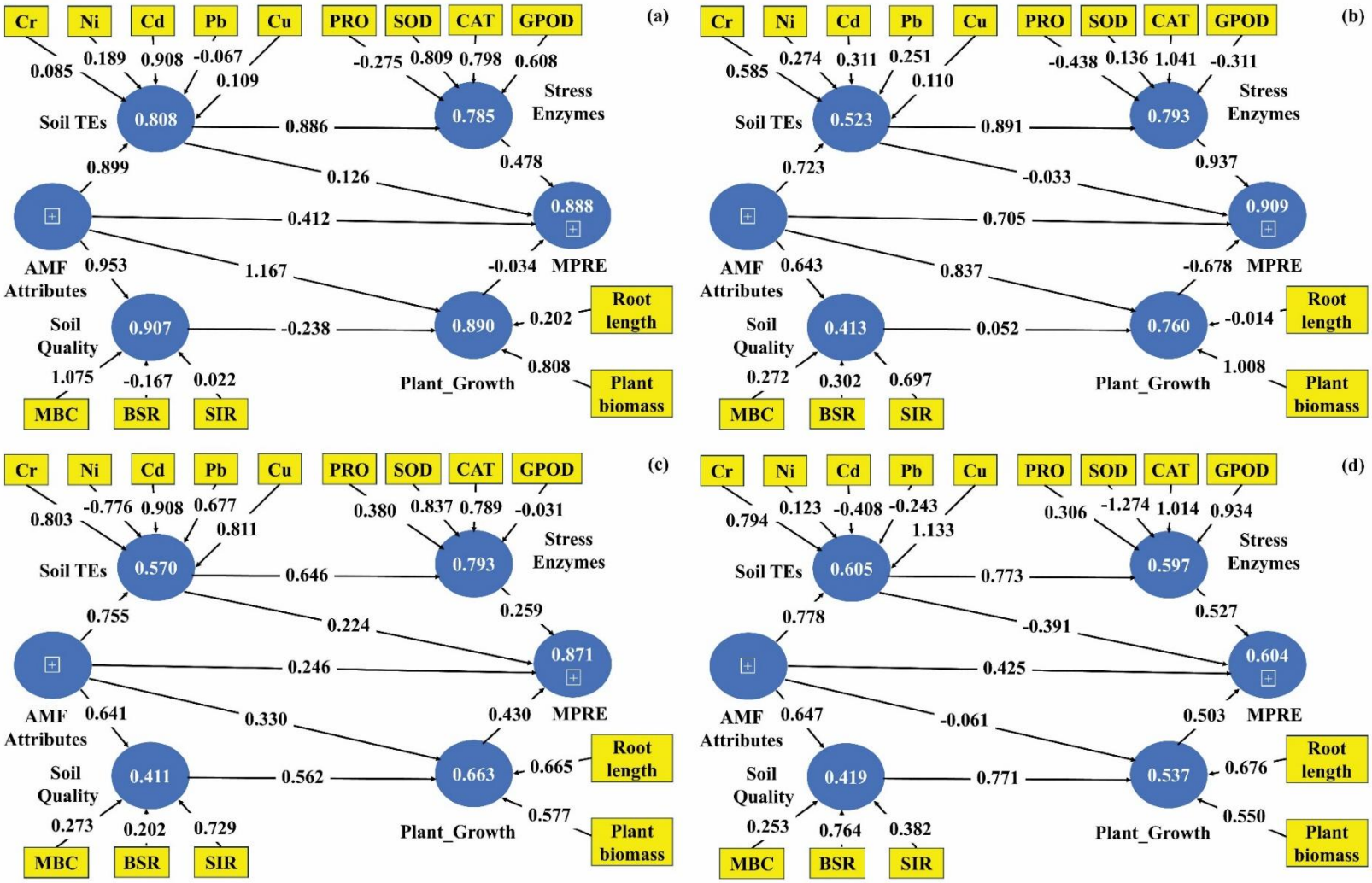

Fig. 63: The partial least squares structural equation modelling (PLS-SEM) through Path analysis diagrams for four different AMF treatments of mycophytoremediation with vetiver plant. Here, (a) for **M1:** *Glomus hoi;* (b) for **M2:** *Funneliformis coronatum*; (c) for **M3:** *Claroideoglomus claroideum*; (d) for **M4:** *Claroideoglomus etunicatum.*

Based on the above findings, M1 AMF (Glomus hoi) proved to be more effective in the mycophytoremediation approach. To assess which AMF attributes (EEG, DEG, TG and CP), influence the accumulation of different PTEs in the vetiver plant's roots, a novel Sobol sensitivity analysis model was performed. The results of the analysis were shown in Fig. 64. The results from the first-order (FOSI) and total-order (TOSI) analyses indicated that TG was the most influential factor for the root accumulation of Ni, Cd, and Pb, compared to other factors. In Fig, for Cr, EEG and DEG were the most influential, while for Cu, CP emerged as the key factor. The presence of *Glomus hoi* in the vetiver root system stimulates the production of glomalin protein, and a high level of colonization enhances the accumulation of toxic PTEs from chromium-asbestos mine waste-contaminated soil. The second-order sensitivity analysis examined the interactions between pairs of model inputs, allowing for the identification of the most influential input pairs by analyzing the variation or interaction between parameters. This model-based analysis highlights the dominance of AMF attributes, showing their superior ability to accumulate various PTEs and enhance the mycophytoremediation potential.

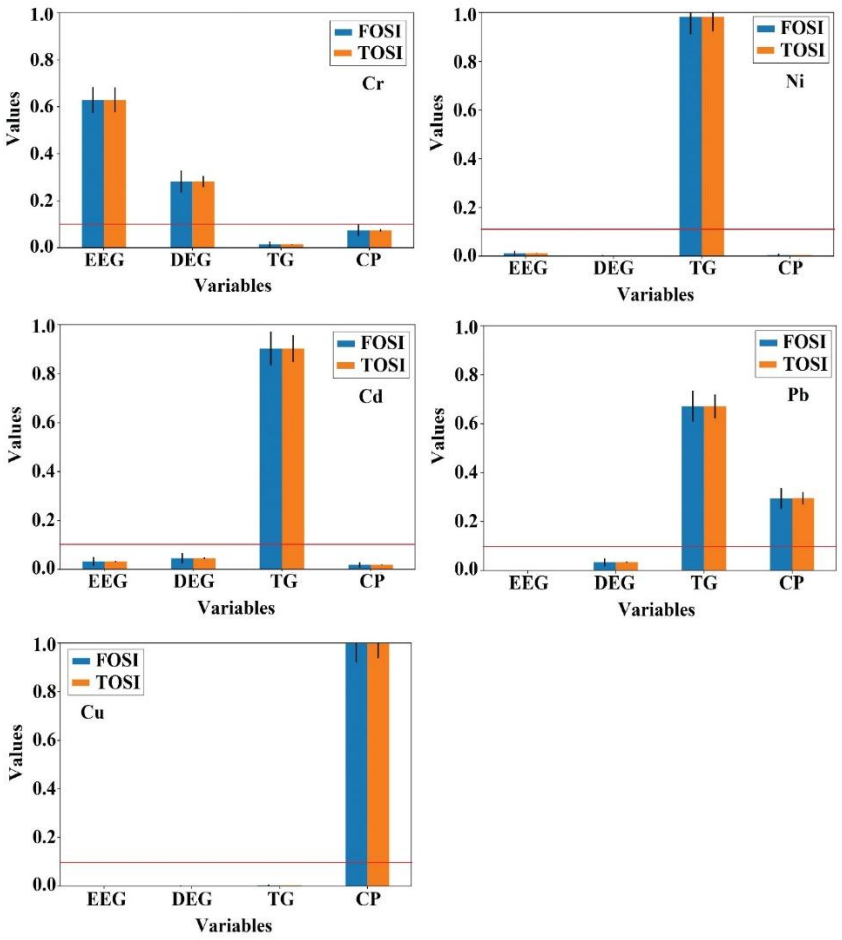

Fig. 64: Evaluation of most sensitive AMF attributes (EEG, DEG, TG, CP) in presence of PTEs in roots (Cr, Ni, Cd, Pb, and Cu) of vetiver plant denoted through Sobol sensitivity analysis

Objective: 4

4.4 Transformation of PTE-enriched vetiver (PTE-EV) and chromium-asbestos mine waste (CAMW) into beneficial organic products utilizing vermi-remediation technology

This objective is divided into two subsections. The first subsection presents the results and discussion related to vermicompost derived from PTE-enriched vetiver (PTE-EV), while the following subsection focuses on vermicompost prepared from chromium-asbestos mine waste (CAMW).

4.4.1 Different properties assessment of vermicomposted PTE-enriched vetiver (PTE-EVVc)

4.4.1.1 Collection of cow dung, PTE-EV, earthworm species, and preparation of vermicompost

The PTE-enriched vetiver plants were harvested following the myco-phytoremediation process, during which the vetiver accumulated a substantial amount of PTEs in both root and shoot tissues. Since the shoot is exposed to the open environment, it poses a risk of re-contaminating the surroundings through shedding. To address this concern, the shoot portions of the PTE-enriched vetiver were collected separately for further management through vermi-remediation technology. The initial characterization of PTE-EV was: pH: 5.81±0.44, Organic carbon: 0.784±0.021%, total PTEs concentration (Cr: 209.58±13.59 mg/kg; Ni: 91.19±4.73 mg/kg; and Pb: 31.42±2.04 mg/kg). Cow dung (CD) was procured from a nearby cattle yard for this experiment. The initial characteristics of cow dung were pH: 6.93±0.37; organic carbon: 1.78±0.08%, with limited PTEs concentration. Adult, uniform-sized (6-7 cm in length) clitellated specimens of *Eisenia fetida* earthworms, identified as active and healthy without abnormalities, were obtained from the institutional earthworm maintenance unit at the Indian Statistical Institute, Jharkhand.

PTE-EV samples were combined with cow dung (CD) in two proportions [1:1 and 1:2 (by weight)], with 2.5 kg of each combination deposited into meticulously cleaned and perforated vermiunits [58 cm × 38 cm × 17 cm]. The mixes underwent pre-composting for approximately one week to ready the feedstock for earthworm incubation. The pre-composting process generally requires 6 to 7 days, contingent upon local meteorological conditions. Pre-composting enables the comprehensive amalgamation of PTE-EV and CD, facilitates the

uniform dispersion of nutrients and pollutants, and creates optimal circumstances for earthworm proliferation and effective remediation (Chakraborty et al., 2022). Earthworms were initially subjected to only PTE-EV based feedstocks, resulting in significant mortality after 10 days (Table 33).

Table 33: Mortality percentage of *Eisenia fetida* in raw PTE-enriched vetiver (PTE-EV)

Time (days)	Count (Earthworms)	Mortality percentage (%)
0	25	0
3	17	32
5	9	64
7	6	76
10	2	99.2

The experiment entailed the amalgamation of PTE-EV with CD in two distinct ratios. Each vermiunit was subsequently combined with *Eisenia fetida* earthworms at a density of 10 worms per kg of substrate. The vermicomposting units utilising PTE-EV based mixes were sustained for 90 days at a moisture content of 50%-60%, with the mixtures being aerated two-times daily. The experiment was performed at the vermiunits of the Indian Statistical Institute in Jharkhand (Fig. 65).

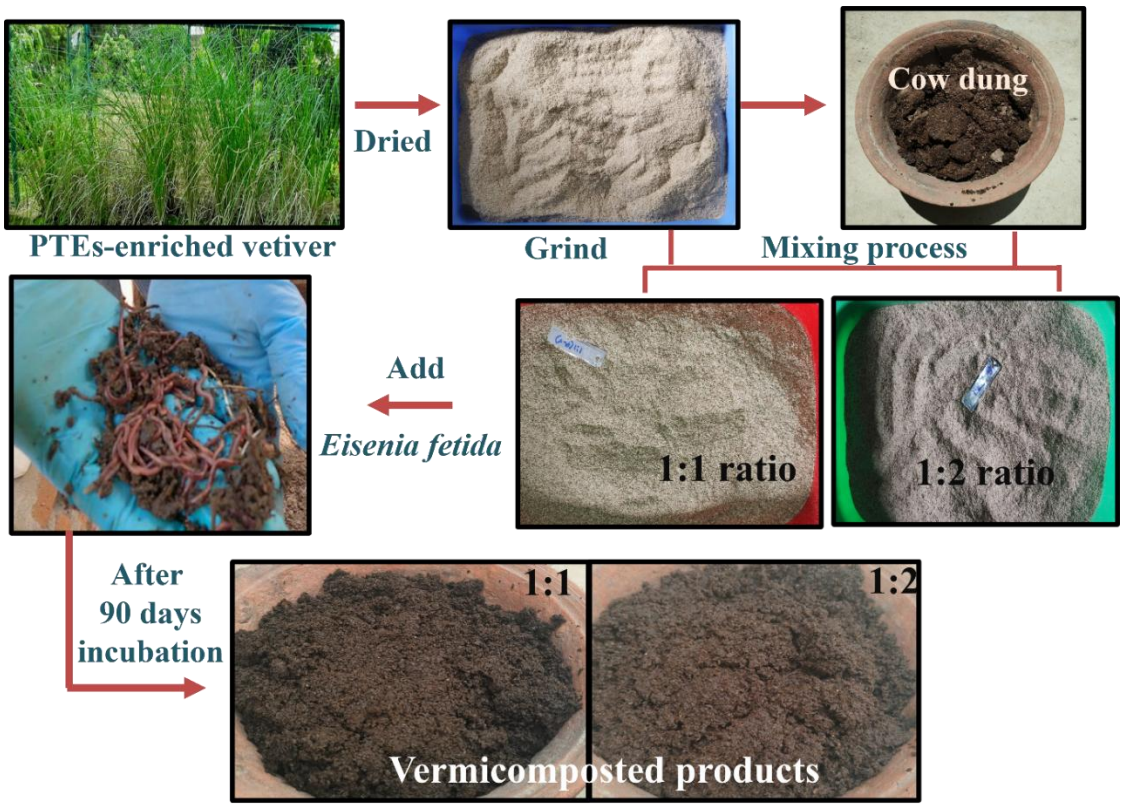

Fig. 65: The pictorial representation of vermi-remediation process of PTE- enriched vetiver

Each treatment was duplicated thrice. Samples were temporally collected from each vermibed (0, 30, 60, and 90 days) during the vermicomposting process to observe temporal variations. The samples were air-dried, sieved, and preserved in zip-lock bags for further analysis according to standard protocol (Page et al., 1982). Furthermore, new samples were obtained at same intervals and stored in sterilised bags at –20°C for microbial analysis (Liu et al., 2011). The subsequent combination of PTE-EV and CD was chosen for the investigation.

Treatment Order	Feedstocks preparation for Earthworms	Mixing Proportions
	Ratio	(Fresh weight based)
T1	1:1	1.25 kg CD + 1.25 kg PTE-EV
T2	1:2	0.83 kg CD + 1.67 kg PTE-EV
T3	-	2.5 kg CD only (Positive control)
T4	-	2.5 kg PTE-EV (negative control)

4.4.1.2 Changes in physico-chemical properties of PTE-EV based vermi-beds

Vermicomposting results in fluctuations in physico-chemical parameters, including pH, total organic carbon (TOC), available nitrogen (Avl N), available phosphorus (Avl P), and exchangeable potassium (Ex. K) in the feedstock (Table 34).

Table 34: Physico-chemical attributes of vermicomposted feedstocks at the initial and final stage with statistical analysis (Mean±SD)

Parameters	0 day			90 days			Statistical Significance	
	T1 (1:1)	T2 (1:2)	T3 (CD)	T1 (1:1)	T2 (1:2)	T3 (CD)	LSD	*p*-values
pH	6.68±0.31	6.47±0.48	6.93±0.23	7.23±0.52	7.39±0.63	7.37±0.44	0.034	0.0015
TOC (%)	1.69±0.03	1.53±0.09	1.18±0.07	1.27±0.04	1.18±0.08	1.21±0.01	0.163	0.0024
Avl. P (mg/kg)	104.36±5.93	94.37±7.98	117.82±9.02	183.24±11.06	159.12±13.11	198.36±11.97	1.46	0.0013
Avl. N (mg/kg)	14.61±0.67	13.29±0.83	15.57±0.73	21.06±1.13	17.44±1.29	23.78±1.61	0.729	0.0043
Ex. K (mg/kg)	158.06±9.04	137.41±11.91	146.85±12.43	289.92±19.22	268.48±23.16	296.74±26.09	0.431	0.0073

T1: Cow dung + PTE-enriched vetiver (1:1); T2: Cow dung + PTE-enriched vetiver (1:2); T3: Cow dung only

In this experiment, the feedstock's pH (T1 and T2) was originally slightly acidic owing to the acidic nature of the raw PTE-EV. Following the vermicomposting process, the pH of the vermibeds was elevated to a neutral level. Mubeen and Hatti (2018) revealed analogous findings, indicating that the calciferous glands of earthworms are essential for neutralising substances. At day 0, the TOC content in the T1 and T3 feedstock exceeded that of the T2 feedstock (LSD= 0.163; p=0.0024). The TOC level considerably decreased after 90 days, following the sequence of vermibeds T2>T3>T1, and the ANOVA revealed a significant treatment interaction effect for TOC. The significant decrease in TOC in vermibeds signifies accelerated mineralisation of organically bound nutrients and the maturation of vermicompost (Sahariah et al., 2015). The Avl. N, Avl. P, and Ex. K values exhibited a significant increase

during the vermicomposting process, with the peak values recorded in T3 and T1, followed by T2 (Table 34). The presence of this nutrient facilitates the growth of earthworms in the vermiunits. Microbial activity and their extracellular enzymes significantly contributed to the enhancement of N–N mineralisation (Sahariah et al., 2015). Potassium-solubilizing microorganisms enhance the availability of potassium in feedstocks (Ghosh et al., 2023). The fast proliferation of P-solubilizing bacteria in the PTE-EV feedstocks presumably induced phosphatase activity, hence expediting phosphorus solubilisation in the feedstocks. Mondal et al. (2020) revealed that the microbial population in the digestive system of earthworms may have enhanced the availability of phosphorus in the feedstocks during vermicomposting.

4.4.1.3 Temporal dynamics of microbial-enzyme activity in different feedstock

The PTE-EV based feedstock was evaluated by analysing variations in important microbial-enzyme activities, including MBC, DHG, FDA, BSR, and SIR. All metrics exhibited substantial increases during the 90-day duration, as demonstrated (Fig. 66). The abundance of PTEs in PTE-enriched vetiver (PTE-EV) adversely affects interspecific interactions among microbial populations and significantly increases microbial toxicity (Tripathy et al., 2014). In this experiment, MBC demonstrated a notable enhancement in both T1 and T2 feedstocks, indicating that the amalgamation of CD and PTE-EV fosters a more favourable environment for microbial proliferation. A two-way ANOVA with a Post-Hoc test (LSD) was conducted to demonstrate considerable temporal variation in microbial-enzymatic activity inside the vermibeds and the interaction impact of treatment and day. The MBC levels in different vermiunits post-incubation were seen in the following order: T3 > T1 > T2 (LSD_{Day} = 1.92; p_{Day} = 0.001) (Fig. 66a). The increase in MBC within the vermiunits suggests that earthworms promoted the proliferation of beneficial bacteria, likely expediting the mineralisation of carbon, phosphorus, and nitrogen (Biruntha et al., 2020).

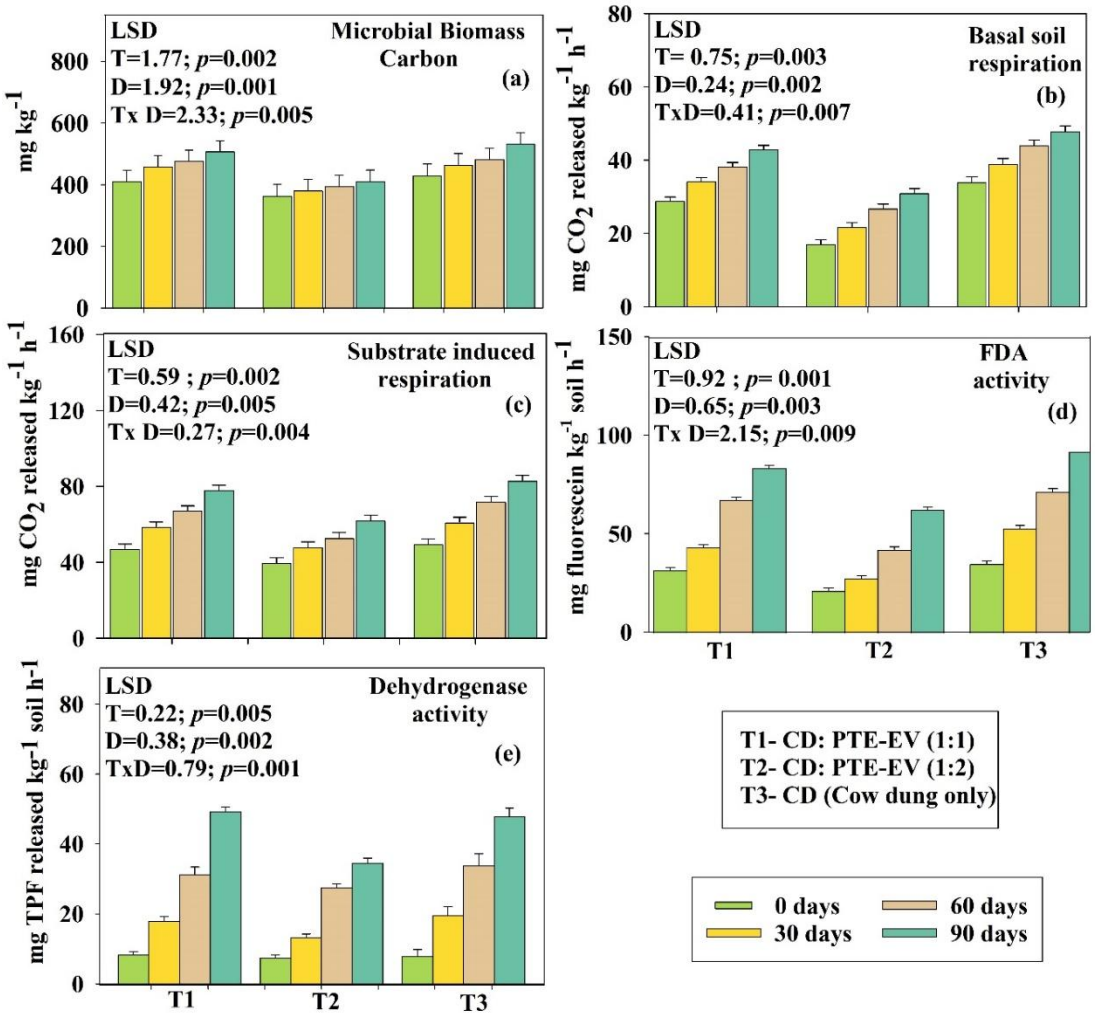

Fig. 66: Temporal dynamics of microbial-enzymatic attributes during vermicomposting process

The study also showed that treatments T1 and T3 displayed substantial levels of FDA and DHG, succeeded by treatment T2, during the entire incubation period (Fig. 66d, e). Treatments initially produced a slight rise in FDA and DHG rates (FDA $p_{Treatment}$ = 0.001, $LSD_{Treatment}$ = 0.92; DHG $p_{Treatment}$ = 0.002; $LSD_{Treatment}$ = 0.38). After a duration of 30 days, the activity of FDA and DHG increased across all treatments. Chakraborty et al. (2022) indicate that the FDA can be decomposed by enzymes such as protease, lipase, and esterase under ideal circumstances that assess the biological activity of vermicomposted treatment. The peak DHG activity was recorded at 90 days in treatment T1 (Fig. 66e). Likewise, the active gut microbiomes of earthworms may enhance metabolic pathways that produce ATP, resulting in elevated dehydrogenase activity (Lipiec et al., 2016). In addition, the BSR and SIR denote the respiration rate of the feedstocks. Basal respiration (BSR) primarily relies on the existence and

function of the indigenous microbial population, which frequently exhibits metabolic inactivity (Banerjee et al., 2024). The elevation in BSR after 90 days was most significant in the T1 treatment combination, followed by T2 ($p_{Day} = 0.002$; $LSD_{Day} = 0.24$) (Fig. 66b). Consequently, the increase in BSR signifies the expansion of indigenous microorganisms that proficiently mitigate toxicity induced by contaminants (Devi et al., 2023). Figure S3e illustrates that treatments T3 and T1 exhibited the highest SIR respiration at 90 days, with treatment S2 following closely after (Fig. 66c). Banerjee et al. (2024) observe that zygomycete bacteria species are indicative of substrate-induced respiration. These bacteria are potent enhancers of plant growth and exhibit robust metabolic activity. The findings demonstrate that earthworms, together with their gut microbiota, effectively mitigated the adverse effects of PTEs (mostly Pb, Ni, and Cr) associated with microbial toxicity in feedstock amended with PTE-EV.

4.4.1.4 Bioavailable PTEs fractions estimation and PTEs removal efficiency by earthworms

This study intended to evaluate the effectiveness of vermi-remediation technology in diminishing the bioavailability of PTEs in vermicomposted products and enhancing their removal by earthworms during the PTE-EV vermicomposting process. The alterations in the bioavailable (BA) pattern of PTEs were examined to understand the dynamics during vermicomposting (Fig. 67 a, b). This investigation indicates that the BA percentages of PTEs (Cr, Ni, and Pb) in the feedstocks were elevated on day 0. Upon the completion of the vermicomposting process at 90 days, the concentration of PTEs in the vermibeds was drastically reduced (Fig. 67a). The existence of BA forms of PTEs influences their toxicity potential because to their accessibility (Amir et al., 2008). In T3, the concentration of bioavailable PTEs was minimal. The bioavailable portions of PTEs, particularly Cr and Ni, in T2 were elevated on day 0, perhaps expediting the *Eisenia fetida*-mediated detoxification of PTEs during vermicomposting. A comparable pattern was documented by Chakraborty et al. (2022) in their investigation of the vermicomposting of tannery sludge waste enriched with PTEs. Research indicates that metallothionein proteins in the gastrointestinal tract of earthworms are crucial for detoxifying PTEs by creating organo-metallic complexes that store PTEs in stable forms for a longer period (Dai et al., 2004). The removal efficiency for Pb was greatest in T1 (6.31 folds) compared to T2 (5.92 folds) (Fig. 67b). Prior research has emphasised the capacity of earthworms to sequester certain elements from various waste materials (Goswami et al., 2014; Sarkar et al., 2023).

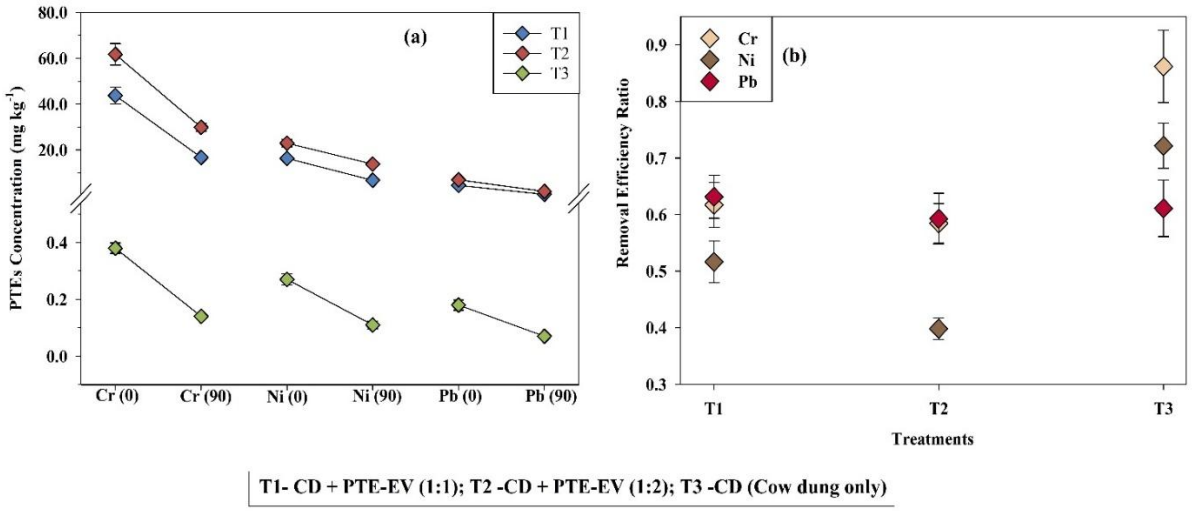

Fig. 67: PTEs dynamics during vermicomposting process. (a) changes in bioavailable PTEs concentration in vermi-beds; (b) PTEs removal efficiency ratio by earthworm

The greatest removal effectiveness was noted for Cr (T1: 6.17 folds, T2: 5.84 folds) and Pb, followed by Ni (T1: 5.16 folds, T2: 3.98 folds), regardless of the treatments applied. The efficacy of earthworms in removing PTEs was essential in eradicating harmful materials from the vermicompost. A more significant decrease in PTE was seen in T1 PTE-enriched vetiver feedstocks with considerable earthworm proliferation. The results indicate that the ideal proportion of cow dung in the feed mixture may efficiently function as a source of carbon and nutrients for earthworms, enabling them to flourish under challenging conditions and successfully execute the restoration process. The data present strong evidence that the starting concentrations of PTEs, their chemical characteristics, and the substrate morphology are essential determinants affecting the form and degree of PTEs reduction in vermicomposting systems (Nannoni et al., 2011).

4.4.1.5 Dynamics of the earthworm population

The dynamics of the earthworm population in PTE-EV based feedstocks during vermicomposting are illustrated (Fig. 68). Population increase is a critical indicator of feedstock appropriateness for earthworm species utilised in vermicomposting. As indicated in the preceding section, earthworms could not endure the raw PTE-EV feedstock in the absence of cow dung, resulting in a substantial population reduction within 10 days (Table S1). The mortality of earthworms in PTE-EV vermibeds was likely attributed to the toxicity of PTEs (mostly Ni, Cr, and Pb) and the deficient nutrition supply. *E. fetida*, as a surface-dwelling

biomass feeder, flourishes optimally on crumbly or granular feedstocks (Das et al., 2020). Conversely, the earthworm population exhibited a substantial increase (T1: 7.88-fold and T2: 5.72-fold) over time in the cow dung mixed PTE-EV-vermibeds in our investigation (Figure S1). After 90 days, the earthworm population in the various feedstocks ranked as follows: T3 > T1 > T2 (p for treatment = 0.001; LSD for treatment = 1.23). The outcome arises from the pH of the feedstocks transitioning to a neutral range and an improvement in nutrient (NPK) levels, which facilitates the proliferation of the earthworm population during vermicomposting. The result was analogous to that of Banerjee et al. (2025).

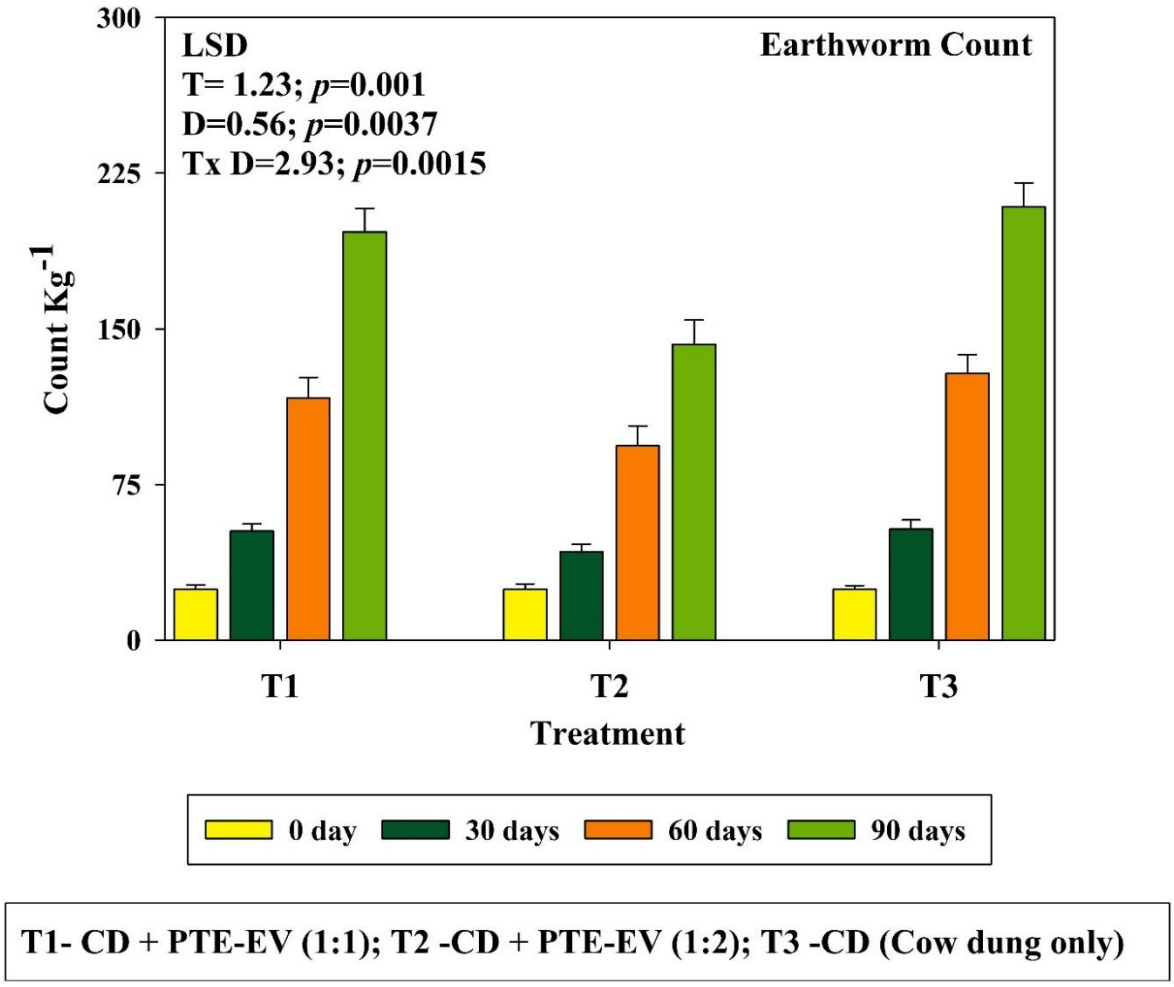

Fig. 68: Earthworm count dynamics during vermicomposting of PTE-EV

4.4.1.6 PTEs content estimation in earthworm gut after the experiment

The earthworm (*Eisenia fetida*) efficiently mitigates the threats associated with PTEs in vermicomposted PTE-EV due to its adeptness in accumulating PTEs. The accumulation of PTEs in the earthworm gut was much greater in T2, as seen in Table 35, followed by T1 and

T3. *E. fetida* shown a propensity to uptake PTEs in the order of Ni > Pb > Cr, irrespective of the treatment situations.

Table 35: Bioaccumulation factor of earthworm (*Eisenia fetida*) in different vermibeds

Treatments	Cr	Ni	Pb
T1 (1:1)	0.44	0.84	0.65
T2 (1:2)	0.44	0.76	0.66
T3 (CD)	0.31	0.57	0.43

The accumulation of PTEs in the earthworm gut may be ascribed to the presence of certain cysteine-rich proteins, such as metallothioneins, which facilitate the chelation of PTEs via their thiol groups (Homa et al., 2016). Concentrations of PTEs, including Ni, Pb, and Cr, in earthworms were enhanced in T2 and T1 mixes, suggesting that the PTE-EV and CD blend fostered favourable circumstances for earthworm growth, hence promoting the bioaccumulation of PTEs. *Eisenia* species serve as efficient bio-accumulators of hazardous PTEs, facilitated by sophisticated cellular defence systems (Suleiman et al., 2017). Earthworms sequester metals such as Ni, Cr, and Pb in stable, organically bound forms within chloragogenous tissues (Stürzenbaum et al., 2017), which remain immobilised and non-toxic in the environment post-mortem, thereby facilitating a sustainable detoxification process for PTEs through vermiremediation technology.

4.4.1.7 The relationship determination between microbial-enzymatic activity and PTEs bioavailability dynamics: An Insight through correlation technique

Pearson's correlation statistics were utilized to examine the impact of bioavailable PTEs on microbial-enzymatic activity. The investigation investigated microbiological characteristics (MBC, DHG, FDA, BSR, SIR) and bioavailable potentially toxic elements (Pb, Cr, Ni). Figure S6 demonstrates a significant negative association (shown by the brown colour) between available PTEs and microbial and enzymatic metrics during the final phase of vermicomposting. This may be ascribed to a significant reduction in the bioavailability of PTEs such as Cr, Pb, and Ni during the maturation period, together with an elevation in microbial activity inside the vermibeds (Fig. 69). Consequently, substantial microbial activity was noted at maturity, ascribed to the diminished harmful effects of PTE-EV. Shi et al. (2013) revealed that correlation analysis efficiently supports the interactions between microorganisms and PTEs.

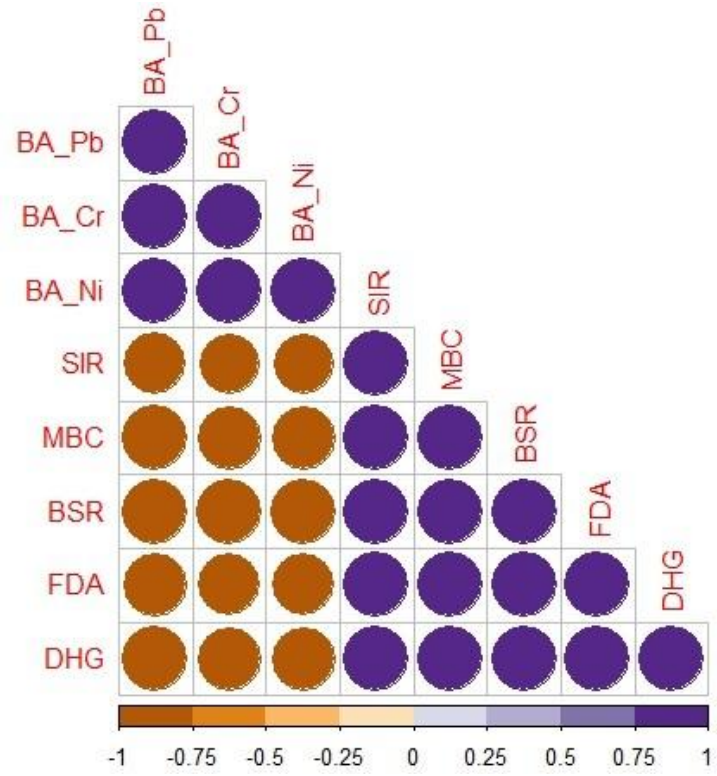

Fig. 69: Pearson-correlation analysis revealed impact of bioavailable PTEs on microbial attributes

4.4.2 Several parameters determination of vermicomposted chromium-asbestos mine waste (CAMW-VC)

4.4.2.1 Acquisition of cow dung, CAMW, and earthworm species

A simple random sampling technique was applied to collect the CAMW from the Roro mine in Jharkhand, India and store into labelled plastic containers. The initial characterization of CAMW was: pH: 6.04±0.22, EC: 0.28±0.1 dS m^{-1}, Organic carbon: 0.19± 0.04%, total PTEs concentration (Cr: 2018.28±88.35 mg/kg; Ni: 1484.88±47.67 mg/kg; Cd: 8.08±0.43 mg/kg; Pb:159.58±7.84 mg/kg; and Cu: 162±8.52 mg/kg) (Banerjee et al., 2023). The cow dung (CD) was collected from an adjacent cattle yard for use in this experiment. The initial properties of cow dung were pH: 7.34±0.41, EC: 0.39±0.02 dS m^{-1}, Organic carbon: 1.41± 0.06%, with negligible PTEs content. Adult, uniform size (6-7 cm in length) clitellated specimens of *Eisenia fetida* earthworms, characterized as active and healthy without deformities, were procured from the institutional earthworm maintenance unit at the Indian Statistical Institute, Jharkhand. This epigeic earthworm (*Eisenia fetida*) facilitates rapid reproduction, adaptability to varying temperature and humidity conditions, high decomposition rate, enhances nutrient content, resilience in toxic metal-contaminated environments, and effectively removes metals. These

characteristics offer a promising choice for vermi-remediation purposes (Bhattacharya and Kim, 2016).

4.4.2.2 Preparation of vermicompost

CAMW samples were mixed with cow dung (CD) in two ratios [1:1 and 1:2 (by weight)], with 25 kg of each mixture placed into thoroughly cleaned (with water), and perforated vermiunits [2.5 feet × 4.75 feet × 1.1 feet] (Fig. 70).

Fig. 70: Pictorial depiction of chromium-asbestos mine waste vermicomposting process

These mixtures were pre-composted for about a week to prepare the feedstock for earthworm incubation. Typically, the pre-composting process takes 6–7 days depending on local weather conditions. Pre-composting serves as an effective method for thermally stabilizing feedstock prior to adding earthworms, enhancing their survival and decomposition efficiency (Hussain et al., 2018). Pre-composting ensures the thorough mixing of CAMW and CD, promotes the even distribution of nutrients and contaminants, and establishes favourable conditions for earthworm proliferation and efficient waste remediation (Chakraborty et al., 2022). This process achieved a stable pH (range of 6.6-6.98) and a feedstock temperature of around 31°C, which are ideal conditions for earthworm activity. The following combination of CAMW and CD were selected for the research.

Treatment	Preparation of Feedstocks for Earthworms	Proportion of mixing
	Ratio	**(Based on Fresh weight)**
T1	1:1	12.5 kg CD + 12.5 kg CAMW
T2	1:2	8.33 kg CD + 16.67 kg CAMW
T3	-	25 kg CD only (Positive control)
T4	-	25 kg CAMW only (negative control)

Earthworms were first exposed to solely CAMW-based feedstocks, and substantial fatality had been identified after a week (Table 36).

Table 36: Mortality percentage of *Eisenia fetida* in raw chromium-asbestos mine waste (CAMW)

Time (days)	Count (Earthworms)	Mortality percentage
0	250	0
3	119	47.6
5	43	17.2
7	11	4.4
8	3	1.2

Thus, the experiment involved combining CAMW with CD in two different ratios. This ratio was determined based on prior research and is applicable to this region (Mondal et al., 2020; Chakraborty et al., 2022). Each vermiunits was then mixed with *Eisenia fetida* earthworms at a density of 10 worms per kg of substrate. The vermicomposting units with CAMW-based mixtures were maintained for 90 days at a moisture level of 50%-60%, with the mixtures being turned twice daily to ensure adequate aeration. Each treatment was replicated three times. During the vermicomposting process, samples were taken temporally from each vermibed (0, 30, 60, and 90 days) to monitor changes over time. The collected samples were air-dried, sieved, and stored in zip-lock bags for further analysis following standard procedure (Page et al., 1982). Additionally, fresh samples were collected at the same intervals and kept in sterilized bags at –20°C for microbial analysis (Liu et al., 2011).

4.4.2.3 Persistence of bioavailable PTEs fractions and removal efficiency by earthworms

This study aimed to estimate the efficacy of vermi-remediation technology in reducing the bioavailability of PTEs and facilitating their removal by earthworms during the CAMW

vermicomposting process. The changes of PTEs bioavailable (BA) pattern were investigated to gain insight dynamics during vermicomposting (Fig. 71a, b). This study reveals that the BA fractions of PTEs (Cr, Cd, Ni, Pb, and Cu) in the feedstocks were higher at day 0. After completion of vermicomposting process at 90 days, PTEs concentration was decreased significantly (Cr_LSD: 1.18; *p*: 0.009; Ni_LSD: 0.78; *p*: 0.004) in the vermibeds. The presence of BA forms of PTEs determines their potential for toxicity as they are easily accessible (Amir et al., 2008). In T3, the concentration of bioavailable PTEs was negligible. The BA form of Ni and Cr was decreased in the following order: T2 (Ni: 80.22%; Cr: 81.69%) ≥ T1 (Ni: 77.24%; Cr: 80.72%) > T3 (Ni: 53.13%; Cr: 62.5%) (Fig. 71a). Since, the bioavailable fractions of PTEs (mainly Cr and Ni) in T2 had higher at day 0 day, that might accelerate the *Eisenia fetida*-mediated detoxification of the PTEs during vermicomposting. A similar trend was reported by Chakraborty et al. (2022) in their study on the vermicomposting of PTEs-rich tannery sludge waste. The reduction in all PTEs levels, highlighted the improved detoxification process through the formation of stable humic substances in the vermiunits (Paul et al., 2020). Studies have shown that the metallothionein proteins in the earthworm's gastrointestinal tract play a key role in detoxifying PTEs by forming organo-metallic complexes that help to sequester PTEs in resistant forms for prolonged periods (Dai et al., 2004). A substantial decrease in BA Pb was seen in T2, but the reduction of BA Cd was most pronounced in T1, followed by T2 (Fig. 1a). The removal efficiency for Cd was highest in T1 (5.12 folds) as compared T2 (4.04 folds) (Fig. 71b). This may result from the low starting concentration of Cd in T1, which likely caused less toxicity to the earthworms, allowing them to absorb Cd more effectively than in T2. Previous studies have highlighted the ability of earthworms to accumulate specific elements from different wastes (Goswami et al., 2014; Sarkar et al., 2023). In case of Cu, the initial concentration was lower as compared with other PTEs across all the vermibeds (Fig. 71b). Additionally, vermicomposting resulted in a 53% decrease in Cu levels in T1 (Fig 1b). The highest removal efficiency was observed in case of Cr, Ni, Cd, and Pb followed by Cu irrespective of treatments. The removal efficiency of PTEs by earthworms played a key role in eliminating hazardous elements from the vermicompost. Overall, greater TE reduction was observed in T1 chromium-mine waste feedstocks exhibiting substantial earthworm proliferation. The results indicate that the equal ratio of (1:1) CAMW and CD mixture in T1 treatment offered the most suitable conditions for earthworm development, promoting the bioaccumulation of toxic PTEs. The findings suggest that the optimal ratio of cow dung in the feed mixture may effectively serve as a carbon and nutrition source for earthworms to thrive in adverse environments and perform the remediation process successfully. These findings

provide compelling evidence that the initial concentrations of PTEs, their chemical properties, and the substrate morphology are critical factors influencing the type and extent of PTEs reduction in vermicomposting systems (Nannoni et al., 2011).

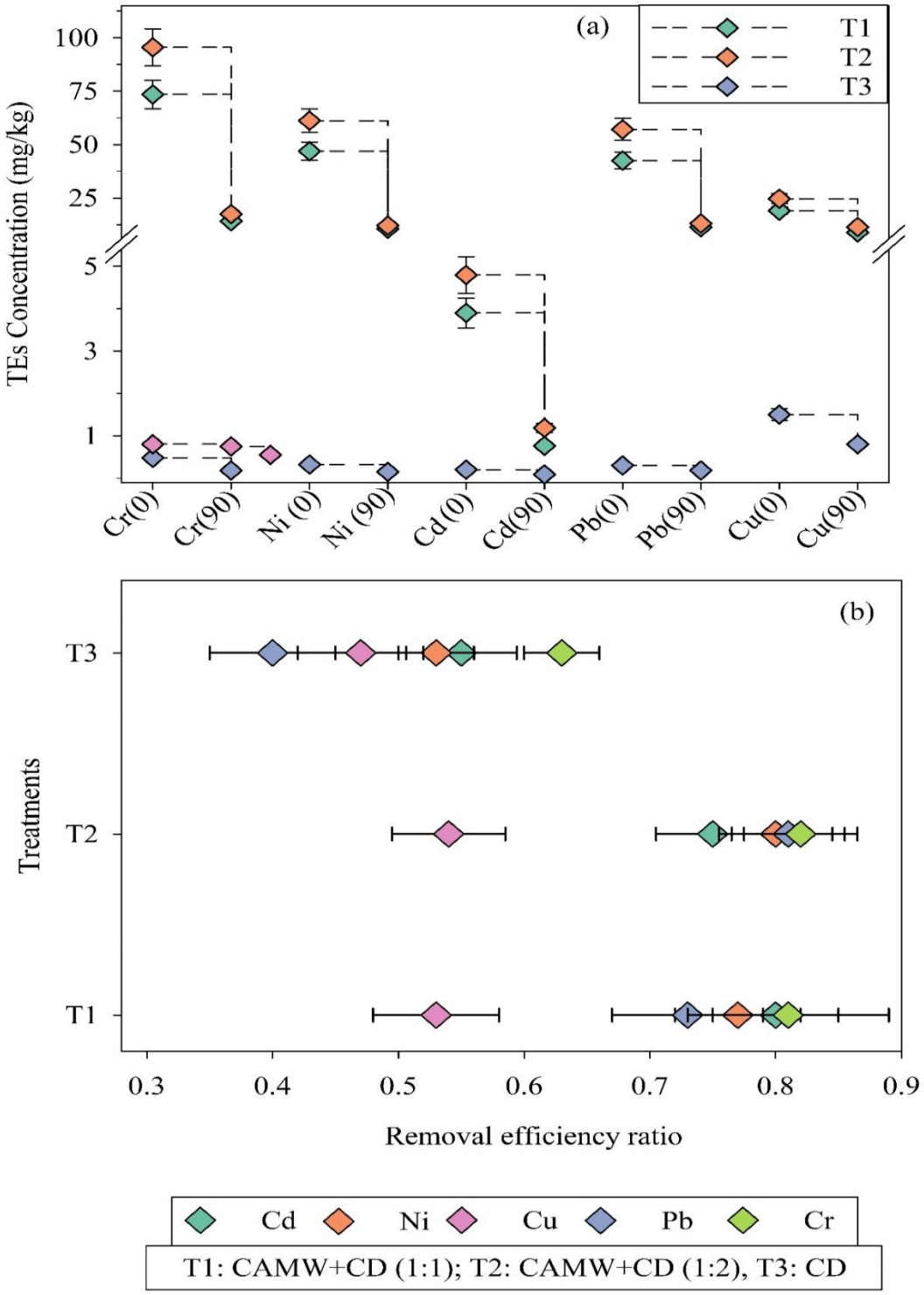

Fig. 71: (a) Variability of PTEs concentration between days 0 and 90 in bioavailable fractions (mg kg^{-1}); (b) The TEs removal efficiency of *Eisenia fetida* during the vermicomposting process. Here, T1: 1:1 [CD:CAMW]; T2: 1:2 [CD:CAMW]; T3: [CD only]

4.4.2.4 Evaluation of earthworm's status during vermicomposting

4.4.2.4.1 Earthworm population dynamics

During vermicomposting, the earthworm population dynamics in CAMW-based feedstocks are shown (Fig. 72). Population growth serves as an important measure of feedstock suitability for earthworm species used in vermicomposting. As noted in the previous section, earthworms were unable to survive in the raw CAMW feedstock without cow dung, and their population significantly declined within a week (Table 36). The mortality of earthworms in CAMW vermibeds was likely caused by the high toxicity of PTEs (mainly Ni, Cr and Pb) and the low nutrient content of the chromium-asbestos mine waste. *E. fetida,* being a surface-dwelling biomass feeder, thrives best in crumbly or granular feedstocks (Das et al., 2020). In contrast, the earthworm population significantly increased (T1: 5.90 fold and T2: 4.93 fold) over time in the cow dung mixed CAMW-vermibeds in this study (Fig. 72). After 90 days, the earthworm population in the different feedstocks followed this order: T3 > T1 > T2 (p for treatment = 0.003; LSD for treatment = 12.90). The result occurs due to the feedstocks' pH shifted towards neutral range, and an enhancement in nutrient (NPK) status, which supports the growth of the earthworm population during vermicomposting. According to Edwards et al., (2010) earthworm species normally grow over a wide range of pH (5 to 11). Remarkably, despite being exposed to CAMW containing toxic elements, the earthworm population growth in T1 was statistically similar to T3 (only cow dung). This finding aligned with statistical test, as the two-way ANOVA revealed a significant increase (LSD_{TxD} = 18.25, p = 0.002) in earthworm population in T1 and T3 feedstocks followed by T2. The earthworm population in T2 was slightly decreased, suggesting an adverse environment due to the feedstock's composition, which contained a doubled ratio of toxic CAMW waste. The initial shock induced by CAMW, due to its slight acidity and PTEs content, could be effectively mitigated by the earthworms over time in T1. This adaptability may be linked to the nature of feedstocks and also unique stress repair mechanisms at the cellular and DNA levels in earthworms, which enhance their resilience to stressful conditions (Vasseur and Bonnard, 2014).

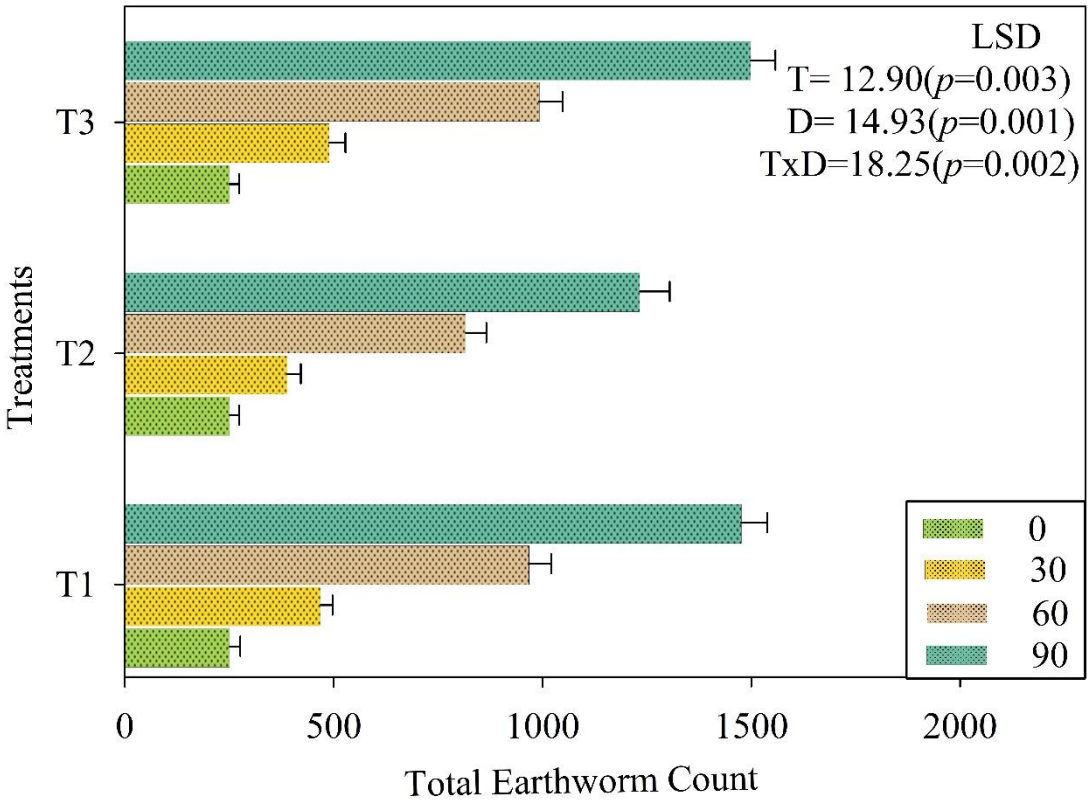

Fig. 72: Temporal variation of earthworm count during vermicomposting. Here, T1: 1:1 [CD:CAMW]; T2: 1:2 [CD:CAMW]; T3: [CD only]

4.4.2.4.2 Analysis of PTEs content in earthworm gut

Earthworm *(Eisenia fetida)* effectively prevents PTEs-related environmental hazards in vermicomposted CAMW owing to its proficient PTEs-accumulating capabilities. PTEs accumulation in earthworm gut was significantly higher in T2 as depicted in Table 37, followed by T1 and T3.

Table 37: Bioaccumulation factor of earthworm (*Eisenia fetida*) in different vermibeds

Treatments	Cr	Ni	Cd	Pb	Cu
T1 (1:1)	2.81	2.58	1.12	1.87	0.88
T2 (1:2)	3.03	2.76	1.27	3.04	0.37
T3 (CD)	0.72	0.80	0.33	0.89	0.51

Overall, *E. fetida* exhibited a tendency to accumulate PTEs in the sequence: Cr > Pb > Ni > Cd > Cu, regardless of the treatment conditions. The tendency of PTEs accumulation in earthworm gut might be attributed to the presence of certain cysteine-rich proteins like metallothioneins which help to chelates PTEs through their thiol groups (Homa et al., 2016). PTEs including Ni, Pb, and Cr levels in earthworms were also elevated in T2 and T1 mixtures, indicating that the

CAMW and CD blend created optimal conditions for earthworm development, enhancing the bioaccumulation of PTEs. *Eisenia* species are effective bio-accumulators of toxic PTEs, supported by advanced cellular defence mechanisms (Suleiman et al., 2017). Notably, earthworms sequester metals like Cd, Ni, Cr and Pb in stable, organically bound forms within chloragogenous tissues (Stürzenbaum et al., 2013), which remain immobilized and non-toxic in the environment even after the worms' lifespan, promoting a sustainable PTEs detoxification process through vermiremediation technology.

4.4.2.4.3 Periodic variation of stress enzymes of earthworms

In earthworms, certain enzymes act as quick and reliable indicators of their physiological response to PTEs toxicity (Łaszczyca et al., 2004). Antioxidant enzymes are considered effective molecular biomarkers of oxidative stress, representing the extent of earthworms' response to toxic PTEs exposure (Zheng et al., 2013). This antioxidant defense system includes enzymes like catalase, superoxide dismutase, and peroxidase, which work to protect cells from oxidative damage. SOD converts two superoxide anion radicals (·O2−) into molecular oxygen and hydrogen peroxide (H_2O_2), while POX and CAT prevent the accumulation of H_2O_2 in cells to maintain cellular homeostasis and counteract the harmful effects of ROS (Chao et al., 2016). Fig. 73(a-c) illustrates the effects of PTEs exposure over periods of 1, 30, 60, and 90 days on the activities of POX, CAT, and SOD in *E. fetida*. In T3 (cow dung), only minimal changes in activity were observed in the earthworms. In contrast, the activities of SOD, CAT, and POX in earthworms fed with CAMW-based feedstocks showed a significant increase from day 1, peaking around day 60, before gradually declining This increase reflects the synthesis of SOD to counteract excess ROS (Chao et al., 2016). The synthesis of CAT and POX activity in earthworms is a response and adaptation mechanism to PTEs stress, enabling the breakdown of H_2O_2. As shown Fig. 73a, 73c the activity of CAT and POX in earthworms significantly increased across all treatments. This rise in CAT, and POX activity during the initial exposure periods was attributed to the elevated concentration of PTEs in the vermibeds. However, by day 90, POX, and CAT activity decreased as the vermicomposted products reached maturity, following the order T2 > T1 > T3. The higher antioxidant enzyme activity observed in the T2 treatment was due to the double ratio of CAMW present, enabling the earthworms to counteract PTEs-induced stress more effectively. In contrast, the antioxidant enzyme activity in T1 was comparable to that in T3, indicating that the earthworms in these treatments successfully mitigated the stress and flourished in the vermibeds. A similar trend is observed with the toxicity effects of soil PTEs on *E. fetida* (Liu et al., 2015). These findings from this research indicate that stress enzymes safeguard earthworm cells from oxidative damage. By 90 days,

PTEs-induced stress was reduced in T1, and earthworm activity remained robust in these vermibeds, highlighting the efficiency of proper vermicomposting process.

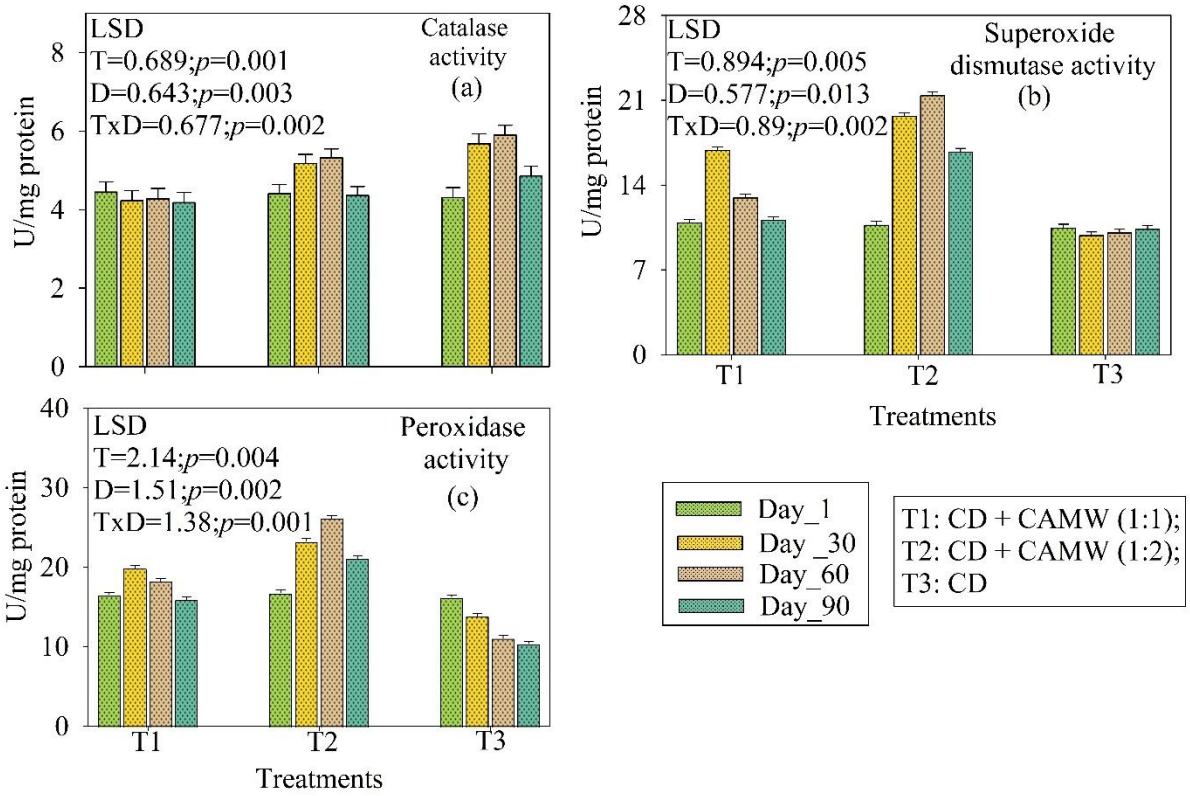

Fig. 73: Dynamics of stress enzymes activity during vermicomposting of various treatment combinations of chromium-asbestos mining waste vermicompost (CAMW). Here, T1: 1:1 [CD:CAMW]; T2: 1:2 [CD:CAMW]; T3: [CD only]

4.4.2.5 Microbial dynamics during vermicomposting process

The CAMW-based feedstock was assessed by examining changes in key microbial activities, including MBC, MBN, MBP, BSR, and SIR. All parameters showed significant increases over the 90-day period, as shown (Fig. 74a-e). The richness of PTEs in CAMW has a detrimental effect on interspecific interactions across microbial communities and greatly enhances microbial toxicity (Tripathy et al., 2014). In this experiment, MBC exhibited a significant increase in both T1 and T2 feedstocks, suggesting that the combination of CD and CAMW creates a more supportive environment for microbial growth. The two-way ANOVA with Post-Hoc test (LSD) was performed to indicates the temporal variation in microbial-enzymatic activities within the vermibeds and the treatment-day interaction effect were significant. The MBC level in various vermiunits after the incubation period was followed the sequence: T3> T1> T2 ($LSD_{Treatment}$ = 1.57; $p_{Treatment}$ = 0.003). Similarly, the CAMW-based feedstock T1 showed a more noticeable increase in MBN (1.70 folds) and MBP (2.78 folds) than T2. This

trend may be due to the stress caused by PTEs in treatment T2, leading to reduced microbial activity (Figure. 74b-c). The rise in MBC, MBP, and MBN in the vermiunits indicates that earthworms facilitated the growth of beneficial bacteria, potentially accelerating the mineralization processes of carbon, phosphorus, and nitrogen (Biruntha et al., 2020).

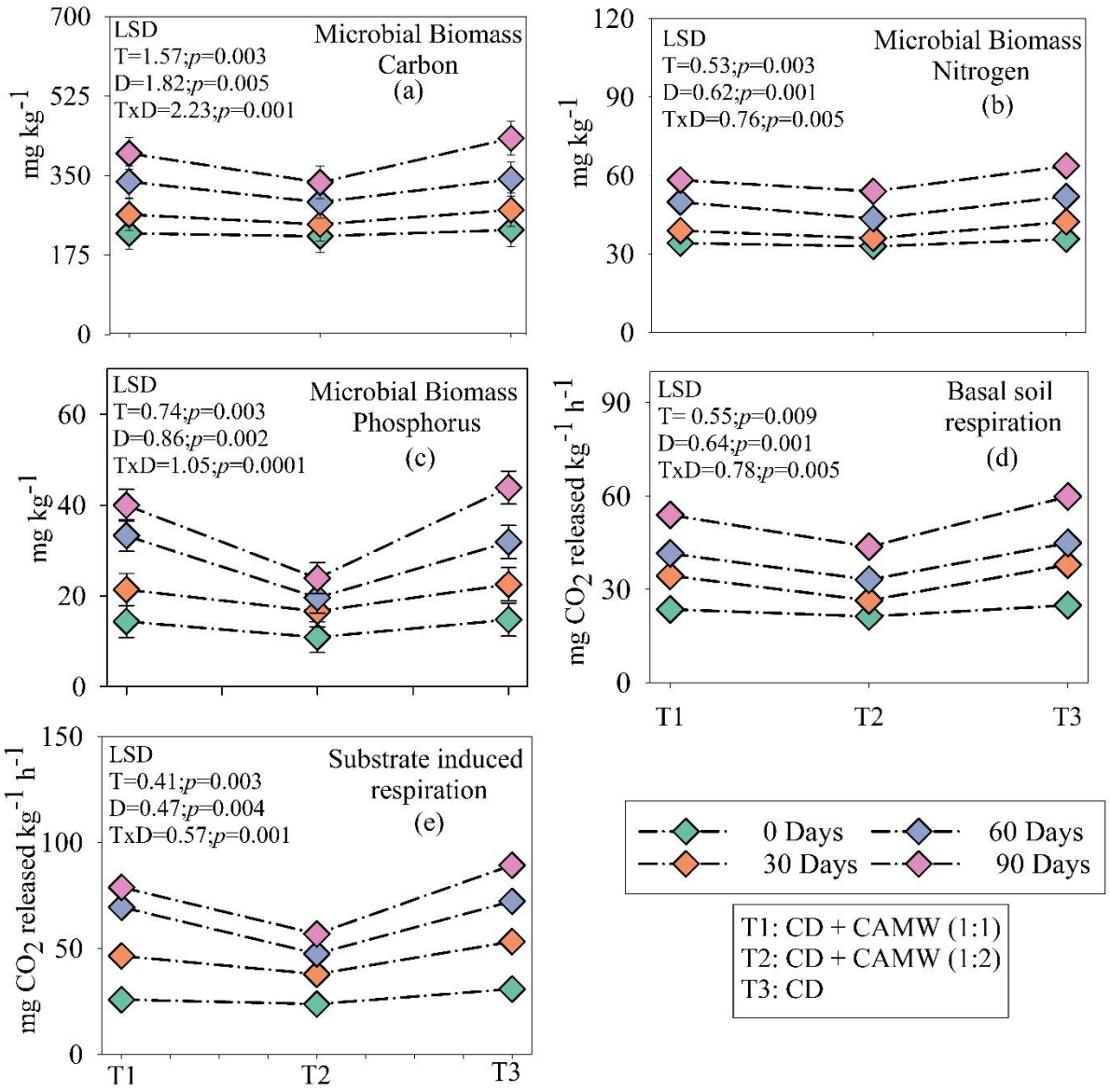

Fig. 74: Periodic Variation in microbiological parameters under different treatment combinations chromium-asbestos mining waste vermicompost (CAMW). Here, T1: 1:1 [CD:CAMW]; T2: 1:2 [CD:CAMW]; T3: [CD only]

Basal respiration (BSR) largely depends on the presence and activity of the native microbial community, which is often metabolically inactive (Banerjee et al., 2024). The present study employs the BSR and SIR to indicate the feedstocks' respiration rate. The increase in BSR after 90 days was most pronounced in the treatment combination of T1, followed by T2 ($p_{Treatment}$ =

0.009; $LSD_{Treatment}$ = 0.55) (Figure. S3d). Therefore, the rise in BSR indicates the proliferation of autochthonous microorganisms that effectively combat toxicity caused by pollutants (Devi et al., 2023). As shown in Fig. 73e, treatment T3 and T1 had the greatest SIR respiration in 90 days, followed by S2. Banerjee et al. (2024) notes that zygomycete microbial species are characteristic of substrate-induced respiration. These microorganisms are strong promoters of plant growth and have highly resilient metabolic activity.

Additionally, microbial activity in the vermibeds was evaluated by analyzing various enzyme activity profiles, including FDA, DHG, U, AP, and BG, which were an important part of the assessment (Fig. 75 f-j). The current research revealed that treatments T1 and T3 exhibited significant levels of FDA and DHG, followed by treatment T2, from the initial phase of the incubation period to its end. Although treatments initially resulted in a minimal increase in FDA and DHG rates (FDA p_{Day} = 0.001, LSD = 0.95; DHG p_{Day} = 0.003; LSD = 0.48). However, after a period of 30 days, the activity of FDA and DHG elevated in all treatments. According to Chakraborty et al. (2022), the FDA can be broken down by enzymes such as protease, lipase, and esterase under optimal conditions which measure the biological activities of vermicomposted treatments. The highest DHG activity was observed at 90 days in treatment T1 (Fig. 75g). Similarly, the active gut microbiomes of earthworms may stimulate metabolic processes that generate ATP, leading to an increase in dehydrogenase activities (Lipiec et al., 2016). These findings indicate that earthworms, together with their gut microbiota, were able to reduce the negative impacts of PTEs (mainly Cr and Ni) induced microbial toxicity in feedstock amendment with CAMW. A precise evaluation of the total hydrolase activity shown by the microorganisms in the vermibeds may be achieved by examining a specific category of enzymes, notably AP, BG, and UR. Therefore, the activity of hydrolase enzymes effectively regulates the concentrations of nutrients, such as phosphorus, carbon, and nitrogen (Aponte et al., 2020). A substantial increase in BG activity (1.77-2.01 folds) was detected in chromium-asbestos mine waste vermiunits after 90 days (LSD_{Day}= 1.05, p_{Day} = 0.001). As shown in Fig. 75j, T1 exhibited more β-D activity than T2 ($LSD_{Treatment}$ = 0.91, $p_{Treatment}$ = 0.004). The BG enzymes, which are cellulolytic enzymes, accelerate the mineralization of organic substances by breaking down bonds of β-D-glucose Significant increases in U activity were seen in T1 ($p_{Tratment}$ = 0.002, p_{Day} = 0.005), followed by T2 ($LSD_{Treatment}$ = 0.90, LSD_{Day} = 1.04) over time (Fig. 2f). The extensive burrowing behavior of earthworms, in addition to gut-assisted nitrogen-fixing bacteria, facilitates aeration in vermipits, thereby increasing the generation of urease and overall nitrogen mineralization (Ge et al., 2020). In T1, and T2, the alkaline phosphatase

activities have shown a substantial ($LSD_{Treatment}$ = 1.87, $p_{Tratment}$ = 0.002) increase of 1.67–2.05 times (Fig. 2i). The enzymes AP and UR are inducible and play a role in breaking down organic materials during the composting process (Sahariah et al., 2015). Urease catalyzes the hydrolysis of organic molecules, producing ammonium-N that remains accessible for plant uptake. On the other hand, phosphatase aids in the conversion of phosphoric esters, indicating a significant diversity in the functional microbial populations within CAMW-based vermibeds (Ghosh et al., 2022). Overall result implies that earthworms enhanced unfavourable feedstock conditions, promoting an ideal environment for microbial proliferation by mitigating CAMW-induced stress during vermicomposting. To support this hypothesis, microbial diversity was assessed using Phospholipid fatty acid profiling.

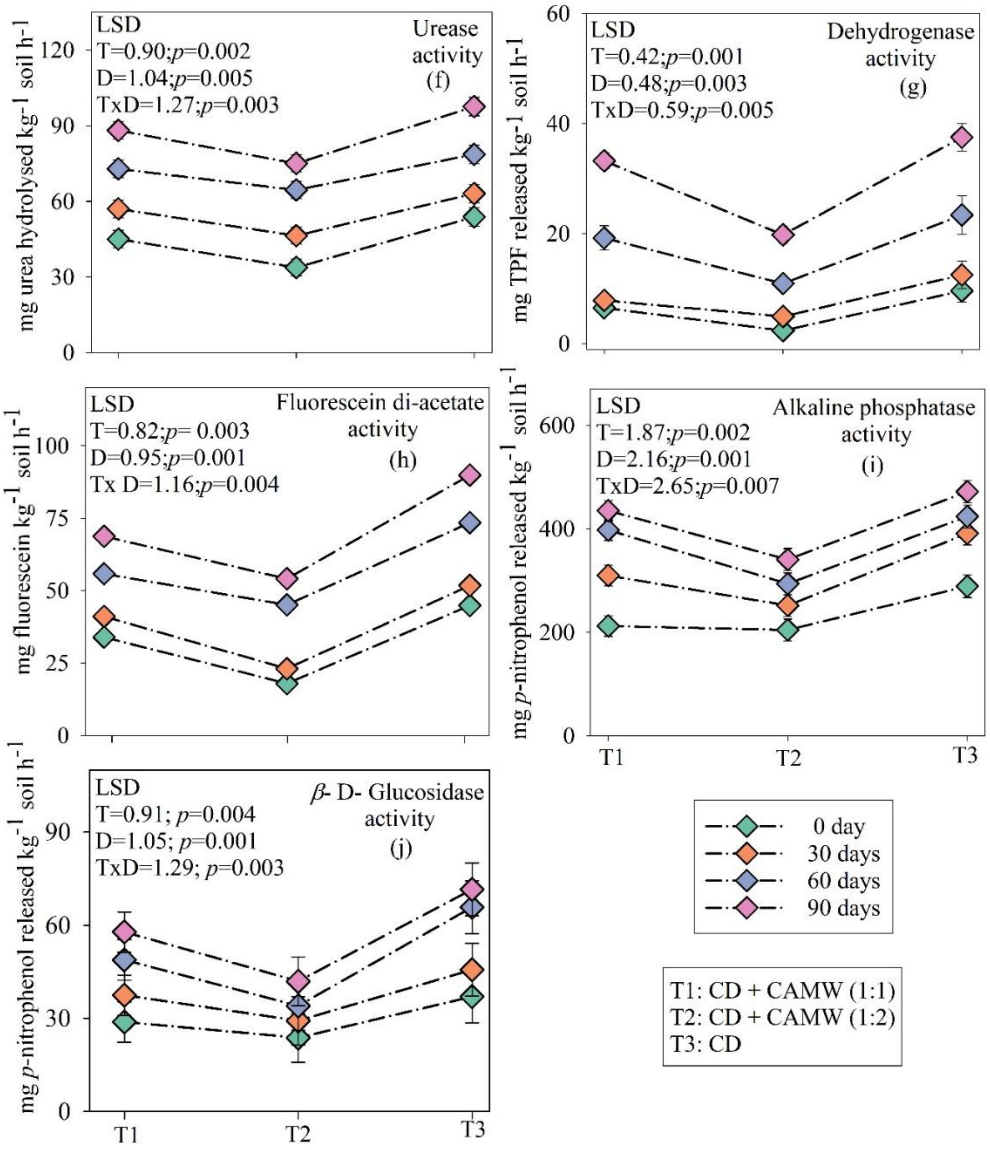

Fig. 75: Temporal dynamics of enzymatic profile activity during CAMW-vermicomposting. Here, T1: 1:1 [CD:CAMW]; T2: 1:2 [CD:CAMW]; T3: [CD only]

4.4.2.6 Alterations in chemical properties and nutrient benefit nutrient ratio of CAMW-based vermibeds

During vermicomposting, the variations in physico-chemical parameters such as pH, EC, organic C (TOC), available N (Avl N), available P (Avl P), and Ex K in the feedstock (Table 38).

Table 38: Physico-chemical attributes of vermicomposted feedstocks at the initial and final stage with statistical analysis (Mean±SD)

	0 day			90 days			Statistical Significance	
Parameters	**T1 (1:1)**	**T2 (1:2)**	**T3 (CD)**	**T1 (1:1)**	**T2 (1:2)**	**T3 (CD)**	**LSD**	***p*-values**
pH	6.78±0.26	6.45±0.31	6.98±0.39	7.14±0.34	7.33±0.49	7.07±0.33	0.021	0.001
EC (ds m^{-1})	0.29±0.01	0.27±0.013	0.23±0.009	0.43±0.014	0.34±0.017	0.47±0.011	0.022	0.006
TOC (%)	1.31±0.04	1.28±0.07	1.37±0.08	0.91±0.02	0.71±0.01	0.83±0.04	0.255	0.004
Avl. P (mg/kg)	163.41±3.19	158.26±4.78	175.09±5.98	274.93±9.76	231.99±10.87	280.89±12.47	1.66	0.007
Avl. N (mg/kg)	11.48±0.32	10.97±0.17	11.76±0.19	13.96±0.43	12.7±0.37	14.2±4.12	0.577	0.002
Ex. K (mg/kg)	174.24±8.46	161.97±7.81	183.96±9.73	436.37±23.77	333.94±17.84	419.87±27.84	0.50	0.009

T1: Cow dung + Chromium-asbestos mine waste (1:1); T2: Cow dung + Chromium-asbestos mine waste (1:2); T3: Cow dung only

*Degree of freedom (df of treatment): 2; Confidence interval: 95%

In this experiment, the feedstock's pH (T1 and T2) was initially mildly acidic due to the acidic character of the raw CAMW. After the vermicomposting process, the vermibeds' pH increased by 1.05–1.13 times, reaching a neutral value. This finding suggests that the decomposition process likely reached a state of equilibrium. Similar results were reported by Mubeen and Hatti (2018), who found that the calciferous glands of earthworms play a crucial role in neutralizing substances. The EC value in T1 increased by 1.48 times from 0 to 90 days, while in T2, it increased by 1.25 times over the same period. At 0 days, the TOC concentration in the T1 and T3 feedstock was higher than that in the T2 feedstock (LSD= 0.255; p=0.04). The TOC level was significantly reduced after 90 days, following the pattern of vermibeds T2>T3>T1, and the ANOVA indicated that the treatment interaction effect was significant for TOC. The BR ratio of organic carbon was the lowest among all attributes across all treatments. The substantial reduction in organic carbon in vermibeds indicates faster mineralization of organically bound nutrients and the maturity of vermicompost (Sahariah et al., 2015). The Avl. N, Avl. P, and Ex. K values showed a substantial rise during the vermicomposting process, with the highest observed values in T3 and T1, followed by T2. Based on the NBR analysis indicated that overall nutrient levels were significantly higher in T1 (Avl. N: 0.21; Avl. P: 0.68; Ex. K: 1.50) compared to T2 (Avl. N: 0.15; Avl. P: 0.46; Ex. K: 1.06).

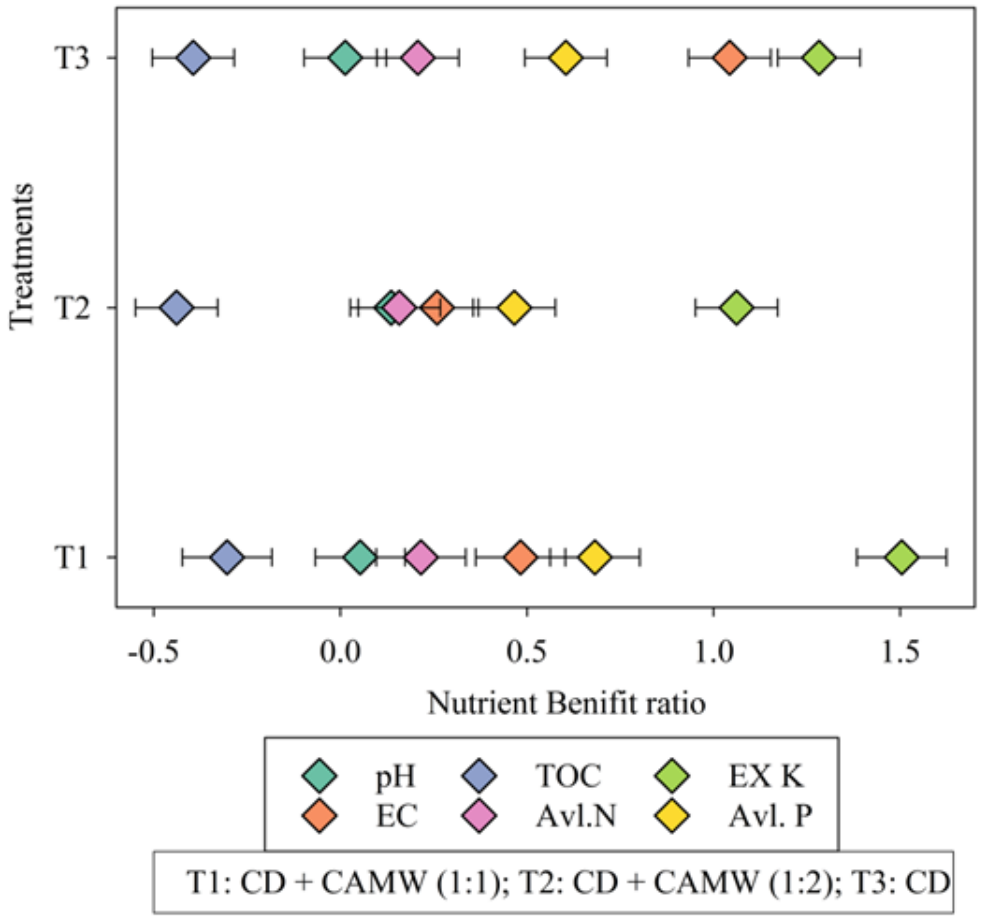

Fig. 76: Assessment of the nutrient benefit ratio of various feedstocks during vermicomposting. Here, T1: 1:1 [CD:CAMW]; T2: 1:2 [CD:CAMW]; T3: [CD only]

(Fig. 76). This nutrient availability supports the growth of earthworms in the vermiunits. These findings indicate that the vermicomposting process, facilitated by *E. fetida*, greatly enhanced the N availability in all feedstocks. Microbial activity, along with their extracellular enzymes, played a key role in promoting further N–N mineralization (Sahariah et al., 2015). Among all attributes, Ex. K exhibited the highest nutrient benefit ratio compared to the others. These results may be attributed to the presence of potassium-solubilizing microorganisms, which increase the availability of potassium in the feedstocks (Ghosh et al., 2023). The rapid increase of the P-solubilizer bacterial population in the CAMW-feedstocks likely stimulated phosphatases, hence accelerating the solubilization of phosphorus in the feedstocks. The data suggest that a notable rise in N and P-specific enzymes, like urease and AP, was the main factor contributing to a substantial increase in the availability of these two crucial macronutrients. As reported by Mondal et al. (2020), the microbial population in the earthworms' digestive system may have increased the availability of P in the feedstocks during vermicomposting. Similarly,

the compaction of organic matter in the earthworm gizzards increases its surface area, which helps improve the availability of potassium (Goswami et al., 2018).

4.4.2.7 Microbial community shifts and diversity in vermibeds: Analysis via PLFA and diversity indices

The PLFA analysis was performed to understand the functional diversity of microbial communities within various CAMW-based vermibeds (Fig. 77). This analysis not only provides insight into the microbial community structure but also reveals shifts in microbial groups under different environmental conditions (Jha et al., 2024). The primary aim of this study was to evaluate CAMW-based feedstock's potential for vermi-remediation, thereby determining the optimal feedstock combination for future applications. The active PLFA levels in the vermibeds showed variation, as illustrated (Fig. 78b). The trend in total PLFA was T3 > T1 > T2 (LSD = 5.08; *p* total PLFA = 0.001). The findings suggest that T3 ≥ T1exhibited greater diversity of both gram-negative and gram-positive bacteria compared to T2 (Gram-negative: *p*=0.001; LSD = 1.17; Gram-positive: *p*= 0.003; LSD = 2.15). This trend shows that T3 had the highest bacterial diversity across all the treatments. Gram-negative bacteria exhibit a high tolerance to challenging environmental conditions (Eberlein et al., 2018). Thus, the relatively lower gram-negative bacterial signatures were observed in the PLFA profiles of T2 and T1 compared to T3. These findings suggest that the increase in gram-positive bacterial communities, along with a decrease in gram-negative populations, likely served as a stress-relieving phenomenon in the CAMW-based vermibeds. Gram-negative bacteria have an outer membrane made of lipopolysaccharides, which enhances their structural integrity, increases the negative charge of the cellular membrane, and protects them from different PTEs stress (Gómez-Brandón et al., 2012). In this research this adaptability might support the microbial population, aiding the degradation of hazardous CAMW. The PLFA study underscored the existence of these bacteria, accentuating their vital function in maintaining stability and microbial activity under PTES stress. Consequently, it was clearly demonstrated that the maturation of vermicompost promotes the proliferation of Gram-positive bacteria while inhibiting the Gram-negative bacteria. The shift from Gram-negative to Gram-positive provide clear evidence for stress adaptation of microbial community caused by toxic PTEs in the vermibeds. This shift enhances microbial resilience, as Gram-positive bacteria have a strong cell wall construction that affords grater resistance to unfavourable environmental conditions. A similar tread was observed in a study related to toxic paper mill wastes vermicomposting

(Ganguly and Chakraborty 2021). PLFA levels for eukaryotes, were significantly higher in T3 [CD] compared to the other treatments, whereas actinomycetes were elevated in T2 (Fig. 77a).

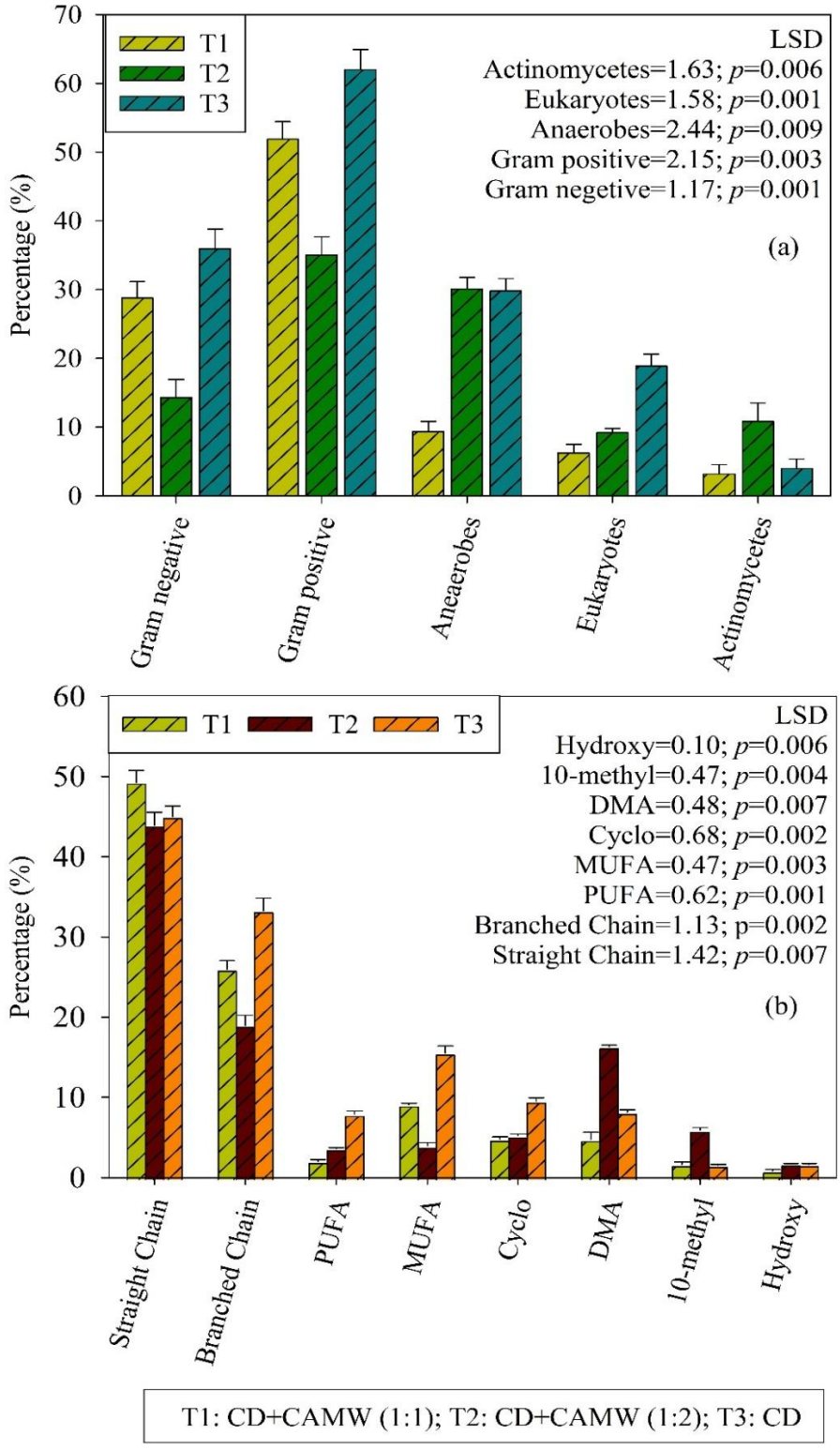

Fig.77: PLFA-based analysis depicted (a) microbial community structure, and (b) fatty acid profile diversity in CAMW-vermicomposted product. Here, T1: 1:1 [CD:CAMW]; T2: 1:2 [CD:CAMW]; T3: [CD only].

The T3 feedstock, made primarily of cow dung, provided a favorable environment for diverse microbial communities. When mixed with CAMW at various ratios, it enhanced CAMW quality, supporting microbial growth and diversity. These findings align well with earlier studies (Devi et al., 2020). Between the two ratios (1:1 and 1:2) of CAMW treatments, microbial proliferation was more effective in treatment T1, with increased levels of straight-chain (LSD: 1.42; p= 0.007), branched-chain fatty acids (LSD: 1.13; p= 0.002), and monounsaturated (MUFA) (LSD: 0.47; p= 0.003), as well as polyunsaturated fatty acids (PUFA) (LSD: 0.62; p= 0.001) and Dimethyl Acetal (DMA) (LSD: 0.48; p= 0.007) in T2. According to Zhao et al. (2018), branched-chain fatty acids serve as reliable markers for sulfate-reducing anaerobic bacteria (*Desulfovibrio sp.*). These findings suggest that earthworms help maintain an aerobic environment. Treatment T3 showed higher levels of MUFA and branched-chain fatty acids (Fig. 77b). The PLFA profiles can be practically interpreted through the stress ratio. Gram-negative bacteria produce monounsaturated fatty acids during active metabolism, which convert to cyclopropane fatty acids when metabolic rates slow due to contaminants (Zhao et al., 2018). The stress indicator, calculated as (cyclopropane17:0 + cyclopropane19:0)/(16:1Ω7c + 18:1Ω7c), reflects stress levels, with a higher ratio indicating greater stress. In this study, the highest stress value was recorded in treatment T2 (p_stress ratio = 0.003; LSD_stress ratio = 0.079) (Fig. 78b).

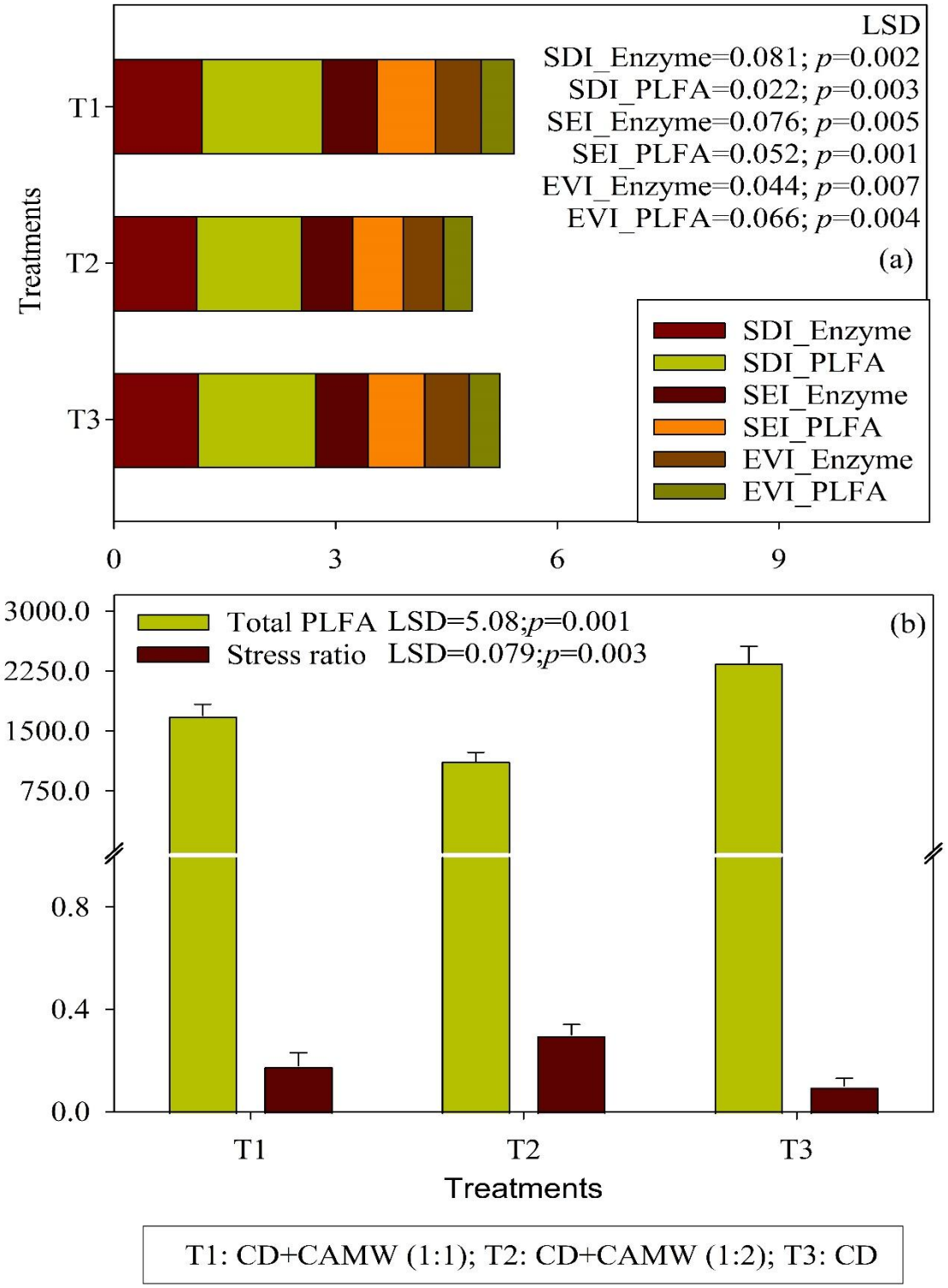

Fig. 78: (a) Alterations in microbial group and enzyme activity Shannon diversity (SDI), evenness (SEE), and E-var (EVI) during vermiconversion of various treatment combinations of chromium-asbestos mining waste vermicompost (CAMW); (b) Changes in total PLFA and stress ratio in different treatments. Here, T1: 1:1 [CD:CAMW]; T2: 1:2 [CD:CAMW]; T3: [CD only]

Also, the stress value in T1 was significantly reduced due to the effectiveness of earthworm- and microbe-mediated PTEs removal along with suitable cow dung incorporation. Microorganisms are known to play an essential role in breaking down organic matter, and earthworm activity helps enhance microbial community structure throughout the vermicomposting process (Devi et al., 2020; Gomez-Brandon et al., 2011). This stress ratio primarily serves as an indicator of microbial stability and health; nevertheless, comprehending these might inform the enhancement of circumstances in vermiremediation process, ensuring more effective microbial activity and waste degradation. Throughout the experiment, treatments T1 and T3 showed increased SDI_PLFA, SDI_enzyme, as well as SEI_PLFA, SEI_enzyme, EVI-PLFA, and EVI-enzyme (Fig. 78a). These findings indicate that T1 also provided a favorable feedstock for earthworm-driven microbial diversity and enzyme activity. In contrast, T2 exhibited notably lower Evar (EVI) indices in-case of both PLFA and enzyme analysis (EVI-PLFA and EVI_enzyme) than T1 and T3, suggesting that CAMW significantly affects the diversity of functional microbial communities. Meanwhile, the high levels in T1 EVI-PLFA and EVI_enzyme suggest that factors like earthworm gut mucus, feeding behavior, and intestinal microbes might have mitigated CAMW-related stress in these vermibeds. Overall, the findings of PLFA indicated that mixing of CAMW and CD (T1 treatment: 1:1ratio) offers a favorable environment for microbial growth and earthworms' activity, mitigation of PTEs, enhance nutrient availability in vermibed, supports the good quality of CAMW-vermicompost.

4.4.2.8 Analysis of PLFA and PTEs Interactions for Sensitivity

Sobol scores for all input variables were analyzed to assess the impact of bioavailable PTEs fractions (Cr, Pb, Ni, Cd, and Cu) on the PLFA profile in vermicompost. Results from the first-order (FOSI) and total-order (TOSI) analyses revealed that gram-positive, gram-negative, and anaerobic microorganisms exhibited greater resilience to Cr, Cd, Pb, and Ni exposure in CAMW-based vermicompost than other community like eukaryotes and actinomycetes (Fig. 79). Such patterns were observed in CAMW-based vermicompost with minimal concentrations of PTEs including Cr, Ni, Cd, and Pb, except Cu. The maximum microbial population demonstrated enhanced survivability against Cu, while Gram-positive bacteria indicated increased tolerance to Cr, Pb, and Ni. Additionally, microorganisms that generate raw fatty acids (straight-chain and branch-chain) demonstrated enhanced survival in response to PTEs stress. These groups exhibited superior resilience relative to other fatty acid, including DMA, Cyclo, MUFA, hydroxyl, and PUFA. In microorganisms, the conversion of raw fatty acids into

MUFA, PUFA, DMA, Cyclo, and Hydroxy types demonstrated distinct correlations. PUFA exhibited a negative association with Cr. Preserving cellular homeostasis during PTEs stress (Cr) is essential for microbial survival, perhaps indirectly affecting PUFA synthesis and stability (Ibarra et al., 2019). DMA showed tolerance towards Ni, Cd, and Pb, whereas Cu was positively associated with PUFA and hydroxy fatty acids under stress conditions. Second-order sensitivity analysis explained the interactions between pairs of the model's inputs, making it possible to identify the most influential input pairs by examining the variation or interaction between two parameters (Jha et al., 2024; Kumar et al., 2020). From this model-based analysis, highlights the dominance of microbial community which helps to detoxify the CAMW and demonstrates tolerance towards different PTEs and improves the efficacy of vermi-remediation technique.

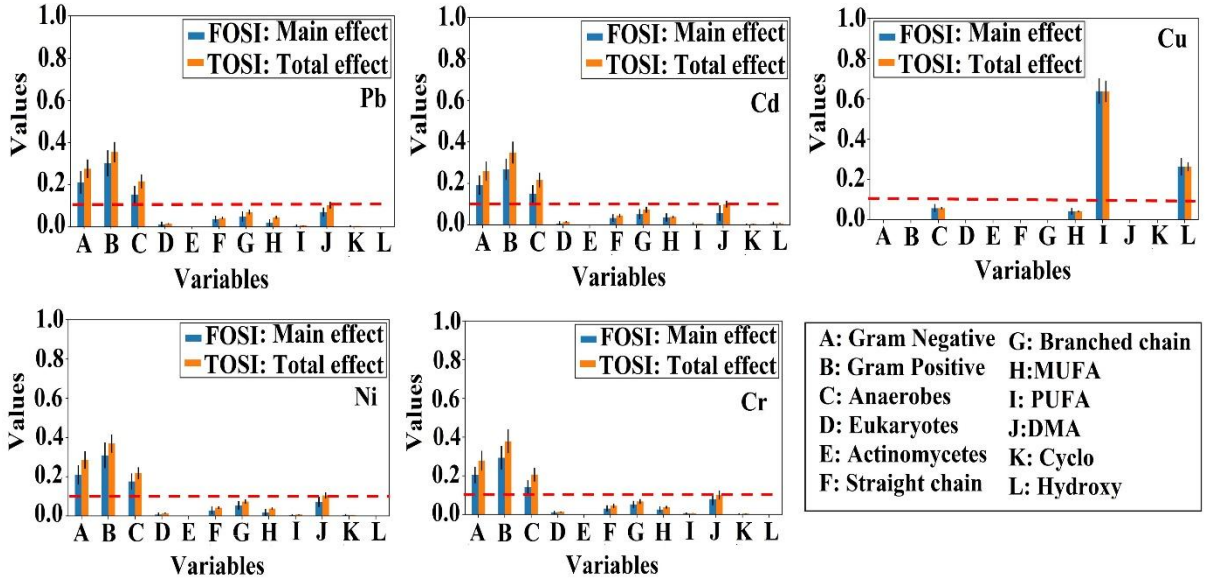

Fig. 79: Quality assessment of vermicomposted CAMW feedstocks utilizing Sobol sensitivity model analysis [first-order and total-order]

4.4.2.9 Evaluate the relationship between microbial diversity and PTEs bioavailability dynamics: An Insight through Correlation technique and PCA

Pearson's correlation statistics were applied to explore how bioavailable PTEs affects microbial diversity. The analysis examined microbial properties (MBC, MBP, MBN, BSR, SIR), enzyme activities (AP, BG, DHG, U, FDA), and available trace elements (Pb, Cr, Cu, Ni, Cd). As illustrated in Fig. 80 a strong negative correlation (denoted by purple color) observed between available PTEs and microbial as well as enzymatic measures in the final vermicomposting phase. This may be attributed to a marked decrease in the bioavailability of PTEs like Cr, Pb, Ni, and Cu at the maturation phase, accompanied by an increase in microbial

activities within the vermibeds (Fig. 80). As a result, significant microbial activity was observed at maturity, attributed to the reduced toxic effects of CAMW. According to Shi et al. (2013) confirmed that correlation analysis effectively validates interactions between microbes and PTEs.

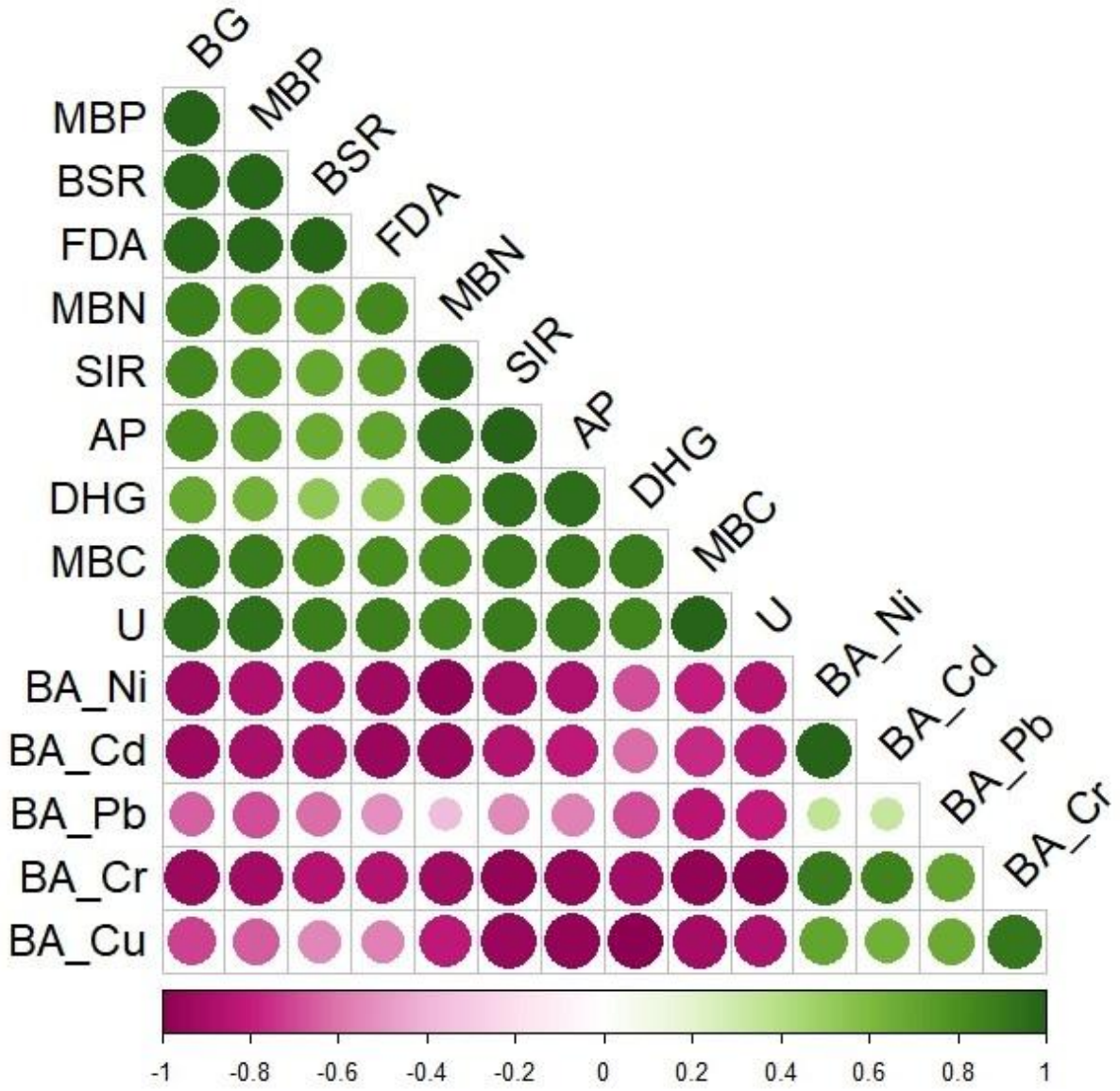

Fig. 80: Correlation plots illustrating the relationships between PTEs bioavailability and microbial-enzymatic activity (each point shows correlation coefficients and their significance value denoted by colors)

A Principal Component Analysis was conducted to investigate the relationship between various concentrations of PTEs, microbial-enzymatic parameters, and the microbial community structure. The analysis revealed that the first two components, Dim-1 and Dim-2, explained 93.4% of the total variance. A closer association between microbial-enzymatic parameters and the PLFA-microbial community structure (Gram positive, Gram negative, actinomycetes, eukaryotes, and Anaerobes) was observed. Furthermore, during vermicomposting, the bioavailable fractions of PTEs were found to decrease as maturity progressed in vermicomposted CAMW (Fig. 81). This result was algin with Chakraborty et al. (2024).

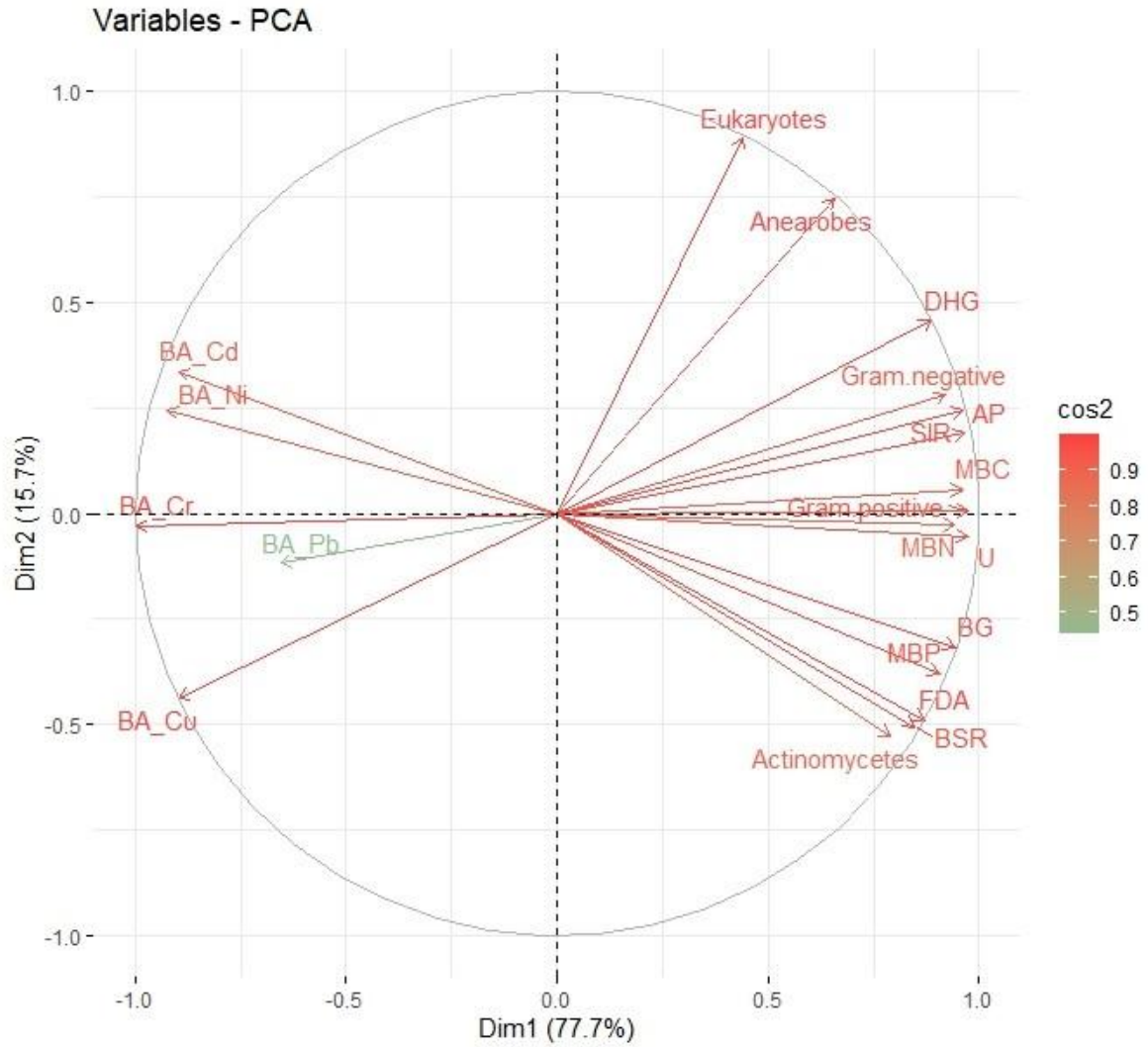

Fig. 81: Principal component analysis demonstrating the relationship among bioavailable trace elements (PTEs), microbial enzymatic characteristics, and microbial community structure

Objective: 5

4.5 Assessing the efficiency of reclaimed vermi-remediating products (PTE-EVVc and CAMW-VC) through pot and field trials

For the purpose of this experiment, four crops—tomato, sesame, chilli, and rice—were selected to evaluate the quality and effectiveness of two vermicomposted products as organic manures. Pot experiments were conducted for tomato, chilli, and sesame, while rice was cultivated under field conditions. The experimental details for each crop are presented sequentially.

4.5.1. Pot experiment with Tomato

Pot experiments for tomato (*Solanum lycopersicum* L.) were conducted during two consecutive winter seasons (November–February) in 2023–2024 at the Indian Statistical Institute's agricultural farm in Jharkhand (Fig. 82).

Fig. 82: Pictorial illustration of tomato cultivation for pot experiment with vermicomposted PTE-enriched vetiver (PTE-EVVc)

A fertilizer regime of 200:150:100 kg/ha (N: P_2O_5: K_2O) was followed for tomato cultivation. Treatment specifications are provided in Table 39, with each treatment replicated three times.

Table 39: Treatment description (Tomato)

Order	Treatment details
T1	Control (No amendment)
T2	Chemical Fertilizer (NPK)100%
T3	Cow dung (CD) 100%
T4	CD 50% + Chemical Fertilizer (NPK) 50%
T5	PTE enriched vetiver vermicompost (PTE-EVVc 1:1) 100%
T6	(PTE-EVVc 1:1) 50% + Chemical Fertilizer (NPK) 50%
T7	(PTE-EVVc 1:2) 100%
T8	(PTE-EVVc 1:2) 50% + Chemical Fertilizer (NPK) 50%

Vermicomposts derived from PTE-enriched vetiver and cow dung were mixed into the potting soil two weeks prior to sowing. Seeds, sourced from the State Seed Corporation, were treated with copper oxychloride before planting. Uniform agronomic practices such as scheduled irrigation, optimal planting density, timely weeding, and integrated pest management were applied across all treatments. After the experiment concluded, various growth and soil-related parameters were assessed following standardized methodologies.

4.5.1.1 Physico-chemical properties estimation after harvest of tomato cultivation

Tomato (*Solanum lycopersicum* L.) was used as the test crop in a pot culture experiment to evaluate the efficacy of vermicomposted PTE-enriched vetiver as a soil supplement. A famous horticultural crop with several health advantages, tomatoes are well-known across the world (Jha et al., 2023). Measurements of the soil properties following tomato cultivation under various treatments are shown in Table 40.

Table 40: Soil physico-chemical and bioavailability PTEs in soil after tomato cultivation under different treatments (Mean±Standard deviation)

Treatments	pH	TOC (%)	Avl. P (mg/kg)	Avl. N (mg/kg)	Ex. K (mg/kg)	BA_Cr (mg/kg)	BA_Ni (mg/kg)	BA_Pb (mg/kg)
T1 (Control soil)	6.63±0.43	0.393±0.021	40.82±3.87	9.72±0.62	144.71±11.23	6.32±0.32	5.29±0.36	4.08±0.27
T2 (NPK fertilizer)	6.77±0.39	0.437±0.018	46.51±3.62	12.63±0.97	173.03±16.07	7.13±0.49	6.37±0.43	6.83±0.53
T3 (Cow dung)	7.21±0.53	0.511±0.023	58.92±4.17	22.24±1.89	196.49±16.53	1.69±0.06	1.43±0.03	0.97±0.04
T4 (Cow dung + NPK fertilizer)	7.29±0.47	0.536±0.027	64.17±5.29	26.97±1.08	204.27±18.66	1.73±0.04	1.29±0.05	0.73±0.031
T5 (1:1 CAMW Vermicompost)	6.98±0.38	0.623±0.031	57.28±4.83	23.67±1.17	191.36±14.22	11.29±0.78	7.01±0.49	5.93±0.29
T6 (1:1 CAMW Vermicompost + NPK fertilizer)	7.16±0.34	0.691±0.029	68.04±5.46	29.6±1.41	212.08±19.17	9.12±0.62	6.29±0.28	5.16±0.36
T7 (1:2 CAMW Vermicompost)	6.81±0.46	0.463±0.024	52.18±4.42	19.26±1.53	179.24±16.41	14.72±1.07	12.56±0.87	11.48±0.97
T8 (1:2 CAMW Vermicompost + NPK fertilizer)	6.89±0.41	0.495±0.032	59.47±4.38	22.03±1.94	188.63±17.92	13.39±1.13	11.74±0.92	9.39±0.78
LSD (Treatments)	0.39	0.27	3.64	1.29	16.19	1.44	1.19	1.037
p-value	0.03	0.04	0.029	0.017	0.036	0.0027	0.0046	0.0012

The study's soil was described as lateritic, poor in organic carbon, moderately acidic, and lacking in NPK nutrients. During tomato cultivation, plots treated with vermiconverted-PTE-enriched vetiver showed a modest increase in soil nutrient levels. The treatment (T6: PTE-EVVc1:1 + NPK fertilizer) had a significantly greater pH rise (towards the neutral range), reaching 7.16±0.34. The treatment (T8: C1:2 + NPK fertilizer) had a pH increase of 6.89±0.41 (p= 0.03). The PTE-enriched vetiver vermicompost's neutral pH is the cause of this pH improvement. Furthermore, the soil's organic carbon (TOC) content increased (0.691±0.029 %) in treatment (T6: PTE-EVVc1:1 + NPK fertilizer), followed by treatment (T4: Cow dung + NPK fertiliser), and treatment (T8: PTE-EVVc1:2 + NPK) (Table 40). The breakdown of organic matter and the leftover agricultural residues affect the amount of TOC available in the soil (Lazcano et al., 2008). By adding organic amendments, the vermicomposting process increases microbial activity, speeds up the mineralisation of soil carbon, and promotes the mineralisation of nutrients like NPK. Furthermore, PTEs are less accessible for plant absorption because they are bound in soil organic matter (Das et al., 2016). Following the sequence T6 > T5 > T2 > T8 > T7 > T1, the vermicomposted PTE-enriched vetiver amendment considerably increased the soil's total NPK levels (Table 40). The combined use of chemical fertilizers and vermicompost may be the cause of this discovery, since it promotes the biological decomposition of organic waste. This process raises the amount of mineralised nitrogen in the soil and encourages the development of microbial communities that solubilise potassium and phosphorus, which in turn triggers the release of a variety of endogenous and exogenous soil enzymes. Vermicompost improves NPK status and lowers the bioavailability of PTEs for plants, according to the results, which are consistent with Sahariah et al. (2020). The findings indicate that recycling PTE-enriched vetiver through vermicomposting by mixing it with cow dung could be an effective strategy for managing plant PTE content residue and minimizing the risk of PTE-induced toxicity in agricultural soils.

4.5.1.2 Determination of biochemical and agronomic perspective across different treatments

Crop production result indicated that PTE-EVVc had a beneficial impact on soil health (Table 41).

Table 41: Biochemical and Agronomic attributes of tomato after harvest (Mean±Standard deviation)

Treatments	Protein	Total Soluble Sugar	Lycopene	Plant shoot length	Plant root length	Yield
	mg 100 g^{-1}	mg 100 g^{-1}	mg 100 g^{-1}	cm	cm	(g $plant^{-1}$)
T1	0.51±0.016	1.97±0.11	5.66±0.42	40.2±2.01	21.3±1.26	190.06±11.73
T2	0.59±0.029	2.19±0.17	6.28±0.46	53.4±3.43	32.9±0.34	240.19±19.51
T3	0.83±0.034	3.09±0.15	7.88±0.38	58.5±3.19	31.4±0.39	337.58±21.94
T4	0.89±0.023	3.64±0.24	8.59±0.34	62.8±2.76	34.8±0.47	349.32±26.95
T5	0.88±0.024	4.70±0.34	7.99±0.53	61.7±2.98	33.1±0.51	346.56±23.21
T6	0.97±0.034	4.87±0.31	8.48±0.43	65.3±2.34	39.8±0.37	360.88±28.13
T7	0.64±0.027	2.49±0.16	7.33±0.54	51.5±4.93	29.4±0.41	312.52±17.37
T8	0.77±0.019	2.67±0.34	7.79±0.57	56.7±3.29	27.2±0.31	300.62±19.01
LSD (Treatments)	1.03	2.3	0.87	9.74	1.59	23.69
p-value	0.006	0.004	0.029	0.006	0.003	0.0017

Treatment T6 was shown to have greater levels of lycopene content (8.48±0.43 mg 100 g^{-1}), total soluble sugar (4.87±0.31 mg 100 g^{-1}), and protein (0.97±0.034 mg 100 g^{-1}) than the other treatments. The improved availability of N, P, and K from vermicompost, which releases nutrients gradually and improves nutrient efficiency and biomass quality more effectively than inorganic fertilizer treatment (T2), is responsible for the higher lycopene, protein, and sugar content in plants treated with PTE-EVVc. The result was in line with the findings of Chakraborty et al. (2024). In similar vein, the PTE-EVVc1:1+NPK (T6) fertilizer treatment yielded (360.88±28.13 g $plant^{-1}$) a remarkably high yield. Furthermore, as shown in Table 41, treatments T6 and T4 produced the highest plant roots and shoots lengths, in comparison with T2. Better root and shoot length growth was demonstrated by the improvement in biochemical characteristics and decreased PTE absorption in plant sections. These findings are consistent with those of Ghosh et al. (2025), who found that crop growth and production are enhanced when organic sources and inorganic fertilisers are combined.

4.5.1.3 Bioavailable PTEs content in soil and different accumulation indices evaluation after harvest

In comparison to initial levels, the statistical analysis (ANOVA) revealed a significant decrease in bioavailable PTEs in soil across all treatments (LSD_{Ni}: 1.19, p_{Ni}: 0.0046; LSD_{Cr}: 1.44, p_{Cr}: 0.0027; LSD_{Pb}: 1.037, p_{Pb}: 0.0012), with the treatment (T6: PTE-EVVc1:1 + NPK fertilizers) exhibiting the most noticeable decrease (Table 40). As seen in Table 42, which highlights the ecological consequences of PTE-enriched vetiver-vermi-transformation, PTEs were assessed using several indices [Plant bio-concentration factor (PBCF) and Plant translocation factors (PTF)] to assess their transportation from soil to plant components (root, shoot, tomato).

Table 42: Different PTEs accumulation indices of tomato plant

Treatments	PBCF_Cr	PTF_Cr	PBCF_Ni	PTF_Ni	PBCF_Pb	PTF_Pb
T1	0.100	0.388	0.048	0.449	0.155	0.734
T2	0.075	0.274	0.023	0.813	0.108	0.510
T3	0.120	0.716	0.154	0.883	0.394	0.457
T4	0.113	0.686	0.152	0.603	0.383	0.585
T5	0.280	0.520	0.559	0.216	0.441	0.442
T6	0.266	0.501	0.341	0.241	0.326	0.720
T7	0.294	0.690	0.353	0.293	0.279	0.683
T8	0.276	0.583	0.332	0.242	0.199	0.650

PTEs (Pb, Cr, and Ni) concentrations in tomatoes were found to be below detectable levels, and absorption was seen to occur in the following order: roots > shoots. PTE absorption in roots is shown by the PBCF study, which shows that in the treated pots, the pattern is Ni > Pb > Cr. Compared to other PTEs, Ni was more prevalent in the treatments, which may have contributed to its high accumulation. A number of variables, including beginning concentration, plant type, and absorption capability, affect the PTEs accumulation. According to Page and Feller (2015), PTEs (mostly Pb, Cr, and Ni) are kept in plant roots by being compartmentalised inside cells or stored in vacuoles, which prevents them from being transported via the xylem. PTF were below 1 in all treatments; the treatment with the lowest PTF (T6: PTE-EVVc1:1 + NPK fertilizers) showed lesser PTE mobility than the treatment (T8: PTE-EVVc1:2 + NPK fertilizers). Understanding bioaccumulation, which was negligible in other treated pots, requires evaluating the transport of PTEs between plant components (root, shoot, and tomato). The findings support those of Chakraborty et al. (2024), who found that adding vermicompost to soil successfully reduces the amount of PTEs that plants absorb.

4.5.2 Pot experiment preparation with Chilli

Pot investigations were executed over two successive (May–August) in 2023–2024 for chilli (*Capsicum annum* L) at the Indian Statistical Institute's agricultural farm in Jharkhand. The required fertilizer dosage of 40:50:60 (N: P_2O_5: K_2O) kg/ha was utilized for chilli cultivation. The treatment details are depicted in Table 43, and each treatment was replicated thrice. Vermicomposted CAMW and cow dung were incorporated into the soil in the pots 2 weeks before sowing.

Table 43: Description of pot experiment (chilli) of treatments

Serial Order	Treatment preparation details
C1	CAMW 1:1 Vermicompost only (100%)
C2	CAMW 1:1 Vermicompost (50%) + NPK fertilizer (50%)
C3	CAMW 1:2 Vermicompost only (100%)
C4	CAMW 1:2 Vermicompost (50%) + NPK fertilizer (50%)
C5	Cow dung only (100%)
C6	Cow dung (50%) + NPK Fertilizer (50%)
C7	NPK Fertilizer (100%)
C8	Control (No input)
C9	Raw chromium-asbestos mine waste only (100%)
C10	Raw chromium-asbestos mine waste (50%) + NPK Fertilizer (50%)

Well-filled seeds obtained from the State Seed Corporation were treated with copper oxychloride prior to being sown. Standard agronomic practices, including irrigation, planting density, periodic de-weeding, and management of pests, were uniformly applied across treatments. After completion of the experiment, different parameters were evaluated based on standard protocol.

4.5.2.1 Changes in soil nutrients and microbial activities among different treatments

Fig. 83 (a-f) depicts the dynamics of physico-chemical properties over time (0 day and post-harvest) among different treatments during the pot experiment. Initially, at 0 day, the soil pH was slightly acidic in nature (range: 6.09±0.36-6.48±0.38) among the treatments. The pH values were C9: 6.09 and C10: 6.16 in the CAMW amended treatments, respectively, on 0 day. After harvest, all the treatments showed an upsurge in the neutral range of 6.59-7.18, except the C9 and C10 treatments (Fig. 83a).

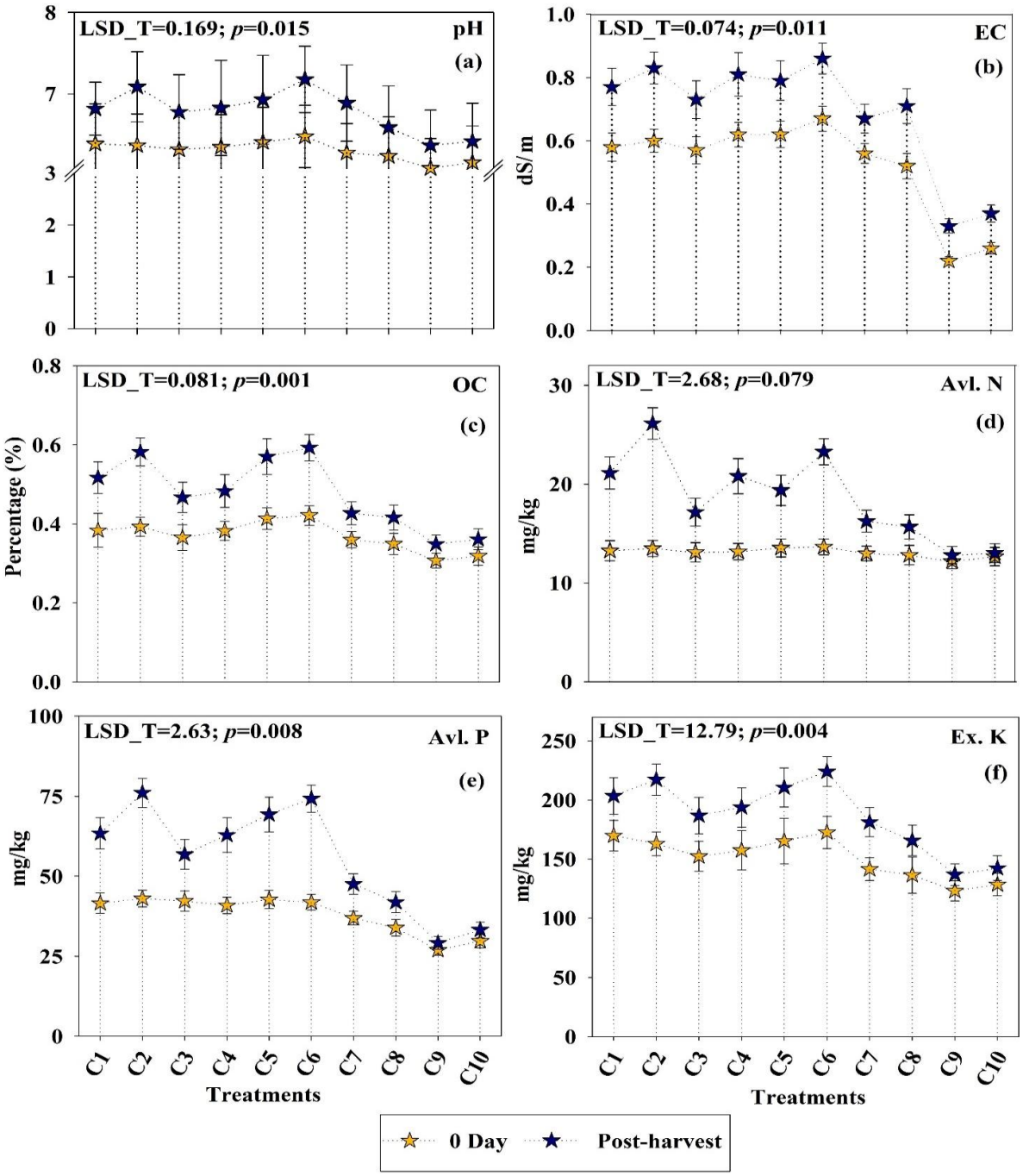

Fig. 83: Changes of soil physico-chemical properties across treatments during the pot experiment

However, CAMW amendment treatments (C9 and C10) tend to exhibit a slightly acidic nature. These findings are consistent with Jha et al. (2024), who found that the incorporation of organic amendments such as vermicomposted CAMW and cow dung could be attributed to the rise in pH among various treatments. Rising pH levels contribute to better plant growth by fostering a more neutral environment, which enhances nutrient absorption and metabolic functions, ultimately helping plants develop more effectively and healthily. The EC levels were elevated in the CAMW vermicompost mixed treatments (C1, C2, C3, and C4) from the beginning to

post-harvest, while the least rise was in raw CAMW waste amended treatments (C9 and C10) (Fig. 83b). Also, the temporal increment of organic carbon was observed significantly (LSD_T: 0.081; *p*: 0.001) in all the treatments from initial to post-harvest (Fig. 83c). The crop residual and organic material decomposition increase the availability of soil organic carbon storage. This observation is similar to previous studies, which showed that carbon from plant residues tends to form clusters within clay structures (Chivenge et al., 2011). This process boosts the humification ratio and leads to a significant increase in organic carbon storage in soil by the time the crop is harvested. Additionally, the other important macronutrients include potassium (Ex. K), nitrogen (Avl. N), and phosphorus (Avl. P) also showed a similar trend in all the treatments except C9 and C10 (raw CAMW amended). Initially, the nutrient content was low, but it escalated at the time of harvest as depicted in Fig. 83(d, e, f). No substantial variation was observed between 0 to post-harvest in the C9 and C10 treatments, likely due to the high levels of PTEs in raw CAMW, which contribute to soil toxicity. The highest nutrient availability was observed in C2 treatment (Ex. K: 217.39±13.17 mg/kg; Avl. P: 76.02±4.60 mg/kg; and Avl. N: 26.14±1.58 mg/kg), where soil is amended with 1:1 CAMW vermicompost (50%) and fertilizer (50%). The combined application of vermicompost/cow dung and chemical fertilizer in C2, and C6 treatments ensures an optimal distribution of mineral nutrients, enhanced microbial activities, and enzymatic attributes, showing the most pronounced results as compared to other treatments. The microorganisms present in vermicompost can boost plant growth by making P and K more available, fixing N, and producing plant growth-promoting substances like indole acetic acid, gibberellic acid, ammonia, and siderophores. Therefore, these nutrient-rich environment support soil fertility, soil health, and plant development (Choudhary et al., 2020; Chakraborty et al., 2024). These results are in line with the findings of Das et al. (2020), who reported that the balanced use of vermicompost and chemical fertilizers significantly enhanced the diversity and growth of microbial communities, which subsequently promoted the release of various endogenous and exogenous enzymes in the soil.

Microorganisms are essential for carbon and nitrogen cycling and act as key indicators of soil health and quality. Evaluating various enzymatic and microbial parameters under different soil amendments offers important insights into the activity of soil microorganisms. In this study, soil microbial and enzymatic activity was assessed at different time intervals (0, 30, 60 days, and post-harvest) across all treatments, as illustrated in Fig. 84(a-h). Temporal dynamics of soil enzymatic activity, including glucosidase, alkaline phosphatase, dehydrogenase, urease, and

fluorescein diacetate significantly varied [LSD_BDG: 4.44, *p*: 0.013; LSD_ALP: 32.17, *p*: 0.001; LSD_DHYG: 5.22, *p*: 0.006; LSD_UR: 4.40, *p*: 0.001; LSD_FDA: 4.23, *p*: 0.02] across all treatments during the pot experiment. Initially, all the enzymatic parameters were higher on 0 day, then showed a significant and gradual decline up to 60 days, followed by a slight increase at the post-harvest stage. At post-harvest, the enzymatic activities were elevated in organic amended treatments (C1, C2, C3, C4, C5, and C6) as compared with the control and raw CAMW contaminated treatments (C9, C10). The least activity was observed in C9 and C10 due to the direct application of raw CAMW waste, which contains high PTEs that negatively affect the microbial population. The highest BDG activity was observed in C6 (BDG: 28.73±1.04 mg of *p*-nitrophenol released/kg soil/h) and C2 (BDG: 26.29±0.86 mg of *p*-nitrophenol released/kg soil/h) followed by C5, C7, and C4 (Fig. 84e). The key role of the BDG enzyme is to decompose organic matter, primarily composed of long-chain β-D-glucose units (Fernández-Gómez et al., 2013). Glucosidase activity is generally reduced in soils with elevated PTEs concentrations; therefore, C9 and C10 showed decreased levels of this enzyme activity. This finding aligns with the results of Jha et al. (2023), who reported that the application of raw waste leads to a reduction in enzymatic activity, while the use of vermicomposted products enhances it.

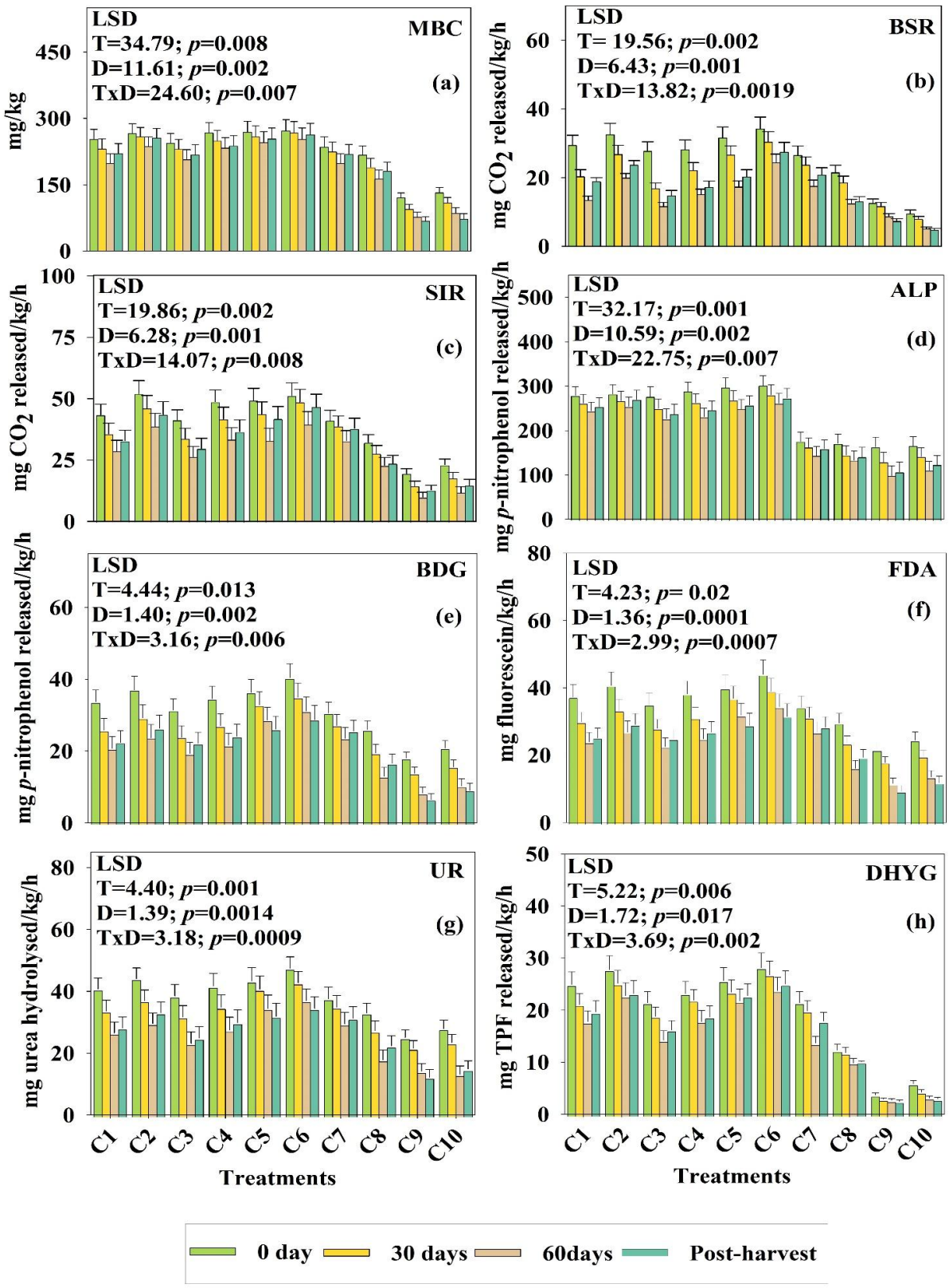

Fig. 84: Temporal dynamics of microbial-enzymatic attributes of various treatments during the pot experiment with chilli as the test crop.

In case of ALP and UR activity, a significant day-wise variation [LSD_ALP: 10.59, *p*: 0.001; LSD_UR: 1.39, *p*: 0.0014] was observed across all treatments. Higher enzyme activity was recorded in C6, C2, C5, and C1, while the lowest activity was determined in C9 and C10 in comparison with the control (C8) (Fig. 84d, g). The results also indicated that the addition of organic matter, such as cow dung or vermicomposted CAMW, enhanced soil enzyme activity. This increase could be attributed to the presence of endoenzymes from active microbial populations and higher accumulation of enzymes within the soil matrix (Jha et al., 2023). These findings are consistent with those of Banerjee et al. (2025), who highlighted the importance of ALP and UR enzymes in the phosphorus and nitrogen cycles of terrestrial ecosystems. In C9 and C10, the presence of PTEs resulting from the application of raw CAMW impacted enzyme activities. These effects may be due to PTEs interacting with enzyme-substrate complexes, causing protein denaturation and impacting both enzyme activity and their synthesis, as stated by Ghosh et al. (2024).

Activities of other enzymes, such as DHYG and FDA, were initially higher at day 0, gradually declined up to 60 days, and showed a slight upsurge at the post-harvest stage across all the treatments except C9 and C10 (Fig. 84f, h). In these two treatments, a decreasing trend was observed over time as the presence of raw CAMW and its associated toxicity, which may have contributed to this finding. In C6 (cow dung + NPK fertilizer) and C2 (1:1 vermicomposted CAMW + NPK fertilizer), the highest enzymatic activity was recorded, while moderate levels of enzymatic activity were observed in C7 and C8. This pattern could be due to the higher levels of organic matter (vermicompost/cow dung combined with chemical fertilizer), which likely promoted greater enzyme production and enhanced the soil's nutrient content over time (Macci et al., 2012). This enhanced enzymatic activity can be linked to the action of the intracellular enzyme DHYG in facilitating the transfer of electrons and hydrogen among various cellular components (Gu et al., 2009). Additionally, the FDA serves as an indicator of the hydrolytic activity within the soil and can be degraded by various enzymes (like esterase, protease, and lipase), reflecting the biological activity within different treatments (Nannipieri et al., 2003).

The soil respiration (BSR and SIR) and microbial biomass carbon (MBC) parameters denote the total activity of microorganisms present in the soil environment. Soil MBC and respiration levels varied across all treatments and showed a gradual decline up to 60 days, considering the chilli plant's growth phase. However, a significant increase in MBC and respiration was observed after harvest. The highest MBC values were observed on day 0 across all treatments.

The incorporation of organic materials such as cow dung or vermicomposted CAMW significantly boosted soil MBC (p = 0.008; LSD = 34.79) compared to the control and treatments with only chemical fertilizers, as shown in Fig. 84a. Earlier findings by Bhattacharya et al. (2012) reported similar outcomes when both organic and inorganic fertilizers were applied together. While chemical fertilizers supply essential nutrients for microbial growth, they fall short in providing the necessary carbon. Notably, the combined use of organic and inorganic amendments meets both nutrient and carbon needs, as evidenced by the elevated soil MBC levels observed in treatments C6 (263.89±13.49 mg/kg) and C2 (256.26±9.17 mg/kg) (Fig. 84a). Additionally, after harvest, the remaining root biomass in the soil serves as an additional substrate that supports microbial growth. Throughout the study period, a significant treatment-specific decline in respiration rates was recorded from day 0 to 60 (p for BSR = 0.001; LSD = 6.43 and p for SIR = 0.001; LSD = 6.28). However, both BSR and SIR showed a slight increase post-harvest except in treatments like C9 and C10, as illustrated (Fig. 84b, c). At post-harvest, the highest respiration levels were observed in treatments C6, followed by C2 and C4. This pattern may be attributed to the enhanced cellular activity resulting from the combined application of organic materials like cow dung and vermicomposted CAMW with inorganic fertilizers. These observations align with the findings reported by Roy et al. (2022). Treatments C9 and C10 consistently exhibited the lowest respiration rates during the study, likely due to the presence of PTEs and the toxic effects of CAMW. Comparable findings have been reported by Rusinowski et al. (2019). Hence, the results suggest that the application of vermicomposted CAMW can enhance soil nutrient availability, boost enzymatic and microbial activity, and create favourable conditions for plant growth and development.

4.5.2.2 Evaluation of the bioavailability of PTEs in soil

The variations in the bioavailable (BA) pattern of PTEs were analyzed to understand their dynamics throughout the pot experiment involving organic and inorganic amendments. PTEs (Ni, Pb, Cr, Cu, and Cd) can interact with different soil components in various ways, resulting in forms that range from readily available to highly resistant. The BA fractions are especially important, as they are easily available in soil and readily accumulated by plants (Banerjee et al., 2023). The water-soluble (WS) and exchangeable (EX) fractions are critical contributors to the potential accumulation of PTEs in soil, and together, these two phases represent the total bioavailable portion. In this study, the bioavailable fraction was significantly (LSD_{Ni}: 6.68, p_{Ni}: 0.001; LSD_{Pb}: 3.20, p_{Pb}: 0.002; LSD_{Cr}: 4.47, p_{Cr}: 0.007; LSD_{Cu}: 1.33, p_{Cu}: 0.009; LSD_{Cd}: 2.70

p_{Cd}: 0.043) decreased in soil across all treatments compared to the initial concentration, except C9 and C10, as these treatments contained raw CAMW as illustrated in Fig. 85. The most pronounced reduction occurred in the treatment (C2: 1:1 vermicompost CAMW + NPK fertilizers) with a decrease of Ni: 3.28 folds, Pb: 4.35 folds, Cr: 2.62 folds, Cu: 2.31 folds, and Cd: 2.43 folds. Treatments amending both organic and inorganic materials led to a significant drop in PTEs concentrations, possibly reflecting a balanced relationship between PTEs availability in the soil and their movement into the crop. Also, PTEs concentrations were negligible in C7 and C8, likely due to the amendment with cow dung. Our findings were aligned with Sarkar et al. (2023).

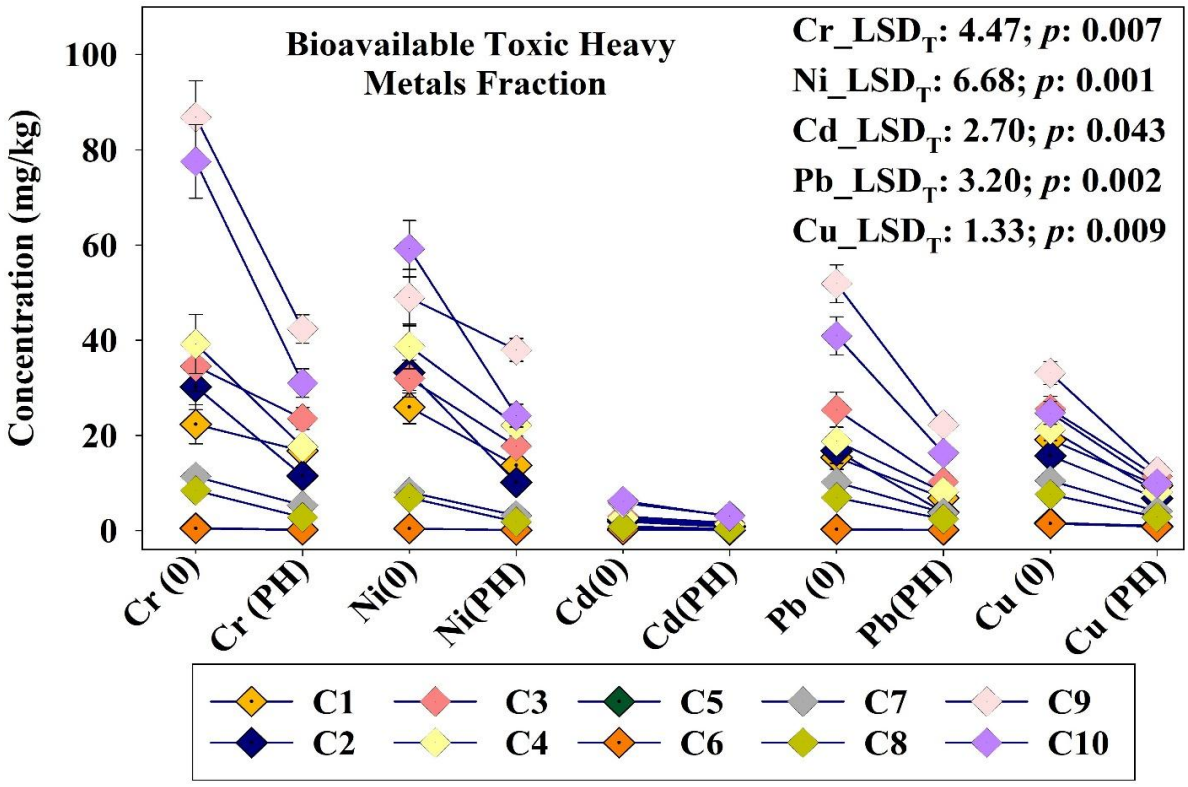

Fig. 85: Dynamics of various bioavailable toxic elements (PTEs) among the treatments

4.5.2.3 Assessing the PTEs accumulation and translocation pattern within chilli plants through different indices

The movement of PTEs within plants was analyzed using several key indicators including plant translocation factor (PTF), plant bioconcentration factor (PBCF), and plant bioaccumulation factor (PBAF), as illustrated in Fig. 86(a-c).

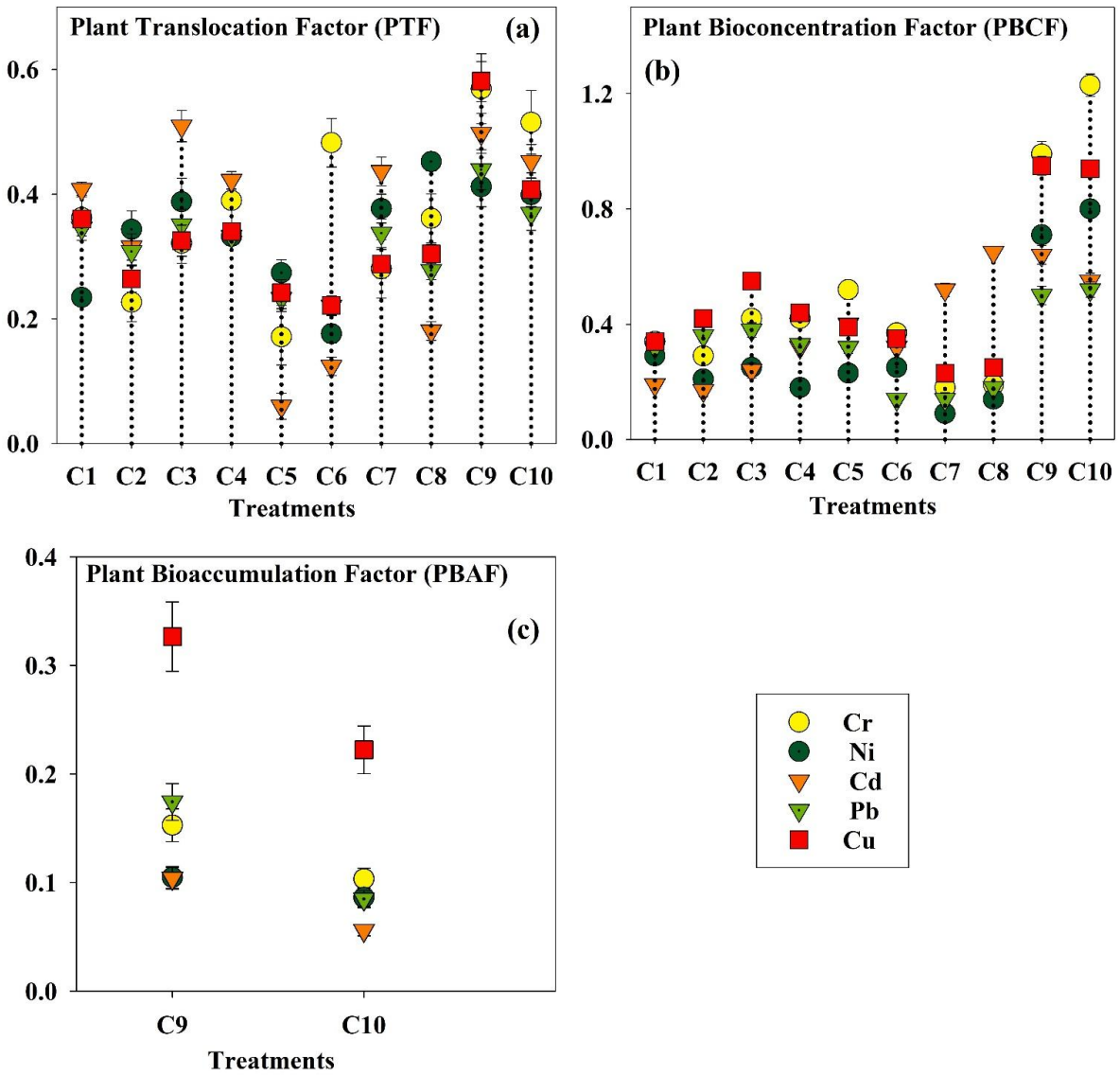

Fig. 86 Different indices to measure the movement and accumulation pattern PTEs in the test crop (chilli) across various treatments

Factors such as microbial interactions, rhizospheric chemistry, root selectivity, and absorption capacity govern the accumulation and translocation of PTEs by plants from soil system (Jha et al., 2024). In this research, the uptake of PTEs from soil to chilli plant is estimated using PBCF, while the transportation of PTEs from root to shoot is determined by PTF. The lowest PTF value for Pb, Cr, and Ni was observed in treatments amended with CAMW vermicompost C2, C3, C1, and C4. According to Page and Feller (2015), the retention of Pb, Cr, and Ni in roots is due to their sequestration in vacuoles or compartmentalization within cells, which restricts their movement through the xylem. The PTF was higher in C9 and C10 treatment for all PTEs as compared to other treatments (Fig. 86a). The PTF values were below 1, indicating limited translocation of PTEs. This reduction in metal movement benefited the growth of the test crop

(chilli). Similarly, the PBCF value mainly focuses on the PTEs uptake in the root section. The maximum PBCF value of Ni, Pb, and Cr was found in the treatment of C9 and C10, which might be due to the direct application of raw CAMW, that contained elevated levels of PTEs, leading to higher accumulation in the root section. In treatments C6 and C7, amended with cow dung, the initial concentration of PTEs was the lowest, resulting in minimum PTF and PBCF values compared to C9 and C10, where raw CAMW was directly applied. The PBCF values were lower in CAMW vermicompost amended treatments (C2, C4, C1, and C3) (Fig. 86b). A similar trend was reported by Chakraborty et al. (2024), indicating that the incorporation of vermicompost into soil can effectively reduce the translocation of toxic elements to plants. Another important indicator used to evaluate the transfer of PTEs from soil to crop grains is the PBAF. The uptake of PTEs in chilli in different organic amended treatments was negligible; therefore, for calculating this index, treatments C9 and C10 were considered, as they involved the direct application of raw CAMW waste. The PBAF values for Cd and Ni were the lowest in treatments C9 and C10, while Cu, Pb, and Cr exhibited the highest PBAF values in these treatments (Fig. 86c). The elevated levels of PTEs in the raw CAMW may be attributed to the accumulation of PTEs in chilli. These findings align with Jha et al. (2024), which indicated that the application of waste resulted in increased accumulation of PTEs in both plant roots and the edible grain segments. Thus, prolonged consumption of such crops may provide health hazards to living entities and adversely affect the ecosystem.

4.5.2.4 Influence of various treatments on biochemical attributes estimation in chilli

The biochemical parameters of chilli, including titratable acidity (TA), total soluble sugar (TSS), ascorbic acid (AA), protein (Pro), lycopene (Lyco), total carotenoids (TCAROT), total chlorophyll (TC), were evaluated across all treatments after harvest and denoted in Fig. 87. The critical components of respiration in fruits (chilli) and key constituents of soluble solids are titratable acidity and soluble sugars, which substantially improve the storage capability of horticulture products (Tigist et al., 2013). Total acidity of fruits (developed mainly from the presence of ascorbic, malic, and citric acids) is denoted by titratable acidity (Samira et al., 2013). The levels of sugar and acid absorbed in fruits predominantly regulate the period of fruit respiration. A decrease in titratable acidity accelerates fruit ripening, thus diminishing the fruit's storage capacity, whereas the total soluble sugar content signifies ripening and senescence of fruits (Samira et al., 2013). The titratable acidity, and total soluble sugar content in chilli were considerably greater in C2 followed by C6, C5, indicating a substantial influence of soil fertility on chilli quality (LSD_TA: 0.705; p: 0.009; LSD_TSS: 1.17, p: 0.008). The lowest activity of

TA and TSS observed in C9 and C10 is attributed to the presence of PTEs in raw CAMW treatments, which may interfere with the formation of sugars and organic acids in chilli. The organic acid, mainly ascorbic acid, was also evaluated across the treatments after post-harvest. The results indicate that AA content in C6, C5, and C2 was maximum as compared with C9 and C10 treatments (Fig. 87). In contrast, organic amendment (vermicompost/cow dung) increases the organic acids and carbohydrate levels in fruits (Zhang et al., 2011). Additionally, organic manuring generally stabilises soil aggregates, hence improving the soil's long-term moisture retention capacity (Wang et al., 2016). Furthermore, sufficient availability of nitrogen and potassium in the soil significantly influences the levels of organic acids and sugars in horticultural crops.

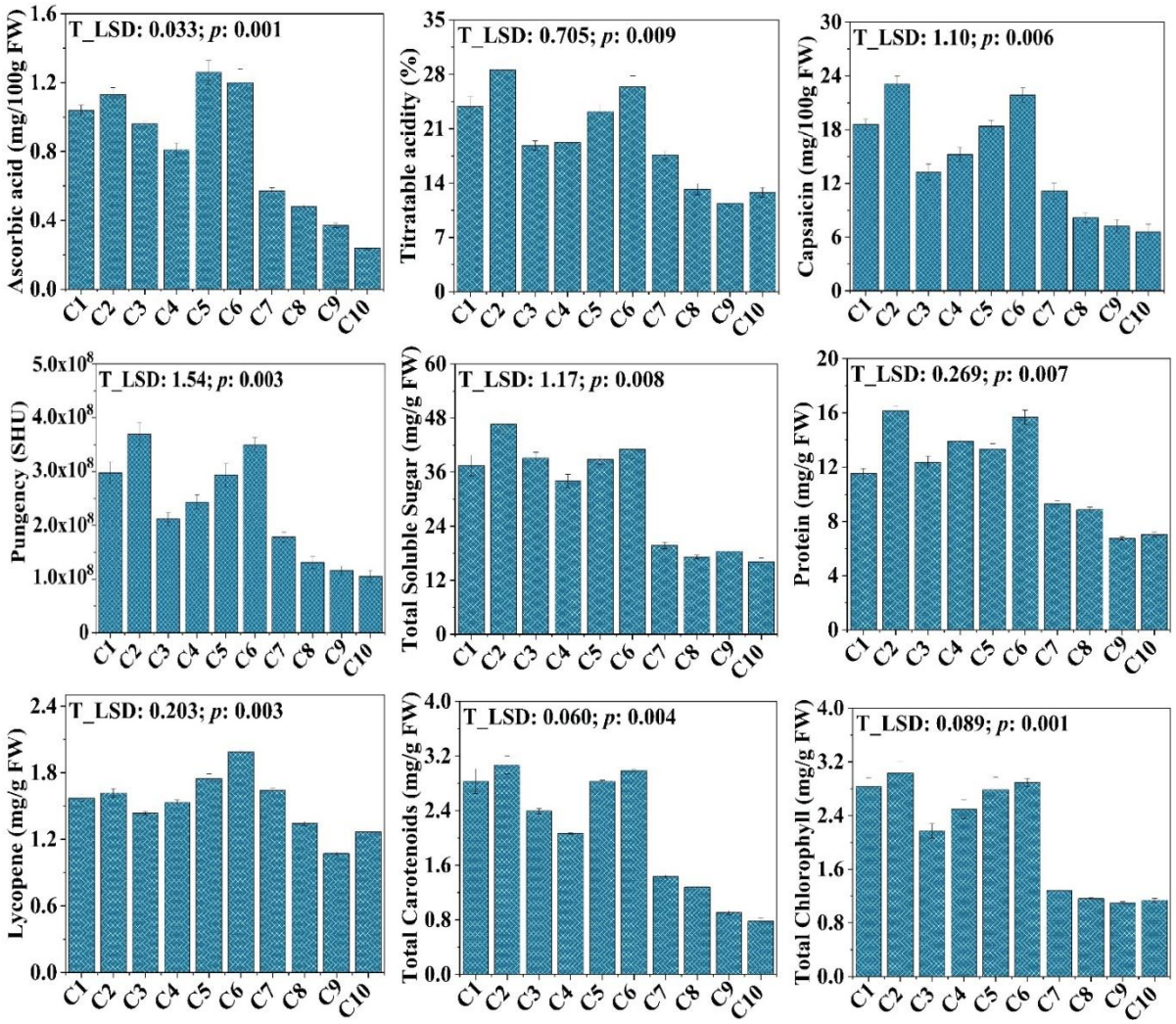

Fig. 87: Analysis of different biochemical parameters of chilli at post-harvest among the treatments during the pot experiment

Likewise, the protein content was significantly (LSD_Pro: 0.269; *p*: 0007) elevated in C2, C6, and C5 compared to C9 and C10 and denoted in Fig. 87. The protein levels were higher under combined application of CAMW vermicompost and inorganic fertilizers (C2: 1.82 folds; C6: 1.77 folds, C4: 1.56 folds) than only CAMW vermicompost (C5: 1.50 folds, C3: 1.39 folds and C1: 1.30 folds) and other treatments. The application of both organic (vermicompost/cow dung) and inorganic sources (NPK fertilizer) provides nitrogen in a highly mineralised form (NO_3^-), which likely resulted in elevated protein levels in chilli (Fallovo et al., 2011). In this study, the total chlorophyll, total carotenoid, and lycopene content in chilli were significant (LSD_TC: 0.089; *p*: 0.001; LSD_TCAROT: 0.060; *p*: 0.004; LSD_Lyco: 0.203, *p*: 0.003) in organic amendment treatment (C6, C2, and C5) as compared to the control (C8) and raw CAMW applied treatments (C9 and C10). The carotenoid synthesis often begins during the ripening phase of crops and is substantially impacted by agricultural practices (Perez-Lopez et al., 2007). The presence of PTEs and low nutrient availability in raw CAMW applied treatments (C9 and C10) disrupts the synthesis of chlorophyll, carotenoid, and lycopene content in chilli (Fig. 87). PTEs may impair the ultrastructure of chloroplasts, disrupt electron transport and thereby affect the photosynthetic process (Shahid et al., 2017). The application of organic manure to soil typically enhances the levels of lycopene and total carotenoid content in chili. The findings of this study support earlier research (Das et al., 2020). Overall, the above findings indicated that the combination of vermicomposted CAMW and chemical fertilizer presents a viable option for integrated nutrient management in crop cultivation.

4.5.2.5 Estimation of capsaicin content and pungency of chilli across all treatments after harvest

Fig. 87 illustrates the variations in capsaicin content (CAPs) and pungency (PUNG) in chilli fruits subjected to various treatments throughout two years of cultivation. A distinctive feature of chilli is the existence of capsaicinoids. The most prevalent molecules are capsaicin, which are the primary contributors to pungency (Tripodi et al., 2019). Pungency is a significant determinant of the quality and market value of chilli (Gangadhar et al., 2012). Overall, both capsaicin and pungency were substantially elevated (LSD_CAPs: 1.10, *p*: 0006; LSD_PUNG: 1.54, *p*: 0.003) in plants cultivated in C2 compared to C8. The elevated capsaicin concentration was also observed in plants cultivated under C1 and C3 (CAMW vermicompost alone). The capsaicin content was elevated 2.82-fold in C2 treatment, followed by 2.67-fold (C6) and 2.24-fold (C5) as depicted in Fig. 87. This revealed that the use of CAMW Vermicompost, in conjunction with inorganic NPK, was effective in enhancing these features in chilli cultivated

in nutrient-depleted soils. Aminifard et al. (2012) demonstrated a 59% enhancement in capsaicin concentration in organically cultivated *C. annuum* plants.

4.5.2.6 Determining the different agronomics attributes of chilli among various treatments

The agronomical characteristics, such as plant height (PH), number of chilli/plant (NCP), length of chilli (LC), fresh weight of individual chilli/plant (FWC), and yield/plant (YC), were evaluated and as shown in Table 44.

Table 44: Agronomical attributes of chilli at post-harvest

Treatments	Plant height (cm)	No. of Chilli/Plant	Length of Chilli (cm)	Fresh Weight of individual Chilli (gm)	Yield/Plant (gm)
C1 (CAMW 1:1 Vermicompost only)	67.42 ± 4.81	34 ± 3.05	6.86 ± 1.41	3.82 ± 0.28	36.74 ± 2.24
C2 (CAMW 1:1 Vermicompost + NPK fertilizer)	72.18 ± 5.57	41 ± 3.51	7.3 ± 0.72	4.63 ± 0.34	47.93 ± 2.86
C3 (CAMW 1:2 Vermicompost only)	57.68 ± 4.45	28 ± 2.56	6.7 ± 0.75	3.71 ± 0.22	29.68 ± 1.82
C4 (CAMW 1:2 Vermicompost + NPK fertilizer)	61.21 ± 3.72	31 ± 1.52	7.03 ± 0.71	3.61 ± 0.26	34.66 ± 2.11
C5 (Cow dung only)	63.97 ± 4.93	33 ± 4.04	7.5 ± 0.62	3.97 ± 0.21	39.67 ± 2.42
C6 (Cow dung + NPK Fertilizer)	69.72 ± 6.38	36 ± 2.51	7.8 ± 0.45	4.54 ± 0.17	44.48 ± 2.71
C7 (NPK Fertilizer)	61.87 ± 4.26	29 ± 2.49	6.4 ± 0.3	3.77 ± 0.13	26.39 ± 1.61
C8 (Control)	53.67 ± 4.14	23 ± 2.08	5.73 ± 0.15	2.86 ± 0.19	21.16 ± 1.29
C9 (Raw chromium-asbestos mine waste only)	42.36 ± 3.27	14 ± 2.52	4.7 ± 0.2	1.03 ± 0.07	11.24 ± 0.68
C10 (Raw chromium-asbestos mine waste + NPK Fertilizer)	49.69 ± 3.83	17 ± 1.15	3.86 ± 0.90	1.69 ± 0.12	15.21 ± 0.92
Treatment (LSD)	3.77	2.17	0.58	0.17	1.62
***p*-value**	0.042	0.184	0.236	0.151	0.006

Various plant attributes, including PH, NCP, LC, and FWC were maximum in C6, followed by C2>C5>C1. The yield was significantly (LSD: 1.62, *p*: 0.006) higher in C2 (2.21-fold) and C6 (2.05-fold) (CAMW vermicompost + NPK fertilizer), and the lowest yield was observed in C9 and C10 (raw CAMW) treatments. This may result from the sustainable utilisation of a combination of inorganic and organic amendments, including cow dung and vermicompost. The finding may result from elevated organic carbon levels and nitrogen availability, as well as the synergistic effect of both inorganic and organic nutrients, which facilitated balanced nutritional absorption in the chilli plant. The findings aligned with Aslam et al. (2022), who illustrate the impact of integrated nutrient management practices on the physiological,

morphological, and yield parameters of chilli. Therefore, the integration of vermicomposted CAMW and chemical fertilizer offers a feasible solution for enhanced crop yield and sustainable waste management practice.

4.5.2.7 Appraise the relationship among different attributes (bioavailable PTEs, microbial attributes, and agronomical parameters): an insight through correlation analysis

A correlation plot was utilised to elucidate the association among different attributes bioavailable PTEs (Ni, Pb, Cu, Cd, and Cr), microbial attributes (MBC, FDA BSR, DHYG, SIR, UR, BDG, and ALP), biochemical traits (AA, TA, TSS, Pro, Lyco, CAPs, PUNG, TCAROT, TC), and agronomical (PH, NCP, LC, FWP, YP) parameters following the harvest of the chilli experiment and illustrated in Fig. 88.

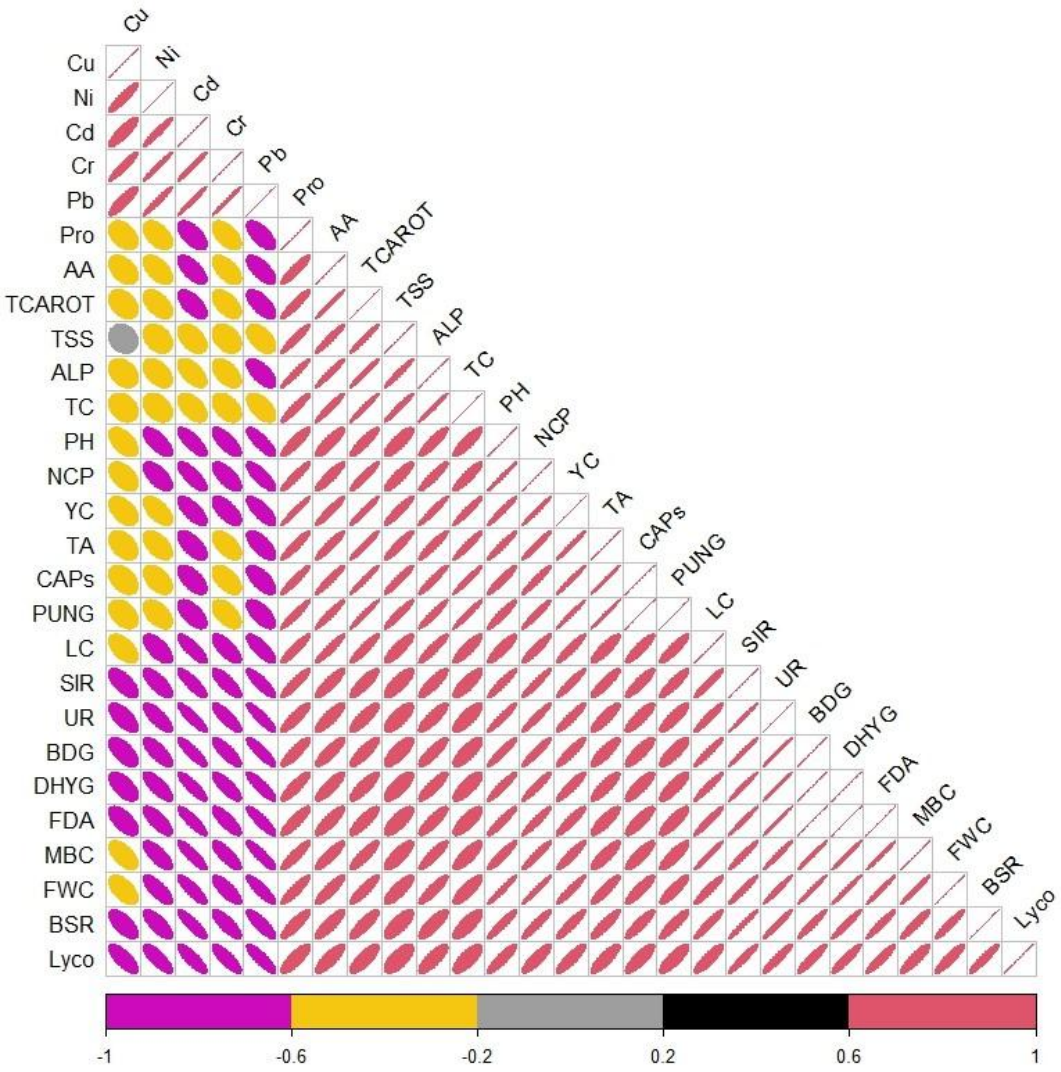

Fig. 88: Pearson Correlation analysis for evaluating the relationship among bioavailable PTEs, microbial-enzymatic parameters, biochemical properties, and agronomical attributes

A significant negative correlation [MBC (rBACr: -0.79, rBACd: -0.86, rBACu: -0.58, rBANi: -0.72, and rBAPb: -0.87), CAPs (rBACr: -0.54, rBACd: -0.60, rBACu: -0.39, rBANi: -0.48, and rBAPb: -0.64), and YP (rBACr: -0.65, rBACd: -0.69, rBACu: -0.48, rBANi: -0.59, and rBAPb: -0.74) was observed between the bioavailable PTEs and microbial, biochemical, and agronomical attributes. This suggests that by the time of harvest, PTEs concentrations had decreased, while microbial activity, organic acids, capsaicin content and agronomic traits showed improvement. Our findings were corroborated by Chakraborty et al. (2024).

4.5.3 Pot experimental details with Sesame

A pot investigation with Sesame (*Sesamum indicum* L.) was conducted from February to May 2023 at the Indian Statistical Institute's agricultural farm in Jharkhand (Fig. 89).

Fig. 89: Pictorial depiction of sesame cultivation

The recommended fertilizer dose of 40:40:20 (N: P_2O_5: K_2O) kg/ha was used, and each treatment was replicated three times. The treatment details are depicted in the Table 45.

Table 45: Treatment description (Sesame)

Order	Treatment combination
S1	Control (No amendment)
S2	Chemical Fertilizer (NPK)100%
S3	Cow dung (CD) 100%
S4	CD 50% + Chemical Fertilizer (NPK) 50%
S5	Chromium-asbestos mine waste Vermicompost (CAMW-VC 1:1) 100%
S6	(CAMW-VC 1:1) 50% + Chemical Fertilizer (NPK) 50%
S7	(CAMW-VC 1:2) 100%
S8	(CAMW-VC 1:2) 50% + Chemical Fertilizer (NPK) 50%

CAMW-VC and cow dung were mixed into the soil in the pots 15 days prior to sowing. Well-filled seeds sourced from the State Seed Corporation were shelled and treated with copper oxychloride (3g/kg) before being sown at a rate of 40 kg/ha. Standard agronomic practices, including planting density, watering, and pest control, were consistent across treatments. At harvest, soil quality, agronomic parameters (shoot length, root length, and yield) biochemical quality (protein, total chlorophyll, total soluble sugar), and bioavailable TEs content were measured using established protocols (Jha et al., 2023; Lowry et al., 1951; Page et al., 1982).

4.5.3.1 Soil physico-chemical properties evaluation

The effectiveness of vermicomposted CAMW as a soil amendment was assessed using a pot culture experiment with sesame (*Sesamum indicum* L.) as the test crop. In India, sesame is primarily grown during the pre-monsoon season on low-fertility lands with minimal external nutrient input and mainly relies on rainfed irrigation (Jha et al., 2023). Table 46 represents soil health status measurements taken before and after sesame cultivation under different treatments. The soil used in this study was characterized as mildly acidic, lateritic with low OC content, and deficient in NPK nutrients. A slight enhancement in soil nutrient levels was observed in plots treated with vermiconverted-CAMW during sesame cultivation. The pH increase was notably higher (towards neutral range) in the treatment (S6: CAMW-VC1:1 + NPK fertilizer), reaching 6.96 ± 0.34, followed by the treatment (S8: CAMW-VC1:2 + NPK fertilizer) at 6.61 ± 0.43 (p = 0.002). This pH improvement is due to the neutral pH of the CAMW-based vermicompost. Additionally, the organic carbon (TOC) level in the soil saw a 1.30-fold rise with treatment (S6: CAMW-VC1:1 + NPK fertilizer), followed by(S4: Cow dung + NPK fertilizer) treatment showed 1.16-fold and S8: CAMW-VC1:2 + NPK treatments, which achieved a 1.13-fold improvement (Table 46). Soil TOC availability is influenced by the decomposition of organic matter and the remaining crop residues (Lazcano et al., 2008). The vermicomposting process introduces organic amendments that accelerate soil carbon mineralization, boost microbial activity, and stimulate the mineralization of nutrients like NPK. Additionally, PTEs are bound in soil organic matter, making them less available for plant uptake (Das et al., 2012). The overall NPK levels in the soil were significantly higher with the vermicomposted CAMW amendment, following the order S6 > S5 > S8 > S7 > S2 > S1(Table 46). This observation may be due to the combined use of vermicompost and chemical fertilizers, which enhances the biological breakdown of organic matter. This process increases mineralized nitrogen in the soil and promotes the growth of phosphorus- and potassium-solubilizing microbial communities, consequently stimulating the release of various

endogenous and exogenous soil enzymes. The findings align with Sahariah et al. (2020) and Gupta et al. (2021), indicating that vermicompost enhances NPK status and reduces the bioavailability of PTEs for plants. The aforementioned findings suggest that the efficient recycling of CAMW in agriculture via vermicomposting (CAMW mixed with cow dung) would be a desirable technique for environmental management while reducing CAMW landfill deposition.

Table 46: Soil vitality status measurements taken before and after sesame cultivation under different treatments (Mean±SD)

Treatments	pH	TOC (%)	Avl. P (mg/kg)	Avl. N (mg/kg)	Ex. K (mg/kg)	Cr (mg/kg)	Ni (mg/kg)	Cd (mg/kg)	Pb (mg/kg)	Cu (mg/kg)
S1 (Control soil)	6.43±0.41	0.489±0.024	33.09±4.13	10.27±0.73	114.33±12.70	8.63±0.41	9.78±0.24	1.11±0.014	9.04±0.19	11.82±0.12
S2 (NPK fertilizer)	6.54±0.46	0.503±0.035	36.18±4.52	13.4±0.74	128.79±14.31	9.53±0.59	10.22±0.37	1.23±0.011	10.48±0.11	12.07±0.14
S3 (Cow dung)	6.72±0.49	0.531±0.044	47.24±5.90	19.1±0.9	174.20±17.13	2.20±0.12	1.87±0.06	0.11±0.012	1.17±0.09	1.37±0.07
S4 (Cow dung + NPK fertilizer)	6.81±0.37	0.569±0.037	52.78±5.59	22.3±0.815	181.64±15.96	1.96±0.09	1.14±0.07	0.09±0.0003	0.87±0.048	1.08±0.04
S5 (1:1 CAMW Vermicompost)	6.88±0.29	0.606±0.041	54.89±6.86	24.16±1.09	185.13±20.57	8.16±0.57	8.57±0.27	0.56±0.07	6.89±0.24	6.18±0.21
S6 (1:1 CAMW Vermicompost + NPK fertilizer)	6.96±0.34	0.636±0.049	62.34±7.79	27.6±1.55	192.92±21.43	7.93±0.43	7.1±0.34	0.49±0.051	5.15±0.34	4.71±0.19
S7 (1:2 CAMW Vermicompost)	6.72±0.39	0.542±0.039	46.79±6.47	17.1±1.44	151.48±19.387	11.32±0.67	9.17±0.53	0.97±0.104	8.74±0.57	9.78±0.57
S8 (1:2 CAMW Vermicompost + NPK fertilizer)	6.61±0.43	0.557±0.042	49.04±6.13	19.49±1.40	179.41±19.93	10.69±0.07	7.14±0.47	0.81±0.101	5.47±0.29	7.49±0.39
LSD (Treatments)	0.45	0.12	3.03	1.38	13.64	1.70	0.94	0.098	1.01	1.06
p-value	0.002	0.05	0.028	0.001	0.05	0.015	0.003	0.004	0.001	0.006

*Degree of freedom (df of treatment): 7; Confidence interval: 95%

4.5.3.2 Estimation of PTEs bioavailability in soil and plant parts

The statistical analysis (ANOVA) showed a notable reduction (LSD_{Cr}: 1.70, p_{Cr}: 0.015; LSD_{Ni}: 0.94, p_{Ni}: 0.003; LSD_{Pb}: 1.01, p_{Pb}: 0.001) in bioavailable (DTPA-extractable) PTEs in soil across all treatments compared to initial levels, with the most pronounced decrease occurring in the treatment (S6: CAMW-VC1:1 + NPK fertilizers) (Table 46). To evaluate PTEs movement from soil to plant parts (root, shoot, pod), PTEs were measured using different indices [$Plant_{concentration\ factor}$ (PCF) and $Plant_{translocation\ factors}$ (PTF)], as shown in Fig. 90, highlighting the ecological effects of CAMW-vermi-transformation. Concentrations of PTEs (Ni, Cd, Cr, Cu, and Pb) in sesame pods were found to be below detectable levels while the uptake was observed following the order: roots > shoots.

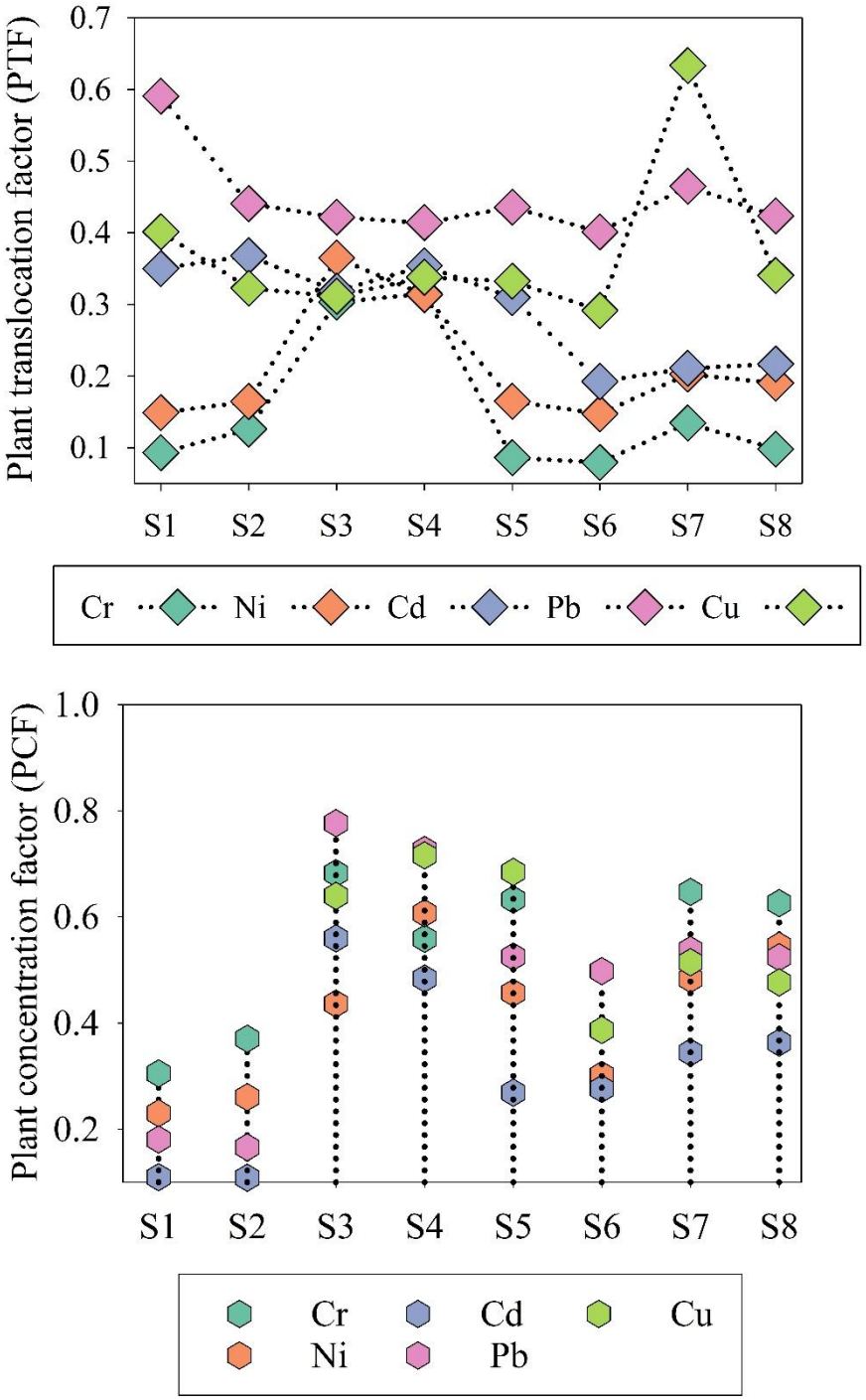

Fig. 90: Plant translocation and plant concentration factor of Sesame in pot experiment

The $Plant_{concentration\ factor}$ (PCF) analysis emphasizes PTEs uptake in roots, with the trend observed as Cr > Pb > Ni > Cu > Cd in the treated pots. The high accumulation of Cr may be attributed to its higher presence in the treatments compared to other PTEs and the least accumulation was observed in Cd. The preference for PTEs accumulation is influenced by factors such as initial concentration, plant species, and uptake potential. PTEs (basically Cr, Pb and Ni) are retained in plant roots by storing it in vacuoles or compartmentalizing it within

cells, which inhibits its transport through the xylem, as described by Page and Feller (2015). All treatments exhibited $Plant_{translocation\ factors}$ (PTF) below 1, with the lowest value found in the treatment (S6: CAMW-VC1:1 + NPK fertilizers), indicating lower PTEs mobility compared to the treatment (S8: CAMW-VC1:2 + NPK fertilizers). Assessing the transfer of PTEs among plant sections (root, shoot, and grain) is essential for understanding bioaccumulation, which remained minimal across other treated pots. The results are consistent with the observations of Goswami et al. (2024), which show that incorporating vermicompost into soil effectively limits the uptake of PTEs into plants.

4.5.3.3 Plant biochemical and agronomic attributes after harvest

Vermicomposted CAMW (CAMW-VC) demonstrated positive effects on soil health, as shown by crop production results (Table 47). The CAMW-VC1:1+NPK (S6) fertilizer treatment produced a notably high yield of 20.98±2.31 g $plant^{-1}$. Similarly, biochemical parameters (protein content, total soluble sugars, and total chlorophyll) were observed to be higher in treatment S6 compared to other treatments. The increased chlorophyll, sugar, and protein content in plants treated with CAMW-VC can be attributed to the enhanced availability of N, P, and K from vermicompost, which releases nutrients gradually, boosting nutrient efficiency and biomass quality more effectively than inorganic fertilizer treatment (S2). Additionally, treatments S6 and S4 resulted in the greatest plant shoot and root lengths, followed closely by S2, as indicated in Table 47.

Table 47: Agronomical and biochemical properties of sesame plant after harvest (Mean±SD)

Treatments	Plant shoot length cm	Plant root length cm	Yield (g $plant^{-1}$)	Protein mg g^{-1}	Total Soluble Sugar mg g^{-1}	Total Chlorophyll mg g^{-1}
S1	60.3±2.21	10.3±0.26	5.36±0.37	37.01±2.16	19.72±1.01	6.01±0.32
S2	84±5.33	11.9±0.34	13.96±1.15	41.24±2.93	31.96±1.72	11.08±0.64
S3	81.5±4.29	11.4±0.39	17.85±1.49	53.06±3.42	40.90±1.57	13.29±0.72
S4	87.8±6.36	12.2±0.47	18.23±1.59	59.35±3.49	46.14±2.41	14.8±0.81
S5	83±3.57	13.3±0.51	19.65±2.12	68.99±4.4	57.03±3.94	15.19±0.89
S6	89.5±6.41	14.1±0.37	20.98±2.31	77.44±5.04	68.77±4.81	17.42±0.94
S7	79.5±4.43	12.1±0.41	12.25±1.11	54.89±4.78	34.89±2.16	12.89±0.56
S8	76.7±3.49	10.2±0.31	13.26±1.01	57.87±3.96	36.47±2.34	14.27±0.76
LSD (Treatments)	3.35	0.36	2.11	4.53	5.9	1.19
p-value	0.008	0.002	0.007	0.003	0.021	0.002

The increase in biochemical attributes and low PTEs uptake in plant parts showed better growth in root and shoot length. This finding aligns with Charan et al. (2024), who reported that

combining organic sources with inorganic fertilizers results in improved yield and crop growth. All of the above findings indicate that the application of CAMW-VC is a good source of organic amendment for agriculture.

4.5.4 Field experiment with Rice

Field trials were conducted over two consecutive growing seasons (July–November) during 2023–2024 for rice cultivation (*Oryza sativa* L) at the agricultural research farm of the Indian Statistical Institute in Jharkhand (Fig. 91).

Fig. 91: Picture showing rice cultivation in the agricultural field

For rice cultivation, a recommended fertilizer dose of 60:30:30 kg/ha (N: P_2O_5: K_2O) was applied. Treatment details are outlined in Table 48, with each treatment replicated three times.

Table 48: Treatment details for rice cultivation in field

Order	Treatment details
R1	Control (No amendment)
R2	Chemical Fertilizer (NPK)100%
R3	Cow dung (CD) 100%
R4	CD 50% + Chemical Fertilizer (NPK) 50%
R5	Chromium-asbestos mine waste Vermicompost (CAMW-VC 1:1) 100%
R6	(CAMW-VC 1:1) 50% + Chemical Fertilizer (NPK) 50%
R7	(CAMW-VC 1:2) 100%
R8	(CAMW-VC 1:2) 50% + Chemical Fertilizer (NPK) 50%

Vermicomposted CAMW and cow dung were incorporated into the soil two weeks prior to sowing. High-quality seeds sourced from the State Seed Corporation were treated with copper oxychloride before planting. Uniform agronomic practices—including irrigation, optimal planting density, regular weeding, and pest control—were maintained across all plots. Upon

completion of the trials, various parameters were assessed following standard evaluation protocols.

4.5.4.1 Determination of physico-chemical attributes across the treatments of rice cultivation

The efficacy of vermicomposted CAMW as a soil amendment was evaluated in a field experiment utilising rice (*Oryza sativa* L.) as the test crop. In India, rice is the predominant staple food and the most widely consumed crop in Asian and South Asian nations. The physico-chemical parameters post-harvest are included in Table 49 from this field investigation. Post-harvest, all treatments exhibited pH values between 6.93 and 7.58, attributable to the incorporation of organic materials such as vermicomposted CAMW and cow dung, which likely contributed to the elevated pH. These findings align with those of Zeb et al. (2020), who reported analogous results in their study of fly ash-based vermicompost applied to rice crops. Soil organic carbon (Table 49) exhibited increases (LSD: 0.38; *p*: 0.026) across all treatments post-harvest. The presence of soil organic carbon is contingent upon the breakdown of organic matter and the remaining crop residue (Lazcano et al., 2008). This observation closely parallels earlier research indicating that residue-derived carbon aggregates within clay structures, binding to soil macro-aggregates, thereby enhancing the humification ratio and significantly elevating SOC storage capacity upon crop harvest (Chivenge et al., 2011). The observed pattern of organic carbon throughout the treatments aligned with Kumar et al. (2023). Correspondingly, the Avl. N content in the soil increased post-harvest, as seen in Table 49. Post-harvest, the highest Avl. N was recorded in treatments R4, R6, and R3 in that order. This result is likely due to the concentrations of organic matter and their biological decomposition, which indicate the existence of mineralised nitrogen in the soil (Turrión et al., 2012). A significant increase in the soil's availability of macronutrients, specifically potassium (Ex. K) and phosphorus (Avl. P), was observed post-harvest. The heightened tendency of Ex. K and Avl. P was most pronounced in treatments R6 (Avl. P: 88.07±6.36 mg/kg; Ex. K: 249.77±18.72 mg/kg) and R4 (Avl. P: 83.27±6.29 mg/kg; Ex. K: 268.45±21.58 mg/kg). The findings align with the observations of Das et al. (2016), indicating that the judicious application of vermicompost in conjunction with chemical fertilizers markedly enhanced the diversity and proliferation of phosphorus and potassium-solubilizing microbial communities, subsequently promoting the release of various endogenous and exogenous enzymes in the soil.

Table 49: Soil physico-chemical and bioavailability PTEs in soil after rice cultivation under different treatments (Mean±Standard deviation)

Treatments	pH	TOC (%)	Avl. N (mg/kg)	Avl. P (mg/kg)	Ex. K (mg/kg)	BA_Cr (mg/kg)	BA_Ni (mg/kg)	BA_Pb (mg/kg)
R1 (Control soil)	6.88±0.51	0.42±0.018	13.68±1.09	58.24±3.29	173.16±12.32	7.29±0.63	6.29±0.51	6.82±0.42
R2 (NPK fertilizer)	6.96±0.44	0.49±0.032	17.57±1.37	66.63±4.63	188.25±14.09	8.13±0.73	7.68±0.67	7.41±0.61
R3 (Cow dung)	7.46±0.63	0.64±0.036	26.62±1.32	78.91±5.81	253.89±19.33	0.93±0.08	0.76±0.04	1.03±0.09
R4 (Cow dung + NPK fertilizer)	7.58±0.49	0.69±0.029	29.68±1.54	83.27±6.29	268.45±21.58	1.13±0.06	0.88±0.07	0.94±0.03
R5 (1:1 CAMW Vermicompost)	7.29±0.38	0.73±0.027	23.61±1.37	79.89±4.22	237.96±17.64	10.29±0.72	9.23±0.65	6.12±0.17
R6 (1:1 CAMW Vermicompost + NPK fertilizer)	7.18±0.36	0.78±0.031	28.65±1.41	88.07±6.36	249.77±18.72	8.12±0.49	5.81±0.22	4.23±0.11
R7 (1:2 CAMW Vermicompost)	6.93±0.47	0.53±0.036	19.72±1.53	69.89±3.17	221.17±16.98	16.72±1.22	14.29±1.01	11.04±1.02
R8 (1:2 CAMW Vermicompost + NPK fertilizer)	6.98±0.52	0.56±0.038	22.79±1.42	73.17±6.11	233.09±21.23	14.39±1.09	13.62±1.12	9.13±0.78
LSD (Treatments)	1.79	0.38	2.73	3.68	14.57	0.73	1.66	0.94
p-value	0.048	0.026	0.0033	0.0021	0.0018	0.001	0.018	0.027

4.5.4.2 Bioavailability of PTEs status evaluation at post-harvest across different treatments

The bioavailability of the different PTEs is dependent upon two fractions: water-soluble phases and exchangeable phases. PTEs from these two phases can easily bioaccumulate in the soil matrix, resulting in PTEs toxicity in the soil. The concentrations of PTEs (Cr, Ni, and Pb) reported in the table indicate that the Cr concentration was notably (LSD: 0.73; *p*: 0.001) low in treatments R6 and R5 (Table 49). Treatments including inorganic and organic amendments markedly decreased concentrations of other PTEs such as nickel (Ni) and lead (Pb), suggesting a balance between the availability of PTEs in the soil and their transfer to the crops. Comparable results were documented (Mondal et al., 2020). He et al. (2021) identified soil pH and organic matter content as primary drivers of the bioavailability of PTEs in the soil. In the field investigation, the concentrations of PTEs such as Pb, Cr, and Ni, which were initially elevated, were decreased in varying ratios due to vermicomposted treatments. These results were analogous to the prior observations made by Sarkar et al. (2023).

4.5.4.3 Estimation of bioconcentration and translocation factor of rice plant after harvest

The movement of PTEs from soil to plants was influenced by many plant attributes, including rhizospheric properties, root selectivity, and absorption physiology (Mondal et al., 2020). The movement of PTEs in plants was examined using various factors, including the plant translocation factor (PTF), which is based on the PTEs content in the root and shoot of the plant, and the plant bioconcentration factor (PBCF), which relies on the concentration of PTEs

in the soil and their uptake by the plant roots. The lowest PBCF value was recorded for Cr, whereas the PBCF value for Pb was notably elevated in treatments R5 and R6 (Table 50). The observed phenomenon may be attributed to the oxidation state of Cr, which quickly dissolves and is assimilated by the crop's roots. The PBCF values for all PTEs were low in treatments R3 and R4. The rationale for the finding was the initially low concentration of PTEs in cow dung. The PTF was minimal in treatment R6 (CAMW-VC1:1 + NPK fertilizers) for all the PTEs. The PTF values were under 1, suggesting restricted translocation of PTEs. The decrease in metal mobility facilitated the development of the test crop, rice.

Table 50: Different indices to determine PTEs accumulation and mobility in rice plant

Treatments	PBCF_Cr	PTF_Cr	PBCF_Pb	PTF_Pb	PBCF_Ni	PTF_Ni
R1	0.087	0.426	0.063	0.842	0.052	0.588
R2	0.102	0.416	0.076	0.542	0.063	0.477
R3	0.313	0.535	0.274	0.516	0.346	0.667
R4	0.232	0.662	0.234	0.471	0.246	0.622
R5	0.451	0.354	0.477	0.364	0.435	0.223
R6	0.387	0.387	0.492	0.332	0.541	0.205
R7	0.319	0.561	0.313	0.503	0.377	0.259
R8	0.326	0.459	0.292	0.418	0.291	0.263

4.5.4.4 Investigation of agronomic properties across different treatments at post-harvest

The various treatments exhibited notable differences in agronomic characteristics (plant height, 1000 grain weight, grain yield, and straw yield) as seen in Table 51. Treatments R6 (131.6±7.46 cm) and R4 (129.5±8.37 cm) had the highest crop heights (p:0.072), followed by R2 (127.5±13.64 cm). The integration of organic sources with inorganic fertilizers has demonstrated superior physical characteristics compared to the exclusive use of chemical fertilizers. Our results align with the findings of Sarker et al. (2024). Treatments R6 and R4 had a greater 1000-grain weight compared to the control treatment R1. Yang et al. (2004) indicated that the integration of chemical fertilizers and organic manure enhanced the weight of 1000 grains. Treatment R6 had the highest straw (p:0.032) and grain (p:0.017) production, followed by treatments R4, R5, and R2. The treatment, including only chemical fertilizers (R2) supplies nutrients for a limited duration because of the rapid mineralisation of nitrogen (Jha et al., 2024). A mix of organic sources and inorganic fertilizers has demonstrated superior grain production benefits compared to the sole use of chemical fertilizers. Inorganic fertilizers and organic manure can boost vegetative development in plants, hence increasing rice straw

production. Mehmood et al. (2018) reported that the use of chemical fertilizers and organic manure improved rice straw yields.

Table 51: Biochemical and agronomic parameters of rice post-harvest (Mean±Standard deviation)

Treatments	Total Chlorophyll	Protein	Total Soluble Sugar	Plant Height	1000 Grain Weight	Straw Yield	Grain Yield
	mg g^{-1}	mg g^{-1}	mg g^{-1}	cm	g	(t ha^{-1})	(t ha^{-1})
R1	6.83±0.41	18.13±1.06	41.07±3.21	120.8±8.53	21.86±1.82	2.20±0.16	1.12±0.08
R2	7.21±0.54	21.95±1.49	44.13±3.71	127.5±13.64	23.65±1.73	2.44±0.19	1.24±0.11
R3	9.34±0.73	28.38±1.34	49.02±3.53	126.3±9.28	25.04±2.71	3.92±0.26	1.72±0.14
R4	9.76±0.64	33.09±2.09	53.48±4.46	128.2±7.17	27.81±2.93	4.18±0.32	1.81±0.13
R5	9.48±0.52	29.71±1.76	51.67±3.82	129.5±8.37	26.29±2.81	3.96±0.24	1.79±0.09
R6	10.87±0.49	34.09±1.43	56.73±3.44	131.6±7.46	28.08±2.04	4.36±0.21	1.88±0.08
R7	8.49±0.66	24.46±1.72	47.94±4.67	121.4±8.19	24.45±2.37	3.67±0.28	1.46±0.12
R8	8.82±0.62	27.79±1.88	49.54±4.04	125.2±12.57	23.19±2.98	3.78±0.23	1.58±0.14
LSD (Treatments)	2.53	3.13	1.76	2.29	1.59	0.43	0.21
***p*-value**	0.002	0.009	0.014	0.072	0.041	0.032	0.017

4.5.4.5 Biochemical parameters estimation at post-harvest of rice experiment

The biochemical parameters, comprising total chlorophyll, protein, and total soluble sugar, were assessed for the harvested rice crops, as illustrated in the Table 51. The total chlorophyll content was elevated in treatments (R6: 10.87±0.49 mg g^{-1}) that utilised a mix of organic and inorganic amendments, consistent with the findings of Gupta et al. (2014). The protein concentration was notably significant (*p*: 0.014) in treatments R6, R4, and R5. The highest protein content recorded in treatment R6 (CAMW-VC1:1 + NPK fertilizers: 34.09±1.43 mg g^{-1}) aligns with the findings of Jha et al. (2024). The total soluble sugar was found to be highest in R6 and R4, followed by R5, with statistical significance (*p*: 0.014). Multiple chemical processes involving sugar are used to provide energy (Xia and Cheng, 2004). The incorporation of organic compost, specifically cow dung and vermicompost, in conjunction with chemical fertilizers, promotes beneficial soil microorganisms and offers a sustainable nutrition supply for plants (Jha et al., 2024).

Therefore, this study emphasizes the potential use of vermicomposted PTE-enriched vetiver and vermicomposted CAMW as organic amendments in agricultural fields, which could improve crop productivity, as demonstrated by our findings. Additionally, exploring the long-term effects of PTE-EVVc and CAMW-VC on soil and plant health would provide deeper insight into the sustainability of the vermi-remediation approach.

Conclusion and Summary

Chapter 5: Conclusion and Summary

The fundamental goal of this study was to characterize soil contaminated by chromite-asbestos mine waste (CAMW) generated from mining activities. It aimed to assess the levels of PTE contamination, predict potential future health risks, and explore various bioremediation strategies (phytoremediation associated with mycorrhiza and vermi-remediation approaches) that could be beneficial for both environmental restoration and agricultural sustainability. This study was conducted to evaluate the source, accumulation, and human health risks associated with PTEs in the soil from the chromite-asbestos mines (Roro mines), in India. In the study area, various indices such as (PI, CI, Igeo and ERI) provided the order of contamination level of PTE in the study area (Site1>Site2>Site3). In accordance with a variety of the indices and hazard indices, exposure to toxic mine tailings poses significant health risks to humans (especially children), with ingestion presenting one of the most important routes of exposure. Also, Monte Carlo simulation combined with the health risk assessment was evaluated the concentration-oriented health risks, and the results showed that all populations (adults and children) had acceptable NCRs for PTEs, while TCRs remained high. By identifying clusters of similar metal content in soil, SOM maps were able to classify the degree of pollution by identifying groups of high and low polluted areas. PMF analysis denotes that natural source (mine) and industrial source (mine industry, mining activity, mine residues) account for the majority of Cr and Ni pollution, while traffic and agriculture account for Cd, Cu, and Pb. Also, the concentration of PTEs mainly Cr and Ni in soil and rice plant parts (roots, shoots, and raw grains) are significantly higher and exceed the permissible limit set by WHO in site 1 and site 2 as compared to site 3. PTEs (mainly Cr and Ni) contaminated rice grain could increase the risk of cancer, based on the results of FIAM-HQ and SAMOE-TCR approaches. This study also provides information regarding the accumulation of each PTE in different rice parts (H, WH, BR, and ST), spatial distribution patterns, dietary risk, and risk evaluation through different indices. The results revealed that mainly Cr and Ni pollution was maximum in agricultural soil and rice parts, and model-based assays like SAMOE, Fuzzy-TOPSIS, and ANN suggest that intake of cooked rice (containing Cr) might be unsafe for humans and animals. MCS-Sensitivity analysis also demonstrated that children were more vulnerable to carcinogenic risk. Through the ML approaches, RF was the best-fit model for Cr and Ni, which contributed the maximum dietary risk in rice parts. From the aforementioned data, it can be inferred that PTEs from chromite mine waste have

leached into the adjacent agricultural soil and were directly affecting the rice components. The majority of living things in South Asian countries use rice as a basic food source; hence, long-term consumption of rice might soon pose the risk of various diseases, including cancer. The survey-based DEMATEL approach also supports the findings that cooked rice and starch rice consumption might be detrimental to health. In addition, this study employed a comprehensive strategy to investigate the spatial associations among different microbial communities subjected to stressful conditions, specifically PTEs and alkalinity-induced stress. The mobility of PTEs enhanced a challenging environment for the soil microbial community. Changes in soil ecophysiology in the impacted areas were mostly caused by extensive mining and inappropriate disposal of hazardous mine waste. This investigation was to identify an optimal model for accurately detecting the specific stressors that lead to changes in the soil microbial community. The noted decrease in microbial diversity and alterations in soil phylogeny within the affected areas were expected to have a significant influence on the overall functioning of the ecosystem. The restoration of the biome and the physiological response of microbial communities in soil were contingent upon the inherent genetic potential present within the microbiome. This study can serve as a benchmark for identifying stressors that contribute to soil health status, enabling the implementation of appropriate agricultural practises or remediation strategies.

Plant–microbe-based bioremediation offers several advantages for environmental cleanup, including eco-friendliness, cost-effectiveness, and the ability to sustainably reduce contaminant levels, making it a promising approach for effective remediation of polluted sites. This study evaluated the effectiveness of vetiver in remediating chromium within a hydroponic setup, demonstrating the potential of this phytoremediation approach. The findings provide a comprehensive understanding of vetiver's capacity for Cr uptake and its suitability for use in chromium removal from contaminated water systems. The most significant reduction of Cr at 75 mg L^{-1} was observed by day 14, along with its accumulation in both the roots and shoots of vetiver, accompanied by variations in agronomic and biochemical traits. These findings offer valuable insights into the chromium tolerance and remediation potential of vetiver, highlighting its effectiveness as a green solution for Cr-removal. Applying vetiver to CAMW-contaminated soil presents both a challenge and an opportunity to enhance remediation efficiency. By incorporating mycorrhizal cultures, the effectiveness of vetiver in managing not only Cr but also a range of other PTE pollutants can be significantly improved, offering a promising and sustainable solution for soil

rehabilitation. Therefore, mycophytoremediation is regarded as a cost-effective, natural, environmentally friendly, and efficient strategy to improve the PTEs removal capabilities of plants used in remediation. Suitable AMF inoculation in vetiver plants promotes root growth, mitigates PTEs toxicity, alters bioavailability of PTEs in soil, and offers a promising approach for restoring soils degraded by chromite-asbestos mining activities. This study highlights the positive impact of specific AMF species including *Glomus hoi, Funneliformis coronatum, Claroideoglomus claroideum,* and *Claroideoglomus etunicatum* on the growth of vetiver planted in field soil containing chromite-asbestos mine wastes. AMF inoculation facilitating better phytoextraction and phytostabilization processes, as well as increased soil enzyme activity. Among the four AMF species tested, *Glomus hoi* and *Funneliformis coronatum* were found to be the most effective for multi-PTEs-polluted sites, enhancing TEs accumulation in vetiver roots while limiting translocation to the shoots. The model-based approaches validate the efficiency of mycophytoremediation potential. This study provides valuable insights into the potential application of the vetiver-AMF (arbuscular mycorrhizal fungi) combination for remediation purposes, demonstrating its effectiveness in mitigating PTEs in contaminated soil. Hence, following the myco-phytoremediation process, vetiver plants enriched with PTEs were harvested, having accumulated significant amounts of contaminants in both roots and shoots. Given the potential risk of environmental re-contamination through shedding from the exposed shoot parts, these portions were separately collected and managed using vermi-remediation technology, offering a sustainable solution for safe disposal and resource recovery. The vermicomposting of PTE-enriched vetiver (PTE-EV) mixed with cow dung (1:1) effectively neutralized acidity, improved NPK content, and stabilized organic carbon mineralization. Earthworm activity was significantly enhanced in these mixtures, contributing to the overall efficiency of the process. Notably, substantial reductions in toxic metals such as Pb, Ni, and Cr were recorded in the vermibeds. Correlation analysis further revealed that increased microbial activity was associated with the reduction of PTEs during vermicomposting. These findings highlight the potential of vermicomposted PTE-EV as a valuable organic amendment for agricultural use, warranting further evaluation through crop-specific trials.

Another aspect, chromite-asbestos mine waste (CAMW), produced in large volumes worldwide, poses a significant environmental challenge due to its high concentrations of PTEs, underscoring the urgent need for effective and sustainable remediation strategies. This study also pioneers the use of vermi-remediation technology to sustainably and efficiently

convert CAMW into valuable fertilizer. The vermicomposting process neutralized CAMW acidity, enhanced NPK levels, and stabilized organic carbon mineralization. Earthworm growth was notably stimulated in the feedstock mixes of CAMW and cow dung (1:1). Earthworms under stress initially showed elevated superoxide dismutase and peroxidase activity, which later decreased as vermicompost matured. The CAMW-based feedstocks also saw increased earthworm reproduction and heightened microbial and enzymatic activity. Additionally, significant reductions in toxic metals (Pb, Ni, Cr, and Cd) were observed within the vermibeds. PLFA analysis revealed valuable insights into how different feedstock mixing ratios impacted stress factors, suggesting that a shift from Gram-negative to Gram-positive bacterial communities and fatty acids profiles (straight chain and branched chain) may serve as a defence mechanism in the vermibeds to mitigate the stress from TEs. In summary, the 1:1 mixture of CAMW and cow dung proved to be especially suitable for the growth and activity of *E. fetida.* The PLFA-model based Sobol sensitivity analysis further validate the high quality of vermicomposted feedstocks, attributed to increased microbial community structure. The study concludes that earthworm-driven vermicomposting effectively detoxifies CAMW, creating nutrient-rich fertilizer for agriculture. Exploring the long-term effects of vermicomposted CAMW on soil health could provide valuable insights and present a compelling avenue for future research.

The overall research paves the way for utilizing vermicomposted PTE_EV and CAMW as an organic amendment in diverse agricultural systems, including tomato, chilli, sesame, and rice, to evaluate its broader applicability, long-term viability, and assessing its impacts on soil microbial diversity across multiple cropping cycles. The research assessed vermicomposted CAMW and vermicomposted PTE-EV combined with organic and inorganic additions, with the objective of enhancing soil health, increasing microbial activity, the growth and development of plant (irrespective of crop) and yield, as well as mitigating PTEs toxicity. The results indicated no immediate impact on soil quality or yield, supporting both vermicomposted products as an advantageous soil conditioner that improves microbiological and chemical qualities without jeopardising crop productivity. The combined application of vermicomposted products and chemical fertilizers reduced PTEs accumulation in plant roots, with minimal or negligible presence detected in the edible portions of the crop. Therefore, this study suggested that both vermicomposted product [1:1 ratio combined with chemical fertilizer] serve as a feasible substitute for conventional organic manure promoting sustainable industrial waste management, and supporting long-term soil resilience.

Bibliography

1. Abbaspour, H., Saeidi-Sar, S., Afshari, H., and Abdel-Wahhab, M. A. (2012). Tolerance of mycorrhiza infected pistachio (*Pistacia vera* L.) seedling to drought stress under glasshouse conditions. J. Plant. Physiol. 169,704–709.
2. Abyaneh, A. S., and Fazaelipoor, M. H. (2016). Evaluation of rhamnolipid (RL) as a biosurfactant for the removal of chromium from aqueous solutions by precipitate flotation. J. Environ. Manage. 165,184–187.
3. Acosta, J. A., Jansen, B., Kalbitz, K., Faz, A., Martínez-Martínez, S., (2011). Salinity increases mobility of heavy metals in soils. Chemosphere 85(8), 1318-1324.
4. Adedeji, O. H., Olayinka, O. O., Tope-Ajayi, O. O., & Adekoya, A. S. (2020). Assessing spatial distribution, potential ecological and human health risks of soil heavy metals contamination around a Trailer Park in Nigeria. *Scientific African*, 10, e00650.
5. Agnihotri, R., Sharma, M. P., Prakash, A., Ramesh, A., Bhattacharjya, S., Patra, A. K., Manna, M. C., Kurganova, I., Kuzyakov, Y., (2022). Glycoproteins of arbuscular mycorrhiza for soil carbon sequestration: Review of mechanisms and controls. Sci. Total. Environ. 806, 150571.
6. Ahmad, W., Alharthy, R. D., Zubair, M., Ahmed, M., Hameed, A., & Rafique, S. (2021). Toxic and heavy metals contamination assessment in soil and water to evaluate human health risk. *Scientific reports*, 11(1), 17006.
7. Akande, F., Ogunkunle, C., and Ajayi, S. (2018). Contamination from petroleum products: Impact on soil seed banks around an oil storage facility in Ibadan, South-West Nigeria. Pollut. 4,515–525.
8. Alam, A. K. M. R., Hossain, A. B. M., Hoque, S., and Chowdhury, D. A. (2018). Heavy metals in wetland soil of Greater Dhaka District, Bangladesh. Pollut. 4,129–141.
9. Alef, K., 1995. Phosphatase activity. Methods in applied soil microbiology and biochemistry
10. Ali H, Khan E, Sajad MA (2013) Phytoremediation of heavy metals—concepts and applications. Chemosphere 91:869–881
11. Alvarez, A.H., Moreno-Sanchez, ´ R., Cervantes, C., (1999). Chromate efflux by means of the *Chr*A chromate resistance protein from *Pseudomonas aeruginosa*. J. Bacteriol. 181, 7398–7400.
12. Alyousef, R. A., Alfaifi, H. J., Zaidi, F. K., & Al-Hashim, M. (2022). Geostatistical and pollution index-based approach for assessing heavy metal pollution in the Cambro-Ordovician Saq Aquifer in Central Saudi Arabia. *Environmental Earth Sciences*, 81(14), 370.
13. Aminifard, M.H., Aroiee, H., Azizi, M., Nemati, H., Jaafar, Z.E., (2012). Effect of humic acid on antioxidant activities and fruit quality of hot pepper (*Capsicum annuum* L.). *J. Herbs. Spices. Med. Plants*. 18, 360–369.
14. Amir H, Lagrange A, Hassaïne N, Cavaloc Y (2013) Arbuscular mycorrhizal fungi from New Caledonian ultramafic soils improve tolerance to nickel of endemic plant species. Mycorrhiza 23:585–595
15. Amir, S., Benlboukht, F., Cancian, N., Winterton, P., & Hafidi, M. (2008). Physico-chemical analysis of tannery solid waste and structural characterization of its isolated humic acids after composting. *Journal of hazardous materials*, *160*(2-3), 448-455.
16. Amna, Ali. N., Masood, S., Mukhtar, T., Kamran, M. A., Rafique, M., Munis, M. F. H., Chaudhary, H. J., (2015). Differential effects of cadmium and chromium on growth, photosynthetic activity, and metal uptake of *Linum usitatissimum* in association with *Glomus intraradices*. *Environ. Monit. Assess.* 187, 1-11.
17. Anandakumar, S., Kalaiselvi, T., Kuttimani, R., Umapathi, M., (2024). Synergistic Effect of Arbuscular Mycorrhizal Fungi and Rhizobium on Glomalin Related Soil Protein and Biochemical Properties of Blackgram Rhizosphere Soil. *J. Soil. Sci. Plant. Nutr. 24*(3), 5534-5551
18. Andra, S. S., Datta, R., Sarkar, D., Makris, K. C., Mullens, C. P., Sahi, S. V., and Bach, S. B. (2009). Induction of Lead-Binding Phytochelatins in Vetiver Grass [*Vetiveria zizanioides* (L.)]. J. Environ. Qual. 38,868-877.

19. Ansari, A., Andalibi, B., Zarei, M., Shekari, F., (2021). Combined effect of putrescine and mycorrhizal fungi in phytoremediation of Lallemantia iberica in Pb-contaminated soils. *Environ. Sci. Pollut. Res. 28*(41), 58640-58659.

20. Aponte, H., Medina, J., Butler, B., Meier, S., Cornejo, P., Kuzyakov, Y., (2020). Soil quality indices for metal (loid) contamination: An enzymatic perspective. Land Degrad Dev 31, 2700–2719

21. Arienzo, M., Christen, E.W., Quayle, W., Kumar, A., (2009). A review of the fate of potassium in the soil–plant system after land application of wastewaters. J Hazard Mater 164, 415–422.

22. Arriagada, C. A., Herrera, M. A., and Ocampo, J. A. (2007). Beneficial effect of saprobe and arbuscular mycorrhizal fungi on growth of Eucalyptus globulus co-cultured with Glycine max in soil contaminated with heavy metals. J. Environ. Manage. 84,93–99.

23. Arshad, M., Silvestre, J., Pinelli, E., Kallerhoff, J., Kaemmerer, M., Tarigo, A., Shahid, M., Guiresse, M., Pradère, P., and Dumat, C. (2008). A field study of lead phytoextraction by various scented Pelargonium cultivars. Chemosphere. 71,2187–2192.

24. Aslam, Z., Ahmad, A., Bashir, S., Hussain, S., Bellitürk, K., Ahmad, J.N., Ullah, E., Tanvir, S., Abbas, T., 2022. Effect of integrated nutrient management practices on physiological, morphological and yield parameters of chilli (*Capsicum annum* L.). *Pak. J. Bot. 54*, 2143-2150.

25. Ayub, S., Siddique, A. A., Khursheed, M. S., Zarei, A., Alam, I., Asgari, E., & Changani, F., (2020). Removal of heavy metals (Cr, Cu, and Zn) from electroplating wastewater by electrocoagulation and adsorption processes. Desalination Water Treatment 179, 263–271.

26. Bahraminia, M., Zarei, M., Ronaghi, A., and Ghasemi-Fasaei, R. (2016). Effectiveness of arbuscular mycorrhizal fungi in phytoremediation of lead-contaminated soil by vetiver grass. Int. J. Phytoremediation. 18,730–737.

27. Baker, A.J.M., S.P. McGrath, C.M.D. Sidoli, and R.S. Reeves. (1994). The possibility of in-situ heavy metal decontamination of polluted soils using crops of metal-accumulating plants. Res. Conserv. Recycl. 11:41–49.

28. Banerjee, R., Goswami, P., Lavania, S., Mukherjee, A., Lavania, U. C., (2019). Vetiver grass is a potential candidate for phytoremediation of iron ore mine spoil dumps. Ecol. Eng. 132, 120-136.

29. Banerjee, S., Ghosh, S., Chakraborty, S., Sarkar, D., Datta, R., Bhattacharyya, P., (2024). Synergistic impact of bioavailable PHEs and alkalinity on microbial diversity and traits in agricultural soil adjacent to chromium-asbestos mines. Environ. Pollut. 350, 124021.

30. Banerjee, S., Ghosh, S., Jha, S., & Bhattacharyya, P. (2025). Innovative green vermi-remediation of chromite-asbestos mine waste: From toxicity reduction to soil-crop-microbe health improvement utilizing novel multimodal statistical approach. *Journal of Environmental Chemical Engineering*, *13*(2), 116019

31. Banerjee, S., Ghosh, S., Jha, S., Kumar, S., Mondal, G., Sarkar, D., Datta, R., Mukherjee, A., & Bhattacharyya, P. (2023). Assessing pollution and health risks from chromite mine tailings contaminated soils in India by employing synergistic statistical approaches. *Science of The Total Environment,* 880, 163228. https://doi.org/10.1016/j.scitotenv.2023.163228

32. Banerjee, S., Ghosh, S., Prajapati, J., & Bhattacharyya, P. (2025). Hidden threats beneath: uncovering the bio-accessible hazards of chromite-asbestos mine waste and their impacts on rice components via multi-machine learning algorithm. *Environmental Geochemistry and Health*, *47*(6), 1-19

33. Bedini, S., Pellegrino, E., Avio, L., Pellegrini, S., Bazzoffi, P., Argese, E., Giovannetti, M., (2009). Changes in soil aggregation and glomalin-related soil protein content as affected by the arbuscular mycorrhizal fungal species Glomus mosseae and Glomus intraradices. *Soil. Biol. Biochem.* 41(7), 1491-1496.

34. Belon, E., Boisson, M., Deportes, I. Z., Eglin, T. K., Feix, I., Bispo, A. O., Galsomies, L., Leblond, S., & Guellier, C. R. (2012). An inventory of

trace elements inputs to French agricultural soils. Sci. Total Environ. 439, 87–95.

35. Beukes, J. P., Dawson, N. F., and van Zyl, P. G. (2010). Theoretical and practical aspects of Cr (VI) in the South African ferrochrome industry. J. South. Afr. Inst. Min. Metall. 110,743–750.
36. Bhattacharya, S. S., & Kim, K. (2016). Utilization of coal ash: Is vermitechnology a sustainable avenue? Renewable & Sustainable Energy Reviews. 58:1376–1386.
37. Bhattacharya, S.S., Iftikar, W., Sahariah, B., Chattopadhyay, G.N., (2012). Vermicomposting converts fly ash to enrich soil fertility and sustain crop growth in red and lateritic soils. *Resour. Conserv. Recycl. 65*, 100–106.
38. Bhattacharyya, K., Sengupta, S., Pari, A., Halder, S., Bhattacharya, P., Pandian, B. J., Chinchmalatpure, A. R., (2021). Characterization and risk assessment of arsenic contamination in soil–plant (vegetable) system and its mitigation through water harvesting and organic amendment. Environ. Geochem. Health 43(8), 2819–2834
39. Bhattacharyya, P., Tripathy, S., Chakrabarti, K., Chakraborty, A., Banik, P., (2008). Fractionation and bioavailability of metals and their impacts on microbial properties in sewage irrigated soil. Chemosphere 72, 543–550.
40. Bhatti, S. S., Kumar, V., Kumar, A., Kirby, J. K., Gouzos, J., Correll, R., Singh, J., Sambyal, V., & Nagpal, A. K. (2020). Potential carcinogenic and non-carcinogenic health hazards of metal (loid) s in food grains. *Environmental Science and Pollution Research,* 27, 17032-17042.
41. Bhuiyan, M. A. H., Karmaker, S. C., Bodrud-Doza, M., Rakib, M. A., Saha, B. B., (2021). Enrichment, sources and ecological risk mapping of heavy metals in agricultural soils of dhaka district employing SOM, PMF and GIS methods. Chemosphere 263, 128339
42. Biruntha, M., Karmegam, N., Archana, J., Selvi, B.K., Paul, J.A.J., Balamuralikrishnan, B., Chang, S.W., Ravindran, B., (2020). Vermiconversion of biowastes with low-to-high C/N ratio into value added vermicompost. Bioresour Technol 297, 122398.
43. Bloise, A., Fornero, E., Belluso, E., Barrese, E., and Rinaudo, C. (2008). Synthesis and characterization of tremolite asbestos fibres. Eur. J. Mineral. 20,1027–1033.
44. Booth, S.C., Weljie, A.M., Turner, R.J., (2015). Metabolomics reveals differences of metal toxicity in cultures of Pseudomonas pseudoalcaligenes KF707 grown on different carbon sources. Front Microbiol 6, 827.
45. Bosso, S. T., & Enzweiler, J. (2008). Bioaccessible lead in soils, slag, and mine wastes from an abandoned mining district in Brazil. *Environmental Geochemistry and Health*, 30, 219-229.
46. Boyrahmadi, M., and Raiesi, F., (2018). Plant roots and species moderate the salinity effect on microbial respiration, biomass, and enzyme activities in a sandy clay soil. Biol Fertil Soils 54, 509-521.
47. Brady, N., (1990). The nature and properties of soils. Macmillan Publishing Company Cranbury 10.
48. Bretaña, B. L. P., Salcedo, S. G., Casim, L. F., & Manceras, R. S., (2019). Growth performance and inorganic mercury uptake of Vetiver (*Chrysopogon zizanoides* Nash) inoculated with arbuscular mycorrhiza fungi (AMF): Its implication to phytoremediation. *J. Agric. Res. Dev. Ext. Tech.* 1(1), 39-47.
49. Brookes, P.C., Landman, A., Pruden, G., Jenkinson, D.S., (1985). Chloroform fumigation and the release of soil nitrogen: a rapid direct extraction method to measure microbial biomass nitrogen in soil. Soil Biol Biochem 17, 837–842
50. Brtnický, M., Pecina, V., Hladký, J., Radziemska, M., Koudelková, Z., Klimánek, M., Vaverková, M. D., (2019). Assessment of phytotoxicity, environmental and health risks of historical urban park soils. Chemosphere 220, 678-686.
51. Bruins, M.R., Kapil, S., Oehme, F.W., (2000). Microbial resistance to metals in the environment. Ecotoxicol Environ Saf 45, 198–207.

52. Bueno, P. C., Bellido, E., Rubí, J. A. M., and Ballesta, R. J. (2009). Concentration and spatial variability of mercury and other heavy metals in surface soil samples of periurban waste mine tailing along a transect in the Almadén mining district (Spain). Environ. Geol. 56,815–824.

53. Burges A, Alkorta I, Epelde L, Garbisu C (2018) From phytoremediation of soil contaminants to phytomanagement of ecosystem services in metal contaminated sites. Int J Phytoremediation 20:384–397

54. Cachada, A., Rocha-Santos, T., and Duarte, A. C. (2018). Soil and pollution: an introduction to the main issues, in: Soil. Pollut. 1,1–28.

55. Cai, L. M., Wang, Q. S., Wen, H. H., Luo, J., Wang, S., (2019). Heavy metals in agricultural soils from a typical township in Guangdong Province, China: Occurrences and spatial distribution. Ecotoxicol. Environ. Safety 168, 184-191.

56. Caicedo-Rivas, G., Salas-Moreno, M., & Marrugo-Negrete, J. (2022). Health risk assessment for human exposure to heavy metals via food consumption in inhabitants of middle basin of the Atrato river in the colombian Pacific. *International Journal of Environmental Research and Public Health*, 20(1), 435.

57. Caporale, A. G., Sarkar, D., Datta, R., Punamiya, P., Violante, A., (2014). Effect of arbuscular mycorrhizal fungi (*Glomus* spp.) on growth and arsenic uptake of vetiver grass (*Chrysopogon zizanioides* L.) from contaminated soil and water systems. *J. Soil. Sci. Plant. Nut. 14*(4), 955-972.

58. Caradonia, F., Francia, E., Morcia, C., Ghizzoni, R., Moulin, L., Terzi, V., and Ronga, D. (2019). Arbuscular mycorrhizal fungi and plant growth promoting rhizobacteria avoid processing tomato leaf damage during chilling stress. Agronomy. 9,299.

59. Casieri, L., Ait Lahmidi, N., Doidy, J., Veneault-Fourrey, C., Migeon, A., Bonneau, L., Courty, P. E., Garcia, k., Charbonnier, M., Delteil, A., Brun, A., Zimmermann, S., Plassard, C., Wipf, D., 2013. Biotrophic transportome in mutualistic plant–fungal interactions. *Mycorrhiza*. 23, 597-625.

60. Central Pollution Control Board of India. (2012). List of waste constituents with concentration limits and Analytical Methods; Class A: Based on leachable concentration limits [Toxicity Characteristic Leaching Procedure (TCLP) or Soluble Threshold Limit Concentration (STLC)]. SCHEDULE II: rule [3(1)(17)(ii)]

61. Chabukdhara, M., & Nema, A.K. (2013). Heavy metals assessment in urban soil around industrial clusters in Ghaziabad, India: probabilistic health risk approach. *Ecotoxicology and Environmental Safety, 87*, 57–64

62. Chai, L., Wang, Y., Wang, X., Ma, L., Cheng, Z., Su, L., Liu, M., 2021. Quantitative source apportionment of heavy metals in cultivated soil and associated model uncertainty. Ecotoxicol. Environ. Safety 215, 112150.

63. Chakraborty, P., Ghosh, S., Banerjee, S., Bhattacharya, S., Bhattacharyya, P., 2024. Evaluating the efficacy of vermicomposted products in rain-fed wetland rice and predicting potential hazards from metal-contaminated tannery sludge using novel machine learning tactic. Chemosphere 358, 142272

64. Chakraborty, P., Sarkar, S., Mondal, S., Agarwal, B.K., Kumar, A., Bhattacharya, S., Bhattacharya, S.S., Bhattacharyya, P., 2022. Eisenia fetida mediated vermi-transformation of tannery waste sludge into value added eco-friendly product: An insight on microbial diversity, enzyme activation, and metal detoxification. J Clean Prod 348, 131368.

65. Chan, M. (2014). Food safety must accompany food and nutrition security. *The Lancet*, 384(9958), 1910-1911. https://doi.org/10.1016/S0140-6736(14)62037-7

66. Chao, G., Jingbo, X., Ji, L., Zhengtao, L., 2016. Biological responses in the earthworm Eisenia fetida exposed to soils near a typical lead acid battery plant. Soil and Sediment Contamination: An International Journal 25, 573–585

67. Charan, K., Bhattacharyya, P., Bhattacharya, S.S., 2024. Vermitechnology transforms hazardous red mud into benign organic input for agriculture: Insights on earthworm-microbe interaction, metal removal, and soil-crop improvement. J Environ Manage 354, 120320.

68. Cheema, A., Garg, N., 2024. Arbuscular mycorrhizae reduced arsenic induced oxidative stress by coordinating nutrient uptake and proline-glutathione levels in *Cicer arietinum* L.(chickpea). *Ecotoxicol. 33*(2), 205-225.

69. Chelangat, A., Gweyi-Onyango, J. P., Korir, N. K., Mwangi, M., 2021. Influence of arbuscular mycorrhizae on callusing and root colonization of tea (*Camellia sinensis*) clones in Kenya. *Asian. Soil. Res. J*. 5, 21-26.

70. Chen X, Wu C, Tang J, Hu S (2005) Arbuscular mycorrhizae enhance metal lead uptake and growth of host plants under a sand culture experiment. Chemosphere 60:665–671

71. Chen, D.K., Yang, S.F., Jiang, Z.Y., Wang, Z.R., Wang, Z.B., & Tian, H. (2023). Spatial distribution, ecological risk and health risk assessment of heavy metals inagricultural soil from Ankang basin, Shaanxi Province. *Heliyon* 9 (12), e22580.

72. Cheng Z (2016) The spatial correlation and interaction between manufacturing agglomeration and environmental pollution. Ecol Indic 61:1024–1032

73. Cheng, P., Zhang, S., Wang, Q., Feng, X., Zhang, S., Sun, Y., Wang, F., 2021. Contribution of nano-zero-valent iron and arbuscular mycorrhizal fungi to phytoremediation of heavy metal-contaminated soil. *Nanomaterials*. *11*(5), 1264.

74. Chezom, D., Chimi, K., Choden, S., Wangmo, T., & Gupta, S. K. (2013). Comparative study of different leaching procedures. *International Journal of Engineering Research and General Science*, 1(2), 23-28. https://doi.org/62dca6a1c736264cf0c8605766482b2c90faa064

75. China SP, Das M, Maiti SK (2014) Phytostabilization of Mosaboni Copper mine tailings: A green step towards waste management. Appl Ecol Environ Res 12:25-32

76. Chivenge, P., Vanlauwe, B., Six, J., 2011. Does the combined application of organic and mineral nutrient sources influence maize productivity? A meta-analysis. *Plant. Soil. 342*, 1–30.

77. Cho, K. H., Sthiannopkao, S., Pachepsky, Y. A., Kim, K. W., & Kim, J. H. (2011). Prediction of contamination potential of groundwater arsenic in Cambodia, Laos, and Thailand using artificial neural network. *Water research*, 45(17), 5535-5544.

78. Chodak, M., Gołebiewski, M., Justyna, M.P., Katarzyna, K., and Maria, N., 2013. Diversity of microorganisms from forest soils differently polluted with heavy metals. Appl Soil Ecol 64,7–14

79. Chodak, M., Gołębiewski, M., Morawska-Płoskonka, J., Kuduk, K., and Niklińska, M., 2015. Soil chemical properties affect the reaction of forest soil bacteria to drought and rewetting stress. Ann Microbiol 65, 1627-1637.

80. Choure, K., Parsai, S., Kotoky, R., Srivastava, A., Rai, P.K., Sharma, A., and Pandey, P., 2021. Comparative metagenomic analysis of two alkaline hot springs of Madhya Pradesh, India and deciphering the extremophiles for industrial enzymes. Front Genet 12, 643423.

81. Chowdhury, N. R., Das, A., Joardar, M., De, A., Mridha, D., Das, R., Rahman, M. M., & Roychowdhury, T. (2020). Flow of arsenic between rice grain and water: Its interaction, accumulation and distribution in different fractions of cooked rice. *Science of the Total Environment*, 731, 138937.

82. Chowdhury, N.R., Das, A., Joardar, M., Mridha, D., De, A., Majumder, S., Mandal, J., Majumdar, A. & Roychowdhury, T. (2022). Distribution of arsenic in rice grain from West Bengal, India: Its relevance to geographical origin, variety, cultivars and cultivation season. In Global arsenic hazard: *Ecotoxicology and remediation*

83. Coban, O., De Deyn, G.B., van der Ploeg, M., 2022. Soil microbiota as game-changers in restoration of degraded lands. Science (1979) 375, abe0725.

84. Coccina, A., Cavagnaro, T. R., Pellegrino, E., Ercoli, L., McLaughlin, M. J., and Watts-Williams, S. J. (2019). The mycorrhizal pathway of zinc uptake contributes to zinc accumulation in barley and wheat grain. BMC Plant. Biol. 19,1–14.

85. Crowley D (2008) Impacts of metals and metalloids on soil microbial diversity and ecosystem function. Revista de la ciencia del suelo y nutrición vegetal 8:6–11

86. Cui, Y., Fang, L., Guo, X., Wang, X., Zhang, Y., Li, P., Zhang, X., 2018. Ecoenzymatic stoichiometry and microbial nutrient limitation in rhizosphere soil in the arid area of the northern Loess Plateau, China. Soil Biol Biochem 116, 11–21.

87. Cunningham, S. D., Anderson, T. A., Schwab, A. P., and Hsu, F. C. (1996). Phytoremediation of soils contaminated with organic pollutants. Adv. Agron. 56,55–114.

88. Daei, G., Ardekani, M. R., Rejali, F., Teimuri, S., and Miransari, M. (2009). Alleviation of salinity stress on wheat yield, yield components, and nutrient uptake using arbuscular mycorrhizal fungi under field conditions. J. Plant. Physiol. 166,617–625.

89. Dai, J., Becquer, T., Rouiller, J.H., Reversat, G., Bernhard-Reversat, F., Nahmani, J., Lavelle, P., 2004. Heavy metal accumulation by two earthworm species and its relationship to total and DTPA-extractable metals in soils. Soil Biol Biochem 36, 91–98.

90. Danesh, Y. R., Tajbakhsh, M., Goltapeh, E. M., Varma, A., 2012. Mycoremediation of heavy metals. In *Fungi as bioremediators*. Berlin, Heidelberg: Springer Berlin Heidelberg. 245-267.

91. Das R, Biswas S, Banerjee ER. 2016. Nutraceutical-prophylactic and therapeutic role of functional food in health. J Nutr Food Sci. 6:4. doi:10.4172/2155-9600.1000527

92. Das S, Dash HR, Chakraborty J (2016) Genetic basis and importance of metal resistant genes in bacteria for bioremediation of contaminated environments with toxic metal pollutants. Applied Microbiology Biotechnology. 100:2967–2984.

93. Das, S., Goswami, L., Bhattacharya, S.S., 2020. Vermicomposting: earthworms as potent bioresources for biomass conversion, in: Current Developments in Biotechnology and Bioengineering. Elsevier, pp. 79–102.

94. Das, S., Teja, K.C., Duary, B., Agrawal, P.K., Bhattacharya, S.S., 2016. Impact of nutrient management, soil type and location on the accumulation of capsaicin in *Capsicum chinense* (Jacq.): One of the hottest chili in the world. *Scientia. Horticulturae*. *213*, 354-366.

95. Dash, D., Patro, H., Tiwari, R. C., & Shahid, M. (2011). Effect of organic and inorganic sources of N on growth attributes, grain and straw yield of rice (Oryza sativa). *International Journal of Pharmaceutical and Life Sciences*, *2*(4), 655-660.

96. de Andrade, S. A. L., da Silveira, A. P. D., Jorge, R. A., de Abreu, M. F., 2008. Cadmium accumulation in sunflower plants influenced by arbuscular mycorrhiza. *Int. J. Phytoremediation.* 10(1), 1-13

97. De Miguel, E., Iribarren, I., Chacon, E., Ordonez, A., & Charlesworth, S. (2007). Risk-based evaluation of the exposure of children to trace elements in playgrounds in Madrid (Spain). *Chemosphere 66, 505–513*

98. Denys, S., Caboche, J., Tack, K., Rychen, G., Wragg, J., Cave, M., Jondreville, C., & Feidt, C. (2012). In vivo validation of the unified BARGE method to assess the bioaccessibility of arsenic, antimony, cadmium, and lead in soils. *Environmental science & technology*, 46(11), 6252-6260.

99. Desai, C., Parikh, R. Y., Vaishnav, T., Shouche, Y. S., and Madamwar, D., 2009. Tracking the influence of long-term chromium pollution on soil bacterial community structures by comparative analyses of 16S rRNA gene phylotypes. Res Microbiol 160, 1-9.

100. Devi, J., Deb, U., Barman, S., Das, S., Bhattacharya, S.S., Tsang, Y.F., Lee, J.-H., Kim, K.-H., 2020. Appraisal of lignocellusoic biomass degrading potential of three earthworm species using vermireactor mediated with spent mushroom substrate: compost quality, crystallinity, and microbial community structural analysis. Science of the Total Environment 716, 135215.

101. Dey, P., Mahapatra, B. S., Juyal, V. K., Pramanick, B., Negi, M.S., Paul, J., Singh, S. P., 2021. Flax processing waste–A low-cost, potential biosorbent for treatment of heavy metal, dye and organic matter contaminated industrial wastewater. Industrial Crops Products 174, 114195

102. Dhalaria, R., Kumar, D., Kumar, H., Nepovimova, E., Kuča, K., Torequl Islam., M., Verma, R., 2020. Arbuscular mycorrhizal fungi as potential agents in ameliorating heavy metal stress in plants. Agronomy. 10(6), 815.

103. Dhaliwal SS, Singh J, Taneja PK, Mandal A (2020) Remediation techniques for removal of heavy metals from the soil contaminated through different sources: a review. Environ Sci Pollut Res 27:1319–1333

104. Dilly, O., Buscot, F., Varma, A., 2005. Microbial energetics in soil. Microorganisms in Soils: Roles in Genesis and Functions. Soil Biol, Springer-Verlag, Berlin, Heidelberg, 3.

105. Dominguez-Nuñez, J. A., Benito, B., Berrocal-Lobo, M., Albanesi, A., 2016. Mycorrhizal fungi: role in the solubilization of potassium. *Potassium solubilizing microorganisms for sustainable agriculture*, 77-98.

106. Dong, H., Zhang, G., Jiang, H., Yu, B., Chapman, L.R., Lucas, C.R., and Fields, M.W., 2006. Microbial diversity in sediments of saline Qinghai Lake, China: linking geochemical controls to microbial ecology. Microb Ecol 51, 65-82.

107. Du, X., Zhu, Y., Han, Q., Yu, Z., 2019. The influence of traffic density on heavy metals distribution in urban road runoff in Beijing. China Environ. Sci. Pollut. Res. 26, 886–895.

108. Duncan, A. E.., de Vries, N., and Nyarko, K. B. (2018). Assessment of heavy metal pollution in the sediments of the River Pra and its tributaries. Water. Air. Soil. Pollut. 229,1–10.

109. Eberlein, C., Baumgarten, T., Starke, S., Heipieper, H.J., 2018. Immediate response mechanisms of Gram-negative solvent-tolerant bacteria to cope with environmental stress: cis-trans isomerization of unsaturated fatty acids and outer membrane vesicle secretion. Appl Microbiol Biotechnol 102, 2583–2593.

110. Edwards, C.A., Arancon, N.Q., Sherman, R.L., 2010. Vermiculture Technology: Earthworms, Organic Waste and Environmental Management. CRC Press, Boca Raton, USA

111. Emran, M., Gispert, M., and Pardini, G. (2012). Patterns of soil organic carbon, glomalin and structural stability in abandoned Mediterranean terraced lands. Eur. J. Soil. Sci. 63,637–649.

112. Equeenuddin, S.M., Tripathy, S., Sahoo, P.K., & Panigrahi, M.K. (2013). Metal behavior in sediment associated with acid mine drainage stream: role of pH. *J Geochem Explor*,124, 230–237.

113. Fall, A. F., Nakabonge, G., Ssekandi, J., Founoune-Mboup, H., Apori, S. O., Ndiaye, A., Badji, A., Ngom, K., 2022. Roles of arbuscular mycorrhizal fungi on soil fertility: contribution in the improvement of physical, chemical, and biological properties of the soil. *Front. Fungal. Biol.* 3, 723892.

114. Fallovo, C., Schreiner, M., Schwarz, D., Colla, G., Krumbein, A., 2011. Phytochemical changes induced by different nitrogen supply forms and radiation levels in two leafy Brassica species. *J. Agric. Food Chem.* 59, 4198–4207.

115. Farhangi-Abriz S and Torabian S (2017) Antioxidant enzyme and osmotic adjustment changes in bean seedlings as affected by biochar under salt stress. Ecotoxicol Environm Saf, 137: 64–70

116. Feng, G., Xie, T., Wang, X., Bai, J., Tang, L., Zhao, H., Wei, W., Wang, M., and Zhao, Y. 2018. Metagenomic analysis of microbial community and function involved in cd-contaminated soil. BMC Microb 18, 1-13.

117. Fernández-Caliani, J. C., Barba-Brioso, C., González, I., and Galán, E. (2009). Heavy metal pollution in soils around the abandoned mine sites of the Iberian Pyrite Belt (Southwest Spain). Water. Air. Soil. Pollut. 200,211–226.

118. Fernández-Gómez, M.J., Díaz-Raviña, M., Romero, E., Nogales, R., 2013. Recycling of environmentally problematic plant wastes generated from greenhouse tomato crops through vermicomposting. *Int. J. Environ. Sci. Technol.* 10, 697–708.

119. Ferreira, S.L.C., da Silva Junior, J.B., dos Santos, I.F., de Oliveira, O.M.C., Cerda, V., & Queiroz, A.F.S. (2022). Use of pollution indices and ecological risk in the assessment of contamination from chemical elements in soils and sediments–Practical aspects. *Trends in Environmental Analytical Chemistry, 35*, e00169

120. Fierer, N., 2017. Embracing the unknown: disentangling the complexities of the soil microbiome. Nat Rev Microbiol 15, 579–590.

121. Fierer, N., Ladau, J., Clemente, J.C., Leff, J.W., Owens, S.M., Pollard, K.S., Knight, R., Gilbert, J.A., McCulley, R.L., 2013. Reconstructing the microbial diversity and function of pre-agricultural Tallgrass soils in the United States. Sci 342,621–624

122. Gangadhar, B.H., Mishra, R.K., Pandian, G., Park, S.W., 2012. Comparative study of color, pungency, and biochemical composition in chili pepper (*Capsicum annuum*) under different light emitting diode treatments. *Hort. Science*. 47, 1729–1735.

123. Ganguly, R. K., & Chakraborty, S. K. 2021. Succession of enzymes and microbial biomarkers in the process of vermicomposting: An insight towards valorization of toxic paper mill wastes using Perionyx excavatus (Oligochaeta; Perrier, 1872). J. Environ Health Sci Eng 19, 1457-1472.

124. Gao, Y., Sun, S., Xing, F., Mu, X., and Bai, Y., 2019. Nitrogen addition interacted with salinity-alkalinity to modify plant diversity, microbial PLFAs and soil coupled elements: A 5-year experiment. Appl Soil Ecol 137, 78-86.

125. García-Galdeano, J.M., Villalón-Mir, M., Medina-Martínez, J., Fonseca-Moor-Davie, S.M., Zamora-Bustillos, J. G., Vázquez-Foronda, L. M., Navarro-Alarcón, M., 2021. Ca and Mg Concentrations in Spices and Growth of Commonly Sporulated and Non-Sporulated Food-Borne Microorganisms According to Marketing Systems. Foods, 10, 1122

126. Ge, M., Zhou, H., Shen, Y., Meng, H., Li, R., Zhou, J., Cheng, H., Zhang, X., Ding, J., Wang, J., 2020. Effect of aeration rates on enzymatic activity and bacterial community succession during cattle manure composting. Bioresour Technol 304, 122928.

127. Gheju, M., Balcu, I., Ciopec, M., 2009. Analysis of hexavalent chromium uptake by plants in polluted soils. *Ovidius University Annals of Chemistry*. 20(1), 127-131.

128. Ghosh, S., Banerjee, S., Prajapati, J., Mandal, J., Mukherjee, A., & Bhattacharyya, P. (2023a). Pollution and health risk assessment of mine tailings contaminated soils in India from toxic elements with statistical approaches. *Chemosphere*, 324, 138267.

129. Ghosh, S., Banerjee, S., Mukherjee, A., & Bhattacharyya, P. (2023b). Appraise potassium chemistry and distribution patterns in tailing soil, India: Through quantity-Intensity relations and multi model statistical methods. *Chemosphere*, *335*, 139184.

130. Ghosh, S., Banerjee, S., Prajapati, J., Mukherjee, A., & Bhattacharyya, P. (2025). Appraisal of Mica-Based Potassium Mobilizing Bacterial Biofertilizers: Revolutionizing Soil Fertility and Plant Growth Employing Multi-Machine Learning Models. *Communications in Soil Science and Plant Analysis*, 1-23.

131. Ghosh, S., Mondal, S., Mandal, J., Mukherjee, A., and Bhattacharyya, P., 2024. Effect of metal fractions on rice grain metal uptake and biological parameters in mica mines waste contaminated soils. J Environ Sci 136, 313-324.

132. Giovannini, L., Palla, M., Agnolucci, M., Avio, L., Sbrana, C., Turrini, A., Giovannetti, M., 2020. Arbuscular mycorrhizal fungi and associated microbiota as plant biostimulants: research strategies for the selection of the best performing inocula. Agronomy 10(1): 106.

133. Gkorezis, P., Daghio, M., Franzetti, A., Hamme, J. D. V., Sillen, W., and Vangronsveld, J. (2016). The interaction between plants and bacteria in the remediation of petroleum hydrocarbons: An environmental perspective. Front. Microbiol. 7,1–27.

134. Gnandi, K., and Tobschall, H. (2002). Heavy metals distribution of soils around mining sites of cadmium-rich marine sedimentary phosphorites of Kpogame and Hahotoe (southern Togo). Environ. Geol. 41,593–600.

135. Göhre, V., Paszkowski, U., 2006. Contribution of the arbuscular mycorrhizal symbiosis to heavy metal phytoremediation. *Planta*. *223*, 1115-1122.

136. Gołębiewski, M., Deja-Sikora, E., Cichosz, M., Tretyn, A., and Wróbel, B., 2014. 16S rDNA pyrosequencing analysis of bacterial community in heavy metals polluted soils. Microb Ecol 67, 635-647.

137. Golui, D., Datta, S. P., Dwivedi, B. S., Meena, M. C., Ray, P., Trivedi, V. K., 2021. A new approach to establish safe levels of available metals in soil with respect to potential health hazard of human. Environ. Earth Sci. 80(19), 1–12.

138. Golui, D., Datta, S. P., Dwivedi, B. S., Meena, M. C., Trivedi, V. K., Jaggi, S., & Bandyopadhya, K. K. (2020). Effectiveness of toxicity characteristics leaching procedure for assessing metal hazards of polluted soils in relation to human health. *Soil and Sediment Contamination: An International Journal*, 29(3), 304-321.

139. Golui, D., Datta, S. P., Dwivedi, B. S., Meena, M. C., Trivedi, V. K., 2020. Prediction of free metal ion activity in contaminated soils using WHAM VII, baker soil test and solubility model. Chemosphere 243, 125408

140. Golui, D., Datta, S. P., Rattan, R. K., Dwivedi, B. S., Meena, M. C., 2014. Predicting bioavailability of metals from sludge-amended soils. Environ. Monitor. Assess. 186(12), 8541–8553

141. Golui, D., Mazumder, D. G., Sanyal, S. K., Datta, S. P., Ray, P., Patra, P. K., Sarkar, S., Bhattacharya, K., 2017. Safe limit of arsenic in soil in relation to dietary exposure of arsenicosis patients from Malda district, West Bengal-A case study. Ecotoxicol. Environ. Safety 144, 227-235

142. Gomez-Brandon, M., Aira, M., Lores, M., Dominguez, J., 2011. Epigeic earthworms exert a bottleneck effect on microbial communities through gut associated processes. PLoS One 6, e24786.

143. González-Villalobos MA, Martinez-Trinidad T, Alarcón A, Plascencia-Escalante FO (2021) Growth and lead uptake by Parkinsonia aculeata L. inoculated with *Rhizophagus intraradices*. Int J Phytoremediation 23:272–278

144. Goswami, A.P., & Kalamdhad, A.S. (2023). Mobility and risk assessment of heavy metals in benthic sediments using contamination factors, positive matrix factorisation (PMF) receptor model, and human health risk assessment. *Environmental Science and Pollution Research 30*, 7056–7074

145. Goswami, L., Mukhopadhyay, R., Bhattacharya, S.S., Das, P., Goswami, R., 2018. Detoxification of chromium-rich tannery industry sludge by Eudrillus eugeniae: insight on compost quality fortification and microbial enrichment. Bioresour Technol 266, 472–481.

146. Goswami, L., Sarkar, S., Mukherjee, S., Das, S., Barman, S., Raul, P., Bhattacharyya, P., Mandal, N.C., Bhattacharya, S., Bhattacharya, S.S., 2014. Vermicomposting of tea factory coal ash: metal accumulation and metallothionein response in Eisenia fetida (Savigny) and Lampito mauritii (Kinberg). Bioresour Technol 166, 96–102.

147. Gravand, F., Rahnavard, A., & Pour, G. M. (2021). Investigation of vetiver grass capability in phytoremediation of contaminated soils with heavy metals (Pb, Cd, Mn, and Ni). *Soil and Sediment Contamination: An International Journal*, *30*(2), 163-186.

148. Gu, Y., Wang, P., Kong, C.H., 2009. Urease, invertase, dehydrogenase and polyphenoloxidase activities in paddy soil influenced by allelopathic rice variety. *Eur. J. Soil Biol. 45*, 436-441.

149. Halter, D., Cordi, A., Gribaldo, S., Gallien, S., Goulhen-Chollet, F., Heinrich-Salmeron, A., Carapito, C., Pagnout, C., Montaut, D., Seby, F., Dorsselaer, A.V., Schaeffer, C., Bertin, P.N., Bauda, P., and ArsenePloetze, F., 2011.Taxonomic and functional prokaryote diversity in mildly arsenic-contaminated sediments. Res Microbiol 162, 877–887.

150. Hamad, R., Balzter, H., and Kolo, K. (2019). Assessment of heavy metal release into the soil after mine clearing in Halgurd-Sakran National Park, Kurdistan, Iraq. Environ. Sci. Pollut. Res. 26,1517-1536.

151. Hamdi, H., Benzarti, S., Aoyama, I., and Jedidi, N. (2012). Rehabilitation of degraded soils containing aged PAHs based on phytoremediation with alfalfa (*Medicago sativa* L.). Int. Biodeterior. Biodegrad. 67,40–47.

152. Handelsman, J., 2004. Metagenomics: application of genomics to uncultured microorganisms. Microbiology and molecular biology reviews 68, 669–685.

153. Hashem, A., Abd Allah, E. F., Alqarawi, A. A., al Huqail, A. A., Egamberdieva, D., and Wirth, S. (2016). Alleviation of cadmium stress in *Solanum lycopersicum* L. by arbuscular mycorrhizal fungi via induction of acquired systemic tolerance. Saudi. J. Biol. Sci. 23,272–281.

154. Hassan, A., Azid, A., Hamid, F. S., Pariatamby, A., Ossai, I. C., 2025. Inoculation of arbuscular mycorrhizal fungi improved phytoremediation ability of *Jatropha multifida* L. in metal/metalloid contaminated landfill soil. *Int. J. Environ. Sci. Technol.* 1-26.

155. Hassan, S. E., Hijri, M., and St-Arnaud, M. (2013). Effect of arbuscular mycorrhizal fungi on trace metal uptake by sunflower plants grown on cadmium contaminated soil. N. Biotechnol. 30,780–787.

156. He Y, Yang R, Lei G, Li B, Jiang M, Yan K, Zu Y, Zhan F, Li Y (2020) Arbuscular mycorrhizal fungi reduce cadmium leaching from polluted soils under simulated heavy rainfall. Environ Pollut 263:114406

157. HemmatiTabar, M., ◌́Amanifar, S., Vatankhah, E., Malekzadeh, E., 2023. Effect of *Claroideoglomus etunicatum* inoculation on nickel phytoremediation and uptake of some micronutrients by maize (*Zea mays* L.). *Agric. Eng.* 46(2), 159-177.

158. Herlina, L., Widianarko, B., and Sunoko, H. R. (2020). Phytoremediation Potential of *Cordyline Fruticosa* for Lead Contaminated Soil. J. Pendidik. IPA. Indones. 9,42-49.

159. Hinojosa MB, Carreira JA, García-Ruíz R, Dick RP (2005) Microbial Response to Heavy Metal–Polluted Soils: Community Analysis from Phospholipid-Linked Fatty Acids and Ester-Linked Fatty Acids Extracts. J Environ Qual 34:1789–1800

160. Homa, J., Stürzenbaum, S. R., & Kolaczkowska, E. 2016. Metallothionein 2 and heat shock protein 72 protect Allolobophora chlorotica from cadmium but not nickel or copper exposure: body malformation and coelomocyte functioning. Arch. Environ Contam Toxicol *71*, 267-277.

161. Hou, D., Li, F., 2017. Complexities surrounding China's soil action plan. Land Degrad. Dev. 28, 2315–2320.

162. Hsu, C.-Y., Chiang, H.-C., Chen, M.-J., Chuang, C.-Y., Tsen, C.-M., Fang, G.-C., Tsai, Y.-I., Chen, N.-T., Lin, T.-Y., Lin, S.-L., 2017. Ambient PM2. 5 in the residential area near industrial complexes: Spatiotemporal variation, source apportionment, and health impact. Science of the Total Environment 590, 204–214.

163. Hu J, Wu S, Wu F, Leung HM, Lin X, Wong MH (2013) Arbuscular mycorrhizal fungi enhance both absorption and stabilization of Cd by Alfred stonecrop (*Sedum alfredii* Hance) and perennial ryegrass (*Lolium perenne* L.) in a Cd-contaminated acidic soil. Chemosphere 93:1359–1365

164. Huang, C. C., Cai, L. M., Xu, Y. H., Wen, H. H., Jie, L., Hu, G. C., Chen, L., Wang, H., Xu, X., & Mei, J. X. (2022). Quantitative analysis of ecological risk and human health risk of potentially toxic elements in farmland soil using the PMF model. *Land Degradation & Development*, 33(11), 1954-1967.

165. Huang, J., Wu, Y., Sun, J., Li, X., Geng, X., Zhao, M., Fan, Z., 2021. Health risk assessment of heavy metal (loid) s in park soils of the largest megacity in China by using Monte Carlo simulation coupled with Positive matrix factorization model. J. Hazard. Mat. 415, 125629.

166. Hussain, N., Chatterjee, S.K., Maiti, T.K., Goswami, L., Das, S., Deb, U., Bhattacharya, S.S., 2021. Metal induced non-metallothionein protein in earthworm: a new pathway for cadmium detoxification in chloragogenous tissue. J Hazard Mater 401, 123357.

167. Hussain, N., Das, S., Goswami, L., Das, P., Sahariah, B., Bhattacharya, S.S., 2018. Intensification of vermitechnology for kitchen vegetable waste and paddy straw employing earthworm consortium: assessment of maturity time, microbial community structure, and economic benefit. J Clean Prod 182, 414–426

168. Ibarra, A. A. G., Wrobel, K., Barrientos, E. Y., Escobosa, A. R. C., Corona, J. F. G., Donis, I. E., Wrobel, K. 2019. Impact of Cr (VI) on the oxidation of polyunsaturated fatty acids in Helianthus annuus roots studied by metabolomic tools. Chemosphere 220, 442-451.

169. IBM., 2013. Indian Bureau of Mines, Ferro-Alloys. Indian Bureau of Mines, Ministry of Mines, Government of India.

170. ICDA. (2022). Statistical Bulletin 2022, Istanbul, Turkey.

171. IRIS., 2020. Integrated Risk Information System-Database. US Environmental Protection Agency

172. IS (1993) Drinking water specifications (1st revision). Bureau of Indian Standards (IS 10500), New Delhi, India. www.bis.org.in/ bis/html/10500.html, accessed Feb 2010, p 1–8

173. Jansa, J., Forczek, S. T., Rozmoš, M., Püschel, D., Bukovská, P., Hršelová, H., 2019. Arbuscular mycorrhiza and soil organic nitrogen: network of players and interactions. *Chem. Biol. Technol. Agric.* 6(1), 1-10.

174. Jha, S., Banerjee, S., Ghosh, S., Verma, A., & Bhattacharyya, P. (2024). Appraisal of Heavy Metal Risk Hazards of Eisenia fetida-Mediated Steel Slag Vermicompost on Oryza sativa L.: Insights from Agro-Scale Inspection and Machine Learning Analytics. *Agriculture*, *14*(11), 2020.

175. Jha, S., Banerjee, S., Ghosh, S., Verma, A., Bhattacharyya, P., 2024. Eisenia fetida-driven vermitechnology for the eco-friendly transformation of steel waste slag into organic amendment: An insight through microbial diversity and multi-model approach. Environ Res 251, 118636

176. Jha, S., Verma, A., Bhattacharyya, P., 2023. Assessing the Effectiveness of Vermicomposted Products and Predicting Potential Hazards From Metal Contaminated Steel Waste Through Multi-model Analysis. Water Air Soil Pollut 234, 679.

177. Jia, H., Wang, H., Lu, H., Jiang, S., Dai, M., Liu, J., and Yan, C. (2016). Rhizodegradation potential and tolerance of Avicennia marina (Forsk.) Vierh in phenanthrene and pyrene contaminated sediments. Mar. Pollut. Bull. 110,112–118.

178. Jiang, H. H., Cai, L. M., Hu, G. C., Wen, H. H., Luo, J., Xu, H. Q., Chen, L. G., 2021. An integrated exploration on health risk assessment quantification of potentially hazardous elements in soils from the perspective of sources. Ecotoxicol. Environ. Safety 208, 111489

179. Jin, Y.L., O'Connor, D., Ok, Y.S., Tsang, D.C.W., Liu, A., Hou, D.Y., 2019. Assessment of sources of heavy metals in soil and dust at children's playgrounds in Beijing using GIS and multivariate statistical analysis. Environ. Int. 124, 320–328.

180. Jo and Biswakarma 2021. Nutrition in Jharkhand. Jharkhand CSO forum. https://jharkhandcsoforum.org/Nutration.php

181. Joergensen, R.G., Wu, J., Brookes, P.C., 2011. Measuring soil microbial biomass using an automated procedure. Soil Biol Biochem 43, 873–876

182. Kabata-Pendias, A., 2011. Trace elements in soils and plants/fourth editions. CRC Taylor and Francis Group, Boca Raton, 505.

183. Kahangwa, C. A., 2022. Application of Principal Component Analysis, Cluster Analysis, Pollution Index and Geoaccumulation Index in Pollution Assessment with Heavy Metals from Gold Mining Operations, Tanzania. J. Geosci. Environ. Protec. 10(4), 303-317

184. Kan, X., Dong, Y., Feng, L., Zhou, M., & Hou, H. (2021). Contamination and health risk assessment of heavy metals in China's lead–zinc mine tailings: A meta–analysis. *Chemosphere*, 267, 128909.

185. Kang, C., Wu, P., Li, Y., Ruan, B., Zhu, N., Dang, Z., 2014. Estimates of heavy metal tolerance and chromium (VI) reducing ability of Pseudomonas aeruginosa CCTCC AB93066: chromium (VI) toxicity and environmental parameters optimization. World J. Microbiol. Biotechnol. 30, 2733–2746

186. Kang, J. Y., Teng, C. H., Chen, F. C., 1996. Effect of capsaicin and cimetidine on the healing of acetic acid induced gastric ulceration in the rat. *Gut. 38*, 832-836.

187. Kapoor, R. T., Mfarrej, M. F. B., Alam, P., Rinklebe, J., Ahmad, P., 2022. Accumulation of chromium in plants and its repercussion in animals and humans. Environ. Pollut. 119044

188. Kaur, G., Sharma, R., Singh, K., and Sharma, P. K., 2015. Delineating bacterial community structure of polluted soil samples collected from cancer prone belt of Punjab, India. Biotech 5, 727-734.

189. Keshri, J., Mishra, A., and Jha, B., 2013. Microbial population index and community structure in saline–alkaline soil using gene targeted metagenomics. Microbiol Res 168, 165-173.

190. Keyhaninejad, N., Curry, J., Romero, J., O'Connell, M.A., 2014. Fruit specific variability in capsaicinoid accumulation and transcription of structural and regulatory genes in Capsicum fruit. *Plant. Sci. 215,* 59-68.

191. Khan, M. A., Ding, X., Khan, S., Brusseau, M. L., Khan, A., Nawab, J., 2018. The influence of various organic amendments on the bioavailability and plant uptake of cadmium present in mine-degraded soil. Sci. Total Environ. 636, 810-817.

192. Khan, N. T., Jameel, N., and Khan, M. J. (2018). A brief overview of contaminated soil remediation methods. Biotechnol. Ind. J. 14,171.

193. Khanam, R., Kumar, A., Nayak, A.K., Shahid, Md, Tripathi, R., Vijayakumar, S.,Bhaduri, D., Kumar, U., Mohanty, S., Panneerselvam, P., Chatterjee, D., Satapathy, B.S., & Pathak, H. (2020). Metal(loid)s (As, Hg, Se, Pb and Cd) in paddy soil:bioavailability and potential risk to human health. *Science of the Total Environment*. 699, 134330.

194. Kien, C. N., Noi, N. V., Son, L. T., Ngoc, H. M., Tanaka, S., Nishina, T., and Iwasaki, K. (2010). Heavy metal contamination of agricultural soils around a chromite mine in Vietnam. Soil. Sci. Plant. Nutr. 56,344–356.

195. Kirchman, D. L. 2002. The ecology of Cytophaga–Flavobacteria in aquatic environments. FEMS Microbiol Ecol 39, 91-100.

196. Kizildag, N., Sagliker, H.A., Darici, C., 2013. Nitrogen mineralisation in some saline soils at Eastern Mediterranean coasts, Turkey. Eurasian J Biosci 7, 95–100.

197. Kohzadi, S., Shahmoradi, B., Ghaderi, E., Loqmani, H., Maleki, A., 2019. Concentration, source, and potential human health risk of heavy metals in the commonly consumed medicinal plants. Biol. Trace Element Res. 187(1), 41–50

198. Kormoker, T., Proshad, R., Islam, M.S., Tusher, T.R., Uddin, M., Khadka, S., Chandra, K., Sayeed, A., 2022. Presence of toxic metals in rice with human health hazards in Tangail district of Bangladesh. Int. J. Environ. Health Res. 32 (1), 40–60

199. Kowitwiwat, A., and Sampanpanish, P. (2020). Phytostabilization of arsenic and manganese in mine tailings using *Pennisetum purpureum* cv. Mott supplemented with cow manure and acacia wood-derived biochar. Heliyon. 6,e04552

200. Kuang, J., Huang, L., He, Z., Chen, L., Hua, Z., Jia, P., Li, S., Liu, J., Li, J., Zhou, J., 2016. Predicting taxonomic and functional structure of microbial communities in acid mine drainage. ISME J 10, 1527–1539.

201. Kumar, A., and Maiti, S. K. (2014). Translocation and bioaccumulation of metals in *Oryza sativa* and *Zea mays* growing in chromite-asbestos contaminated agricultural fields, Jharkhand, India. Bull. Environ. Contam. Toxicol. 93,434–441.

202. Kumar, A., Maiti, S., 2015. Assessment of potentially toxic heavy metal contamination in agricultural fields, sediment, and water from an abandoned chromite-asbestos mine waste of Roro hill, Chaibasa, India. Environ. Earth Sci. 74, 2617–2633.

203. Kumar, D., Singh, A., Kumar, P., Jha, R.K., Sahoo, S.K., Jha, V., 2020. Sobol sensitivity analysis for risk assessment of uranium in groundwater. Environ Geochem Health 42, 1789–1801

204. Kumar, S. N., Mishra, B. B., Kumar, S., Mandal, J., 2021. Organo-arsenic complexation studies explaining the reduction of uptake of arsenic in wheat grown with contaminated irrigation water and organic amendments. Water Air Soil Pollut. 232, 118

205. Kumar, S., Banerjee, S., Ghosh, S., Majumder, S., Mandal, J., Roy, P. K., & Bhattacharyya, P. (2024). Appraisal of pollution and health risks associated with coal mine contaminated soil using multimodal statistical and Fuzzy-TOPSIS approaches.

206. Kumari, P. B., Singh, Y. K., Mandal, J., Shambhavi, S., Sadhu, S. K., Kumar, R., Ghosh, M., Raj, A., Singh, M., 2021. Determination of safe limit for arsenic contaminated irrigation water using solubility free ion activity model (FIAM) and Tobit Regression Model. Chemosphere 270, 128630.

207. Kumari, S. M. P., and Prabina, B. J. (2019). Protection of tomato, Lycopersicon esculentum from wilt pathogen, *Fusarium oxysporum* f. sp. lycopersici by arbuscular mycorrhizal fungi, *Glomus* sp. Int. J. Curr. Microbiol. Appl. Sci. 8,1368–1378.

208. Kurdiya, K., Meena, J. K., Khedia, R., Sharma, K. C., & Sharma, M. (2020). Comparative Studies of Effects of Fertilizers and Manures on Biochemical Characteristics of Sesame (Sesamum indicum L.) Plant. *Research Journalr of Agriculturall Science*, *11*, 1266-1271.

209. Lagomarsino, A., Benedetti, A., Marinari, S., Pompili, L., Moscatelli, M.C., Roggero, P.P., Lai, R., Ledda, L., Grego, S., 2011. Soil organic C variability and microbial functions in a Mediterranean agroforest ecosystem. Bio Fertil Soils. 47, 283-291.

210. Lam CM, Lai HY (2018) Effect of inoculation with arbuscular mycorrhizal fungi and blanching on the bioaccessibility of heavy metals in water spinach (*Ipomoea aquatica* Forsk.). Ecotoxicol Environ Saf 162:563–570

211. Łaszczyca, P., Augustyniak, M., Babczyńska, A., Bednarska, K., Kafel, A., Migula, P., Wilczek, G., Witas, I., 2004. Profiles of enzymatic activity in earthworms from zinc, lead and cadmium polluted areas near Olkusz (Poland). Environ Int 30, 901–910.

212. Lazcano, C., Gómez-Brandón, M., & Domínguez, J. (2008). Comparison of the effectiveness of composting and vermicomposting for the biological stabilization of cattle manure. *Chemosphere*, *72*(7), 1013-1019.

213. Lee CG, Chon HT, Jung MC (2001) Heavy metal contamination in the vicinity of the Daduk Au–Ag–Pb–Zn mine in Korea. Appl Geochem 16:1377–1386

214. Li F, Yang F, Chen, Y, Jin H, Leng, Y, Wang J (2020) Chemical reagent-assisted phytoextraction of heavy metals by Bryophyllum laetivirens from garden soil made of sludge. Chemosphere 253:126574

215. Li, F., Li, Z., Mao, P., Li, Y., Li, Y., McBride, M. B., Wu, J., & Zhuang, P. (2019). Heavy metal availability, bioaccessibility, and leachability in contaminated soil: effects of pig manure and earthworms. *Environmental Science and Pollution Research*, 26, 20030-20039.

216. Li, K., Cui, S., Zhang, F., Hough, R., Fu, Q., Zhang, Z., Gao, S., An, L., 2020. Concentrations, possible sources and health risk of heavy metals in multi-media environment of the Songhua River, China. Int. J. Environ. Res. Public Health 17(5), 1766.

217. Li, S., Wu, J., Huo, Y., Zhao, X., and Xue, L., 2021. Profiling multiple heavy metal contamination and bacterial communities surrounding an iron tailing pond in Northwest China. Sci Total Environ 752, 141827.

218. Li, X., Bond, P. L., Van Nostrand, J. D., Zhou, J., and Huang, L., 2015. From lithotroph-to organotroph-dominant: directional shift of microbial community in sulphidic tailings during phytostabilization. Sci Rep 5, 12978

219. Likuku, A.S., Mmolawa, K.B., $ Gaboutloeloe, G.K. (2013). Assessment of heavy metal enrichment and degree of contamination around the copper-nickel mine in the Selebi Phikwe Region, Eastern Botswana. *Environment and Ecology Research. 1,* 32 – 40

220. Limmer, M., and Burken, J. (2016). Phytovolatilization of organic contaminants. Environ. Sci. Technol. 50,6632–6643.

221. Lindsay W L. and Norvell W A. 1978. Development of a DTPA soil test for zinc, iron, manganese and copper. Soil Science Society of America Journal 42 (3): 421–8

222. Lins CEL, Cavalcante UMT, Sampaio EVSB, Messias AS, Maia LC (2006) Growth of mycorrhized seedlings of *Leucaena leucocephala* (Lam.) de Wit. in a copper contaminated soil. Appl Soil Ecol 31:181–185

223. Lipiec, J., Frąc, M., Brzezińska, M., Turski, M., Oszust, K., 2016. Linking microbial enzymatic activities and functional diversity of soil around earthworm burrows and casts. Front Microbiol 7, 1361.

224. Liu L, Gong Z, Zhang Y, Li P (2014) Growth, cadmium uptake and accumulation of maize (*Zea mays* L.) under the effects of arbuscular mycorrhizal fungi. Ecotoxicol 23:1979–1986

225. Liu, A., Hamel, C., Hamilton, R. I., Ma, B. L., Smith, D. L., 2000. Acquisition of Cu, Zn, Mn and Fe by mycorrhizal maize (*Zea mays* L.) grown in soil at different P and micronutrient levels. *Mycorrhiza.* 9, 331-336.

226. Liu, D., Zhang, R., Wu, H., Xu, D., Tang, Z., Yu, G., Xu, Z., Shen, Q., 2011. Changes in biochemical and microbiological parameters during the period of rapid composting of dairy manure with rice chaff. Bioresour Technol 102, 9040–9049.

227. Liu, J., Mo, A., Ni, J., Fan, X., & Jiang, Y. (2023). Selenium Reduces Rice Plant Tissues Cadmium and Increases the Yield, Quality, and Edible Safety of Rice Grain, and May Affect the Taste of Cooked Rice. *Journal of Soil Science and Plant Nutrition*, 1-9.

228. Liu, J., Zheng, Q., Pei, S., Li, J., Ma, L., Zhang, L., Niu, J. & Tian, T. (2024). Ecological and health risk assessment of heavy metals in agricultural soils from northern China. *Environmental Monitoring and Assessment*, *196*(1), pp.1-19.

229. Liu, K., Chen, L., Zhang, W., Lin, K., Zhao, L., 2015. EPR detection of hydroxyl radical generation and oxidative perturbations in lead-exposed earthworms (Eisenia fetida) in the presence of decabromodiphenyl ether. Ecotoxicology 24, 301–308.

230. Liu, L., Liu, Q., Ma, J., Wu, H., Qu, Y., Gong, Y., Yang, S., An, Y, Zhou, Y., 2020. Heavy metal(loid)s in the topsoil of urban parks in Beijing, China: concentrations, potential sources, and risk assessment. Environ. Pollut. 260, 114083.

231. Lopez, S., Goux, X., Echevarria, G., Calusinska, M., Morel, J.L., Benizri, E., 2019. Community diversity and potential functions of rhizosphere-associated bacteria of nickel hyperaccumulators found in Albania. Science of the Total Environment 654, 237–249.

232. Lopez-L ´ opez, ´ A., Yarza, P., Richter, M., Suarez-Su ´ arez, ´ A., Anton, ´ J., Niemann, H., Rossello-M ´ ora, ´ R., 2010. Extremely halophilic microbial communities in anaerobic sediments from a solar saltern. Environ Microbiol Rep 2, 258–271.

233. Lothe, A. G., Hansda, A., and Kumar, V. (2016). Phytoremediation of Copper-Contaminated Soil Using *Helianthus annuus*, *Brassica nigra*, and *Lycopersicon esculentum* Mill.: A Pot Scale Study. Environ. Qual. Manage. 25,63–70.

234. Lowry, O.H., Rosebrough, N.J., Farr, A.L., Randall, R.J., 1951. Protein measurement with the Folin phenol reagent. J biol Chem 193, 265–275

235. Luo, L., Ma, Y., Zhang, S., Wei, D., Zhu, Y. G., 2009. An inventory of trace elements inputs to agricultural soils in China. J. Environ. Manage. 90, 2524–2530.

236. Ma, Q., Qu, Y.Y., Zhang, X.W., Shen, W.L., Liu, Z.Y., Wang, J.W., Zhang, Z.J., Zhou, J.T., 2015. Identification of the microbial community composition and structure of coalmine wastewater treatment plants. Microbiol. Res. 175, 1–5.

237. Ma, Y., Rajkumar, M., Oliveira, R. S., Zhang, C., Freitas, H., 2019. Potential of plant beneficial bacteria and arbuscular mycorrhizal fungi in phytoremediation of metal-contaminated saline soils. *J. Hazard. Mater. 379*, 120813.

238. Macci, C., Doni, S., Peruzzi, E., Masciandaro, G., Mennone, C., Ceccanti, B., 2012. Almond tree and organic fertilization for soil quality improvement in southern Italy. *J. Environ. Manag. 95*, S215-S222.

239. Mackay, J. E., Cavagnaro, T. R., Stöver, D. S. M., Macdonald, L. M., Grønlund, M., Jakobsen, I. 2017. A key role for arbuscular mycorrhiza in plant acquisition of P from sewage sludge recycled to soil. *Soil. Biol. Biochem.* 115, 11-20.

240. Mahammad, S., Islam, A., Shit, P. K., Islam, A. R. M. T., & Alam, E. (2023). Groundwater level dynamics in a subtropical fan delta region and its future prediction using machine learning tools: sustainable groundwater restoration. *Journal of Hydrology: Regional Studies*, 47, 101385.

241. Maity, S., Biswas, R., & Sarkar, A., 2020. Comparative valuation of groundwater quality parameters in Bhojpur, Bihar for arsenic risk assessment. Chemosphere 259, 127398.

242. Mandal, J., Golui, D., Raj, A., Ganguly, P., 2019. Risk assessment of arsenic in wheat and maize grown in organic matter amended soils of Indo-Gangetic plain of Bihar, India. Soil Sediment Cont.: An Int. J. 28(8), 757–772.

243. Manyiwa, T., and Ultra Jr, V. U. (2022). Soil Amendments and Arbuscular Mycorrhiza Influenced the Growth and Heavy Metal Accumulation of *Colosphospermum Mopane* (Kirk Ex Benth.) In Heavy Metal Contaminated Soil. Soil. Sediment. Contam. Int. J. 31,81–96.

244. Medina, A., Vassileva, M., Barea, J. M., Azcón, R., 2006. The growth-enhancement of clover by Aspergillus-treated sugar beet waste and *Glomus mosseae* inoculation in Zn contaminated soil. *Appl. Soil. Ecol.* 33(1), 87-98.

245. Meena, M. L., Gehlot, V. S., Meena, D. C., Kishor, S., Kumar, S., & Meena, J. K. (2017). Impact of Biofertilizers on Growth, Yield and Quality of Tomato (Lycopersicon esculentum Mill) Cv. Pusa Sheetal. Journal of Pharmacognosy and Phytochemistry, 6(4), 1579-1583.

246. Meena, R., Datta, S. P., Golui, D., Dwivedi, B. S., Meena, M. C., 2016. Long-term impact of sewage irrigation on soil properties and assessing risk in relation to transfer of metals to human food chain. Environ. Sci. Pollut. Res. 23(14), 14269–14283.

247. Mehmood, S., Saeed, D. A., Rizwan, M., Khan, M. N., Aziz, O., Bashir, S., ... & Shaheen, A. (2018). Impact of different amendments on biochemical responses of sesame (Sesamum indicum L.) plants grown in lead-cadmium contaminated soil. *Plant Physiology and Biochemistry*, *132*, 345-355.

248. Meyer E, Londoño DMM, de Armas RD, Giachini AJ, Rossi MJ, Stoffel SCG, Soares CRFS (2017) Arbuscular mycorrhizal fungi in the growth and extraction of trace elements by *Chrysopogon zizanioides* (vetiver) in a substrate containing coal mine wastes. Int J Phytoremediation 19:113-120

249. Midhat, L., Ouazzani, N., Hejjaj, A., Ouhammou, A., Mandi, L., 2019. Accumulation of heavy metals in metallophytes from three mining sites (Southern Centre Morocco) and evaluation of their phytoremediation potential. Ecotoxicol Environ Saf 169, 150–160.

250. Mileusnić, M., Mapani, B. S., Kamona, A. F., Ružičić, S., Mapaure, I., Chimwamurombe, P. M., 2014. Assessment of agricultural soil contamination by potentially toxic metals dispersed from improperly disposed tailings, Kombat mine, Namibia. J. Geochem. Exp. 144, 409-420.

251. Mishra, A., Bhattacharya, A., and Mishra, N. (2019). Mycorrhizal symbiosis: An effective tool for metal bioremediation. New and Future Developments in Microbial Biotechnology and Bioengineering, 113–128.

252. Mishra, R., Sinha, V., Kannan, A., Upreti, R.K., 2012. Reduction of chromium-VI by chromium resistant lactobacilli: a prospective bacterium for bioremediation. Toxicol. Int. 19, 25

253. Mitra, D., Uniyal, N., Panneerselvam, P., Senapati, A., and Ganeshamurthy, A. N. (2020). Role of mycorrhiza and its associated bacteria on plant growth promotion and nutrient management in sustainable agriculture. Int. J. Life. Sci. Appl. Sci. 1

254. Mohammadi, K., Khalesro, S., Sohrabi, Y., Heidari, G., 2011. A review: beneficial effects of the mycorrhizal fungi for plant growth. J. Appl. Environ. Biol. Sci. 1(9), 310-319.

255. Mohan D, Pittman Jr CU, Bricka M, Smith F, Yancey B, Mohammad J, Steele PH, Alexandre-Franco MF, Gómez-Serrano V, Gong H (2007) Sorption of arsenic, cadmium, and lead by chars produced from fast pyrolysis of wood and bark during bio-oil production. J Colloid Interface Sci 310:57–73

256. Mondal, A., Das, S., Sah, R. K., Bhattacharyya, P., & Bhattacharya, S. S. (2017). Environmental footprints of brick kiln bottom ashes: Geostatistical approach for assessment of metal toxicity. *Science of the Total Environment,* 609, 215-224.

257. Mondal, A., Goswami, L., Hussain, N., Barman, S., Kalita, E., Bhattacharyya, P., Bhattacharya, S.S., 2020. Detoxification and eco-friendly recycling of brick kiln coal ash using Eisenia fetida: a clean approach through vermitechnology. Chemosphere 244, 125470

258. Moorhead, D.L., Rinkes, Z.L., Sinsabaugh, R.L., Weintraub, M.N., 2013. Dynamic relationships between microbial biomass, respiration, inorganic nutrients and enzyme activities: informing enzyme-based decomposition models. Front Microbiol 4, 223.

259. Moreira, L. J., da Silva, E. B., Fontes, M. P., Liu, X., & Ma, L. Q. (2018). Speciation, bioaccessibility and potential risk of chromium in Amazon forest soils. *Environmental pollution*, 239, 384-391

260. Morikawa, H., and Erkin, Ö. C. (2003) Basic processes in phytoremediation and some applications to air pollution control. Chemosphere. 52,1553–1558.

261. Mridha, D., Ray, I., Sarkar, J., De, A., Joardar, M., Das, A., Roychowdhury, N., Acharya, K., & Roychowdhury, T. (2022). Effect of sulfate application on inhibition of arsenic bioaccumulation in rice (Oryza sativa L.) with consequent health risk assessment of cooked rice arsenic on human: A pot to plate study. *Environmental Pollution*, 293, 118561.

262. Mubeen, H., Hatti, S.S., 2018. Earthworms diversity of Koppal district with the updated information on genus Thatonia of Hyderabad–Karnataka region, Karnataka, India. J Asia Pac Biodivers 11, 482–493.

263. Mukherjee, P., Dutta, J., Roy, M., Thakur, T. K., & Mitra, A. (2024). Plant growth-promoting rhizobacterial secondary metabolites in augmenting heavy metal (loid) phytoremediation: An integrated green in situ ecorestorative technology. *Environmental Science and Pollution Research*, *31*(44), 55851-55894.

264. Mwirichia, R., Cousin, S., Muigai, A. W., Boga, H. I., and Stackebrandt, E., 2011. Bacterial diversity in the haloalkaline Lake Elmenteita, Kenya. Curr Microbiol 62, 209-221.

265. Najmeddin, A., Keshavarzi, B., Moore, F., Lahijanzadeh, A., 2018. Source apportionment and health risk assessment of potentially toxic elements in road dust from urban industrial areas of Ahvaz megacity Iran. Environ. Geochem. Health 40(4), 1187–1208.

266. Nakagawa, K., Yu, Z., Berndtsson, R., Hosono, T., 2020. Temporal characteristics of groundwater chemistry affected by the 2016 Kumammoto earthquake using Self-organizing maps. J. Hydrol. 582, 124519.

267. Nakamura, S., Cui, J., Zhang, X., Yang, F., Xu, X., Sheng, H., & Ohtsubo, K. I. (2016). Comparison of eating quality and physicochemical properties between Japanese and Chinese rice cultivars. *Bioscience, Biotechnology, and Biochemistry*, 80(12), 2437-2449.

268. Nakmee, P. S., Techapinyawat, S., and Ngamprasit, S. (2016). Comparative potentials of native arbuscular mycorrhizal fungi to improve nutrient uptake and biomass of Sorghum bicolor Linn. Agric. Nat. Resour. 50,173–178.

269. Nanjundappa, A., Bagyaraj, D. J., Saxena, A. K., Kumar, M., Chakdar, H., 2019. Interaction between arbuscular mycorrhizal fungi and *Bacillus* spp. in soil enhancing growth of crop plants. *Fungal. Boil. Biotechnol.* 6(1), 23.

270. Nannipieri, P., Ascher, J., Ceccherini, M., Landi, L., Pietramellara, G., Renella, G., 2017. Microbial diversity and soil functions. *Eur. J. Soil Sci. 68*(1), 12-26.

271. Nannoni, F., Protano, G., Riccobono, F., 2011. Uptake and bioaccumulation of heavy elements by two earthworm species from a smelter contaminated area in northern Kosovo. Soil Biol Biochem 43, 2359–2367.

272. Narendrula-Kotha, R., and Nkongolo, K. K., 2017. Bacterial and fungal community structure and diversity in a mining region under long-term metal exposure revealed by metagenomics sequencing. Ecol Genet Genom 2, 13-24

273. Navarro-Noya, Y. E., Jan-Roblero, J., del Carmen González-Chávez, M., Hernández-Gama, R., and Hernández-Rodríguez, C., 2010. Bacterial communities associated with the rhizosphere of pioneer plants (*Bahia xylopoda* and *Viguiera linearis*) growing on heavy metals-contaminated soils. Antonie Van Leeuwenhoek 97, 335-349.

274. Nawab, J., Ghani, J., Khan, S., Xiaoping, W., 2018. Minimizing the risk to human health due to the ingestion of arsenic and toxic metals in vegetables by the application of biochar, farmyard manure and peat moss. J. Environ. Manage. 214, 172-183.

275. Nawab, J., Khan, N., Ahmed, R., Khan, S., Ghani, J., Rahman, Z., Khan, F., Wang, X., Muhammad, J., Sher, H., 2019. Influence of different organic geo-sorbents on Spinacia oleracea grown in chromite mine-degraded soil: a greenhouse study. J. Soils Sediments 19, 2417-2432.

276. Nawab, J., Khan, S., Shah, M.T., Khan, K., Huang, Q., Ali, R., 2015. Quantification of heavy metals in mining affected soil and their bioaccumulation in native plant species. Int. J. Phyt., 17, 801–813.

277. Nawab, J., Li, G., Khan, S., Sher, H., Aamir, M., Shamshad, I., Khan, A., Khan, M. A., 2016. Health risk assessment from contaminated foodstuffs: a field study in chromite mining-affected areas northern Pakistan. Environ. Sci. Pollut. Res. 23, 12227-12236.

278. Neisi, A., Farhadi, M., Angali, K. A., & Sepahvand, A. (2024). Health risk assessment for consuming rice, bread, and vegetables in Hoveyzeh city. *Toxicology Report,* 12, 260-265.

279. Nielsen, S., Minchin, T., Kimber, S., Zwieten, L., Gilbert, J., Munroe, P., Joseph, S., and Thomas, T., 2014. Comparative analysis of the microbial communities in agricultural soil amended with enhanced biochars or traditional fertilizers. Agric Ecosyst Environ 191,73–82.

280. Nordlund, S., and Ludden, P.W., 2004. Post-translational regulation of nitrogenase in photosynthetic bacteria. In Genetics and regulation of nitrogen fixation in free-living bacteria. Dordrecht: Springer Netherlands. 175-196.

281. Nosrati K, Collins AL (2019) A soil quality index for evaluation of degradation under land use and soil erosion categories in a small mountainous catchment, Iran. J Mt Sci 16:2577–2590

282. Nossent, J., Elsen, P., Bauwens, W., 2011. Sobol'sensitivity analysis of a complex environmental model. *Environ. Model. Softw.* 26(12), 1515-1525

283. Olaniran, A.O., Balgobind, A., Pillay, B., 2013. Bioavailability of heavy metals in soil: impact on microbial biodegradation of organic compounds and possible improvement strategies. Int J Mol Sci 14, 10197–10228.

284. Oluwasola, H., Oluoye, O., Mohammad Bashir, S., Odewole, O. A., Onyeka Abugu, H., Akpomie, K. G., Aishatu Umar, M., 2021. Geochemical and health risk assessment of heavy metals concentration in soils around Oke-Ere mining area in Kogi State, Nigeria. Int. J. Environ. Anal. Chem. 103, 1-16.

285. Omeka, M. E., Igwe, O., Unigwe, C. O., 2022. An integrated approach to the bioavailability, ecological, and health risk assessment of potentially toxic elements in soils within a barite mining area, SE Nigeria. Environ. Monit. Assess. 194(3), 1-30

286. Onuoha, S. C., Anelo, P. C., Nkpaa, K. W., 2016. Human health risk assessment of heavy metals in snail (*Archachatina marginata*) from four contaminated regions in Rivers State, Nigeria. Am. Chem Sci J, 11(2), 1–8

287. Orłowska, E., Przybyłowicz, W., Orlowski, D., Turnau, K., and Mesjasz-Przybyłowicz, J. (2011). The effect of mycorrhiza on the growth and elemental composition of Ni-hyperaccumulating plant *Berkheya coddii* Roessler. Environ. Pollut. 159,3730–3738.

288. Oshunsanya, Suarau. Odutola., Yong, Li., Hanqing, Yu., 2019. "Vetiver grass hedgerows significantly reduce nitrogen and phosphorus losses from fertilized sloping lands." *Sci. Total Environ.* 661 86-94.

289. Ostad-Ali-Askari, K., Shayannejad, M., & Ghorbanizadeh-Kharazi, H. (2017). Artificial neural network for modeling nitrate pollution of groundwater in marginal area of Zayandeh-rood River, Isfahan, Iran. *KSCE Journal of Civil Engineering*, 21, 134-140.

290. Ozyhar, T., Marchi, M., Facciotto, G., Bergante, S., Luster, J., 2022. Combined application of calcium carbonate and NPKS fertilizer improves early-stage growth of poplar in acid soils. For Ecol Manage 514, 120211.

291. Page, A.L., Miller, R.H., Keeney, D.R., 1982. Methods of Soil Analysis. Part 2. SSSA, Madison, WI.

292. Page, V., Feller, U., 2015. Heavy metals in crop plants: transport and redistribution processes on the whole plant level. Agronomy 5, 447–463.

293. Pandey, B., Singh, S., Roy, L. B., Shekhar, S., Singh, R. K., Prasad, B., Singh, K. K. K., 2021. Phytostabilization of coal mine overburden waste, exploiting the phytoremedial efficacy of lemongrass under varying level of cow dung manure. *Ecotoxicol. Environ. Saf.* 208, 111757

294. Parniske, M. (2008). Arbuscular mycorrhiza: the mother of plant root endosymbioses. Nat. Rev. Microbiol. 6,763–775.

295. Patra, D. K., Pradhan, C., & Patra, H. K. (2018). An in situ study of growth of Lemongrass Cymbopogon flexuosus (Nees ex Steud.) W. Watson on varying concentration of Chromium (Cr+ 6) on soil and its

bioaccumulation: Perspectives on phytoremediation potential and phytostabilisation of chromium toxicity. *Chemosphere*, *193*, 793-799.

296. Paul, D., Kumbhare, S.V., Mhatre, S.S., Chowdhury, S.P., Shetty, S.A., Marathe, N. P., Shouche, Y.S., 2016. Exploration of microbial diversity and community structure of Lonar Lake: the only hypersaline meteorite crater lake within basalt rock. Frontiers microbiol 6, 1553.
297. Paul, S., Goswami, L., Pegu, R., Bhattacharya, S.S., 2020. Vermiremediation of cotton textile sludge by Eudrilus eugeniae: Insight into metal budgeting, chromium speciation, and humic substance interactions. Bioresour Technol 314, 123753.
298. Pei, Y., Yu, Z., Ji, J., Khan, A., Li, X., 2018. Microbial community structure and function indicate the severity of chromium contamination of the Yellow River. Frontiers microbiol 9, 38.
299. Peralta-Videa J.R, Lopez ML, Narayan M, Saupe G, Gardea-Torresdey J (2009) The biochemistry of environmental heavy metal uptake by plants: implications for the food chain. Int J Biochem Cell Biol 41:1665–1677
300. Pereira, L. B., Vicentini, R., and Ottoboni, L. M., 2014. Changes in the bacterial community of soil from a neutral mine drainage channel. PLoS One 9, e96605.
301. Pérez-López, A. J., del Amor, F. M., Serrano-Martínez, A., Fortea, M. I., Núñez-Delicado, E., 2007. Influence of agricultural practices on the quality of sweet pepper fruits as affected by the maturity stage. *J. Sci. Food. Agric. 87*(11), 2075-2080.
302. Perronnet, K., Schwartz, C., Gérard, E., and Morel, J. L. (2000). Availability of cadmium and zinc accumulated in the leaves of *Thlaspi caerulescens* incorporated into soil. Plant. Soil. 227, 257-263.
303. Peter, L., Clausen, W., Broholm, M. M., Gosewinkel, U., and Trapp, S. (2017). Test of aerobic TCE degradation by willows (Salix viminalis) and willows inoculated with TCE-cometabolizing strains of *Burkholderia cepacia*. Environ. Sci. Pollut. Res. 24,18320–18331.
304. Phillips, J. M., Hayman, D. S., 1970. Improved procedures for clearing roots and staining parasitic and vesicular-arbuscular mycorrhizal fungi for rapid assessment of infection. *Trans. Br. Mycol. Soc.* 55(1), 158-IN18
305. Piearce, T. G., Oates, K., & Carruthers, W. J. (1990). A fossil earthworm embryo (Oligochaeta) from beneath a Late Bronze Age midden at Potterne, Wiltshire, UK. Journal of Zoology. 220: 537–542
306. Pirsaheb, M., Hadei, M., & Sharafi, K. (2021). Human health risk assessment by Monte Carlo simulation method for heavy metals of commonly consumed cereals in Iran-Uncertainty and sensitivity analysis. *Journal of food composition and analysis*, 96, 103697.
307. Prasad, B. C. N., Shrivastava, R., Ravishankar, G.A., 2005. Capsaicin: a promising multifaceted drug from *Capsicum* spp. *Evidence-Based Integrative Medicine*, *2*, 147-166.
308. Proshad, R., Islam, M., Idris, A. M., 2022. Uncertainty Analysis in Receptor Model with Sources Identification and Risks Apportionment of Toxic Metal (oid) s in Agricultural Soils Around Industrial Areas in Bangladesh. Water Air Soil Pollut. 233(8), 1-26.
309. Pugnaloni, A., Giantomassi, F., Lucarini, G., Capella, S., Bloise, A., di Primio, R., and Belluso, E. (2013). Cytotoxicity induced by exposure to natural and synthetic tremolite asbestos: an in vitro pilot study. Acta. Histochem. 115,100–112.
310. Pulford, I. D., Watson, C., and McGregor, S. D. (2001). Uptake of chromium by trees: prospects for phytoremediation. Environ. Geochem. Health. 23,307–311.
311. Punamiya, P., Datta, R., Sarkar, D., Barber, S., Patel, M., and Das, P. (2010). Symbiotic role of *Glomus mosseae* in phytoextraction of lead in vetiver grass [*Chrysopogon zizanioides* (L.)]. J. Hazard. Mater. 177,465–474.
312. Qing, X., Yutong, Z., & Shenggao, L. (2015). Assessment of heavy metal pollution and human health risk in urban soils of steel industrial city (Anshan), Liaoning, Northeast China. *Ecotoxicology and environmental safety,* 120, 377-385.

313. Quideau, S.A., McIntosh, A.C.S., Norris, C.E., Lloret, E., Swallow, M.J.B., Hannam, K., 2016. Extraction and analysis of microbial phospholipid fatty acids in soils. J Vis Exp.

314. Raj, D., Kumar, A., Maiti, S. K., 2022. Health Risk Assessment of Children Exposed to the Soil Containing Potentially Toxic Elements: A Case Study from Coal Mining Areas. Metals 12(11), 1795.

315. Ramnarain, Y.I., Ansari, A.A., Ori, L., 2019. Vermicomposting of different organic materials using the epigeic earthworm Eisenia foetida. International Journal of Recycling of Organic Waste in Agriculture 8, 23–36.

316. Ramnarain, Y.I., Ansari, A.A., Ori, L., 2019. Vermicomposting of different organic materials using the epigeic earthworm Eisenia foetida. Int. J. Recycl. Org. Waste Agric. 8, 23–36.

317. Ramsey, P.W., Rillig, M.C., Feris, K.P., Holben, W.E., Gannon, J.E., 2006. Choice of methods for soil microbial community analysis: PLFA maximizes power compared to CLPP and PCR-based approaches. Pedobiologia (Jena) 50, 275–280.

318. Rasheed, F., Zafar, Z., Waseem, Z. A., Rafay, M., Abdullah, M., Salam, M. M. A., Mohsin, M., and Khan, W. R. (2020). Phytoaccumulation of Zn, Pb, and Cd in *Conocarpus lancifolius* irrigated with wastewater: does physiological response influence heavy metal uptake. Int. J. Phytoremediation. 22,287-294.

319. Ravindran, B., Wong, J. W. C., Selvam, A., & Sekaran, G. (2016). Influence of microbial diversity and plant growth hormones in compost and vermicompost from fermented tannery waste. Bioresource Technology. 217:200–204.

320. Reichl, C., Schatz, M., and Zsak, G. (2020). World mining data 2020. Federal Ministry of Agriculture, Regions and Tourism: Vienna, Austria, 35:265.

321. Rengasamy, P., 2002. Clay dispersion. In 'Soil physical measurement and interpretation for land evaluation'.(Eds BM McKenzie, K Coughlan, H Cresswell) pp. 200–210.

322. Rengasamy, P., 2006. Soil salinity and sodicity. Growing crops with reclaimed wastewater 125–138.

323. Rengasamy, P., Greene, R.S.B., Ford, G.W., 1986. Influence of magnesium on aggregate stability in sodic red-brown earths. Soil Research 24, 229–237.

324. Rengasamy, P., Marchuk, A., 2011. Cation ratio of soil structural stability (CROSS). Soil Res 49, 280-285

325. Riesenfeld, C.S., Schloss, P.D., Handelsman, J., 2004. Metagenomics: genomic analysis of microbial communities. Annu. Rev. Genet. 38, 525–552.

326. Robinson, B. H., Leblanc, M., Petit, D., Brooks, R. R., Kirkman, J. H., and Gregg, P. E. (1998). The potential of Thlaspi caerulescens for phytoremediation of contaminated soils. Plant. Soil. 203,47-56.

327. Roy, A., Bhattacharya, T., 2022. Ecological and human health risks from pseudo-total and bio-accessible metals in street dusts. Environ. Monit. Assess. 194(2), 1-26.

328. Roy, M., Pandey, V. C., 2020. Role of microbes in grass-based phytoremediation. Phytoremediation Potential of Perennial Grasses. Elsevier, Amsterdam, 303–327.

329. Roy, S., Sarkar, D., Datta, R., Bhattacharya, S.S., Bhattacharyya, P., 2022. Assessing the arsenic-saturated biochar recycling potential of vermitechnology: Insights on nutrient recovery, metal benignity, and microbial activity. *Chemosphere*, *286*, 131660.

330. Rusinowski, S., Szada-Borzyszkowska, A., Zieleźnik-Rusinowska, P., Małkowski, E., Krzyżak, J., Woźniak, G., Sitko, K., Szopiński, M., McCalmont, J. P., Kalaji, H. M., Pogrzeba, M., 2019. How autochthonous microorganisms influence physiological status of *Zea mays* L. cultivated on heavy metal contaminated soils?. *Environ. Sci. Pollut. Res. 26*, 4746-4763.

331. Sahariah, B., Das, S., Goswami, L., Paul, S., Bhattacharyya, P., & Bhattacharya, S. S. (2020). An avenue for replacement of chemical fertilization under rice-rice cropping pattern: Sustaining soil health and organic C pool via MSW-based vermicomposts. *Archives of Agronomy and Soil Science*, *66*(10), 1449-1465.

332. Sahariah, B., Goswami, L., Kim, K.-H., Bhattacharyya, P., Bhattacharya, S.S., 2015. Metal remediation and biodegradation potential of earthworm species on municipal solid waste: A parallel analysis between *Metaphire posthuma* and *Eisenia fetida*. Bioresour Technol 180, 230–236

333. Saif-Ud-Din, A. S., Hussain, S., Hussain, J., Luqman, M., Hussain, J., & Ali, S. (2022). Evaluation of heavy metal contamination in indigenous fruits and associated human health risk: evidence from Fuzzy-TOPSIS approach. *Glob. NEST*. J 24, 435-444.

334. Sakakibara, M., Watanabe, A., Inoue, M., Sano, S., and Kaise, T. (2010). Phytoextraction and phytovolatilization of arsenic from as-contaminated soils by Pteris vittata. Proc. Annu. Int. Conf. Soils. Sediments. Water. Energy. 12,26.

335. Salari, H., Amooaghaie, R., Mozafari, H., Ghorbanpour, M., Sedaghati, E., 2024. Impact of two arbuscular mycorrhizal fungi species on arsenic tolerance and accumulation in safflower (*Carthamus tinctorius* L.). *BMC Plant Biol. 24*(1), 1-17.

336. Saminathan, S. K., Sarkar, D., Andra, S. S., & Datta, R. (2010). Lead fractionation and bioaccessibility in contaminated soils with variable chemical properties. *Environmental Pollutants & Bioavailability*, 22(4), 215. https://doi.org/558424a108ae7bc2f4481ede

337. Samira, A., Woldetsadik, K., Workneh, T.S., 2013. Postharvest quality and shelf life of some hot pepper varieties. *J. Food. Sci. Technol. 50*, 842-855.

338. Sand, S., Concha, G., Öhrvik, V., & Abramsson, L. (2015). Inorganic arsenic in rice and rice products on the Swedish market. *National Food Agency*, Livsmedelsverket (rapport nr 16/2015a).

339. Saran, A., Fernandez, L., Cora, F., Savio, M., Thijs, S., Vangronsveld, J., and Merini, L. J. (2020). Phytostabilization of Pb and Cd polluted soils using Helianthus petiolaris as pioneer aromatic plant species. Int. J. Phytoremediation. 22,459–467.

340. Sarkar, D., & Datta, R. (2003). A modified in-vitro method to assess bioavailable arsenic in pesticide-applied soils. *Environmental Pollution*, 126(3), 363-366.

341. Sarkar, S., Ghosh, S., Banerjee, S., & Bhattacharyya, P. (2023). Evaluation of oil sludge vermicompost for integrated nutrient management in rain fed wetland rice (Oryza sativa L.): SAMOE, FIAM and Fuzzy TOPSIS approach.

342. Sarma, H., Narayan, M., Peralta-Videa, J.R., Lam, S.S., 2022. Exploring the significance of nanomaterials and organic amendments—Prospect for phytoremediation of contaminated agroecosystem. Environmental Pollution 308, 119601.

343. Schindler, F. V., Mercer, E. J., and Rice. J. A. (2007). Chemical characteristics of glomalin-related soil protein (GRSP) extracted from soils of varying organic matter content. Soil. Biol. Biochem. 39,320–329.

344. Schloter, M., Dilly, O., Munch, J.C., 2003. Indicators for evaluating soil quality. Agric Ecosyst Environ 98, 255–262.

345. Schneegurt MA, Jain JC, Menicucci JA, Brown SA, Kemner KM, Garofalo DF, Quallick MR, Neal CR, Kulpa CF (2001) Biomass byproducts for the remediation of wastewaters contaminated with toxic metals. Environ Sci Technol 35:3786–3791

346. Schnrer, J., Rosswall, T., 1982. Fluorescein diacetate hydrolysis as a measure of total microbial activity in soil and litter. Appl. Environ. Microbiol. 43, 1256-1261.

347. Seleiman, M.F., Ali, S., Refay, Y., Rizwan, M., Alhammad, B.A., El-Hendawy, S.E., 2020. Chromium resistant microbes and melatonin reduced Cr uptake and toxicity, improved physio-biochemical traits and yield of wheat in contaminated soil. Chemosphere 250, 126239.

348. Sengupta, S., Bhattacharyya, K., Mandal, J., Bhattacharya, P., Halder, S., Pari, A., 2021. Deficit irrigation and organic amendments can reduce dietary arsenic risk from rice: Introducing machine learning-based prediction models from field data. Agric. Ecosyst. Environ. 319, 107516.

349. Setia, R., Dhaliwal, S. S., Singh, R., Kumar, V., Taneja, S., Kukal, S. S., & Pateriya, B. (2021). Phytoavailability and human risk assessment of heavy metals in soils and food crops around Sutlej river, India. *Chemosphere*, 263, 128321.

350. Shahid, M., Dumat, C., Khalid, S., Schreck, E., Xiong, T., Niazi, N.K., 2017. Foliar heavy metal uptake, toxicity and detoxification in plants: A comparison of foliar and root metal uptake. *J. Hazard. Mater. 325*, 36-58.

351. Shanker, A. K., Cervantes, C., Loza-Tavera, H., and Avudainayagam, S. (2005). Chromium toxicity in plants. Environ. Int. 31,739–753.

352. Shao, Y., Xu, X., Wang, L., Han, J., Katuwal, H. B., Jiao, S., & Qiu, G. (2023). Human dietary exposure to heavy metals via rice in Nepal. *International Journal of Environmental Research and Public Health*, 20(5), 4134.

353. Sharma, S., Pradhan, K., Satya, S., Vasudevan, P., & Khas, H. (2005). Potentiality of Earthworms for Waste Management and in Other Uses - A Review. Journal of American Science. 1.

354. Shi, Z., Cao, Z., Qin, D., Zhu, W., Wang, Q., Li, M., Wang, G., 2013. Correlation models between environmental factors and bacterial resistance to antimony and copper. PLoS One 8, e78533.

355. Shieh, J. I., Wu, H. H., & Huang, K. K. (2010). A DEMATEL method in identifying key success factors of hospital service quality. Knowledge-Based Systems, 23(3), 277-282.

356. Shrestha, B., Lipe, S., Johnson, K. A., Zhang, T. Q., Retzlaff, W., and Lin, Z. (2006). Soil hydraulic manipulation and organic amendment for the enhancement of selenium volatilization in a soil-pickleweed system. Plant. Soil. 288,189–196.

357. Singh, G., Pankaj, U., Chand, S., Verma, R. K., 2019. Arbuscular mycorrhizal fungi-assisted phytoextraction of toxic metals by *Zea mays* L. from tannery sludge. *Soil. Sediment. Contam.* 28(8), 729-746.

358. Singh, P. K., Singh, M., and Vyas, D. (2010). Biocontrol of fusarium wilt of chickpea using arbuscular mycorrhizal fungi and *Rhizobium leguminosorum* biovar. Caryologia. 63,349–353.

359. Singh, S., Mishra, H., Suprasanna, P., 2021. Evaluation of arsenic remediation, morphological and biochemical response by *Vetiveria zizanoides* L. plants grown on artificially arsenic contaminated soil: A field study. *Ecol. Eng.* 168, 106267.

360. Siyar, R., Ardejani, F. D., Farahbakhsh, M., Norouzi, P., Yavarzadeh, M., & Maghsoudy, S. (2020). Potential of Vetiver grass for the phytoremediation of a real multi-contaminated soil, assisted by electrokinetic. Chemosphere, 246, 125802.

361. SLUSI., 2013. Annual Report. Soil and Land Use Survey of India, Ministry of Agriculture and Farmers Welfare, IARI, New Delhi, p. 112

362. Smiles, D.E., Smith, C.J., 2004. A survey of the cation content of piggery effluents and some consequences of their use to irrigate soils. Soil Research 42, 231–246.

363. Smith, S, E., and Smith, F. A. (2011). Roles of arbuscular mycorrhizas in plant nutrition and growth: new paradigms from cellular to ecosystem scales. Annu, Rev. Plant. Biol. 62,227–250.

364. Smith, S. E., and Read, D. J. (2010). Mycorrhizal symbiosis. Academic press.

365. Solís-Domínguez, F. A., Valentín-Vargas, A., Chorover, J., and Maier, R. M. (2011). Effect of arbuscular mycorrhizal fungi on plant biomass and the rhizosphere microbial community structure of mesquite grown in acidic lead/zinc mine tailings. Sci. Total. Environ. 409,1009–1016.

366. Spagnoletti, F. N., Cornero, M., Chiocchio, V., Lavado, R. S., and Roberts, I. N. (2020). Arbuscular mycorrhiza protects soybean plants against Macrophomina phaseolina even under nitrogen fertilization. Eur. J. Plant. Pathol. 156,839–849

367. Stürzenbaum, S.R., Höckner, M., Panneerselvam, A., Levitt, J., Bouillard, J.S., Taniguchi, S., Dailey, L.A., Khanbeigi, R.A., Rosca, E. V, Thanou, M., 2013. Biosynthesis of luminescent quantum dots in an earthworm. Nat Nanotechnol 8, 57–60.

368. Suleiman, H., Rorat, A., Grobelak, A., Grosser, A., Milczarek, M., Płytycz, B., Kacprzak, M., Vandenbulcke, F., 2017. Determination of the performance of vermicomposting process applied to

sewage sludge by monitoring of the compost quality and immune responses in three earthworm species: Eisenia fetida, Eisenia andrei and Dendrobaena veneta. Bioresour Technol 241, 103–112.

369. Sun, B., Zhang, L., Yang, L., Zhang, F., and Norse, D. (2012). Agricultural non-point source pollution in China: Causes and mitigation measures. AMBIO. 41,370–379.
370. Sun, Y., Xie, Z., Li, J., Xu, J., Chen, Z., & Naidu, R. (2006). Assessment of toxicity of heavy metal contaminated soils by the toxicity characteristic leaching procedure. *Environmental Geochemistry and Health,* 28, 73-78.
371. Suthar, S., Mutiyar, P. K. & Singh, S. Vermicomposting of milk processing industry sludge spiked with plant wastes. Bioresour. Technol. 116: 214–219, 2012.
372. Taghavi, M., Bakhshi, K., Zarei, A., Hoseinzadeh, E., & Gholizadeh, A. (2024). Soil pollution indices and health risk assessment of metal (loid) s in the agricultural soil of pistachio orchards. *Scientific Reports*, 14(1), 8971. https://doi.org/10.1038/s41598-024-59450-4
373. Tahir, A., Afzal, I., Khalid, E., Razzaq, M., & Arif, M. A. R. (2023). Rice seed longevity in the context of seed moisture contents and hypoxic conditions in the storage environment. *Seed Science Research*, *33*(1), 39-49.
374. Tang, J., Zhang, J., Ren, L., Zhou, Y., Gao, J., Luo, L., Yang, Y., Peng, Q., Huang, H., Chen, A., 2019. Diagnosis of soil contamination using microbiological indices: A review on heavy metal pollution. J Environ Manage 242, 121–130.
375. Tangahu, B. V., Sheikh Abdullah, S. R., Basri, H., Idris, M., Anuar, N., and Mukhlisin, M. (2011). A review on heavy metals (As, Pb, and Hg) uptake by plants through phytoremediation. Int. J. Chem. Eng. 1-31.
376. Taylor, R. (1990). Interpretation of the correlation coefficient: a basic review. *Journal of diagnostic medical sonography,* 6(1), 35-39.
377. TCLP, U., (1990). EPA method 1311. Washington, US.
378. Tebo, B.M., Davis, R.E., Anitori, R.P., Connell, L.B., Schiffman, P., Staudigel, H., 2015. Microbial communities in dark oligotrophic volcanic ice cave ecosystems of Mt. Erebus, Antarctica. Front Microbiol 6,1–14
379. Tejada, M., Gómez, I., Hernández, T., García, C., 2010. Utilization of vermicomposts in soil restoration: effects on soil biological properties. Soil Science Society of America Journal 74, 525–532.
380. Tessier, A. N. D. R. E., Campbell, P. G., & Bisson, M. A. R. C. (1982). Particulate trace metal speciation in stream sediments and relationships with grain size: implications for geochemical exploration. *Journal of Geochemical Exploration*, *16*(2), 77-104
381. Thatoi, H., Das, S., Mishra, J., Rath, B. P., and Das, N. (2014). Bacterial chromate reductase, a potential enzyme for bioremediation of hexavalent chromium: a review. J. Environ. Manage. 146,383–399.
382. Tian, S.H., Liang, T., Li, K.X., Wang, L.Q., 2018. Source and path identification of metals pollution in a mining area by PMF and rare earth element patterns in road dust. Sci. Total Environ. 633, 958–966
383. Tigist, M., Workneh, T.S., Woldetsadik, K., 2013. Effects of variety on the quality of tomato stored under ambient conditions. *J. Food. Sci. Technol. 50*, 477-486.
384. Tong, R., Cheng, M., Yang, X., Yang, Y., Shi, M., 2019. Exposure levels and health damage assessment of dust in a coal mine of Shanxi Province, China. Process Saf. Environ. Protec. 128, 184–192.
385. Treseder, K. K., Holden, S. R., 2013. Fungal carbon sequestration. *Science*, 339(6127), 1528-1529.
386. Tripathi, S., Chakraborty, A., Chakrabarti, K., and Bandyopadhyay, B. K., 2007. Enzyme activities and microbial biomass in coastal soils of India. Soil Biol Biochem, 39, 2840-2848.
387. Tripathy, S., Bhattacharyya, P., Mohapatra, R., Som, A., Chowdhury, D., 2014. Influence of different fractions of heavy metals on microbial ecophysiological indicators and enzyme activities in century old municipal solid waste amended soil. Ecol Eng 70, 25–34.
388. Tripodi, P., Ficcadenti, N., Rotino, G.L., Festa, G., Bertone, A., Pepe, A., Caramanico, R., Migliori, C. A., LoScalzo, R., 2019. Genotypic and environmental effects on the agronomic, health-related

compounds and antioxidant properties of chilli peppers for diverse market destinations. *J. Sci. Food. Agric. 99*, 4550-4560.

389. Turner, M. A., and Rust, R. H. (1971). Effects of chromium on growth and mineral nutrition of soybeans. Soil. Sci. Soc. Am. J. 35,755–758.
390. Turrión, M. B., Lafuente, F., Mulas, R., López, O., Ruipérez, C., & Pando, V. (2012). Effects on soil organic matter mineralization and microbiological properties of applying compost to burned and unburned soils. *Journal of environmental management*, *95*, S245-S249.
391. Ugbede, F. O., Akpolile, A. F., Oladele, B. B., Agbajor, G. K., & Popoola, F. A. (2024). Ingestion exposure and committed health risk of natural radioactivity and toxic metals in local rice sold in Enugu urban markets. *International Journal of Environmental Analytical Chemistry*, 104(5), 1202-1222.
392. USEPA (United States Environmental Protection Agency). 2021 Region 3, Hazardous Waste Management Division, Office of Superfund Programs,1650 Arch St. Philadelphia, PA 19103-2029, EPA903-F-94-001 - February 1994.Original Author: Dr. Roy L. Smith, retired EPA. https://www.epa.gov/risk/use-monte-carlo-simulation-risk-assessments
393. USEPA, 1989. Risk assessment guidance for superfund. *Human Health Evaluation*. part A. 1, 1–74
394. USEPA., 2014. EPA Positive Matrix Factorization (PMF) 5.0 Fundamentals and User Guide. U.S. Environment Protection Agency (Washington DC).
395. Valenzuela-Encinas, C., Neria-González, I., Alcántara-Hernández, R. J., Estrada-Alvarado, I., Zavala-Díaz de la Serna, F. J., Dendooven, L., and Marsch, R., 2009. Changes in the bacterial populations of the highly alkaline saline soil of the former lake Texcoco (Mexico) following flooding. Extremophiles 13, 609-621.
396. Valverde, A., Tuffin, M., and Cowan, D.A., 2012. Biogeography of bacterial communities in hot springs: a focus on the actinobacteria. Extremophiles 16, 669-679.
397. Vasseur, P., Bonnard, M., 2014. Ecogenotoxicology in earthworms: a review. Curr Zool 60, 255–272.
398. Vaverková MD, Maxianová A, Winkler J, Adamcová D, Podlasek A (2019) Environmental consequences and the role of illegal waste dumps and their impact on land degradation. Land Use Policy 89
399. Verma, R., Kumar, D., Nagraik, R., Sharma, A., Tapwal, A., Puri, S., Kumar, H., Kumari, A., Nepovimova, E., & Kuca, K. (2021). Mycorrhizal inoculation impact on Acorus calamus L.-An ethnomedicinal plant of western Himalaya and its in silico studies for anti-inflammatory potential. *Journal of ethnopharmacology*, *265*, 113353.
400. Vig, A.P., Singh, J., Wani, S.H., Dhaliwal, S.S., 2011. Vermicomposting of tannery sludge mixed with cattle dung into valuable manure using earthworm Eisenia fetida (Savigny). Bioresour Technol 102, 7941–7945.
401. Vos, C. M., Tesfahun, A. N., Panis, B., de Waele, D., and Elsen, A. (2012). Arbuscular mycorrhizal fungi induce systemic resistance in tomato against the sedentary nematode Meloidogyne incognita and the migratory nematode *Pratylenchus penetrans*. Appl. Soil. Ecol. 61,1–6.
402. Wahocho, N.A., Zeshan Ahmed, S., Jogi, Q., Talpur, K.H., Leghari, S.J., 2016. Growth and productivity of chilli (*Capsicum annuum* L.) under various nitrogen levels. *Sci. Int.* 28.
403. Wang M, Zhu Y, Cheng L, Andserson B, Zhao X, Wang D, Ding A (2018) Review on utilization of biochar for metal-contaminated soil and sediment remediation. J Environ Sci 63:156–173
404. Wang, C. C., Li, M. Y., Yan, C. A., Tian, W., Deng, Z. H., Wang, Z. X., Xiang, P., 2022. Refining health risk assessment of heavy metals in vegetables from high geochemical background areas: Role of bioaccessibility and cytotoxicity. Process Saf. Environ. Protec. 159, 345-353.
405. Wang, C. C., Zhang, Q. C., Kang, S. G., Li, M. Y., Zhang, M. Y., Xu, W. M., Xiang, P., & Ma, L. Q. (2023). Heavy metal (loid) s in agricultural soil from main grain production regions of China: Bioaccessibility and health risks to humans. *Science of the Total Environment*, 858, 159819.

406. Wang, F., Liu, X., Shi, Z., Tong, R., Adams, C. A., Shi, X., 2016. Arbuscular mycorrhizae alleviate negative effects of zinc oxide nanoparticle and zinc accumulation in maize plants–a soil microcosm experiment. *Chemosphere*. *147*, 88-97.

407. Wang, G., Xia, X., Yang, J., Tariq, M., Zhao, J., Zhang, M., Huang, K., Lin, K., Zhang, W., 2020. Exploring the bioavailability of nickel in a soil system: physiological and histopathological toxicity study to the earthworms (Eisenia fetida). J Hazard Mater 383, 121169

408. Wang, M., Zhu, Y., Cheng, L., Andserson, B., Zhao, X., Wang, D., and Ding, A. (2018). Review on utilization of biochar for metal-contaminated soil and sediment remediation. J. Environ. Sci. 63,156–173.

409. Wang, X., Jia, Z., Liang, L., Yang, B., Ding, R., Nie, J., Wang, J., 2016. Impacts of manure application on soil environment, rainfall use efficiency and crop biomass under dryland farming. *Sci. Rep. 6*, 20994.

410. Wang, Y. J., He, X. H., Meng, L. L., Zou, Y. N., Wu, Q. S., 2023. Extraradical mycorrhizal hyphae promote soil carbon sequestration through difficultly extractable glomalin-related soil protein in response to soil water stress. *Microbial. Ecol.* 86(2), 1023-1034.

411. Wang, Y., & Cheng, H. (2023). Soil heavy metal (loid) pollution and health risk assessment of farmlands developed on two different terrains on the Tibetan Plateau, China. *Chemosphere*, 335, 139148.

412. Wang, Y., Duan, X., Wang, L., 2020. Spatial distribution and source analysis of heavy metals in soils influenced by industrial enterprise distribution: case study in Jiangsu Province. Sci. Total Environ. 710, 134953.

413. Wani, S. H., Sanghera, G. S., Athokpam, H., Nongmaithem, J., Nongthongbam, R., Naorem, B. S., Athokpam, H.S. (2012). Phytoremediation: Curing soil problems with crops. Afr. J. Agric. Res. 7:3991-4002.

414. Wei, X., Gao, B., Wang, P., Zhou, H., & Lu, J. (2015). Pollution characteristics and health risk assessment of heavy metals in street dusts from different functional areas in Beijing, China. *Ecotoxicology and environmental safety*, 112, 186-192. https://doi.org/10.1016/j.ecoenv.2014.11.005

415. Weissmannová, H.D., & Pavlovský, J. (2017). Indices of soil contamination by heavy metals–methodology of calculation for pollution assessment (minireview). *Environmental Monitoring and Assessment*, 616

416. WHO., 1996. World Health Organization Permissible limits of heavy metals in soil and plants. Switzerland

417. Wright, S. F., and Upadhyaya, A. (1996). Extraction of an abundant and unusual protein from soil and comparison with hyphal protein of arbuscular mycorrhizal fungi. Soil. Sci. 161,575–586.

418. Wu QS, Li Y, Zou YN, He XH (2015) Arbuscular mycorrhiza mediates glomalin-related soil protein production and soil enzyme activities in the rhizosphere of trifoliate orange grown under different P levels. Mycorrhiza 25:121–130

419. Wu, S.C., Wong, C.C., Shu, W.S., Khan, A.G., Wong, M.H. (2010) Mycorrhizo-remediation of lead/zinc mine tailings using vetiver: a field study. Int J Phytoremediation 13:61–74

420. Xiao, R., Guo, D., Ali, A., Mi, S., Liu, T., Ren, C., Li, R., Zhang, Z., 2019. Accumulation, ecological-health risks assessment, and source apportionment of heavy metals in paddy soils: a case study in Hanzhong, Shaanxi, China. Environ. Pollut. 248,349–357.

421. Xiong, L., Deng, Q., Tucker, G.J., McDowell, D.L., and Chen, Y., 2012. Coarse-grained atomistic simulations of dislocations in Al, Ni and Cu crystals. Int J Plasticity 38, 86-101.

422. Xu, W.H., Jian, H., Liu, Y.G., Zeng, G.M., Li, X., Zhang, W., 2015. Bioreduction of chromate by an isolated Bacillus anthracis Cr-4 with soluble Cr (III) product. Water Air Soil Pollut. 226, 1–9.

423. Yan, L., Lu, M., Riaz, M., Tong, K., Yu, H., Gao, G., & Niu, Y. (2025). Exogenous proline enhances salt acclimation in soybean seedlings: Modifying physicochemical properties and controlling proline metabolism through the ornithine-glutamate dual pathway. *Ecotoxicology and environmental safety*, *294*, 118012.

424. Yan, X., Luo, X., Zhao, M., (2016). Metagenomic analysis of microbial community in uranium-contaminated soil. Appl. Microbiol. Biotechnol. 100, 299–310.

425. Yang, X., Cheng, B., Gao, Y., Zhang, H., & Liu, L. (2022). Heavy metal contamination assessment and probabilistic health risks in soil and maize near coal mines. *Frontiers in Public Health*, 10, 1004579.

426. Yang, Y., Ge, Y., Tu, P., Zeng, H., Zhou, X., Zou, D., Wang, K., Zeng, Q., 2019. Phytoextraction of Cd from a contaminated soil by tobacco and safe use of its metal enriched biomass. J. Hazard. Mater. 363, 385–393.

427. Yang, Z., Wang, Y., Shen, Z., Niu, J., Tang, Z., (2009). Distribution and speciation of heavy metals in sediments from the mainstream, tributaries, and lakes of the Yangtze River catchment of Wuhan, China. J. Hazard. Mater. 166, 1186–1194

428. Ye LL, Chen YS, Chen YD, Qian LW, Xiong WL, Xu JH, Jiang JP (2020) Phytomanagement of a Chromium-contaminated Soil by a High-value Plant: Phytostabilization of Heavy Metal Contaminated Sites. BioResour 15:3545-3565

429. Yoon, J. M., Oliver, D. J., and Shanks, J. V. (2008). Phytotransformation of 2,4-dinitrotoluene in Aradidopsis thaliana: Toxicity, fate and gene expression studies in vitro. Biotechnol. Program. 22,1524–1531.

430. Yu, B., Wang, Y., & Zhou, Q. (2014). Human health risk assessment based on toxicity characteristic leaching procedure and simple bioaccessibility extraction test of toxic metals in urban street dust of Tianjin, China. *PLoS One*, 9(3), e92459.

431. Yu, B., Wang, Y., & Zhou, Q. (2014). Human health risk assessment based on toxicity characteristic leaching procedure and simple bioaccessibility extraction test of toxic metals in urban street dust of Tianjin, China. *PLoS One*, 9(3), e92459.

432. Zakir, H. M., Quadir, Q. F., Mollah, M. Z. I., (2021). Human health risk assessment of heavy metals through the consumption of common foodstuffs collected from two divisional cities of Bangladesh. Exposure Health 13(2), 253–268.

433. Zayed, A., Lytle, C. M., Qian, J. H., and Terry, N. (1998). Chromium accumulation, translocation and chemical speciation in vegetable crops. Planta. 206,293–299.

434. Zazouli, M. A., Mahdavi, Y., Bazrafshan, E., and Balarak, D. (2014). Phytodegradation potential of bisphenolA from aqueous solution by *Azolla Filiculoides*. J. Environ. Health. Sci. Eng. 12,66.

435. Zeb, A., Li, S., Wu, J., Lian, J., Liu, W., & Sun, Y. (2020). Insights into the mechanisms underlying the remediation potential of earthworms in contaminated soil: A critical review of research progress and prospects. *Science of the Total Environment*, *740*, 140145.

436. Zeng, F., Ali, S., Zhang, H., Ouyang, Y., Qiu, B., Wu, F., Zhang, G., (2011). The influence of pH and organic matter content in paddy soil on heavy metal availability and their uptake by rice plants. Environ. Poll. 159(1), 84–91.

437. Zeng, X.F., Wang, Z.W., Wang, J., Guo, J.T., & Zhuang, J. (2015). Health risk assessment of heavy metals via dietary intake of wheat grown in Tianjin sewage irrigation area. *Ecotoxicology* 24 (10), 2115–2124.

438. Zhan F, Li B, Jiang M, Li T, He Y, Li Y, Wang Y (2019) Effects of arbuscular mycorrhizal fungi on the growth and heavy metal accumulation of bermudagrass [*Cynodon dactylon* (L.) Pers.] grown in a lead–zinc mine wasteland. Int J Phytoremediation 21:849–856

439. Zhang Z, Wang Q, Wang H, Nie S, Liang Z (2017) Effects of soil salinity on the content, composition, and ion binding capacity of glomalin-related soil protein (GRSP). Sci Total Environ 581:657–665

440. Zhang, H.Y., Wang, Y., Xiao, S., Wang, H., Wang, J.H., and Feng, L. (2017). Rapid detection of Cr (VI) ions based on cobalt (II)-doped carbon dots. Biosensors Bioelectronics 87, 46-52.

441. Zhang, N., Ren, Y., Shi, Q., Wang, X., Wei, M., Yang, F., (2011). Effects of vermicompost on quality and yield of watermelon. China Veg. 6, 76–79 (in Chinese with English abstract).

442. Zhao X, Sun Y, Huang J, Wang H, Tang D (2020) Effects of soil heavy metal pollution on microbial activities and community diversity in different land use types in mining areas. Environ Sci Pollut Res 27:20215–20226

443. Zhao, C., Wang, Yong, Wang, Yue, Wu, F., Zhang, J., Cui, R., Wang, L., Mu, H., 2018. Insights into the role of earthworms on the optimization of microbial community structure during vermicomposting of sewage sludge by PLFA analysis. Waste Management 79, 700–708.

444. Zhao, F.J., Wang, P., (2020). Arsenic and cadmium accumulation in rice and mitigation strategies. Plant Soil 446(1), 1–21.

445. Zheng, K., Liu, Z., Li, Y., Cui, Y., Li, M., (2013). Toxicological responses of earthworm (*Eisenia fetida*) exposed to metal-contaminated soils. Environmental Science and Pollution Research 20, 8382–8390.

446. Zhong W, Li J, Chen Y, Shu W, Liao B (2012) A study on the effects of lead, cadmium and phosphorus on the lead and cadmium uptake efficacy of *Viola baoshanensis* inoculated with arbuscular mycorrhizal fungi. J Environ Monitor 14:2497–2504

447. Zhou, H., Zhou, X., Zeng, M., Liao, B. H., Liu, L., Yang, W. T., Wu, Y. M., Qui, Q. Y., & Wang, Y. J. (2014). Effects of combined amendments on heavy metal accumulation in rice (Oryza sativa L.) planted on contaminated paddy soil. *Ecotoxicology and Environmental Safety,* 101, 226-232.

448. Zhu X, Song F, Liu F (2017) Arbuscular mycorrhizal fungi and tolerance of temperature stress in plants. Arbuscular mycorrhizas and stress tolerance of plants 163–194

frontiers | Frontiers in Environmental Science

TYPE Systematic Review
PUBLISHED 10 January 2025
DOI 10.3389/fenvs.2024.1532169

OPEN ACCESS

EDITED BY
Pavol Midula,
Czech University of Life Sciences Prague, Czechia

REVIEWED BY
Sudipta Tripathi,
Ramakrishna Mission Vivekananda Educational and Research Institute, India
Raktim Pal,
Tea Research Association, India

*CORRESPONDENCE
Pradip Bhattacharyya,
pradip.bhattacharyya@gmail.com

RECEIVED 22 November 2024
ACCEPTED 12 December 2024
PUBLISHED 10 January 2025

CITATION
Banerjee S, Mandal J, Sarkar D, Datta R and Bhattacharyya P (2025) A review and meta-analysis of the efficacy of arbuscular mycorrhizal fungi in remediating toxic metals in mine-affected soils.
Front. Environ. Sci. 12:1532169.
doi: 10.3389/fenvs.2024.1532169

A review and meta-analysis of the efficacy of arbuscular mycorrhizal fungi in remediating toxic metals in mine-affected soils

Sonali Banerjee[1], Jajati Mandal[2], Dibyendu Sarkar[3], Rupali Datta[4] and Pradip Bhattacharyya[1]*

[1]Agricultural and Ecological Research Unit, Indian Statistical Institute, Giridih, Jharkhand, India, [2]School of Science, Engineering & Environment, University of Salford, Salford, United Kingdom, [3]Department of Civil, Environmental, and Ocean Engineering, Stevens Institute of Technology, Hoboken, NJ, United States, [4]Department of Biological Science, Michigan Technological University, Houghton, MI, United States

Mines are natural reservoirs of various minerals, metals, and metalloids. Several heavy metals (HMs), such as Pb, Cd, Cr, Cu, and Ni, are major anthropogenic pollutants that cause severe environmental pollution. The accumulation of these toxic HMs in soils has raised several concerns for crop growth, food safety, and marketing. Physiological and biochemical processes in plants are severely impacted by HMs, disrupting normal metabolic activities and reducing biomass production. Phytoremediation plays a pivotal role in addressing HM contamination by offering an eco-friendly, economical, and holistic solution. Similarly, arbuscular mycorrhizal fungi (AMF) play a significant role by forming a symbiotic relationship with plant roots. In this association, plants provide root exudates, while AMF enhance plant growth under heavy metal stress by supplying essential nutrients, minerals, and water. These fungi also improve nutrient status, soil quality, and ecosystem stability. The present review and meta-analysis encompass an examination of the global distribution of toxic HMs in mining-affected areas. Furthermore, the study highlights the role of various plant species and microbes, particularly AMF, in mitigating HM stress and its impact on plant growth and nutrition. The meta-analysis also evaluates the efficacy of AMF as a remediation strategy for HM-impacted mine soils.

KEYWORDS

mines, heavy metals, phytoremediation, arbuscular mycorrhizal fungi, meta-analysis

1 Introduction

Human-driven activities such as agriculture, mining, industrial processes, and the extensive use of fertilizers and pesticides have escalated the demand for land resources since the twentieth century (Cheng, 2016). Heavy metal pollution, desertification of land, ecological imbalance of land, soil erosion, land degradation, environmental damage, and decreased soil fertility are all major environmental factors that have severe effects on soil, water, and air (Nosrati and Collins, 2019; Vaverková et al., 2019). Heavy metal (HM) pollution is a global phenomenon. Metal mining and mineral ore processing have a dual effect on the economy and the environment. From one perspective, they provide economic benefits to the country, and simultaneously, they cause environmental pollution. Abundant and active mines are the primary source of toxic HMs. During the rainy season, due to heavy

Science of the Total Environment 880 (2023) 163228

Contents lists available at ScienceDirect

Science of the Total Environment

journal homepage: www.elsevier.com/locate/scitotenv

Assessing pollution and health risks from chromite mine tailings contaminated soils in India by employing synergistic statistical approaches

Sonali Banerjee [a], Saibal Ghosh [a], Sonam Jha [a], Sumit Kumar [a], Gourav Mondal [a], Dibyendu Sarkar [b], Rupali Datta [c], Abhishek Mukherjee [a], Pradip Bhattacharyya [a,*]

[a] Agricultural and Ecological Research Unit, Indian Statistical Institute, Giridih, Jharkhand 815301, India
[b] Stevens Institute of Technology, Department of Civil, Environmental, and Ocean Engineering, Hoboken, NJ 07030, USA
[c] Department of Biological Science, Michigan Technological University, MI, USA

HIGHLIGHTS

- Mines and Mining activities pose the greatest ecological threats.
- The Chromite-Asbestos Mine's agroecosystem was contaminated with potentially toxic elements (PTEs), particularly Cr and Ni.
- PTE bioavailability may shed light on soil-crop-human transit and boost their presence in food chains.
- Studies using FIAM-HQ and SAMOE-TCR show PTEs (Cr and Ni) contaminated rice grain may increase cancer risk.
- Integrate the health risk assessment with the positive matrix factorization to identify pollution sources

GRAPHICAL ABSTRACT

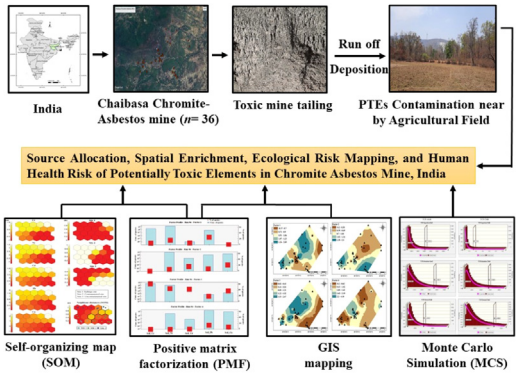

ARTICLE INFO

Editor: Deyi Hou

Keywords:
Chromite -asbestos mine
Potentially toxic elements
Soil and health risk evaluation
Multi-model analysis
Source apportionment

ABSTRACT

Potentially toxic elements (PTEs) contamination in the agricultural soil can generate a detrimental effect on the ecosystem and poses a threat to human health. The present work evaluates the PTEs concentration, source identification, probabilistic assessment of health hazards, and dietary risk analysis due to PTEs pollution in the region of the chromite-asbestos mine, India. To evaluate the health risks associated with PTEs in soil, soil tailings and rice grains were collected and studied. The results revealed that the PTEs concentration (mainly Cr and Ni) of total, DTPA-bioavailable, and rice grain was significantly above the permissible limit in site 1 (tailings) and site 2 (contaminated) as compared with site 3 (uncontaminated). The Free ion activity model (FIAM) was applied to detect the solubility of PTEs in polluted soil and their probable transfer from soil to rice grain. The hazard quotient values were significantly higher than the safe (FIAM-HQ < 0.5) for Cr (1.50E + 00), Ni (1.32E + 00), and, Pb (5.55E + 00) except for Cd (1.43E − 03), Cu (5.82E − 02). Severity adjustment margin of exposure (SAMOE) results denote that the PTEs contaminated raw rice grain has high health risk [Cr_{SAMOE}: 0.001; Ni_{SAMOE}: 0.002; Cd_{SAMOE}: 0.007; Pb_{SAMOE}: 0.008] for humans except for Cu. The Positive matrix factorization (PMF) along with correlation used to apportion the source. Self-organizing map (SOM) and PMF analysis identified the source of pollution mainly from mines in this region. Monte Carlo simulation (MCS) revealed that TCR (total carcinogenic risk) cannot be insignificant and children were the maximum sufferers relative to adults via ingestion-pathway. In the spatial distribution map, the region nearer to mine is highly prone to ecological risk with respect to PTEs pollution. Based on appropriate and reasonable evaluation methods, this work will help environmental scientists and policymakers' control PTEs pollution in agricultural soils near the vicinity of mines.

* Corresponding author.
E-mail address: pradip.bhattacharyya@gmail.com (P. Bhattacharyya).

http://dx.doi.org/10.1016/j.scitotenv.2023.163228
Received 29 December 2022; Received in revised form 29 March 2023; Accepted 29 March 2023
Available online 3 April 2023

Environ Geochem Health (2025) 47:212
https://doi.org/10.1007/s10653-025-02500-1

ORIGINAL PAPER

Hidden threats beneath: uncovering the bio-accessible hazards of chromite-asbestos mine waste and their impacts on rice components via multi-machine learning algorithm

Sonali Banerjee · Saibal Ghosh · Jyoti Prajapati · Pradip Bhattacharyya

Received: 24 October 2024 / Accepted: 3 April 2025

Abstract The chromite-asbestos mining leaves behind tonnes of toxic waste, contaminating nearby agricultural fields with potentially toxic elements (PTEs). Over time, wind and water erosion spread these pollutants, severely impacting the ecosystem, food chain, and human health. This study evaluates the bioaccessible (stomach and intestinal phases) and leachable forms of PTEs, emphasizing the health and dietary risks associated with PTE pollution in this region. The study result indicates that the leachable and bio-accessible PTEs concentrations in agricultural soil, mainly Cr and Ni, were higher in zone 1 (mine tailings dumping area) and zone 2 (tailings contaminated soil) than zone 3 (uncontaminated soil). PTEs content in rice parts, mainly in boiled rice, showed moderate risk in the SAMOE model from Cr (0.011) and Ni (0.013) while in rice (without husk), it indicated high (class 5) dietary risk. The Fuzzy-TOPSIS, artificial neural network, and Monte-Carlo simulation models all demonstrated that Cr was the major contributor to anthropogenic risk. Compared to adults (5.08E-05), children (1.88E-03) were more vulnerable to total carcinogenic risk via ingestion pathway. Machine learning methods have been implemented to forecast the effects of leachable PTEs on soil-rice systems and possible health hazards associated with consuming food from the chromite-asbestos waste-contaminated zone. The survey-based Fuzzy-DEMATEL technique also showed that consumption of starch and cooked rice were the most crucial factors influencing the population's health risk. Overall, the implications of the statistical model may aid in assessing potential health hazards and enhancing regulations for ecosystem preservation.

Keywords Hazardous PTEs · Health risk · Taylor · Fuzzy-DEMATEL · Anthropogenic hazards

Introduction

The global industrialization of the mining industry, especially in developing countries (China, India, and Bangladesh), has led to an increase in the concentration of potentially toxic elements (PTEs) in aquifers, crops, and agricultural soils as a result of mining, mine effluents, and mine tailing waste deposition (Pradhan et al., 2020; Zhu et al., 2018). The contamination of PTEs in the environment occurs from natural sources, including weathering, erosion, and eroding of the parent rock. Similarly, anthropogenic

Supplementary Information The online version contains supplementary material available at https://doi.org/10.1007/s10653-025-02500-1.

S. Banerjee · S. Ghosh · P. Bhattacharyya (✉)
Agricultural and Ecological Research Unit, Indian Statistical Institute, Giridih, Jharkhand 815301, India
e-mail: pradip.bhattacharyya@gmail.com

J. Prajapati
Department of Mathematics, Institute of Chemical Technology, Mumbai, India

Published online: 17 May 2025

Environmental Pollution 350 (2024) 124021

Contents lists available at ScienceDirect

Environmental Pollution

journal homepage: www.elsevier.com/locate/envpol

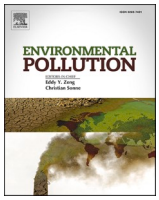

Synergistic impact of bioavailable PHEs and alkalinity on microbial diversity and traits in agricultural soil adjacent to chromium-asbestos mines☆

Sonali Banerjee [a], Saibal Ghosh [a], Shreya Chakraborty [a], Dibyendu Sarkar [b], Rupali Datta [c], Pradip Bhattacharyya [a,*]

[a] Agricultural and Ecological Research Unit, Indian Statistical Institute, Giridih, Jharkhand, 815301, India
[b] Stevens Institute of Technology, Department of Civil, Environmental, and Ocean Engineering, Hoboken, NJ, 07030, USA
[c] Department of Biological Science, Michigan Technological University, Michigan, USA

ARTICLE INFO

Keywords:
PHEs
Alkalinity
Soil bacterial diversity
Geospatial pattern
Multi-model approaches

ABSTRACT

Soil microbial communities undergo constant fluctuations, particularly in response to environmental factors. Although the deposition of toxic mine waste is recognized for introducing potentially hazardous elements (PHEs) into the soil, its specific impacts on microbial communities remain unclear. This study aims to explore the combined effects of soil alkalinity and bioavailable PHEs on microbial diversity and traits in agricultural soil adjacent to a chromium-asbestos mining area. By employing a comprehensive analysis, this study indicated that microbiological attributes were reduced in contaminated areas (zone 1), whereas both the levels of bioavailable PHEs (CrWs: 31.08 mg/kg, NiWs: 13.90 mg/kg) and alkalinity indices (CROSS, MCAR, MH) were significantly higher. The spatial distribution of soil alkalinity and bioavailable PHEs, primarily originating from chromium-asbestos mines, has been determined. This study also elucidates the negative relationship between soil stressors (Alkalinity and PHEs) and microbial activities (soil enzymatic activity, microbial respiration, and biomass carbon). The vector's length exhibited a notable difference between zone 1 (0.51) and zone 2 (0.32), indicating a substantial limitation on carbon (C). Also, the investigation of soil bacterial diversity unveiled notable disparities in the prevalence of microbial populations inside zone 1. *Proteobacteria* constituted 57.18% of the total population indicating a noteworthy prevalence in the contaminated soils. Finally, the random forest (RF) algorithm from machine learning was selected and proven to be a robust choice in Taylor diagrams for predicting the causative stressors responsible for the deterioration of soil microbial health. Therefore, this research offers insights into the health and resilience of soil microbial communities under synergistic stress conditions, which will aid environmentalists in planning future interventions and improving sustainable farming techniques.

1. Introduction

Soil is the natural habitat for a diverse range of living organisms, encompassing plants, animals, and microorganisms (Kuang et al., 2016). Microorganisms, being the most predominant group present on Earth, serve a vital role in maintaining the biological activity and biodiversity within the soil. Since soil microorganisms are highly sensitive to changes in their environment, they are frequently used as accurate stress indicators of the environment (Schloter et al., 2003). Nevertheless, both anthropogenic and natural stressors have the potential to induce disturbances in microbial biodiversity. The alteration of microbial communities is strongly linked to variations in physicochemical factors, such as pH, temperature, and cationic stress (Xiong et al., 2012). Additionally, imbalances in nutrient levels (Zhang et al., 2017), improper agricultural practices (such as pesticide and chemical fertilizer usage), industrial effluents, mining activities, and the presence of toxic potential hazardous elements (PHEs) have been recognized as key factors that influence changes in microbial communities (Sarma et al., 2022;

☆ This paper has been recommended for acceptance by Prof. Wen-Xiong Wang.
* Corresponding author.
E-mail address: pradip.bhattacharyya@gmail.com (P. Bhattacharyya).

https://doi.org/10.1016/j.envpol.2024.124021
Received 2 December 2023; Received in revised form 15 April 2024; Accepted 20 April 2024
Available online 22 April 2024

Journal of Environmental Chemical Engineering 13 (2025) 116019

Contents lists available at ScienceDirect

Journal of Environmental Chemical Engineering

journal homepage: www.elsevier.com/locate/jece

Innovative green vermi-remediation of chromite-asbestos mine waste: From toxicity reduction to soil-crop-microbe health improvement utilizing novel multimodal statistical approach

Sonali Banerjee [a], Saibal Ghosh [a,b], Sonam Jha [a], Pradip Bhattacharyya [a,*]

[a] Agricultural and Ecological Research Unit, Indian Statistical Institute, Giridih, Jharkhand 815301, India
[b] Department of Analytical Services, Tocklai Tea Research Institute, Jorhat, Assam 785008, India

ARTICLE INFO

Keywords:
Chromite-asbestos mine waste
PLFA profiling
Sobol sensitivity analysis
Toxic elements bioavailability
Sesame Crop

ABSTRACT

Chromite-asbestos mine waste (CAMW), a highly toxic byproduct induces significant environmental contamination, currently lacks sustainable recycling solutions. This study aimed to assess the potential of vermi-remediation technology for transforming hazardous CAMW into valuable agricultural resources. The key objectives were to determine the suitable feedstock combination for effective vermi-remediation, offer new insights regarding microbe-toxic elements (TEs) interactions during vermicomposting, and validate the efficacy of *Eisenia fetida* by examining the CAMW-induced alterations in microbial community structure, TEs removal, and nutrient dynamics. To achieve this goal, cow dung (CD) was combined with CAMW at ratios (1:1 and 1:2) for large-scale vermicomposting, with results compared to CD alone. The findings revealed that earthworm counts in CAMW-vermibeds increased by 4.89–5.92 times. Bioavailable TEs levels (Ni, Cd, Cr, Pb, and Cu) were significantly reduced up to 80 % in vermibeds. Additionally, CAMW-rich mixtures [T1: CD+CAMW (1:1)] saw significant acidity neutralization, improved organic carbon mineralization, and increased NPK levels. Vermicomposting showed greater microbial proliferation and enzyme activity in T1 Species-diversity and phospholipid fatty acid (PLFA)analysis revealed that the structure of microbial communities and fatty acid profiles showed substantial variation with varying CAMW content in vermibeds. Further Sobol analysis demonstrated the susceptibility and resilience of microbial populations in response to certain TEs. Ultimately, CAMW-vermicompost application boosted sesame growth and improved soil health with negligible TEs transfer. Overall, we believe this study provides an initial step towards understanding the eco-friendly transformation of toxic CAMW into beneficial organic soil amendments, promoting sustainable mine-waste management and ecosystem health.

1. Introduction

Soil health is essential for sustainable agricultural development, which is vital for securing food supplies and supporting terrestrial ecology [78]. However, extensive industrialization and the modernization of various farming practices, especially the overuse of pesticides and chemical fertilizers along with mining activities and the careless disposal of mine waste containing toxic elements (TEs: Ni, Cd, Cr, Cu, and Pb), have resulted in the contamination of adjacent farmlands, thereby reducing crop yield and quality worldwide [68]. Chromite-asbestos mine waste (CAMW) disperses rapidly due to environmental influences like heavy rainfall, strong winds, and natural processes such as weathering and erosion. Human activities further accelerate this spread, all contributing to significant harm to the

Abbreviations: CAMW, Chromite-asbestos mine waste; CD, Cow dung; TEs, Toxic elements; Avl. N, Available Nitrogen; Avl. P, Available Phosphorus; EX. K, Exchangeable Potassium; EC, Electrical conductivity; TOC, Total organic carbon; PLFA, Phospholipid fatty acid; VCT, Vermi-remediation technology; PCA, Principal component analysis; RSD, Relative standard deviation; BAF, Bioaccumulation factor; SOD, Super oxide dismutase; CAT, Catalase; POX, Peroxidase; NBR, Nutritional benefit ratio; MBC, Microbial biomass carbon; MBN, Microbial biomass nitrogen; MBP, Microbial biomass phosphorus; SIR, Substrate-induced respiration; BSR, Basal soil respiration; BG, β-glucosidase; U, Urease; AP, Alkaline phosphatase; DHG, Dehydrogenase; FDA, Fluorescein diacetate; SDI, Shannon diversity index; SEI, Shannon evenness index; EVI, Evar index; VC, Vermicompost; PCF, Plant concentration factor; PTF, Plant translocation factor; BA, Bioavailable; CAMW-VC, Chromite-asbestos mine waste Vermicompost; MUFA, Monounsaturated fatty acids; PUFA, Polyunsaturated fatty acids; DMA, Dimethyl Acetal.

* Corresponding author.
E-mail address: pradip.bhattacharyya@gmail.com (P. Bhattacharyya).

https://doi.org/10.1016/j.jece.2025.116019
Received 26 November 2024; Received in revised form 25 February 2025; Accepted 27 February 2025
Available online 27 February 2025

Science of the Total Environment 989 (2025) 179884

Contents lists available at ScienceDirect

Science of the Total Environment

journal homepage: www.elsevier.com/locate/scitotenv

Enhancing mycophytoremediation potential of *Chrysopogon zizanioides* in chromite-asbestos mine waste soil using arbuscular mycorrhizal fungi: A natural bioaccelerator for soil ecosystem rehabilitation

Sonali Banerjee [a], Saibal Ghosh [a,b], Sonam Jha [a], Sumit Kumar [a], Dibyendu Sarkar [c], Rupali Datta [d], Pradip Bhattacharyya [a,*]

[a] *Agricultural and Ecological Research Unit, Indian Statistical Institute, Giridih 815301, Jharkhand, India*
[b] *Department of Analytical Services, Tocklai Tea Research Institute, Jorhat, 785008, Assam, India*
[c] *Stevens Institute of Technology, Department of Civil, Environmental, and Ocean Engineering, Hoboken, NJ 07030, USA*
[d] *Department of Biological Science, Michigan Technological University, MI, USA*

HIGHLIGHTS

- Natural bio-accelerator "Arbuscular mycorrhizal fungi" enhances mycophyt oremediation
- *Glomus hoi* increased TEs accumulation (Ni: 27.44 %, Cr: 21.74 %) in vetiver roots
- Higher Glomalin production and colonization depicted in presence of *Glomus hoi*
- PLS-SEM and Sobol models validates AMF presence enhances phytoremediation
- AMF mitigates TEs toxicity, promote plant growth, and improve soil health quality

GRAPHICAL ABSTRACT

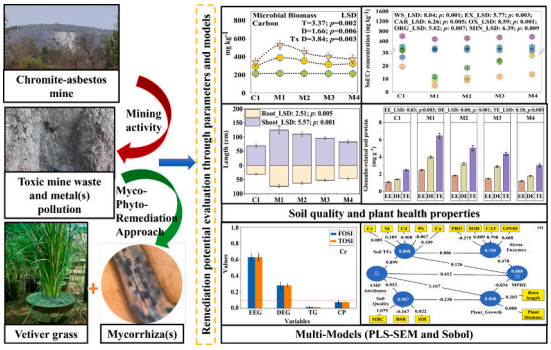

ARTICLE INFO

Editor: Paromita Chakraborty

Keywords:
Mycophytoremediation
Chromite-asbestos mine waste
PLS-SEM
Glomalin
Sobol analysis

ABSTRACT

Soil contamination with toxic elements (TEs) has become a serious environmental issue in recent decades. Bio-based approaches especially, "phytoremediation-associated with arbuscular mycorrhizal fungi (AMF)" has emerged as a promising, eco-friendly and sustainable technology worldwide. The present investigation assessed the impact of AMF on the growth and TEs accumulation abilities of vetiver (*Chrysopogon zizanioides)* in a soil containing chromite-asbestos mine wastes. Among the four different AMF species tested—*Glomus hoi*, *Funneliformis coronatum*, *Claroideoglomus claroideum*, and *Claroideoglomus etunicatum*—*Glomus hoi* (M1) showed high efficiency in improving soil quality, mitigating TEs stress and promoting healthy plant growth. In comparison with control plant (devoid of AMF), the higher accumulation of TEs in the roots (Ni: 27.44 %, Cr: 21.74 %) was observed in presence of *Glomus hoi* and TEs concentration in soil was reduced in bioavailable phase. A periodic increase in microbial-enzymatic activity was found across all AMF inoculums, with the M1 treatment (microbial biomass carbon: 527.66 mg kg^{-1}) exhibiting highest microbial activity as compared with control. The AMF infection resulted in heightened antioxidant activity, which mitigated TE-induced stress in vetiver plants.

* Corresponding author.
E-mail address: pradip.bhattacharyya@gmail.com (P. Bhattacharyya).

https://doi.org/10.1016/j.scitotenv.2025.179884
Received 19 April 2025; Received in revised form 31 May 2025; Accepted 9 June 2025